Technische Universität Braunschweig

Network Partner of

International Network on Sustainable Water Management in Developing Countries

ex)(ceed SWINDON

Water Perspectives in Emerging Countries

Integrating Ecosystems in Coastal Engineering Practice (INECEP)

Rodolfo Silva and Valeria Chávez (Eds.)

Summer School in Puerto Morelos, Mexico – September 2017

Funded by:

Federal Ministry for Economic Cooperation and Development

exceed EXCELLENCE CENTERS FOR EXCHANGE AND DEVELOPMENT

DAAD

Water Perspectives in Emerging Countries

Integrating Ecosystems in Coastal Engineering Practice (INECEP)

Rodolfo Silva and Valeria Chávez

Proceedings of the Summer School

September 18-30, 2017 – Puerto Morelos, Mexico

Dieses Werk ist copyrightgeschützt und darf in keiner Form vervielfältigt werden noch an Dritte weitergegeben werden.
Es gilt nur für den persönlichen Gebrauch.

Dieses Werk ist copyrightgeschützt und darf in keiner Form vervielfältigt werden noch an Dritte weitergegeben werden.
Es gilt nur für den persönlichen Gebrauch.

Water Perspectives in Emerging Countries

Integrating Ecosystems in Coastal Engineering Practice (INECEP)

Rodolfo Silva and Valeria Chávez

Proceedings of the Summer School

September 18-30, 2017 – Puerto Morelos, Mexico

Issue Editors

Prof. Dr. Rodolfo Silva Casarin
Universidad Nacional Autónoma de México, Instituto de Ingeniería, CDMX, México;
RSilvaC@iingen.unam.mx

Prof. Valeria Chávez Cerón
Universidad Nacional Autónoma de México, Instituto de Ingeniería, CDMX, México;
VChavezC@iingen.unam.mx

Exceed Chairman & Editor-in-Chief

Prof. Dr.-Ing. Norbert Dichtl
Technische Universität Braunschweig, Institute of Sanitary and Environmental Engineering, Braunschweig, Germany
n.dichtl@tu-bs.de

Publishing Editor

Prof. em. Dr. mult. Dr. h.c. Müfit Bahadir
Technische Universität Braunschweig, Leichtweiss Institute, Exceed, Braunschweig, Germany;
m.bahadir@tu-bs.de

This publication was financed by the German Academic Exchange Service (DAAD) and the Federal Ministry for Economic Cooperation and Development (BMZ).

All rights reserved including translation into foreign languages. The publication or parts thereof may not be reproduced in any form without permission from the publishers.

Printed in Germany by Cuvillier Verlag, Göttingen, Germany

Dieses Werk ist copyrightgeschützt und darf in keiner Form vervielfältigt werden noch an Dritte weitergegeben werden.
Es gilt nur für den persönlichen Gebrauch.

Bibliografische Information der Deutschen Nationalbibliothek
Die Deutsche Nationalbibliothek verzeichnet diese Publikation in der
Deutschen Nationalbibliografie; detaillierte bibliografische Daten sind im Internet
über http://dnb.d-nb.de abrufbar.
1. Aufl. - Göttingen: Cuvillier, 2017

© CUVILLIER VERLAG, Göttingen 2017
Nonnenstieg 8, 37075 Göttingen
Telefon: 0551-54724-0
Telefax: 0551-54724-21
www.cuvillier.de

Alle Rechte vorbehalten. Ohne ausdrückliche Genehmigung des Verlages ist
es nicht gestattet, das Buch oder Teile daraus auf fotomechanischem Weg
(Fotokopie, Mikrokopie) zu vervielfältigen.
1. Auflage, 2017
Gedruckt auf umweltfreundlichem, säurefreiem Papier aus nachhaltiger Forstwirtschaft.

ISBN 978-3-7369-9661-8
eISBN 978-3-7369-8661-9

Dieses Werk ist copyrightgeschützt und darf in keiner Form vervielfältigt werden noch an Dritte weitergegeben werden.
Es gilt nur für den persönlichen Gebrauch.

CONTENT

Dieses Werk ist copyrightgeschützt und darf in keiner Form vervielfältigt werden noch an Dritte weitergegeben werden.
Es gilt nur für den persönlichen Gebrauch.

Dieses Werk ist copyrightgeschützt und darf in keiner Form vervielfältigt werden noch an Dritte weitergegeben werden.
Es gilt nur für den persönlichen Gebrauch.

PREFACE

In September 2011 and September 2013, the EXCEED-SWINDON Project organised two-week Summer Schools on “Flood Risk Analysis and Management” at Bahir Dar University, Ethiopia, and “Coastal Erosion and Management for Safer Coasts in a Changing Climate” in Tamandare, Brazil, respectively. Given their success, a similar Summer School “Integrating Ecosystems in Coastal Engineering Practice (INECEP)” was organised in Puerto Morelos, Mexico, September 18-30, 2017.

The lecturers in charge of teaching on the course were:

Angel Borja	AZTI, Spain
Andres F. Osorio	UNAL, Colombia
Brigitta van Tussenbroek	ICMYL-UNAM, Mexico
Edgar Escalante	ICMYL-UNAM, Mexico
Edgar Mendoza	Instituto de Ingeniería-UNAM, Mexico
Eleonora Carol	CONICET-UNLP, Argentina
Gladys Bernal Franco	UNAL, Colombia
Hocine Oumeraci	TU Braunschweig, Germany
Ismael Mariño-Tapia	CINVESTAV, Mexico
Katie Arkema	Stanford University, US
Malva Mancuso	UFSM-FW, Brazil
Ma. Luisa Martínez	INECOL, A.C., Mexico
Milton Asmus	FURG, Brazil
Patricia Moreno-Casasola	INECOL, A.C., Mexico
Pedro Pereira	UFPE, Brazil
Rodolfo Silva	Instituto de Ingeniería-UNAM, Mexico
Sheila J.J. Heymans	Scottish Marine Institute, UK
Tjeerd Bouma	Royal Netherlands Institute of Sea Research, NL

The Summer School sessions included class lectures, exercises and discussions. During the classes, the participants from nine countries were equipped with essential state-of-the art knowledge concerning coastal ecosystems, their functioning and interaction with traditional man-made infrastructure, and their evaluation. Modelling concepts and approaches to quantify the degradation and renovation of ecosystems by and after natural disturbances were also covered. The most promising methods/strategies/tools to integrate eco-system engineering solutions for coastal protection at different scales (local to regional) were discussed. The participants also carried out field work in three different ecosystems: beach and dunes, coral reefs, and wetlands. The participants had the opportunity to present and to discuss in group discussions case studies from their own countries with the aim of identifying the most appropriate solutions. Twenty six chapters written by the attendees were selected and are presented in this book.

Valeria Chávez and Rodolfo Silva – Coordinators of INECEP Summer School
Instituto de Ingeniería-UNAM, Mexico

Dieses Werk ist copyrightgeschützt und darf in keiner Form vervielfältigt werden noch an Dritte weitergegeben werden.
Es gilt nur für den persönlichen Gebrauch.

ECOSYSTEM-BASED ADAPTATIONS FOR STEPPED REVETMENTS: AN APPLICATION TO STRAND, SOUTH AFRICA

Talia Schoonees[1]

[1]Ludwig Franzius Institute, Leibniz University Hannover, Nienburger Str. 4, 30167 Hannover, Germany, schoonees@lufi.uni-hannover.de

Keywords: Coastal Structure, Ecosystem-based Adaptations, Stepped Revetment

Abstract

Conventional hard coastal structures such as stepped revetments have significant environmental impacts. This paper investigates how a conventional stepped revetment can be adapted to mitigate or to reduce its environmental impacts. As a first step, the potential environmental impacts of a conventional stepped revetment are identified. Considering these impacts, possible ecosystem-based adaptations are proposed. Since the feasibility of these adaptations will differ from site to site, a case study is selected to investigate the implementation of an ecosystem-based stepped revetment. The study site and its environmental and ecological conditions are described. A discussion on the site selection for the implementation of a possible ecosystem-based stepped revetment is also included. Finally, an ecosystem-based stepped revetment is proposed for the study site.

1 Introduction

Even though there has been a shift towards the implementation of soft shoreline protection measures, hard coastal structures still form a vital component of coastal protection strategies. Hard coastal structures have generally been designed with little or no consideration of their potential impacts on the environment. One solution to address this shortcoming in the traditional design procedure is to incorporate ecosystem-based adaptations for traditional coastal structures.

A stepped revetment is classified as a hard coastal structure (non-erosive). From a coastal engineering point of view, the main advantage of a stepped revetment (in comparison to a smooth slope revetment or dike) is that the steps on the revetment create roughness elements which results in a reduction of wave run-up and wave overtopping. In addition, a stepped revetment is multi-functional. It can be an aesthetical coastal protection measure that promotes tourism and recreation by providing access to water areas, creating walkways and/or serve as a bench (Figures 1 and 2). An economic advantage of a stepped revetment is that the steps can be constructed with precast concrete elements. Stepped revetments are typically applied as coastal structure in cities, where available space is constrained.

Dieses Werk ist copyrightgeschützt und darf in keiner Form vervielfältigt werden noch an Dritte weitergegeben werden.
Es gilt nur für den persönlichen Gebrauch.

One main disadvantage of a conventional stepped revetment is its potential environmental impacts. However, ecosystem-based adaptations to a conventional stepped revetment can mitigate or reduce its environmental impacts.

2 General

2.1 Objectives

The overall objective of this research is to develop ecosystem-based adaptations for stepped revetments to mitigate or to reduce its environmental impacts. General adaptations will be considered. However, the environmental, ecological and social conditions of the site, where the structure will be implemented, have to be taken into account in order to develop optimal ecosystem-based adaptations for a specific case. A study site in Strand, South Africa was selected as a case study to consider the implementation of an ecosystem-based stepped revetment. (Note that the author has not been involved in the design and construction of the seawall that is presently (July 2017) being built at the Strand. Neither have the designer and contractor of the seawall been part of this hypothetical case study.)

The paper defines the scope of the research and gives an overview of previous studies on stepped revetments. The prospective methodology to reach the research objectives is described. The focus then shifts to the case study for Strand, South Africa. A description of the Strand study site and its environmental and ecological conditions are presented. Social conditions at a study are also very important, but are not in the scope of this study. Finally, an adaptation for a stepped revetment for the case study is proposed.

Figure 1: Stepped revetment at Margate, United Kingdom

Dieses Werk ist copyrightgeschützt und darf in keiner Form vervielfältigt werden noch an Dritte weitergegeben werden.
Es gilt nur für den persönlichen Gebrauch.

Figure 2: Stepped sea organ at Zadar, Croatia

2.2 Background

The traditional thinking of engineers often causes them to perceive environmental considerations as a 'chore' that comes as part of the profession. When an engineer has this mind-set, optimal and innovative coastal engineering solutions, which are also favourable or less harmful to the environment, will not be achieved. Since research on stepped revetments is ongoing, it is possible to include environmental considerations for stepped revetments in the development of design guidelines.

This research aims to complement the research project *waveSTEPS*. Project *waveSTEPS* is funded by the German Federal Ministry of Education and Research (BMBF) through the German Coastal Engineering Research Council (KFKI, 03KIS118 and 03KIS119) and focusses on the development of design guidelines for conventional stepped revetments. The investigation to develop an ecosystem-based stepped revetment is not within the scope of project waveSTEPS and is the focus of this paper.

2.3 Definitions

For this paper a stepped revetment is defined as a coastal defence constructed parallel to the coast to reduce the impacts of waves. A conventional stepped revetment is defined as an impermeable concrete structure typically located at the back of a beach (Figure 1) or at waterfront areas (Figure 2).

For a design water level, wave height and wave period, the crest level for a stepped revetment will be determined by the allowable wave run-up or wave overtopping. Wave run-up is defined as the maximum vertical distance above the still water level, to which a wave rushes up on the stepped

Dieses Werk ist copyrightgeschützt und darf in keiner Form vervielfältigt werden noch an Dritte weitergegeben werden.
Es gilt nur für den persönlichen Gebrauch.

revetment. Wave overtopping occurs when wave action discharges water over the crest of the stepped revetment and is defined as the discharge of water (m^3/s) over 1 meter of crest length.

In [1], two approaches are described, whereby ecology is integrated into coastal protection measures. The first approach is to use ecosystem engineering species that change their environment. An example of the first approach is to use organisms (such as mussels or seagrass) to trap sediment and to attenuate waves. The second approach is to adapt coastal structures to enhance local biodiversity and ecosystem functioning.

The focus of this paper will only include the second approach. Therefore, the adaptations to a conventional stepped revetment are aimed at enhancing the ecological value of the structure. Only ecosystem-based adaptations in small (<10 cm) to medium (1-10 m) spatial scales will be considered. Microscale adaptations such as building material composition and surface roughness are not within the scope of the research [2].

2.3 Previous studies on stepped revetments

Research on stepped revetments has a history of more than 60 years. A thorough summary and evaluation on this research history of stepped revetments is provided by [3]. Through the literature review, which includes almost 30 publications, [3] identified a number of areas where additional research on stepped revetments are required.

Firstly, no comprehensive study could be identified that conducted physical model tests on a wide range of dimensionless parameters. Due to different scales and boundary conditions of the model tests, it is not possible to develop empirical predictions for wave run-up, wave overtopping, and the wave impacts. Therefore, there is a need for systematic research to provide generic design guidelines for stepped revetments. The knowledge gaps identified by [3] were the research motivation for the comprehensive study of [4].

[4] conducted an experimental and theoretical study of the wave-induced response of stepped revetments. Physical model tests were conducted for a large range of geometric and hydraulic boundary conditions. Based on these model tests, [4] derived empirical predictions for wave reflection, wave run-up, wave overtopping, and the wave loads of stepped revetments.

Although [4] presents predictions applicable for a wide range of dimensionless parameters, there are still certain ranges of boundary conditions with little or no data points. The project *waveSTEPS* aims to focus on these certain ranges of boundary conditions. Another uncertainty is the scale effects that the model tests are subjected to. As part of *waveSTEPS,* the scale effects will be assessed by conducting full scale model tests.

The development of ecosystem-based adaptations for stepped revetments complements the present research and will raise new research questions for future research.

Dieses Werk ist copyrightgeschützt und darf in keiner Form vervielfältigt werden noch an Dritte weitergegeben werden.
Es gilt nur für den persönlichen Gebrauch.

3 Methodology

This section describes the methodology that was followed to achieve the research objectives. As a first step, the general potential environmental impacts of stepped revetments are described. This step is important to consider, since the ecosystem-based adaptations aim to mitigate or to reduce the environmental impacts.

Once the key environmental impacts have been identified, three possible adaptations will be considered based on literature research. Since the adaptations will differ from site to site, the study site at Strand, South Africa is considered. A description of the environmental and ecological conditions for Strand is given. These conditions are taken into account in order to select the most suitable adaptation for the study site, which is the final step of the methodology.

4 Results and Discussion

4.1 Environmental impacts

Environmental impacts are defined as any modifications (deliberate or accidental) made to the environment and/or biological resources by anthropogenic activities [5]. When environmental impacts are considered it is important to take into account that these impacts are subjected to different spatial and temporal scales. For this research, only impacts in terms of the local spatial scale (1-10 km) are considered, since the ecosystem-based adaptations are aimed to reduce or to mitigate environmental impacts on the local scale.

A stepped revetment will cause changes to the coastal environment in terms of wave conditions and sediment transport (erosion and deposition patterns). In the case of a stepped revetment, constructed along a shoreline that experiences long-term net erosion, the shoreline will migrate landward resulting in loss of beach width. The revetment also interrupts the sand supply between the beach and backshore which influences the cross-shore transport processes. The changes in the sediment transport also impacts the characteristics in terms of grain size, content of organic matter, and redox conditions [5].

The changes of the coastal environment in turn affect the composition, abundance, and trophic structure of the benthos [5, 6]. The construction of a stepped revetment will also result in a loss of soft-bottom habitats and associated fauna and flora as well as result in an increase in (artificial) hard-bottom substrata [5]. Fish and mobile fauna are to be affected as well. When a stepped revetment is built in an environment, which has mostly sandy habitats, changes in the local biodiversity can be a consequence [5, 7].

4.2 Ecosystem-based adaptations

This section considers three possible adaptations to conventional stepped revetments to reduce or mitigate the environmental impacts of stepped revetments. The suitability of the adaptations should be based on the environmental, ecological and social conditions of a specific site, and should consider whether the functionality of the structure is retained (coastal safety, recreational value, multi-functionality, providing safe access).

Dieses Werk ist copyrightgeschützt und darf in keiner Form vervielfältigt werden noch an Dritte weitergegeben werden.
Es gilt nur für den persönlichen Gebrauch.

4.2.1 Incorporating vegetation

To provide habitat and to improve aesthetical value of stepped revetments, sections of native vegetation can be incorporated to the steps on the revetment. The incorporation of vegetation in combination with harder material is one of the principles of the broad term 'living shorelines' [8]. One disadvantage of this adaptation is that the construction of such a stepped revetment with vegetated sections can be challenging. Good monitoring and maintenance is required, especially as it is uncertain if the vegetation growth will be successful.

4.2.2 Porosity sections

Adding porosity to a stepped revetment has the benefits that wave run-up can be reduced and habitats can be created. However, adding porosity to a stepped revetment by means of rock-filled sections can have a negative impact on a stepped revetment's recreational function, as rough structures are not convenient to sit or walk on. As an alternative, porosity can be added by incorporating a prototype habitat enhancement unit as the BIOBLOCK. The BIOBLOCK offers multiple habitat types while simultaneously dissipating wave energy [2].

4.2.3 Rock pools

Artificial rock pools can be added to coastal structures to add habitat to hard coastal structures [2, 7]. Not only can the rock pools add intertidal habitats and increase the diversity of species, but also a recreational feature to the coastal structure.

4.3 Case study

4.3.1 General

Strand is located on the north-eastern coast of one of South Africa's largest natural bays (approx. 1000 km^2), False Bay (Figure 3). The Bay's opening is orientated to the south and situated in the Atlantic Ocean.

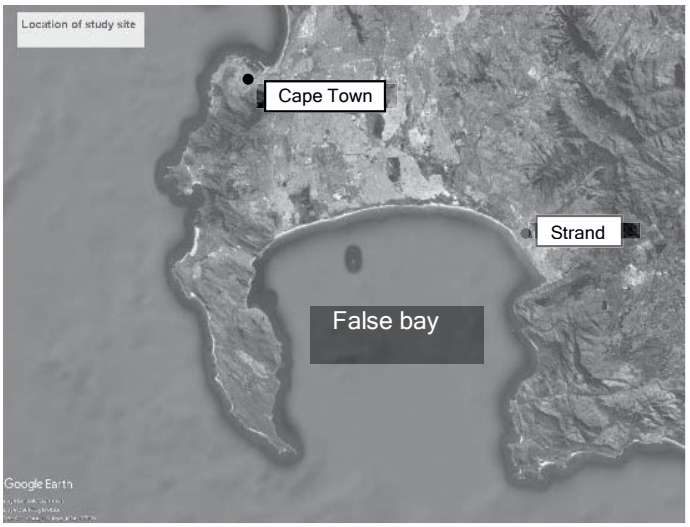

Figure 3: Location of Strand in the north-east of False Bay

Dieses Werk ist copyrightgeschützt und darf in keiner Form vervielfältigt werden noch an Dritte weitergegeben werden.
Es gilt nur für den persönlichen Gebrauch.

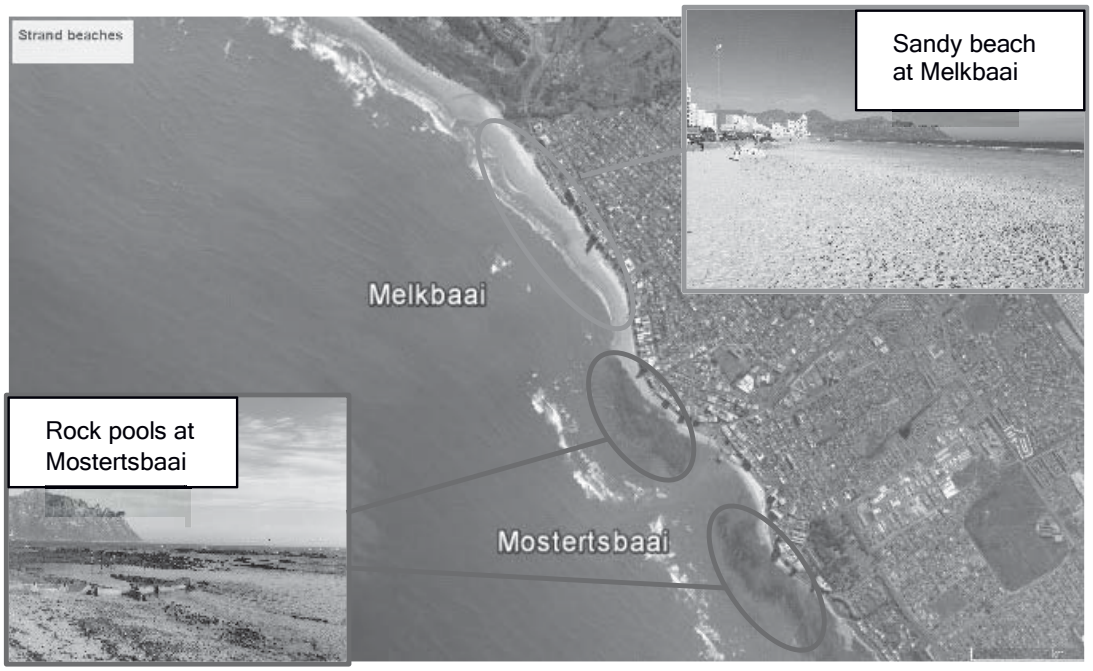

Figure 4: Location of Strand's beaches

The coastal town of Strand has a population of over 55,500 people [9]. Strand attracts many locals and tourists to its popular recreational beaches, Melkbaai and Mostertsbaai (Figure 4). Melkbaai, the northern beach, stretches over approximately 1.5 km. The beach is sandy and offers good conditions for swimming and other recreational activities such as kitesurfing. Mostertsbaai is characterised by its rock reefs and is popular for fishing and exploring the sea life in the rock pools.

Strand's coastline is regularly subjected to storm events. A scenic road, Beach Road, and an adjacent promenade stretch along the coastline (Figure 5). High rise buildings are located landwards along Beach road. The present coastal defences comprise natural sand dunes, vertical seawalls and recurved seawalls. The natural dunes along the coastline have been damaged due to human intervention and, therefore, do not provide sufficient safety. The vertical seawall was constructed in the 1940s and originally designed to prevent wind-blown sand from the dunes to reach the adjacent pavement and road [10]. Therefore, the vertical seawall was not designed to offer protection against overtopping. Since the dunes are damaged and the vertical seawall has reached the end of its design life, the coastline is left vulnerable to storm events.

The pictures presented in Figure 6 are not an uncommon sight along Strand's coastline and illustrate the severity of the wave overtopping events.

In order to address the hazardous wave overtopping events that Strand experiences, coastal protection measures need to be implemented. One possible coastal protection measure is to implement a stepped revetment. A stepped revetment would provide safe access to the beach while simultaneously protecting the hinterland from overtopping.

Dieses Werk ist copyrightgeschützt und darf in keiner Form vervielfältigt werden noch an Dritte weitergegeben werden.
Es gilt nur für den persönlichen Gebrauch.

Figure 5: Promenade and Beach Road along Strand's coastline

However, in 2016, the refurbishment of the seawall along Strand's coastline commenced, which will take place in three project phases. Phase 1 is currently under construction. The new coastal defence is a recurved wall constructed from precast elements (Figure 7).

Even though Strand's municipality already selected a new coastal defence strategy, the hypothetical case study for implementing a stepped revetment at Strand is valuable. Strand with its sandy beaches, partly rocky shoreline and abundant marine life make it a representing location for a case study to investigate ecosystem-based adaptations for stepped revetments.

In the next subsections, the environmental conditions (wind, waves, and beach characteristics), ecological conditions (habitats and species) as well as the site selection for the ecosystem-based stepped revetment will be discussed.

Figure 6: Wave overtopping events at Strand

Dieses Werk ist copyrightgeschützt und darf in keiner Form vervielfältigt werden noch an Dritte weitergegeben werden.
Es gilt nur für den persönlichen Gebrauch.

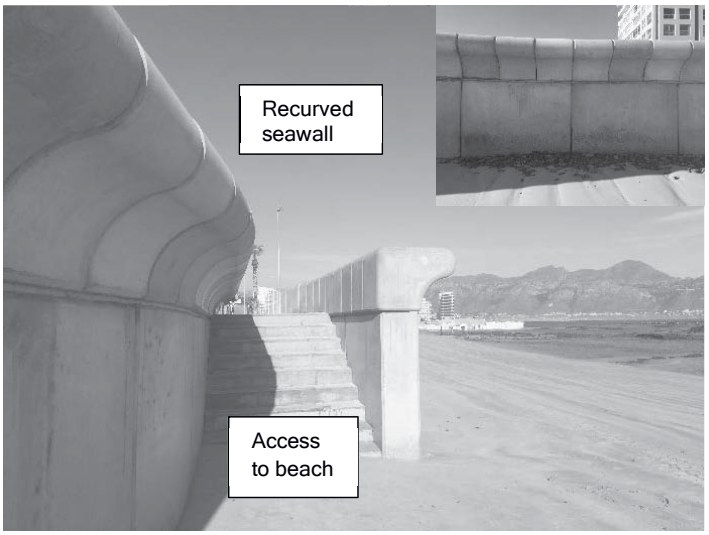

Figure 7: New recurved seawall

4.3.2 Environmental conditions

Strand is not only known for its beaches but also for being windy. It is estimated that Strand annually experiences only between 14.6 to 18.3 percent of the time calm conditions, i.e. defined as wind velocities below 8.6 m/s [11]. During winter, Strand predominantly experiences northerly wind conditions, while during the other seasons a south-easterly wind is dominant [10]. Based on 11 years of wind measurements, the average wind speed is 4 m/s [10].

Strand experiences semi-diurnal tides with mean spring tidal range of approximately 1.5 m [12].

Strand's coastline is mostly exposed to waves from a south-westerly (SW) to south-south-westerly (SSW) direction. The mean nearshore significant wave height at 15 m below the Mean Sea Level (MSL) is 1.13 m, while the significant wave height with a 1 year return period at 15 m below MSL is 3.40 m with a peak wave period of 13 s [11].

The beaches at Strand are on average between 30 and 100 m wide and characterised by mild beach slopes. The average beach slope is approximately 1:67. As a consequence, the beaches have wide surf zones. The sediment at the study site is classified as fine with a mean diameter of D_{50} = 0.15 mm [11].

Furthermore, the beaches of Strand are classified as dissipative. In other words, most of the wave energy is dissipated in the surf zone. Dissipative beaches are characterised by their finer sediments, mild slopes, wide surf zones, and wide beach widths. This classification, therefore, confirms the beach characteristics of Strand as described above. In addition, dissipative beaches have multiple lines of breakers, which are also distinctive in Strand [11].

The potential for aeolian sand transport is high because of the wide beaches and the windy conditions.

Dieses Werk ist copyrightgeschützt und darf in keiner Form vervielfältigt werden noch an Dritte weitergegeben werden.
Es gilt nur für den persönlichen Gebrauch.

4.3.3 Ecological conditions

(This section is not meant as a complete or comprehensive overview of the ecology. It gives rather few facts that can serve as background for the case study, enabling engineers to apply adaptations.)

The Strand coastline offers habitat to a vast array of species. The habitats are divided into two types; namely sandy beaches and rocky shores.

Sandy beaches are dynamic systems as they are continuously influenced by wind, waves and currents. Three main zones can be distinguished for sandy beaches: the surf zone, the beach (including the intertidal and backshore zones) and the dunes. Dune vegetation is essential as it stabilises dunes while simultaneously providing habitat for beach fauna. The moist areas between sand grains provide habitat to meiofauna, which is important for breaking down organic matter and recycling nutrients. The intertidal zone is habitat to a large number of species, including plough snails, sand mussels and crabs. Offshore the sandy beach, zooplankton as well as a variety of fish species can be found [13, 14].

The rocky outcrops along Mostertsbaai serve as habitat to a number of species. The rock habitat can be divided into four distinct zones: the infratidal, the cochlear, the balanoid, and the littorina zones. The infratidal is habitat to sea urchins, mussels, starfish etc., and is only exposed above water during extreme low tides. The cochlear zone is located between low water neap and low water spring tide. This zone is named after the organism, which is most common in this zone, the pear limpet (*Scutellastra cochlear*). The balanoid zone is covered by high tide twice a day and offers habitat to mussels, anemones and barnacles. The last zone, the littorina zone, is the uppermost zone and is located between high water spring tide and high water neap tide. The most common organism in this zone is the *Littorina* snail. These rocky reefs are also habitat to a number of fish species including the Roman (*Chrysoblephus laticeps*) and Galjoen (Dichistius capensis) [13, 14].

4.3.4 Site Selection

To minimise the effect of a stepped revetment on the Strand environment, it is important to investigate what the most suitable location for such a coastal structure would be. A description of the current coastal defences along the coastline of Melkbaai and Mostertsbaai follows.

Figure 8 indicates the three different zones along Melkbaai. The northern part of Melkbaai, indicated as Zone A is protected by vegetated dunes and a vertical seawall. The vertical seawall is located on the landward side of the dunes. Currently, this zone offers sufficient coastal safety.

Zone B offers inadequate protection since the dune system has been damaged and the crest level of the seawall is too low. In addition, the seawall has reached the end of its design life.

Dieses Werk ist copyrightgeschützt und darf in keiner Form vervielfältigt werden noch an Dritte weitergegeben werden.
Es gilt nur für den persönlichen Gebrauch.

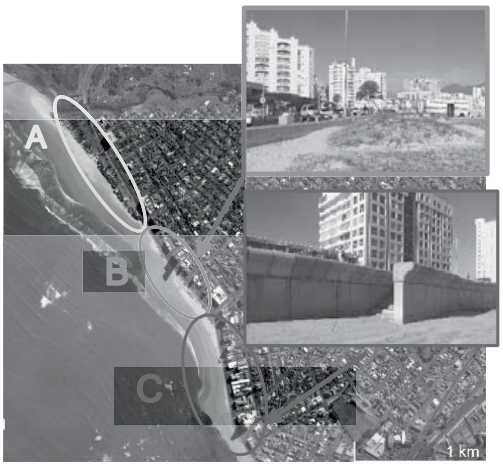

Figure 8: Coastal defences along Melkbaai's coast

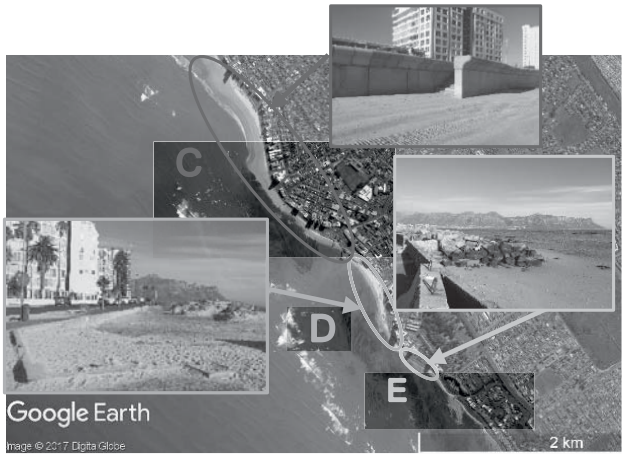

Figure 9: Coastal defences along Mostertsbaai's coast

The newly constructed seawall is located in Zone C (Figures 8 and 9). The seawall consists of a recurve sited on top of a vertical wall. The wall is constructed of precast concrete units. Zone D offers insufficient coastal safety, as the seawall has a very low crest level (Figure 9). Zone E is protected by a rock revetment, which stretches over approximately 150 m and is located seawards of the original seawall. This rock revetment was implemented as emergency temporary protection measure after a storm in 2008. This protection is currently still in place [10].

When selecting the most suitable site for a stepped revetment, a number of aspects need to be considered. (Note the aspects mentioned here is not an exhaustive list.) Firstly, the stepped revetment has to be able to provide sufficient coastal safety at the particular site for the design wave conditions and water level. In addition, the local conditions such as available space, the beach level and the level of the hinterland, should be considered. As the promenade along the beachfront is popular for tourism, the line of site to the beach for promenade and road users should preferably not be affected. Furthermore, as the stepped revetment will provide access to the beach and promote tourism, the structure should be implemented at an attractive location for

Dieses Werk ist copyrightgeschützt und darf in keiner Form vervielfältigt werden noch an Dritte weitergegeben werden.
Es gilt nur für den persönlichen Gebrauch.

recreation. Aeolian sand transport is another aspect that should be taken into consideration in the site selection. Moreover, the selected site should also be based on, where the environmental impacts would be a minimum. In the case of Strand, it should be considered that along some stretches of the coast, and where there is space, it would be more beneficial to restore the damaged dune system. As the focus of the present research is to develop ecosystem-based adaptations for stepped revetments, and not to provide design recommendations, the only criteria for the site selection will be the minimisation of environmental impacts.

One hypothetical location for a stepped revetment has been selected (Figure 10). The developed ecosystem-based adaptations for stepped revetments will be considered for this location. The selected location is situated along the rocky outcrops in Mostertsbaai. This location is popular for walking at the rock pools as well as swimming in the tidal pool (location indicated in Figure 10). This particular location was selected for its recreational value and the potential low environmental impacts of the stepped revetment in this location than along the sandy beaches.

Figure 10: Possible locations to implement a stepped revetment

4.3.5 Selection of ecosystem-based adaptation for study site

In order to select the most suitable adaptation for the study site, the environmental, ecological and spatial conditions of the study site are taken into account. The adaptations to include porosity or rock pools would be the most suitable options as the selected location is characterised by rock habitats with no significant vegetation at the particular site. As the addition of porosity to the stepped revetment can have negative impacts on the recreational value of the stepped revetment, the option to include artificial rock pools in the stepped revetment is the preferred adaptation for the selected location. Furthermore, the rock pools can add additional recreational value to the structure and potentially offer the best resemblance to the current rock habitats. The rock pools offer mitigation by creating novel habitats.

5 Conclusions

The research investigates how the ecological value of stepped revetments can be increased by including ecosystem-based adaptations to conventional stepped revetments. Potential

Dieses Werk ist copyrightgeschützt und darf in keiner Form vervielfältigt werden noch an Dritte weitergegeben werden.
Es gilt nur für den persönlichen Gebrauch.

environmental impacts of stepped revetments have been described and three potential ecosystem-based adaptations were proposed. Only small to medium adaptations are considered. As the feasibility of the adaptations is subjected to conditions and characteristics at a particular location, a site at Strand, South Africa was selected as hypothetical location to implement a stepped revetment. The most suitable adaptation for the selected location has been identified to include artificial rock pools in the stepped revetment. The rock pools offer novel habitats and imitate the existing natural rock pools found along the coastline.

It is recommended that further research should be done for the detail design of the rock pools in order to determine the quantitative impacts of rock pools on coastal safety and the ecological value of these structures.

6 Acknowledgement

The author would like to express her gratitude to DAAD and Exceed Swindon for funding the Integrating Ecosystems in Coastal Engineering Practice (INECEP) Summer School. Great thanks go to UNAM and the Ludwig Franzius Institute at Leibniz University Hannover that made the participation of the author at the summer school a reality.

7 References

1. Borsje, B.W., van Wesenbeeck, B.K., Dekker, F., Paalvast, P., Bouma, T.J., van Katwijk, M.M., de Vries, M.B.: How ecological engineering can serve in coastal protection. Ecological Engineering 37, 113-122 (2011)
2. Firth, L.B., Thompson, R.C., Bohn, K., Abbiati, M., Airoldi, L., Bouma, T.J., Bozzeda, F., Ceccherelli, V.U., Colangelo, M.A., Evans, A., Ferrario, F., Hanley, M.E., Hinz, H., Hoggart, S.P.G., Jackson, J.E., Moore, P., Morgan, E.H., Perkol-Finkel, S., Skov, M.W., Strain, E.M., van Belzen, J., Hawkins, S.J.: Between a rock and a hard place: Environmental and engineering considerations when designing coastal defence structures. Coastal Engineering 87, 122-135 (2014)
3. Kerpen, N.B., Schurmann, T.: Stepped revetments–Revisited. Proceedings of the 6th International Conference on the Application of Physical Modelling in Coastal and Port Engineering and Science (Coastlab16), pp. 10-13 (2016)
4. Kerpen, N.B.: Experimental and theoretical study of the wave-induced response of stepped revetments. vol. Ph.D. Leibniz University Hannover (2017)
5. Airoldi, L., Abbiati, M., Beck, M.W., Hawkins, S.J., Jonsson, P.R., Martin, D., Moschella, P.S., Sundelöf, A., Thompson, R.C., Åberg, P.: An ecological perspective on the deployment and design of low-crested and other hard coastal defence structures. Coastal Engineering 52, 1073-1087 (2005)
6. Martin, D., Bertasi, F., Colangelo, M.A., de Vries, M., Frost, M., Hawkins, S.J., Macpherson, E., Moschella, P.S., Satta, M.P., Thompson, R.C., Ceccherelli, V.U.: Ecological impact of coastal

Dieses Werk ist copyrightgeschützt und darf in keiner Form vervielfältigt werden noch an Dritte weitergegeben werden.
Es gilt nur für den persönlichen Gebrauch.

defence structures on sediment and mobile fauna: Evaluating and forecasting consequences of unavoidable modifications of native habitats. Coastal Engineering 52, 1027-1051 (2005)

7. Bulleri, F., Chapman, M.G.: The introduction of coastal infrastructure as a driver of change in marine environments. Journal of Applied Ecology 47, 26-35 (2010)
8. NOAA: Guidance for considering the use of living shorelines. National Oceanic and Atmospheric Administration (NOAA) (2015)
9. Statistics South Africa: Census 2011: Strand. www.statssa.gov.za (2011)
10. Roux, G.B.: Reduction of seawall overtopping at the Strand. vol. M.Sc. Stellenbosch: Stellenbosch University, South Africa (2013)
11. Van der Merwe, C.: A synthesis of the coastal geophysical characteristics of sandy beaches along the South African coastline. vol. M.SC. Stellenbosch--Stellenbosch University, South Africa (2017)
12. South African Navy Hydrographic Office (SANHO): South African tide tables. South African Navy, Tokai, South Africa, (2007)
13. City of Cape Town: Beaches: A diversity of coastal treasures, City of Cape Town: Environmental Resource Management Department. (2009)
14. City of Cape Town: Helderberg Marine Protected Area Management Plan. (2009)

Dieses Werk ist copyrightgeschützt und darf in keiner Form vervielfältigt werden noch an Dritte weitergegeben werden.
Es gilt nur für den persönlichen Gebrauch.

COASTAL ECOSYSTEM SERVICES PROVIDED BY CORAL REEFS AT TESORO ISLAND, COLOMBIA

Juan D. Osorio-Cano[1,2], Andrés F. Osorio[1,2], Juan C. Alcérreca-Huerta[3], Hocine Oumeraci[4]

[1] Research Group in Oceanography and Coastal Engineering, OCEANICOS, jdosori0@unal.edu.co

[2] Department of Geosciences and Environment, Universidad Nacional de Colombia at Medellín

[3] Department of Zooplancton and Oceanography, CONACYT-ECOSUR Campus Chetumal

[4] Technische Universität Braunschweig, Leichtweiß Institute for Hydraulic Engineering and Water Resources, Braunschweig, Germany

Keywords: Bottom roughness, Coral Reefs, Ecosystem Services, Numerical modelling, Wave damping

Abstract

Coral reefs are coastal environments along a large number of world's coastlines, which constitute protection against sea waves and provide shelter and food for at least 25% of the ocean species. Pressure from tourism, fishing and recreation are among the anthropogenic activities that generate high impacts over the conservation and preservation of these natural habitats. Understanding the ecosystem services provided by coral reefs is fundamental for determining their value and contribution for reducing damages due to human actions combined with the effects of natural extreme events and climate change, which also contributes to coastal erosion and flooding hazards. A lack of knowledge currently exists in Latin American countries for the quantification of ecosystem services provided by coral reefs and the appropriate methodologies to support decision-makers and coastal managers. For this purpose, the current work considers a multidisciplinary approach aiming to combine results from hydrodynamic studies with biological factors, particularly regarding wave-transformation processes and energy dissipation under normal and extreme wave climate conditions. A typical fringing reef from the Colombian Caribbean Sea is selected as case study to quantify specific ecosystem services for practical socio-economic and environmental solutions in those regions, in which coral reefs predominate.

1 Introduction

Tourism, fisheries and ecosystem conservation have a large economic and environmental impact in tropical countries both islander and continental coastal ecosystems (e.g., coral reefs, beaches, seagrass beds, and mangrove forests). These natural habitats provide several ecosystem services such as coastal protection, fishing, navigation, food, and shelters. Wave energy dissipation is among the hydrodynamic processes in coral reefs relevant for its contribution to the ecosystem services as protecting barriers against waves under different water levels, and eventually protects

Dieses Werk ist copyrightgeschützt und darf in keiner Form vervielfältigt werden noch an Dritte weitergegeben werden.
Es gilt nur für den persönlichen Gebrauch.

coastal infrastructure and communities from coastal erosion and flooding. However, in recent decades, they have been subjected to strong anthropogenic pressure and extreme events due to natural causes as well as to climate change.

A case study corresponding to a small island located at the northern side of Rosario Archipelago called Tesoro Island at the Colombian Caribbean Sea (Fig. 1) is herein presented to analyse the ecosystem services provided by coral reefs and their hydrodynamic processes. Declared as Natural National Park in 1988, the archipelago is formed by 28 islands [1]. Its protection and conservation attended to the needs of preserving coral reefs, associated ecosystems (sea grass, mangroves) as well as the fauna and flora that inhabit these environments.

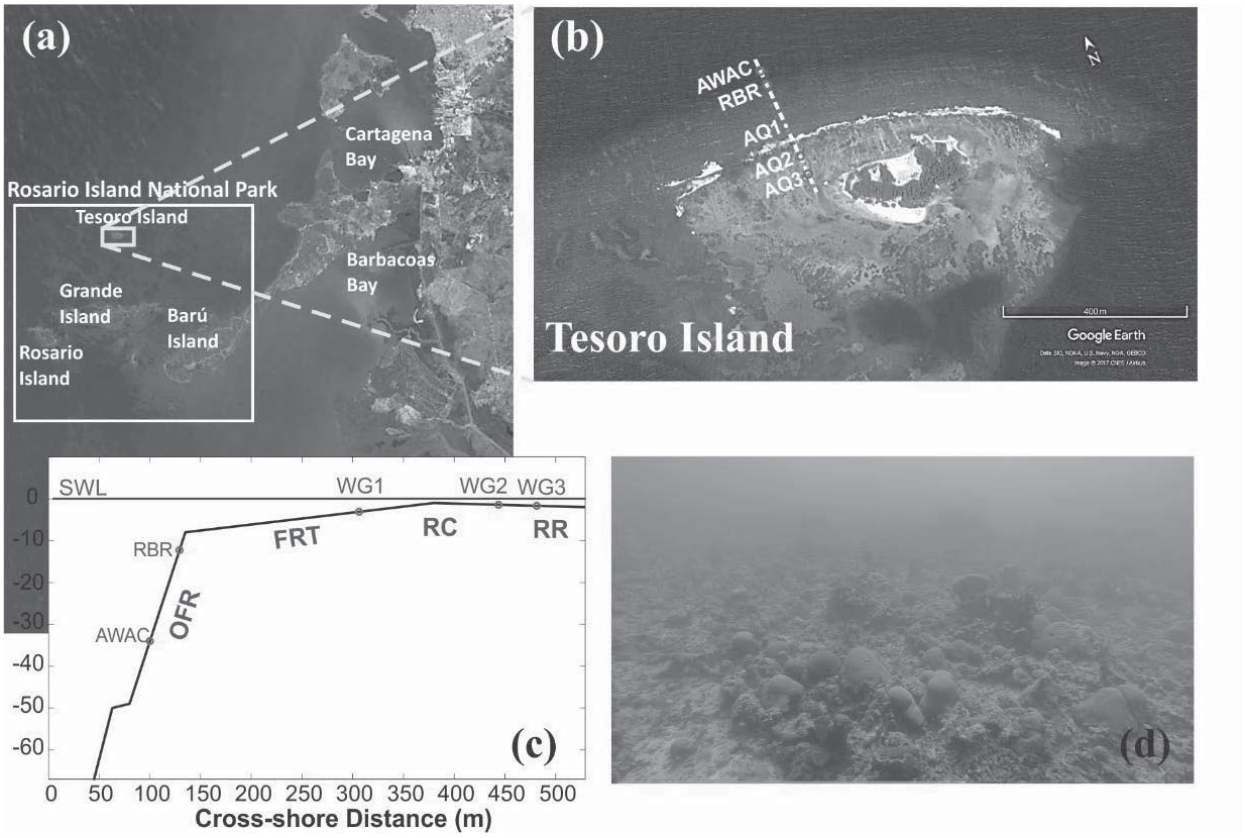

Figure 1: (a, b) Location of Tesoro Island in the Rosario Islands National Natural Park, Cartagena, Colombia - Caribbean Sea. White dashed line shows the reef profile location analysed. (c) Coral reef profile and main geomorphological characteristics: outer fore-reef (OFR); fore reef terrace (FRT); reef crest (RC) and rear reef (RR), and (d) current coral reef degradation over the FRT at Tesoro Island.

Scenarios of coastal ecosystem degradation should be understood in order to properly account the impacts such as coastal erosion/flooding. Further ecosystem services provided by these natural habitats lies on the integration of different disciplines for combining the hydrodynamic studies with biological issues in order to onset practical socio-economic and environmental solutions [2-4]. Assessing ecosystem services, considering both physical and environmental processes, is highly

Dieses Werk ist copyrightgeschützt und darf in keiner Form vervielfältigt werden noch an Dritte weitergegeben werden.
Es gilt nur für den persönlichen Gebrauch.

relevant to enhance and to map out potential prospects for services such as tourism, fishing and land conservation. However, this might also depend on the values and priorities exercised by people in the coming decades.

The case study will focus on the effectiveness of a coral reef ecosystem for: (i) enhancing wave energy dissipation, (ii) providing coastal erosion and flooding, and (iii) evidencing the changing of hydrodynamic conditions in complex systems with high bottom roughness. These results aim to provide insights for coastal managers and decision-makers for further development of strategies in favour of natural habitats restoration. Moreover, the use of coastal ecosystems as eco-engineering solutions for coastal protection over traditional "grey" infrastructure constitutes an environmental friendly and innovative solution with large benefits to both environmental protection and human activity development. Thus, this paper conducts a comprehensive analysis of the current situation of the coral reefs at Tesoro Island and possible management action for improving the ecosystem services provided by coral reefs.

2 Materials and Methods

2.1 Description of the study area and diagnosis of current situation

Caribbean Coasts are worldwide known for tourism developments; the quality of the beaches is cited by most tourists as the main feature of a successful holiday. They also provide areas of recreation and enjoyment for local people throughout the region and, therefore, have a large cultural value in addition to their economic importance in attracting overseas visitors. However, it has recently been estimated that 70% of beaches on the islands of the Caribbean are eroding at rates of between 0.25 m and 9 m per year [5].

Particularly for the study area in the Rosario Archipelago, 58% of the coral reef cover has died and live corals decreased by 25% between 1995 and 2000, according to the Caribbean Sea Ecosystem Assessment Team [5]. In Rosario Archipelago, the erosive activity has been constant for the last 50 years as a consequence of continuous wave action and rising sea levels [6]. Anthropogenic intervention for tourism activities (e.g., change in coastal land- and sea-use) has caused significant changes to the geomorphologic setting of the coast. In Tesoro Island, the situation is critical, since it is exposed directly to NNE-NW waves and has lost around 48.7% of its territory. Moreover, the decline in fisheries catches (from 63,700 t in 1978 to 7,850 t in 1998) is another crucial indicator of the environmental degradation caused by reduced water quality and sewage pollution.

The barrier reef of Tesoro Island (approximately 2.5 km in length and 1.5 km in width, displaying an ovoid shape, as shown in Fig. 1b) provides different geomorphological features and coral species distribution [7]. The reef profile and the main geomorphological features (Fig. 1c) include (i) a sloping outer fore-reef (OFR) with an inclination angle around 40 degrees and between 8 and 50 m deep. The live coral grows reaching more than 30 m in depth on the fore reef slope, colonized by platy corals, especially *Montastrea franksi* and *Agaricia* spp (Fig. 2a); (ii) a fore-reef terrace (FRT) also referred as inner fore-reef with depths varying from 2 and 9 m and slopes below 2 degrees of inclination. It is the largest zone of the reef, forming a circular shape and

Dieses Werk ist copyrightgeschützt und darf in keiner Form vervielfältigt werden noch an Dritte weitergegeben werden.
Es gilt nur für den persönlichen Gebrauch.

characterized by a low relief spur and groove system. It's basal substratum is composed of dead *Acropora palmata* stands, which are replaced gradually by algae and sponge's colonization; (iii) a shallow top reef crest (RC) between 0 - 2 m deep lying at the breaker zone and composed of buttresses of the hydrocoral *Millepora complanata* and the zoanthids *Palythoa* spp., and (iv) a rear reef (RR), which is a narrow flat located behind the crest platform, ranging from 0.5 to 1.5 m depth and formed by pavements with shallow grooves and scattered growth of *Porites porites* and *P. astreoides* corals. The total length of the reef profile is about 700 m.

The benthic communities are composed of a group of species adapted to determined environmental conditions related to water depth, wave exposure, and the basic type of substratum. The Island is not currently damaged by tourism or any other anthropogenic pressure, as it is only occupied by a permanent military post for the Colombian Army. However, since the area is exposed directly to the incoming waves without any dissipation due to other islands or structures, the erosion processes are critical and highly relevant. Additionally, the reef has a high rate of coral mortality, especially of *Acropora palmata*. This species of coral is of particular interest due to its geometrical characteristics and its ability to survive in moderate to high energy environments associated with the incident waves and currents (e.g., between the fore reef terrace and reef crest, Fig. 1c). Its branches and the global structure of its coral colonies play an important role on the wave energy dissipation due to bottom friction. However, there is still a gap of knowledge regarding the contribution to the wave damping caused by its roughness and, consequently, on the ecosystem services provided.

Field data recorded between Nov. 2013 and Feb. 2014 in the framework of the research project entitled "Extreme Events in the Pacific and Caribbean Coastal Island Ecosystems" sponsored by COLCIENCIAS are available for the valuation of the coastal protection services based on wave attenuation provided by Tesoro Island. Wave conditions were measured hourly at five locations along a cross-shore transect (white dashed line in Fig. 1b) as follows:

On the outer fore reef, an Acoustic Doppler Current profiler (ADCP) from Nortek Instruments (AWAC 1200 kHz) was deployed (Fig. 2a) to measure the incoming waves and current profiles. Between the fore reef terrace and the rear reef, a pressure sensor from RBR Instruments and three pressure sensors from Aquatec Group were deployed to measure the decreasing wave height due to wave breaking and bottom friction. With the aim to measure meteorological variables during the field survey, a weather station Davis Vantage-Vue was permanently located on top of the main building of the Research Center, Education and Recreation (CEINER in Spanish) inside the National Natural Park, Corales Islas del Rosario (Colombian Caribbean). Table 1 summarizes the description of all equipment used during the field campaign. Finally, a bathymetry profile (Fig. 1c) was obtained with a mono-has Eco sounder.

Dieses Werk ist copyrightgeschützt und darf in keiner Form vervielfältigt werden noch an Dritte weitergegeben werden.
Es gilt nur für den persönlichen Gebrauch.

Table 1: Field Instrument locations and deployment Information

Site	Mean Depth (m)	Instrument	Conditions Measured
OFR	32.0	ADCP (AWAC)	Waves & Currents
OFR	12.8	RBR	waves
FRT	2.0	WG1	waves
RR	1.5	WG2	waves
RR	1.0	WG3	waves
Meteo	+15	Weather station	Hydroclimatology

3 Results and Discussion

3.1 Physical processes description and ecosystem services analysis for eco-engineering management tools

The significant wave height (Hs) and peak period obtained for each sensor during the field campaign at Tesoro Island, Colombia (Nov. 18-23, 2013) are shown in Fig. 2b. The range of conditions supported by coral reefs over the different sections of a profile clearly shows the services that the reef provides. The total dissipation after wave propagation along the reef reaches a percentage up to 95% between the outer fore reef and the rear reef (including dissipation due to wave breaking and bottom friction). Furthermore, even the significant wave height reached values up to Hs=2.0 m at the RBR-location, the wave height at the rear reef never exceeded Hs=0.30 m (WG3), which becomes highly relevant for promoting long-term stable conditions in reef lagoons and the protection of the shoreline against a wide range of wave conditions. Moreover, larger wave heights are noticed over the RBR-location than in other sections of the reef profile so that the OFR presents the location, in which the most energetic conditions over the reef structure are found.

In addition to the wave height results, it can be observed in Fig. 2b that the wave period is also being modified by the reef structure. For instance, the measurements of the aqualoggers in the rear reef on November 20th exhibit small wave heights (Hs < 0.2 m) but associated to long wave periods (Tp=8.0-9.5 s), which is in contrast to the wave height (Hs=0.40 m) and wave period (Tp= 7s) in the outer fore-reef (AWAC location). The later may induce different hydrodynamic processes, which are related to the physical features and wave dissipation effects that the reef bottom roughness and reef geomorphology induce, affecting also the development of flora and fauna along the reef profile.

Dieses Werk ist copyrightgeschützt und darf in keiner Form vervielfältigt werden noch an Dritte weitergegeben werden.
Es gilt nur für den persönlichen Gebrauch.

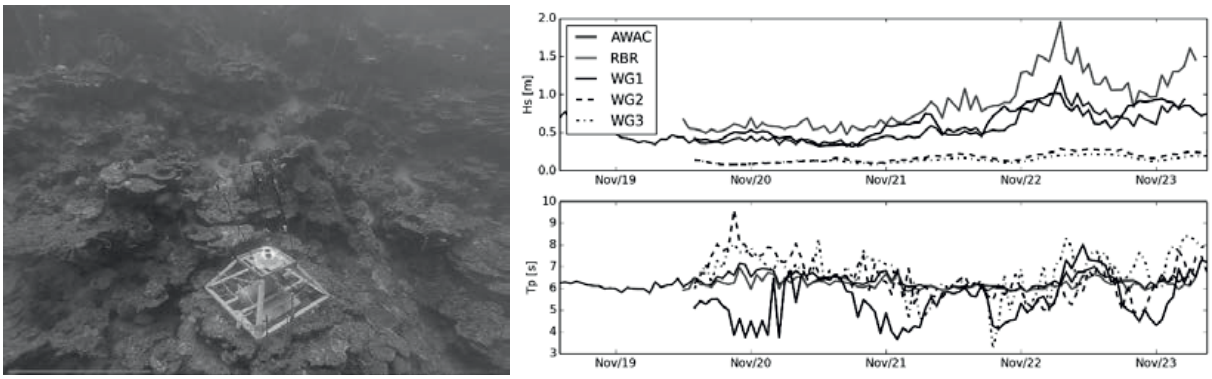

Figure 2: (a - left) Outer-fore reef features and deployment of the AWAC sensor. (b - right) Wave parameters (Hs, Tp) obtained from field measurements along the reef profile at Tesoro Island, Colombia (November 18-23, 2013).

The field measurement results provide an insight into the transformation of the physical processes due to variations of the reef structure and reef roughness, and possible implications for the protection of the shoreline, maintenance of stable conditions in the reef lagoon, and effects over the species that inhabit the fringing reef. However, a more detailed description of the contribution of reefs is detailed in this section, specifically accounting for (i) wave dissipation in coral reefs considering numerical modelling results and field observations, and (ii) ecosystem management tools in order to support integrated ecosystem management.

3.1.1 Wave dissipation in coral reefs

The physical processes involved in wave energy dissipation are strongly induced by steep slopes, heterogeneous bathymetry, and large bottom roughness. Complex wave transformation processes such as refraction, shoaling, reflection, and wave breaking are normally found together with an enhancement of frictional energy dissipation [8-10]. In order to account for wave damping and wave energy dissipation due to bottom friction, the most important aspects are related to the roughness and porosity of the reef surface, highly correlated with the coral colonies density as well as with the species distribution along the reef. In shallow waters with large bottom roughness, the total wave energy dissipation due to bottom friction can be a primary component of the total wave energy dissipation [11-14].

Advances in computational and numerical modelling provide tools that could enhance the quantification of the contribution of coral species on wave height attenuation. Within this context, Computational Fluid Dynamics (CFD) arises as a valuable tool for describing in detail the wave energy dissipation process over fringing reefs. Locations, where energy dissipation is higher and the determination of processes related to this damping such as turbulence, boundary layer deployment, and development of wave-induced currents are among the knowledge gain for a better understanding of the interaction between physical processes with biological issues. Thus, CFD modelling by considering available field data from Tesoro Island are briefly presented here as well as in Osorio-Cano et al. [15]. A quantitative analysis of the energy dissipation considering the modelling of two scenarios of reef roughness (i) a smooth reef surface to represent a reef without

Dieses Werk ist copyrightgeschützt und darf in keiner Form vervielfältigt werden noch an Dritte weitergegeben werden.
Es gilt nur für den persönlichen Gebrauch.

corals, and (ii) a rough surface to account for the presence of *A. palmata* (Fig. 3b and 3c) along the outer fore reef (OFR) and fore-reef terrace (FRT) according to the description is made by [7].

Wave propagation of different regular wave conditions (H, T) and see water levels were carried out for better understanding the wave damping processes along the reef profile. Figure 4a exemplarily shows the comparison between a smooth (without corals) and rough condition (with corals) of the wave height evolution along the reef profile from a single test (H=0.75 m, T=11 s). The results clearly illustrate the difference of significant wave height (Hs), which is reduced up to 10% at the rear reef only as consequence of the rough reef bottom. The main differences are obtained close to the reef crest, where differences in zero moment wave height (H_{m0}) reach values up to 55%. An enhanced wave shoaling induces a wave breaking for rough scenarios, while for smooth conditions wave dissipation occurs uniformly along the FRT and wave breaking closer to the reef crest. Fig. 4b shows the evolution of the wave energy spectrum between the incident condition (black solid line, taken at x=50 m) and the transmitted energy at x = 340 m for both scenarios (smooth and rough reef surface). In addition, the spectral energy associated with the high frequency harmonics is reduced considerably (see red dashed line in Fig. 4b). The latter confirms the importance of considering bottom roughness in numerical models as well as on the effects that it induces on physical processes, and, consequently, on the development of biological processes and species establishment, which again alter the hydrodynamics in a dynamic equilibrium.

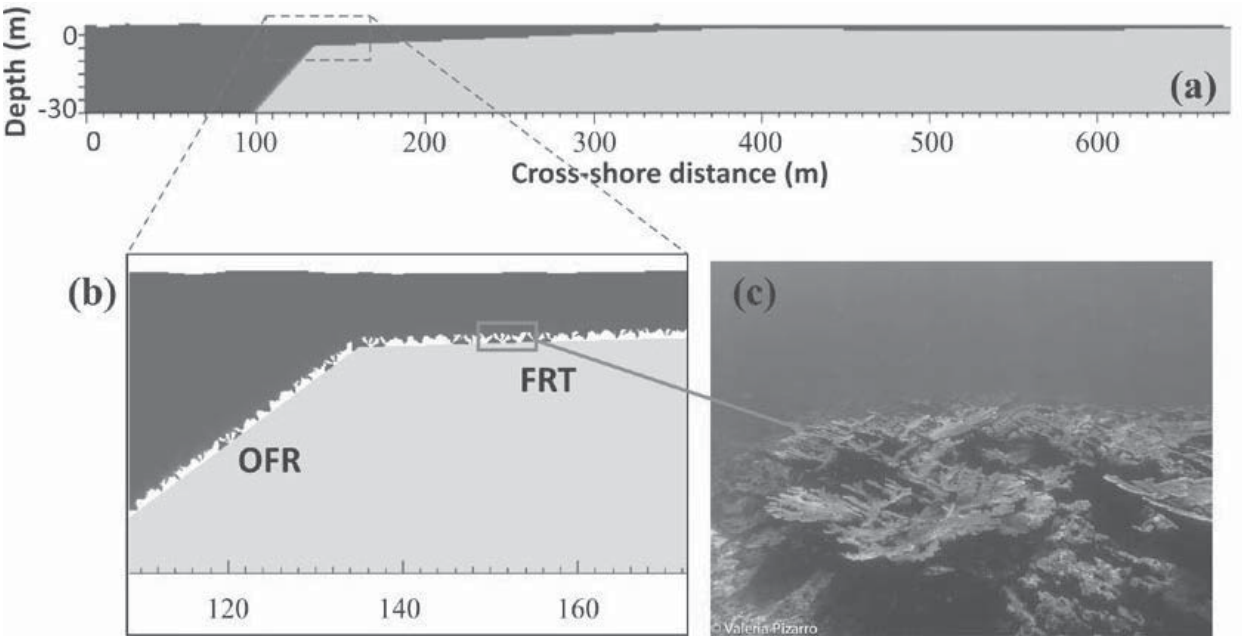

Figure 3: Cross-shore reef profile of Tesoro Island implemented in the OpenFoam model and numerical mesh details of (a) smooth impermeable reef surface, (b) highly rough reef surface around the outer fore reef (OFR), and (c) fore reef terrace (FRT) represented by 2D projections of healthy coral colonies of *A. palmata* from the Colombian Caribbean.

Dieses Werk ist copyrightgeschützt und darf in keiner Form vervielfältigt werden noch an Dritte weitergegeben werden.
Es gilt nur für den persönlichen Gebrauch.

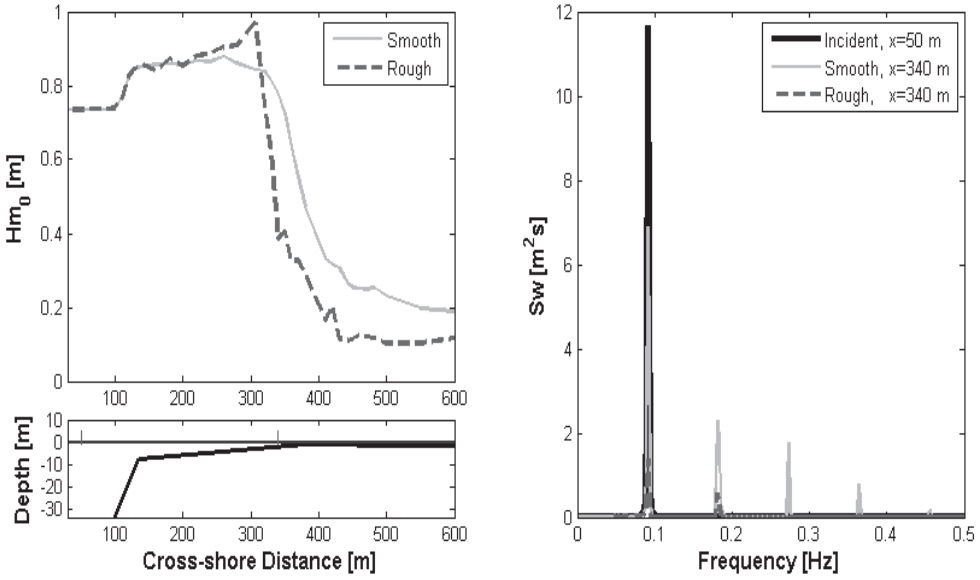

Figure 4: (a) Wave height evolution along coral reef profile, and (b) comparison of wave energy spectrum between smooth (grey line) and rough (red dashed line) reef mesh at x=340 m. (H = 0.75 m, t = 11s).

In addition to the aforementioned results, Osorio-Cano et al. [16] has shown the use of other computational models such as XBeach [17] as part of a methodological framework to study coastal ecosystems as wave damping structures. The analysis was focused on the impact of coral roughness on wave setup, wave runup, coastal erosion, and flooding.

The same reef profile from Tesoro Island was considered and complemented with a sandy beach profile with a slope of 1:20 in order to quantify the effect of wave damping due to bottom friction. A sensitivity analysis was made by considering different short wave friction values (f_w) to represent the coral roughness instead of considering the real shape of corals, since limitations are still found for morphodynamic models such as XBeach. The friction coefficient ranged between 0.01 and 1.0, where the lower limit is associated with a smooth sandy beach bottom, while the highest value represents very high bottom roughness with a 100% coral cover of healthy massive and branched coral species. The impact of coral roughness on the beach profile was made assuming an erosion area factor defined as $\lambda=W/A_i$, where W is the amount of sand removed ($W^{(-)}$) or transported ($W^{(+)}$) by the wave-induced cross-shore transport, and A_i is an influence area defined between two different sea water levels (as illustrated in Fig. 5 by the black dashed triangle). Z_{s0}=2.0 m represents an extreme sea water level scenario associated with high tide level and a storm surge event at the Colombian Caribbean.

According to [16], results indicate that under storm conditions there is a great influence of bottom roughness, as variations on the f_w value exhibit differences up to 40% on the affected erosion area. Therefore, bottom roughness parameterization is highly relevant for the proper implementation into more robust numerical models (e.g., CFD modelling -> Morphodynamics models) as well in

Dieses Werk ist copyrightgeschützt und darf in keiner Form vervielfältigt werden noch an Dritte weitergegeben werden.
Es gilt nur für den persönlichen Gebrauch.

order to highlight the importance of preserving coastal ecosystems to improve the ecosystem services that they provided.

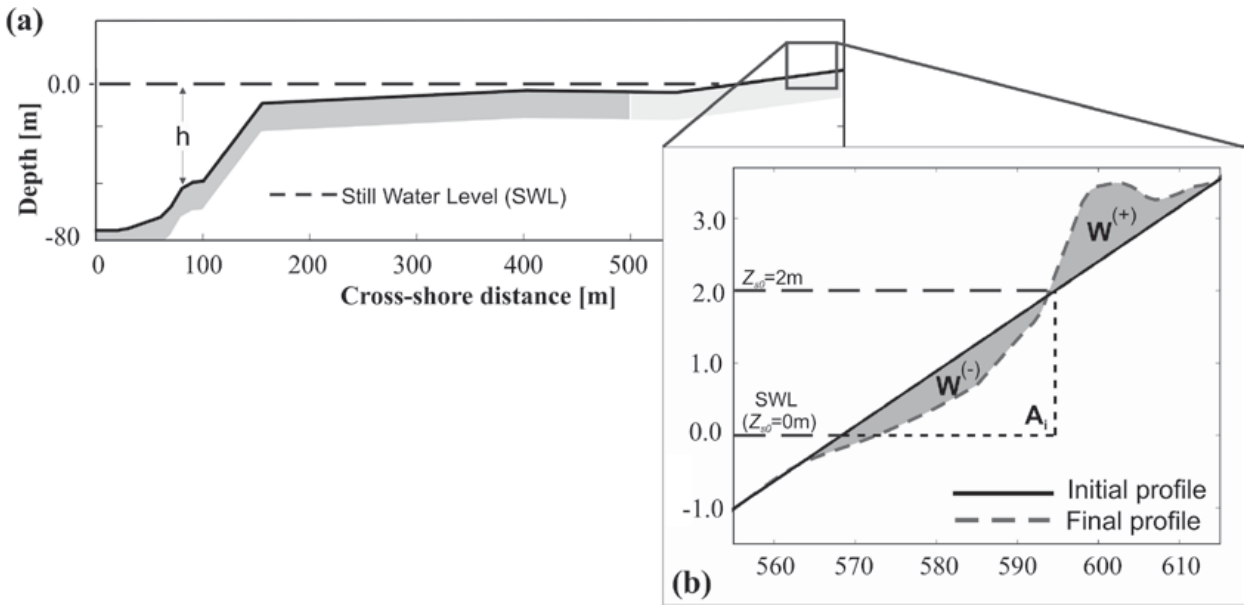

Figure 5: (a) Reef profile used for numerical simulations with XBeach model, and (b) definition of main variables to account for beach erosion. Adapted from [16]

3.1.2 Ecosystem management tools

Frameworks and tools that can support an integrated ecosystem assessment to inform decision-making globally and at multiple scales are: Integrated Valuation of Ecosystem Services and Tradeoffs - InVEST [18, 19]; Artificial Intelligence for Ecosystem Services – ARIES [20, 21]; LUCI - formerly Polyscape [22]; Multi-scale Integrated Models of Ecosystem Services/Marine Integrated Decision Analysis - MIMES/MIDAS [23]; Ecosystem Portfolio Model - EPM [24] among others. More details about each model, their performance, limitations, and scale of modelling can be found in Bagstad et al. [25].

If compared with CFD or morphodynamic models for assessing physical processes, this type of models are able to produce functions that define changes in an ecosystem's structure and function that are likely to affect the value of ecosystems services. In Latin America, a small number of countries (e.g., Mexico, Brazil, Chile, and Colombia) have joined the idea of promoting interdisciplinary groups to implement natural or hybrid solutions as innovative coastal defence mechanisms with opportunities for adaptation to climate variability and climate change [26, 27]. The integration process of research fields is a challenging task, so the impacts into the ecosystems and their services can be quantified numerically and not only qualitatively. The assessment of biological characteristics (species composition and bottom roughness) from natural habitats can be better understood, by means of their explicit inclusion into numerical models to account, for example, on the relationships for inducing and supporting wave energy dissipation and morphodynamic changes.

Dieses Werk ist copyrightgeschützt und darf in keiner Form vervielfältigt werden noch an Dritte weitergegeben werden.
Es gilt nur für den persönlichen Gebrauch.

Besides the contribution made by different authors [2-4, 19, 28, 29], there is still a lack of knowledge in understanding scenarios of coastal habitats degradation and the management actions that should be taken to preserve the ecosystem services provided by coral reefs, and to determine their economic values in terms of reducing damages caused by coastal erosion and flooding at short, medium and long-term horizons. The use of these habitats as coastal protection strategies has not been entirely adopted yet as an engineering practice and mechanism of adaptation to climate change. Nevertheless, in the last decade, research and development of ecosystem-based approaches have advanced considerably, including an improved understanding of biophysical processes and the interaction between engineering structures and coastal ecosystems [26]. Additionally, the advances in valuation, modelling and mapping of ecosystem services as well as methodological frameworks and eco-engineering tools [19, 21, 28] have allowed the recognition of coastal ecosystems from an engineering point of view for their use as a coastal protection mechanism in the face of global change.

CFD tools and numerical models for assessing the physics of coastal processes are effective tools for a very detailed and better understanding of physical processes; however, limitations are found as they require high computational costs and knowledge capabilities about all physical process and numerical issues involved. Thus, these models cannot be directly used for management and decision making, however, can be used as a complement with morphodynamic models to help coastal managers to take proper decisions.

4 Conclusions

Reduction of risk from coastal hazards and the preservation/restoration of natural habitats like coral reefs, seagrass and mangroves are scarce and, unfortunately, non-integrated and multidisciplinary approaches are fully developed for understanding the ecosystem services these environments offers. This has become a common issue in Latin America and the Caribbean, where natural defence structures are not considered over traditional infrastructure [27].

Poor or ineffective communication between scientists, coastal zone managers, and policy makers is a major problem, while end-users often claim that research findings cannot easily be put to practical use [30]. Therefore, engineers/scientists should provide objective information and tools, which in direct collaboration with managers can be of interest for decision makers. In this way, the relevance of natural habitats and the recognition of ecosystem services by scientists/engineers, managers, and decision-makers can be performed. Identification of the potential of coastal ecosystems to be considered for traditional coastal protection schemes should be based on the implementation and improvement of both ecosystem management tools and modelling of physical processes [16]. In this sense, a multidisciplinary approach is needed, as the knowledge of each discipline may contribute to optimize the functionality of these ecosystems and motivate ecological restoration processes. Similarly, inputs are obtained to quantify the degree of degradation or renewal of ecosystems before and after an extreme event, and their impact on the ecosystem services they typically provide [2, 28].

Dieses Werk ist copyrightgeschützt und darf in keiner Form vervielfältigt werden noch an Dritte weitergegeben werden.
Es gilt nur für den persönlichen Gebrauch.

The findings from numerical studies as well as field measurements in Tesoro Island [15, 16] can be used to encourage strategies for coral reefs restoration and the use of artificial reefs as green infrastructure for coastal protection. Up to now, reef restoration programs are being implemented by governmental authorities and volunteers at Rosario Archipelago and San Bernardo National Natural Park, where through propagation techniques (Coral Tree Nursery®) corals are first grown in nurseries and then out-planted in strategically selected locations along the reef. These practices should be promoted, as green infrastructure has shown positive impacts in terms of wave energy reduction and coastal protection in the Colombian Caribbean.

5 Acknowledgement

The work done by J. D. Osorio-Cano is part of his PhD thesis and is supported by COLCIENCIAS in the framework of the research project entitled “Study of wave energy dissipation in natural structures and their response to extreme events” – Internal Code: 111866044690. The authors also acknowledge the DAAD and Exceed Swindon for the financial support for academic exchanges and the participation at the Summer School INECEP 2017 “Integrating Ecosystems in Coastal Engineering Practice”.

6 References

1. Cendales, M.H., Sea, S., Díaz, J.M.: Geomorfología y unidades ecológicas del complejo de arrecifes de las Islas del Rosario y Barú (Mar Caribe, Colombia). vol. XXVI, 497-510 (2002)
2. Ferrario, F., Beck, M.W., Storlazzi, C.D., Micheli, F., Shepard, C.C., Airoldi, L.: The effectiveness of coral reefs for coastal hazard risk reduction and adaptation. Nature communications 5, 3794-3794 (2014)
3. Quataert, E., Storlazzi, C., Van Rooijen, A., Cheriton, O., Van Dongeren, A.: The influence of coral reefs and climate change on wave-driven flooding of tropical coastlines. Geophysical Research Letters 42, 6407-6415 (2015)
4. Storlazzi, C.D., Brown, E.K., Field, M.E., Rodgers, K., Jokiel, P.L.: A model for wave control on coral breakage and species distribution in the Hawaiian Islands. Coral Reefs 24, 43-55 (2005)
5. Carsea: Caribbean Sea Ecosystem Assessment (CARSEA), A sub-global component of the Millennium Ecosystem Assessment (MA). Caribbean Marine Studies Special Ed, 85-85 (2007)
6. Restrepo, J.C., Otero, L., Casas, A.C., Henao, A., Gutiérrez, J.: Shoreline changes between 1954 and 2007 in the marine protected area of the Rosario Island Archipelago (Caribbean of Colombia). Ocean & Coastal Management 69, 133-142 (2012)
7. Sánchez, J.A.: Benthic communities and geomorphology of the Tesoro Island coral reef, Colombian Caribbean. An. Inst. Invest. Mar. Punta Betín 24, 55-77 (1995)
8. Lugo-Fernández, A., Roberts, H.H., Suhayda, J.N.: Wave transformations across a Caribbean fringing-barrier Coral Reef. Continental Shelf Research 18, 1099-1124 (1998)

Dieses Werk ist copyrightgeschützt und darf in keiner Form vervielfältigt werden noch an Dritte weitergegeben werden.
Es gilt nur für den persönlichen Gebrauch.

9. Monismith, S.G.: Hydrodynamics of Coral Reefs. Annual Review of Fluid Mechanics 39, 37-55 (2007)

10. Young, I.R.: Wave Transformation Over Coral Reefs. 94, 9779-9789 (1989)

11. Falter, J.L., Atkinson, M.J., Merrifield, M.A.: Mass-transfer limitation of nutrient uptake by a wave-dominated reef flat community. Limonology And Oceanography 49, 1820-1831 (2004)

12. Lowe, R.J., Falter, J.L., Bandet, M.D., Pawlak, G., Atkinson, M.J., Monismith, S.G., Koseff, J.R.: Spectral wave dissipation over a barrier reef. Journal of Geophysical Research 110, 1-16 (2005)

13. Lowe, R.J., Falter, J.L., Koseff, J.R., Monismith, S.G., Atkinson, M.J.: Spectral wave flow attenuation within submerged canopies: Implications for wave energy dissipation. Journal of Geophysical Research 112, 1-14 (2007)

14. Nelson, R.C.: Hydraulic roughness of coral reef platforms. Applied Ocean Research 18, 265-274 (1996)

15. Osorio-Cano, J.D., Alcérreca, J.C., Zapata-Tamayo, L.M., Osorio, A.F., Toro, F.M., Oumeraci, H.: Numerical modelling of wave energy dissipation over a submerged reef, study Case: Tesoro Island, Colombia. pp. abstract ID 26301-abstract ID 26301, Granada, Spain (2015)

16. Osorio-Cano, J.D., Osorio, A.F., Peláez-Zapata, D.S.: Ecosystem management tools to study natural habitats as wave damping structures and coastal protection mechanisms. Ecological Engineering (In Press, 2017)

17. Roelvink, D., van Dongeren, A.R., McCall, R.T., Hoonhout, B., van Rooijen, A., van Geer, P., de Vet, L., Nederhoff, K., Quataert, E.: XBeach Technical Reference: Kingsday Release (2015)

18. Kareiva, P., Tallis, H., Ricketts, T.H., Daily, G.C., Polasky, S.: Natural Capital: Theory and Practice of Mapping Ecosystem Services. Oxford University Press, Oxford (2011)

19. Sharp, E.R., Chaplin-kramer, R., Wood, S., Guerry, A., Tallis, H., Ricketts, T., Authors, C., Nelson, E., Ennaanay, D., Wolny, S., Olwero, N., Vigerstol, K., Penning, D., Mendoza, G., Aukema, J., Foster, J., Forrest, J., Cameron, D., Arkema, K., Lonsdorf, E., Kennedy, C., Verutes, G., Kim, C.-k., Guannel, G., Papenfus, M., Toft, J., Mar, M., Bernhardt, J., Griffin, R., Glowinski, K., Chaumont, N., Perelman, A., Lacayo, M., Hamel, P., Vogl, A.L., Rogers, L., Bierbower, W., Denu, D., Sharp, C., Mandle, M.: InVEST +VERSION+ User's Guide. The Natural Capital Project. Stanford University, University of Minnesota, The Nature Conservancy, and World Wildlife Fund (2016)

20. Bagstad, K.J., Villa, F., Johnson, G.W., Voigt, B.: ARIES (Artificial Intelligence for Ecosystem Services): A guide to models and data, version 1.0. Aries report series no. 1, 122-122 (2011)

21. Villa, F., Bagstad, K., Johnson, G., Voigt, B.: Scientific instruments for climate change adaptation: Estimating and optimizing the efficiency of ecosystem service provision. Economia Agraria y Recursos Naturales 11, 83-98 (2011)

Dieses Werk ist copyrightgeschützt und darf in keiner Form vervielfältigt werden noch an Dritte weitergegeben werden.
Es gilt nur für den persönlichen Gebrauch.

22. Jackson, B., Pagella, T., Sinclair, F., Orellana, B., Henshaw, A., Reynolds, B., McIntyre, N., Wheater, H., Eycott, A.: Polyscape: A GIS mapping framework providing efficient and spatially explicit landscape-scale valuation of multiple ecosystem services. Landscape and Urban Planning 112, 74-88 (2013)

23. Boumans, R., Roman, J., Altman, I., Kaufman, L.: The Multiscale Integrated Model of Ecosystem Services (MIMES): Simulating the interactions of coupled human and natural systems. Ecosystem Services 12, 30-41 (2015)

24. Labiosa, W.B., Forney, W.M., Esnard, A.M., Mitsova-Boneva, D., Bernknopf, R., Hearn, P., Hogan, D., Pearlstine, L., Strong, D., Gladwin, H., Swain, E.: An integrated multi-criteria scenario evaluation web tool for participatory land-use planning in urbanized areas: The Ecosystem Portfolio Model. Environmental Modelling & Software 41, 210-222 (2013)

25. Bagstad, K.J., Semmens, D.J., Waage, S., Winthrop, R.: A comparative assessment of decision-support tools for ecosystem services quantification and valuation. Ecosystem Services 5, 27-39 (2013)

26. Burcharth, H.F., Zanuttigh, B., Andersen, T.L., Lara, J.L., Steendam, G.J., Ruol, P., Sergent, P., Ostrowski, R., Silva, R., Martinelli, L., Nørgaard, J.Q.H., Mendoza, E., Simmonds, D., Ohle, N., Kappenberg, J., Pan, S., Nguyen, D.K., Toorman, E.A., Prinos, P., Hoggart, S., Chen, Z., Piotrowska, D., Pruszak, Z., Schönhofer, J., Skaja, M., Szmytkiewicz, P., Szmytkiewicz, M., Leont'yev, I., Angelelli, E., Formentin, S.M., Smaoui, H., Bi, Q., Sothmann, J., Schuster, D., Li, M., Ge, J., Lendzion, J., Koftis, T., Kuznetsov, S., Puente, A., Echavarri, B., Medina, R., Díaz-Simal, P., Rodriguez, I.L., Maza, M., Higuera, P.: Innovative Engineering Solutions and Best Practices to Mitigate Coastal Risk. Elsevier, pp. 55-170 (2015)

27. Silva, R., Lithgow, D., Esteves, L.S., Martínez, M.L., Moreno-Casasola, P., Martell, R., Pereira, P., Mendoza, E., Campos-Cascaredo, A., Winckler Grez, P., Osorio, A.F., Osorio-Cano, J.D., Rivillas, G.D.: Coastal risk mitigation by green infrastructure in Latin America. Proceedings of the Institution of Civil Engineers - Maritime Engineering MAEN-2016-, 1-16 (2017)

28. Duarte, C.M., Losada, I.J., Hendriks, I.E., Mazarrasa, I., Marbà, N.: The role of coastal plant communities for climate change mitigation and adaptation. Nature Climate Change 3, 961-968 (2013)

29. Guannel, G., Ruggiero, P., Faries, J., Arkema, K., Pinsky, M., Gelfenbaum, G., Guerry, A., Kim, C.K.: Integrated modeling framework to quantify the coastal protection services supplied by vegetation. Journal of Geophysical Research C: Oceans 120, 324-345 (2015)

30. Davidson, M., Van Koningsveld, M., de Kruif, A., Rawson, J., Holman, R., Lamberti, A., Medina, R., Kroon, A., Aarninkhof, S.: The CoastView project: Developing video-derived Coastal State Indicators in support of coastal zone management. Coastal Engineering 54, 463-475 (2007)

Dieses Werk ist copyrightgeschützt und darf in keiner Form vervielfältigt werden noch an Dritte weitergegeben werden.
Es gilt nur für den persönlichen Gebrauch.

WAVE ENERGY DISSIPATION ON THE CARIBBEAN INSULAR CORAL REEFS OF COLOMBIA

Johann K. Delgado[1], Andrés F. Osorio[1], Francisco M. Toro[1], Juan D. Osorio-Cano[1]

[1]Research Group in Oceanography and Coastal Engineering, OCEANICOS, Department of Geosciences and Environment, Nacional University of Colombia at Medellín, Colombia, jkdelgadog@unal.edu.co, afosorioar@unal.edu.co, fmtoro@unal.edu.co, jdosorio0@unal.edu.co

Key words: Coral Reefs, Degradation, Roughness, Wave dissipation, XBeach

Abstract

The numerical model XBeach was employed to simulate two typical Colombian coral reefs. A fringing and a barrier type reefs under healthy and degraded conditions were compared in terms of their capability to dissipate the wave energy through bottom friction and wave breaking. Laboratory experiments were used to calibrate and validate some modelled results. A significant difference was found between both coral reefs. The bottom friction dissipation is dominated in the fringing reef. By contrast, the barrier reef loses almost all the wave energy by wave breaking.

1 Introduction

The coral reefs are extremely diverse ecosystems and play a key role in the productivity of the coastal areas [1]. The rise in wave energy close inshore due to coral mortality (degradation) is affecting the coral reef environments in all tropical areas. Previous studies reported more energetic wave attacks, which compromise infrastructure, coastline protection, and economy stability of coastal communities. However, some of these places lack government presence, and continuous and systematic monitoring. As a result, the effects of natural and human threats are hardly quantified.

Colombia possesses about 2,860 km^2 of coral reef areas within the Caribbean Sea. They are able to be divided in oceanic and continental coral reefs. Former consists of the San Andrés and Providencia Archipelago (SPA) and represents the greatest percentage of the coral area (76.5%). It is formed by three inhabited Islands (San Andrés, Old Providence, and Santa Catalina) and several atolls and banks (Courtown, Albuquerque, Serrana, Roncador, Quitasueño, Serranilla, and Bajo Nuevo). They are located approximately 700 km off the Colombian continental coast [2, 3]. By contrast, latter involves all coral reefs within continental coastal waters, of which Rosario Island Archipelago (RIA) belongs to. RIA includes 27 Islands, even though, the Grande, Rosario, and Tesoro Islands are the most representative in terms of their size, environment (the presence of vulnerable ecosystems and protected areas), and socio-economic characteristics (human settlements and tourism) [4].

Dieses Werk ist copyrightgeschützt und darf in keiner Form vervielfältigt werden noch an Dritte weitergegeben werden.
Es gilt nur für den persönlichen Gebrauch.

Despite oceanic and continental coral reefs of Colombia are in the Caribbean, they present natural and human threats in different manners. In contrast to RIA, SPA is exposed to storm conditions as extreme winds, waves, and surges due to hurricanes and cold fronts presence [5]. As an illustration, between 1988 and 2016, a total of 7 hurricanes hit or passed close to the Colombian Island Serrana Cay. [6] presented an estimation of the extreme wave height over the Colombian Seaflower Biosphere Reserve (SBR), including Serrana Island, during the hurricane Fifi (1974), Carmen (1974), Greta (1978), Joan (1988), Iris (2001), Dean (2007), and Felix (2007). In accordance with this reference extreme wave heights were from 3.2 m to 7 m throughout events. These results are in agreement with other authors, who have detected Hs > 5m during hurricane events in the Old Providence Island [5], as well as changes in peak periods were noticed, periods between 8 s and 10 s were the most frequent ones during these events [5, 7].

Human activities have also affected strongly the coral reef environments, in particular through sediment fluxes from rivers, oil spills, and untreated sewage pollution, followed by solid wastes (mainly domestic), industrial pollution, and pesticides [8-10]. Particularly, RIA has been impacted by prolonged and significant muddy plumes of the Magdalena River. Some studies have shown that the current cover of live coral in Rosario Islands is only 33% in comparison with previous decades [10]. Under similar conditions, coral reefs in San Andrés Island have been jeopardized mainly by sewage. High values of biologically available nitrogen and phosphorous, which were up to 13 times above the maximum recommended for coral reefs health, were detected during the monitoring period 2000-2005. Hence, a nutrient enrichment has been detected that has a negative impact on coral reproduction and its calcification, decreasing the growth rate of the reef, and producing chronic diseases [8]. Regionally, Caribbean reefs have been devastated by population declines of coral species as *Acropora cervicornis* and *A. palmata* [11, 12]. In a particular case, estimated coral mortality for Serrana Cay Island (SPA) in the 1990s was around 50% [13], while the average for all Colombian Caribbean Reefs Areas was 38% [12]. In consequence, seabed has been changing from coral rough structures to algae colonies. For summarizing the threat intensities that affects the Colombian coral reefs, the Table 1 shows the degree of affectation (qualitatively) for several Colombian coral reefs. It is classified in null, minimum, medium and high degree. For a complete list of areas and threats see [2].

In order to investigate challenges as SPA as RIA face and to take into account the necessity to obtain accurate and practical information for understanding attenuation and wave transformation mechanisms in degraded scenarios, a scale model of a representative fringing reef profile was built based on bathymetric information from RIA. Previously, [14] has already used this configuration with satisfactory results. The model is installed in the wave flume at the National University of Colombia. Then, the numerical model (XBeach) was calibrated using the laboratory results to assess several climatic scenarios for the same profile and for a characteristic idealized barrier profile. This last one is based on bathymetry observations made in Serrana Cay Island.

Dieses Werk ist copyrightgeschützt und darf in keiner Form vervielfältigt werden noch an Dritte weitergegeben werden.
Es gilt nur für den persönlichen Gebrauch.

Table 1: Degree of affectation for some oceanic and continental Colombian coral reefs (Adapted from [2]).

	San Andrés	Old Providence	Cay Islands	Rosario
Hurricanes	Medium	High	Medium	Null
Warming	Medium	Medium	Medium	High
Diseases	High	Medium	Medium	Medium
Sediment fluxes	Null	Minimum	Null	High
Waste water	Medium	Minimum	Null	Medium

2 Study area and methodology

2.1 Serrana Cay Island

The Colombian Seaflower Biosphere Reserve (SBR) is the largest marine protected area (MPA) in the Caribbean and the second one in Latin America [15]. The SBR has a large reef system that includes SPA extending over 500 km [16]. One of the most representative atolls in the area is Serrana Cay Island. It is an extensive reef complex, about 322 km^2, with a windward reef wall that attains a total length of nearly 45 km [3]. Serrana possesses a high biodiversity, and biological and economic productivity concentrated in marine ecosystems (coral reefs). It also provides a variety of valuable ecosystem services, including coastal risk reduction for the complete MPA [17]. Due to its remote location and lack of government interest, Serrana has been an unexplored territory in terms of the scientific knowledge.

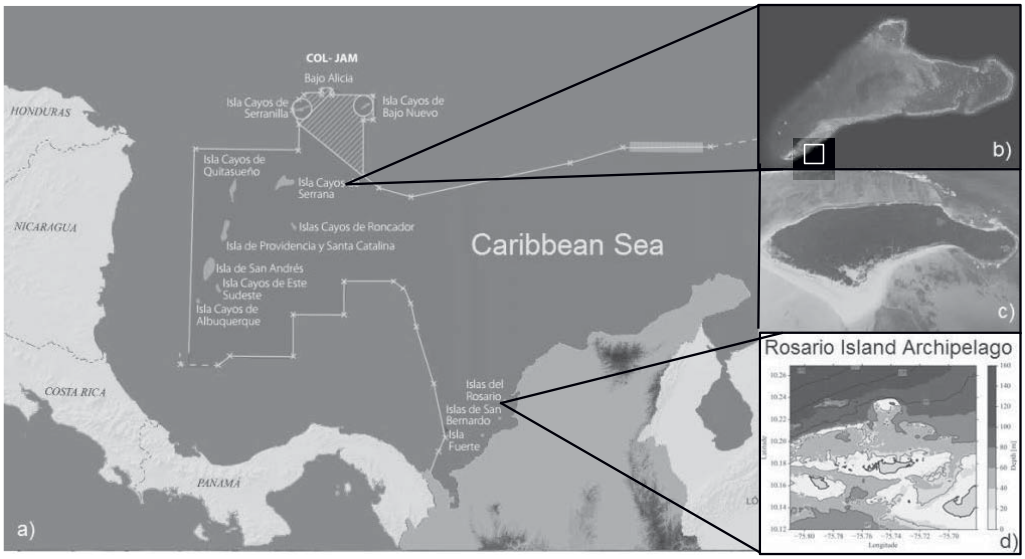

Figure 1: a) Colombian insular territories within the Caribbean Sea (Adapted from schematic map of Colombia, CCO), b) Reef complex of Serrana Cay Island including emerged land and the complete barrier reef, c) Detail of the emerged land, South West Cay, and d) Bathymetric scheme of Rosario Island Archipelago.

Dieses Werk ist copyrightgeschützt und darf in keiner Form vervielfältigt werden noch an Dritte weitergegeben werden.
Es gilt nur für den persönlichen Gebrauch.

As part of a Colombian National Program, a scientific expedition was carried out to investigate biotic and abiotic factors of the Island during August 2016. The main goal was to assess the degree of damage of natural system (marine species, reefs, coastal vegetation, and beaches, among others) from changing like sea levels, climate variability (macro climatic phenomena (e.g., ENSO) and extreme events, among others), and human interventions (oil industry, extensive fishing). However, the strong environmental conditions did not allow obtaining primary oceanographic information about current velocities, wave conditions, and tide sea level during the field work. Fortunately, bathymetric, sediments, morphology (from aerial photography), and meteorological information could be collected. That approach requires different methodologies as physical and numerical modelling, which are able to explore the existing and future coral reef development.

2.2 Rosario Island Archipelago

The Rosario Island Archipelago is a 145 km^2 offshore coral reef in Barbacoas Bay, the major continental coral reef system in Colombia that belongs to the Colombian MPA's [10]. Three primary geomorphological units form the archipelago: (1) fringing reefs, (2) marine terraces, and (3) emerged areas (islands).The fringing reefs are separated from the island coastline by narrow, shallow channels with bottoms covered by calcareous sands and gravel [4]. The Archipelago's marine dynamics are influenced significantly by how both the intensity and seasonality of the trade winds effects wave propagation in the shallow waters and rising sea levels. Most of the year (November-July), the archipelago wave system is dominated (72%) by the presence of swells from the north-northeast (NNE), which have average heights and periods of 0.71 ± 0.4 m and 6.3 ± 1.7 s, respectively [4]. The Figure 1 shows the location of SPA and RIS within Caribbean Sea.

2.3 Experimental Methods

Different approaches were used for investigating the effect of coral degradation on water wave dissipation due to bottom friction and wave breaking. Firstly, a physical model of a representative fringing reef profile was mounted in the wave flume at the National University of Colombia. The flume is 25 m long, 1 m width, and 1 m height. The model has a geometry scale 1:30, and the kinematic scale was obtained assuming equal Froude number as prototype as model. Two monochromatic cases of wave heights (H = 0.07 m and 0.1 m) and a couple on periods (T = 0.7 s and 1.3 s) were carried out. These scenarios were based on climate wave available information for the RIA [4, 18]. These cases represent higher conditions above the average wave heights and periods. Variations in the tide level were not considered. The Table 2 presents the cases modelled and their parameters. Each case was run on RIS and Serrana profile. The model reef profile was built with wood laminated board. These pieces have small friction, even though the friction factor was estimated (f_w = 0.03). The equation proposed by Kamphuis (1978) was employed for calculating the best fit. A total of eight free surface probes were installed in the wave flume. The measurements recorded were used to estimate the significant wave height and wave period along the flume. The sensors were enumerated 1-8 from left to right. The first two sensors determined the incident wave in deep waters and in the beginning of the fore reef terrace, respectively. The other ones, except of 8, were positioned on the middle of the fore reef terrace before the breaking zone. The sensor number 8 measured after the wave breaking for estimating the total loss of

Dieses Werk ist copyrightgeschützt und darf in keiner Form vervielfältigt werden noch an Dritte weitergegeben werden.
Es gilt nur für den persönlichen Gebrauch.

energy. The laboratory experiments were performed three times for evaluating the repetitive independency. Afterwards, the XBeach Model was calibrated and validated using laboratory results.

The Open Source XBeach Model is a two-dimensional model (with two approaches: (1) spectral action balance equation for hydrostatic mode, and (2) Non-Linear Shallow Water Equations for non-hydrostatic mode) for wave propagation, long waves and mean flow, sediment transport and morphological changes of the nearshore area, beaches, dunes and back barrier during storms (http://oss.deltares.nl/web/xbeach/). It has been employed in several studies for calculating wave run-up, infragravity, and very low frequency wave motions on an atoll reef with satisfactory results [14, 19, 20].

3 Results and discussion

The numerical results using $f_w = 0.3$ are in agreement with the laboratory recordings. Changes in the parameter f_w have been included in this study. [21] recommend some values for different seabed conditions, from 0.08, for 75% - 100% sand, to 0.2 for 75%-100% live coral or dead uneroded coral or tall (>30 cm) boulders, although f_w is able to be greater than this value [14, 22, 23]. Particularly, $f_w = 0.05,\ 0.1,\ 0.2,\ \text{and}\ 0.3$ have been selected for considering an ample range of possibilities.

The friction effect on waves was more representative in RIA than in Serrana Island. A monotonic decrease of energy is observed when the wave cross over the fore reef terrace. Before that, wave has already interacted with the fore reef, even though just a significant dissipation is observed for CR03). For the other modelled cases, there is not any effect of the roughness on the wave conditions in that part of the reef. In the case of Serrana profile, all cases present the same behaviour. The dissipation on both fore reef and lagoon due the friction is minimal; indeed it is explained by the large slope and depth (~20m), respectively. The difference in dissipated energy between the roughest case and the smoothest one holds constant. That difference is generated likely by the interaction flow-seabed during the wave breaking. For both fringing and barrier reefs, the wave heights increase about 10% due to the friction reduction; however, the performance presents a similar pattern for all cases. For RIA, a convex and progressive decreasing of the wave heights was observed from the fore reef terrace to the crest where the rate of energy dissipation reducing while in Serrana Island the wave heights fall and rapidly they change.

Table 2: Modelled wave cases. The subindex means model (m) and prototype (p)

Case	H_m [m]	T_m [s]	H_p [m]	T_p [s]
CR01	0.07	1.0	2.1	5.48
CR02	0.07	1.3	2.1	7.12
CR03	0.10	1.0	3.0	5.48
CR04	0.10	1.3	3.0	7.12

Dieses Werk ist copyrightgeschützt und darf in keiner Form vervielfältigt werden noch an Dritte weitergegeben werden.
Es gilt nur für den persönlichen Gebrauch.

The approaches employed in this study allowed to explore the different behaviours, in which bottom friction and wave breaking take place in the hydrodynamic processes. The imminent degradation, what is exposed the Colombian coral reefs, will have a severe effect on the oceanic and continental coastal areas, although there is a lack of data, studies, and official reports about the current and future coral reef states. In this order, the understanding of changes in hydrodynamic mechanisms allows integrating ecosystems in coastal engineering practice and coastal management.

Despite physical and numerical tools represent satisfactory approaches for studying processes such as wave dissipation, set-up, run up, sediment transport, and flood levels, it is crucial to obtain primary information as wave climate, damage by natural and human threats, progressive effects on the coast and others. It is a pivotal element in the decision-making performance.

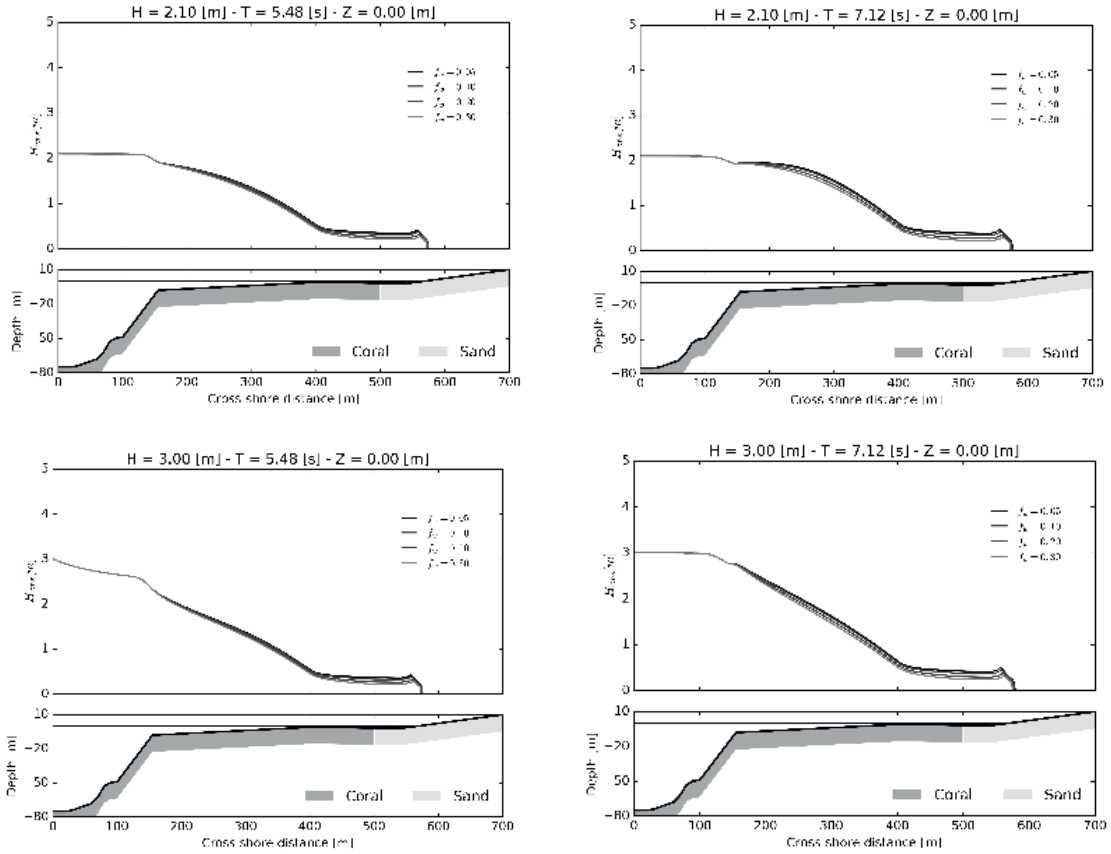

Figure 2: Wave height on RIA reef profile

Dieses Werk ist copyrightgeschützt und darf in keiner Form vervielfältigt werden noch an Dritte weitergegeben werden.
Es gilt nur für den persönlichen Gebrauch.

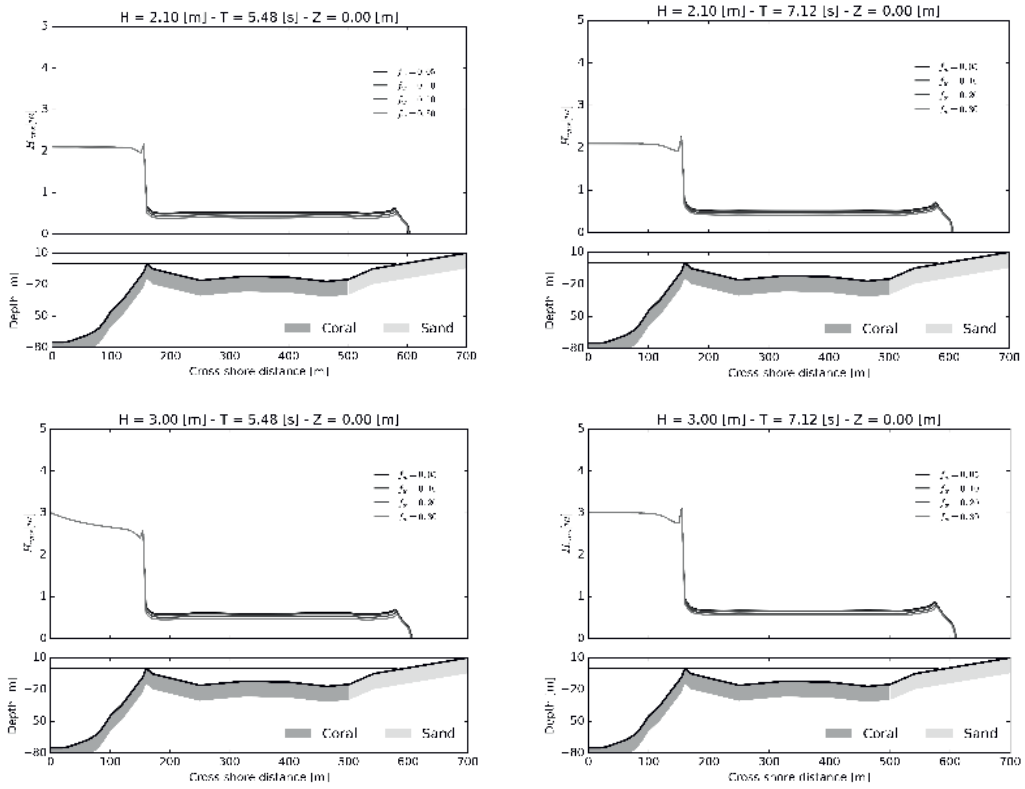

Figure 3: Wave height on Serrana reef profile

4 Conclusions

The comparison presented between fringing and barrier coral reefs provides a general approximation about the possible wave conditions within Colombian coral reefs. This study helps to explore the consequences of coral degradation in a remote and poorly gauged Island. Also, it becomes a first step of an accomplished experiment for exploring other processes such as coral uptake, coral breaking, and design conditions for coastal engineering projects. Remarkable differences were found between fringing and barrier type reefs, the mechanisms, which are involved into dissipation energy, have different contributions depend on bathymetry conditions. Prolonged time periods under stronger wave attacks could affect the morphodynamics of the beaches. More efforts should be made for studying the consequences on the shoreline.

5 Acknowledgments

The authors thank DAAD and Exceed Swindon Project for the financial and technical support to participate at the Summer School on “Integrating Ecosystems in Coastal Engineering Practice”. We also thank all the lecturers and the attendees for their comments and assistances to this study. This work is part of the Master thesis of the main author and is supported by COLCIENCIAS and the National University of Colombia at Medellín in the project “Study of wave energy dissipation in natural structures and their response to extreme events” – Internal Code: 111866044690. We also thank Juan Camilo Amaya for his support with the numerical modelling.

Dieses Werk ist copyrightgeschützt und darf in keiner Form vervielfältigt werden noch an Dritte weitergegeben werden.
Es gilt nur für den persönlichen Gebrauch.

6 References

1. CORDIO: Coral reef degradation in the Indian Ocean: status report 2002. CORDIO, University of Kalmar, Sweden (2002)
2. Diaz, J., Barrios, L., Cendales, H., Garzón-Ferreira, J., Geister, J., López-Victoria, M., Ospina, G., Parra-Velandia, F., Pinzón C, J., Vargas-Angel, B., Zapata, F., Zea, S.: Áreas Coralinas de Colombia (2000)
3. Garzón-Ferreira, J., Díaz, J.M.: The Caribbean coral reefs of Colombia. In: Cortes, J. (ed.) Latin America Coral Reefs, pp. 275-301. Elsevier Science B.V., Amsterdam, The Netherlands (2003)
4. Restrepo, J.C., Otero, L., Casas, A.C., Henao, A., Gutiérrez, J.: Shoreline changes between 1954 and 2007 in the marine protected area of the Rosario Island Archipelago (Caribbean of Colombia). Ocean & Coastal Management 69, 133-142 (2012)
5. Bernal, G., Osorio, A.F., Urrego, L., Peláez, D., Molina, E., Zea, S., Montoya, R.D., Villegas, N.: Occurrence of energetic extreme oceanic events in the Colombian Caribbean coasts and some approaches to assess their impact on ecosystems. Journal of Marine Systems 164, 85-100 (2016)
6. Lizano-Rodríguez, O.G.: Simulación de la altura máxima de ola en huracanes con trayectorias similares en el mar Caribe y su relación con los impactos costeros generados. Boletín Científico CIOH. 29, 8-26 (2011)
7. Chen, S.S., Curcic, M.: Ocean surface waves in Hurricane Ike (2008) and Superstorm Sandy (2012): Coupled model predictions and observations. Ocean Modelling 103, 161-176 (2016)
8. Gavio, B., Palmer-Cantillo, S., Mancera, J.E.: Historical analysis (2000–2005) of the coastal water quality in San Andrés Island, SeaFlower Biosphere Reserve, Caribbean Colombia. Marine Pollution Bulletin 60, 1018-1030 (2010)
9. Restrepo, J.D., Park, E., Aquino, S., Latrubesse, E.M.: Coral reefs chronically exposed to river sediment plumes in the southwestern Caribbean: Rosario Islands, Colombia. Science of The Total Environment 553, 316-329 (2016)
10. Restrepo, J.D., Zapata, P., Díaz, J.M., Garzón-Ferreira, J., García, C.B.: Fluvial fluxes into the Caribbean Sea and their impact on coastal ecosystems: The Magdalena River, Colombia. Global and Planetary Change 50, 33-49 (2006)
11. Carpenter, K.E., Abrar, M., Aeby, G., Aronson, R.B., Banks, S., Bruckner, A., Chiriboga, A., Cortés, J., Delbeek, J.C., DeVantier, L.: One-third of reef-building corals face elevated extinction risk from climate change and local impacts. Science 321, 560-563 (2008)
12. Jackson, J., Cramer, K., Donovan, M., Lam, V.: Status and trends of Caribbean coral reefs: 1970-2012. Global Coral Reef Monitoring Network, IUCN, Gland, Switzerland. 304 pp. (2014)

Dieses Werk ist copyrightgeschützt und darf in keiner Form vervielfältigt werden noch an Dritte weitergegeben werden.
Es gilt nur für den persönlichen Gebrauch.

13. Sánchez M, J.A.: Benthic communities and geomorphology of the Tesoro Island coral reef, Colombian Caribbean. Boletín de Investigaciones Marinas y Costeras - INVEMAR 24, 55-77 (1995)

14. Osorio-Cano, J.D., Osorio, A.F., Peláez-Zapata, D.S.: Ecosystem management tools to study natural habitats as wave damping structures and coastal protection mechanisms. Ecological Engineering (*In press, 2017*)

15. Guarderas, A.P., Hacker, S.D., Lubchenco, J.: Current Status of Marine Protected Areas in Latin America and the Caribbean (Estado Actual de las Áreas Marinas Protegidas en Latinoamérica y el Caribe). Conservation Biology 22, 1630-1640 (2008)

16. Mow, J.M., Howard, M., Delgado, C.M., Tabet, S.: Promoting Sustainable Development: A Case Study of the Seaflower Biosphere Reserve. Prospects 33, 303-312 (2003)

17. van Zanten, B.T., van Beukering, P.J.H., Wagtendonk, A.J.: Coastal protection by coral reefs: A framework for spatial assessment and economic valuation. Ocean & Coastal Management 96, 94-103 (2014)

18. Osorio, A.F., Montoya, R.D., Ortiz, J.C., Peláez, D.: Construction of synthetic ocean wave series along the Colombian Caribbean Coast: A wave climate analysis. Applied Ocean Research 56, 119-131 (2016)

19. Quataert, E.: Wave runup on atoll reefs. Civil Engineering and Geosciences. Hydraulic Engineering. TU Delft. M.Sc. Thesis (2015)

20. Quataert, E., Storlazzi, C., van Rooijen, A., Cheriton, O., van Dongeren, A.: The influence of coral reefs and climate change on wave-driven flooding of tropical coastlines. Geophysical Research Letters 42, 6407-6415 (2015)

21. Sheppard, C., Dixon, D.J., Gourlay, M., Sheppard, A., Payet, R.: Coral mortality increases wave energy reaching shores protected by reef flats: Examples from the Seychelles. Estuarine, Coastal and Shelf Science 64, 223-234 (2005)

22. Lowe, R.J., Falter, J.L., Bandet, M.D., Pawlak, G., Atkinson, M.J., Monismith, S.G., Koseff, J.R.: Spectral wave dissipation over a barrier reef. Journal of Geophysical Research: Oceans 110, 1-16 (2005)

23. Monismith, S.G., Rogers, J.S., Koweek, D., Dunbar, R.B.: Frictional wave dissipation on a remarkably rough reef. Geophysical Research Letters 42, 4063-4071 (2015)

Dieses Werk ist copyrightgeschützt und darf in keiner Form vervielfältigt werden noch an Dritte weitergegeben werden.
Es gilt nur für den persönlichen Gebrauch.

ASSESSMENT OF WAVE ATTENUATION PERFORMANCE OF SEAWEED

Sanaz Hadadpour

Leichtweiss-Institute for Hydraulic Engineering and Water Resources (LWI), Department of Hydromechanics and Coastal Engineering, Technische Universität Braunschweig, Beethovenstr. 51a, 38106 Braunschweig, Germany, s.hadadpour@tu-braunschweig.de

Keywords: Coastal vegetation, Hydraulic model tests, Seaweed, Wave attenuation, Wave-vegetation interaction

Abstract

Due to the importance of beaches as one of the most important natural resources, many investigations on shoreline protection have been conducted. In addition to beach nourishment and structures such as jetties and breakwaters, which can protect the shoreline by dissipating and reflecting wave energy, the consideration of vegetation for shore protection and related eco-engineering issues has been increasingly addressed in recent publications. Since the interaction processes between hydrodynamics and plants structures are complex, there is an increasing demand for understanding the physical processes taking place in the vegetated areas and improving the current modelling approaches. Therefore, this study aims to improve the understanding of the attenuation of waves by submerged vegetation. For this purpose, hydraulic model tests have been carried out in a wave flume to study the effects of vegetation parameters (density and flexibility) and wave parameters (wave height and period) on wave attenuation using an artificial seaweed meadow subject to different wave conditions. For the effects of wave parameters, it was found that higher dissipation is induced by larger wave heights, and wave attenuation decreases for longer waves. For the effects of vegetation parameters, the results showed that wave attenuation increases with higher density and stiffness of the vegetation.

1 Introduction

Coastal areas are very complex and sensitive regions, which are extremely important in terms of economic, social and environmental value. Hence, providing protection against coastal erosion becomes one of the most significant current issues and a large number of studies have been conducted on the development of shore protection concepts and approaches. In addition to hard structures such as jetties and breakwaters, which can protect the shoreline by dissipating and reflecting wave energy, the vegetation role in shore protection is increasingly considered as a potential component of sustainable coastal defence schemes. Coastal vegetation is able to enhance wave attenuation [1-6] and can act as natural buffer zone against coastal flood during storms. Additionally, aquatic vegetation has the ability to increase the stability of shorelines through the root systems, thus reducing shoreline erosion. This might explain the evolution from hard structures to more adaptive nature-based and hybrid shore protection schemes by combining hard and soft solutions, which is increasingly observed since few years in coastal engineering.

Dieses Werk ist copyrightgeschützt und darf in keiner Form vervielfältigt werden noch an Dritte weitergegeben werden.
Es gilt nur für den persönlichen Gebrauch.

Given the significant protective role of coastal vegetation in the context of climate change and eco-system management of coastal zones, and the high complexity of the processes underlying the interactions of vegetation with waves and currents (see Figure 1), understanding and modelling the mechanisms associated with these interactions are increasingly becoming the research focus in several coastal countries worldwide. Despite the recognition of the major role of coastal vegetation as a natural shore protection, the engineering evaluation or design related information on plants exposed to waves are still not sufficient. Therefore, the aim of this study is to further develop the understanding of the wave attenuation performance of coastal vegetation and their interactions with waves with a focus on some types of coastal vegetation, seaweeds.

Figure 1: Interaction of wave and seaweed (from: https://flic.kr/p/7wfqgk)

From the review of the existing literature regarding vegetation effects on wave attenuation, there is evidence that the vegetation can reduce flow velocities and wave heights, and attenuate wave energy. This attenuation effect can be used for coastal protection. In addition, vegetation fields in coastal area have the capability to provide a habitat for a variety of valuable organisms [7] and result in sedimentation and stabilization of the bed [8], and hence, could be important in coastal managements [9]. These features result in a positive feedback not only in coastal protection but also in coastal eco-system conservation [10].

The role of vegetation in wave attenuation has been proven for several plant communities such as saltmarsh [5], kelp [11], seagrass [12], and mangroves [13]. Using physical models can help to gain a better insight into the biophysical interactions and the processes involved. However, it should be mentioned that due to requirements with respect to plant health, resilience and adaptation to different and changing environmental conditions using live vegetation in hydraulic laboratories is limited [14]. As an alternative, many researchers used abiotic surrogates to investigate their effects on waves and currents [6, 14].

Geometrical plant properties such as stem and shoot dimensions, and density (i.e. number of plants per unit area) may strongly affect the biophysical interactions [5, 12, 15-18]. Other significant parameters, which intensively affect the drag imposed on the vegetation and play a key role in wave attenuation, are the mechanical parameters, in particular buoyancy and stiffness [6, 7, 19, 20].

Dieses Werk ist copyrightgeschützt und darf in keiner Form vervielfältigt werden noch an Dritte weitergegeben werden.
Es gilt nur für den persönlichen Gebrauch.

In addition, some efforts have been made to numerically simulate the interaction of the vegetation with hydrodynamics [21, 22], in which validation has been carried out using surrogate plants. Although visual observations have been undertaken in order to better investigate the ability of the physical models to mimic the real vegetation [6, 23], a more quantitative approach is favoured to make the results transferable between laboratory experiments, field observations and numerical models.

Furthermore, a highly coupled and non-linear interaction between waves and vegetation has been identified [24]. Such dissipation may change with plant density, wave conditions, current velocity, and drag coefficient. The drag forces on vegetation due to waves and currents, commonly described by a drag coefficient, play an important role in the energy dissipation process [25].

In coastal area, tidal currents can also play an important role together with the incident waves in wave dissipation process [25]. However, to the author's knowledge, there are only very few studies, which investigated the effect of currents on the wave-attenuating capacity of the plants [3, 6, 25, 26].

Different laboratory tests and field measurement have indicated that wave attenuation by vegetation depends on both incident wave and canopy parameters (e.g. [11, 14, 25, 27, 28]). In summary, most of previous studies showed that the higher vegetation density, the higher wave energy attenuation. Moreover, it was found that the wave energy dissipation also depends on the stiffness of the plant stems, and higher dissipation resulted from stiffer plant stems. Furthermore, the submergence ratio (i.e. the ratio of the water depth to canopy height) was taken into account as an effective parameter, which showed an inverse relationship to the wave damping resulting in higher wave energy attenuation for lower submergence ratios.

The overall objective of this study is was to determine the effect of seaweed field on wave attenuation in order to find how seaweeds may affect incoming waves. Therefore, hydraulic model tests were carried out to study the influencing parameters to determine the role of vegetation density and flexibility, and incoming wave parameters (wave height and period) on wave damping.

2 Materials and Methods

2.1 Study area

In this study, hydraulic model tests have been carried out in the 1 m wide flume of Twin Wave Flume (TWF) at the Leichtweiss-Institute (LWI), TU Braunschweig within the MERMAID project (FP7-OCEAN.2011-1 "Multi-use offshore platforms") to study the effects of vegetation parameters (density and flexibility) and wave parameters (wave height and period) on wave attenuation.

The full floating seaweed culture installation in the North Sea (Figure 2) is considered as the area of study [29], thus forming the basis for the hydraulic model tests in a 1:30 scale. The original H-floater profiles are 10 m wide, 6 m high, and their tube diameter is around 30 cm. These H-floaters were placed every 25 m. The dimension of the entire seaweed field was 125 x 10 m.

Dieses Werk ist copyrightgeschützt und darf in keiner Form vervielfältigt werden noch an Dritte weitergegeben werden.
Es gilt nur für den persönlichen Gebrauch.

Figure 2: Observations from North Sea seaweed installation [29]

Different wave conditions were generated in order to reproduce the wave conditions from the North Sea (Table 1), where the full seaweed culture installation is placed in a water depth of 20 m.

Table 1: Wave conditions in the North Sea and in the LWI wave flume (model scale 1:30)

Description of wave conditions	Prototype values		Froude-scaled model values	
	H_{m0} [m]	T_p [s]	H_{m0} [m]	T_p [s]
Mild - Most common	1.5	6	0.05	1.1
	3	8	0.1	1.5
Storm - 1% condition	4	9	0.13	1.6
	4.5	9.5	0.15	1.7
	6	11	0.2	2
Extreme - 1/10 year storm	7.4	13	0.25	2.4

2.2 Set-up of model tests and test program

As mentioned above, the narrower flume of the TWF consists of two parallel flumes (2 m and 1 m wide), both being about 90 m long and 1.25 m deep. The walls and the bottom of the flume are made of bricks and concrete, respectively. Two rubble mound slopes are constructed at one end of each flume to absorb wave energy and to reduce reflection effects. At the opposite end of the flume, a twin wave maker is installed. The observation windows are placed within the outer wall of the 2 m wide flume for observing the cross section and the hydraulic processes. The arrangement and dimensions of TWF are shown in Figure 3.

Dieses Werk ist copyrightgeschützt und darf in keiner Form vervielfältigt werden noch an Dritte weitergegeben werden.
Es gilt nur für den persönlichen Gebrauch.

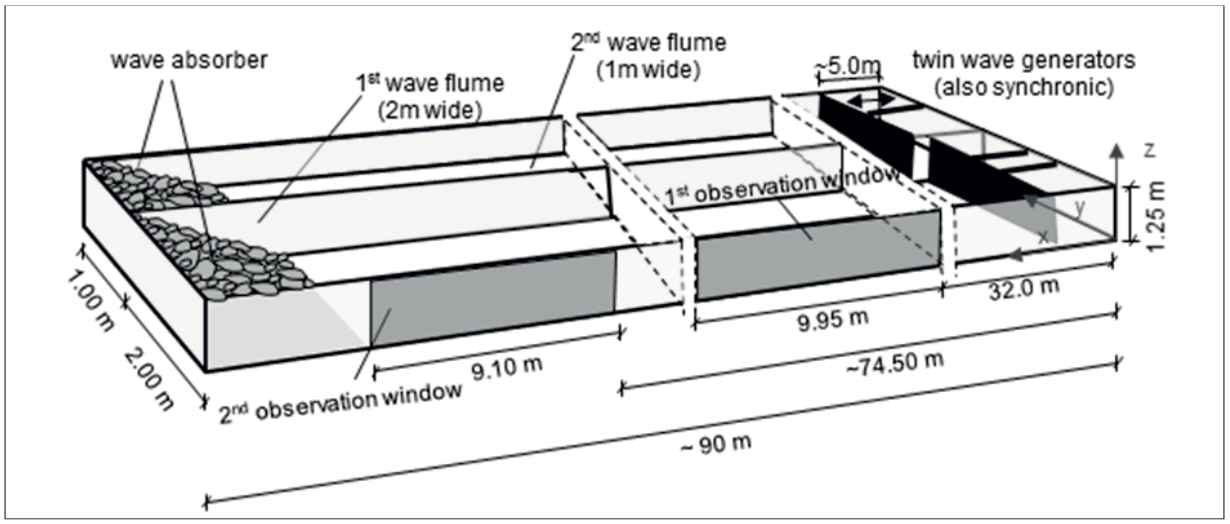

Figure 3: Arrangement and dimensions of the Twin Wave Flume of LWI

The waves are generated by two identical wave generators of piston type, which can be operated simultaneously or independently. The wave paddles can generate solitary waves as well as regular and irregular waves up to about 0.30 m height and 5 s period. Figure 4 shows the twin wave paddles of LWI and the wave types, which can be generated.

To simulate a seaweed farm, the H-shaped profiles with seaweed strings in between are considered (the same as Hortimare design of floating seaweed culture installation, see [29]).

A series of experiments was performed for regular waves propagating over an artificial seaweed field with a length of 4.2 m, which is placed approximately 40 m from the wave maker, in order to reproduce wave conditions of the North Sea. For this purpose, two different types of materials (rigid and flexible) were used for preparing the artificial seaweeds. Moreover, two different densities of the seaweed field (i.e. 10 lines and 5 lines of artificial seaweeds) were considered. Figure 5 shows the model set-up in the TWF of LWI.

Ten resistance wave gauges were used to measure the free surface oscillations in front, along and behind the seaweed field for each test run. Two arrays of wave gauges with predefined distances were installed to analyse wave reflections. Moreover, two Acoustic Doppler Velocimeters (ADVs) were used to measure the flow velocity in front and behind of the seaweed field.

The wave conditions and the parameters of the artificial seaweed (surrogate) tested in the wave flume are reported in Table 2.

Dieses Werk ist copyrightgeschützt und darf in keiner Form vervielfältigt werden noch an Dritte weitergegeben werden.
Es gilt nur für den persönlichen Gebrauch.

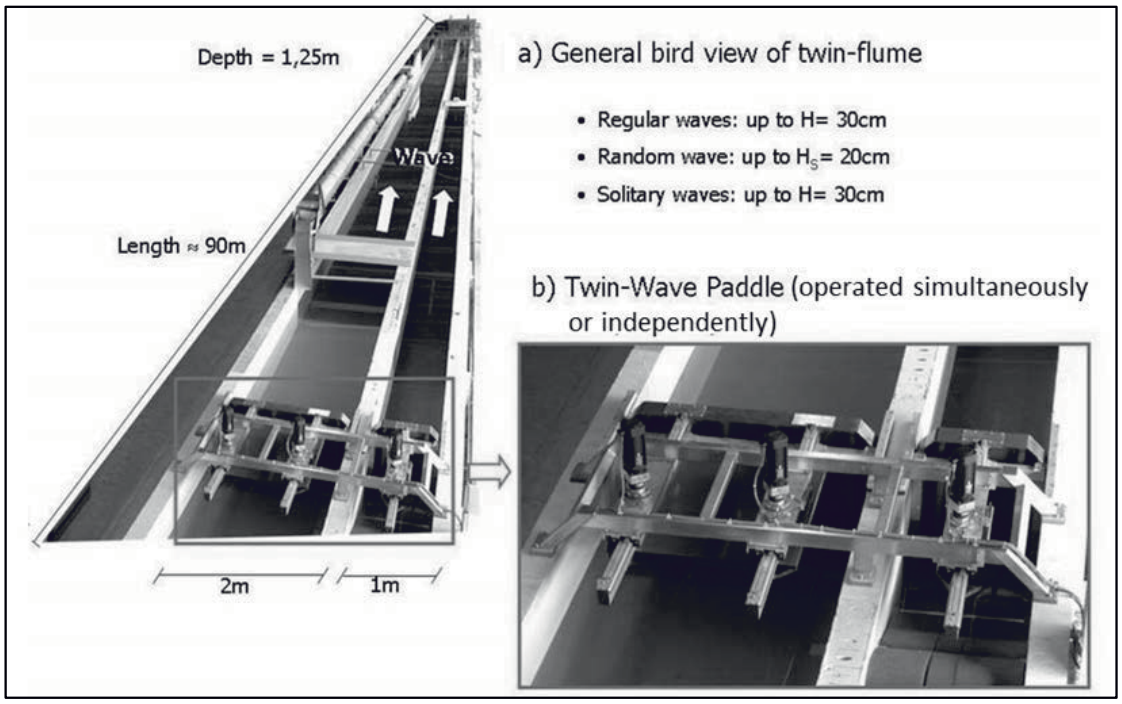

Figure 4: Twin wave paddles of LWI and possible types of waves

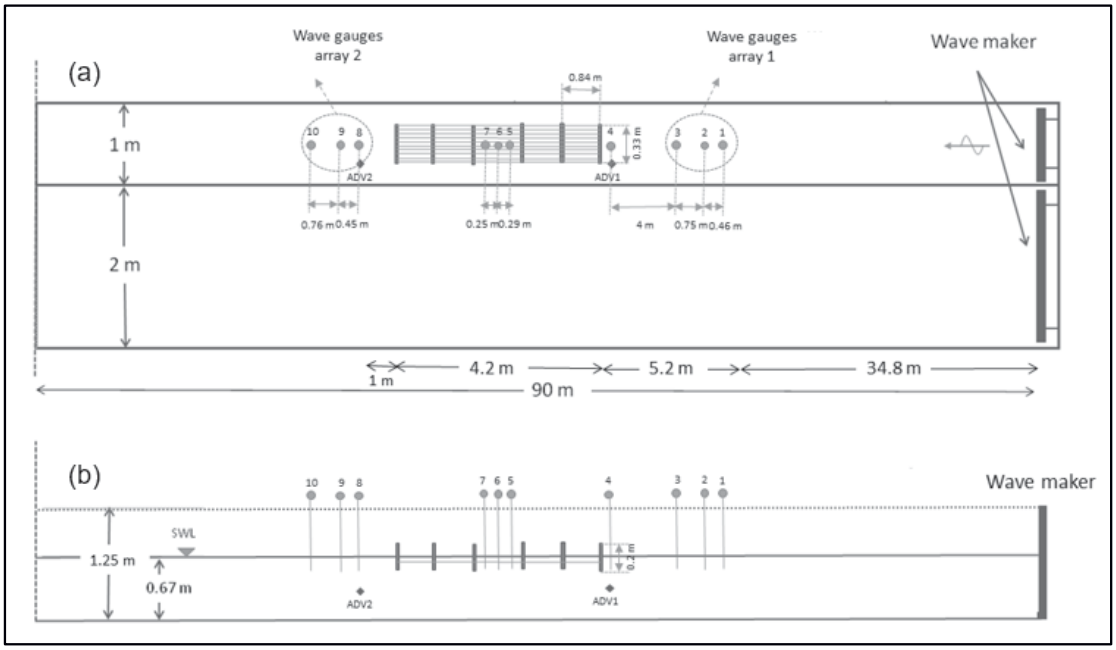

Figure 5: Experimental set-up in the TWF of LWI: (a) Plan view (b) Longitudinal cross section view

Dieses Werk ist copyrightgeschützt und darf in keiner Form vervielfältigt werden noch an Dritte weitergegeben werden.
Es gilt nur für den persönlichen Gebrauch.

Table 2: Testing programme for regular waves in the wave flume (model scale 1:30)

Wave types	Surrogate material	Surrogate size, (cm)	Density of seaweed farm	Incident wave height, H (m)	Wave period, T (s)	Wavelength, λ (m)	Deepwater steepness, H/λ (-)
Regular waves	Fluor elastomer	7	5 strings	0.05	0.9	1.26	0.04
					1.5	3.51	0.01
				0.1	1.4	3.06	0.03
					2.2	7.55	0.01
	Cylindrical wooden rods		10 strings	0.15	1.4	3.06	0.05
					2.2	7.55	0.02
				0.2	1.5	3.51	0.06
					2.6	10.55	0.02

3 Results and Discussion

The wave analysis was performed on each time series measured in the wave flume using L-Davis tools (LWI Data Analysis and Visualization Software). The previous studies concluded that the wave attenuation due to vegetation depends not only on the vegetation characteristics, but also on the wave parameters.

Therefore, different kinds of graphs were plotted to investigate the relative importance of the different parameters influencing the wave attenuation. For this purpose, the percentage of wave height reduction was calculated as a measure of the wave attenuation performance within the seaweed field:

$$\%\ Reduction = \left(\frac{H_{i,behind} - H_{i,front}}{H_{i,front}} \right) \times 100 \quad (1)$$

where $H_{i,\ front}$ and $H_{i,behind}$ are the measured wave height in front of and behind the seaweed field, respectively.

Dieses Werk ist copyrightgeschützt und darf in keiner Form vervielfältigt werden noch an Dritte weitergegeben werden.
Es gilt nur für den persönlichen Gebrauch.

To investigate the influence of vegetation characteristics on wave damping, the percentage of wave height reduction versus two different materials used for preparing artificial seaweed was plotted. Figure 6 shows these graphs for (a) 5 lines and (b) 10 lines of seaweed including eight different combinations of wave heights and periods.

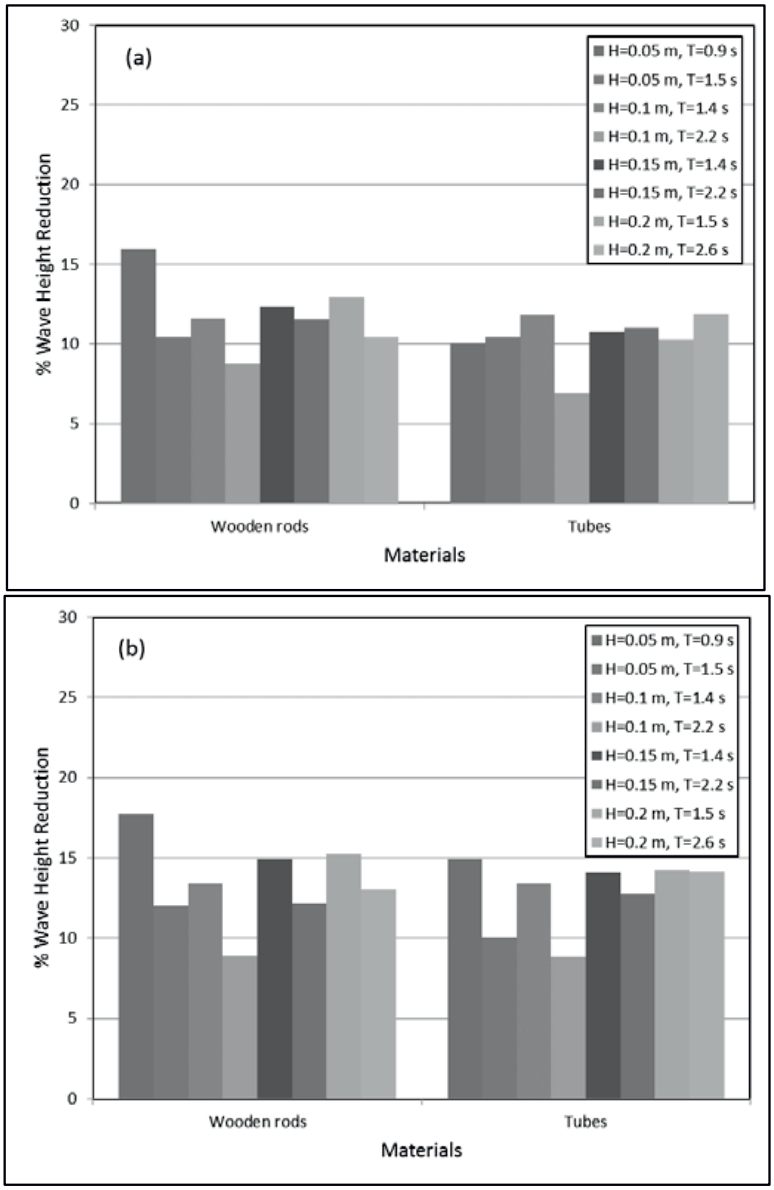

Figure 6: The percentage of wave height reduction for (a) 5 lines and (b) 10 lines of seaweed

To investigate the influence of wave parameters on wave attenuation through the seaweed field, the percentage of wave height reduction was plotted versus the generated wave height (called nominal wave height) for different wave periods, and the generated wave period (called nominal wave period) considering two wave periods for each wave height in Figures 7 and 8, respectively. From the Figures, it can be seen that as the wave height increases, the amount of attenuation due to vegetation enhances.

Dieses Werk ist copyrightgeschützt und darf in keiner Form vervielfältigt werden noch an Dritte weitergegeben werden.
Es gilt nur für den persönlichen Gebrauch.

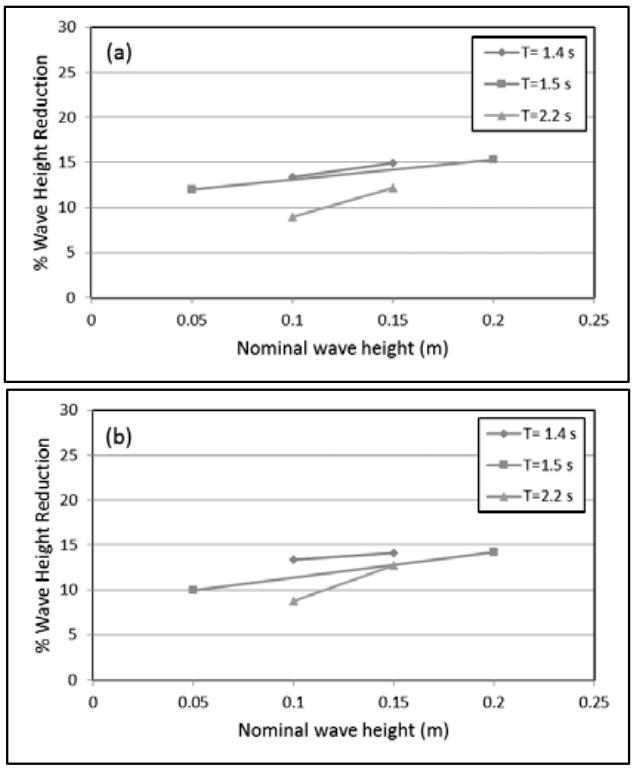

Figure 7: Wave attenuation (determination of nominal *wave height*) for 10 lines of seaweed: (a) Wooden rods, (b) Tubes

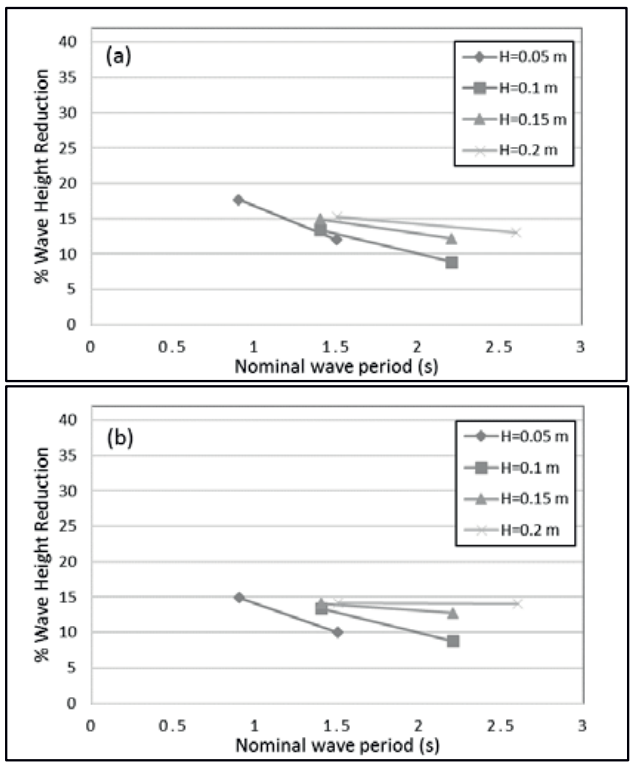

Figure 8: Wave attenuation (determination of nominal *wave period*) for 10 lines of seaweed: (a) Wooden rods, (b) Tubes

Dieses Werk ist copyrightgeschützt und darf in keiner Form vervielfältigt werden noch an Dritte weitergegeben werden.
Es gilt nur für den persönlichen Gebrauch.

Table 3: Total percentage of wave height reduction and the average percentage of wave height reduction per meter of seaweed field for wooden rods and tubes

Density	H_{m0}	T_p	Wooden rods		Tubes	
			Total	Per Meter	Total	Per Meter
5 Lines	0.05	0.9	16%	4%	10%	2%
		1.5	10%	3%	10%	2%
	0.10	1.4	12%	3%	12%	3%
		2.2	9%	2%	7%	2%
	0.15	1.4	12%	3%	11%	3%
		2.2	12%	3%	11%	3%
	0.20	1.5	13%	3%	10%	2%
		2.6	10%	3%	12%	3%
10 Lines	0.05	0.9	18%	4%	15%	4%
		1.5	12%	3%	10%	2%
	0.10	1.4	13%	3%	13%	3%
		2.2	9%	2%	9%	2%
	0.15	1.4	15%	4%	14%	3%
		2.2	12%	3%	13%	3%
	0.20	1.5	15%	4%	14%	3%
		2.6	13%	3%	14%	3%

Experiments showed an inverse relationship between the percentage of wave height reduction and wave period. In all cases, the shorter period showed a higher amount of wave damping.

The total percentage of energy loss through the seaweed field as well as the average of energy attenuation per meter of the seaweed field for two different materials, including two densities (i.e. 5 lines and 10 lines of seaweed) are summarized in Table 3.

The results for the wave height attenuation are in a good agreement with the results found in the literature [14, 25, 28, 29]. The wave height reduction showed the same trends for both materials (rigid and flexible), which were used for preparing the artificial seaweeds. The results show that the vegetation stiffness affects the amount of wave height damping: with rigid members, in most cases, the wave height is reduced by an extra 1- 3% compared to flexible members. Moreover, it was found that the vegetation density affects wave attenuation: with the higher vegetation density (10 lines of seaweeds) the wave height decreases only by 1- 4% more than the lower density with 5 lines of seaweeds.

Dieses Werk ist copyrightgeschützt und darf in keiner Form vervielfältigt werden noch an Dritte weitergegeben werden.
Es gilt nur für den persönlichen Gebrauch.

Regarding the wave parameters, it is demonstrated that the percentage of wave attenuation has a direct relationship with incident wave height, and the larger incident wave height leads to the higher amount of energy dissipation. In addition, an inverse relationship between the percentage of wave attenuation and wave period was found, showing that wave attenuation decreases for longer periods, i.e. waves with shorter periods show a higher amount of energy dissipation.

The experimental results show a total wave height reduction of nearly 7- 18% through the total length of the seaweed field. For both rigid and flexible vegetation elements, the wave height was reduced an average of 2– 4% per meter of wave propagation.

4 Conclusions

Through flume experiments, the impact of vegetation characteristics (stem density and flexibility) and wave properties (wave height and period) on wave decay were studied. As expected, wave attenuation by vegetation depends not only on the wave conditions but also on the vegetation properties. Attending to the vegetation characteristics, meadow density and stiffness influence the wave damping rates. It has been shown that higher stiffness (up to 3%) as well as higher density (up to 4%) enhances the loss of wave height. Furthermore, wave damping increases with increasing wave height and decreasing wave period.

However, a number of knowledge gaps including seasonal impacts on dissipation potential, determination of vegetation-induced damping under combined waves and currents, meadow length impacts on attenuation, and the damping coefficient through the vegetation field still exist. Due to the importance of vegetation for shore protection, it is planned to consider some of these knowledge gaps and to substantially improve the understanding of the highly complex hydrodynamic processes involved in the wave-vegetation interaction in the future works. This goal will be mainly achieved through a numerical model.

5 Acknowledgement

The author would like to gratefully acknowledge DAAD and Exceed Swindon for the financial support to make the participation at the Summer School possible. I really do appreciate Prof. Dr. Rodolfo Silva Casarín and his team for all the time and effort they put into making the Summer School a very special event. In addition, the financial support of this study by the EU within the MERMAID project (FP7-OCEAN.2011-1 “Multi-use offshore platforms") as well as the nice collaboration within this project is gratefully acknowledged. After the completion of MERMAID, a PhD scholarship is gratefully provided by the DAAD for this research topic. I also thank Dr. Maike Paul and Jan-Joost Schouten for their support and help.

6 References

1. Augustin, L.N., Irish, J.L., Lynett, P.: Laboratory and numerical studies of wave damping by emergent and near-emergent wetland vegetation. Coastal Engineering 56, 332-340 (2009)
2. Husrin, S.: Attenuation of solitary waves and wave trains by coastal forests. (2013)

Dieses Werk ist copyrightgeschützt und darf in keiner Form vervielfältigt werden noch an Dritte weitergegeben werden.
Es gilt nur für den persönlichen Gebrauch.

3. Losada, I.J., Maza, M., Lara, J.L.: A new formulation for vegetation-induced damping under combined waves and currents. Coastal Engineering 107, 1-13 (2016)

4. Mendez, F.J., Losada, I.J.: An empirical model to estimate the propagation of random breaking and nonbreaking waves over vegetation fields. Coastal Engineering 51, 103-118 (2004)

5. Möller, I., Spencer, T., French, J.R., Leggett, D.J., Dixon, M.: Wave Transformation Over Salt Marshes: A Field and Numerical Modelling Study from North Norfolk, England. Estuarine, Coastal and Shelf Science 49, 411-426 (1999)

6. Paul, M., Bouma, T.J., Amos, C.L.: Wave attenuation by submerged vegetation: -combining the effect of organism traits and tidal current. Marine Ecology Progress Series 444, 31-41 (2012)

7. Bouma, T.J., De Vries, M.B., Low, E., Peralta, G., Tánczos, I.C., van de Koppel, J., Herman, P.M.J.: Trade-offs related to ecosystem engineering: a case study on stiffness of emerging macrophytes. Ecology 86, 2187-2199 (2005)

8. Gacia, E., Duarte, C.M.: Sediment Retention by a Mediterranean Posidonia oceanica Meadow: The Balance between Deposition and Resuspension. Estuarine, Coastal and Shelf Science 52, 505-514 (2001)

9. Temmerman, S., Meire, P., Bouma, T.J., Herman, P.M.J., Ysebaert, T., De Vriend, H.J.: Ecosystem-based coastal defence in the face of global change. Nature 504, 79-83 (2013)

10. van der Heide, T., van Nes, E.H., van Katwijk, M.M., Olff, H., Smolders, A.J.P.: Positive feedbacks in seagrass ecosystems–evidence from large-scale empirical data. PloS one 6, e16504, https://doi.org/10.1371/journal.pone.0016504 (2011)

11. Dubi, A., Tørum, A.: Wave Damping by Kelp Vegetation. Coastal Engineering 1994, 142-156 (1995)

12. Paul, M., Amos, C.L.: Spatial and seasonal variation in wave attenuation over Zostera noltii. Journal of Geophysical Research: Oceans 116, C08019, (2011), DOI 10.1029/2010JC006797

13. Strusinska-Correia, A., Husrin, S., Oumeraci, H.: Tsunami damping by mangrove forest: a laboratory study using parameterized trees. Natural Hazards and Earth System Sciences 13, 483-503 (2013)

14. Paul, M., Henry, P.-Y.T.: Evaluation of the use of surrogate Laminaria digitata in eco-hydraulic laboratory experiments. Journal of Hydrodynamics, Ser. B 26, 374-383 (2014)

15. Boller, M.L., Carrington, E.: The hydrodynamic effects of shape and size change during reconfiguration of a flexible macroalga. Journal of Experimental Biology 209, 1894-1903 (2006)

16. Bouma, T.J., Vries, M.B.D., Herman, P.M.J.: Comparing ecosystem engineering efficiency of two plant species with contrasting growth strategies. Ecology 91, 2696-2704 (2010)

Dieses Werk ist copyrightgeschützt und darf in keiner Form vervielfältigt werden noch an Dritte weitergegeben werden.
Es gilt nur für den persönlichen Gebrauch.

17. Bradley, K., Houser, C.: Relative velocity of seagrass blades: Implications for wave attenuation in low-energy environments. Journal of Geophysical Research: Earth Surface 114, F01004, (2009), DOI 10.1029/2007JF000951

18. Fonseca, M.S., Koehl, M.A.R.: Flow in seagrass canopies: The influence of patch width. Estuarine, Coastal and Shelf Science 67, 1-9 (2006)

19. Denny, M., Gaylord, B.: The mechanics of wave-swept algae. Journal of Experimental Biology 205, 1355-1362 (2002)

20. Nepf, H.M., Koch, E.W.K.: Vertical secondary flows in submersed plant-like arrays. Limnology and Oceanography 44, 1072-1080 (1999)

21. Dijkstra, J.T., Uittenbogaard, R.E.: Modeling the interaction between flow and highly flexible aquatic vegetation. Water Resources Research 46, W12547, (2010), DOI 10.1029/2010WR009246

22. Luhar, M., Nepf, H.M.: Flow-induced reconfiguration of buoyant and flexible aquatic vegetation. Limnology and Oceanography 56, 2003-2017 (2011)

23. Folkard, A.M.: Hydrodynamics of model Posidonia oceanica patches in shallow water. Limnology and Oceanography 50, 1592-1600 (2005)

24. Koch, E.W., Barbier, E.B., Silliman, B.R., Reed, D.J., Perillo, G.M.E., Hacker, S.D., Granek, E.F., Primavera, J.H., Muthiga, N., Polasky, S., Halpern, B.S., Kennedy, C.J., Kappel, C.V., Wolanski, E.: Non-linearity in ecosystem services: temporal and spatial variability in coastal protection. Frontiers in Ecology and the Environment 7, 29-37 (2009)

25. Hu, Z., Suzuki, T., Zitman, T., Uittewaal, W., Stive, M.: Laboratory study on wave dissipation by vegetation in combined current–wave flow. Coastal Engineering 88, 131-142 (2014)

26. Li, C.W., Yan, K.: Numerical Investigation of Wave–Current–Vegetation Interaction. Journal of Hydraulic Engineering 133, 794-803 (2007)

27. Augustin, L.N.: Laboratory experiments and numerical modeling of wave attenuation through artificial vegetation. (2010)

28. Koftis, T., Prinos, P., Stratigaki, V.: Wave damping over artificial Posidonia oceanica meadow: A large-scale experimental study. Coastal Engineering 73, 71-83 (2013)

29. Hulsman, H., Schipper, J.: Wave attenuation potential of floating seaweed installations. In: 5th Mermaid meeting, Athen (2014)

Dieses Werk ist copyrightgeschützt und darf in keiner Form vervielfältigt werden noch an Dritte weitergegeben werden.
Es gilt nur für den persönlichen Gebrauch.

INTERACTION BETWEEN REEFS AND BEACH MORPHOLOGY IN PONTAL DO CUPE BEACH, BRAZIL

Karoline Angélica Martins[1], Pedro de Souza Pereira[2], Luciana Slomp Esteves[3]

[1] Laboratory of Geological Oceanography, Oceanography Department Federal University of Pernambuco. Av. Arquitetura s/n 50740-550. Recife, Pernambuco, Brazil, karol.martins@msn.com

[2] Laboratory of Marine Geology, Oceanography Department, Federal University of Pernambuco. Av. Arquitetura s/n 50740-550. Recife, Pernambuco, Brazil

[3] Department of Life & Environmental Sciences, Faculty of Science and Technology, Bournemouth University. Talbot Campus, Poole, Dorset, BH12 5BB

Keywords: Beach morphology, Beach profile, Coastal protection, Reef, Ecosystem services.

Abstract

Reefs provide substantial protection to the coast by reducing wave energy before it reaches the shore, which is also considered an ecosystem service of coastal protection. Wave transformations over reefs influence the beach morphology, which is primarily determined by wave breaking height, wave peak period and sediment size. Pontal do Cupe Beach, located in the Brazilian northeast, at Pernambuco state was taken as a model to evaluate the reef's influence over the beach morphology. This beach is characterized by the presence of a parallel reef line in certain parts of the coast, often covered by corals, calcareous algae and molluscs. A Principal Component Analysis confirmed the existence of five beach profile clusters, distinguished by their morphology. One cluster represents the morphology of beaches right in front of the reef lee, another denotes the morphology of beaches under the influence of wave diffraction, and the other three clusters indicate the beaches with less influence of the reef's protection. Through clusters mean profiles it was possible to identify morphological features associated with wave transformation gradients, such as the existence of berm on exposed profiles and a marked low tide terrace on protected profiles.

1 Introduction

The benefits of coral reefs through supply, regulation, culture and support ecosystem services are fundamental to human well-being [1]. The most relevant services provided by coral reefs are: coastal protection, maintenance of species biodiversity, provision of food, recreation and beautiful landscape [2]. All those services generate an estimated contribution of US$ 800 billion to global economy [3].

Studies have shown that up to 97% of wave energy is dissipated when propagated over reefs, and a decrease in wave height of 20-47% depending on the depth of the reef and its extension [4, 5]. With similar effects, submerged breakwaters have been considered an environmental friendly

Dieses Werk ist copyrightgeschützt und darf in keiner Form vervielfältigt werden noch an Dritte weitergegeben werden.
Es gilt nur für den persönlichen Gebrauch.

solution to protect beaches from erosion [6]. In order to design effective projects, it is important to understand how the beach profile would change due to different reef configurations.

The ecosystem service of coastal protection provided by coral reefs is due to wave attenuation, which promotes sediment deposition, reduces erosion and favours beach stability. By altering the hydrodynamic conditions, corals can build auspicious environment for other ecosystems to develop such as seagrass beds and mangroves [7]. In turn, mangroves and seagrasses help to bind marine and terrestrial sediments, reducing coastal erosion and the concentration of suspended sediments, which favours the corals.

The degree of wave attenuation is influenced by the reef's cross-shore bathymetric profile, the barrier's height and width, and surface roughness [4, 8]. One study indicates that the relative rate of wave energy dissipation on a Caribbean fringing reefs under normal hydrodynamics conditions was between 75% and 85% [4]. Without corals on the reef crest the wave energy dissipation function would decrease to 57% and 66%. Implying that, under normal conditions, about 20% of wave energy dissipation can be attributed to coral friction. These results are based on an idealized two-dimensional reef and assumes that wave energy dissipation by coral reefs only occurs when the waves break over the reef [9].

The coastal protection service provided by coral reefs is estimated to be worth US$ 2,000-1,000,000 per km of coastline based on the average costs required to create the same level of coastal protection by artificial means. The wide range of value concerns the level of urbanization, population density and tourist activity. However, within the next 50 years, the net value of benefit loss from reef-associated shoreline protection could be in the order of 10-20% of the current provisioning [10].

Coastal protection service of reefs will continue to be provided if reef growth/accretion keeps pace with rising waters. However, coral reefs are being degraded worldwide mostly because of overfishing, bleaching and biotic threats [10].

The surfing area holds most of the control of beach morphology and coastal hydrodynamics [11]. The offshore boundary of beach controlling processes is the wave's breaker zone. The energy fluctuations imposed by waves, tides and currents manifest in the beach morphology in terms of temporal and spatial variations of shape, width, slope, frequency of secondary morphological features, erosive characteristics and hydrodynamics [12].

Usually, gently sloped dissipative beach profiles may erode under high-energy conditions, this erosion is mainly limited to dune scarping with no expressive change of foreshore slope or beach surfaces level. Also, the vertical and horizontal mobility of such beaches is restricted, and the profile envelope is relatively narrow. The opposite steeply reflective beach is significantly more susceptible to erosion as substantial amounts of incident wave energy can propagate towards the

Dieses Werk ist copyrightgeschützt und darf in keiner Form vervielfältigt werden noch an Dritte weitergegeben werden.
Es gilt nur für den persönlichen Gebrauch.

shoreline. Intermediate beach states, between dissipative and reflective, are characterized by alongshore variable morphology [13, 14].

Beach elevation, morphology and volume changes can be assessed by comparing surveys taken along the same profile line on different periods. The magnitude of seasonal variations in the beach profile can be identified. Spatial variations of beach profiles can also be assessed by comparing data, which have been collected on the same date from a series of adjacent profiles lines along the coast [15].

Regarding the assessment of the beach profile equilibrium, some models are used to estimate sandy beach profiles that represent a dynamic equilibrium condition between wave climate and sediments, making it possible to identify erosion or accretion trends. For example, the Bruun-Dean model was tested for a beach with characteristics similar to Pontal do Cupe Beach and concluded that the model yielded a good fit, though may require some adjustments for a better fit [16].

Therefore, the aim of this paper is to assess the environmental services of coastal protection provided by the Cupe reef, throughout spatial variation of beach profile along the coast, comprising an area in front of the reef lee and a the adjacent segments on both sides of it.

2 Methods

2.1 Study area

In order to evaluate the effect of reef on the dry beach morphology, the Pontal do Cupe Beach was chosen as a case study. This beach is in the northeast of Brazil, at Pernambuco state. It is characterized by the presence of reefs parallel to the coast [17], formed mainly by beachrocks often covered by corals, calcareous algae and molluscs [18]. At low tide, especially during spring tide, the reef top of Pontal do Cupe Beach is emerged, confining masses of water that form natural pools and channels (Fig. 1).

The coastal waters of northeast Brazil favour the formation of beachrocks due to the super saturation of calcium carbonate, warm water temperatures and a mesotidal system that generates a drying and wetting cycle of the foreshore. These factors allow the precipitation of calcium carbonate [19]. The rocks of Pontal do Cupe Beach region were formed about 6,000 years ago in the Holocene period [19].

Petrographic studies of beachrocks in the study area revealed that the mean granulometry of these rocks varies from medium to coarse sand fraction, with the presence of some interlayered granules and pebbles [19]. The carbonate cement, found in the samples, consists of calcite with a high magnesium content that characterizes a depositional environment under strong marine influence, specifically in the intertidal zone. Due to the existence of the reef, the local bathymetry exhibits a complex pattern.

Dieses Werk ist copyrightgeschützt und darf in keiner Form vervielfältigt werden noch an Dritte weitergegeben werden.
Es gilt nur für den persönlichen Gebrauch.

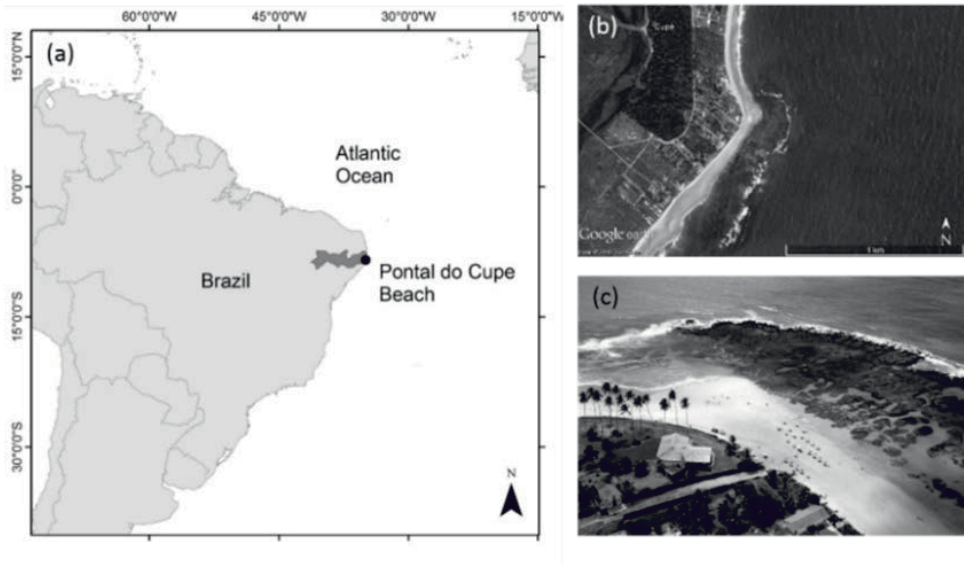

Figure 1: (a) Location of Pontal do Cupe Beach at the Northeast of Brazil; (b) Satellite image of Pontal do Cupe Beach; (c) Aerial view of Pontal do Cupe Beach coastal reefs detail (photo by Silvio Vasconcelos).

The local coastal zone of Pontal do Cupe Beach is composed of Holocene sediments from the Quaternary period (medium and fine sand), which are deposited over the crystalline base of the Borborema Province from the Precambrian age. The sediment is siliceous and carbonate and the grain size are mostly medium sand [17].

The southern part of the Cupe beach, protected by the reef, has predominantly fine sand with the occurrence of medium and very fine sand. The central part has predominantly medium sand with frequent occurrence coarse sand are predominantly found. Northern part has predominantly medium sand; in these last two parts fine sand is present in less significance.

The coastal zone of Pernambuco has a tropical Atlantic climate with annual average temperature of 24 °C and annual average rainfall of 2,000 mm during raining months, with a dry period for the rest of the year.

The wind regime is governed generally by atmospheric pressure distribution; blowing predominantly from the southeast (SE), southeast trade winds. The wave regime responds to the winds. The main wave direction is from ESE with average height of 1.66 m and peak periods of 8.85 s, being this dominate throughout the year. The east southeast incoming waves determine the sediment transport by longshore drift to the North. The beaches close to Cupe generally have a slightly concave morphology and their slope varies basically according to the granulometry of the sediments that constitute them, as well as the characteristics of the incident wave climate [20], both as a result of the shelter degree caused by the reef.

According to tide data provided by the Brazilian Directory of Hydrography and Navigation, the tidal range in the region is mesotidal, with average amplitude of 1.67 m. The mean amplitude during

Dieses Werk ist copyrightgeschützt und darf in keiner Form vervielfältigt werden noch an Dritte weitergegeben werden.
Es gilt nur für den persönlichen Gebrauch.

spring tide is 2.07 m and during neap tides 0.97 m; however it can reach 2.8 m during equinoctial tide. Due to its period of 12.42 hours the local tide is semidiurnal and results mainly from astronomical forcing, while the meteorological tide has no significant effect on the coast [8].

2.2 Field work

The survey of the beach topography was done through beach profiles between the coordinates UTM E 281.100,00 and 281.800,00; and UTM N 9.064.000,00 and 9.066.200,00 Zone 25S - SIRGAS 2000, comprising an area of approximately two kilometres long. In November 2014, during a spring tide, it was measured 34 profiles every 60 m of beach.

All profiles extended from the dune toe, often delimitated by vegetation, until approximately 1 m depth, considering the local Mean Water Level (MWL), covering the backshore region to the outermost portion of the low tide terrace. The data was collected walking using a kinematic GPS, which records at regular intervals of 5 seconds with a GNSS (global navigation satellite system).

The survey was performed with Trimble Kinematic GPS models R3 and R4, using a rover and a base. The base was positioned at the IBGE (Brazilian Institute of Geography and Statistics) geodetic station number 93804. The data were post processed in Trimble Business Center© software. Terrain latitude, longitude and elevation were obtained with 10^{-3} m of precision. The SIRGAS 2000 datum, which is official in Brazil, was used.

2.3 Data analysis

The profile survey data was plotted using SANDS software for calculating the cross-sectional area of each location. To enable consistent comparison, calculation of profile area was confined by the MWL, defined at 0.1412 m [21] (Fig. 2). Data interpolation to assess the beach sediment volume beach was done creating a TIN (Triangular Irregular Networks) that represents the surface morphology at ArcGIS®.

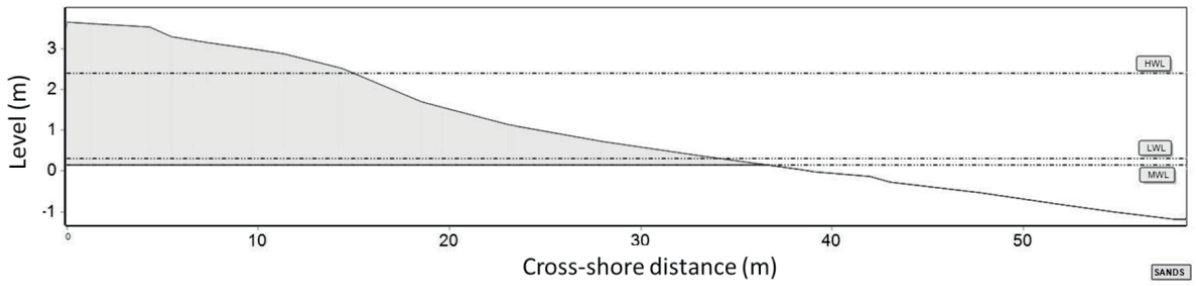

Figure 2: Area of dry profiles above the Mean Water Level.

Data mining was applied to select the most representative morphologies along the beach. This is effective in selecting common features and equilibrium shapes from large data sets. These techniques extract features from the data, providing a more compact and manageable representation of some of the important properties contained in them. To identify the beach

Dieses Werk ist copyrightgeschützt und darf in keiner Form vervielfältigt werden noch an Dritte weitergegeben werden.
Es gilt nur für den persönlichen Gebrauch.

profile clusters, a multivariate data analysis was applied: Principal Component Analysis & Classification (PCA), using STATISTICA®.

3 Results and Discussion

3.1 Profiles clustering

Through PCA it was possible to identify five mean clusters at Pontal do Cupe Beach (Fig. 3). These clusters were defined based on the top three principal components (PCs), which explain 68% of the variability between the profiles (Table 1). The first factor explains mostly the variation of the first 20 m and between chainage 70-80 m. The second factor, explains the profiles variation between 15-25 m and 60-70 m. The third factor explains mainly the variation between the chainage 25-45 m. These cover most of the profiles length (around 90 m).

Table 1: Five first principal components and the percent of variation explained.

PCs	Eigenvalue	% Total	Cumulative
1	7.66	33.31	33.31
2	4.16	18.08	51.39
3	3.86	16.78	68.17
4	2.72	11.83	80.00
5	1.33	5.79	85.79

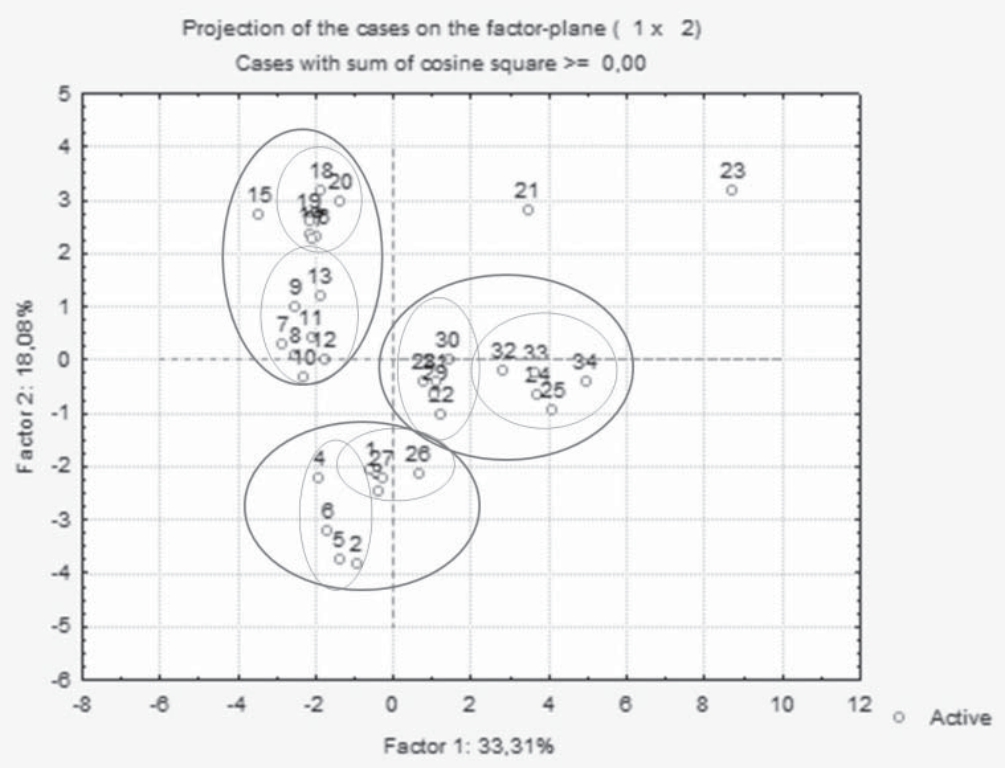

Figure 3: Example of a case plot factor between the first and second eigenvalues.

Dieses Werk ist copyrightgeschützt und darf in keiner Form vervielfältigt werden noch an Dritte weitergegeben werden.
Es gilt nur für den persönlichen Gebrauch.

3.2 Profiles description

In this section, a description on the morphological features of the five different profile types is presented (Fig. 4).

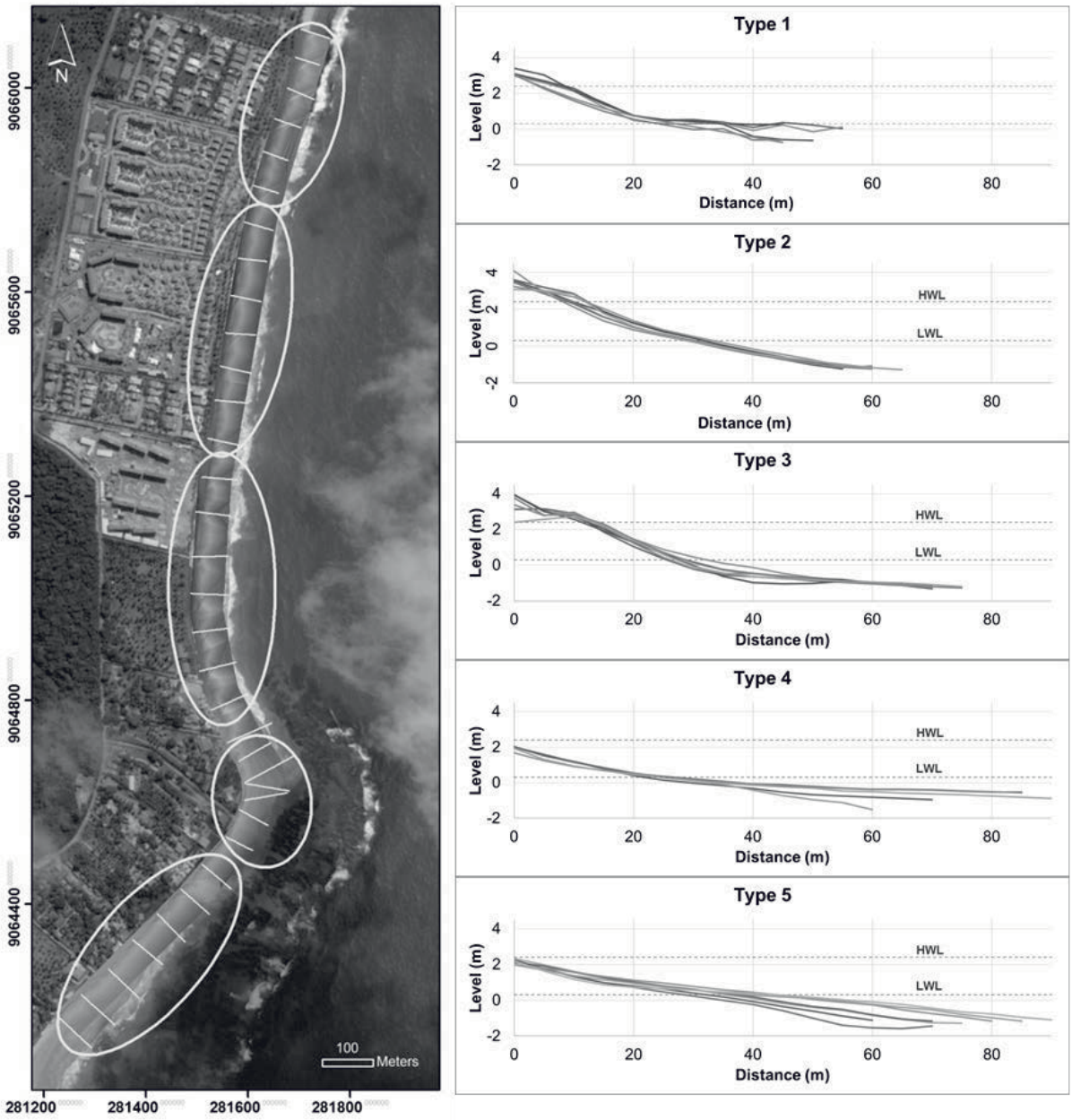

Figure 4: Left: Position of profiles clusters along the coast, the yellow lines mark the position of measured profiles; Right: Graphs of the five profiles types identifies at PCA.

Type 1: Beach profiles of type 1 are relatively free from the reef influence and are exposed to the wave climate. Its behaviour is controlled primarily by the incident waves and secondly by the tide. The profiles present two key features, an upper berm and a low tide terrace. Some of these profiles may be influenced by another reef formation northward. At this area, the wave

Dieses Werk ist copyrightgeschützt und darf in keiner Form vervielfältigt werden noch an Dritte weitergegeben werden.
Es gilt nur für den persönlichen Gebrauch.

approaches the coast with a small degree that generates a northward longshore current. The dry profile has a mean area of 48 m^2.

Type 2: Beach profiles of type 2 are relatively free from the reef influence and its behaviour is mainly controlled by waves. In the beach sector of type 2 profiles, rip currents, cusps and mega-cusps can be present [20] (Fig. 4 left). Although the morphology is controlled by waves, it is possible to observe the tide's influence in the profile morphology. The mean dry beach profile area is 54 m^2.

Type 3: Beach profiles of type 3 are under reef influence due to wave diffraction and the morphology is modified by the tide. The profiles show a steep and narrow high tide terrace and a gentle and long intertidal profile, similar to the morphology observed in other beaches at Pernambuco cost [22]. The break in the profile slope at the beach face indicates a tide effect on the profile [11]. The mean dry beach profile area is 50 m^2.

Type 4: These beach profiles are under reef influence due to wave energy dissipation. Their morphology is mainly controlled by tide as observed in other nearby beaches where reefs occur at the shore face [22]. The profiles have a low gradient beach face and a long and shallow low tide terrace, with no three-dimensional features occurrence. It is evident in Figure 4 that this is the only sector where cusps are absent. However, during winter, cusps can form on the high tide terrace [22]. These beaches are characterized by a dissipative profile followed by a low tide terrace [11, 20]. The mean dry beach profile area is 22 m^2.

Type 5: Similar to type 4, beach profiles of type 5 are under reef influence and their morphology is primarily controlled by tide and secondly by waves dissipation over the reef. The beach face is wider and the low tide terrace is less marked than at adjacent profiles of type 4. The foreshore morphology of these profiles could not be evaluated due to constructions on shore. The mean dry profile area is 37 m^2.

The propagation of waves to the coast in areas with reefs is modulated by the interaction with reefs surface and tides [23]. In Pontal do Cupe Beach, where the upper part of the reefs emerges during low tide, the amount of wave energy in their lee is highly reduced. At high tide the reef crest depth increases and the wave dissipation diminishes, allowing the transmission of waves to the shore [24].

Following the conceptual model of beach morphodynamic stages influenced by tides [11], Pontal do Cupe Beach could be classified as reflective during high tide and low tide terrace at low tide, except the profiles behind the reef, which could be classified as dissipative during high tide and low tide terrace at low tide. The wave's process over the reef explains the formation of tombolos and saliences on the lee side of the reef due to a gradient of longshore sediment transport. The morphology of the profiles indicates that the foreshore sediment volume was higher at sectors dominated by waves than in those modified by tide.

Dieses Werk ist copyrightgeschützt und darf in keiner Form vervielfältigt werden noch an Dritte weitergegeben werden.
Es gilt nur für den persönlichen Gebrauch.

4 Conclusions

Reefs can have a significant effect on nearshore wave climate and the adjacent beach morphology. As a result, beaches protected by reefs present less three-dimensional features than the ones exposed to waves; the latter will also have a wider foreshore. Knowledge about the morphology of beach profiles in the lee side of reefs may help improving conceptual beach models that predict change as a function of wave, tide, and sediment parameters. Better understanding the effects of reefs can be useful to inform policymaking and beach management related to tourism and the coastal protection ecosystem service. Further studies on temporal evolution of beach profiles could provide better understanding on reef influence over the coastal morphology.

5 Acknowledgement

This publication is one of the results of the Latin American Regional Network global collaborative project “EXCEED-SWINDON project — Excellence Center for Development Cooperation – Sustainable Water Management in Developing Countries”. The beach surveys are part of the project “Rip currents dynamics” funded by CNPq (process 484180/2012-6). The author, K.A. Martins, would also like to thank CNPq and CAPES for granting her Doctorate scholarship.

6 References

1. Albert, J.A., Olds, A.D., Albert, S., Cruz-Trinidad, A., Schwarz, A.M.: Reaping the reef: Provisioning services from coral reefs in Solomon Islands. Marine Policy 62, 244-251 (2015)
2. Moberg, F., Folke, C.: Ecological goods and services of coral reef ecosystems. Ecological Economics 29, 215-233 (1999)
3. Cesar, H., Burke, L., Pet-soede, L.: The Economics of Worldwide Coral Reef Degradation. Cesar Environmental Economics Consulting, Arnhem, and WWF-Netherlands 14, 23-23 (2003)
4. Ferrario, F., Beck, M.W., Storlazzi, C.D., Micheli, F., Shepard, C.C., Airoldi, L.: The effectiveness of coral reefs for coastal hazard risk reduction and adaptation. Nature communications 5, 3794-3794 (2014)
5. Lugo-Fernández, A., Roberts, H.H., Wiseman, W.J.: Tide effects on wave attenuation and wave set-up on a Caribbean coral reef. Estuarine Coastal and Shelf Science 47, 385-393 (1998)
6. Silva, R., Mendoza, E., Mariño-Tapia, I., Martínez, M.L., Escalante, E.: An artificial reef improves coastal protection and provides a base for coral recovery. Journal of Coastal Research 75, 467-471 (2016)
7. Barbier, E.B., Hacker, S.D., Kennedy, C., Kock, E.W., Stier, A.C., Silliman, B.R.: The value of estuarine and coastal ecosystem services. Ecological Monographs 81, 169-193 (2011)
8. Costa, M.B.S.F., Araújo, M., Araújo, T.C.M., Siegle, E.: Influence of reef geometry on wave attenuation on a Brazilian coral reef. Geomorphology 253, 318-327 (2016)

Dieses Werk ist copyrightgeschützt und darf in keiner Form vervielfältigt werden noch an Dritte weitergegeben werden.
Es gilt nur für den persönlichen Gebrauch.

9. Van Zanten, B.T., Van Beukering, P.J.H., Wagtendonk, A.J.: Coastal protection by coral reefs: A framework for spatial assessment and economic valuation. Ocean and Coastal Management 96, 94-103 (2014)

10. Spalding, M., Kramer, P., Green, E., Greenhalgh, S., Nobles, H., Kool, J.: Economic implications of coral reef degradation. In: Burke, L., Maidens, J. (eds.) Reefs at Risk in the Caribbean, pp. 52-59. World Resources Institute, Washington, DC (2004)

11. Masselink, G., Short, A.D.: The effect of tide range on beach morphodynamics and morphology: a conceptual beach model. Journal of Coastal Research 9, 785-800 (1993)

12. Calliari, L.J., Muehc, D., Hoefel, F.G., Toldo Jr, E.: Morfodinâmica praial: uma breve revisão. Brazilian Journal of Oceanography 51, 63-78 (2003)

13. Wright, L.D.: Beach cut in relation to surf zone morphodynamics. 17th International Conference on Coastal Engineering, vol. 61, pp. 978-996. ASCE, Sydney, Australia (1980)

14. Wright, L.D., Short, A.D.: Morphodynamic variability of surf zones and beaches: A synthesis. Marine Geology 56, 93-118 (1984)

15. Cooper, N.J., Leggett, D.J., Lowe, J.P.: Beach-profile measurement, theory and analysis: Practical guidance and applied case studies. Journal of the Chartered Institution of Water and Environmental Management 14, 79-88 (2000)

16. Rollnic, M., Medeiros, C.: Equilibrium Beach Profile in the Presence of Beachrocks. Journal of Coastal Research 75, 452-456 (2016)

17. Dominguez, J.M.L., Bittencourt, A., Leão, Z., Azevedo, A.: Geologia Do Quaternário Costeiro Do Estado De Pernambuco. Revista Brasileira de Geociências 20, 208-215 (1990)

18. Ferreira, B.P., Maida, M.: Monitoramento dos Recifes de Coral do Brasil: situação e perspectivas. Ministério do Meio Ambiente, Secretaria de Biodiversidade e Florestas, Brasília (2006)

19. Ferreira Júnior, A.V., Araújo, T.C.M., Vieira, M.M., Neumann, V.H., Gregório, M.d.N.: Petrologia dos arenitos de praia (Beachrocks) na costa central de Pernambuco. Geociencias 30, 545-559 (2011)

20. Mallmann, D., Pereira, P., Santos, F., Facanha, P.: Classificação morfodinâmica das praias arenosas de Ipojuca (Pernambuco, Brasil) através da análise semântica de imagens de satélite pancromáticas. Pesquisas em Geociencias 41, 169-190 (2014)

21. Mesquita, A.R.D., Franco, A.d.S., Harari, J.: On mean sea-level along the Brazilian coast. Geophysical Journal of the Royal Astronomical Society 87, 67-77 (1986)

22. Pereira, P.d.S., de Araujo, T.C., Vaz Manso, V.d.A.: Tropical Sandy Beaches of Pernambuco State. In: Short, A.D., Klein, A. (eds.) Brazilian Beach Systems, vol. 10, pp. 251-279. Springer, Florida (2016)

Dieses Werk ist copyrightgeschützt und darf in keiner Form vervielfältigt werden noch an Dritte weitergegeben werden.
Es gilt nur für den persönlichen Gebrauch.

23. Beetham, E.P., Kench, P.S.: Wave energy gradients and shoreline change on Vabbinfaru platform, Maldives. Geomorphology 209, 98-110 (2014)

24. Martins, K.A., Pereira, P.d.S., Silva-Casarín, R., Nogueira Neto, A.V.: The Influence of Climate Change on Coastal Erosion Vulnerability in Northeast Brazil. Coastal Engineering Journal 59, 25-25 (2017)

Dieses Werk ist copyrightgeschützt und darf in keiner Form vervielfältigt werden noch an Dritte weitergegeben werden.
Es gilt nur für den persönlichen Gebrauch.

CHANGES IN COASTAL ECOSYSTEMS' ROLE AGAINST HURRICANE AND STORM SURGE AT ANA MARIA GULF, CUBA

Yandy Rodríguez Cueto[1,2], Rodolfo Silva[3]

[1]Postgraduate in Civil Engineering, Faculty of Engineering, National Autonomous University of Mexico, Ave. Universidad 3000, Colonia UNAM-CU, Delegación Coyoacán, Ciudad de México, yandyro84@gmail.com

[2]Research Center for Coastal Ecosystems, Avenida Los Almácigos, Cayo Coco, Morón, Ciego de Ávila, CP 64900

[3]Engineering Institute, National Autonomous University of Mexico, Ave. Universidad 3000, Colonia UNAM-CU, Delegación Coyoacán, Ciudad de México

Keywords: change of covers, coastal exposure, ecosystems' role, human activities, natural habitat's ranking

Abstract

The Terrain Categorization (TERCAT) tool from ENVI identified change of covers from 1975 to 2014. The covers include Sand, Mud, Rocks, Seagrass, Dry Crops, Green Crops, Inland Water Bodies, Mangrove, Natural Vegetation, and No Vegetation. Natural habitat's ranking and drag coefficient assigned to each cover represent a measure of coastal exposure. Crops and No Vegetation express if human activities have induced coastal exposure changes. Results show an increment of Natural Vegetation and decrement of covers related to crops and no vegetation. The study area has a highly coastal exposure due to the natural habitat's ranking 5, which is the most representative one. Changes in covers do not generate great changes in coastal exposure. The reduction of covers identified with human activities and the increase of Natural Vegetation prove that human activities do not affect the coastal exposure. The cover profiles near to Palo Alto harbor and Júcaro town have less mangrove width than those long away, making it more exposed to coastal flooding. It is possible to identify two different zones taking into account changes of both natural habitats ranking for coastal exposure and drag coefficient from 1975 to 2014.

1 Introduction

Coastal and marine ecosystems play an important role in coastal protection against hurricane and storm surge, not only by reducing coastal flood penetration, but also providing ecosystems good and services that help people to resist and to recover from storm surge and hurricane impacts. Coastal habitats reduce by approximately 50% the proportion of people and property along the US coastline that are most exposed to storms and sea-level rise [1]. Coastal ecosystems provide coastal protection especially in tropical and sub-tropical regions and are a vital component of natural environment of Earth [2]. The surge amplitude decreases at a rate of 40-50 cm/km across

Dieses Werk ist copyrightgeschützt und darf in keiner Form vervielfältigt werden noch an Dritte weitergegeben werden.
Es gilt nur für den persönlichen Gebrauch.

the mangrove forest and at a rate of 20 cm/km across the areas with a mixture of mangrove islands with open water.

Each ecosystem has a drag coefficient value that reduces the water movement into land. Additionally, the combination of several ecosystems in front of coastal towns and villages could be a better solution to protect them against flooding and storm surge. Two aspects are important to assess coastal ecosystem's role in coastal protection: presence and type of the ecosystem, and fragmentation of them.

The rate of reduction of surge through mangrove appears to range between 5 and 15 cm/km (observed reduction rates [7]) up to 50 cm/km (well-validated numerical models [3])

Dissipation is relatively great in canopies of increased density, height and width. Vegetation Dissipation Potential varies between 5–40% when canopies width increase from 0.5 to 1.5 km. Width seems slightly more important than density and height [4]. [1] indicates where conservation and restoration of reefs and vegetation have the greatest potential to protect coastal communities against flood and sea-level rise.

The capacity of vegetation to reduce the water depth is minimal for the narrow vegetation belt (100 m). Percentage of maximum reduction of storm surge height ranges between 17.3% and 21.7% behind the vegetation on the 1:500 ground slope for both 200 m and 300 m vegetation belt, respectively. In addition, it is clear that widening the vegetation belt definitely increases the reduction of maximum water depth behind the vegetation [5].

Both [6] and [3] consider the presence of channels and pools as likely to decrease the ability of mangrove to reduce peak water levels, because the water is able to pass more easily along the rivers and penetrate further inland [7]. For this reason, the fragmentation of ecosystems is a variable to take into account.

The objectives of this paper are to determine, how the coastal ecosystems' variations have caused changes in coastal exposure to hurricanes and storm surge, as well as to identify, which zones have experienced the highest variations in the period of time 1975 to 2014. Additionally, how coastal ecosystems' role against hurricanes and storm surge has changed in this period of time.

2 Materials and Methods

2,621 km^2 of Ana Maria gulf (27.9%) represent the study area, including land zone until 10 m above mean sea level. This area includes one town, two harbors, and one beach. Total area and the amount of patches allow analyzing changes over time per each cover (Figure 1).

Landsat images from 1975 to 2014 with 30 m spatial resolution pixel were classified. Terrain Categorization (TERCAT) tool from ENVI software allowed to develop classification process. The Terrain Categorization (TERCAT) tool creates classes clumping pixels with similar spectral properties. These

Dieses Werk ist copyrightgeschützt und darf in keiner Form vervielfältigt werden noch an Dritte weitergegeben werden.
Es gilt nur für den persönlichen Gebrauch.

classes may be either user-defined or automatically generated by the classification algorithm. The TERCAT tool provides all of the standard ENVI classification algorithms.

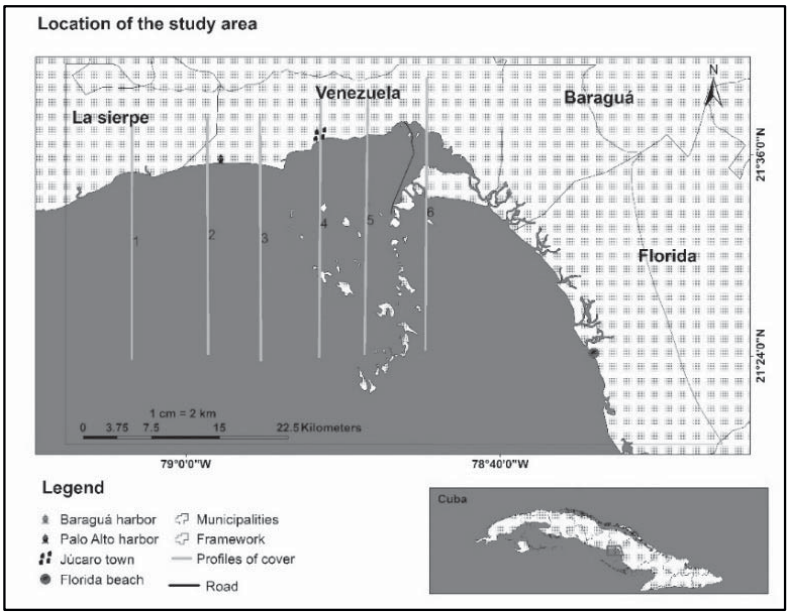

Figure 1: Location of the study area and profiles of cover analyzed

Drag coefficient and natural habitats' ranking represent a measure of coastal exposure. Drag coefficient for several ecosystems from [3] and [4] were adjusted to our categories of land cover. Natural habitats' ranking for coastal exposure, modified from [8], were assigned to covers identified during classification process. The results of both natural habitats ranking and drag coefficient adjustment are shows in Table 1.

Table 1: Natural habitats' ranking for coastal exposure and drag coefficient for each cover identified (adjusted from [3, 8])

Cover	Ranking	Drag coefficient
Sand	5	0.040
Green Crops	2	0.037
Natural Vegetation	1	0.100
Dry Crops	3	0.034
Mud	5	0.020
Inland Water Bodies	2	0.000
Mangrove	1	0.140
No Vegetation	5	0.090
Seagrass	4	0.125
Rocks	1	0.090

Dieses Werk ist copyrightgeschützt und darf in keiner Form vervielfältigt werden noch an Dritte weitergegeben werden.
Es gilt nur für den persönlichen Gebrauch.

Natural vegetation was considered in ranking 1 corresponding with coastal forest of [8]. Sand was included in ranking 5 because is mostly related to sea bottom. About drag coefficient, No vegetation and Rocky have 0.090 like Barren land while Mangrove have 0.140 corresponding to Woody wetland and according to Liu *et al*. (2013) [9]. Unconsolidated shore considered Sand and Mud, although Muddy is lightly inferior. Finally, Natural vegetation was considered like Mixed forest [3]. The amount patches of covers identified characterizes fragmentation of the area.

3 Results

3.1 Land cover classification

Classification dropped 10 types of covers including Sand, Mud, Seagrass, Rocks, Natural Vegetation, Mangrove, Green Crops, Dry Crops, Inland Water Bodies, and No Vegetation.

Classifications show that the most important cover in the area is Mud, with the highest values of area to 1975, 1986, 1997, and 2014. In 2006, the most representative cover was Seagrass. The most fragmented cover varied among years. If Seagrass was the most fragmented cover in 1975, in 2014 No Vegetation occupied this site.

Table 2: Area of coversidentified during classification process for each year (km^2)

Cover	1975		1986		1997		2006		2014	
	Area	%	Area	%	Area	%	Area	%	Area	%
Sand	434	16.5	197	7.51	35.0	1.34	106	4.06	18.5	0.71
Green Crops	132	5.02	122	4.66	343	13.1	157	5.98	108	4.11
Natural Vegetation	88.9	3.39	353	13.5	401	15.3	524	20.0	530	20.2
Dry Crops	263	10.0	21.5	0.82	20.9	0.80	4.22	0.16	0.38	0.01
Mud	1,044	39.8	1,175	44.8	1,221	46.6	624	23.8	1,216	46.4
Inland Water Bodies	40.8	1.56	69.7	2.66	12.4	0.47	114	4.34	77.3	2.95
Mangrove	167	6.36	308	11.7	113	4.32	80.7	3.08	124	4.73
No Vegetation	262	9.99	77.9	2.97	61.8	2.36	73.2	2.79	113	4.32
Seagrass	179	6.81	295	11.2	393	15.0	933	35.6	399	15.2
Rocks	12.1	0.46	1.88	0.07	19.0	0.73	4.88	0.19	34.8	1.33

The total amount of patches from 1975 to 2014 has decreased. The highest value of patches corresponds to Green Crops cover in 1997 although Seagrass, in 1975, and No Vegetation, in 1997, show a big value too. The minimum value corresponds to Dry Crops in 2014 with only one entity. Rocks present the lowest values between 1975 and 2006, but it is related with its lowest area too. The amount of patches in total area was reduced from 1975 to 2014, with maximum value in 1997.

Dieses Werk ist copyrightgeschützt und darf in keiner Form vervielfältigt werden noch an Dritte weitergegeben werden.
Es gilt nur für den persönlichen Gebrauch.

Table 3: Amount of patches computed per each cover identified

Number	Cover	1975	1986	1997	2006	2014
1	Sand	19	24	25	11	8
2	Green Crops	43	71	110	62	51
3	Natural Vegetation	58	39	24	30	16
4	Dry Crops	67	19	27	6	1
5	Mud	73	73	53	68	32
6	Inland Water Bodies	26	66	29	34	49
7	Mangrove	41	37	56	55	44
8	No Vegetation	53	67	102	53	63
9	Seagrass	102	41	61	44	40
10	Rocks	5	4	15	3	20
	Total	487	441	502	366	324

3.2 Natural habitats' ranking for coastal exposure

Natural habitats' rankings for coastal exposure (from [8]) were assigned to each cover to compute the temporal and spatial variation of costal exposure in relation to cover changes.

The Figures 2 and 3 show the percentage of the area corresponding to each natural habitat's ranking as well as the amount of patches per each ranking. Clearly, ranking 5 is the most representative ranking for coastal exposure in the area and has the biggest amount of patches assigned for all years analyzed.

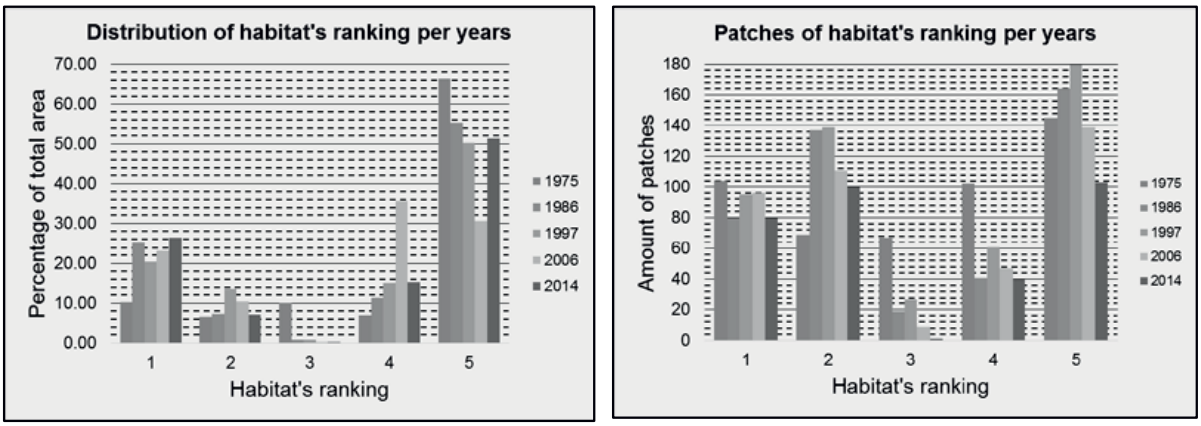

Figure 2: Percentage and patches of habitats' ranking for coastal exposure in the study area from 1975 to 2014

Another important element is the fact that the area has a little amount of patches and extension in middle ranking 3, and the opposite rankings 1 and 5 group the biggest amount of area and patches. Additionally, ranking 2 groups more patches than ranking 1.

Dieses Werk ist copyrightgeschützt und darf in keiner Form vervielfältigt werden noch an Dritte weitergegeben werden.
Es gilt nur für den persönlichen Gebrauch.

The amount of patches in ranking 5 as well as the total extension of this ranking decreases from 1975 to 2014. The amount of patches in ranking 1 decreases from 1975 to 2014, although the extension of this ranking increases in this period of time. For ranking 3, both patches and extension decrease from 1975 to 2014.

The covers identified change between years as part of the spatial and temporal evolution of the study area. Those changes were identified in terms of natural habitats' ranking and drag coefficient to compute the change of coastal exposure due to the changes of cover identified.

Changes of habitats' ranking values between years reveal that the biggest amount of patches and extension are grouping in 0 (no changing), -1 and 1 (Figure 3). From 1975 to 1986, there is more extension, and patches in negative habitats ranking change values more than in positive ones. For the rest of couple of years, there is a similar behavior in positive and negative habitats' ranking changes values. In this case, the changes in two ranking values are the smallest for both extension and patches.

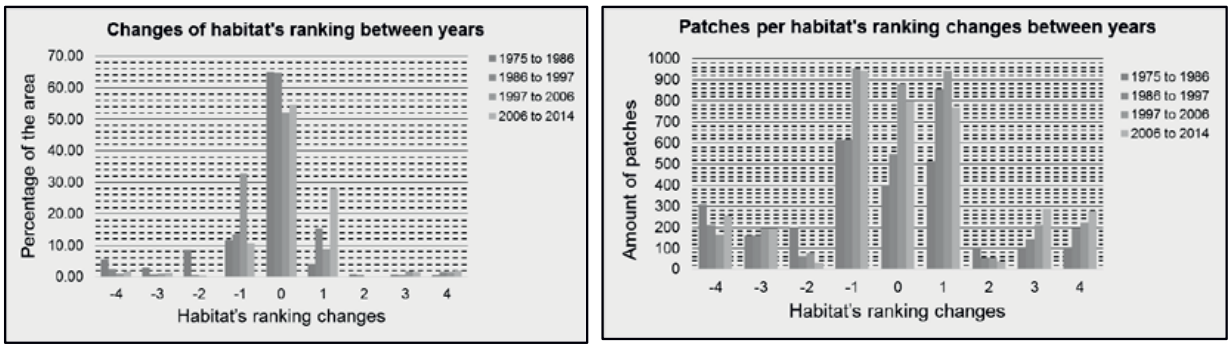

Figure 3: Percentage and patches per habitats' ranking changes values in the study area from 1975 to 2014

From the spatial perspective, the changes of natural habitat's ranking for coastal exposure shows two different areas in emerged land. As one can see in the map (Figure 4), the eastern part of the area has a different behavior from the northern part. From 1975 to 1986, there is not a big difference in changes of ranking, showed by the same colors in both parts. From 1986 to 1997, northern part has a predominant orange color (change of ranking equal to 1), while eastern part has a presence of all colors of the classification. From 1997 to 2006, orange to red colors (change of ranking from 1 to 4) are present in eastern part, while light green color (change of ranking equal to -1) is predominant in northern part. From 2006 to 2014, positive changes associated to orange and red colors (from 1 to 4 in changes of ranking) are predominant in northern part, while positive and negative changes (associated to red and green colors, respectively) are present in eastern part.

Dieses Werk ist copyrightgeschützt und darf in keiner Form vervielfältigt werden noch an Dritte weitergegeben werden.
Es gilt nur für den persönlichen Gebrauch.

In sea bottom, changes are very different from one period to another. Areas with positive changes in one period show negative changes in the next one. The biggest changes take place between 1997-2006 and 2006-2014, where areas with negatives changes in first period have positive changes in second one.

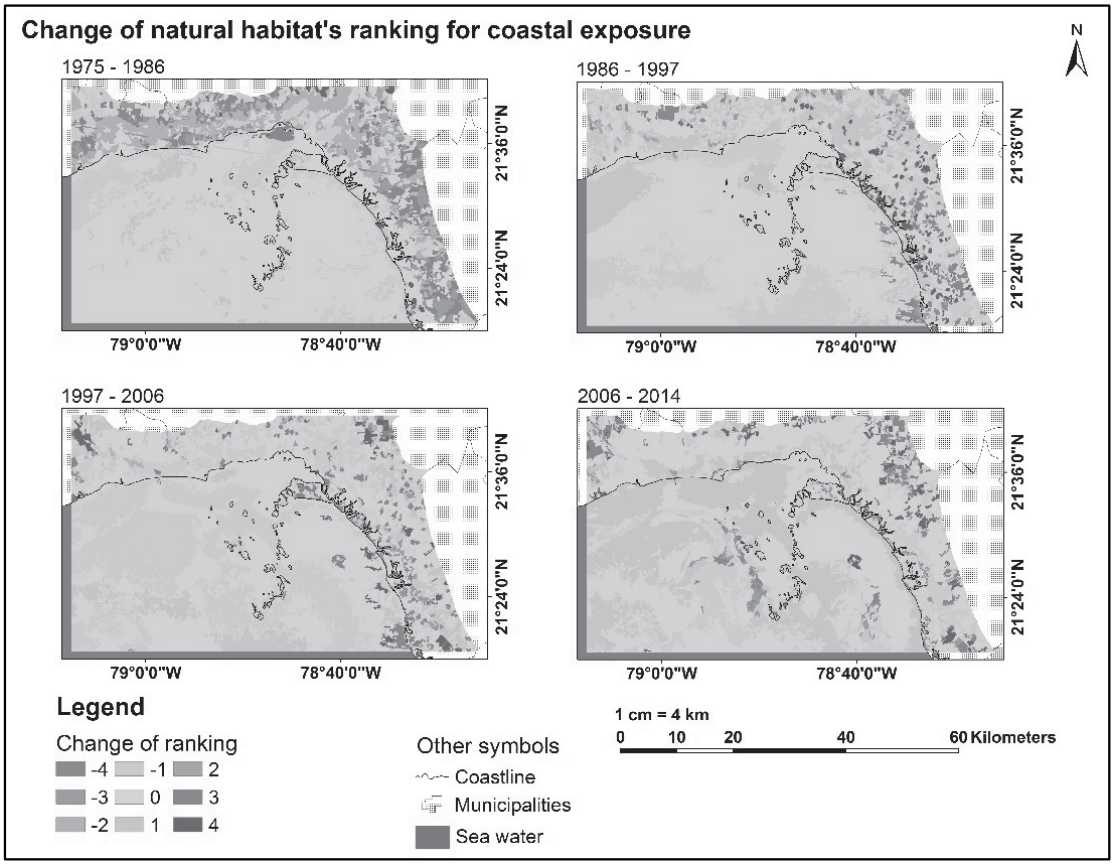

Figure 4: Spatial representation of changes of natural habitats' ranking for coastal exposure from 1975 to 2014

3.3 Drag coefficient.

The analysis of drag coefficient reveals that the most predominant drag coefficient value is 0.020, associated to Mud, while in emergent land the most important coefficient is 0.034, associated to Natural Vegetation (Figure 5).

The area associated to drag coefficient values of 0.034, 0.037, 0.040, and 0.140 decreases from 1975 to 2014, while the area associated to values of 0.000, 0.030, 0.100 and 0.125 increases in this period. The most important increment in drag coefficient values is associated to 0.100, which increases from 3.39% to 20.2% in the period 1975 to 2014. The most important decrement is associated to 0.040 that decreases from 16.5% to 0.44% from 1975 to 2014.

Dieses Werk ist copyrightgeschützt und darf in keiner Form vervielfältigt werden noch an Dritte weitergegeben werden.
Es gilt nur für den persönlichen Gebrauch.

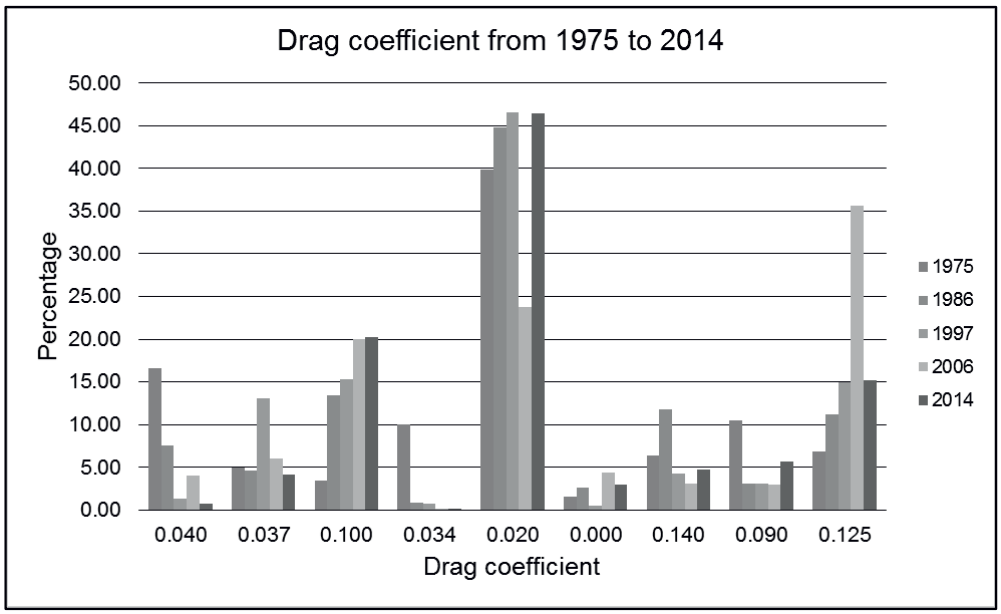

Figure 5: Percentages associated to each drag coefficient from 1975 to 2014

About drag coefficient changes, the biggest part of the area remains without changes from 1975 to 2014. Except from 1986 to 1997, where negative changes are bigger than positive ones, the positive changes occupy a bigger area than negative ones in the rest of the couple of years analyzed (Figure 6).

From the spatial point of view, one can identify two different areas in the map. One represented by eastern part of the area, and another represented by northern part. Different predominant changes take place in those areas, as one can see in the maps.

From 1975 to 1986, orange and light green colors (negative and small positive changes, respectively) are predominant in eastern part, while intense green colors (big positive changes) are predominant in northern part. From 1986 to 1997, there are not predominant colors in eastern part by the presence of all kind of colors, while orange and red colors (medium and big negative changes) are predominant in northern part. Different changes take place from 1997 to 2006, while green colors (positive changes) are predominant in northern part, orange and red colors (negative changes) are predominant in eastern part. From 2006 to 2014, there are not big changes in the area, but there is a big difference between eastern and northern part of the area. While green color (positive changes) is present in eastern area, orange and red colors (negative changes) are present in northern area.

Dieses Werk ist copyrightgeschützt und darf in keiner Form vervielfältigt werden noch an Dritte weitergegeben werden.
Es gilt nur für den persönlichen Gebrauch.

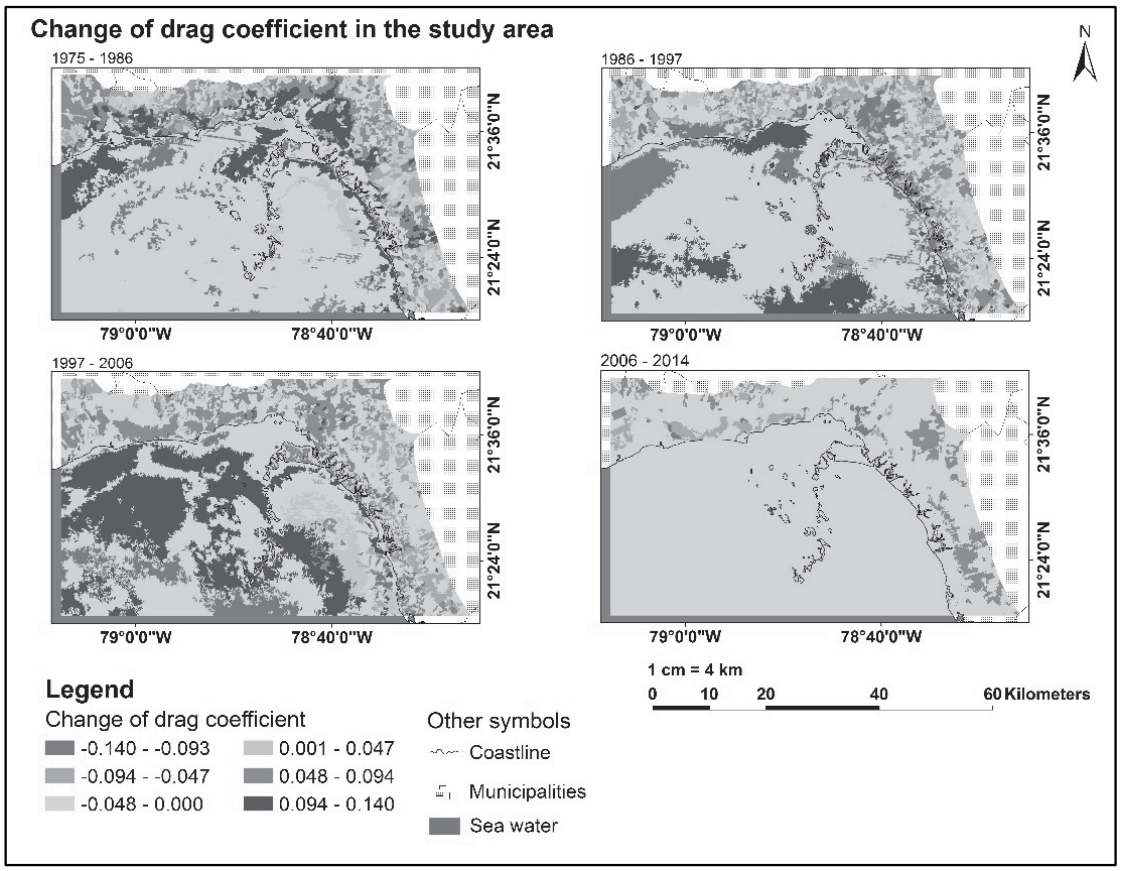

Figure 6: Spatial representation of drag coefficient changes from 1975 to 2014

3.4 Sea-Land profiles of covers.

Six sea-land profiles explain the behavior of covers identified and the evolution of their width from 1975 to 2014 (Figure 7).

The most important element in those profiles is the change of both cover width and presence from 1975 to 2014, which is represented by color width in each graph above. Each color corresponds to one cover, and each graph corresponds to one profile. Seawater is located in top of each profile, and coastline is around five kilometers from zero.

The predominant element in sea bottom is Mud, although Seagrass is present in all profiles, and in some cases occupy a bigger distance than Mud. In emerged land, Natural Vegetation and crops are the most important covers.

In profile 1, Mangrove width varies from 0.76 km in 1975 to 2.49 km in 1986, but from 1997 to 2014 the width is almost constant. Natural Vegetation varies from 2.59 km in 1986 to 3.59 km in 2006, without presence in 1975 and 1997, and from 2006 to 2014 it is almost constant. The presence of Mud experienced a big reduction in 2006, but the rest of the years it was the most predominant sea bottom cover. Dry Crops reduced his width and presence from 1975 to 2014.

Dieses Werk ist copyrightgeschützt und darf in keiner Form vervielfältigt werden noch an Dritte weitergegeben werden.
Es gilt nur für den persönlichen Gebrauch.

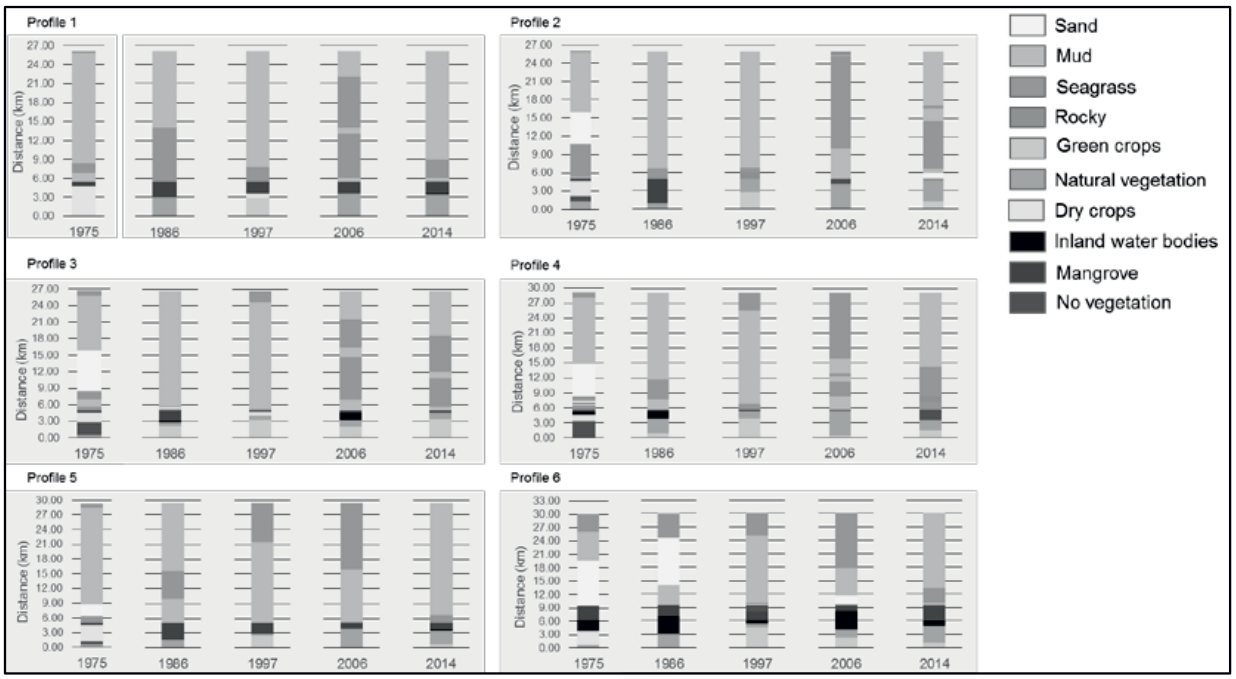

Figure 7: Evolution of covers per each profile employed from 1975 to 2014

In profile 2, Sand appears in 1975 but is absent from 1986 to 2006, and appears again in 2014 with a very narrow band. Mud is predominant except in 2006, when Seagrass occupies the biggest extension in sea bottom. Mangrove is absent in 1997 and 2006, but occupies around 4 km in 1986. In 1975 and 2014, Mangrove is very narrow. In 1975 and 2006, No Vegetation is present with about 1 km of width. Dry Crops are present in 1975 but disappear from 1986 to 2014, and Natural Vegetation and Green Crops occupy his place.

In profile 3, the relevant aspect is the alternation of Mud and Seagrass as predominant sea bottom, and disappearance of Sand from 1986 to 2014. Mangrove is almost absent, except in 1986, where it occupies around 2 km width. Inland Water Bodies appear in 2006 with about 1 km width, and crops are predominant in emerged land covers. No Vegetation disappears from 1986 to 2014, with about 2 km in 1975.

Profile 4 passes at western part of Júcaro town. Changes in covers reveal the presence of No Vegetation in 1975 and 2014, with Inland Water Bodies only in 1986. Mangrove is almost absent, except in 1975 with about 1 km width, and 2006 with less than 1 km width. Natural Vegetation and crops are predominant in land covers, and Mud is predominant in sea bottom, except in 2006, when Seagrass is widest. It is the unique profile with presence of Rocks about 1km width.

Profile 5 experienced a reduction of Mangrove width from 1986 to 2014 and disappearance of Sand in the same period. Mud is predominant in sea bottom, and Natural Vegetation appears as predominant from 2006 to 2014. No Vegetation and Dry Crops are present only in 1975.

Dieses Werk ist copyrightgeschützt und darf in keiner Form vervielfältigt werden noch an Dritte weitergegeben werden.
Es gilt nur für den persönlichen Gebrauch.

Inland Water Bodies are present in profile 6 from 1975 to 2014, with reduction of Mangrove from 1975 to 2006 and an expansion of this in 2014. Alternation of sea bottom cover is peculiar in this profile, with Sand as predominant cover in 1975 and 1985, Mud as predominant in 1997 and 2014, and Seagrass as predominant in 2006.

4 Discussion

A predominant cover of Mud, the reduction of Mangrove extension and a predominant natural habitat ranking for coastal exposure in Figure 4 and 5 show a highly exposure area. However, reduction of total patches from 1975 to 2014 reveals a less fragmented area that supposes a better protection against coastal flooding. Reduction of patches in natural habitat ranking 5 as well as the area of this ranking decreases the fragmentation and coastal exposure. This, added to the fact that patches of ranking 1 decrease and extension of these ranking increases, produces a reduction of coastal exposure to coastal flooding.

The reduction of mangrove extension and the increment of amount of patches produce a slightly reduction of Mangrove protection in the study area between 1975 and 2014. Additionally, the increment of inland water bodies also increases the coastal exposure to coastal flooding penetration.

In contrast, the increment of Natural Vegetation cover reveals a reduction of human impact on the area and low impact of human activities in coastal exposure. The reduction in fragmentation supports this approach, because cover fragmentation is typical in agricultural and residential activities. Additionally, reduction of Green Crops and Dry Crops reveals an abandon of agricultural activities and expansion of Natural vegetation.

Changes in natural habitat's ranking for coastal exposure between -1 and 1 and predominant no changes reveal that changes in covers do not generate great changes in coastal exposure. No change in drag coefficient around 50% and positive changes bigger than negative ones support this fact. Only between 1986 and 1997, the negative changes in drag coefficient were bigger than positive changes, corresponding to the fact that positive changes in natural habitat's ranking were bigger too. This shows the fact that human activities in this period generated an increment of coastal exposure.

From the spatial point of view, one can identify two areas in emerged land: eastern and northern. Eastern part is more exposed than the northern one. This corresponds to the fact that changes on natural habitat's ranking for coastal exposure in eastern part are bigger than northern one, and positive changes are predominant in eastern part of the area, while negative changes are predominant in northern part. This demonstrates a different use and intervention of human activities in eastern and northern parts of the study area.

Dieses Werk ist copyrightgeschützt und darf in keiner Form vervielfältigt werden noch an Dritte weitergegeben werden.
Es gilt nur für den persönlichen Gebrauch.

Another spatial differentiation deals with different profiles of covers analyzed. Profiles near to Palo Alto harbor and Júcaro town show reduction and absence of mangrove, generating major coastal exposure than those profiles far away from those places. This means little protection of mangrove to town and harbor.

Presence of mangrove around 2 km width in profiles 1, 5 and 6 supposes a continuous and better protection in these zones from 1975 to 2014. Additionally, a reduction around 50% of storm surge height is expected due to mangrove width about 2 km in profiles 1, 5 and 6 according to [3].

Badola and Hussain (2005) [10] found that in the mangrove-protected village, damage to houses and other adverse effects were lowest, while crop yields and other positive factors were least impacted. Thus, it is expected that profiles 1, 5 and 6 suffer less impact than profiles 2, 3 and 4 due to presence of mangrove in front part.

5 Conclusions

The area has suffered important changes in relation to covers identified from 1975 to 2014. Those changes do not cause very big changes in coastal exposure and drag coefficient, although the area is classified as highly exposure zone. Reduction of Mangrove extension causes an increment of coastal exposure, but increment of Natural Vegetation counteracts this. Reduction of fragmentation increases protection by reducing the channel among mangrove and other covers. Human activities do not cause big changes on natural habitat's ranking for coastal exposure and drag coefficient. It is possible to differentiate two areas, where changes on both natural habitat's ranking for coastal exposure and drag coefficient are different. It is necessary to include anthropogenic landscapes in further analysis in order to know the role of crops or secondary vegetation in coastal exposure and protection against coastal flooding.

6 Acknowledgements

Authors are thankful to German Academic Exchange Service (DAAD), Excellence Center for Development Cooperation, Sustainable Water Management (EXCEED/ SWINDON), and Technical University of Braunschweig (TUBS) for their financial and technical supports, enabling to participate at the Summer School Integrating Ecosystems in Coastal Engineering Practice (INECEP).

7 References

1. Arkema, K.K., Guannel, G., Verutes, G., Wood, S.A., Guerry, A., Ruckelshaus, M., Kareiva, P., Lacayo, M., Silver, J.M.: Coastal habitats shield people and property from sea-level rise and storms. Nature Climate Change 3, 913-918 (2013)
2. Silva, R., Martínez, M.L., Hesp, P.A., Catalan, P., Osorio, A.F., Martell, R., Fossati, M., Miot da Silva, G., Mariño-Tapia, I., Pereira, P., Cienguegos, R., Klein, A., Govaere, G.: Present and Future Challenges of Coastal Erosion in Latin America. Journal of Coastal Research SI-71, 1-16 (2014)

Dieses Werk ist copyrightgeschützt und darf in keiner Form vervielfältigt werden noch an Dritte weitergegeben werden.
Es gilt nur für den persönlichen Gebrauch.

3. Zhang, K., Liu, H., Li, Y., Xu, H., Shen, J., Rhome, J., Smith, T.J.: The role of mangroves in attenuating storm surges. Estuarine, Coastal and Shelf Science 102, 11-23 (2012)

4. Sheng, Y.P., Lapetina, A., Ma, G.: The reduction of storm surge by vegetation canopies: Three-dimensional simulations. Geophysical Research Letters 39, L20601, (2012), DOI: 10.1029/2012GL053577

5. Das, S.C., Iimura, K., Tanaka, N.: Effects of coastal vegetation species and ground slope on storm surge disaster mitigation. Coastal Engineering Proceedings; No 32 (2010): Proceedings of 32nd Conference on Coastal Engineering, Shanghai, China, 2010. DOI 10.9753/icce.v32.currents.24 (2011)

6. Krauss, K.W., Doyle, T.W., Doyle, T.J., Swarzenski, C.M., From, A.S., Day, R.H., Conner, W.H.: Water level observations in mangrove swamps during two hurricanes in Florida. Wetlands 29, 142 (2009)

7. McIvor, A., Spencer, T., Möller, I., Spalding, M.: Storm surge reduction by mangroves. Natural coastal protection series: report 2. Cambridge Coastal Research Unit Working Paper 41, 35 (2012)

8. Sharp, R., Tallis, H.T., Ricketts, T., Guerry, A.D., Wood, S.A., Chaplin-Kramer, R., Nelson, E., Ennaanay, D., Wolny, S., Olwero, N., Vigerstol, K., Pennington, D., Mendoza, G., Aukema, J., Foster, J., Forrest, J., Cameron, D., Arkema, K., Lonsdorf, E., Kennedy, C., Verutes, G., Kim, C.K., Guannel, G., Papenfus, M., Toft, J., Marsik, M., Bernhardt, J., Griffin, R., Glowinski, K., Chaumont, N., Perelman, A., Lacayo, M., Mandle, L., Hamel, P., Vogl, A.L., Rogers, L., Bierbower, W.: InVEST +VERSION+ User's Guide. The Natural Capital Project. The Nature Conservancy and World Wildlife Fund (2015)

9. Liu, H., Zhang, K., Li, Y., Xie, L.: Numerical study of the sensitivity of mangroves in reducing storm surge and flooding to hurricane characteristics in southern Florida. Continental Shelf Research 64, 51-65 (2013)

10. Badola, R., Hussain, S.A.: Valuing ecosystem functions: an empirical study on the storm protection function of Bhitarkanika mangrove ecosystem, India. Environmental Conservation 32, 85-92 (2005)

Dieses Werk ist copyrightgeschützt und darf in keiner Form vervielfältigt werden noch an Dritte weitergegeben werden.
Es gilt nur für den persönlichen Gebrauch.

WAVELET AS ROUGHNESS INDICATOR FOR CORAL REEF BATHYMETRIC PROFILES

César Armando Acevedo Ramírez[1], Ismael Mariño-Tapia[1]

[1]CINVESTAV (Sea Resources Department) Antigua Carretera a Progreso km 6 S/N, Merida, Yucatan; cesar.acevedo.2708@gmail.com

Keywords: Coral-Reef, Roughness, Structural-Complexity, Wavelet

Abstract

Coral reefs are complex, productive and fragile systems, which are affected by multiple variables acting at several scales. However, properly evaluating and measuring roughness in these systems represent technical and logistic challenges, including water motion (breaking waves), shallowness, and coral fragility. Therefore, selection of a suitable method within the variety of existing possibilities is very important. The present work compares different analysis tools for roughness evaluation on bathymetric profiles: Rugosity Index (RI), Standard Deviation (SD), Spectral Analysis (Fourier Analysis), and Wavelet Analysis. Cross-reef bathymetric profiles were performed in the Puerto Morelos reef system in Quintana Roo, Mexico. A pentamaran (dim: 2 x 1.5 m) was equipped with an ADCP used as an echosounder (~30 cm resolution) and a differential GPS. The Wavelet analysis was the only one capable of evaluating roughness height, length at different scales (0.3 to 30 m) and its spatial location along the profile. Thus, this tool is adequate to find relations between roughness and phenomena at different scales through profiles.

1 Introduction

Structural complexity measurements have an important role on surveying biological and physical coral reef processes. This structural complexity results in increased habitat heterogeneity by providing refuge and attachment points for coral, algae and invertebrates [1, 2]. On the other hand, coral reef structural complexity is an important part of wave energy dissipation by bottom friction [3-6]. Moreover, the complexity of Caribbean corals has declined nonlinearly over the last 40 years [7], and the length of time it takes for reefs to collapse following coral mortality are unknown [8]. Although there is a general agreement on the importance of structural complexity, there are no any standard measurement techniques or metrics for quantifying it [9]. Therefore, it is not only important to develop a robust way to measure structural complexity, but also to define a concept with biological and physical meanings.

There are conceptual and logistic challenges trying to describe this structural complexity. First of all, coral reefs are complex and diverse systems, in which multiple physical and biological processes vary in space and time [10]. In fact, the ocean floor is characterized by variability on all scales, from millimeter polyp structures up to the ocean basins [11]. Therefore, as was noted by Aronson (1994) [10], *"the question of the appropriate scales, at which to search for pattern and process, is fundamental to unravelling these multiple parameters connections"*. Secondly,

Dieses Werk ist copyrightgeschützt und darf in keiner Form vervielfältigt werden noch an Dritte weitergegeben werden.
Es gilt nur für den persönlichen Gebrauch.

measurements on reef environments implies several logistic and technical problems as high water motion (principally, at breaking point), and instruments resolution for the small scales complexity.

In spite of multi-scale characteristics of floor complexity, measurement of rugosity in coral reef environments has generally relied on the chain method [2]. This method is dimensionless and does not take into account any scale parameter. It is calculated from the ratio between the actual surface distance on the reef, measured by draping a chain over the floor, and a linear distance that is measured with transect tape [2, 12]. It is assumed to be a measurement of spatial heterogeneity [12]. This method was universally accepted because it was simple and inexpensive, but large numbers of samples must be taken to provide a robust measure of rugosity due to often high spatial heterogeneity in coral reef environments and subjectivity, in how the diver placed the chain along the transect [13]. Furthermore, this is an imprecise descriptor of the structural complexity [13].

More recently, several alternatives have been developed to the chain method. [1] used a field profile gauge and analyses each 3 m profile with several indicators: standard deviation, coefficient of variation, angular standard deviation, among others. [9, 14] obtained profiles from a digital elevation model using lidar and multibeam-sonar, respectively, and then expressed roughness as fractal dimension. [15] used an echo sounder and variance, skewness, entropy, power spectral slope, and anisotropy as indicators. Finally, [2, 16] used Structure From Motion (SFM) algorithms, in underwater and aerial (drone) videos to obtain microbathymetries and then used the ratio between area and the *planar area* (analogous to chain method in two dimensions) as indicator.

Here, we present the wavelet as a new method to express roughness from bathymetric profiles. To compare this method, we selected one of the most common indictors, the rugosity index (RI) and some new indicators: Fourier spectrum [13] and Four Time Standard Deviation [4, 6].

2 Methodology

2.1 Study Area

"El Parque Nacional Arrecife de Puerto Morelos" (PNAPM) is a marine protected area and Ramsar site (wetland of international importance). It is located between Puerto Morelos that is a small village (9000 inhabitants) and Cancun that is the most recognized touristic city of Mexico [17, 18]. PNAPM encloses a semi-continuous fringing reef system that is part of Mesoamerican Barrier Reef, the largest barrier reef on the Western Hemisphere. This fringing reef surrounds a reef lagoon that its wide is from 550 m (its southern part) up to 3000 m (its northern part) with a mean depth of 3.5 m [19].

2.2 Cross-barrier reef profiles

Three areas were selected based on previous fieldwork observations. Limones, a high reef cover zone in the northern side of PNAPM (blue profile, Figure 1), a middle reef cover zone in front of "Unidad Acedémica Sistemas Arrecifales Puerto Morelos", belonging to the National Autonomous University of Mexico (black profile, Figure 1), and finally very degraded zone that was previously

Dieses Werk ist copyrightgeschützt und darf in keiner Form vervielfältigt werden noch an Dritte weitergegeben werden.
Es gilt nur für den persönlichen Gebrauch.

dredged and is located southern part of PNAPM (red profile, Figure 1). In each zone, a reef profile was carried out with a system that consists of a pentamaran (approx. size 1.5 x 1 x 0.4 m) with the following installed instruments: a differential-GPS (DGPS-Leica 1200) and an Acoustic Doppler Profiler (ADP; Hydrosurveyor, SonTek). Profiles were measured from the ocean side of the reef (front reef), over the coral reef and through the reef lagoon, ending near to coastline. The system is moving by boat in the lagoon and swimming over shallow sections (reef crest). Profiles measured provide high-resolution bathymetry (approx. 0.3 m). They were named based on its reef cover as high cover profile (HCP), middle cover profile (MCP), and low cover profile (LCP).

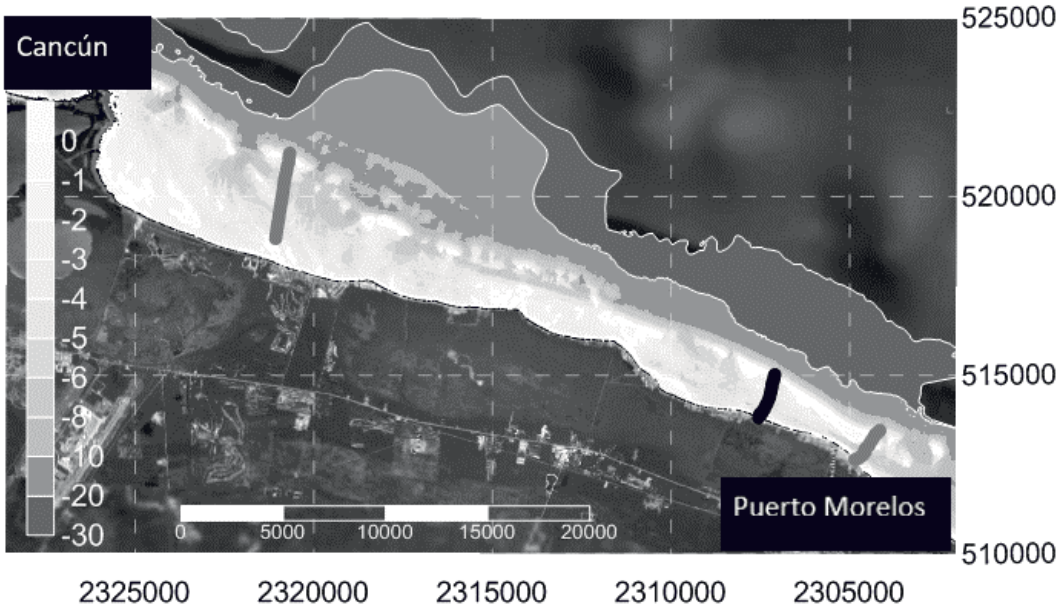

Figure 1: Study area map. The three coloured lines represent reef profiles selected to this study

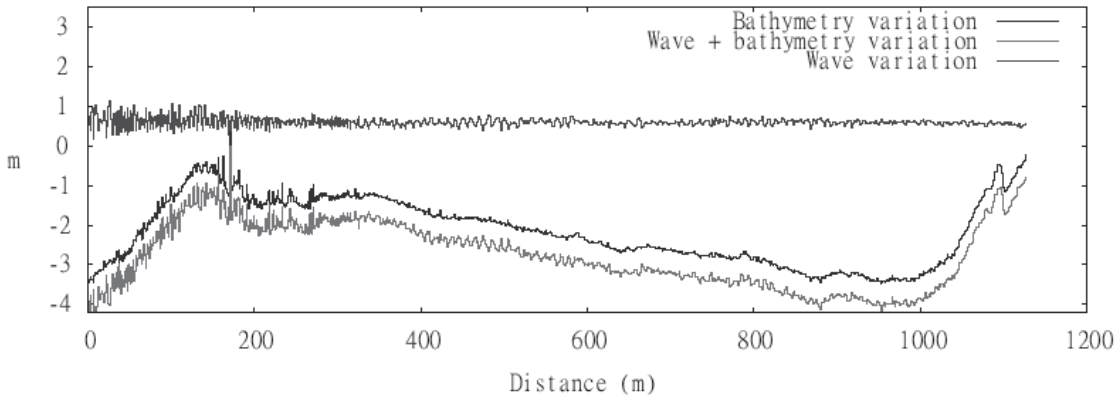

Figure 2: Obtaining Small Bathymetry Fluctuation Series (SBFS) [middle line] from resting Differential-GPS (Wave variation) [top line] to ADCP signal (wave + bathymetry variation) [bottom line]

Data treatment and analysis were performed using Matlab 8.3.0.532 (R2014a). Treatment for cross-barrier profiles consist of (a) delete deficient data from DGPS and ADP, (b) obtain bathymetry profiles (depth variation) by removing DGPS time series (wave variation) from ADP

Dieses Werk ist copyrightgeschützt und darf in keiner Form vervielfältigt werden noch an Dritte weitergegeben werden.
Es gilt nur für den persönlichen Gebrauch.

(wave + bathymetry variation), (c) convert time series to spatial domain calculating distance between each of the DGPS points, (d) interpolate to homogenizes distance to 0.02 m, (e) eliminate linear trend, and (f) finally, the signal is divided by smooth filter (3 0m) into small (high pass) and large scales (low pass) (Figure 2). The final product is a Small Scale Bathymetry Fluctuation Signal (SBFS) that corresponds to individual reef colonies, patch reefs, and other structures of this size (0.3 to 30 m), and a Large Scale Bathymetry Fluctuation (LSBF) corresponding to structural feature like reef crest, reef slope, and reef front (Figure 3 and Figure 4).

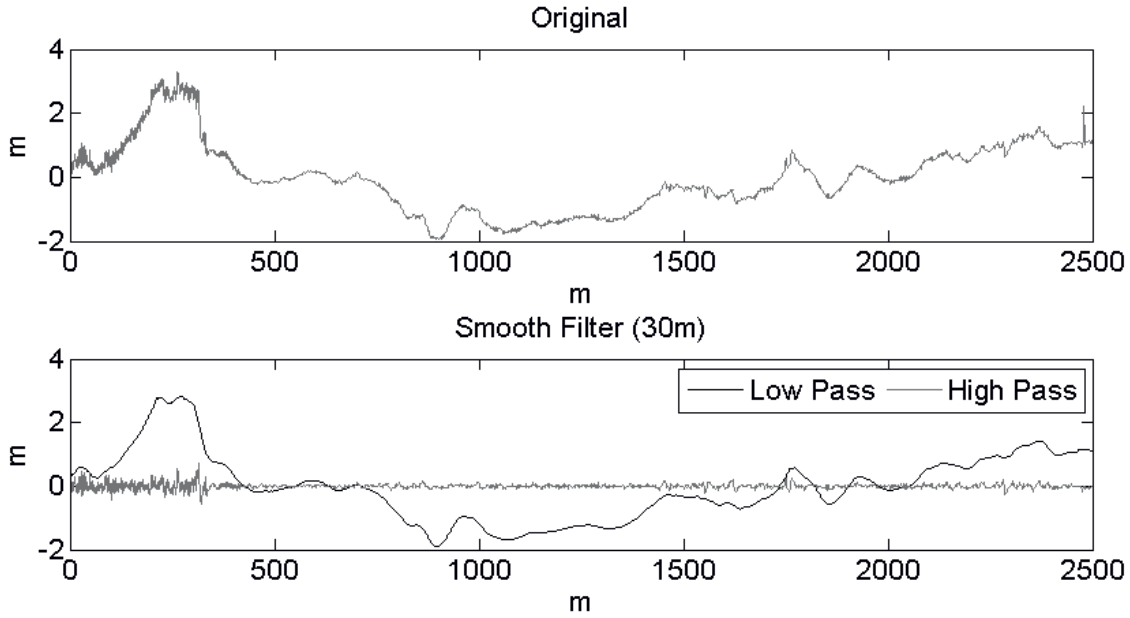

Figure 3: Smooth filter. [top] Original series; [bottom] low pass (LBFS) on black and high pass (SBFS) on red

In case of the index rugosity (RI) and Four Times Standard Deviation (FTSD), a sensibility test to evaluate windows lengths was performed, determining the highest indicator value for each window length (Figure 4). It was found that five meter is the optimal evaluation windows length, because it has a high value and at least 16 points to perform the calculus. Therefore, RI and FTSD were calculated in five-meter segments throughout the profile.

RI = contour/segment length [20]

$$\text{FTSD}(\text{Four Times Standard Deviation}) = \sigma x4$$

Throughout each profile, Fourier analysis was performed using Welch's overlapped segment averaging estimator available in MATLAB®, with a Hanning window of size 2048 (40.96 m) and 50% overlap.

Wavelet analysis was implemented following the methodology and scripts of [21]. Using a Morlet's wavelet with $\omega_0 = 6$, thus, the wavelet scale and Fourier frequency are almost equal, with a factor

Dieses Werk ist copyrightgeschützt und darf in keiner Form vervielfältigt werden noch an Dritte weitergegeben werden.
Es gilt nur für den persönlichen Gebrauch.

of 1.03 [21]. Similar to Fourier Spectrum, Wavelet is expressed finally as wavelet power spectra (WSP), but to make easy the comparison of different wavelets it is desirable to fine a common normalization [21]. For normalization, it was also followed the method proposed by [21]. To evaluate Wavelet magnitude in terms of variance, one can take WPS without normalization and select some interesting scales to average. In this case, WPS from 0.5 to 5 m scales were averaged and expressed as four times the deviation standard.

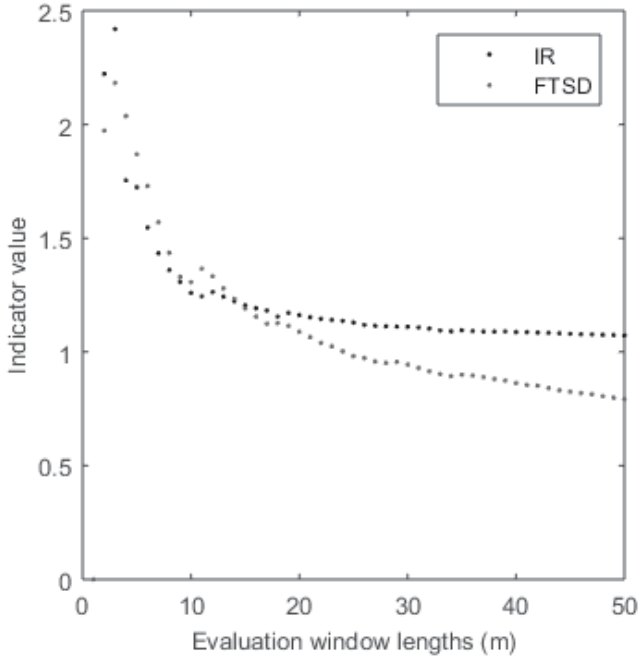

Figure 4: Sensibility test to evaluate windows lengths, using the highest indicator value for each window length

3 Results

3.1 Reef profile features

Based on the reef profile and field observation, it was found that LCP (Figure 5 [top]) is almost flat from the fore reef (0 m) to back reef (650 m). In the lagoon, there are two section between 800 m and 950 m, and between 1000 m and 1100 m that have a high vertical variability, with large scale characteristics (wider features, > 15 m), probably due to sand features. In the case of MCP, there are two high vertical variability sections but with short scale characteristics (narrow features < 15 m), over the fore reef (0 to 80 m) and the back reef (120 to 200 m), respectively. The vertical variability in these sections (fore and back reef) is related to coral structures (field work observations). Finally, the HCP shows a large section (0 to 380 m) of high vertical variability and short scale characteristics that are also related to coral structures (field work observations).

Dieses Werk ist copyrightgeschützt und darf in keiner Form vervielfältigt werden noch an Dritte weitergegeben werden.
Es gilt nur für den persönlichen Gebrauch.

3.2 Rugosity Index

The RI is close to 1 (the lowest possible value) throughout the LCP (Figure 6). On the reef area (first 200 m), the MCP has RI values around 1.1 and a maximum RI value of 1.18 in the back reef (120 to 200 m). The HCP has the highest RI value 1.38 on the front reef (first 100 m) and rougher zone (RI 1.1 to 1.3) between 0 and 400 m (reef zone), in contrast, between 480 to 2500 m (lagoon) RI close to 1.

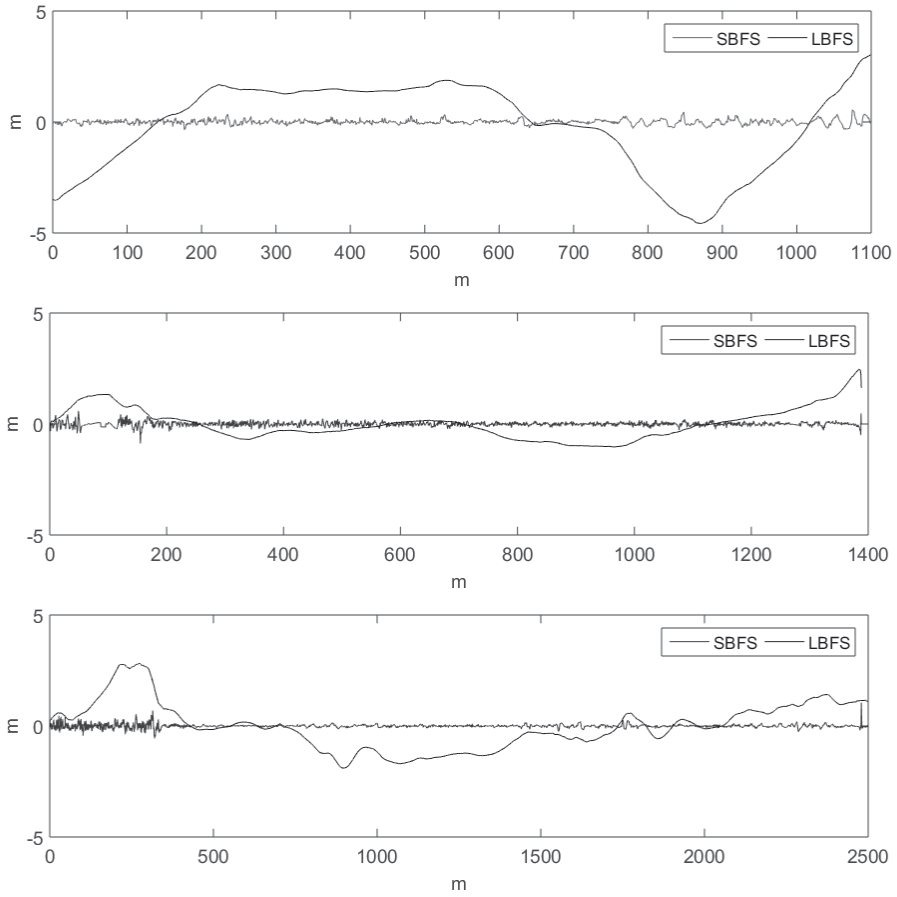

Figure 5: SBFS and LBFS from each of the profiles analysed; [top] LCP, [middle] MCP and [bottom] HCP

3.3 Four times standard deviation (FTSD)

In general, FTSD appears to be more sensible than RI (Figure 7). In fact, using FTSD lagoon appears to be rougher than using RI. In case of LCP, it shows high FTSD values close to the beach (800 to 1100 m). MCP has a similar tendency than using the RI, but there is more contrast between reef and lagoon roughness using FTSD than with RI. An interesting feature of MCP is that over the crest reef (approx. 60 to 110 m) FTSD decreases dramatically from 1.1 to 0 m, and then come back to 1.1 on the back reef (110 to 200 m). Finally, the HCP has the same tendency as using the RI, but it seems that difference is increased among profiles using FTSD. Another feature in HCP is that back reef is the roughest zone using FTSD. In contrast, using the RI the front reef is the roughest. In both MCP and HCP roughness values (0.5 up to 1.6 m) are close to object heights (coral heads) throughout each profile (Field work observations).

Dieses Werk ist copyrightgeschützt und darf in keiner Form vervielfältigt werden noch an Dritte weitergegeben werden.
Es gilt nur für den persönlichen Gebrauch.

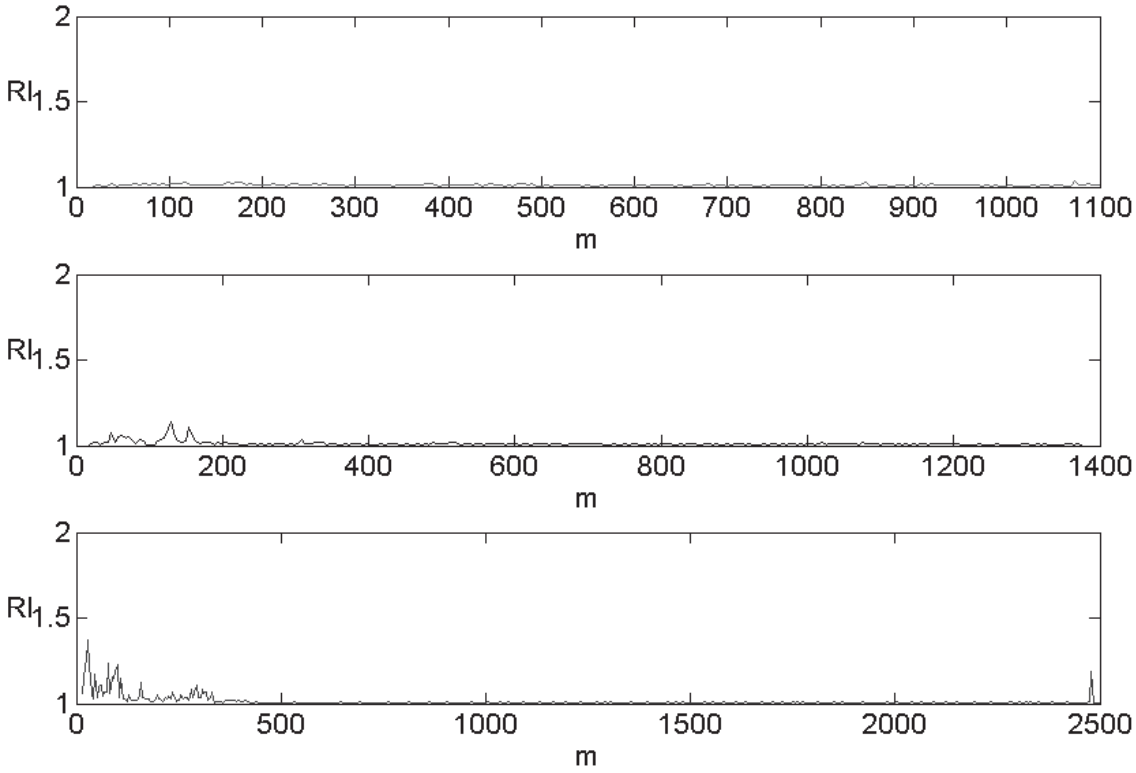

Figure 6: Rugosity Index (RI) for segments of 5m; [top line] LCP, [middle line] MCP, and [bottom line] HCP.

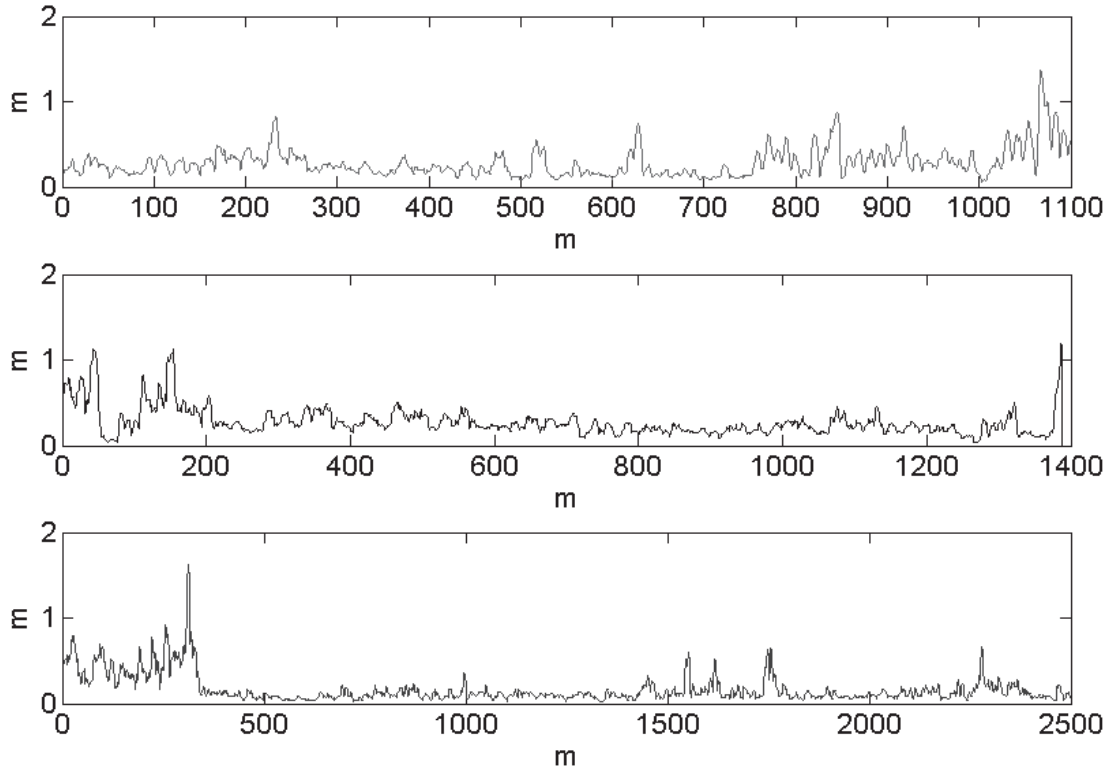

Figure 7: Four times the standard deviation for 5 m segments; [top line] LCP, [middle line] MCP, and [bottom line] HCP.

Dieses Werk ist copyrightgeschützt und darf in keiner Form vervielfältigt werden noch an Dritte weitergegeben werden.
Es gilt nur für den persönlichen Gebrauch.

3.4 Fourier analysis

Fourier analysis results are presented in Figure 8. MCP and HCP have more Power Spectra Energy (PSE) in their short wavenumbers (0.1 to 1 cycle per meter [cpm], equivalent to objects between 1 and 10 m) than in their large wavenumbers (< 0.1 cpm, i.e., >10 m). In contrast, LCP has only a peak at 0.0488 cpm (equivalent to wider features, around 20 m).

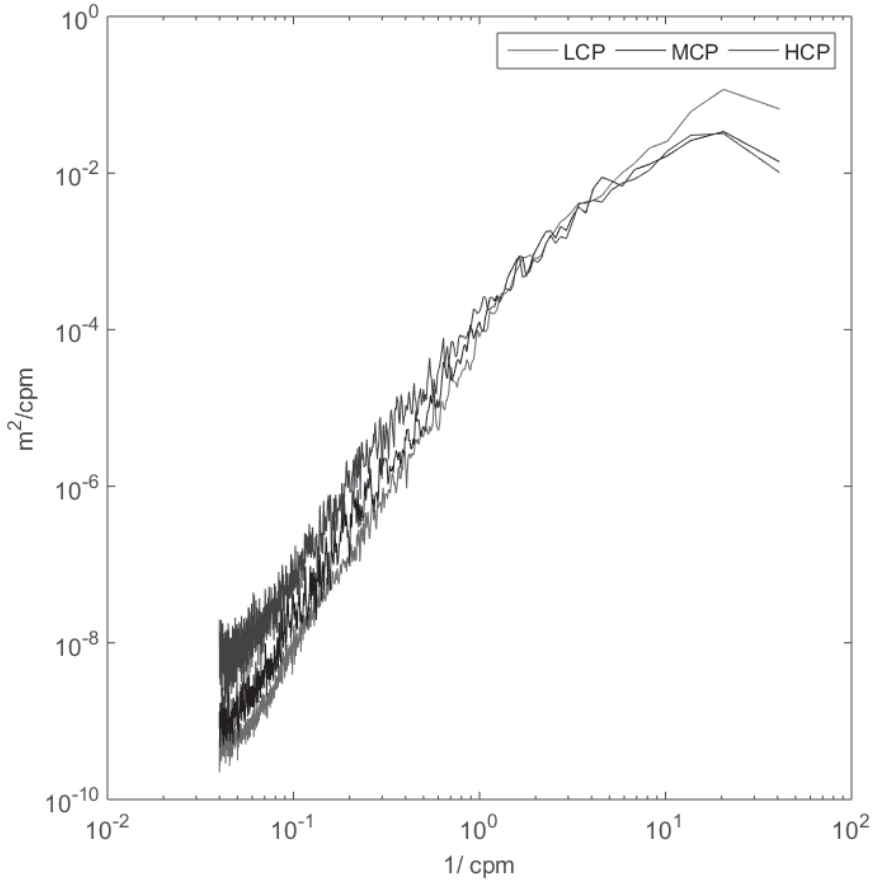

Figure 8: Fourier analysis for each profile; [red line] LCP, [black line] MCP, and [blue line] HCP

3.5 Wavelet

Figure 9 shows the normalized wavelet graph of each profile (LCP, MCP and HCP). X axis, such as in RI and FTSD, represents the linear space between the beginning and the end of profile, and Y axis represents horizontal scales (width of features). In this case, as results were normalized, the coloured axis shows how variance is distributed throughout profile and its horizontal scales (0 to 30 m). This consideration is important because as normalized wavelets, all of them have a variance equal to 1. Another possibility is to express Wavelet directly as variance or standard deviation, and then it is possible to compare profiles by their magnitudes.

Wavelet of LCP (Figure 9, top) shows that most WPS is concentrated at scales between 10 to 30 m and at the end of profile (780 to 1100 m). In the case of MCP, most energy is between 0 and 200 m

Dieses Werk ist copyrightgeschützt und darf in keiner Form vervielfältigt werden noch an Dritte weitergegeben werden.
Es gilt nur für den persönlichen Gebrauch.

(reef zone). Moreover, back reef appears to have the highest WPS values among all scales (0.5 to 30 m). Finally, the HCP has a similar variance distribution than MCP. Most WPS is located at reef zone (between 0 and 450 m) and the roughest zone is the back reef.

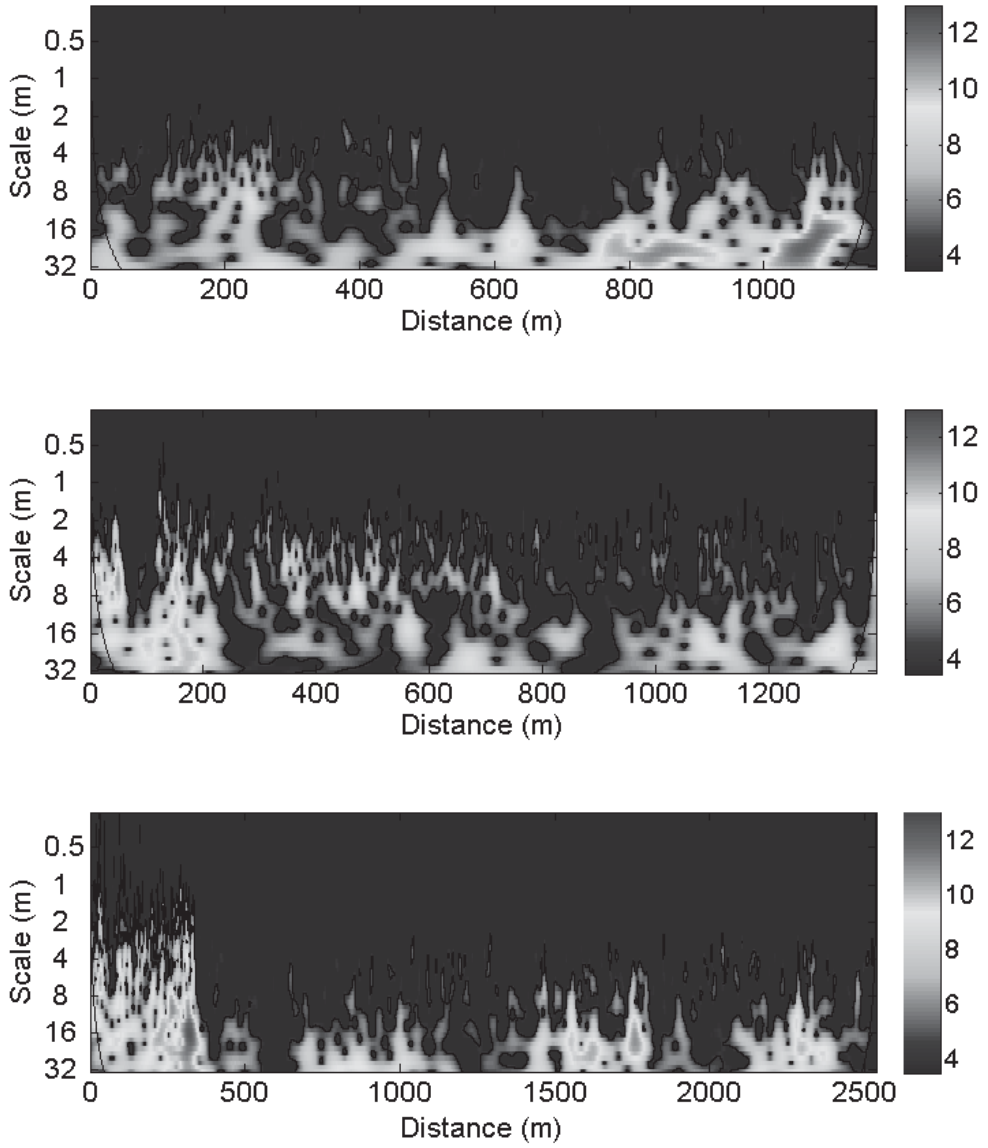

Figure 9: Normalized wavelet; [top] LCP, [middle] MCP, and [bottom] HCP

3.6 Wavelet FTSD

FTSD from wavelet (FTSDW) has a similar tendency as FTSD, but without noise from bigger scales. This feature is clear in the LCP, where FTSDW is almost zero throughout profile. In contrast, FTSD of LCP shows some roughness at large scales (10 to 30 m). From the FTSDW results it is also clear that back reef is the roughest zone at MCP and HCP. Furthermore, HCP has the roughest zone (1.5 m) and a large rough region (400 m).

Dieses Werk ist copyrightgeschützt und darf in keiner Form vervielfältigt werden noch an Dritte weitergegeben werden.
Es gilt nur für den persönlichen Gebrauch.

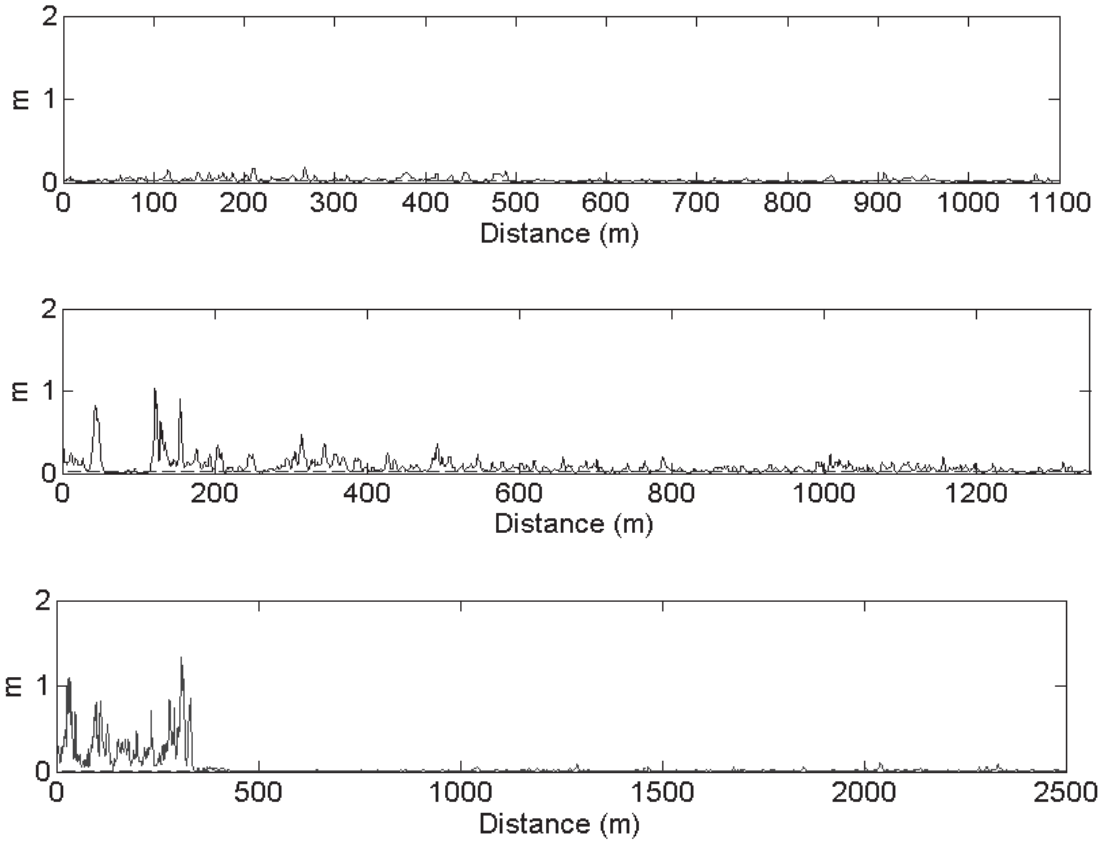

Figure 10: Four times the standard deviation from Wavelet analysis; [top line] LCP, [middle line] MCP, and [bottom line] HCP

4 Discussion

Indicators

Each roughness indicator offers different information. RI is a dimensionless indicator that is assumed to be a measurement of spatial heterogeneity [12]. However, RI does not give any direct information about objects contained throughout profiles. In this sense, RI could be an ambiguous indicator. In fact, [1] showed that profiles with a very different structure can have similar RI values. FTSD has a very interesting improvement; its value can be related with the height of objects. It can be, in some way, similar to significant wave height (Hs). Hs is calculated as four times standard deviation (4.004xSD) of wave elevations time series [22, 23]. Hs represents the average height of the third part with the highest waves and is a useful indicator that is common to express wave conditions [22]. This indicator has a statistical support, wave time series have a Rayleigh distribution [23]. Although profiles used in this study have also a Rayleigh distribution, it is necessary to confirm this characteristic in other reef systems. Fourier analysis is useful to divide series variance among frequencies. In a spatial series, this vertical variance is in function of objects height (for example coral reefs), and wavenumber (frequency in spatial series) is related to the horizontal scale of objects (width) and their incidence rate. The main problem Fourier analysis is that profiles lose their spatial distribution. Moreover, trying to apply Fourier analysis to small segments represents a loss of statistical significance. Finally, wavelet is a useful analysis that allows

Dieses Werk ist copyrightgeschützt und darf in keiner Form vervielfältigt werden noch an Dritte weitergegeben werden.
Es gilt nur für den persönlichen Gebrauch.

expressing roughness as variance on several scales and without losing its spatial distribution (in contrast to Fourier analysis). In this sense, Wavelet analysis is the best indicator because one gets roughness, height and width of object estimations throughout profiles at several scales.

Probably the most important characteristic of Wavelet analysis is that it shows results at several scales. An inherent feature of the ocean floor is that it has variance at all scales [11]. Therefore, it is important to have the capacity to divide this variance among scales and to choose the scale (or scales) of interest. For example, in the FTSD analysis, there is a lot of variance from large scales in lagoon zones. If one is interested in coral communities (horizontal scales from 0.5 to 5 m) this large scale variance can be seen as noise. Using FTSDW it is easy to select interesting scales (for example, 0.5 to 5 m). In fact, as [10] explained, most processes, for example wave dissipation as well complexity, have an inherent multi-scale characteristic. Therefore, a multi-scale analysis is needed to find interactions among processes and roughness.

In general, RI values on three profiles that are very low (< 1.38). It is important to note that measurement method (ADCP-differential GPS) has a maximum resolution of 0.3 m and average resolution of 0.5 m on reef zones. In contrast, typical chain methods have resolutions around 5 cm (in function of link size). Therefore, one cannot expect to find the same values. In the case of FTSD, [6] found similar values in their coral reef system (0.37 to 1.25 m). Although a direct comparison is not possible, Rogers' results (FTDS between 1.1 and 2.5 m) [6] show that the results presented here are coherent. Moreover, they coincide with field work observations. All indicators show HCP as the roughest one, and the reef zone is rougher than the lagoon zone. Inside the reef zone, FTSD and Wavelet show back reef as the roughest. In fact, these results coincide with a monitoring between 2005 and 2013 in PNAPM by [24]. In the other hand, RI shows that front reef is rougher than back reef in the HCP. It can be due to RI is less sensible than FTSD or Wavelet.

Measurement method

RI is the only indicator that can be obtained from chain method data. Chain method is an inexpensive but also is an imprecise measurement method. [25] demonstrates that chain method not only change among repetition, but also among users. Moreover, over more complex zones these changes tend to increase [25]. In contrast, accuracy of method used here is independent of user and complexity of bottom. Another problem of chain method is that to simulate measurement at different scales, it is necessary to change sizes of links of the chain and to repeat the measurement, something that also increases uncertainty and errors. The other indicators need a digital bathymetric profile (DBP). DBP can be obtained from expensive methods as ADCP/DGPS (used here), LIDAR or multibeam systems and from inexpensive methods such as Dustan's method [13] that uses pressure sensors, McCornick's method [1] that uses a mechanical profile gauge, or even the video-SFM method proposed by [2] and [16]. Each of these measurement methods has different resolution and costs. Therefore, one can choose each method in function of scales that one needs to evaluate, and the budget that one has. Moreover, a combined method should give more information, for example, to use ADCP/DGPS method and to complement it with high resolution method as video-SFM method.

Dieses Werk ist copyrightgeschützt und darf in keiner Form vervielfältigt werden noch an Dritte weitergegeben werden.
Es gilt nur für den persönlichen Gebrauch.

5 Acknowledgements

The authors thank INECEP committee and INECEP Summer School (INECEP-SS) assistants for their helpful suggestions during the INECEP-SS, also a special acknowledgment to EXCEED for the INECEP-SS and publication facilities. This study was funded through a scholarship from CONACYT (MEXICO) and LAPCOF (CINVESTAV- Merida).

6 References

1. McCormick, M.I.: Comparison of field methods for measuring surface topography and their associations with a tropical reef fish assemblage. Marine Ecology Progress Series 112, 87-96 (1994)
2. Storlazzi, C.D., Dartnell, P., Hatcher, G.A., Gibbs, A.E.: End of the chain? Rugosity and fine-scale bathymetry from existing underwater digital imagery using structure-from-motion (SfM) technology. Coral Reefs 35, 889-894 (2016)
3. Ferrario, F., Beck, M.W., Storlazzi, C.D., Micheli, F., Shepard, C.C., Airoldi, L.: The effectiveness of coral reefs for coastal hazard risk reduction and adaptation. Nature Communications 5, 1-9 (2014)
4. Lowe, R.J., Falter, J.L., Bandet, M.D., Pawlak, G., Atkinson, M.J., Monismith, S.G., Koseff, J.R.: Spectral wave dissipation over a barrier reef. Journal of Geophysical Research 110, C04001 (2005)
5. Monismith, S.G., Rogers, J.S., Koweek, D.A., Dunbar, R.B.: Frictional wave dissipation on a remarkably rough reef. Geophysical Research Letters 4063-4071 (2015)
6. Rogers, J.S., Monismith, S.G., Koweek, D.A., Dunbar, R.B.: Wave dynamics of a Pacific Atoll with high frictional effects. Journal of Geophysical Research: Oceans 121, 350-367 (2016)
7. Alvarez-Filip, L., Alvarez-Filip, L., Dulvy, N.K., Dulvy, N.K., Gill, J.a., Gill, J.a., Côté, I.M., Côté, I.M., Watkinson, A.R., Watkinson, A.R.: Flattening of Caribbean coral reefs: region-wide declines in architectural complexity. Proceedings. Biological sciences / The Royal Society 276, 3019-3025 (2009)
8. Alvarez-Filip, L., Côté, I.M., Gill, J.a., Watkinson, A.R., Dulvy, N.K.: Region-wide temporal and spatial variation in Caribbean reef architecture: is coral cover the whole story? Global Change Biology 17, 2470-2477 (2011)
9. Zawada, D.G., Brock, J.C.: A Multiscale Analysis of Coral Reef Topographic Complexity Using Lidar-Derived Bathymetry. Journal of Coastal Research 10053, 6-15 (2009)
10. Aronson, R.B., Edmunds, P.J., Precht, W.F., Swanson, D.W., Levitan, D.R.: Large-scale, long-term monitoring of Caribbean coral reefs: simple, quick, inexpensive techniques. Atoll Research Bulletin 42, 777-778 (1994)

Dieses Werk ist copyrightgeschützt und darf in keiner Form vervielfältigt werden noch an Dritte weitergegeben werden.
Es gilt nur für den persönlichen Gebrauch.

11. Bell, T.H.: Mesoscale sea floor roughness. Deep Sea Research Part A, Oceanographic Research Papers 26, 65-76 (1979)

12. Risk, M.J.: Fish diversity on a coral reef in The Virgin Islands. Atoll Research Bulletin 153, 1-6 (1972)

13. Dustan, P., Doherty, O., Pardede, S.: Digital Reef Rugosity Estimates Coral Reef Habitat Complexity. PLoS ONE 8, e57386-e57386 (2013)

14. Zawada, D.G., Piniak, G.A., Hearn, C.J.: Topographic complexity and roughness of a tropical benthic seascape. Geophysical Research Letters 37, 1-6 (2010)

15. Jaramillo, S., Pawlak, G.: AUV-based bed roughness mapping over a tropical reef. Coral Reefs 30, 11-23 (2011)

16. Casella, E., Collin, A., Harris, D., Ferse, S., Bejarano, S., Parravicini, V., Hench, J.L., Rovere, A.: Mapping coral reefs using consumer-grade drones and structure from motion photogrammetry techniques. Coral Reefs 36, 269-275 (2017)

17. Fonatur: FONATUR. http://www.fonatur.gob.mx/es/proyectos_desarrollos/cancun/index.asp. *(Accessed on October 1, 2017)*

18. INEGI: INEGI. http://www.microrregiones.gob.mx/catloc/contenido.aspx? *(Accessed on October 1, 2017)*

19. Coronado, C., Candela, J., Iglesias-Prieto, R., Sheinbaum, J., López, M., Ocampo-Torres, F.: On the circulation in the Puerto Morelos fringing reef lagoon. Coral Reefs 26, 149-163 (2007)

20. Graham, N.a.J., Nash, K.L.: The importance of structural complexity in coral reef ecosystems. Coral Reefs 32, 315-326 (2012)

21. Torrence, C., Compo, G.P.: A practical guide to wavelet analysis. Bams 79, 61 (1998)

22. Emery, W.J., Thomson, R.E.: Data Analysis Methods in Physical Oceanography. Oceanographic Literature Review, vol. 45, pp. 728. Elsevier, Poland (2014)

23. Goda, Y.: Random seas and desing of maritime structures. World Scientific (2000)

24. Rodríguez-Martínez, R.E., Ruíz-Rentería, F., van Tussenbroek, B., Barba-Santos, G., Escalante-Mancera, E., Jordán-Garza, G., Jordán-Dahlgren, E.: Environmental state and tendencies of the Puerto Morelos CARICOMP site, Mexico. Revista de Biologia Tropical 58, 23-43 (2010)

25. Wilding, T.A., Palmer, E.J.L., Polunin, N.V.C.: Comparison of three methods for quantifying topographic complexity on rocky shores. Marine Environmental Research 69, 143-151 (2010)

Dieses Werk ist copyrightgeschützt und darf in keiner Form vervielfältigt werden noch an Dritte weitergegeben werden.
Es gilt nur für den persönlichen Gebrauch.

RIP CURRENTS IN AN INTERMEDIATE BEACH WITH A NATURAL SUBMERGED ROCKY BANK

Francisco F. Criado-Sudau[1], Douglas D. Nemes[1], Marcos N. Gallo[1]

[1]Laboratório de Dinâmica de Sedimentos Coesivos, Programa de Pós-graduação de Engenharia Naval e Oceânica, Universidade Federal do Rio de Janeiro - COPPE, Rio de Janeiro, Brasil, franciscofabian@oceanica.ufrj.br

Keywords: Risk scale, Surf zone, Morphodynamic Variability

Abstract

Rip currents are strong transverse seaward directed flows, part of the hydrodynamic of oceanic beaches, being the main reason for lifeguard rescues efforts and drownings all over the world. To obtain in situ measures in the surf zone is a challenge due to the high energy, which is typical of these environments. A significant dataset was created during 25 field experiments (01/2015–01/2016) under low and high wave energy conditions. Eulerian and lagrangian surveys were carried out by an ADCP and human drifters, respectively. The Reserva Beach presented three zones considering the rip currents´ frequency and intensity, two lateral zones classified like “risk zones” and a central, classified as safety zone. The largest rip currents speeds were typically observed during high and shore-normal wave conditions. A threshold for significant wave height was identified (1.5-2) that determines the highest rip current velocities, from them on higher waves do not increase rip currents intensity. This study aims to characterize the rip currents of Reserva Beach in order to support a rip current forecast scale for the beaches of Rio de Janeiro, considering the wave parameters, tide influence, and the beach morphodynamic. The analysis of the in situ measurements should help in the calibration and validation of a hydrodynamic numerical model meaning to extend the risk scale along the coast of Rio de Janeiro.

1 Introduction

Rip currents are strong transverse seaward directed flows, part of the hydrodynamic of oceanic beaches, being the main reason for lifeguard rescues efforts and drownings all over the world [1-4]. Rip currents are strongly related to the beach morphology [5, 6] and influence the near shore sediment transport [7]. Submerged structures like rocky banks could affect the rip currents behaviour (location and strength); in these cases they are known as topographic rips [8]. Bathymetry longshore variations induce the wave breaking in diverse locations [9], thus produce alongshore different sea levels and, therefore, pressure gradients, which generate the rip currents. Rip currents intensity increases with significant wave height, wave period and when the wave direction is shore normal [1, 5, 10-13].

The tide also influences the rip current strength, which increases during low tidal elevations [1, 5, 6, 14-22]. In addition to the tidal elevation, the tidal currents may have a considerable effect in the

Dieses Werk ist copyrightgeschützt und darf in keiner Form vervielfältigt werden noch an Dritte weitergegeben werden.
Es gilt nur für den persönlichen Gebrauch.

currents behaviour in meso- or macro-tidal environments. Bruneau *et al.* [14] found in a meso/macro-tidal beach a strong asymmetry of rip current intensity, with stronger velocities during ebb than during flood; this asymmetry was even stronger between low and mid tide. Such asymmetries were not found in micro-tidal environments.

Despite rip currents becoming more researched in the last decades, studies using in situ data are lacking due to the difficulties with installing instruments under the high energetic conditions, which dominate the surf zones of open beaches. A way to get in situ measurements in these zones is using drifters, which represent the course and velocity of the currents. This methodology began to be used by Shepard and Inman [15] and has been improved with advances in the geographic information systems until the present time, being applied in several nearshore studies. The human drifters, used by some authors [6, 16], are especially appropriate in studies related to beach safety since they are the most legitimate representation of a swimmer being pushed by a rip current. Despite the non-linear processes suppose a challenge for numerical models in shallow water, numerical modelling has been improved and used to understand the rip currents behaviour [14, 17] increasing the number of publication during the last two decades [18]. 68 fatalities in 2016 and 31 until June 24, 2017 (NOAA) were related to rip currents in the United States. During the first 26 days of 2016, 8196 rescues were carried out by the lifeguards along Rio de Janeiro beaches, an average of 220 rescues per day for the first three months of 2017 [19], most of them probably related to the rip currents. In 1991, Lushine *et al.* [20] created the Lushine Rip Current Scale relating the number of rescues to the main wave parameters to forecast rip currents. Since then, several authors [1, 21-28] adapted or created new forecast scales for different beaches.

This study aims to create a rip current forecast scale for the beaches of Rio de Janeiro, based on an extensive data collection performed on a beach with a submerged rocky bank and topographic rip currents. In situ measurements analysis should help the calibration and validation of a hydrodynamic numerical model to forecast the rip currents in this particular beach, with the intention to extend this forecast for Rio the Janeiro to beaches with similar characteristics all over the world.

2 Study area

The Reserva Beach is classified an intermediate beach, the type found most commonly around the world [29] with micro-tidal regime and wave domination. The E-W beach orientation leaves it exposed to the highest energetic waves from meteorological systems of the South Atlantic Ocean. The longest waves usually come from S, SSW, SSE and the shortest one from southeast, thus the waves reach the beach with angles between -20º and 11º (considering 0º normal to the coastline, positive and negative angles have west and east components, respectively). Significant wave heights (Hs) in the breaking zone were between 0.2-3.2 m and periods (T) between 6-17 seconds. The study area presented tide heights ranging from 1.2 to 0.31 m. Reserva Beach's profile can be characterized by 1:13 slope and 0.400 mm (d50) sediment grain size in the surf zone. A natural rocky bank is present in the surf, with a mean depth in the breaking zone of 3.27 m. The surf zone is one of the most dynamic environments of the planet [7], therefore, the presence of the rocky

Dieses Werk ist copyrightgeschützt und darf in keiner Form vervielfältigt werden noch an Dritte weitergegeben werden.
Es gilt nur für den persönlichen Gebrauch.

bank allowed the fixation of oceanographic instruments. The Reserva Beach is a very popular beach with intense rip currents and a high number of rescues and drownings, located in the Rio de Janeiro state (23° 0'50.48" S and 43°23'9.78" W), Brazil (Figure 1).

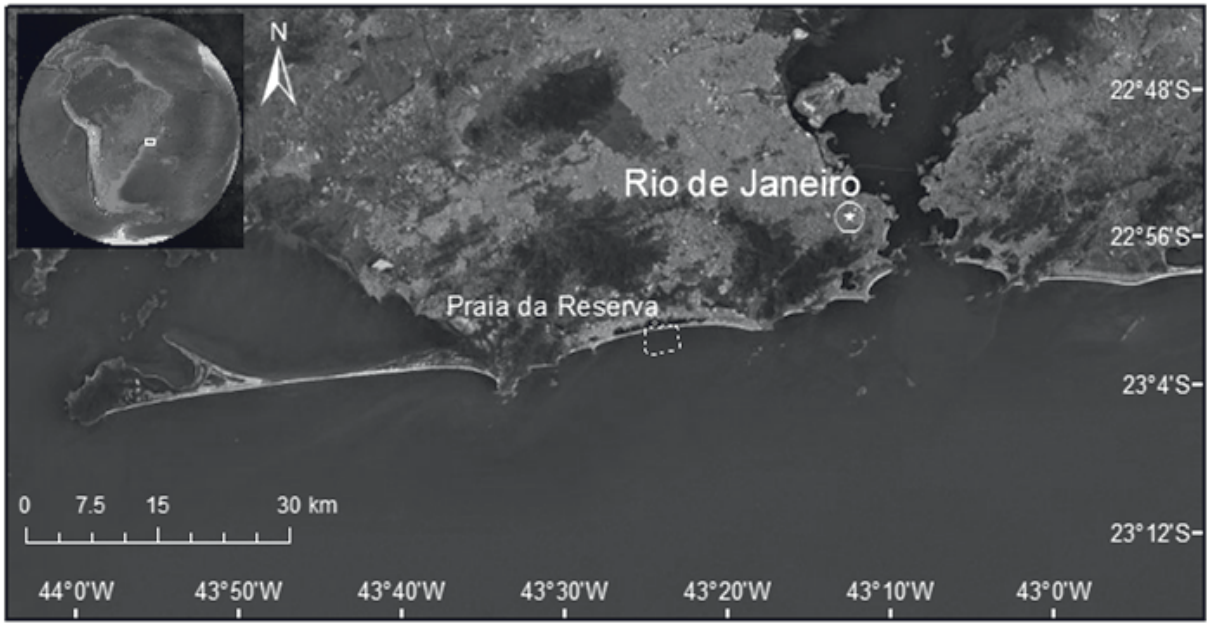

Figure 1: Study area

3 Experimental

With the purpose to characterize the rip currents behaviour at the Reserva Beach under different wave and tidal conditions, 25 field experiments were carried out along the year of 2015. Each field experiment was carried out after the mains meteorological events, which changed the beach morphology. In each field experiments, lagrangian measurements through human drifters and eurelian measurements using ADCP were conducted (Table 1).

Waves and currents measurements were obtained using the following instruments: 1 ADCP (Acustic Doppler Current Profiler, 1MHz), Aquadopp from NORTEK, and 2 GPSs Garmin Etrex10. The ADCP was fixed in the same location for all field campaigns. This was possible due to the presence of the rocky bank. The ADCP was anchored waveward of the rocky bank (23° 0'50.67"S, 43°23'9.70"O) during surveys. The tide and wave parameters were recorded using a pressure sensor 0.9 m above the bottom, with a deployment profile interval of 2048 seconds and with 2048 samples taken of the wave's measurements. The current data were recorded at 2 Hz in profile intervals of 1024 seconds with an average interval of 900 seconds. Two researchers, who meet the required skills for working in environments as energetic as the surf zone of Reserva Beach, carried out the survey operation. Lagrangian measurements were made through human drifters, consisting of a swimmer carrying a GPS and drifting with the rip current. The main advantages of this kind of drifters are that it is the most legitimate way to represent a swimmer in a rip current; it is a cheap methodology; and it represents not only the most superficial water layer but also the depth until 1.5 m. The morphodynamic variabilities were obtained by beach profiles spaces every

Dieses Werk ist copyrightgeschützt und darf in keiner Form vervielfältigt werden noch an Dritte weitergegeben werden.
Es gilt nur für den persönlichen Gebrauch.

12 m alongshore, covering a total length of 500 m longshore and 130 m cross-shore. The morphodynamic data were interpolated obtaining so a 3D morphologic feature configuration. The bathymetry was extended offshore using the field and nautical chart data.

Table 1: Summary of the field measurements: TM = Topographic measurement, ADCP = Acustic Doppler Current Profiler, HD = Human Drifters, "x" with measurements, "-" without measurements

Nº	Date	TM	ADCP	HD	Nº	Date	TM	ADCP	HD
1	29/01/15	x	-	x	14	14/08/15	x	-	x
2	28/04/15	x	-	x	15	31/08/15	x	-	x
3	10/05015	-	-	x	16	10/09/15	x	x	x
4	11/05/15	x	-	x	17	16/09/15	x	x	x
5	18/05/15	x	-	x	18	14/10/15	x	x	x
6	25/05/15	x	-	x	19	21/10/15	x	-	x
7	01/06/15	x	-	x	20	11/11/15	x	x	x
8	08/06/15	x	-	x	21	20/11/15	x	-	x
9	17/06/15	-	-	x	22	14/12/15	x	x	x
10	01/07/15	-	x	x	23	21/12/16	x	x	x
11	20/07/15	x	x	x	24	13/01/16	x	x	x
12	29/07/15	x	x	x	25	28/01/16	x	x	x
13	05/08/15	x	x	x					

4 Description and analysis

The diversity of the wave systems that reach the Reserva Beach, as well as the different tidal heights generate several hydrodynamic behaviours, which are classified into three flow patterns: rip currents, circulation cells, and longshore currents. This study is focused in the rip currents. The boundary conditions that characterized the study area are described below.

4.1 Boundary conditions

Throughout the study, the hydrodynamic behaviour of the Reserve Beach under different wave and tidal conditions were monitored. The tide heights ranged from 1.2 to 0.31 m, while the main wave parameters (Hs, Tp and θ) ranged from 0.2 to 3.2 m, 6 to 17 seconds, and 160 to 191º, respectively. Considering the relative tide range (RTR) [30], the beach was wave-dominated for each field experiment (RTR values smaller than 3).

The ADCP measured waves and currents for 12 field experiments, which were classified in four scenarios (SSE-SW; SSW-SSE; N-WC; I-M), as described below.

4.1.1 Scenario south-southeast waves and south-west currents (SSE-SW)

The incident waves (SSE) dominate the boundary conditions, generating rip currents, which leave the beach with SSW component. Longshore currents presented west direction (Figure 2). This behaviour was observed during field experiments 12 and 20.

Dieses Werk ist copyrightgeschützt und darf in keiner Form vervielfältigt werden noch an Dritte weitergegeben werden.
Es gilt nur für den persönlichen Gebrauch.

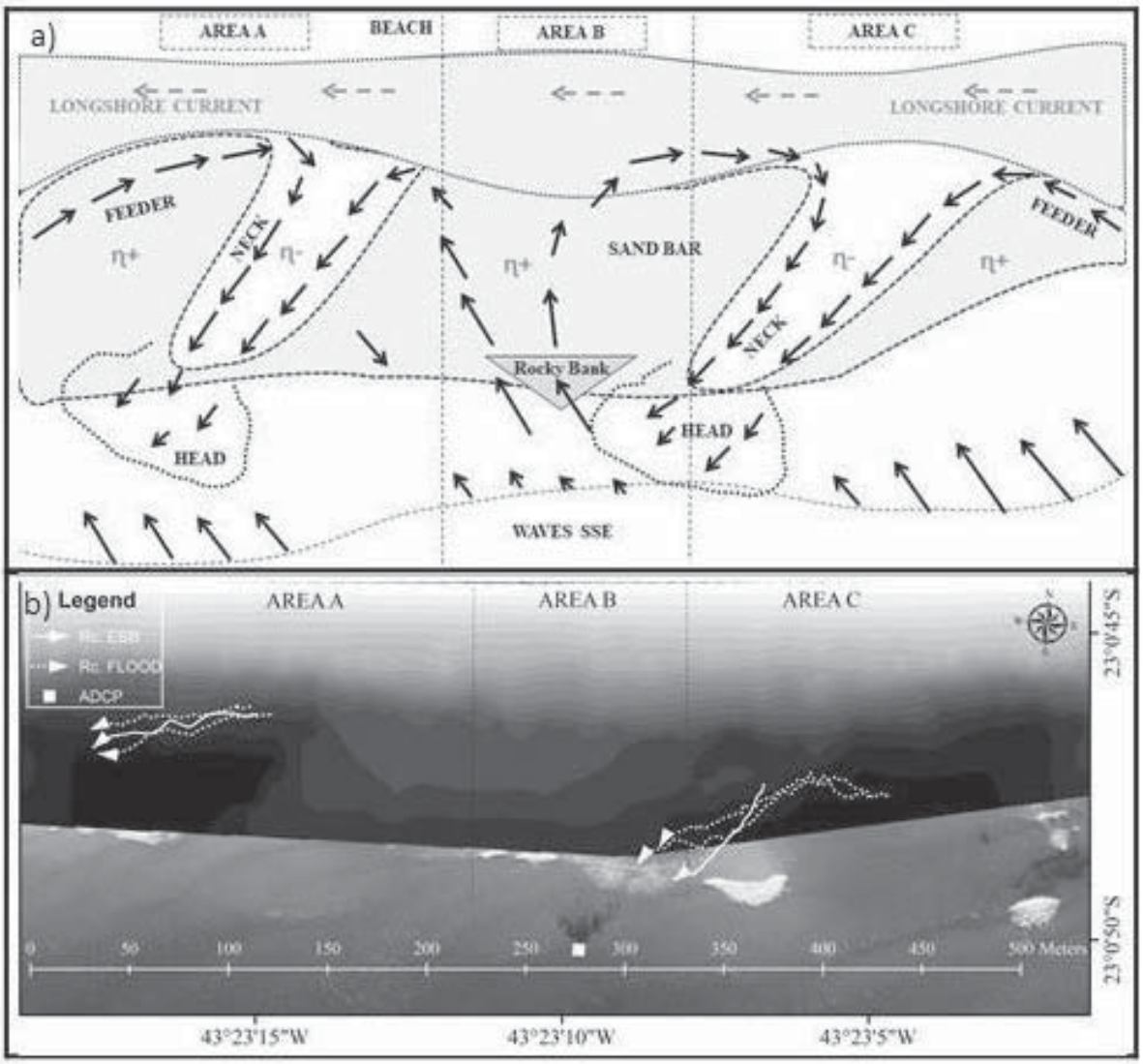

Figure 2: (a) Theoretical scheme representing the expected hydrodynamic behaviour of the surf zone with incident waves from SSE in grey shallow zones. η+: high wave set-up, η-: low wave set-up represents the sea level at the sea surface; (b) Measured rip currents tracks (Rc.) and position of the ADCP. Dark colours represent deeper areas.

4.1.2 Scenario south-southwest waves and south-southeast currents (SSW-SSE)

In this scenario, south-southwest waves dominate the boundary condition, generating rip currents that propagate in a south-southeast direction and longitudinal currents in an easterly direction (Figure 3). This behaviour was observed only during the field experiment number 25, following the same logic as the hydrodynamic behaviour of the first Scenario (SSE-SW) but for waves coming from SSW.

Dieses Werk ist copyrightgeschützt und darf in keiner Form vervielfältigt werden noch an Dritte weitergegeben werden.
Es gilt nur für den persönlichen Gebrauch.

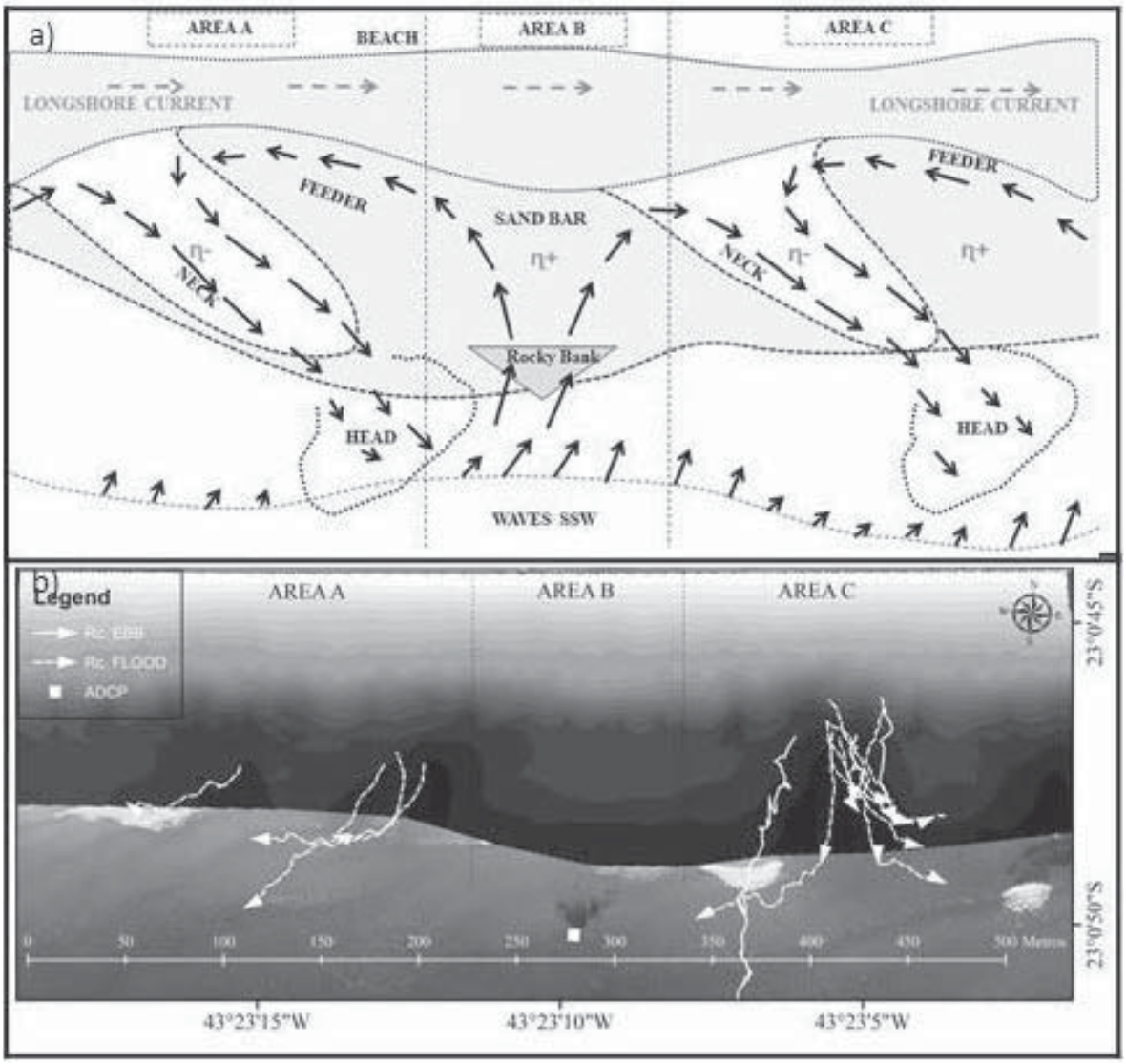

Figure 3: (a) Theoretical scheme representing the expected hydrodynamic behaviour of the surf zone with incident waves from SSW in grey shallow zones. η+: high wave set-up, η-: low wave set-up represents the sea level of the surface of the sea; (b) Measured rip currents tracks (Rc.) and position of the ADCP. Dark colours represent deeper areas.

For both scenarios (SSE-SW/SW-SSE), the waves dominate the hydrodynamics tilting the currents in the opposite direction to the angle of incidence. The velocity profile and directions of currents were homogeneous along the water column.

4.2.3 Scenario (N-WC): waves and currents normal to the beach

This scenario assemble field experiments, in which the wave incidence and the currents registered by the ADCP were normal to the beach (field experiments 11, 13, 16, 17, 22, 23 and 24).

The scenario (NWC) is divided into two cases. The first one and most common presented a sand bar after the submerged structure in the shadow area and two rips on both sides, respectively

Dieses Werk ist copyrightgeschützt und darf in keiner Form vervielfältigt werden noch an Dritte weitergegeben werden.
Es gilt nur für den persönlichen Gebrauch.

(Figure 4). In the second case, only one rip was formed in the shadow deeper area and two sand bars appear in both sides, were the shallows areas induce the wave breaking.

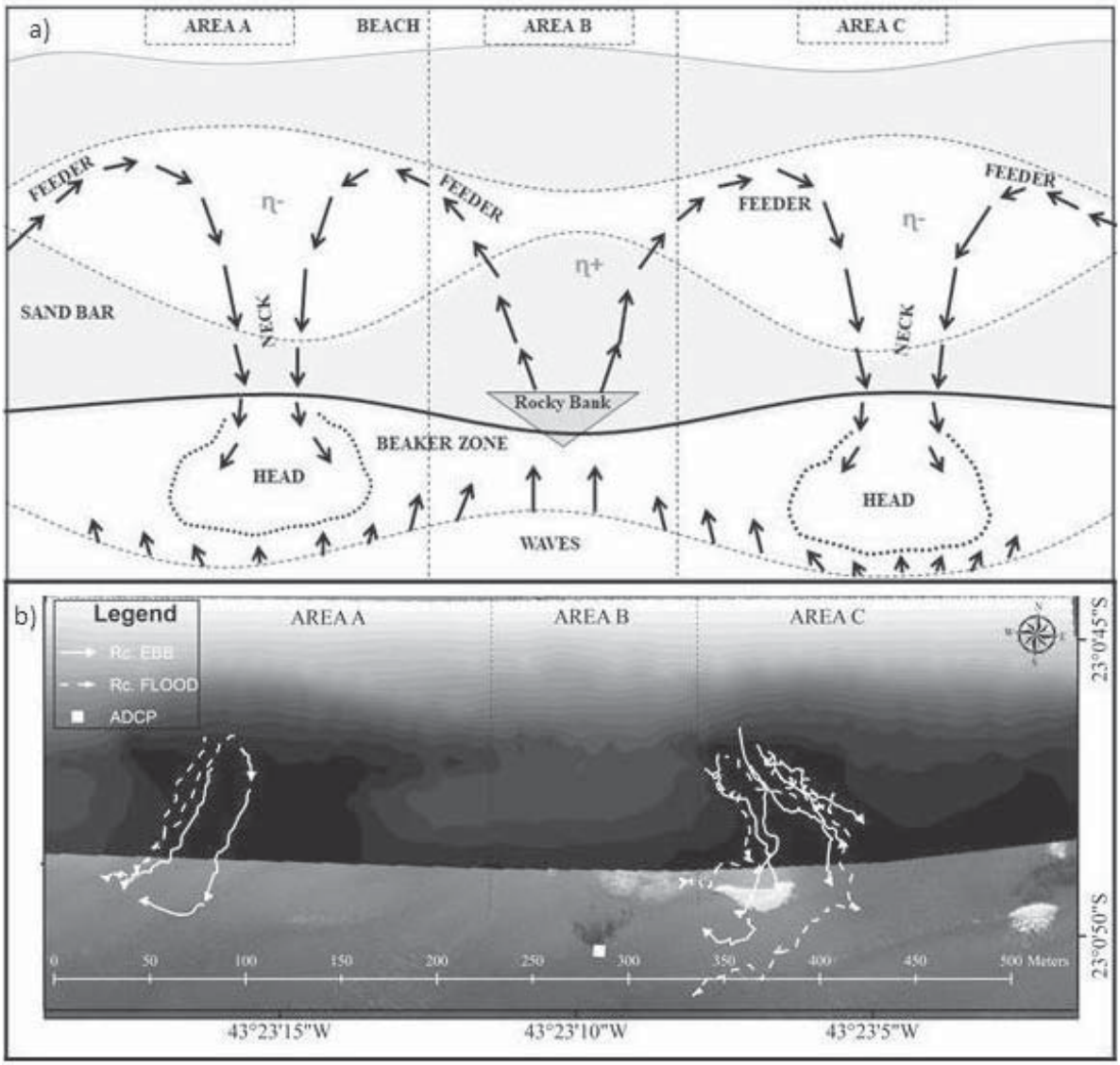

Figure 4: (a) Theoretical scheme representing the expected hydrodynamic behaviour of the surf zone with incident waves from S in grey shallow zones. η+: high wave set-up, η-: low wave set-up represents the sea level of the surface of the sea; (b) Measured rip currents tracks (Rc.) and position of the ADCP. Dark colours represent deeper areas.

4.2.4 Scenario inherited-morphology (I-M):

This particular scenario happened during the field experiment 18. With SSE waves, rip currents flowing to the SSW were expected, but in this case the rip currents flowed in the opposite direction from the incoming waves (Figure 5).

Dieses Werk ist copyrightgeschützt und darf in keiner Form vervielfältigt werden noch an Dritte weitergegeben werden.
Es gilt nur für den persönlichen Gebrauch.

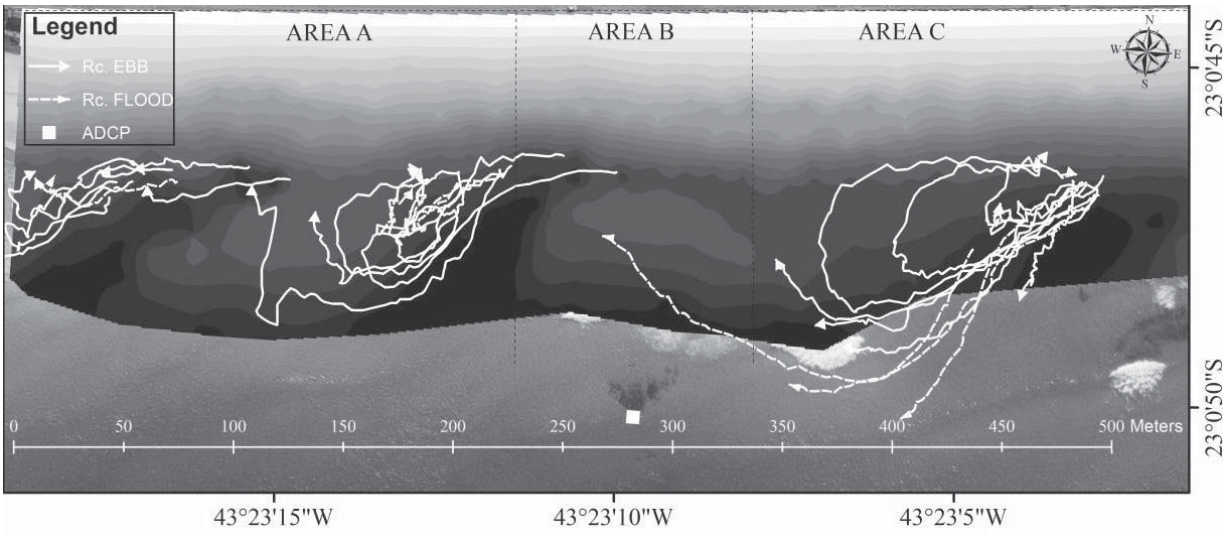

Figure 5: Measured rip currents tracks (Rc.) and position of the ADCP. Dark colours represent deeper areas.

The previous state with incidence waves from SSW shaped the morphodynamics of the surf zone generating rip channels with SSW orientation. When the field experiment was carried out, the new wave field (SSE) had not been acting for long enough to reshape the beach morphodynamic. Consequently, the rip currents were fixed to these inherited rips, flowing in the opposite direction of the waves. The surf zone morphodynamic is, therefore, a determining factor for the rip currents, as observed by other authors [5, 6].

There was observed a relationship between the main wave parameters (significant wave height, Hs; period, T; wave direction, θ), the tidal range, and the rip currents measured in the Reserva Beach. An increase of the rip currents velocity is observed as the height of the waves increases, until reaching a threshold of 1.5 m. The increase of the waves´ period supposes a decrease of the intensity of the currents. This is because large wave periods (swell and storms), which correspond to high wave heights, are conditions that favour the resetting of the surf zone morphodynamics. Energetic events "reset" the beach morphodynamic, leading to the formation of uniform shore parallel bar [31, 32]. Thus, longshore bar-trough morphodynamic state (LBT) is dominant; therefore, the longshore pressure gradients decrease and consequently do the rip current intensity. What one would expect for an intermediary beach is that after the storm, rhythmic features began to appear, indicating the recovery of the beach [29]. The frequency of the total reset of the beach will depend on the frequency, with which these energy events happen. During this study, 4 reset events were recorded, corresponding to the field experiments 5, 6, 9 and 18 (Figure 6).

Dieses Werk ist copyrightgeschützt und darf in keiner Form vervielfältigt werden noch an Dritte weitergegeben werden.
Es gilt nur für den persönlichen Gebrauch.

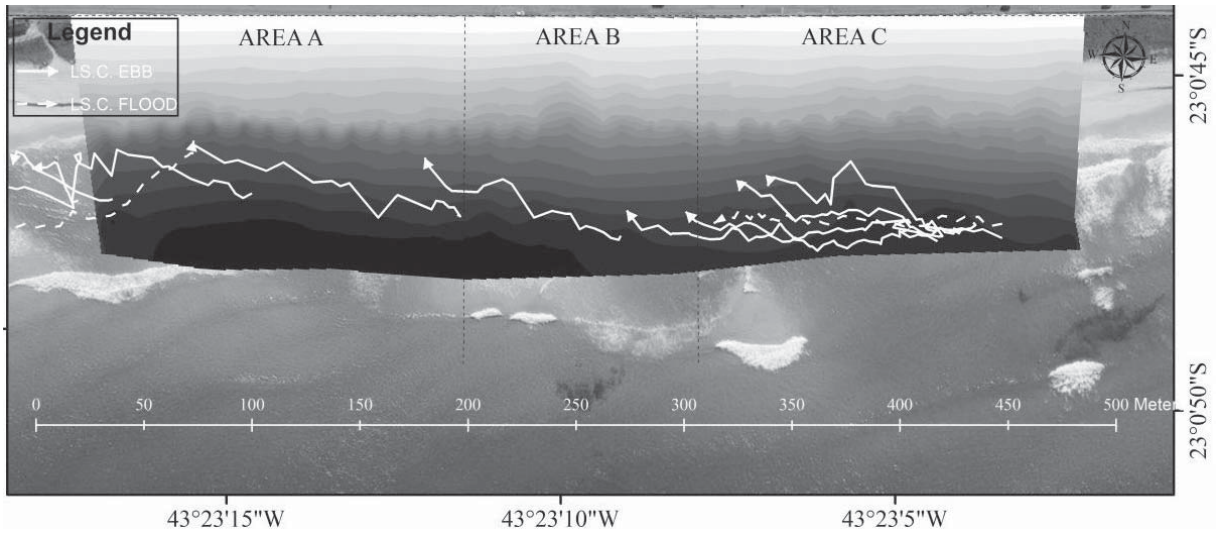

Figure 6: Beach morphodynamic after “reset” events whit the hydrodynamic dominated by longshore currents.

When relating the direction of the incident wave with the velocity of the rip currents, it is observed that for normal waves (+/- 5º) the intensity of the currents is larger, obtaining smaller speeds as the incidence angles becomes more oblique. It can also be verified that the rip currents are more frequent when the waves are normal to the beach, as pointed out by [33].

In order to verify the tidal effect on the rip currents, velocities and direction, averages for each hour were surveyed and analysed during the complete tidal range (Figure 7).

The intensity of the rip currents increases progressively from the end of the high tide (hours 4-5), corresponding to the minimum speed peak, until near the low tide (hours 7-8), where the maximum speed peak is reached (Figure 7), as observed in numerous studies [1, 5, 6, 30, 33-39]. According to the classification by [40], the Reserva Beach is micro-tidal, explaining so, that the asymmetry of the rip currents was insignificant. The tidal currents did not influence the magnitude of the rip currents; however, the decrease in the sea level during low tide was significant for the rip currents intensity (as observed between hours 6 and 9 in Figure 7).

The rip current velocity is strongly influenced by the water depth (Figure 8), this phenomenon was also observed by Brander and Short [5] in the rip-neck velocities.

This phenomenon agrees with the modulation previously found (Figure 7), greater velocities during the low tide (lower depth) and lower velocities during the high tide (higher depth).

Dieses Werk ist copyrightgeschützt und darf in keiner Form vervielfältigt werden noch an Dritte weitergegeben werden.
Es gilt nur für den persönlichen Gebrauch.

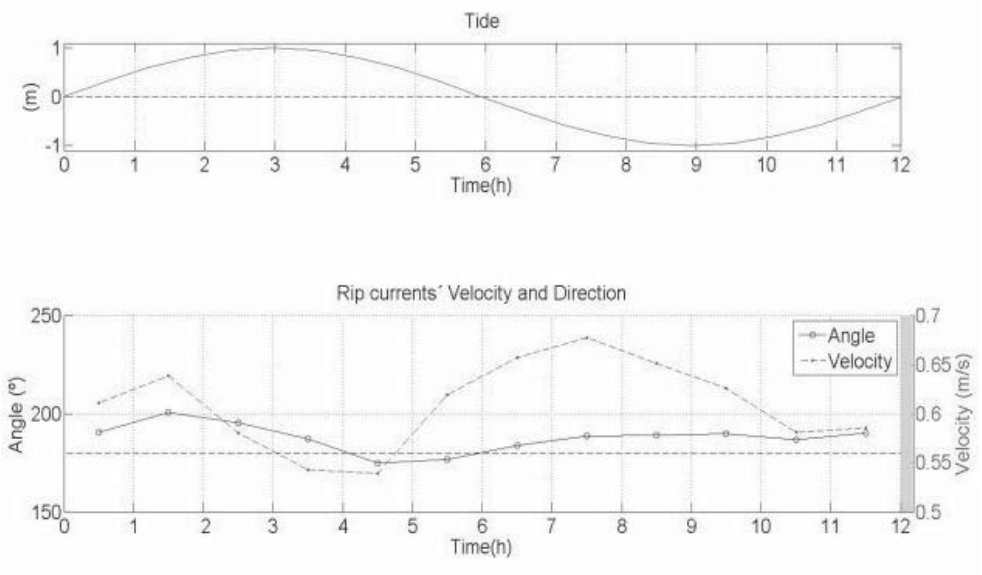

Figure 7: Average velocities and directions of the rip currents along the tidal cycle. *top*: tidal cycle, *bottom*: velocity and average angles per hour during the tidal cycle. The discontinuous line marks 180º (normal to the beach) larger angles with SSW and smaller angles with SSE components.

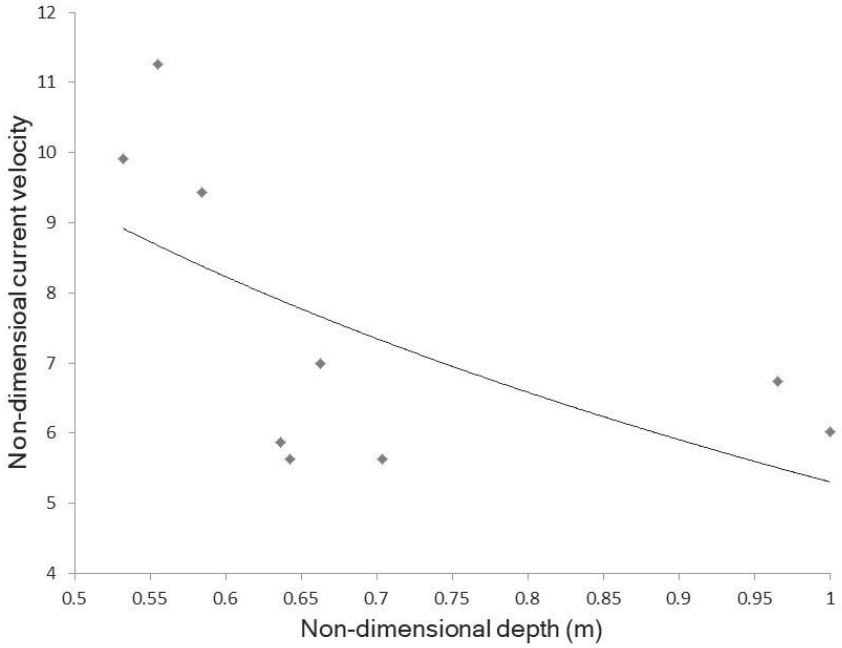

Figure 8: Relationship between non-dimensional rip current velocity and non-dimensional water depth

Dieses Werk ist copyrightgeschützt und darf in keiner Form vervielfältigt werden noch an Dritte weitergegeben werden.
Es gilt nur für den persönlichen Gebrauch.

5 Conclusions

The rich dataset obtained in the Reserva Beach and the well-known hydro and morphodynamic processes that take place in encouraged the authors to create a rip current forecast scale for the beaches of Rio de Janeiro. In situ data from rip currents, the main wave parameters, and the different beach states will be the basis to develop the rip currents scale. A risk scale, able to predict the rip currents´ behaviour could be a powerful tool, providing an effective forecast for lifeguards and beach goers, being thus a useful tool for the beach safety management.

A numerical model to represent the hydrodynamics of the beach will be used, supported by the field data from the Reserva Beach. When the numerical model is able to represent the hydrodynamic for the different beach states and, therefore, to simulate the rip currents, it will be compared with the risk scale. After the calibration and validation, its use could be extended for different places with beaches that meet similar characteristics as the study area.

The analysis of the in situ measurements could help in the calibration and validation of a hydrodynamic numerical model to forecast the rip currents in this particular beach, with the intention of extends this forecast along the coast of Rio the Janeiro.

6 Acknowledgement

The authors are grateful to the organizing committee from Integrating Ecosystems in Coastal Engineering in Puerto Morelos 2017 for financial support, which made possible to participate at this event. This summer school was funded by the DAAD and Exceed Swindon. Special thanks to the many volunteers, who helped with the fieldwork (Cohesive Sediment Dynamic Laboratory LDSC/COPPE/UFRJ). The first and second authors were supported by a scholarship from the CAPES Foundation (Ministry of Education) and the FAPERJ Foundation (Rio de Janeiro State).

7 References

1. Dusek, G., Seim, H.: A Probabilistic Rip Current Forecast Model. Journal of Coastal Research 29, 909-925 (2013)
2. Gensini, V.A., Ashley, W.S.: An examination of rip current fatalities in the United States. Natural Hazards 54, 159-175 (2010)
3. Hoefel, F., KLEIN, A.d.F.: Environmental and social decision factors of beach safety in the central northern coast of Santa Catarina, Brazil. Notas Téc. FACIMAR 2, 155-166 (1998)
4. Sherker, S., Williamson, A., Hatfield, J., Brander, R., Hayen, A.: Beachgoers' beliefs and behaviours in relation to beach flags and rip currents. Accident Analysis & Prevention 42, 1785-1804 (2010)
5. Brander, R.W., Short, A.D.: Flow kinematics of low-energy rip current systems. Journal of Coastal Research 17, 468-481 (2001)

Dieses Werk ist copyrightgeschützt und darf in keiner Form vervielfältigt werden noch an Dritte weitergegeben werden.
Es gilt nur für den persönlichen Gebrauch.

6. Bruneau, N., Castelle, B., Bonneton, P., Pedreros, R., Almar, R., Bonneton, N., Bretel, P., Parisot, J.-P., Sénéchal, N.: Field observations of an evolving rip current on a meso-macrotidal well-developed inner bar and rip morphology. Continental Shelf Research 29, 1650-1662 (2009)

7. Short, A.D.: Handbook of beach and shoreface morphodynamics. John Wiley & Sons Ltd. Baffins Lane, Chinchester (1999)

8. Short, A.: Australian rip systems—friend or foe. Journal of Coastal Research 50, 7-11 (2007)

9. Bowen, A.J.: Rip currents: 1. Theoretical investigations. Journal of Geophysical Research 74, 5467-5478 (1969)

10. Dalrymple, R.A., MacMahan, J.H., Reniers, A.J., Nelko, V.: Rip currents. Annual Review of Fluid Mechanics 43, 551-581 (2011)

11. Haller, M.C., Dalrymple, R.A., Svendsen, I.A.: Experimental study of nearshore dynamics on a barred beach with rip channels. Journal of Geophysical Research: Oceans 107(C6), 3061 (2002)

12. MacMahan, J.H., Thornton, E.B., Reniers, A.J.: Rip current review. Coastal Engineering 53, 191-208 (2006)

13. Winter, G., van Dongeren, A.R., de Schipper, M.A., van Thiel de Vries, J.S.M.: Rip currents under obliquely incident wind waves and tidal longshore currents. Coastal Engineering 89, 106-119 (2014)

14. Bruneau, N., Bertin, X., Castelle, B., Bonneton, P.: Tide-induced flow signature in rip currents on a meso-macrotidal beach. Ocean Modelling 74, 53-59 (2014)

15. Shepard, F., Inman, D.L.: Nearshore water circulation related to bottom topography and wave refraction. Eos, Transactions American Geophysical Union 31, 196-212 (1950)

16. MacMahan, J., Brown, J., Brown, J., Thornton, E., Reniers, A., Stanton, T., Henriquez, M., Gallagher, E., Morrison, J., Austin, M.J., Scott, T.M., Senechal, N.: Mean Lagrangian flow behavior on an open coast rip-channeled beach: A new perspective. Marine Geology 268, 1-15 (2010)

17. Reniers, A.J., MacMahan, J., Thornton, E., Stanton, T., Henriquez, M., Brown, J., Brown, J., Gallagher, E.: Surf zone surface retention on a rip‐channeled beach. Journal of Geophysical Research: Oceans 114, C10010 (2009)

18. Castelle, B., Scott, T., Brander, R.W., McCarroll, R.J.: Rip current types, circulation and hazard. Earth-Science Reviews 163, 1-21 (2016)

19. Corpo de Bombeiros Militar do Rio de Janeiro: 10/08/17, (2017) http://www.cbmerj.rj.gov.br/index.php?option=com_sppagebuilder&view=page&id=163.

Dieses Werk ist copyrightgeschützt und darf in keiner Form vervielfältigt werden noch an Dritte weitergegeben werden.
Es gilt nur für den persönlichen Gebrauch.

20. Lushine, J.B.: A study of rip current drownings and related weather factors. In: Natl. Wea. Dig. Citeseer, (1991)

21. Austin, M.J., Scott, T.M., Russell, P.E., Masselink, G.: Rip Current Prediction: Development, Validation, and Evaluation of an Operational Tool. Journal of Coastal Research 29, 283-300 (2012)

22. Engle, J.A.: Formulation of a rip current forecasting technique through statistical analysis of rip current-related rescues. University of Florida Florida, USA (2003)

23. Kumar, S.A., Prasad, K.: Rip current-related fatalities in India: a new predictive risk scale for forecasting rip currents. Natural hazards 70, 313-335 (2014)

24. Lascody, R.L.: East central Florida rip current program. National Weather Digest 22, 25-30 (1998)

25. Nelko, V., Dalrymple, R.A.: Rip currents: mechanisms and observations. Coastal Engineering 2008: (In 5 Volumes), pp. 888-900. World Scientific (2009)

26. Sembiring, L., van Dongeren, A., Winter, G., Roelvink, D.: Dynamic Modelling of Rip Currents for Swimmer Safety on a Wind-Sea–Dominated Mesotidal Beach. Journal of Coastal Research 32, 339-353 (2015)

27. Sembiring, L., van Dongeren, A., Winter, G., van Ormondt, M., Briere, C., Roelvink, D.: Nearshore bathymetry from video and the application to rip current predictions for the Dutch Coast. Journal of Coastal Research, Special Issue 70, 354-359 (2014)

28. Yoon, S.B., Park, W.K., Choi, J.: Observation of Rip Current Velocity at an Accidental Event by using Video Image Analysis. Journal of Coastal Research, Special Issue 72, 16-21 (2014)

29. Wright, L.D., Short, A.D.: Morphodynamic variability of surf zones and beaches: A synthesis. Marine Geology 56, 93-118 (1984)

30. Masselink, G., Short, A.D.: The effect of tide range on beach morphodynamics and morphology: a conceptual beach model. Journal of Coastal Research 9, 785-800 (1993)

31. Holman, R.A., Symonds, G., Thornton, E.B., Ranasinghe, R.: Rip spacing and persistence on an embayed beach. Journal of Geophysical Research: Oceans 111, C01006 (2006)

32. Turner, I.L., Whyte, D., Ruessink, B.G., Ranasinghe, R.: Observations of rip spacing, persistence and mobility at a long, straight coastline. Marine Geology 236, 209-221 (2007)

33. MacMahan, J.H., Thornton, E.B., Stanton, T.P., Reniers, A.J.H.M.: RIPEX: Observations of a rip current system. Marine Geology 218, 113-134 (2005)

34. Aagaard, T., Greenwood, B., Nielsen, J.: Mean currents and sediment transport in a rip channel. Marine Geology 140, 25-45 (1997)

35. Aagaard, T., Vinther, N.: Cross-Shore Currents in the Surf Zone: Rips or Undertow? Journal of Coastal Research 561-570 (2008)

Dieses Werk ist copyrightgeschützt und darf in keiner Form vervielfältigt werden noch an Dritte weitergegeben werden.
Es gilt nur für den persönlichen Gebrauch.

36. Austin, M.J., Masselink, G., Scott, T.M., Russell, P.E.: Water-level controls on macro-tidal rip currents. Continental Shelf Research 75, 28-40 (2014)

37. Scott, T., Masselink, G., Austin, M.J., Russell, P.: Controls on macrotidal rip current circulation and hazard. Geomorphology 214, 198-215 (2014)

38. Scott, T., Russell, P., Masselink, G., Wooler, A., Short, A.: High volume sediment transport and its implications for recreational beach risk. In: Proceedings 31st International Conference on Coastal Engineering. ASCE, Hamburg, Germany, pp. 4250-4262. (Year)

39. Sonu, C.J.: Field observation of nearshore circulation and meandering currents. Journal of Geophysical Research 77, 3232-3247 (1972)

40. Davies, J.: A morphogenic approach to world shorelines. Zeitschrift für Geomorphologie 8, 127-142 (1964)

Dieses Werk ist copyrightgeschützt und darf in keiner Form vervielfältigt werden noch an Dritte weitergegeben werden.
Es gilt nur für den persönlichen Gebrauch.

OCEANOGRAPHIC CONDITIONS LINKED TO THE ARRIVAL AND DEPARTURE OF *SARGASSUM SPP.* ON A FRINGING REEF LAGOON IN PUERTO MORELOS, QUINTANA ROO

Diana Berriel-Bueno[1], Ismael Mariño-Tapia [1], Elena Ojeda-Casillas [2], Cecilia Enriquez-Ortiz[3], Tonatiuh Mendoza-Ponce[2], A. David García-Barrera [2]

[1]Departamento de Recursos del Mar, CINVESTAV-Mérida. Antigua carretera a Progreso Km 6, Cordemex, 97310 Mérida, Yucatán. México, diana.berriel@cinvestav.mx

[2]Instituto de Ingeniería, Universidad Nacional Autónoma de México, Puerto de Abrigo s/n, 92718, Sisal, México

[3]Facultad de Ciencias, Universidad Nacional Autónoma de México, Puerto de Abrigo s/n, 92718, Sisal, México

Keywords: Atypical *Sargassum* influx, Coastal video-monitoring, Fringing reef lagoon, *Sargassum* dispersion, *Sargassum* modelling

Abstract

Massive atypical influx of *Sargassum spp.* has been reported from 2011 to 2016 across the Caribbean Sea and Gulf of Mexico's coasts. It is believed that this atypical influx was originated in the North Equatorial Recirculating Region (NERR), and because of the tropical characteristics of the surrounding water the *Sargassum* reservoir found the ideal conditions for establishing and growing. Under normal conditions, *Sargassum*'s role as a nutrient input source benefits the benthic community and the coastal vegetation, while in contrast, huge accumulations of *Sargassum* lead to anoxic conditions resulting in the eutrophication of the environment. In the Mexican Caribbean, the coastline of Quintana Roo was the most affected one. Around 9,700 m^3 of *Sargassum* were removed monthly per kilometer of beach, and at Puerto Morelos fringing reef lagoon, more than 6,600 m^3/km washed ashore. Wave and wind forces are the main drivers of the circulation of the reef lagoon, so the coupled wave-hydrodynamic Delft3D-SWAN model was used to simulate *Sargassum* inflow and outflow oceanographic conditions in the lagoon. Additionally, cover areas of *Sargassum* were obtained from imagery analysis from a fixed coastal video monitoring system installed during the massive arrival event.

1 Introduction

During summer 2015, an unprecedented influx of *Sargassum spp.*, a brown pelagic macroalgae, washed along the coast of several Caribbean beaches affecting coastal ecosystems and becoming an important health and economic issue. Holopelagic *Sargassum*, represented by two species *Sargassum natans* and *Sargassum fluitans* [1, 2], is commonly found at the Sargasso Sea, a region near Bermuda, which is surrounded by the North Atlantic gyre.

Dieses Werk ist copyrightgeschützt und darf in keiner Form vervielfältigt werden noch an Dritte weitergegeben werden.
Es gilt nur für den persönlichen Gebrauch.

It is known that under normal conditions *Sargassum* travels annually across the Caribbean and the Gulf of Mexico through a cyclic path known as the *Sargassum* Loop System [3]. The circulation path starts when the Azores high pressure system lies upon the Sargasso Sea (Figure 1), causing winds strong enough to rip off *Sargassum* mats from the gyre. *Sargassum* mats can be distinguished from satellite and aircraft imagery as long rows floating in the direction of the wind (similar to Langmuir cells) of less than 0.5 m of diameter [4]. This mats then enter to the Caribbean Sea by 3 passages (Windward, Mona and Anegada) located on the Antilles. Inside the Caribbean, *Sargassum* is carried northward by the Carribean current and then into to the Gulf of Mexico. The path ends on the northwest Atlantic with the *Sargassum* driven by the Florida current back into the Sargasso Sea [3, 5].

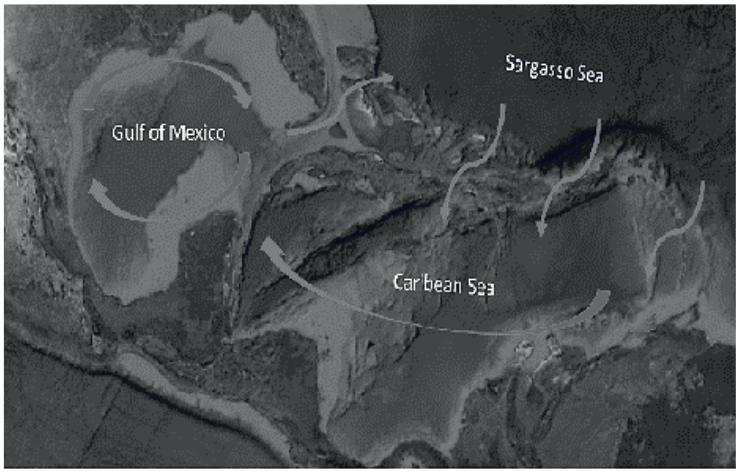

Figure 1: *Sargassum* Loop System

Nevertheless, since 2011 the atypical arrival of *Sargassum* mats has been reported in places as far as the west coast of Africa and northern Brazil [6, 7], suggesting the existence of a new reservoir located inside the North Equatorial Recirculating Region (NERR) located between 3°N to about 10°N in the tropical Atlantic (Figure 2). This reservoir may have stablished as the result of an ocean-scale over accumulation of *Sargassum* occurred in 2011, which then spread throughout the NEER in 2012 and stablished inside the gyre due to warmer nutrient-rich surrounding water [8].

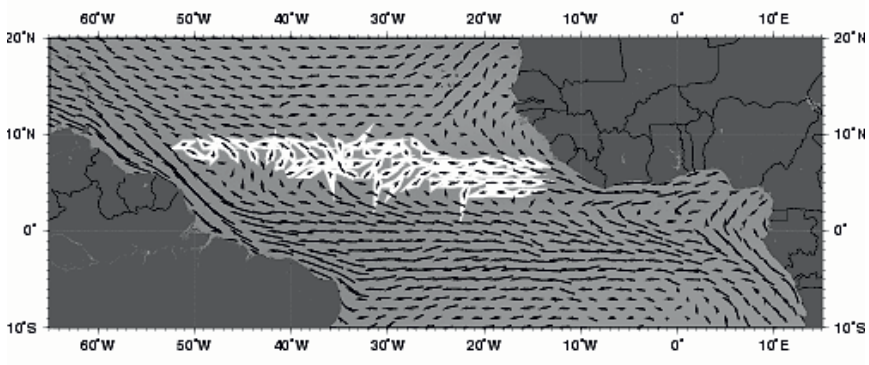

Figure 2: Location of the North Equatorial Recirculating Region

Dieses Werk ist copyrightgeschützt und darf in keiner Form vervielfältigt werden noch an Dritte weitergegeben werden.
Es gilt nur für den persönlichen Gebrauch.

On the open ocean, *Sargassum* serves as spawning area and nursery to sea turtles and fish (some of them of commercial importance), provides shelter to marine birds, fish, invertebrates and other marine organisms [9]. At normal amounts, *Sargassum* landings benefit the benthic community providing nutrients derived from its decomposition; it also stimulates the growth of coastal vegetation and prevents beach erosion during its arrival [10, 11]. On the contrary, great amounts of *Sargassum* represent a major problem to the ecosystem. Huge rafts of *Sargassum* prevent the light to penetrate, leading to the death of submerged aquatic vegetation and corals. Also, the input of excess nutrients to the system derived from high decomposition rates, leachates, and H_2S formation becomes difficult to assimilate by the system, causing the eutrophication of the area covered by *Sargassum* [8]. Additionally, beach morphology could be modified due to *Sargassum* removal performed by nearby hotels, in which heavy machinery is used to collect the algae leading to the compacting of sand and the erosion of the beach [12, 13].

In the Mexican Caribbean, massive landings of *Sargasssum* occurred during late summer 2015 (Figure 3). Quintana Roo was the state with the most affected coastline by *Sargassum* over accumulation, being Benito Juarez and Tulum the municipalities with most *Sargassum* removed (37,859 and 19,382 m^3 in total, respectively). About 9,726 m^3 of *Sargassum* accumulated monthly per kilometer of coastline. And although most of it was remove, more than 90% of the beaches remained uncleaned, becoming a public health problem and causing environmental hazard [8, 12].

Figure 3: *Sargassum* invasion to Puerto Morelos beach during summer 2015

1.1 State-of-the-art

In order to understand the causes of *Sargassum* over accumulation on the beach, it is of utmost importance to assess the regional and local conditions driving the permanence of *Sargassum* on coastal areas. Specifically, on Puerto Morelos reef lagoon there is mainly journalistic information about the massive arrivals and a list of the amount of *Sargassum* collected throughout the event provided by the Ministry of Environment and Natural Resources of Quintana Roo and the National Commission of Natural Protected Areas. Nevertheless, as a product of the devastating effects, a Technical-Scientific Committee was formed by the academic community and some governmental institutions in order to provide information about the *Sargassum* atypical arrivals with investigations on course [12]. Additionally, investigations of the ecological damages caused by the

Dieses Werk ist copyrightgeschützt und darf in keiner Form vervielfältigt werden noch an Dritte weitergegeben werden.
Es gilt nur für den persönlichen Gebrauch.

massive *Sargassum* landings of 2015 in Puerto Morelos showed a devastating effect on nearshore seagrass meadows that resulted in a 61.6–99.5% loss of below ground biomass [8]. Also, Silva et al. [14] reported the decline of an artificial coral reef constructed 120 m offshore for coastal protection caused by low pH, anoxic conditions, nutrient excess, and poor water transparency during the massive *Sargassum* event.

To date, no explanation has been established related to the circulation of *Sargassum* in the reef lagoon. However, the general circulation of the reef lagoon of Puerto Morelos has been studied before. Coronado et al. [15] showed using 4 acoustic doppler profilers distributed in the vicinity of the lagoon that there is a surface flow induced by the breaking waves entering the lagoon and a strong flow leaving the lagoon through the north and south channels. Also, [16, 17] used the WAPO/COCO, SWAN/Delft3D, and SWASH models, respectively, to model the wave-induced circulation in the reef lagoon under hurricane conditions. Similarly, [18] used the Delft3D model to describe the mechanisms that govern the circulation of the reef lagoon.

With the aim of contributing to the understanding of this unprecedented phenomenon, the objective of this study is to describe the oceanographic and atmospheric conditions driving the permanence and dispersion of *Sargassum* in the fringing reef lagoon of Puerto Morelos during *Sargassum* atypical arrivals.

1.2 Study area diagnostic

Puerto Morelos fringing reef lagoon is located on the northeaster region of the Yucatán Peninsula between 20.8478° N and 86.8755° W, 30 km south of Cancun (Figure 4). The region is home to various ecosystems including coastal dunes, mangrove wetlands, seagrass beds, and coral reefs, all of whom being of special importance because of multiple roles such as protection from natural hazards (hurricanes, storms and floods) that are very common to the zone, mitigation of storm surge and debris movement, wave energy attenuation, sediment capture, erosion reduction, shelter and nursery of several marine species including birds, turtles, fish, and invertebrates, among others [19, 20].

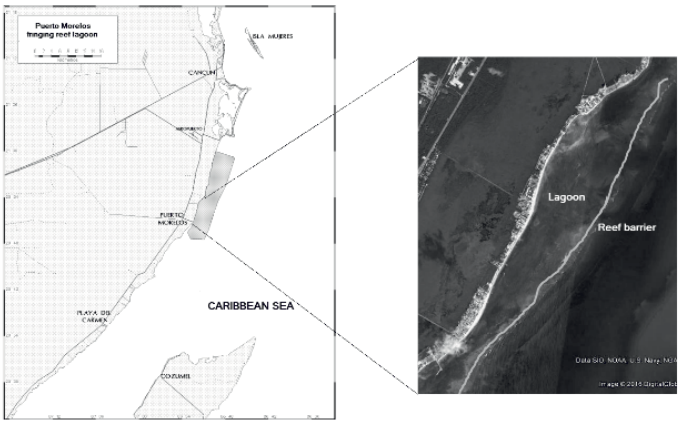

Figure 4: Puerto Morelos fringing reef lagoon location

Dieses Werk ist copyrightgeschützt und darf in keiner Form vervielfältigt werden noch an Dritte weitergegeben werden.
Es gilt nur für den persönlichen Gebrauch.

Easterly Trade Winds dominate the region with average speed between 3-9 m/s. Offshore, waves are generated by the Trade Winds, while inside the lagoon waves are largely attenuated after breaking on the reef. Offshore, average wave height is about 0.8 m with a wave period between 6-8 s with a microtidal regime prevailing on the lagoon. The circulation inside the reef lagoon is primarily influenced by incident wave energy with an external influence of the Yucatan Current [15]. It is connected to the ocean by two inlets on the north and a dredged navigational channel (up to 8 m depth) on the southern end. Water influx between the lagoon and the sea is controlled by wave height and sea level, with wave-induced flows moving into the lagoon and strong flows exiting through the channels [19]. The reef extends 4 km alongshore, creating a shallow reef lagoon of 3-4 m depth and a variable width between 500-1500 m. The fore reef slope is 0.023 at depths of 20-25 m. Salinity ranges from 35.3 to 36 g/kg. The major terrestrial nutrient input drivers are submarine ground water discharges with high phosphorus (75 to 217 kg P/km*year) and nitrogen ($2.4x10^3$ kg N/km*year) concentrations. Pollution has been attributed to the lack of wastewater treatment and heavy tourism [21].

The main income in the region remains on touristic activities with about 15 million visitors to Quinta Roo per year. The second most important economic activity is fishing, being fish and lobster the principal fisheries [12].

During *Sargassum* landfall to Puerto Morelos beach, between 6.6 and $9.6x10^3$ m^3/km of seaweed was washed ashore by the waves and wind, creating a rotting mass that kept growing as *Sargassum* continue arriving. In addition to the rotting mass, animals such as fish, turtles and some invertebrates were trapped by the seaweed and died of suffocation because they could not find their way out of the *Sargassum,* or due to anoxic conditions. The nitrogen input during the peak months of the *Sargassum* event was 3.8 to 11.6 times greater than the whole input from the aquifer in the Yucatan Peninsula of a single year, causing the eutrophication of the area. Because of the great amount of *Sargassum* lying on the beach, heavy machinery was used for its removal, leading to the destruction of turtle nests, compacting sand, and resulting in beach erosion due to the removal of over 60% of sand from the total volume of the *Sargassum* pile [12].

2 Materials and Methods

In order to contribute to the understanding of these atypical massive arrival events, the circulation of *Sargassum* inside the lagoon was modelled using the coupled wave-hydrodynamic numerical model Delft3D-SWAN with waves and wind as forcing parameters. A 17 day simulation was performed using wind and wave conditions from peak and low periods of *Sargassum* coverage on the beach and sea. Such conditions were based on a time series of *Sargassum* coverage obtained from a series of digital images taken from a fixed video system (SIRENA) installed at the Academic Unit Puerto Morelos Reef System from the National Autonomous University of Mexico during the atypical arrival event. It should be mentioned that the SIRENA system was thought to be installed for a project related to coastline change monitoring, thus the images of the *Sargassum* event were obtained from mid-September to December 2015.

Dieses Werk ist copyrightgeschützt und darf in keiner Form vervielfältigt werden noch an Dritte weitergegeben werden.
Es gilt nur für den persönlichen Gebrauch.

The areas covered by *Sargassum* on the images were obtained using a MATLAB routine based on the Otsu method for segmentation by thresholding. The method helps separating objects in the image based on their maximum variance or optimum threshold. In this case, it separates *Sargassum* from coastal vegetation, sand, and water, resulting in *Sargassum* coverage polygons (Figure 5) that were orthorectified to obtain a corrected image in real world coordinates and then to estimate the coverage areas (Figure 6).

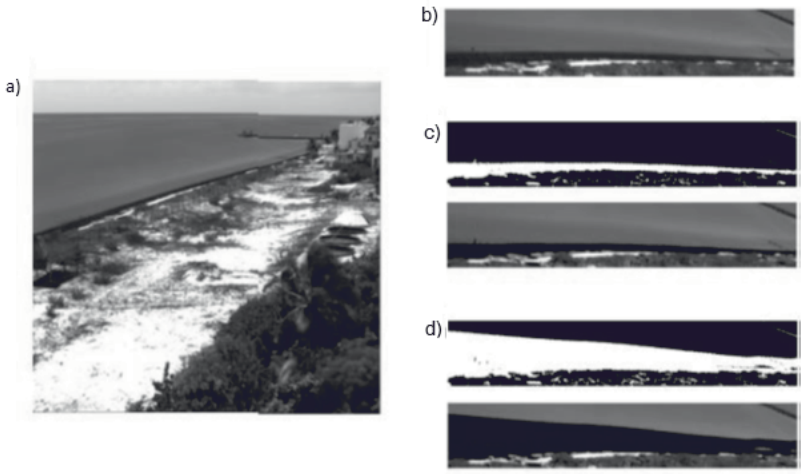

Figure 5: (a) Resulting image of SIRENA video system, (b) Selected regions of interest to be processed, (c and d) Detection of *Sargassum* coverage on the beach and water using Otsu method

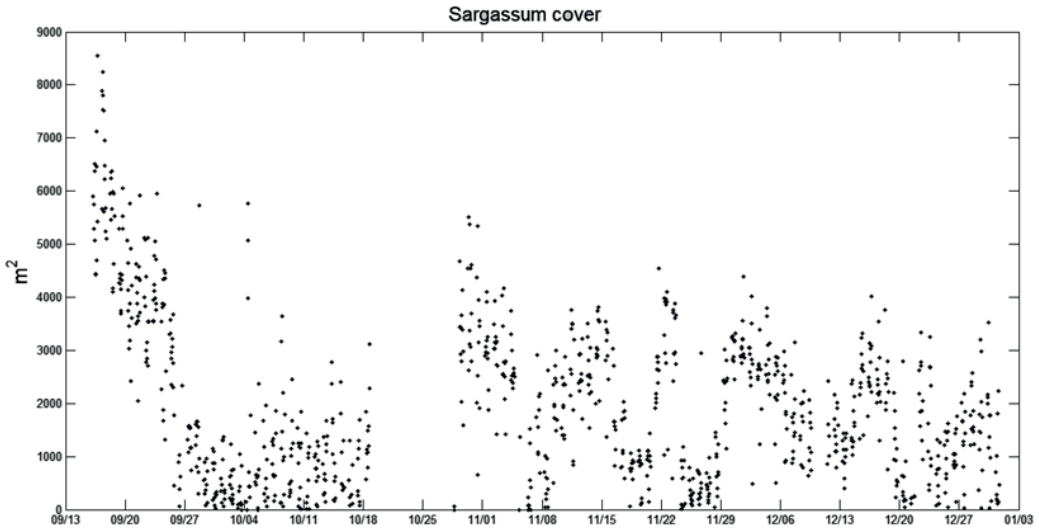

Figure 6: *Sargassum* coverage time series during 2015 atypical event. Coverage areas are estimated from September 16 to December 31.

For model validation, wind and tide data were obtained from the Academic Service of Meteorological and Oceanographical Monitoring of the National Autonomous University of Mexico

Dieses Werk ist copyrightgeschützt und darf in keiner Form vervielfältigt werden noch an Dritte weitergegeben werden.
Es gilt nur für den persönlichen Gebrauch.

in Puerto Morelos. Wave data were taken from station 42056 of NOAA National Buoy Data Center, located on the Yucatán basin.

To simulate the permanence inside the lagoon and the seaward dispersion of *Sargassum* from the lagoon, 6 punctual discharges located along the fore reef were used during a 17 day simulation.

3 Results and Discussion

Little is known about the conditions behind the massive arrival of *Sargassum* to the coasts of the Caribbean, but some studies focused on tracking back the *Sargassum* path based on sighting reports and satellite imagery, leading to the creation of two forecast systems. The first one is called the SEAS (*Sargassum* Early Advisory System) program by Texas A&M University, who has already been forecasting the arrival of *Sargassum* to the coast of Texas since 2010 and extended its watch to the Caribbean Sea. The SEAS program based their watching system in Landsat 8 satellite images and on reports from the public, reaching an accuracy of 97% with a 7 day prevision [3]. The second forecasting system is the SaWS (*Sargassum* Watch System) program developed by the University of South Florida, which forecasts mainly Florida, but also the Caribbean Sea, Bahamas and the western tropical Atlantic. Its forecasting system is based on drifting buoys data and satellite imagery from MODIS (Moderate Resolution Imaging Spectroradiometer), VIIRS (Visible Infrared Imaging Radiometer Suit), and Landsat 8. *Sargassum* is detected with a Floating Algae Index, and its circulation path is estimated with the HYCOM model [22]. Although these programs remain active there is still a need to propose local or regional circulation models so that specific paths along the coast could be described and critical areas for the accumulation of *Sargassum* could be detected.

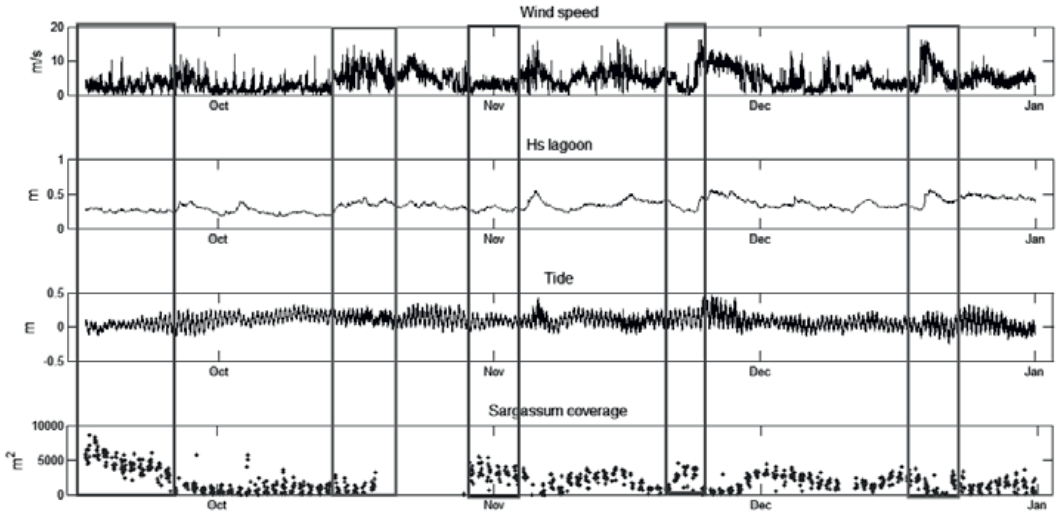

Figure 7: Oceanographic variables and *Sargassum* coverage time series from mid September to December 31. Low wind and wave conditions, and high *Sargassum* coverage are indicated inside the first, third and fourth rectangles. High wind and wave conditions and low *Sargassum* coverage are indicated inside the second and fifth rectangles.

Dieses Werk ist copyrightgeschützt und darf in keiner Form vervielfältigt werden noch an Dritte weitergegeben werden.
Es gilt nur für den persönlichen Gebrauch.

Two peaks of *Sargassum* accumulation were observed in the reef lagoon of Puerto Morelos: One in mid-September being the highest accumulation, and the other one in November. Comparing the results obtained from the time series of *Sargassum* coverage with the oceanographic variables driving the circulation of the reef lagoon (wind and wave), it is observed that when low wind and wave conditions (~4 m/s and ~0.3 m, respectively) prevail, *Sargassum* coverage on the beach increases. On the other hand, when wind was between 10 and 15 m/s, *Sargassum* coverage was at its lowest (Figure 7). During the atypical event of *Sargassum* arrival, it was observed that there was a reduction in the amount of seaweed arriving to the beach by the end of 2015 and by mid-2016, *Sargassum* was reported just from few beaches of Cancun and Playa del Carmen [12].

Results from the hydrodynamic simulation showed weak outflows on the northern entrance of the reef lagoon. The maximum velocity reached by the flows was between 0.06 and 0.07 m/s, which can lead to the increase of the residence time of both water and *Sargassum* inside the lagoon due to low dynamics (Figure 8).

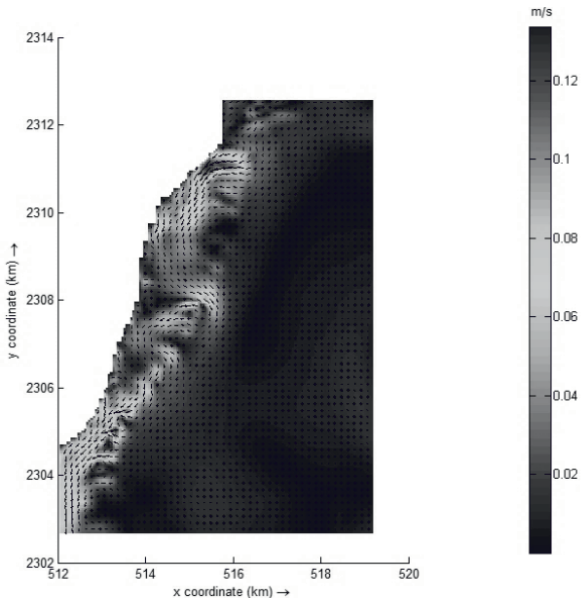

Figure 8: Results of the coupled wave-hydrodynamic model for boundary conditions of Hs=0.3 m, Tp=6s, θ= 90°, Simulation for low wave and wind conditions

During strong wind and wave conditions, it can be observed strong outflows at the northern and southern entrances and also strong inflows at the reef tops (Figure 9). This could lead to a more dynamic circulation inside the lagoon and to the reduction of the residence time. It was reported that during the atypical events, the seaweed was carried away from the lagoon during small storms events [12].

Dieses Werk ist copyrightgeschützt und darf in keiner Form vervielfältigt werden noch an Dritte weitergegeben werden.
Es gilt nur für den persönlichen Gebrauch.

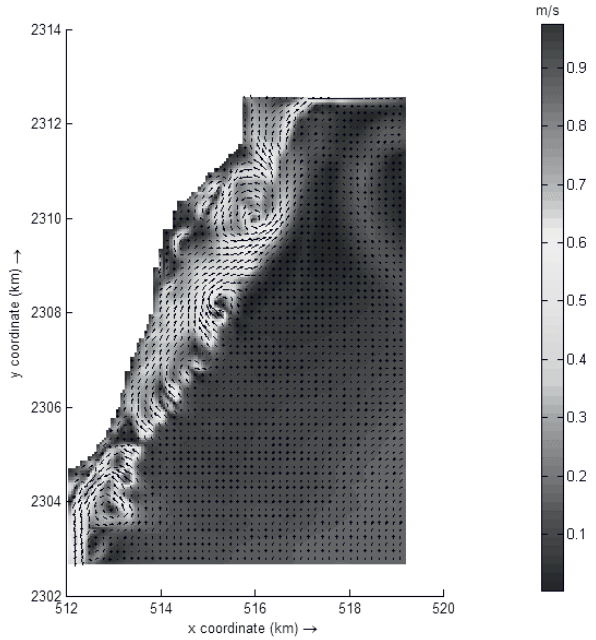

Figure 9: Results of the coupled wave-hydrodynamic model for boundary conditions of Hs=1.75 m, Tp=10s, θ=135°, Simulation for high wave and wind conditions

Punctual discharges showed a major flux of *Sargassum* in the northern entrance. By day 8 of the simulation, the maximum accumulation of *Sargassum* inside the reef lagoon was observed, especially on the northern entrance (Figure 10a). This could be explained by low wave conditions (< 0.36 m) and wind less than 4 m/s (Figure 11). By day 13, an increase of wind velocity (above 5 m/s) and of wave height (> 0.42 m) was observed, which leads to the decrease in *Sargassum* accumulation inside the lagoons. Nevertheless, a persistent accumulation on the southern entrance was observed (Figure 10b).

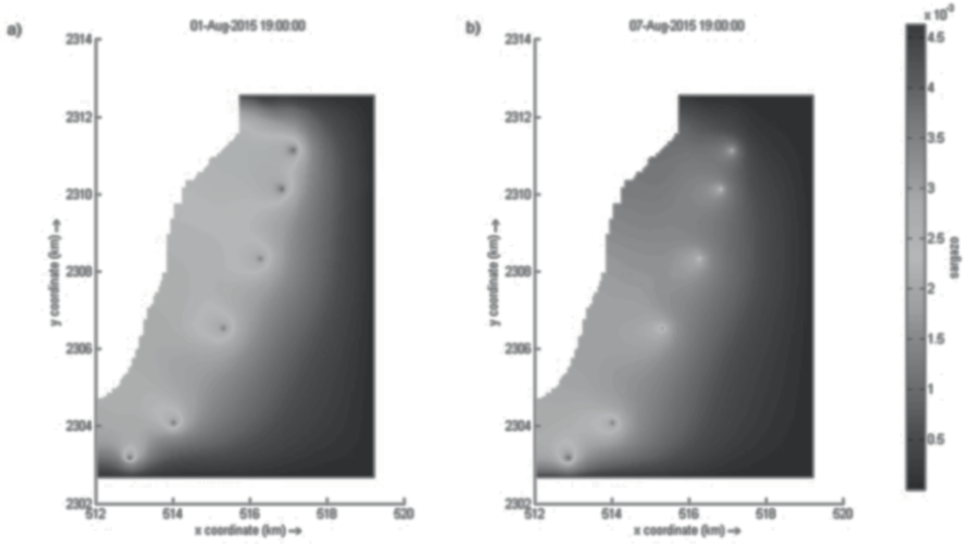

Figure 10: (a) Simulation results showing *Sargassum* maximum accumulation inside the reef lagoon, (b) Simulation results showing *Sargassum* decrease inside the reef lagoon.

Dieses Werk ist copyrightgeschützt und darf in keiner Form vervielfältigt werden noch an Dritte weitergegeben werden.
Es gilt nur für den persönlichen Gebrauch.

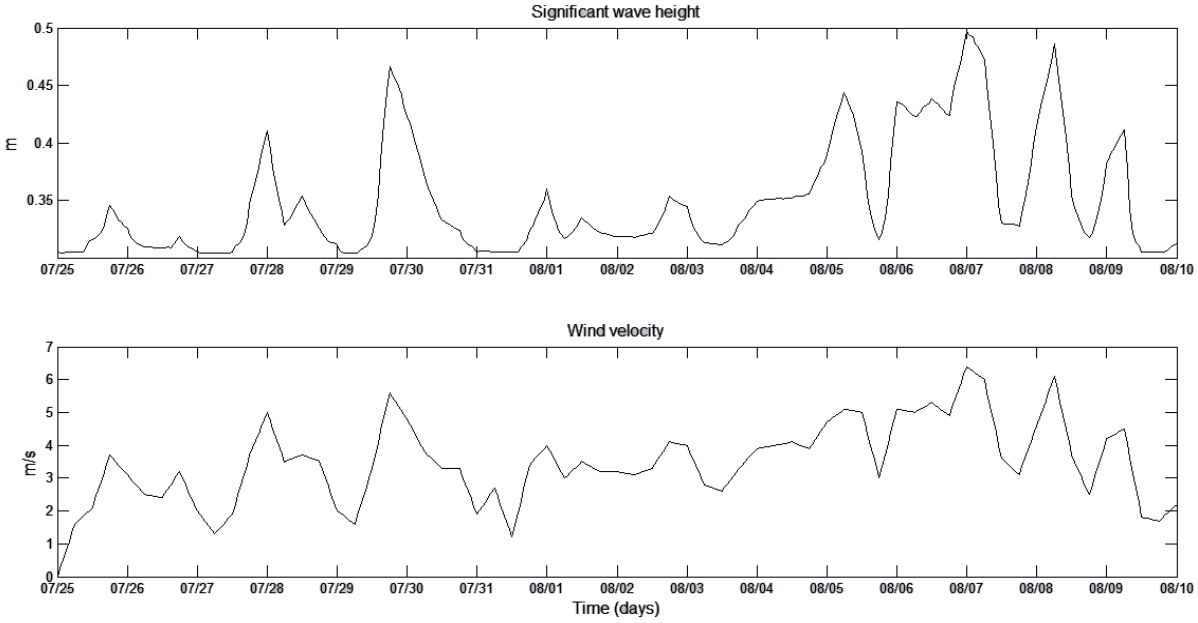

Figure 11: (Top) Significant wave height time series obtained from the 17-day simulation. (Bottom) Wind velocity time series obtained from the 17-day simulation.

4 Conclusions

As preliminary conclusions, it can be said that the permanence of *Sargassum* on the beach is driven by low swell conditions, sporadic wind gusts, and high tide range. Its dispersion is favoured under intense swell conditions, which in turn generate a wide swash zone promoting the lagoon circulation and hence the circulation of *Sargassum*. Nevertheless, it is still important to identify vulnerable areas to the over accumulation of *Sargassum* so that measures against the effects of atypical arrivals could be implemented in a way that do not compromise the welfare of the coastal environment and its associated wildlife and flora.

5 Acknowledgments

Thanks to the Academic Service of Meteorological and Oceanographic Monitoring of the UASA of the ICML of the National Autonomus University of Mexico (UNAM), MSc. Francisco Gerardo Ruiz Rentería, MSc. José Edgar Escalante Mancera and Ing. Miguel Ángel Gómez Reali, for the wind and tide data provided, to the Institute of Engineering of UNAM through the internal project 5341 “Implementation of a video monitoring station to obtain indicators of vulnerability to erosion” for providing the images for *Sargassum* segmentation analysis.

Authors are also thankful to Federal Ministry for Economic Affairs and Energy, Germany (BMWi), German Academic Exchange Service (DAAD), Excellence Center for Development Cooperation, Sustainable Water Management (EXCEED/ SWINDON), and Technical University of Braunschweig (TUBS) for their financial and technical supports, enabling to participate at the Summer School on Integrating Ecosystems in Coastal Engineering Practice (INCECP), September 2017 in Puerto Morelos, Mexico.

Dieses Werk ist copyrightgeschützt und darf in keiner Form vervielfältigt werden noch an Dritte weitergegeben werden.
Es gilt nur für den persönlichen Gebrauch.

6 References

1. Huffard, C.L., von Thun, S., Sherman, A.D., Sealey, K., Smith, K.L.: Pelagic Sargassum community change over a 40-year period: temporal and spatial variability. Marine Biology 161, 2735-2751 (2014)
2. Széchy, M.T.M.d., Guedes, P.M., Baeta-Neves, M.H., Oliveira, E.N.: Verification of Sargassum natans (Linnaeus) Gaillon (Heterokontophyta: Phaeophyceae) from the Sargasso Sea off the coast of Brazil, western Atlantic Ocean (2012)
3. Frazier, J.: Advanced Prediction of the Intra-Americas Sargassum Season through Analysis of the Sargassum Loop System Using Remote Sensing Technology. vol. M.Sc. Texas A & M University (2014)
4. Marmorino, G.O., Miller, W.D., Smith, G.B., Bowles, J.H.: Airborne imagery of a disintegrating Sargassum drift line. Deep Sea Research Part I: Oceanographic Research Papers 58, 316-321 (2011)
5. Gavio, B., Rincón-Díaz, M.N., Santos-Martinez, A.: Massive quantities of pelagic sargassum on the shores of San Andres island, southwestern Caribbean. Acta Biológica Colombiana 20, 239-241 (2015)
6. Johnson, D., Ko, D., Franks, J., Moreno, P., Sanchez-Rubio, G.: The Sargassum invasion of the Eastern Caribbean and dynamics of the Equatorial North Atlantic. Proceedings of the 65th Gulf and Caribbean Fisheries Institute 65, 102-103 (2013)
7. Smetacek, V., Zingone, A.: Green and golden seaweed tides on the rise. Nature 504, 84-88 (2013)
8. van Tussenbroek, B.I., Hernández Arana, H.A., Rodríguez-Martínez, R.E., Espinoza-Avalos, J., Canizales-Flores, H.M., González-Godoy, C.E., Barba-Santos, M.G., Vega-Zepeda, A., Collado-Vides, L.: Severe impacts of brown tides caused by Sargassum spp. on near-shore Caribbean seagrass communities. Marine Pollution Bulletin 122, 272-281 (2017)
9. Laffoley, D.d.A., Roe, H., Angel, M., Ardron, J., Bates, N., Boyd, L., Brooke, S., Buck, K., Carlson, C., Causey, B.: The protection and management of the Sargasso Sea: The golden floating rainforest of the Atlantic Ocean: Summary Science and Supporting Evidence Case. 44 (2011)
10. Chelazzi, L., Colombini, I.: Influence of Marine Allochthonous Input on Sandy Beach Communities. Oceanography and Marine Biology, An Annual Review, Volume 41, pp. 115-159. CRC Press (2003)
11. Webster, D., Taylor, Roberts: A quantitative investigation of the role of Sargassum accumulation plays in inhibiting sand erosion on Galveston Island's west-end beaches. Symposium conducted at the meeting of the Sargassum Symposium, Corpus Christi, TX. (2008)

Dieses Werk ist copyrightgeschützt und darf in keiner Form vervielfältigt werden noch an Dritte weitergegeben werden.
Es gilt nur für den persönlichen Gebrauch.

12. Rodríguez-Martínez, R., Tussenbroek, B., Jordán-Dahlgren, E.: Afluencia masiva de sargazo pelágico a la costa del Caribe mexicano (2014-2015). Caribe Mexicano, pp. 352-365. Universidad Nacional Autónoma de México, Instituto de Ciencias del Mar y Limnología, Unidad Académica Puerto Morelos, Mexico (2016)

13. Webster, R.K., Linton, T.: Development and implementation of Sargassum early advisory system (SEAS). Shore & Beach 81, 1 (2013)

14. Silva, R., Mendoza, E., Mariño-Tapia, I., Martínez, M., Escalante, E.: An artificial reef improves coastal protection and provides a base for coral recovery. Journal of Coastal Research SI 75, 467-471 (2016)

15. Coronado, C., Candela, J., Iglesias-Prieto, R., Sheinbaum, J., López, M., Ocampo-Torres, F.J.: On the circulation in the Puerto Morelos fringing reef lagoon. Coral Reefs 26, 149-163 (2007)

16. Marino-Tapia, I., Silva, R., Enriquez, C., Mendoza-Baldwin, E., Escalante-Mancera, E., Ruiz-Rentería, F.: Wave transformation and wave-driven circulation on natural reefs under extreme hurricane conditions. Proceedings of 32nd Conference on Coastal Engineering, pp. n. 32, p. waves.28, Shanghai, China (2011)

17. Torres-Freyermuth, A., Mariño-Tapia, I., Coronado, C., Salles, P., Medellín, G., Pedrozo-Acuña, A., Silva, R., Candela, J., Iglesias-Prieto, R.: Wave-induced extreme water levels in the Puerto Morelos fringing reef lagoon. Natural Hazards and Earth System Sciences 12, 3765-3773 (2012)

18. Enriquez, C., Mariño-Tapia, I., Valle-Levinson, A., Torres-Freyermuth, A., Silva-Casarín, R.: Mechanisms driving the circulation in a fringing reef lagoon: a numerical study. Book of Abstracts of the Physics of Estuaries and Coastal Seas Symposium, (2012)

19. Ruiz de Alegria-Arzaburu, A., Mariño-Tapia, I., Enriquez, C., Silva, R., González-Leija, M.: The role of fringing coral reefs on beach morphodynamics. Geomorphology 198, 69-83 (2013)

20. Spalding, M.D., Ruffo, S., Lacambra, C., Meliane, I., Hale, L.Z., Shepard, C.C., Beck, M.W.: The role of ecosystems in coastal protection: Adapting to climate change and coastal hazards. Ocean & Coastal Management 90, 50-57 (2014)

21. Hernández-Terrones, L., Rebolledo-Vieyra, M., Merino-Ibarra, M., Soto, M., Le-Cossec, A., Monroy-Ríos, E.: Groundwater Pollution in a Karstic Region (NE Yucatan): Baseline Nutrient Content and Flux to Coastal Ecosystems. Water, Air, Soil Pollution 218, 517-528 (2011)

22. Hu, C., Murch, B., Barnes, B., Wang, M., Maréchal, J., Franks, J., Lapointe, B., Goodwin, D., Schell, J., Siuda, A.: Sargassum watch warns of incoming seaweed. Eos - Earth & Space Science News 97 (2016) https://doi.org/10.1029/2016EO058355

Dieses Werk ist copyrightgeschützt und darf in keiner Form vervielfältigt werden noch an Dritte weitergegeben werden.
Es gilt nur für den persönlichen Gebrauch.

LONG-TERM BEACH AND COASTAL DUNE DYNAMICS IN RESPONSE TO NATURAL AND HUMAN-MADE FACTORS

M. Luisa Martínez[1], Rosario Landgrave[1], Rodolfo Silva[2], Patrick Hesp[3]

[1] Red de Ecología Funcional, Instituto de Ecología, A.C., Xalapa, Veracruz, Mexico, marisa.martinez@inecol.mx

[2] Laboratorio de Costas y Puertos, Instituto de Ingeniería, UNAM, Mexico City, Mexico

[3] Beach and Dune Systems (BEADS) Laboratory, College of Science and Engineering, Flinders University, South Australia, 5041

Keywords: Breakwaters, Coastal Dunes, Mexico, Mobile Dune Stabilization, Urbanization

Abstract

This study took place in Playa Chachalacas, located in the central region of the Gulf of Mexico. The goal of this study was to understand the long-term consequences of modifying sediment dynamics through the combined effect of dune stabilization and the construction of breakwaters for shoreline protection. With aerial images from different years, the following items were analyzed: (a) stabilization of the mobile dune; (b) shoreline dynamics and changes at the river mouth, located down-drift from the dunefield; and (c) urbanization along the shoreline. Data show that the cover of grasses and shrubs increased rapidly. In some points, there was intense erosion along the shoreline and accretion in others. The breakwaters promoted accretion but exacerbated erosion down-drift, with notable changes in the inlet. Finally, urbanization has occurred at a fast rate, and mostly parallel to the shoreline. The results indicate that different factors affect sediment dynamics: (a) warm and wet climate promoted vegetation growth and sediment stabilization; (b) the breakwaters solved the erosion problem locally, but generated intense erosion down-drift; and (c) urbanization along the coast resulted in ecosystem loss and increased risks to flooding. Indeed, management and development plans for coastal environments need to consider the dynamic nature of the coastline.

1 Introduction

In Mexico, coastal dunes are abundant: they cover nearly 800,000 ha and occur on both the Pacific and Atlantic coasts. In particular, the state of Veracruz, which is located in the central region of the Gulf of Mexico, has the second largest area of coastal dunes, only surpassed by Baja California Sur. The dunes of Veracruz are diverse, dynamic, and heterogeneous [1] with parabolic and transgressive dunefields being abundant, but foredunes and foredune plains are also common. These dunes have varying degrees of mobility, ranging from largely mobile to completely stabilized by vegetation, and their conservation status is also very variable. Because degradation and fragmentation have been expanding rapidly on Mexican coastal dune systems, less than 50% of the

Dieses Werk ist copyrightgeschützt und darf in keiner Form vervielfältigt werden noch an Dritte weitergegeben werden.
Es gilt nur für den persönlichen Gebrauch.

original landforms and their attendant vegetation are well preserved [1]. However, in the state of Veracruz, most of the dunes (85%) are degraded at some level.

Different factors affect the dynamics of coastal dunes in Mexico. First, the yearly impact of hurricanes and cold fronts bring about intense storm surges, which oftentimes result in severe erosion that can modify their natural patterns, when human interference is present. Erosion can be a natural process that occurs on the coasts and plays a key role in shoreline dynamics. However, it becomes problematic when (a) human intervention modifies hydro-sedimentary dynamics and, thus, natural beach processes are altered, and (b) infrastructure is threatened, especially when it is built too close to the beach and on erosive coasts. Specifically, the state of Veracruz is amongst the states most exposed to waves and storm surges induced by hurricanes and cold fronts, whose impact may cover many kilometres along the coast, affecting large regions.

On top of these hydrometeorological phenomena, human impact is also extensive. The richness of natural resources of the coast has historically provided relevant trading opportunities to society. In this sense, the modification and human encroachment along the coast of the state of Veracruz began several centuries ago with the construction of the Port of Veracruz in 1519 [2], which was built on top of coastal dunes. Gradually but constantly, the alteration of the coasts of Veracruz has continued to the present days and is coupled with a demographic explosion and urban expansion. Currently, 7.6 million people inhabit the state of Veracruz, of which 28% (2.2 million) live less than 20 km from the coastline and 20% (1.5 million) live in low elevation coastal zones of less than 10 m above sea level. As urban encroachment on the coast expands, so does the human impact. In brief, the current situation of the coasts of Veracruz is like that of other regions: an increasing human population and urbanization with high risks to storm exposure and erosion, and increasing degradation.

A good example of the situation described above occurs in Playa de Chachalacas, a mostly national tourist destination [3], located in the central region of the Gulf of Mexico. In this location, the dunefield is wide in the north and narrows to a thin coastal strip in the south (Figure 1). The coastal transgressive dunefield in the northern portion of Playa Chachalacas is among the tallest and largest in Mexico. It covers 3,200 ha (4 x 8 km) and dunes reach up to 40 m in height. The dominant winds blow almost parallel to the coast and the dunefield is, therefore, migrating along-coast from the north to the south. Some of these dunes are unique in Mexico in terms of their geomorphological attributes, and include different types, such as foredunes, transverse and barcahnoid dunes, parabolic dunes, transverse dune trailing ridges, and gegenwall ridges, among others [4, 5]. These dunes are extremely diverse: they are very mobile near the ocean, but inland, they become gradually stabilized by both natural (coastal shrubland and tropical rainforest) and anthropogenic vegetation (croplands, rangelands). Specialized plant species such as *Chamaecrista chamaecristoides*, *Palafoxia lindenii, Croton punctatus*, and *Diphysa robinioides* grow on the conserved and mobile dunes. All of them are tolerant to burial by sand and, thus, are considered as psammophytes [6, 7]. Furthermore, *C. chamaecristoides* and *P. lindenii* are endemic to Mexican coastal dunes [8].

Dieses Werk ist copyrightgeschützt und darf in keiner Form vervielfältigt werden noch an Dritte weitergegeben werden.
Es gilt nur für den persönlichen Gebrauch.

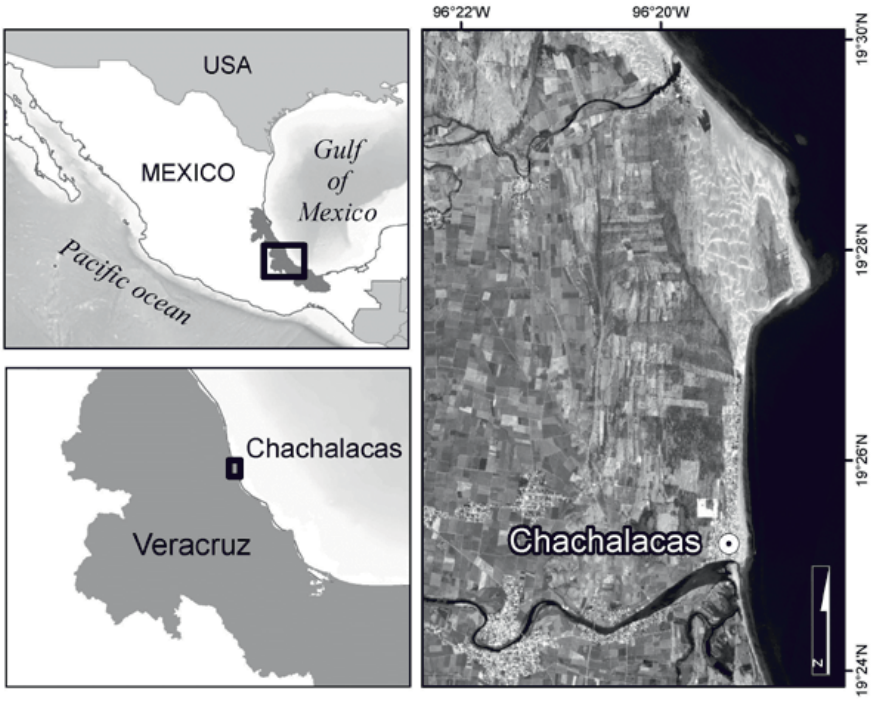

Figure 1: Location of the study sites in the Mexican Gulf of Mexico

In recent years, four phenomena have occurred in the location that modified the natural dynamics of the beach and dune system. First, a relatively large fraction of the dunes has become stabilized through the natural growth of vegetation as well as by crop plantations. This resulted in a reduced sand movement to the south (Figure 2). Second, the south-eastern margin of the larger northern transgressive dunefield has been both accreting (bulging) eastwards and changing shape over time, and this has led to a natural westwards realignment of the down-drift beach. Thus, beach erosion has become acute in the southern area, and because of this, two breakwater structures were built, likely further exacerbating erosion rather than assisting in reducing the erosion. Third, urban development has occurred along the coast, and coastal squeeze is increasing [9]. And fourth, the increasing use of off-road vehicles on the mobile dunes has further degraded the system: plants are destroyed and are then unable to hold the sand. In consequence, the protective role of the biogeomorphologically dynamic dunes is diminished as the dunes and plants deteriorated. Additionally, the destruction of the dunes decreases the scenic beauty of the area, which is another ecosystem service highly valued by tourists [10].

The aim of this study was to understand the long-term changes of Playa Chachalacas, the adjacent dunes, and river mouth, in order to infer the causes and consequences of modifying sediment dynamics by means of the combined effect of dune stabilization, and hard infrastructure used for coastal protection. The working hypothesis was that probably the dynamic equilibrium of the area is shifting to a new state with modified sedimentary dynamics, because this very large dune system is functioning differently.

Dieses Werk ist copyrightgeschützt und darf in keiner Form vervielfältigt werden noch an Dritte weitergegeben werden.
Es gilt nur für den persönlichen Gebrauch.

2 Methods

2.1 Mobile dune stabilization

Changes in vegetation cover were analysed over time from 2006 to 2017, through interpretation of aerial photographic images, and by using eCognition Developer 8.7 to generate different land cover polygons. These polygons were then classified manually, one by one, into the following categories: coastal shrubland, grassland, and bare sand (mobile dunes). The area used for this analysis included originally mobile, semi-mobile, and stabilized dunes (Figure 2). The study focused on the mobile dune area because this is where vegetation changes occurred more rapidly and were thus more evident. After identification of different land covers in each observation date, changes in the surface of each land cover type were calculated over time.

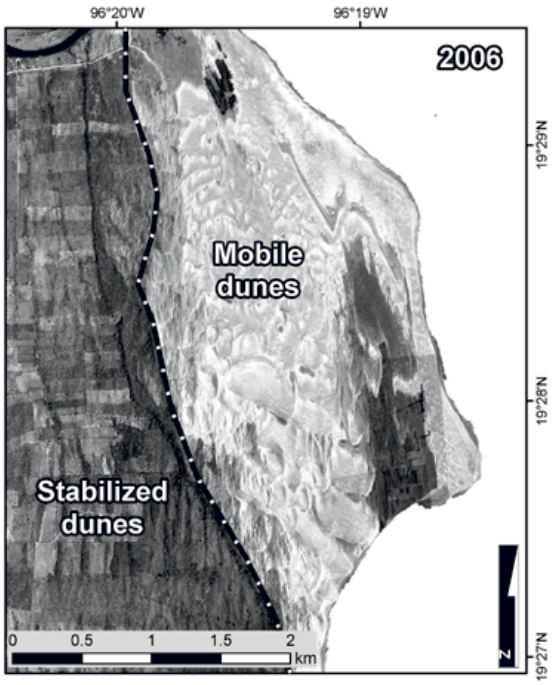

Figure 2: Aerial image from 2006 showing the largely mobile dune area in which changes in vegetation cover were analysed.

2.2 Shoreline dynamics and changes at the river mouth of Río Actopan

The shoreline of Playa Chachalacas and adjacent areas have changed drastically over the last decades, owing to natural factors as well as human-related actions such as the construction of two breakwaters offshore (Figure 3). Shoreline dynamics was analysed along the dunefield and all the way south to the mouth of Río Actopan. To achieve this, the following images were used: a 1995 mosaic of orthophotos from INEGI; 14 rectified aerial photographs from 2006 that were rectified through 112 control points; and Google Earth Images from 2017 with 100 control points that were the same as the 2006 images. On each image, the landward limit of the coastline was identified as the landward limit of the wet beach, which was the only way that allowed for the determination of

Dieses Werk ist copyrightgeschützt und darf in keiner Form vervielfältigt werden noch an Dritte weitergegeben werden.
Es gilt nur für den persönlichen Gebrauch.

the shoreline position, given the quality of the images at hand. A base line was traced, parallel to the shoreline, and here, every 20 m, additional lines were traced, perpendicular to the baseline, which were 400 m long, giving a total of 609 perpendicular lines. Following this, the intersection points between the perpendicular lines and the different coastlines were obtained, and with this, erosion and accretion rates were calculated by measuring the distance between the intersection points from different observation dates.

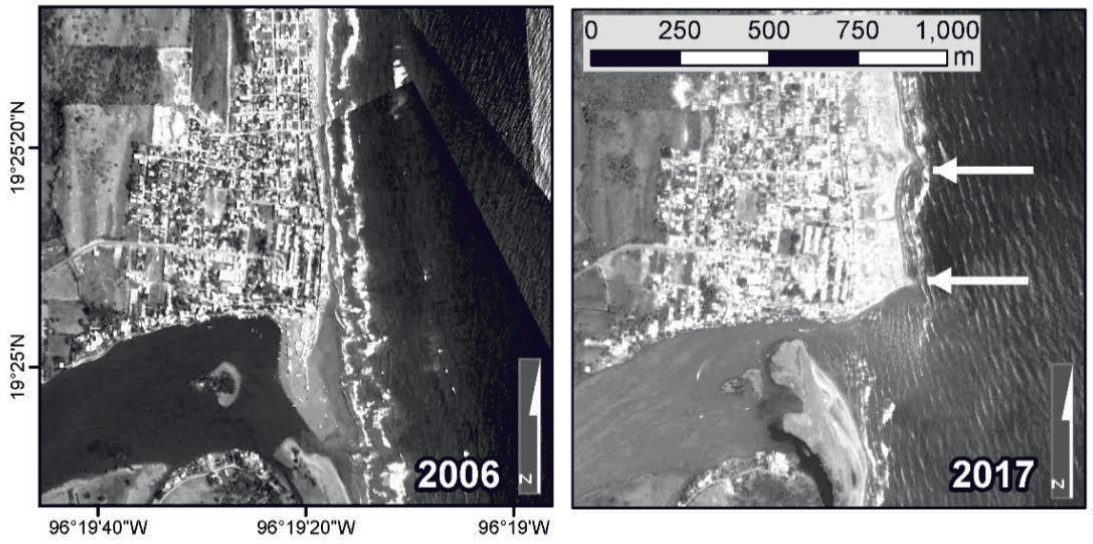

Figure 3: Shoreline changes in southern Playa Chachalacas after the construction of two breakwaters (shown by the yellow arrows). Note the marked change in the position of the shoreline and barrier system south of the river inlet in 2017

2.3 Urbanization

Using the same aerial images described above, eCognition Developer 8.7 was used as a multiresolution segmentation process with 30 as a scale parameter and 0.1 as a shape index. The result of this segmentation process was a layer of polygons that was exported in a shapefile format. Once the polygons were ready, each one was analysed manually, so that those corresponding to urban areas were recognized. The same procedure was performed for the three observation dates, and with this, changes in the urbanized surface were analysed over time.

3 Results

3.1 Transgressive dunefield stabilization and changes

The transgressive dunefield has changed rapidly during the last decades. Firstly, a large amount of sand was deposited on the southern arc-shore of the dunefield, which will, eventually, move south to the river mouth. Furthermore, the most easterly buldge of the dunefield also accreted a big deal.

Dieses Werk ist copyrightgeschützt und darf in keiner Form vervielfältigt werden noch an Dritte weitergegeben werden.
Es gilt nur für den persönlichen Gebrauch.

Vegetation cover also varied drastically. From 2006 to 2017, the vegetated area in the study site expanded and changed rapidly. In the aerial image analyses (Figure 4), data show that the area covered by bare sand, grasslands on stabilized dunes, and rangelands (grasslands for cattle) decreased, while grasslands on previously mobile dunes and coastal shrubland increased (Table 1). The relative increase (or decrease) of each land use was variable. The original area covered with grasslands on the mobile dunes, and coastal shrubland, increased by 14% and 50%, respectively. In turn, the area covered with bare sand (mobile dunes) decreased by 11%, rangelands decreased 18%, and, noteworthy, grasslands on stabilized dunes decreased by 80%. The rate of mobile dune colonization by grasses was 8.6 ha/yr. Evidence of natural succession taking place was observed, also occurring at a relatively fast rate, with grasslands in general (located previously on mobile or stabilized dunes) turning into coastal shrubland as well as abandoned grasslands for cattle also turning into shrubland (Table 1). Only 35.1 ha previously occupied by grasslands on mobile dunes became bare sand, probably owing to the natural movement of the dunefield. The above shows a rapid "greening" of the dune-field in Chachalacas, but notably, much of this is located on either the dunefield western margin or in the eastern deflation plain (Figure 4, Table 1).

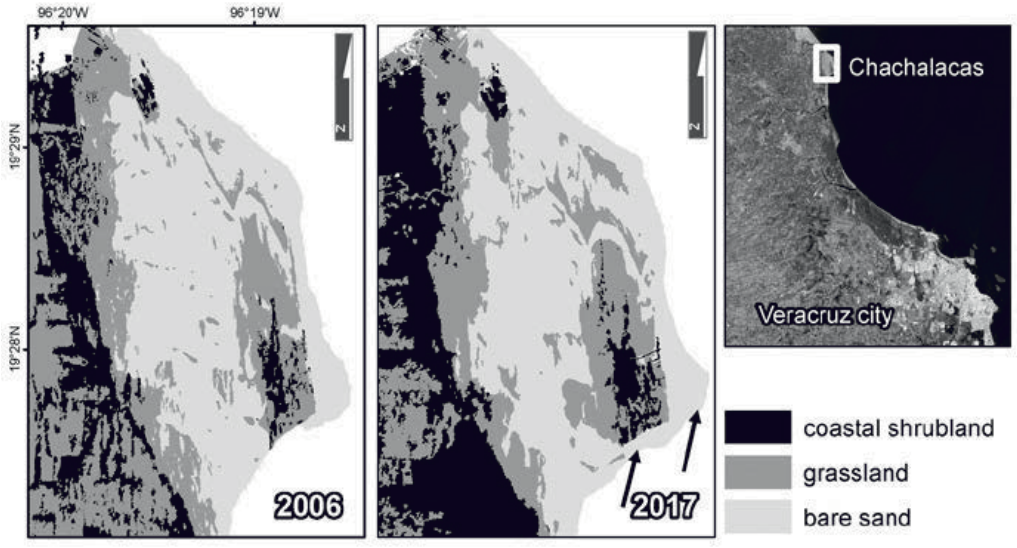

Figure 4: Aerial analyses of land cover changes from 2006 to 2017 on the largely mobile transgressive dunefield system from Chachalacas, located in the northern portion of the study region. The arrows show areas where much sand has been deposited

3.2 Shoreline changes

The analyses of shoreline changes revealed that it is very dynamic and heterogeneous. From 1995 to 2006 (Figure 5a), erosion was intense and occurred throughout most of the area, in most of our analysis points, with minimal accretion at some points. The contrary was observed from 2005 to 2017 after the construction of the breakwaters (Figure 5b). The accretion occurred during the last decade was larger than the erosion from previous years, and thus, the net change over the 20 year observation period was mostly positive, with some points showing an accretion higher than 200 m (Figure 5c).

Dieses Werk ist copyrightgeschützt und darf in keiner Form vervielfältigt werden noch an Dritte weitergegeben werden.
Es gilt nur für den persönlichen Gebrauch.

Table 1. Changes in the area covered by natural vegetation on a mobile dune system from Chachalacas, located in the central region of the Gulf of Mexico, from 2006 to 2017. The most relevant changes are highlighted in gray.

	2017					
	Bare sand	Grassland on mobile dunes	Grassland on stabilized dunes	Grassland for cattle	Coastal shrubland	TOTAL (2006)
2006						
Bare sand	372	86.5	0.4	0.1	1.4	460
Grassland on mobile dunes	35.1	132	3.6	0.5	28.2	200
Grassland on stabilized dunes	0.1	0.6	5.4	1.3	72.9	80.3
Grassland for cattle	0	0	0.7	40.9	28.9	70.5
Coastal shrubland	1.7	8.4	6.1	14.9	171	202
TOTAL (2017)	409	228	16.2	57.7	303	

The location of the erosion and accretion points was variable along the coast of Playa Chachalacas (Figure 6). The coast around the northern headland, where the dune-field is located, had some erosion from 1995 to 2006 (in the southern limit), but it expanded in the following decade on both the northern, NE, and southern margins. In turn, the beach to the south was quite stable from 1995 to 2006, with moderate erosion at the river mouth. After the breakwaters were built, the beach accreted intensely, especially on the northern spit of the river mouth of Río Actopan. Here, accretion was greater than 100 m, yielding a rate of accretion of 10 m/yr. Certainly, this retention of sediments has affected the shoreline down-drift. As the beach accreted, the shoreline south of Rio Actopan has had severe erosion, greater than 50 m over a ten-year period by 5 m/yr.

3.3 Urbanization

The urban area almost doubled during the last two decades, and this has mostly occurred along the shoreline (Figure 7). The original settlement was located along 1,890 m of the coast, and in 2017 the urbanized area occupies 3,060 m along the shoreline. The rate of urban expansion was different for each decade, being higher from 1995-2006 (2.3 ha/yr) than from 2006-2017 (1.2 ha/yr). Overall, the urban encroachment was 3.5 ha/yr from 1995-2017. Interestingly, the original settlement was established along the coast, but it also covered areas inland. Nevertheless, more recent urbanization has occurred parallel to the coastline at less than 200 m from the beach. The most recent buildings (hotels) are located almost at the base of the dune-field, which is highly risky, because the system is still largely mobile.

Dieses Werk ist copyrightgeschützt und darf in keiner Form vervielfältigt werden noch an Dritte weitergegeben werden.
Es gilt nur für den persönlichen Gebrauch.

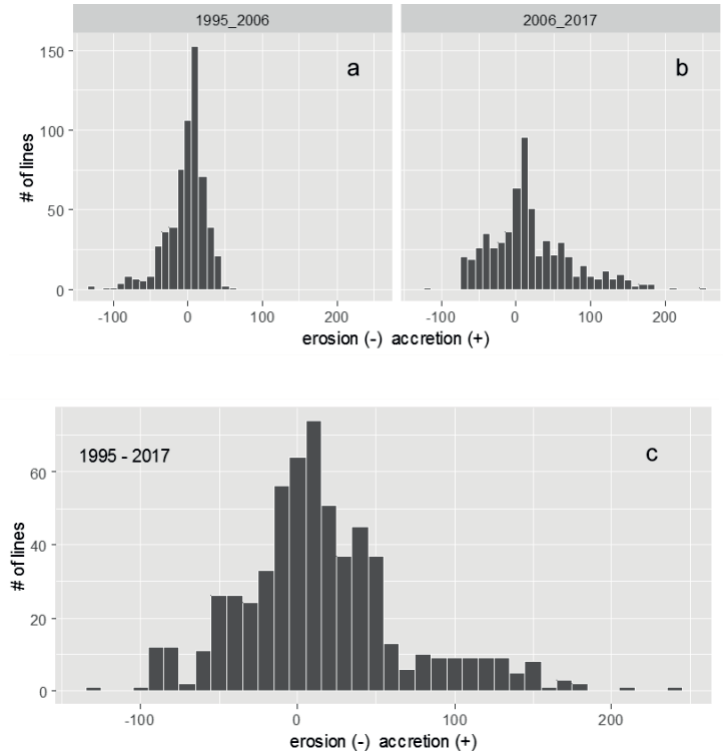

Figure 5: Histogram showing the calculated erosion and accretion at the intersection points between a base lane and the traced shorelines from three observation periods

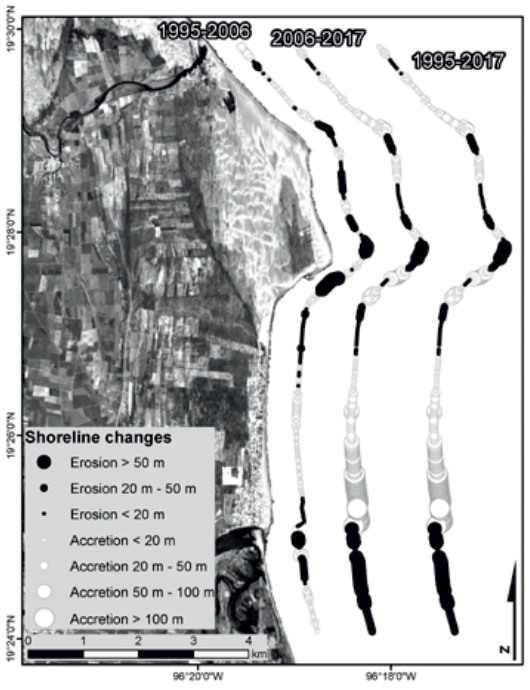

Figure 6: Changes along the shoreline of Playa Chachalacas (central region of the Gulf of Mexico) and adjacent dune-field headland and the river mouth of Río Actopan

Dieses Werk ist copyrightgeschützt und darf in keiner Form vervielfältigt werden noch an Dritte weitergegeben werden.
Es gilt nur für den persönlichen Gebrauch.

4 Discussion

The analyses show that Playa Chachalacas and adjacent dunes and river mouth are very dynamic, owing to both natural processes and human-related factors. The greening of the dune area in terms of mobile dune colonization and ecological succession is notable and has occurred at a relatively rapid rate. Natural changes in the shoreline around the transgressive dunefield to the north have also been significant. In addition, human activities have also modified the environment at a fast rate by means of a rapid urban development along the coastline, on top of the foredunes, and through the construction of two breakwaters. The result of these combined natural and human-related processes is that the sediment dynamics has changed drastically.

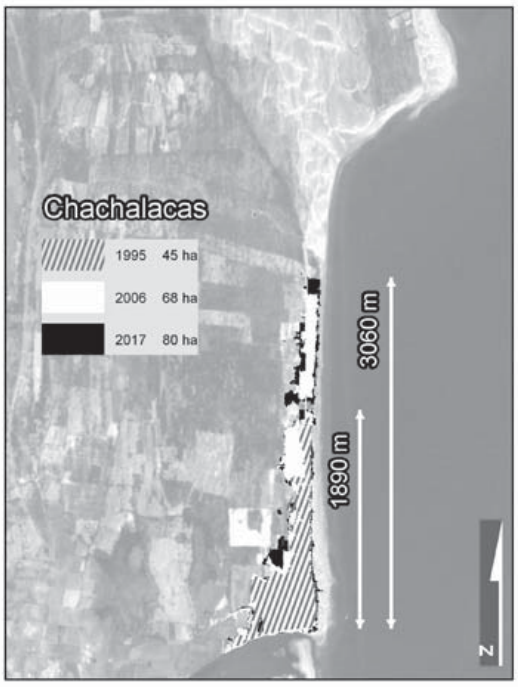

Figure 7: Expansion of the urban area during two decades, in the southern portion of Playa Chachalacas

The greening of the mobile dunes is probably related to changes in the regional climate. The data from the last four decades show that the climate was wetter and warmer in the 1990's and 2000's than in the other decades (Figure 8). Considering both annual accumulated precipitation and mean temperature (Figure 8a), and accumulated precipitation and mean temperature during the growing season (from June to October) it is evident that the weather in the 80's was cooler and dryer than in the 1990´s and 2000´s, which probably assisted in keeping the dunes more mobile. These contrasts are more marked in the analyses of the rainy season, when precipitation was more than 300 mm higher than in the 1980's. Similar trends seem to follow for the 2010's, because data from the rainy season of 2017 are obviously missing, and there are three more years to go to complete the decade, but the values are already very close to the 1980's.

Dieses Werk ist copyrightgeschützt und darf in keiner Form vervielfältigt werden noch an Dritte weitergegeben werden.
Es gilt nur für den persönlichen Gebrauch.

The influence of climate on coastal dune dynamics is well known in the literature. For example, Hesp notes that coastal vegetation changes are more marked and rapid in the tropics and sub-tropics than in temperate regions [4]. Previous studies have found that coastal dunes and vegetation dynamics are associated with climate changes and meteorological events. In Southern Brazil, an increased precipitation and decreased wind power were correlated with the rapid stabilization of coastal transgressive dunefields by Miot da Silva and Hesp [11, 12], and Miot da Silva et al. [13]. Martinho et al [14] also found a similar pattern in southern Brazil as did Ribau-Mendes and Giannini [15]. In turn, Clemmensen et al. [16] determined that dune stabilization in Denmark was associated with a decreased storminess in the summer that resulted in less disturbance and sand movement. In addition to weather, seed dispersers (such as rabbits) and grazing may also determine dune colonization or mobilization [17, 18].

It is important to highlight that, even though dune stabilization has occurred at a fast rate, the system has remained largely mobile with intense sand movement to the south arc shoreline of the dunefield. That is, it seems like changes on the southern beach that leads to the river mouth depend on how the transgressive dunefield and bulge change, and on how much sand moves down-drift. The above means that, in this case, the greening process did not interfere with the dynamics of the beach south the dunefield.

Another factor that is largely affecting sediment dynamics on the beach of Chachalacas are the breakwaters and the built infrastructure on the foredunes. No doubt, the breakwaters modified sediment dynamics, generating an intense accumulation on the northern side of the river mouth, but producing erosion to the south of it. These changes have occurred at a very fast rate, and they do not seem to have stabilized. It is possible that the river mouth will continue to accrete on the northern side and generate further erosion and risk of flooding on the southern side. An example of how tempering with shoreline dynamics may result in drastic changes is that of Boca de Cuautla, in the state of Nayarit on the Pacific coast of Mexico [19]. Here, between 1974 and 1976, an artificial inlet was built, and it was 40 m wide and 2 m deep. Because of the large volume of water and its great speed, this inlet has been changing ever since, and nowadays, it is 1,700 m wide and 20 m deep [20]. Therefore, the inlet of Rio Actopan needs to be monitored regularly after the construction of the breakwaters so that the huge problem of Boca de Cuautla is not repeated. Incorrect diagnoses usually entail the inadequate implementation of solutions, which, in addition to having an economic cost, usually severely affects the functioning of ecosystems.

Dieses Werk ist copyrightgeschützt und darf in keiner Form vervielfältigt werden noch an Dritte weitergegeben werden.
Es gilt nur für den persönlichen Gebrauch.

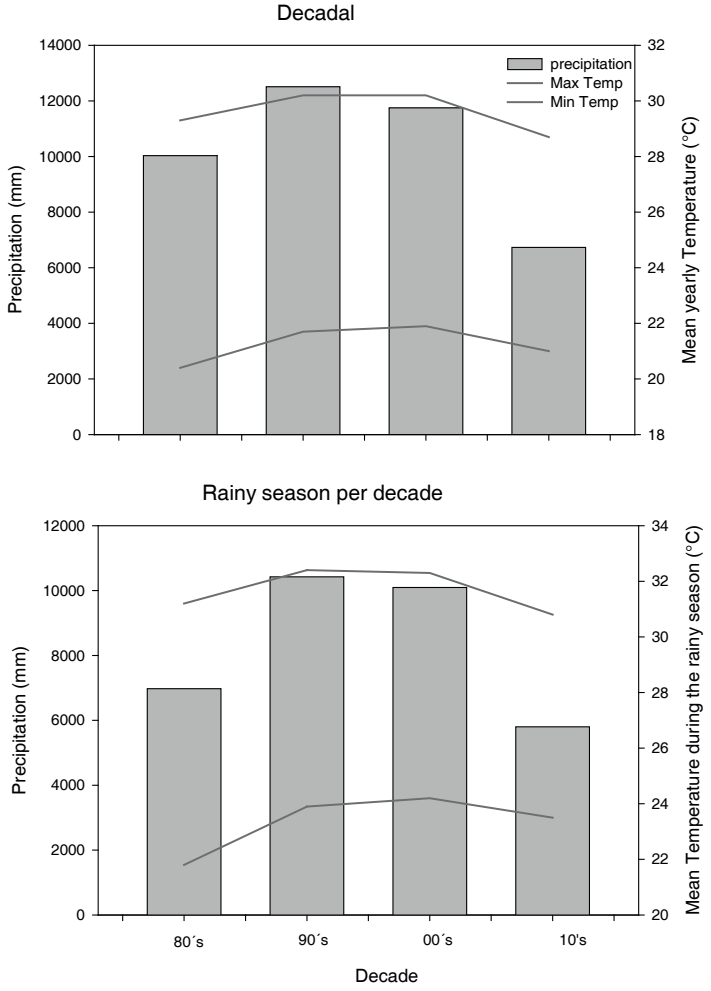

Figure 8: Total precipitation and mean maximum and minimum temperatures during four decades, considering a) yearly data, and b) the rainy season (June to October). Data from the weather station of La Mancha (Veracruz), located on the coast, 20 km north from the study site

Finally, urban development on the foredunes can also affect the natural vegetation of the beach and dunes, and modify sediment dynamics as well. For example, Lucrezi et al. [21] observed that dune width, species richness and composition, and plant height were altered as infrastructure development increased. This shows how coastal dunes are sensitive to varying levels of human impact. Similarly, Pérez-Maqueo et al. [22] found that tourism on the beach also affects community structure and composition. However, in this case, the authors found that changes were not significant when tourism was moderate or low. This shows the close interrelationship between ecosystem structure and function with the socioeconomic relevance of the coastal environment, which is critical to coastal management decisions. The protective role of coastal ecosystems has been widely demonstrated [23-28], so it is past time to determine an adequate balance between how much of the natural habitat needs to be preserved, and how much can be allocated to human development; furthermore, how this development should be created.

Dieses Werk ist copyrightgeschützt und darf in keiner Form vervielfältigt werden noch an Dritte weitergegeben werden.
Es gilt nur für den persönlichen Gebrauch.

5 Conclusions

In Playa Chachalacas, the results show that different factors affect sediment dynamics: (a) a warm and wet climate has promoted a rapid vegetation growth, expansion and successional species turnover, stabilizing portions of the transgressive dunefield at a fast rate; (b) inadequately built infrastructure for shoreline protection solved the erosion problem locally, but has altered the dynamics of the river mouth located down-drift, with the possibility of a greater risk for the population, because of marked rivermouth morphological variations and altered water flows with a greater risk of flooding; and (c) urbanization has occurred along the coastline on top of the foredunes and resulted in ecosystem loss. Furthermore, urbanization may reduce the ability of the beach to absorb changes from either natural or human-related origins. Thus, building too close to the beach has exposed infrastructure to the natural erosion zone. This would probably have not occurred if these hotels and restaurants had been built several meters behind the erosion area.

These processes are occurring in many coastal areas of the world, and are likely to be worsened by climate change scenarios with increased storminess and rising sea levels [9, 24]. Considering the above, and the increasing demand and interest for coastal tourism in general, and in Chachalacas in particular [10, 25], management plans should be made carefully, while considering the dynamic nature of the coastline. The protection of natural dune landforms, plant species richness and composition, and vegetation zonation are critical not only for their intrinsic values, but also because, as this example shows, their dynamism is a fundamental attribute that is too often ignored. Public awareness, but in particular local authority awareness, education, and an increased will to balance development with nature is fundamental to achieve better management of the coast, to reduce hazards, and to protect and to preserve the nature.

6 Acknowledgments

This research was financed by CEMIE-Océano. Also, the authors thank the EXCEED-SWINDON project, DAAD and their respective institutions for the support provided. This publication is one of the results of the summer course, “Integrating Ecosystems in Coastal Engineering Practice-INECEP-2017,” funded by the Federal Ministry for Economic Cooperation and Development, the EXCEED-SWINDON project and DAAD.

7 References

1. Martínez, M.L., Moreno-Casasola, P., Espejel, I., Jiménez-Orocio, O., Infante-Mata, D., Rodríguez-Revelo, N.: Diagnóstico de las dunas costeras de México. CONAFOR. Guadalajara, Jalisco. 350 pp. (2014)
2. Martinez, M.L., Silva, R., Lithgow, D., Mendoza, E., Flores, P., Martínez, R., Cruz, C.: Human impact on coastal resilience along the coast of Veracruz, Mexico. Journal of Coastal Research 77, 143-153 (2017)

Dieses Werk ist copyrightgeschützt und darf in keiner Form vervielfältigt werden noch an Dritte weitergegeben werden.
Es gilt nur für den persönlichen Gebrauch.

3. Mendoza-González, G., Martínez, M., Lithgow, D., Pérez-Maqueo, O., Simonin, P.: Land use change and its effects on the value of ecosystem services along the coast of the Gulf of Mexico. Ecological Economics 82, 23-32 (2012)

4. Hesp, P.: Coastal dunes in the tropics and temperate regions: location, formation, morphology and vegetation processes. Coastal Dunes, pp. 29-49. Springer (2008)

5. Hesp, P., Martinez, M., da Silva, G.M., Rodríguez-Revelo, N., Gutierrez, E., Humanes, A., Laínez, D., Montaño, I., Palacios, V., Quesada, A.: Transgressive dunefield landforms and vegetation associations, Doña Juana, Veracruz, Mexico. Earth Surface Processes and Landforms 36, 285-295 (2011)

6. Martinez, M.L., Moreno-Casasolai, P.: Effects of burial by sand on seedling growth and survival in six tropical sand dune species from the Gulf of Mexico. Journal of Coastal Research 406-419 (1996)

7. Moreno-Casasola, P.: Sand movement as a factor in the distribution of plant communities in a coastal dune system. Plant Ecology 65, 67-76 (1986)

8. Álvarez-Molina, L.L., Martínez, M.L., Lithgow, D., Mendoza-González, G., Flores, P., Ortíz-García, S., Moreno-Casasola, P.: Biological flora of coastal dunes and wetlands: Palafoxia lindenii A. Gray. Journal of Coastal Research 29, 680-693 (2013)

9. Martínez, M.L., Mendoza-González, G., Silva-Casarín, R., Mendoza-Baldwin, E.: Land use changes and sea level rise may induce a “coastal squeeze” on the coasts of Veracruz, Mexico. Global Environmental Change 29, 180-188 (2014)

10. Mendoza-González, G., Martínez, M.L., Guevara, R., Pérez-Maqueo, O., Howard, A.: Sun sea and sand tourism: the value of ocean view and proximity to the coast. Sustainable Tourism (in press), (2017)

11. Miot da Silva, G., Hesp, P.A.: Increasing rainfall, decreasing winds, and historical changes in Santa Catarina dunefields, southern Brazil. Earth Surface Processes and Landforms 38, 1036-1045 (2013)

12. Miot da Silva, G.M., Hesp, P.: Coastline orientation, aeolian sediment transport and foredune and dunefield dynamics of Moçambique Beach, Southern Brazil. Geomorphology 120, 258-278 (2010)

13. Miot da Silva, G., Martinho, C.T., Hesp, P., Keim, B.D., Ferligoj, Y.: Changes in dunefield geomorphology and vegetation cover as a response to local and regional climate variations. Journal of Coastal Research 65, 1307-1312 (2013)

14. Martinho, C.T., Hesp, P.A., Dillenburg, S.R.: Morphological and temporal variations of transgressive dunefields of the northern and mid-littoral Rio Grande do Sul coast, Southern Brazil. Geomorphology 117, 14-32 (2010)

Dieses Werk ist copyrightgeschützt und darf in keiner Form vervielfältigt werden noch an Dritte weitergegeben werden.
Es gilt nur für den persönlichen Gebrauch.

15. Ribau-Mendes, V., Fonseca-Giannini, P.C.F.: Coastal dunefields of south Brazil as a record of climatic changes in the South American Monsoon System. Geomorphology 246, 22-34 (2015)

16. Clemmensen, L., Hansen, K.W.T., Kroon, A., D., A.: A.: Storminess variation at Skagen, northern Denmark since AD 1860: Relations to climate change and implications for coastal dunes. Aeolian Research 15, 101-112 (2014)

17. Gallego-Fernandez, J.B., Muñoz-Valles, S., Dellafiore, C.: Spatio-temporal patterns of colonization and expansion of *Retama monosperma* on developing coastal dunes. Journal of Coastal Conservation 19, 577-587 (2015)

18. Roskin, J., Katra, I., Blumberg, D.G.: Late Holocene dune mobilizations in the northwestern Negev dunefield, Israel: A response to combined anthropogenic activity and short-term intensified windiness. Quaternary International 303, 10-23 (2013)

19. Ramírez-Zavala, J.R., Cervantes Escobar, A., Ramírez Zavala, J.: El ambiente biofísico de marismas nacionales, Sinaloa, y criterios básicos para la gestión de su integridad ecológica. Marismas Nacionales Sinaloa 53-116 (2012)

20. Franco-Ochoa, C., Mendoza-Baldwin, E., Silva-Casarín, R., Ruiz-Martínez, G.: Hydro‐morphologic Revision of the Cuautla Channel at Nayarit, Mexico. CLEAN – Soil, Air, Water 40, 920-925 (2012)

21. Lucrezi, S., Saayman, M., Van der Merwe, P.: Influence of infrastructure development on the vegetation community structure of coastal dunes: Jeffreys Bay, South Africa. Journal of Coastal Conservation 18, 193-211 (2014)

22. Pérez-Maqueo, O., Martínez, M.L., Nahuacatl, R.C.: Is the protection of beach and dune vegetation compatible with tourism? Tourism Management 58, 175-183 (2017)

23. Barbier, E.B.: A global strategy for protecting vulnerable coastal populations. Science 345, 1250-1251 (2014)

24. Feagin, R.A., Sherman, D.J., Grant, W.E.: Coastal erosion, global sea-level rise, and the loss of sand dune plant habitats. Frontiers in Ecology and the Environment 3, 359-364 (2005)

25. Piñar-Álvarez, M.Á., Wojtarowski-Leal, A., Martínez-Vázquez, M.L.: Dunas costeras en Veracruz, México: Conservación y uso para la cohesión social desde la percepción local. Regions and Cohesion 7, 40-68 (2017)

26. Salgado, K., Martinez, M.L.: Is ecosystem-based coastal defense a realistic alternative? Exploring the evidence. Journal of Coastal Conservation 1-12 (2017)

27. Silva, R., Martínez, M., Odériz, I., Mendoza, E., Feagin, R.: Response of vegetated dune–beach systems to storm conditions. Coastal Engineering 109, 53-62 (2016)

28. Temmerman, S., Meire, P., Bouma, T.J., Herman, P.M., Ysebaert, T., De Vriend, H.J.: Ecosystem-based coastal defence in the face of global change. Nature 504, 79-83 (2013)

Dieses Werk ist copyrightgeschützt und darf in keiner Form vervielfältigt werden noch an Dritte weitergegeben werden.
Es gilt nur für den persönlichen Gebrauch.

MORPHODYNAMIC VARIABILITY OF BEACHES IN COSTA VERDE, COLOMBIA

Oriana Daza[1], German Rivillas-Ospina[2], Yeison Berrio[1], Marianella Bolivar[1], Guillermo Acuña[1], Rodolfo Silva[3], Edgar Mendoza[3], Angélica Felix[3], Gabriel Ruiz[4]

[1]Universidad Del Norte, Civil and Environmental Engineering Department, Sustainable Development Institute, Km 5 Puerto Colombia, Barranquilla, Atlántico, Colombia, boriana@uninorte.edu.co

[2]Universidad Del Norte, Civil and Environmental Engineering Department, Sustainable Development Institute, PIANC COLOMBIA, Km 5 Puerto Colombia, Barranquilla, Atlántico, Colombia

[3]Instituto de Ingeniería, Universidad Nacional Autónoma de México, 04510, Ciudad de México, México

[4]Departamento de Recursos del Mar, Centro de Investigación y Estudios Avanzados – Politécnico Nacional, Carretera Puerto Progreso Km, Mérida, Yucatán, México

Keywords: sediment transport model, coastal erosion, statistical parameters, morphology, dynamic equilibrium, SANDY®

Abstract

The stability of coastal ecosystems depends greatly on the sediment balance, so understanding the sediment fluxes and their spatial distribution is a key issue for understanding the stability of a dune beach system. This research considers the analysis of statistical parameters of grain size distribution on the Costa Verde coast, Colombia in order to determine its stability status. Theoretical and numerical models are used to predict the sediment transport direction and volume. The physical processes of the coastal zone are evaluated based on combined analyses of the coastline evolution, the geomorphology, the effect of hydrodynamics, and the anthropogenic impacts. The results show that better management policies must be developed in order to reduce beach erosion and to promote a sustainable use of the coastal zone.

1 Introduction

It is well known that the construction of residential, recreational, port and tourism infrastructure endangers coastal ecosystems and alters the services these provide. Beach degradation is commonly caused by human intervention, rigidizing the systems and not letting the coastal area adapt to changes under hydro-meteorological conditions. For human settlement and economic activities that are continued in degraded coastal areas, policies of protection and conservation must be strengthened.

Dieses Werk ist copyrightgeschützt und darf in keiner Form vervielfältigt werden noch an Dritte weitergegeben werden.
Es gilt nur für den persönlichen Gebrauch.

The main causes of erosion are sea level rise, extreme storm events, lack of sediment availability, and badly planned coastal protection infrastructure. One of the first signs that a beach is unstable is the imbalance in sediment fluxes. A quantitative analysis of sediment transport rates is critical in understanding erosion and accretion processes. The use of theoretical models to quantify sediment transport and to evaluate sediment volume lost or arriving in a littoral cell is a successful, widespread practice [1, 2].

Colombia has 2,445 km of coast on the Caribbean Sea, of which 1,182 km have been classified as erosive, 813 km as stable and 450 km in accretion, according to studies carried out by [3]. These authors also stated that over the last 34 years there has been a serious problem of erosion all along the Colombian Caribbean coast, particularly in Magdalena department, 306 km in length, which has an erosion rate of 15 m/yr. This strip extends from the town of Ciénaga to the Cuatro Bocas wetland. The coastline has gently curving beaches, limited by rocky protrusions or cliffs (Figure 1). In this kind of system, sediment transport is independent of the adjacent beaches and governed by wave diffraction at the limits. The geometry of the beach is thus oriented in response to the local wave climate [4], although marine structures produce environmental impacts along the coast by modifying sediment transport patterns. In 1953, a jetty was built at the mouth of the Magdalena River, called Bocas de Cenizas in order to improve navigation to the port of Barranquilla. However, the jetty drives sediments transported by the Magdalena River directly into deep water, and they do not return to the beach. This is one of the main causes of erosion on the Salamanca barrier island in the Ciénaga Grande of Santa Marta and the Coastal Lagoon of Pajaral [3].

Sediment transport is related to morphodynamic processes and the resulting topography of a coastal system. When a beach is controlled by diffraction, for example rocky headlands, sediments accumulate in the sheltered zone and in other areas, where energy is concentrated and erosion occurs [5]. Several empirical methodologies are available to assess the sediment transport rate, e.g., (i) Energy flux method, (ii) Coastal current evaluation method, and (iii) Dimensional analysis, as proposed by [2]. Such formulations are limited by the parameters they include, since they must be characterized at each study site and may vary seasonally and locally. The first method (CERC formula) is based on the wave energy, considering a submerged weight transport rate, which, as described by [6], is proportional to the energy flow in the breaking zone. The second method applies the Longuet-Higgins model in order to establish the energy flux along the coast. Finally, the model proposed by [2] relates the sediment transport rate to a series of parameters such as the bottom slope and the mean diameter of the beach sediment [6].

In order to identify the trajectories of the sedimentary material based on the "Grain Size Trend Analysis (GSTA)", the spatial change of the sediment characteristics has been investigated. In order to explain sedimentation rates, various proposals have been made, such as the variation of particle size in relation to the direction of motion, analysis of the combination of statistical parameters such as D50, classification and asymmetry, and dimensional models that include a mesh of dimensionless vector "transport vectors" for comparison of texture variables and establishing sediment direction patterns [7]. The objective of this research was to determine the applicability

Dieses Werk ist copyrightgeschützt und darf in keiner Form vervielfältigt werden noch an Dritte weitergegeben werden.
Es gilt nur für den persönlichen Gebrauch.

of theoretical models based on the comparison of a two-dimensional sediment transport model, which was validated with field data.

2 Study Area

The study area is located in the municipality of Costa Verde, on the Colombian Caribbean, in the department of Magdalena, and has the geographic coordinates 11°2'9.07"N - 74°14'34.59"O and 11°06'35.19"N - 74°50'39.48"O. The littoral cell is approximately 73 km long, and divided into three sub-cells as shown in Figure 6.

The main wind direction is northwest, with an average maximum speed of 39 m/s, according to Interactive Platform of the Institute of Hydrology, Meteorology and Environmental Studies of Colombia (IDEAM in Spanish) [8]. The area studied includes ecosystems such as lagoons, wetlands, mangroves, seagrass and vegetation in the dunes and tributaries. The area also has hard coastal protection structures (suspected to have worsened the erosion problems) and low density urbanization.

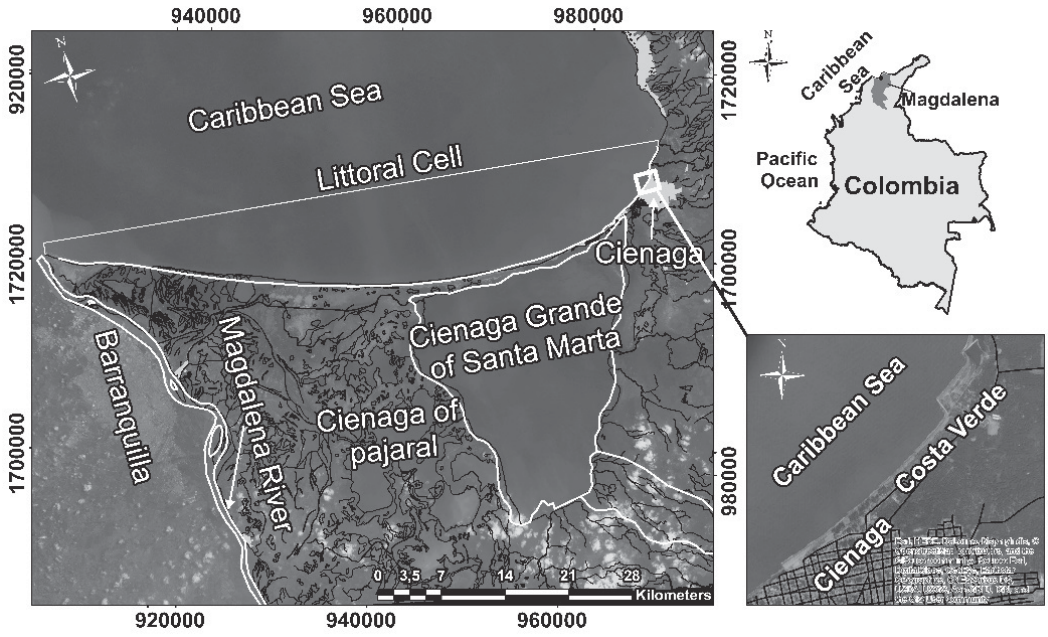

Figure 1: Geographical location of the study site

3 Materials and methods

3.1 Physical characterization of sediment samples

The methodology used for the physical characterization of the samples consisted of performing standard grain size distribution tests. The granulometric analysis of coarse and fine aggregates was performed according to the standards of National Institute of Roads of Colombia (INV E – 213- 13, INVIAS in Spanish) with the series of sieves described by ASTM (American Society for Testing Materials). The percentage weight retained on each sieve is input for the application, and the statistical parameters were estimated by the SANDY© routine by[9].

Dieses Werk ist copyrightgeschützt und darf in keiner Form vervielfältigt werden noch an Dritte weitergegeben werden.
Es gilt nur für den persönlichen Gebrauch.

Twenty sediment samples (10 from the breaker zone and 10 from the shoreline) were taken during the dry season, and 28 samples from the breaker zone and the dune were collected under extreme wave conditions. The statistical-mathematical equations used to determine the mean diameter, standard deviation, and statistical bias, respectively, are:

$$\bar{d} = \frac{\emptyset_{16} + \emptyset_{50} + \emptyset_{86}}{3}$$

$$s = \frac{\emptyset_{84} + \emptyset_{16}}{4} + \frac{\emptyset_{95-\emptyset_5}}{4}$$

$$sesg = \frac{\emptyset_{16} + \emptyset_{84} - 2\emptyset_{16}}{2(\emptyset_{84} - 2\emptyset_{16})} + \frac{\emptyset_5 + \emptyset_{95} - 2\emptyset_{50}}{2(\emptyset_{95} - \emptyset_5)}$$

Where ***d*** is the mean diameter, ***s*** the standard deviation, and ***sesg*** the statistical skewness. Figure 2 shows the points in the dune and in the breaker zone where the samples were taken.

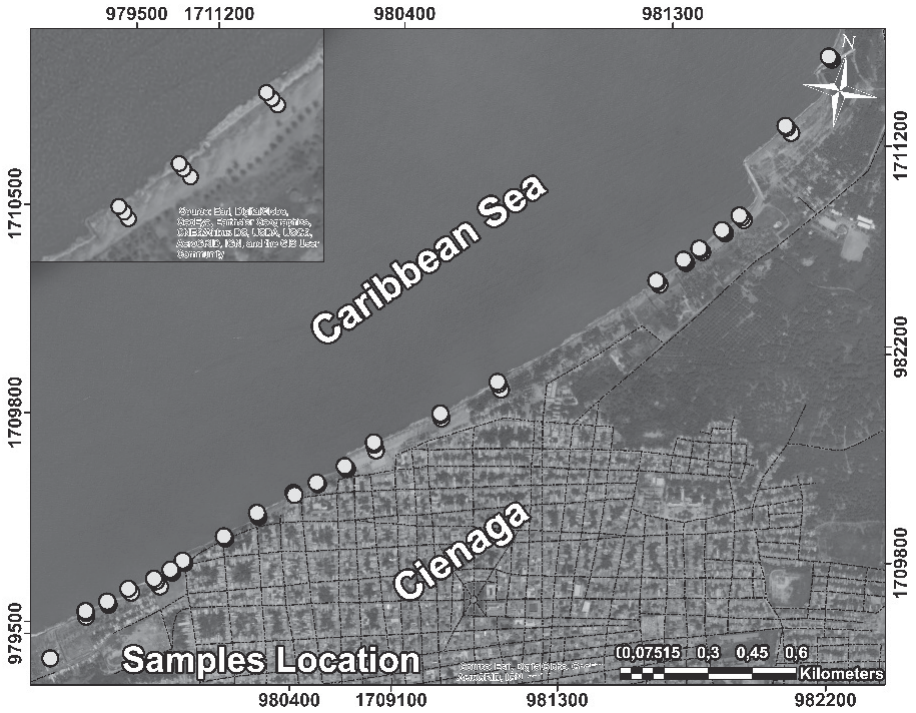

Figure 2: Sediment samples of Costa Verde

3.2 Geomorphology of the coastal area and evolution of the shoreline

The geomorphology of the system was analyzed from field monitoring and historical data review. The littoral cell was divided into sub-cells, which are very different with regard to coastal ecosystems and natural limitations within the systems, such as rivers, cliffs, or maritime infrastructures. The historical evolution of the shoreline was carried out from Landsat satellite images from 1973 to 2017.

Dieses Werk ist copyrightgeschützt und darf in keiner Form vervielfältigt werden noch an Dritte weitergegeben werden.
Es gilt nur für den persönlichen Gebrauch.

3.3 Wave climate

The maritime climate analysis of the area was taken from the WAVEWATCH III database with a coordinate point of 11.4154 ° N -74.08325 ° W, for a time series from 1979 to 2007. Figure 3a shows that a significant wave height of 1.63 m occurs with a 50% of exceedance probability, and a wave height of 2.64 m has a probability of 95%. Regarding the joint probability distributions of significant wave height and peak period as well as of significant wave height and incoming direction, a period of 7 s with a direction of 45° were identified as the most likely ones (Figure 3c).

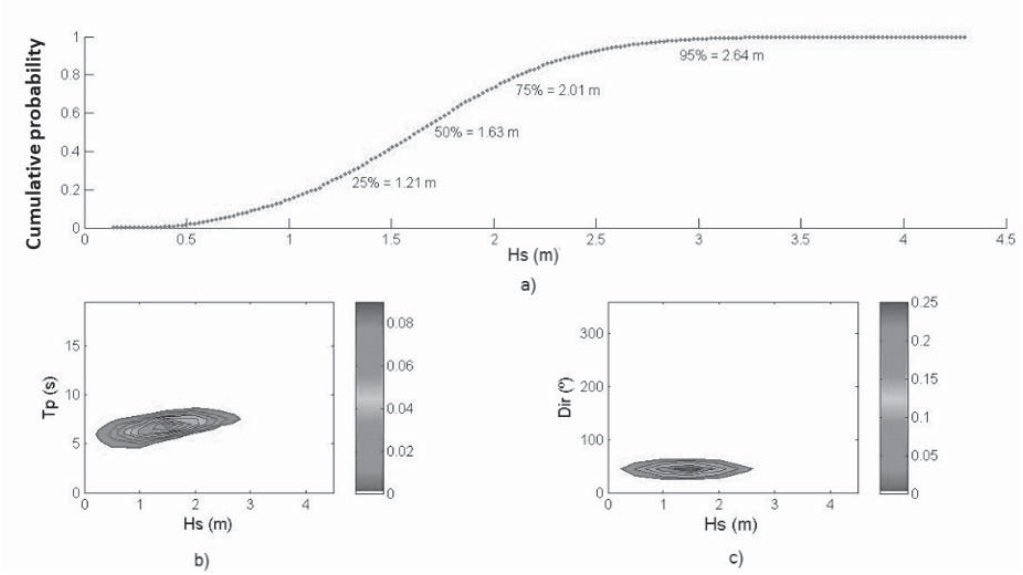

Figure 3: Wave climate characterization at Costa Verde: (a) Wave height exceedance probability, (b) wave height-peak period joint probability distribution, (c) wave height-wave direction joint probability distribution

From the data available, the extremal wave regime was defined as that with 95% of exceedance probability. Figure 4a shows the relation between the extreme wave heights and the incident direction.

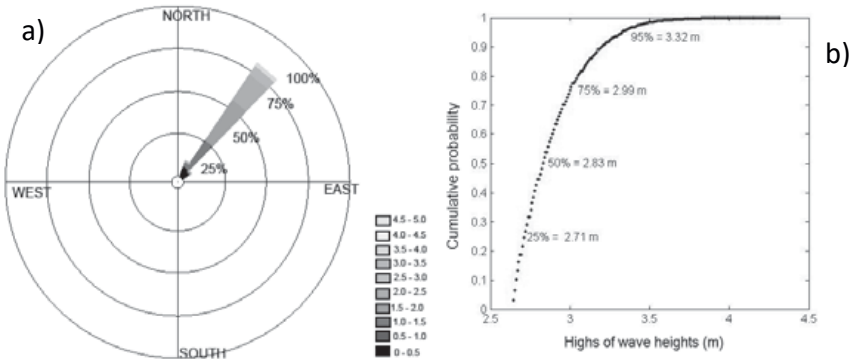

Figure 4: (a) Wave rose and (b) Cumulative probability

Dieses Werk ist copyrightgeschützt und darf in keiner Form vervielfältigt werden noch an Dritte weitergegeben werden.
Es gilt nur für den persönlichen Gebrauch.

4 Results and Discussion

4.1 Physical characterization of sediments

The obtained statistical parameters from the granulometric analysis of sediment samples, taken during the dry season, show average diameters (D50) between 0.19 mm and 0.35 mm, as seen in Figure 5a, which shows the variation of D50 along the coast. The dispersion of the distribution of the sediment samples was classified as well sorted, skewed and very leptokurtic, according to the standard deviation, the skewness coefficient and the kurtosis, respectively. The results show a concentration of particle sizes according to the probability distribution function. This means that during the dry season, there is little sediment supply, which induces erosion. However, as the particle size tends to be heterogeneous, the coast is in quasi-static equilibrium, having regression of the coastline due to skewness and standard deviation. The system is dynamic given that beach presents a large range of sediment particle diameters.

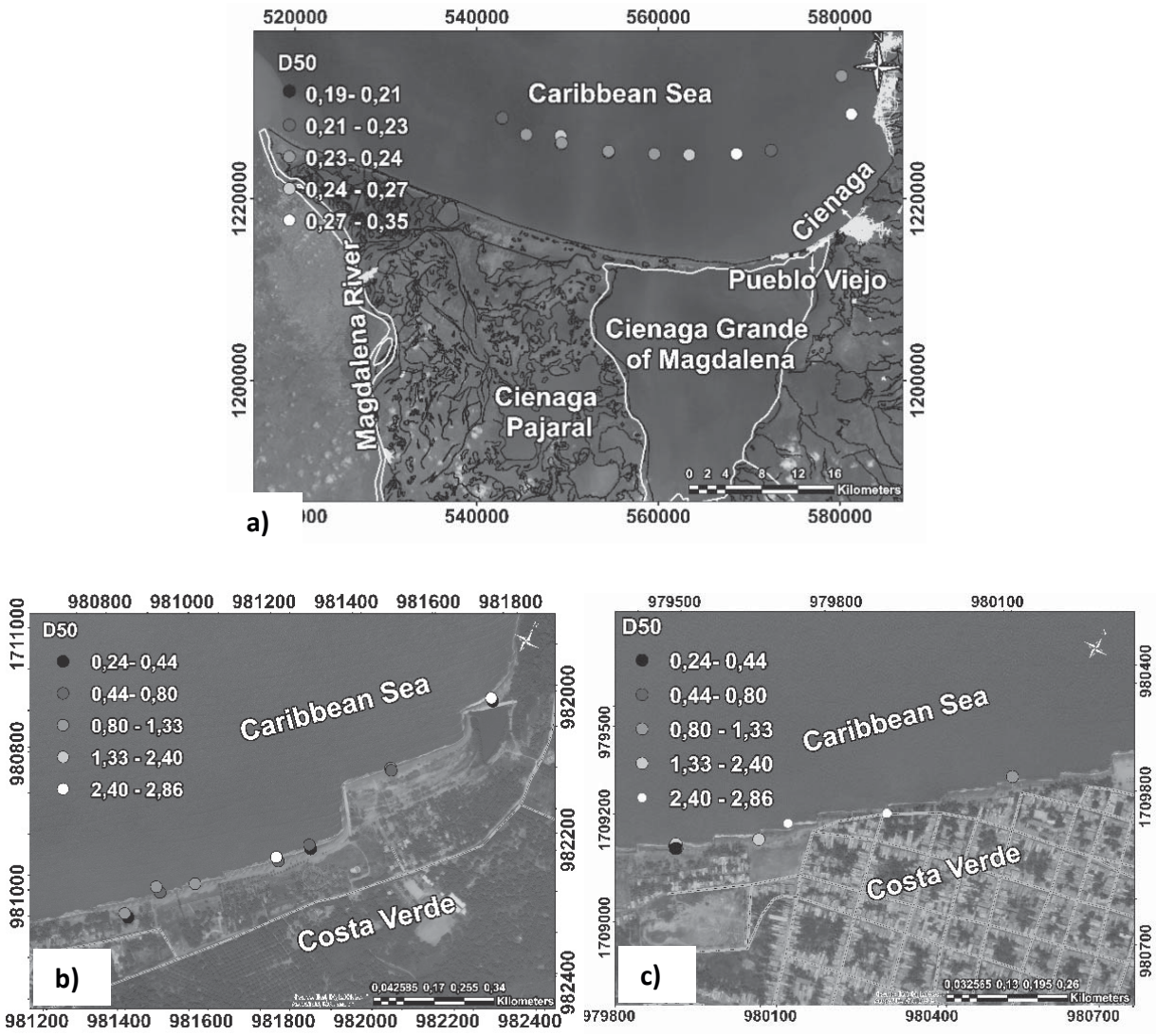

Figure 5: Average diameter during (a) summer season in study zone, (b) winter season in Costa Verde, and (c) winter season in Ciénaga municipality

Dieses Werk ist copyrightgeschützt und darf in keiner Form vervielfältigt werden noch an Dritte weitergegeben werden.
Es gilt nur für den persönlichen Gebrauch.

The distribution of grain size in the winter season, when extreme conditions are presented, shows a large variation of the diameter D50 between 0.24 mm and 2.86 mm, as can be seen in Figure 5b and 5c. According to the granulometric analysis, the sedimentary material is classified as coarse sand. The sediments fall within the very well sorted and mesokurtic classifications.

4.2 Geomorphology of the coast

The littoral cell was divided in three sub-cells, shown in the Figure 6. Sub-cell 1 is from Cordoba River to Pueblo Viejo; sub-cell 2 is from the mouth of Ciénaga Grande of Santa Marta to the emerging structure crosswise to the coast; and sub-cell 3 goes from the structure crosswise to the system to the mouth of the Magdalena River, Bocas de Cenizas.

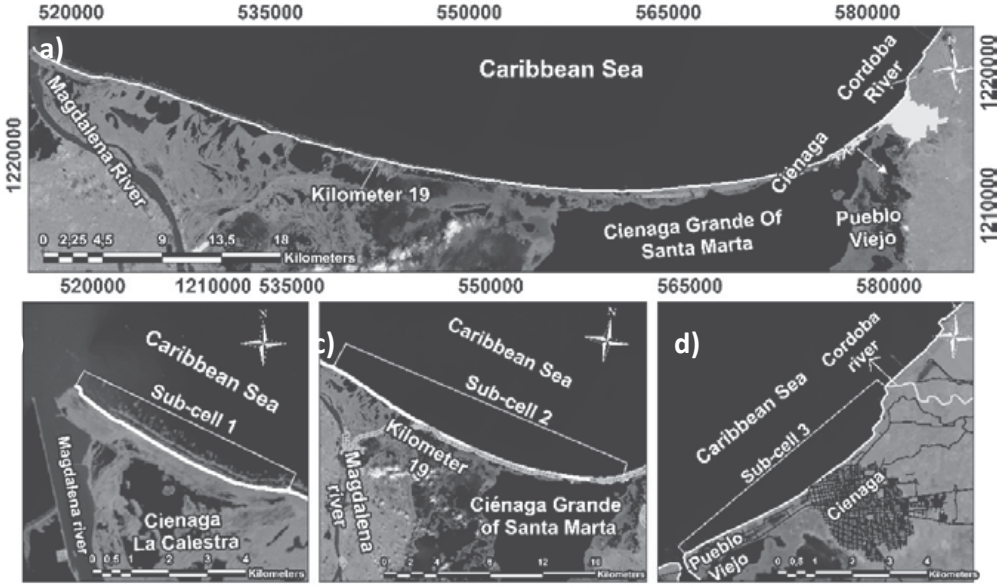

Figure 6: (a) Littoral cells of the study site, (b) sub-cell close to Bocas de Ceniza river mouth, (c) sub-cell from coastal structure to Ciénaga Grande tidal channel, (d) sub-cell from tidal channel to Costa Verde

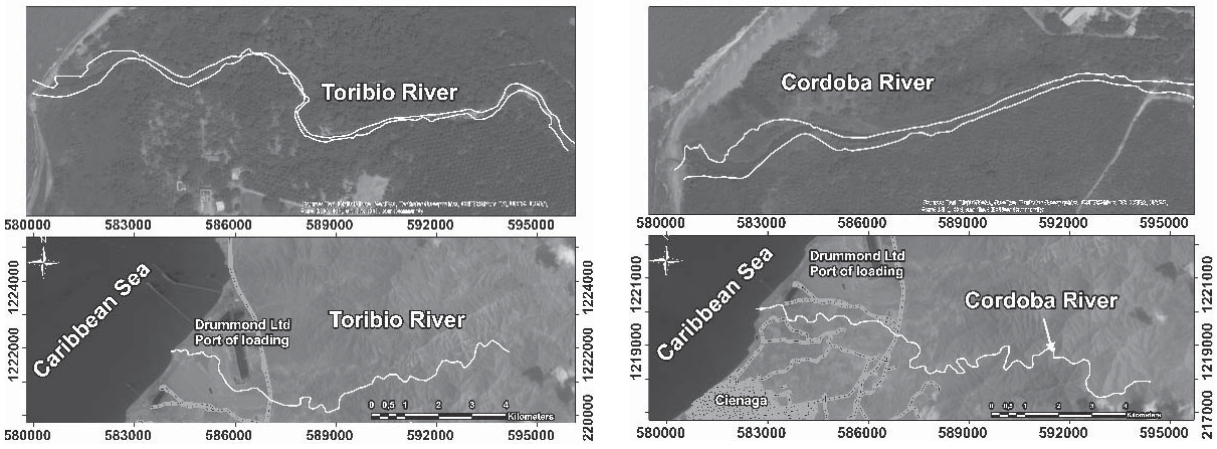

a) b)

Figure 7: Alluvial effluents: river mouths (a) Toribio and (b) Cordoba (GoogleEarth®, 2016)

Dieses Werk ist copyrightgeschützt und darf in keiner Form vervielfältigt werden noch an Dritte weitergegeben werden.
Es gilt nur für den persönlichen Gebrauch.

Figure 7 shows the rivers that generate greatest sediment support in the coastal system of Costa Verde. These are mainly the Toribio River with a watershed area of 101 km^2 and an average flow of 4.6 m^3/s, the Cordoba River with 63.9 km length, a watershed of 120 km^2 and a mean flow of 7.2 m^3/s**,** in addition, the Gaira River with a length of 32.3 km, a catchment area of 105 km^2, and an average flow 2.5 m/s. On the other hand, the rivers feeding Ciénaga Grande of Santa Marta make less of the contribution to sediment transport. This wetland has an area of 4,280 km^2, depths that vary from 2 to 6 meters [10] and three tributaries.

Among the bodies of water, which are in the evaluated cell, are the Ciénaga Grande of Santa Marta, Pajaral wetland, Cuatro Bocas wetland, and Tigre wetland. The sector has a dune system with vegetation, berms, craggy coastline, coastal plains, mangroves, coastal lagoons, and megacusps. The sediments are light gray and dark in all sections. There is also a discontinuity in relation to sediment transport in the Costa Verde area, because the breakwaters generate accretion to the northeast and erosion to the southwest of each one, as observed in the field monitoring carried out.

The beaches between Cuatro Bocas wetland and the second mouth of the Great Magdalena Swamp are characterized as straight and without cliffs, and the stabilized dunes are surrounded by vegetated and flooded areas. According to the SGC platform in the geological Atlas of Colombia, alluvial deposits and alluvial plains predominate along the Costa Verde coast and Port Drummond. In the area surrounding the Ciénaga Grande de Santa Marta are deposits of gravel and sand accumulated on beaches, and muds, rich in organic matter associated with the development of mangroves. Finally, where the Boca Cenizas wetland ends there are paludal deposits (i.e., marshes).

4.3 Shoreline Evolution

The time evolution of the coastline does not present significant changes in relation to the dynamics of the system (regression or advance of the shoreline). It was observed that a regression of the shoreline at kilometer 19 (Figure 8a), at the height of the Ciénaga (Figure 8b), shows a loss of 0.37 km of beach from 1973 to 2016. Figure 8c shows that the coast of the municipality of Ciénaga has not changed much in position, while the mouth of the Ciénaga Grande of Santa Marta is an active ecosystem, which tends to be less static, as coastal lagoons usually are. It is worth noting that the protection structures along the coast contributed to the instability of the beach and have not generated much contribution of sediment to the system, as they were poorly designed and planned.

4.4 Diagnostics

When assessing the probable causes and consequences of the instability of this coastline, it is worth remembering that there are 23 structures in the area (21 geotubes and 2 groynes) that are inadequate. They were built without considering the local morphology and hydrodynamics. In addition, sediments are extracted from the Cordoba River to be used as construction materials for the inhabitants of Costa Verde, which explains partially the deficit of sediments. The beaches

Dieses Werk ist copyrightgeschützt und darf in keiner Form vervielfältigt werden noch an Dritte weitergegeben werden.
Es gilt nur für den persönlichen Gebrauch.

adjacent to the mouth of the Toribio River are metastable with a moderate amount of sediment. The littoral morphodynamics can be defined as follows: In sub-cell 1, the beaches are reflective, having no wide breaking zones and plunging type of wave breaking; In sub-cell 2, there is a breaking wave type collapsing, from being a reflective to a dissipative beach, due to the greater breaking area; Finally, sub-cell 3 remains dissipative up to Bocas of Cenizas. The recession of the shoreline began in 1980 and was moderately stable until 1990, and then from 1999, the mouth of the Ciénaga Grande of Santa Marta began to recover by itself until 2009. In 2011, the breakwater built in Cabo Viejo changed the morphodynamics of the system.

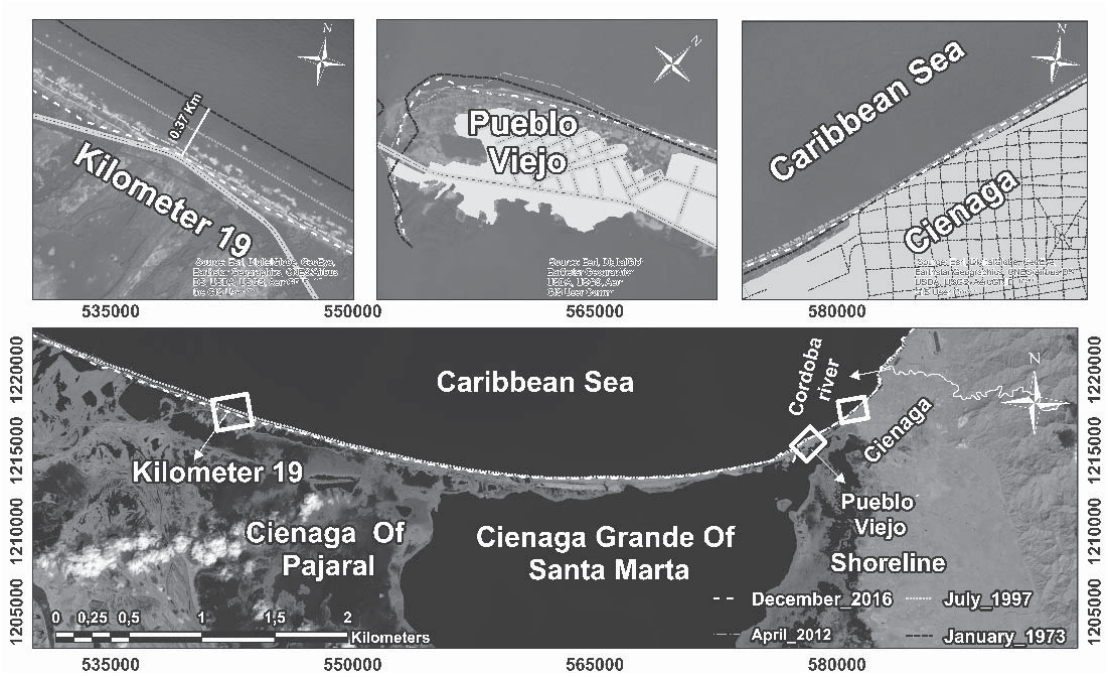

Figure 8: Shoreline evolution of study area. a) Kilometer 19, b) Pueblo Viejo, and c) Ciénaga municipality

From the above, it could be deduced that the actual sediment sources are not sufficient to keep the beaches stable. This would seem to justify the construction of hard structures. But if the dynamics of the coast and the connectivity between the coastal ecosystems had been considered, measures could have been undertaken that offered more success.

5 Conclusions

Costa Verde beach systems have great morphodynamic variability, explained through the seasonal transition of sediment grain size and the sedimentary imbalance that increases the erosion problems. It is suggested that the artificial structures should be removed and an alternative means employed to solve the problem. A coastal management plan is needed, that eventually considers artificial sediment nourishment and relocation of the infrastructure at risk. In addition, sediment transport models and monitoring should be applied in order to assess the situation. Appropriate regulations and oriented policies can help in this process.

Dieses Werk ist copyrightgeschützt und darf in keiner Form vervielfältigt werden noch an Dritte weitergegeben werden.
Es gilt nur für den persönlichen Gebrauch.

6 References

1. Córdova López, L.F., Torres Hugues, R.: Modelo Matemático Para la Determinación del Transporte Longitudinal Para Playas del Caribe. Tecnología y Ciencias del Agua II, 127-140 (2011)
2. Kamphuis, J.W.: Alongshore sediment transport rate. Journal of Waterway, Port, Coastal, and Ocean Engineering 117, 624-624 (1991)
3. Rangel-Buitrago, N.G., Anfuso, G., Thomas, A.: Coastal erosion along the Caribbean coast of Colombia : Magnitudes , causes and management. Ocean and Coastal Management 114, 129-144 (2015)
4. Van Rijn, L.: Coastal erosion control based on the concept of sediment cells. Conscience project Final Report (2010). http://www. leovanrijn-sediment. com/papers/Coastalerosion2012. pdf (accessed 1 May 2016)
5. da Silva, G.V., Toldo, E.E., da F. Klein, A.H., Short, A.D., Woodroffe, C.D.: Headland sand bypassing - quantification of net sediment transport in embayed beaches, Santa Catarina Island north shore, southern Brazil. Marine Geology 379, 13-27 (2016)
6. Vera, L.: Comparación de Tasa Anual de Transporte de Sedimentos de la Playa en la Isla Jambelí, utilizando formulación sugerida por varios autores. Acta Oceanográfica del Pacífico 14, 21-24 (2007)
7. Sánchez, A., Carriquiry, J., Barrera, J., Estela López-Ortiz, B.: Comparación de modelos de transporte de sedimento en la Bahía Todos Santos, Baja California, México. Boletin de la Sociedad Geologica Mexicana 61, 13-24 (2009)
8. Instituto de Hidrología: Meteorología y Estudios Ambientales de Colombia (IDEAM), 2016. “visorAtlasVientos @ atlas.ideam.gov.co,” 2016. [Online]. Available: Visor Atlas de Vientos.
9. Ruiz-Martinez, G., Rivillas-Ospina, G.D., Mariño-Tapia, I., Posada-Vanegas, G.: SANDY: A Matlab tool to estimate the sediment size distribution from a sieve analysis. Computers and Geosciences 92, 104-116 (2016)
10. Ministerio de Agricultura y Desarrollo Rural, Gobernación del Magdalena, Fondo Nacional de Fomento Hortifrutícola, Asociación Hortifrutícola de Colombia, Sociedad de Agricultores y Ganaderos del Valle del Cauca: Plan Frutícola Nacional. Desarrollo de la fruticultura en el Magdalena, Santa Marta, Colombia (2006)

Dieses Werk ist copyrightgeschützt und darf in keiner Form vervielfältigt werden noch an Dritte weitergegeben werden.
Es gilt nur für den persönlichen Gebrauch.

SALINIZATION OF MARSHES IN ARGENTINA: NATURAL VS. ANTHROPOGENIC FACTORS

Eleonora Carol[1], María del Pilar Alvarez[2], Yanina L. Idaszkin[2], Lucia Santucci[1]

[1]Centro de Investigaciones Geológicas. Consejo Nacional de Investigaciones Científicas y Técnicas (CONICET) Universidad Nacional de La Plata (UNLP) Argentina, eleocarol@fcnym.unlp.edu.ar

[2]Instituto Patagónico para el Estudio de los Ecosistemas Continentales, Consejo Nacional de Investigaciones Científicas y Técnicas (CONICET) Argentina

Keywords: Argentinian coast, coastal wetland, embankment, salt marshes, soil salinity

Abstract

In the littoral zone of Argentina, marsh environments under arid, semi-arid and humid conditions are numerous. In this work, salt marshes located in Río de la Plata Estuary, Bahía Blanca Estuary, San Antonio Bay, and San Jorge Gulf were studied aiming at understanding the processes that determine the occurrence of evaporites in salt marshes, and analyzing the importance of natural and anthropogenic factors. QuickBird and Google Earth images were used to identify the geomorphologic, anthropogenic and hydrological characteristics, and selected samples were examined under a binocular magnifying glass, through X-ray diffraction (XRD) and scanning electron microscopy (SEM). The four studied marshes are located along a latitudinal gradient on the Argentina Atlantic coast, where the climatic conditions are wet in the northern sector and arid in the marshes of the southern sector. The tidal conditions change from north to south as micro-tidal in Ajó marsh, meso-tidal in Bahía Blanca, and macro-tidal in San Antonio and Fracasso marshes. In each area, contrasting climatic conditions, tidal and anthropogenic influence and hydrological characterization were studied both the anthropogenic and the natural factors condition the soils marshes salinization. Although it is expected that a greater amount of salts occur in arid marshes soils, it was observed that salt development in altered marshes with humid climates are more important. This shows the high negative influence that an anthropogenic modification can have over sensitive ecosystems as the marshes.

1 Introduction

Salt marshes occur worldwide, being sparse in the tropics, where they are replaced by mangroves [1]. They develop in estuarial and/or intertidal areas, where the slow movement of water generates the accumulation of fine sediments, which are then colonized by vegetation typically resistant to both immersion and hyper-salinity. Although marshes remain exposed to air most of the day, they are subject to periodic flooding due to water level oscillations in the adjacent water bodies [1, 2]. In turn, incoming tide water carves channels and builds the intricate salt marsh creek system [3]. The amplitude of the tide and the elevation of the ground regulate the formation and growth of the marsh [3, 4]. The frequency of the tidal flow rules the salinity fluctuations and the

Dieses Werk ist copyrightgeschützt und darf in keiner Form vervielfältigt werden noch an Dritte weitergegeben werden.
Es gilt nur für den persönlichen Gebrauch.

oxygen regimes, which determines microbial productivity and influences plant zonation that supports the whole marsh food web [5]. The ecology of salt marsh plants depends on a combination of multiple factors [6] such as flooding frequency, soil salinity, and water logging, whereas for most species, salinity is the primary control factor of plant distribution [7]. Hydrological modifications in salt marshes worldwide have affected their structure and function, altering their spatial extent and distribution [8]. Many abiotic factors, such as the spatiotemporal flow pattern and the soil salinity, are strongly influenced by the modifications in the hydrological conditions.

Most of the coastal wetlands of Argentina are Ramsar sites or natural reserve areas [9]. Due to this, there are several investigations about these environments, many of them oriented to characterize biodiversity, highlighting their importance as migratory bird whereabouts [10-12]. Likewise, many studies are focused on the distribution of the plant species that characterize the marshes [13-16]. Ecological studies focused on vegetation, soils and climate, evidencing the existence of latitudinal variations in the marshes located along the Argentine coast [17]. However, in general little is known about the natural and anthropogenic conditioning factors affecting the salinization processes occurring in these marshes. As the transport, dissolution, and/or precipitation of salts are mainly determined by local hydrological characteristics, it is hoped to find out, how the different natural and anthropogenic factors affect the hydrological functioning of wetlands and influence the salinization processes.

In the littoral zone of Argentina, marsh environments under arid, semi-arid, and humid conditions are numerous; however, few evaporitic salts formation studies have been undertaken [18, 19]. Nevertheless, these studies deal with particular issues, while an integral study of marshes along a latitudinal gradient is still lacking. The objective of this work is to assess, which processes condition the occurrence of evaporites in salt marshes of the littoral of Argentina (Fig. 1), through analyzing the importance of natural and anthropogenic factors. For this purpose, four marshes with contrasting climatic conditions, tidal and anthropogenic influences were studied. This would make it possible to visualize the different salinization problems affecting the marshes, and to generate management guidelines to be used at the regional level.

2 Methodology

This study was conducted in salt marshes located in Río de la Plata Estuary, Bahía Blanca Estuary, San Antonio Bay and San Jorge Gulf (Fig. 1). In these marshes, QuickBird/Google Earth images (taken in 2016) were used to identify the geomorphologic, anthropogenic (embankment, road, drainages) and hydrological characteristics, which were later verified in field surveys. The hydrological characterization of each area was carried out taking into consideration climate and tidal data. The annual and seasonal variations in the rainfall and temperature regime as well as their influence on the real evapotranspiration were estimated as suggested by Thornthwaite and Mather [20]. In those sectors with salinization evidences, salt precipitates formed in the most surficial sediments were collected and stored hermetically in order not to alter the humidity conditions. Then, those samples were examined under a binocular magnifying glass and through

Dieses Werk ist copyrightgeschützt und darf in keiner Form vervielfältigt werden noch an Dritte weitergegeben werden.
Es gilt nur für den persönlichen Gebrauch.

X-ray diffraction (XRD) with a Philips X'Pert PRO diffractometer. Some samples were selected to be examined by a Jeol JSM 6460 LV scanning electron microscope with an EDAX PW7757/78 X-ray energy-scattering micro-analyzer (SEM-EDS), which was used to determine the qualitative composition of certain minerals.

Finally, the obtained results of the four marshes were contrasted in order to evaluate which factors (natural or anthropogenic) are more relevant in the salinization processes of marshes.

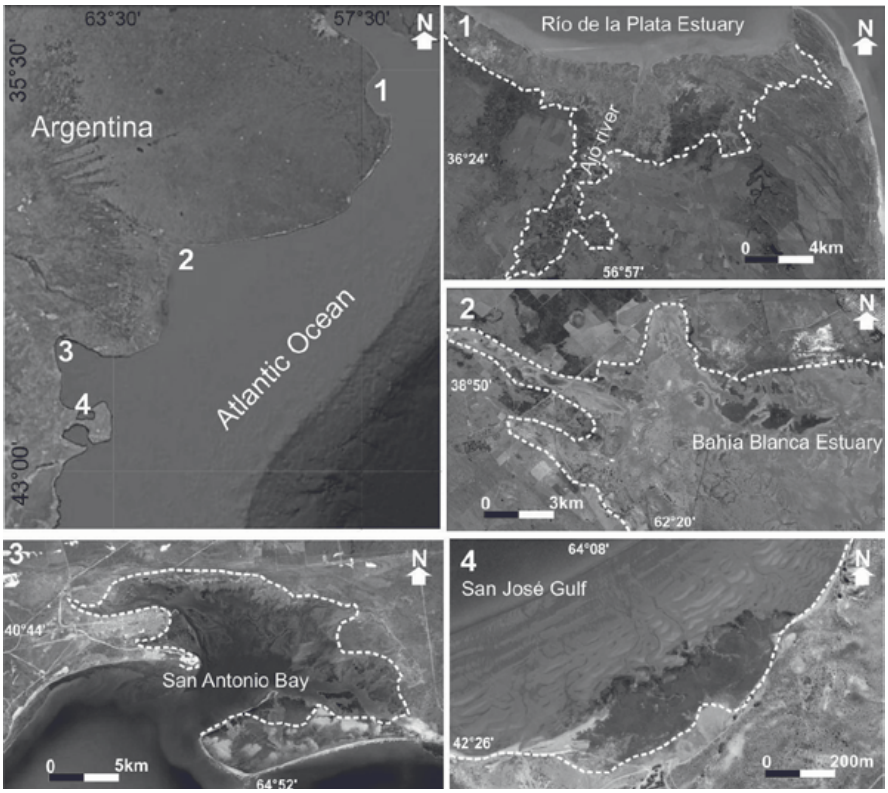

Figure 1: Location of the selected salt marshes of the Argentina Atlantic coast. The white dotted lines show the upper limit of the marsh areas.

3 Results

The four marshes selected have different tidal and climatic characteristics, and a different degree of anthropogenic influence.

3.1 Río de la Plata Estuary

The littoral of the outer Río de la Plata estuary constitutes an extensive marsh that reaches its greatest extent at the southern end (Fig. 1). In this sector, the tide enters the marsh along a large tidal channel named Ajó River, which also receives the contribution of continental courses and is regulated by floodgates. Even though the estuary has a semidiurnal micro-tidal regime (tidal amplitude minor to 2 m). This region has a humid subtropical climate that is mild with no dry season, constantly moist (year-round rainfall). Seasonality is moderate (Köppen-Geiger classification: Cfa). The mean annual precipitation (Servicio Meteorológico Nacional -SMN-1995-

Dieses Werk ist copyrightgeschützt und darf in keiner Form vervielfältigt werden noch an Dritte weitergegeben werden.
Es gilt nur für den persönlichen Gebrauch.

2010) is around 930 mm and the Potential evapotranspiration (ET0) around 820 mm. The monthly ET0 only overcomes the monthly precipitation in November, December and January, being the rest of the year the precipitation higher than the ET0 (Fig. 2).

Farms have been set up within the Ajó marsh, whose main activity is livestock farming. The development of this activity modifies the marsh hydrologically. The analysis of the satellite images and field observations showed that there are numerous embankments that cut across the tidal channels, leaving sectors of the marsh out of the tidal cycle (Fig. 3). All of the embankments are made of soil and generally lack drains, or, if present, they are broken or blocked by sediments. During extraordinary high tides (greater than 1.50 m a.s.l.), the tide overtops the embankments and floods the isolated marsh areas. Subsequently, at low tide, the embankments prevent the tidal flow from draining, causing the area to remain waterlogged until the water infiltrates or evaporates completely.

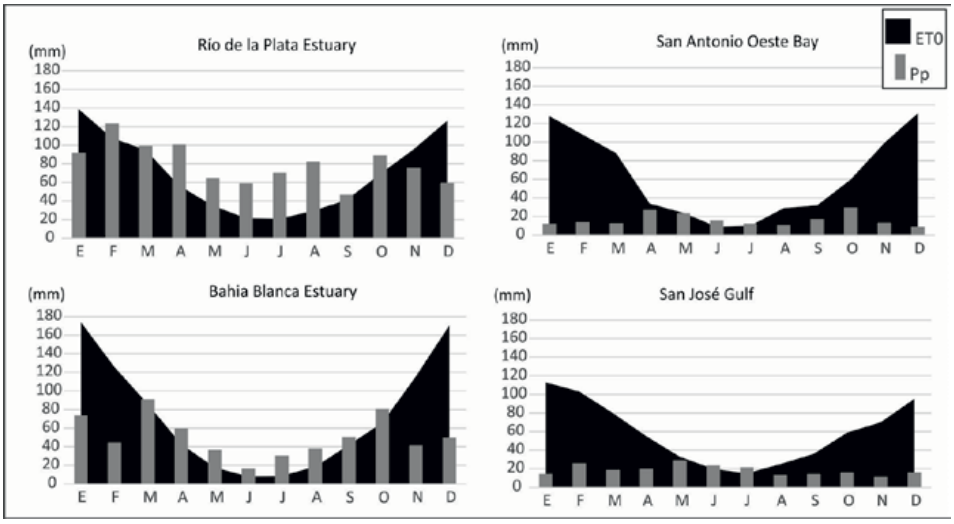

Figure 2: Mean monthly potential evapotranspiration (ET0) and precipitation (Pp) distribution for the four studied areas

In field surveys, the formation of evaporites was observed in a large portion of the embanked marsh areas. The evaporites that precipitated over clayey sediments shows abundant desiccation cracks, while those formed over sandy sediments develops a patina and produce agglomerates due to the cementation of the grains (Fig. 3). The XRD and SEM determinations showed that halite and gypsum are the main evaporitic minerals that precipitate in the soils. In turn, in the natural marsh areas, no saline precipitates were observed.

Dieses Werk ist copyrightgeschützt und darf in keiner Form vervielfältigt werden noch an Dritte weitergegeben werden.
Es gilt nur für den persönlichen Gebrauch.

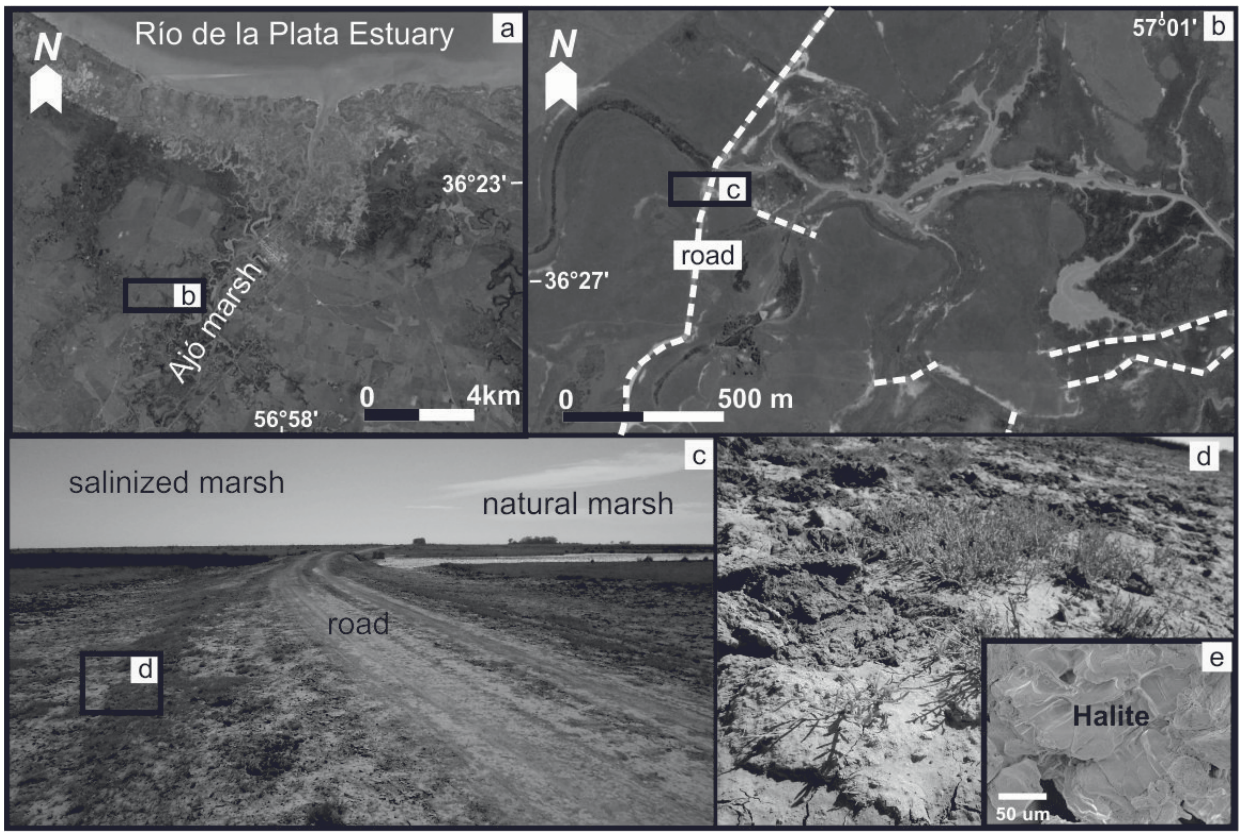

Figure 3: (a) Ajó marsh; (b) Detail of embankment area (white dotted lines) and route; (c) Photograph showing how the route embankment obstructs the tidal flow separating a natural marsh area and a salinized one ; (d) Detail of a zone with saline precipitates formation; (e) SEM image showing grains of halite-coated sediment

3.2 Bahía Blanca Estuary

This area has a meso-mareal tidal regime with mean amplitude of 3 m. Although Bahía Blanca has also a humid subtropical climate with year-round rainfall, the mean annual values of precipitation (SMN-1995-2010) and ET0 are 614 mm and 875 mm, respectively. The analysis of the relationship between both variables showed that the ET0 overcomes the precipitation from November to March, and the rest of the year the precipitation is just slightly higher (Fig. 2). In the coastal sector of the estuary, a wide marsh is developed, which is interrupted by route embankments in the most continental sectors (Fig. 4a and b). In some sectors, the embankment reaches 1.5 km in length with only one drainage. It is worth mentioning that, while the marsh sectors that are affected by the embankment develop large saline surfaces, those are not affected by the embankment, showing only few saline precipitates (Fig. 4c). In the affected areas, the halite develops above the marsh soils in layers of more than 5 cm thick (Fig. 4d). Significant amounts of salts are also recorded in other areas of the marsh that have locally embankments.

Dieses Werk ist copyrightgeschützt und darf in keiner Form vervielfältigt werden noch an Dritte weitergegeben werden.
Es gilt nur für den persönlichen Gebrauch.

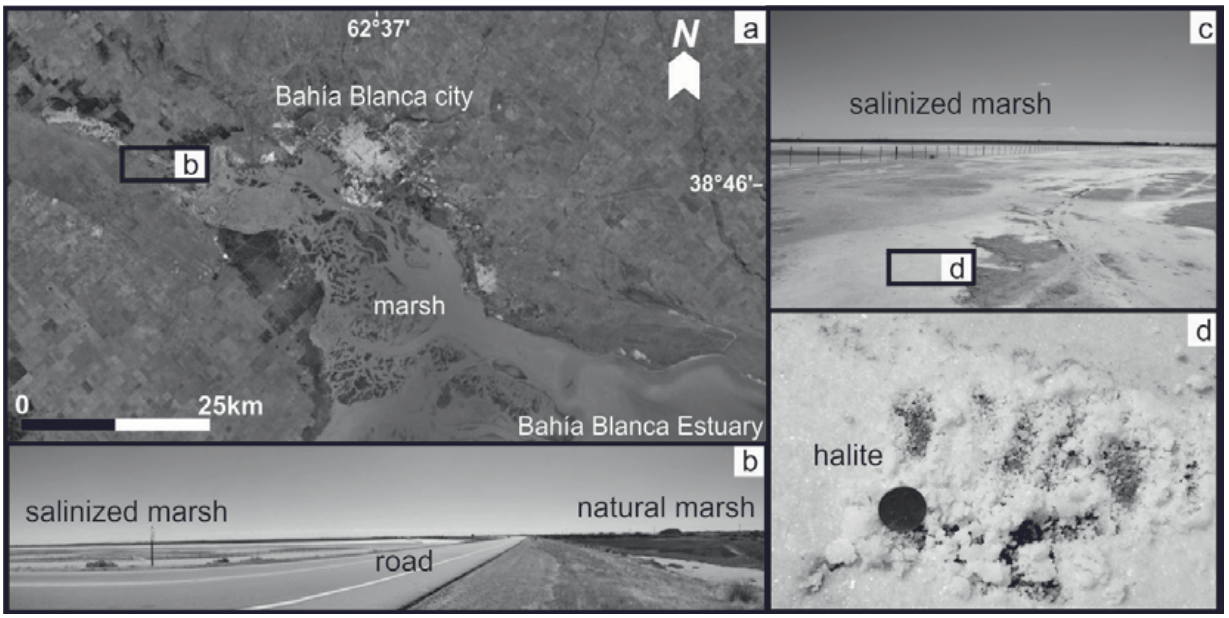

Figure 4: (a) Bahía Blanca marsh; (b) Photograph showing how the embankment of the route obstructs the tidal flow separating an area of natural marsh and a salinized one; (c) Photograph of the salinized marsh; (d) Detail of the halite precipitates that cover the salinized marsh sector

3.3 San Antonio marsh

This salt marsh is located surrounding the San Antonio Bay and has a strictly marine system with a semidiurnal macro-tidal regime (tidal amplitude between 9 and 4 m) crossed by several tidal channels (Fig. 1). The climate is semi-arid with a mean annual precipitation around 200 mm (SMN 1995-2010) and an annual ET0 of 750 mm (Köppen-Geiger classification: BSk). The monthly ET0 highly overcomes the precipitation in most part of the year except of June and July, when it is almost equal (Fig. 2). San Antonio Oeste city is located in the upper part of the marsh and along an old coastal spit. The routes and roads encircling the city are located either on the spike or surrounding the marsh in its upper part. Only few tidal channels in the high sector are crossed by these roads (Fig. 5a and b). This arrangement allows the natural flow to be almost unchanged. Salinization processes in the upper part of the marsh are mainly due to natural causes. Only in a sector, where a tidal channel is interrupted by a route, the development of a saline surface is identified (Fig 5c, d and e).

Dieses Werk ist copyrightgeschützt und darf in keiner Form vervielfältigt werden noch an Dritte weitergegeben werden.
Es gilt nur für den persönlichen Gebrauch.

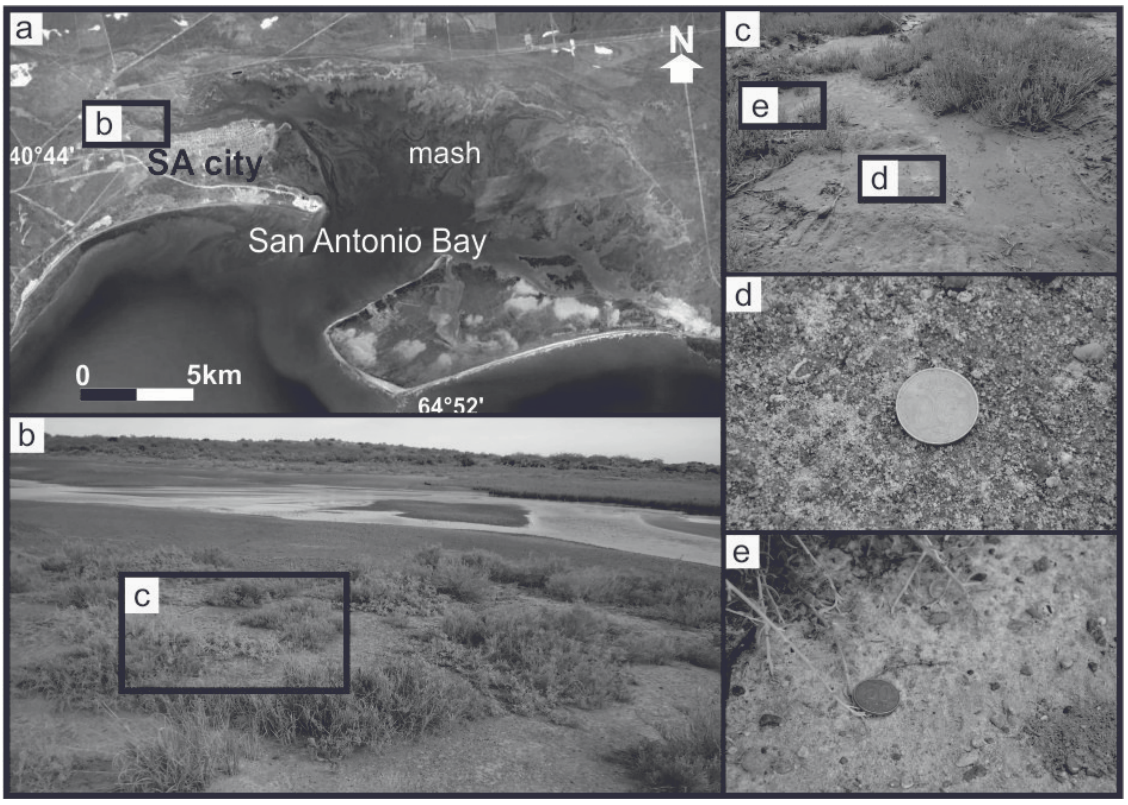

Figure 5: (a) San Antonio mash, San Antonio (SA) city; (b) Photography of the marsh area; (c, d and e) Details of areas with saline precipitates

3.4 Fracasso marsh

This salt marsh, located at the eastern coast of San José Gulf within Península Valdés, consists of an open coast and a bay marsh with no inflow from permanent surface water courses (Fig. 1). The tidal regime is semidiurnal, macro-tidal type, with amplitudes of approximately 4 m at quadrature and up to 9 m at syzygy. Its climate is semi-arid (Köppen-Geiger classification: BSk) characterized by an annual precipitation of 230 mm, with no definite trend throughout the year, and a mean annual temperature of 13.4 °C, fluctuating between mean extremes of 6.4 °C in July and 20.4 °C in January. The annual potential evapotranspiration reaches 704 mm and the distribution of Pp and ET0 throughout the year is similar to the San Antonio area (Fig. 2). The arid climate plus the seawater flooding, promote the salinization process. This process takes place mainly at the high topographic sectors, were the flooding occurs only at the syzygy high tides, while at quadrature the evapotranspiration rules. The evaporate minerals occur as really thin layers mostly at the upper marsh and over the levees of the tidal channels (Fig. 6b and c). Although depending on the topographic position, different types of evaporites were registered; there is a predominance of halite composition (Fig. 6c and d). Unlike in other study cases, Fracasso marsh is relatively isolated from the effect of developed urban centers, being only affected by small communities of artisanal fishermen extracting fish and shellfish in a seasonal way. In agreement with that, this marsh does not present anthropogenic modifications, and the mentioned salt crusts are only developed due to natural causes.

Dieses Werk ist copyrightgeschützt und darf in keiner Form vervielfältigt werden noch an Dritte weitergegeben werden.
Es gilt nur für den persönlichen Gebrauch.

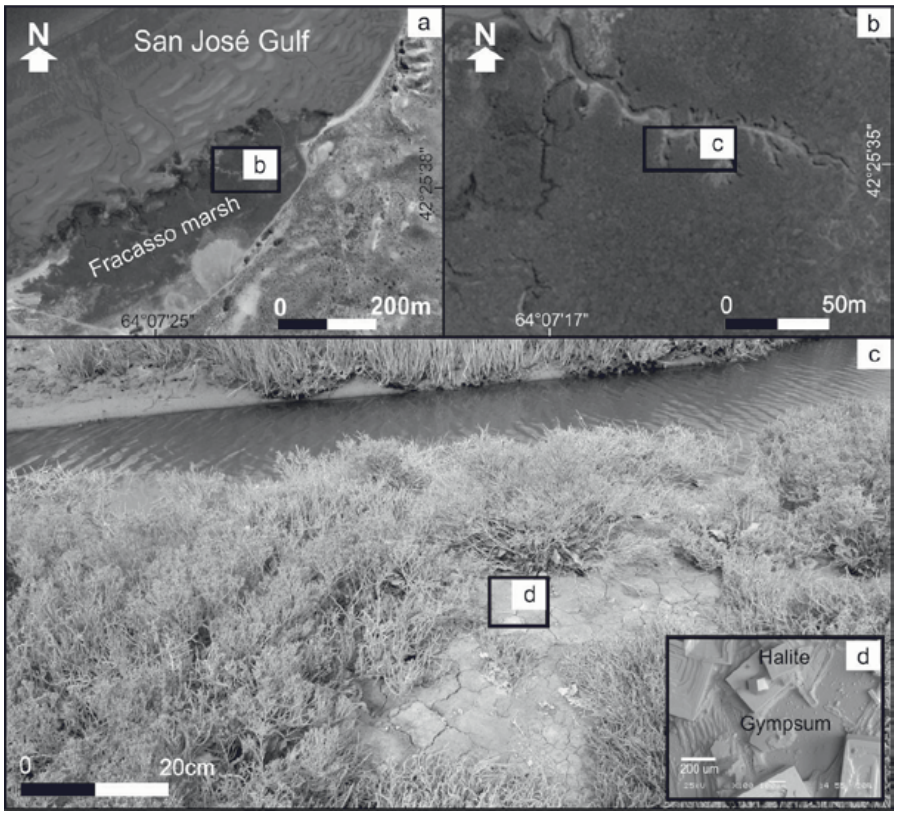

Figure 6: (a) Fracasso marsh; (b) Tidal channel detail; (c) Photograph of the marsh soil with saline precipitates; (d) SEM photography of saline precipitates

4 Discussion

The precipitation of evaporite minerals in marsh areas is determined by natural factors such as the climatic characteristics, tidal flow salinity, and the amplitude differences between the syzygy tides and quadrature tides, as well as soils types and topography [21]. The climatic characteristics condition the water balance and consequently the relationship between precipitation and evapotranspiration. As a product of the total evaporation of tidal water, the formation of saline precipitates occurs, requiring that real evapotranspiration exceeds precipitation [22]. Tidal flow salinity determines the quantity and type of salts that can be precipitated by total evaporation. Marshes with sea water influence will form more saline precipitates than those, where the tidal flow is influenced by the discharge of fresh water from rivers. On the other hand, if there is a great difference between height and amplitude of tides in syzygy and quadrature, the highest marsh sectors, which are flooded in the high tides of syzygy, are not flooded in the quadrature tides. If sea water from high tides of syzygy is accumulated, it can evaporate completely during the quadrature period [6].

The comparative analysis of the studied marshes allow to settle that anthropogenic modifications affecting the hydrological dynamic can promote the salinization of marsh soils and encourage the saline precipitates formation. Embankments of tidal flow or routes embankments with scarce or without drainage are engineering structures that modify the hydrological functioning of the

Dieses Werk ist copyrightgeschützt und darf in keiner Form vervielfältigt werden noch an Dritte weitergegeben werden.
Es gilt nur für den persönlichen Gebrauch.

marshes. The embankments limit the tidal flow, but during extraordinary tides the high tide can overcome them, causing the flooding of marsh areas that are usually isolated by the same embankment. Subsequently at low tide, the tidal water cannot drain efficiently and accumulates for long periods, and then it may be evaporated completely. Drainage system is usually scarce in routes embankments and has a higher level than the marsh; a similar hydrological situation can take place when the high tide exceeds the drainage level, and at low tide, only part of the tidal flow can drain back into the sea, evaporating the remaining flow.

Both the natural and the anthropogenic factors are different in the four marshes studied. The Ajó marsh is developed in a humid climate area, where the precipitation overcomes the potential evapotranspiration most part of the year, with favourable conditions for salt precipitate formation only between November and January (Fig. 2). The influence of the Río de la Plata discharge reduces the salinity of the tidal flow that floods periodically. This determines that the formed salt precipitates are considerably smaller than those formed in the other marshes that present a sea water influence. Finally, the tidal regime is micro-tidal without marked differences between the high tides of quadrature and syzygy. Consequently, there are not minor or greater flooding tides regulated by quadrature or syzygy cycles, respectively. Considering the natural factors, the saline precipitates formation in the Ajó marsh is highly unlikely, however, these were observed in several sectors of the marsh. Its formation agrees with the presence of tidal flow contention embankments and routes embankments. During extraordinary tides, the tidal flow surpasses the embankment and then, when it cannot drain, it evaporates resulting in the formation of salts over the soils surface. However, climatic characteristics and the high control of precipitation over evapotranspiration make the salts formation unstable because they are dissolved by rainfall and occasionally by the high atmospheric humidity of the region [19].

The Bahía Blanca marsh is developed in a humid subtropical climate area, where potential evapotranspiration far exceeds rainfall between November and February, while in the rest of the year rainfall slightly exceeds potential evapotranspiration (Fig. 2). The tidal flow that floods the marsh has a clear contribution of seawater without fluvial courses influencing the hydrology. It has a meso-tidal regime with mean amplitude of 3 m. All these climatic and tidal characteristics determine that the salt precipitates can be formed naturally, and that in natural areas of the marsh thin crusts were formed. When these natural conditions are combined with embankment effects, salinization highly increases, as observed in the marsh sector isolated by the route embankments. The tidal water that enters in extraordinary or syzygy tides accumulates and evaporates completely forming layers of halite precipitates.

San Antonio and Fracasso marshes have similar climatic and tidal characteristics. The climate is semi-arid in both marshes and evapotranspiration far exceeds the few precipitations almost all the year (Fig. 2). The tidal regime is macro-tidal with a marked difference between the high tides of quadrature and syzygy. This determines that saline precipitates formation naturally occurs in the soils of both marshes, a characteristic that has been observed in the field surveys. Halite salts occur in thin crusts or overlying the sediment grains mainly in the higher sectors of the marshes

Dieses Werk ist copyrightgeschützt und darf in keiner Form vervielfältigt werden noch an Dritte weitergegeben werden.
Es gilt nur für den persönlichen Gebrauch.

that are only flooded during high tides of syzygy. It is important to note that there are no embankments that increase the salts formation processes in these two marshes. Although San Antonio marsh has some human impacts, the embankments that limit the marsh show only few affected areas.

5 Conclusions

The obtained results show how both the anthropogenic and the natural factors condition the soils marshes salinization. The four studied marshes are located along a latitudinal gradient on the Argentina Atlantic coast, where the climatic conditions are wet in the northern sector and arid in the marshes of the southern sector. The tidal conditions change from north to south as micro-tidal in Ajó marsh, meso-tidal in Bahía Blanca, and macro-tidal in San Antonio and Fracasso marshes. Depending on the natural factors, it is expected that only in San Antonio and Fracasso marshes stable salt precipitates will occur, in Bahía Blanca marsh, salt crusts will occur mainly in summer and in Ajó marsh is very unlikely to form saline precipitates. However, both in Bahía Blanca and Ajó marshes anthropogenic factors related to embankments construction determine the formation of saline precipitates, which causes the salinization of the marsh soils to the extent of making great salines such as in Bahía Blanca. Despite of the development of salinization in humid climates, they are much more important than those formed under natural conditions in arid climates. This shows the high negative influence that an anthropogenic modification can have over sensitive ecosystems as the marshes.

6 Acknowledgement

The authors are very indebted to the Excellence Center for Exchange and Development (Exceed) and German Academic Exchange Service (DAAD) that made the participation at the event possible, and to the Agencia Nacional de Promoción Científica y Tecnológica (National Agency for Scientific and Technological Promotion) and the Consejo Nacional de Investigaciones Científicas y Técnicas (National Council for Scientific and Technological Research) of Argentina for financially supporting this study by means of their grants, PICT 2013 – 2248 and PICT 2012 – 687. They also want to thanks the Aluar S.A.I.C. for the SEM determinations.

7 References

1. Adam, P.: Saltmarsh Ecology. Cambridge University Press (1993)
2. Bertness, M.D.: The ecology of Atlantic shorelines. Sinauer Associates Sunderland, MA, USA (1999)
3. Fagherazzi, S., Kirwan, M.L., Mudd, S.M., Guntenspergen, G.R., Temmerman, S., D'Alpaos, A., van de Koppel, J., Rybczyk, J.M., Reyes, E., Craft, C., Clough, J.: Numerical models of salt marsh evolution: Ecological, geomorphic, and climatic factors. Reviews of Geophysics 50,n/a-n/a (2012)
4. Morris, J.T., Sundareshwar, P.V., Nietch, C.T., Kjerfve, B., Cahoon, D.R.: Responses of coastal wetlands to rising sea level. Ecology 83,2869-2877 (2002)

Dieses Werk ist copyrightgeschützt und darf in keiner Form vervielfältigt werden noch an Dritte weitergegeben werden.
Es gilt nur für den persönlichen Gebrauch.

5. Crain, C.M., Gedan, K., Dionne, M.: Tidal restrictions and mosquito ditching in New England marshes. University of California Press: Berkely, CA, USA (2009)

6. Silvestri, S., Defina, A., Marani, M.: Tidal regime, salinity and salt marsh plant zonation. Estuarine, Coastal and Shelf Science 62,119-130 (2005)

7. Watson, E.B., Byrne, R.: Abundance and diversity of tidal marsh plants along the salinity gradient of the San Francisco Estuary: implications for global change ecology. Plant Ecology 205,113 (2009)

8. Richardson, C.J., Reiss, P., Hussain, N.A., Alwash, A.J., Pool, D.J.: The Restoration Potential of the Mesopotamian Marshes of Iraq. Science 307,1307 (2005)

9. Canevari, P., Blanco, D.E., Bucher, E.H., Castro, G., Davidson, I.: Humedales de la Argentina: clasificación, situación actual, conservación y legislación. Wetlands International (1999)

10. Bala, L.O., D Amico, V.L., Stoyanoff, P.: Migrant shorebirds at Peninsula Valdes, Argentina: report for the year 2000. BULLETIN-WADER STUDY GROUP 98,14-19 (2002)

11. Blanco, D.E.: Situación actual de los chorlos y playeros migratorios de la zona costera patagónica. Fundación Patagonia Natural, Chubut (Argentina). Plan Integrado de la Zona Costera Patagónica. (1995)

12. Musmeci, L.R., de los Ángeles Hernández, M., Bala, L.O., Scolaro, J.A.: Use of Peninsula Valdes (Patagonia Argentina) by migrating Red Knots (Calidris canutus rufa). Emu 112,357-362 (2012)

13. Bortolus, A., Schwindt, E., Bouza, P.J., Idaszkin, Y.L.: A Characterization of Patagonian Salt Marshes. Wetlands 29,772-780 (2009)

14. Idaszkin, Y.L., Bortolus, A.: Does low temperature prevent Spartina alterniflora from expanding toward the austral-most salt marshes? Plant Ecology 212,553-561 (2011)

15. Idaszkin, Y.L., Bortolus, A., Bouza, P.J.: Flooding Effect on the Distribution of Native Austral Cordgrass Spartina densiflora in Patagonian Salt Marshes. Journal of Coastal Research 30, 59-62 (2014)

16. Isacch, J.P., Costa, C.S.B., Rodríguez-Gallego, L., Conde, D., Escapa, M., Gagliardini, D.A., Iribarne, O.O.: Distribution of saltmarsh plant communities associated with environmental factors along a latitudinal gradient on the south-west Atlantic coast. Journal of Biogeography 33,888-900 (2006)

17. Isla, F.I., Espinosa, M., Gerpe, M.S., Iantanos, N., Menone, M.L., Miglioranza, K.S.B., Ondarza, P.M., Gonzalez, M., Bertola, G., Aizpun, J.E.: Patagonian salt marshes: the soil effects on the NDVI response. Thalassas 26,23-31 (2010)

18. Alvarez, M.d.P., Carol, E., Bouza, P.J.: Precipitation/dissolution of marine evaporites as determinants in groundwater chemistry in a salt marsh (Península Valdés, Argentina). Marine Chemistry 187,35-42 (2016)

Dieses Werk ist copyrightgeschützt und darf in keiner Form vervielfältigt werden noch an Dritte weitergegeben werden.
Es gilt nur für den persönlichen Gebrauch.

19. Carol, E.S., Alvarez, M.d.P., Borzi, G.E.: Assessment of factors enabling halite formation in a marsh in a humid temperate climate (Ajó Marsh, Argentina). Marine Pollution Bulletin 106,323-328 (2016)

20. Thornthwaite, C.W.: Instructions and tables for computing potential evapotranspiration and the water balance. Drexel Institute of Technology, Centerton, NJ (EUA). Laboratory of Climatology (1957)

21. Warren, J.K.: Evaporites:Sediments, Resources and Hydrocarbons. Springer Berlin Heidelberg (2006)

22. Babel, M., Schreiber, B.: Geochemistry of Evaporites and Evolution of Seawater (2014)

Dieses Werk ist copyrightgeschützt und darf in keiner Form vervielfältigt werden noch an Dritte weitergegeben werden.
Es gilt nur für den persönlichen Gebrauch.

MODELLING AND MANAGEMENT OF STORM-DRIVEN SALTWATER INTRUSION IN FRESHWATER AQUIFERS: THE CASE OF NEAR BREMERHAVEN, GERMANY

Saber M. Elsayed[1], Hocine Oumeraci[1]

[1]Division of Hydromechanics and Coastal Engineering, Leichtweiß-Institute for Hydraulic Engineering and Water Resources, Technische Universität Braunschweig, Beethovenstraße 51a, 38106 Braunschweig, Germany, s-m.elsayed@tu-braunschweig.de

Keywords: Aquifers contamination; Coastal floods; Seawater intrusion; Storm surge; Wave overtopping.

Abstract

Coastal floods represent a significant humanitarian and socioeconomic hazard. Therefore, coastal barriers such as dunes, dykes and other engineered structures are often required as structural mitigation measures against coastal flooding. However, during extreme conditions (e.g., extreme storm surges), overtopping waves and/or floods resulting from breaching of coastal barriers may still be a threat. In fact, they can induce, in addition to direct physical damages, further types of long-term damages. The most important long-term effect of coastal floods is saltwater intrusion (SWI) into coastal aquifers induced by the vertical infiltration of the salt water behind the overtopped and/or breached coastal barriers. Such vertical SWI increases the salinity of the originally fresh groundwater, which indeed represents a major decrease of the water quality, possibly with significant environmental effects that can hinder possible sustainable development in coastal zones. This paper, therefore, highlights this problem through a case study in northern Germany, where coastal floods from the North Sea might represent a real threat to freshwater aquifers. Moreover, through the case study, the paper attempts to briefly summarise the state-of-the-art in modelling and mitigating storm-driven saltwater intrusion.

1 Introduction

Coastal areas and coastal aquifers are highly vulnerable environments and may experience severe impacts from coastal storms [1]. With global warming and sea level rise, many coastal systems may experience accelerated coastal erosion, coastal barrier breaching, coastal flooding, and subsequent seawater intrusion into fresh groundwater [2-6]. Changing climate might lead to changes in the frequency, intensity, spatial extent, and duration and timing of weather events, possibly resulting in unprecedented extreme events [7-10]. Extreme storm surges, subsequent coastal barrier erosion/breaching, and induced coastal flooding have the potential to result in severe direct and indirect consequences [11, 12]. The direct consequences might, for instance, be associated with damages to lifelines and infrastructures as well as with fatalities and injured people, while interruption of production processes represents an example of indirect economic damages that can be accounted for in flood risk assessments (e.g., [13]). Nevertheless, groundwater contamination owing to infiltrating seawater behind overtopped/breached coastal

Dieses Werk ist copyrightgeschützt und darf in keiner Form vervielfältigt werden noch an Dritte weitergegeben werden.
Es gilt nur für den persönlichen Gebrauch.

defences during and after coastal floods, as shown in Fig 1, represents one of the main indirect damages that are often not included in flood risk assessments.

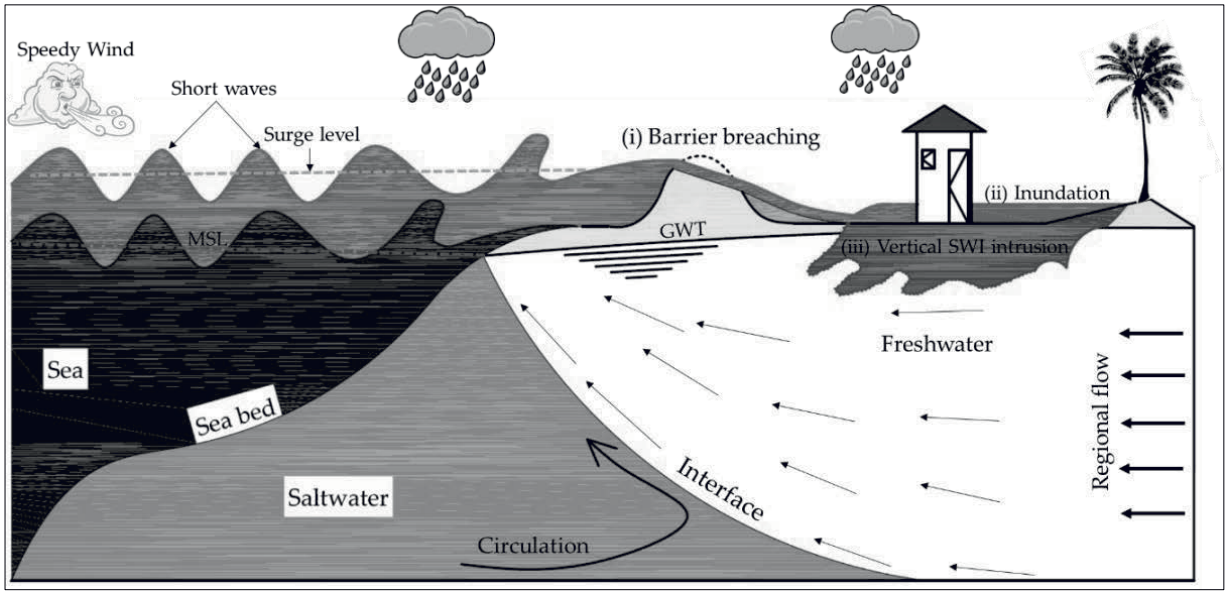

Figure 1: Sea/land boundary during an extreme storm surge, where a coastal barrier is directly attacked by propagating sea waves riding on the surge level, thus possibly causing barrier breaching, induced coastal inundation, and subsequent vertical SWI.

In fact, SWI during and after extreme events has a substantial impact on the dynamics of coastal aquifers as well as on the salinity distribution in such aquifers [1, 4-6, 14-16]. Even a moderate storm surge event may significantly affect the usability of coastal aquifers for many years [17, 18]. Vertical SWI contaminates the originally fresh groundwater by increasing its salinity, which may thus significantly reduce the water quality and the environmental values of groundwater, and possibly hinder any possible sustainable development in coastal zones exposed to flooding. Therefore, it is important to understand the effects of storm surges and the induced hinterland inundation on the water quality of coastal aquifers. Hence, this study aims at highlighting this problem through the case study near Bremerhaven, northern Germany, where any possible coastal flood from the North Sea might be a real threat to freshwater aquifers there. For the latter purpose, this paper is structured as follows: Section 2 describes the properties of the case study; Section 3 presents the state-of-the-art review in modelling storm-driven saltwater intrusion at the case study near Bremerhaven; Section 4 presents a brief overview of possible mitigation measures that may possibly mitigate aquifers contamination induced by a flood event, while Section 5 attempts to provide a brief summary of the results and conclusions drawn.

2 Case study

The following case study makes use of hydrogeological data and geophysical information available from the studies [4-6] for the same study area. The site selected for the case study belongs to the German Bight, which is situated north of Bremerhaven, northern Germany (Fig. 2).

Dieses Werk ist copyrightgeschützt und darf in keiner Form vervielfältigt werden noch an Dritte weitergegeben werden.
Es gilt nur für den persönlichen Gebrauch.

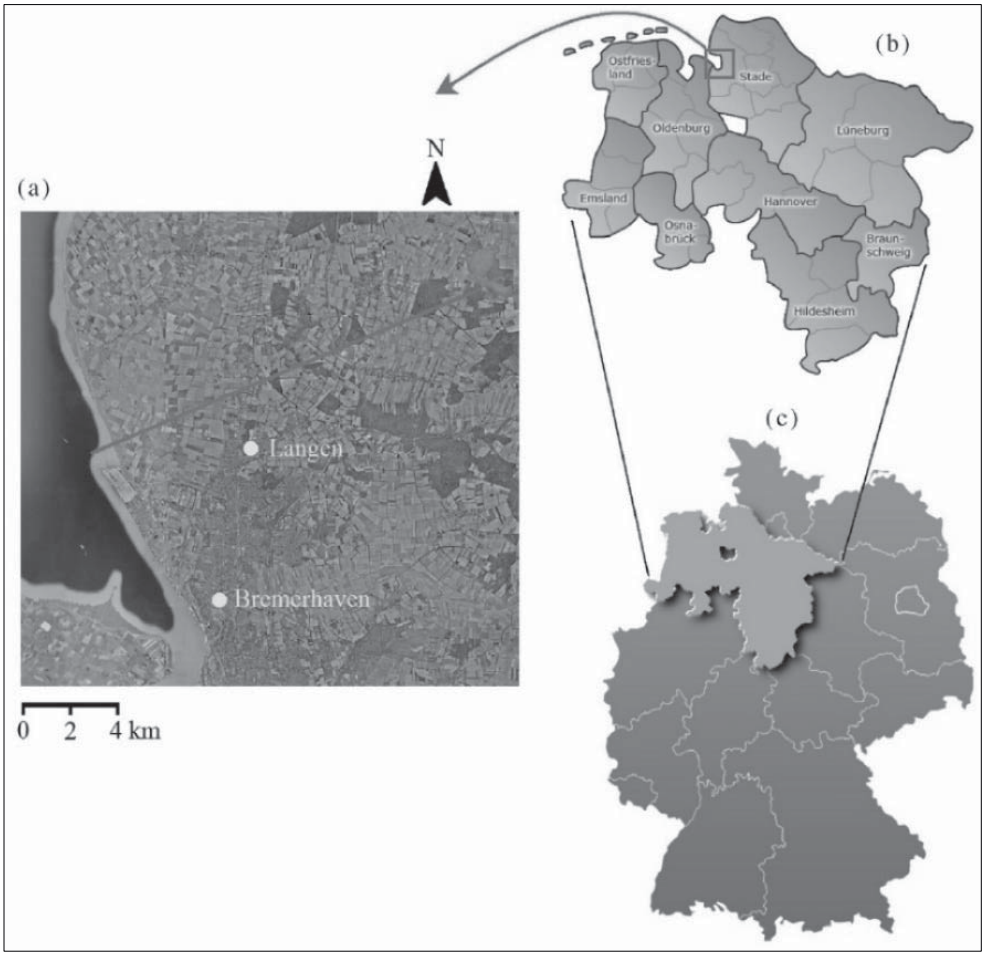

Figure 2: Location of the study area: (a) selected cross section near Bremerhaven (red line), (b) state of Niedersachsen (Lower Saxony), and (c) Germany [4]

In the German Bight, increases in wind velocity are expected in the future [6], which may enhance the probability of higher and longer storm surges. The river Weser discharges into the German Bight, and the catchment of the lower part of this river incorporates several cities, major ports, a variety of industries as well as agriculture, including livestock farming. The latter makes it crucial to study the impact of possible storm surge event on the sustainable development at this zone of Germany. The discharge of the river Weser results in dilation of the seawater in the North Sea near the study area, and thus reduces the average seawater concentration from 35,000 mg/L to 25,000 mg/L [4-6]. A 12 km long cross shore cross-section is considered, which is perpendicular to the coastline, as indicated by the red line in Fig. 2a. Therefore, the study area consists of a two-dimensional vertical cross-section of an unconfined coastal aquifer initially saturated with fresh water (salt concentration = 0.0 mg/L). The ground surface elevation (Fig. 3) was obtained from a digital elevation model (DEM) showing that the seaside (west) has a minimum seafloor bathymetry of −20.6 (m.a.s.l.). The inland area is protected by a dyke with a height of 7.3 m.a.s.l., whereas the elevation of the area behind the dyke ranges from 0.5 m.a.s.l. to 14.66 m.a.s.l. A constant domain bottom elevation of −100 m.a.s.l. is used as the aquifer bottom, which is considered impermeable.

Dieses Werk ist copyrightgeschützt und darf in keiner Form vervielfältigt werden noch an Dritte weitergegeben werden.
Es gilt nur für den persönlichen Gebrauch.

Groundwater level at the landside boundary was measured to be 4.0 m.a.s.l., and the effective groundwater surcharge (precipitation minus evapotranspiration) is estimated to be 300 mm/yr.

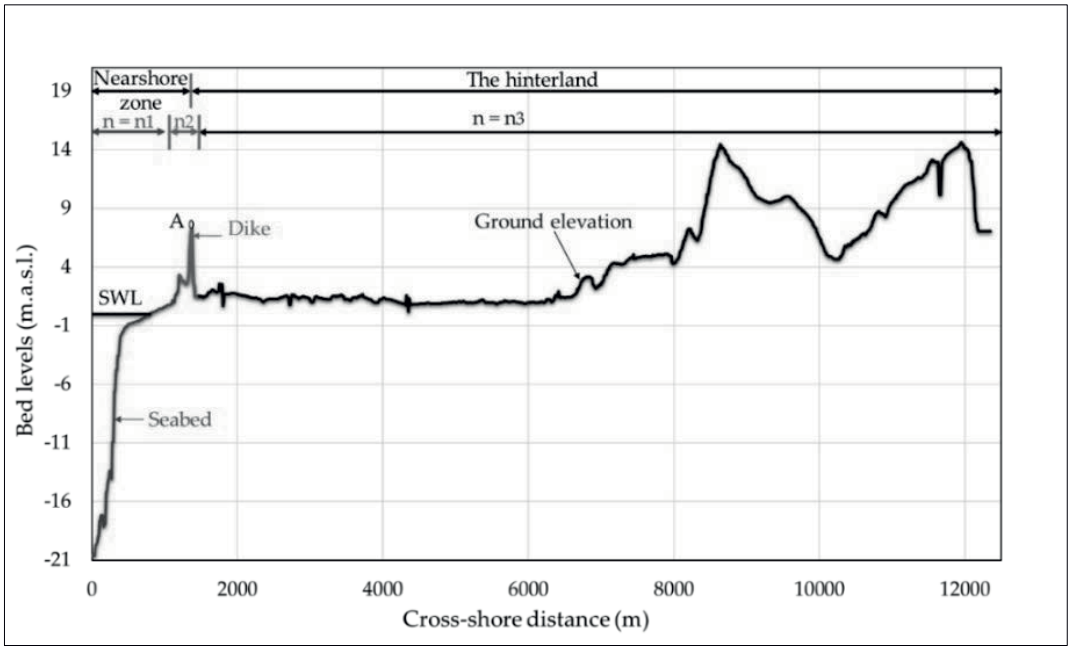

Figure 3: Bathymetry and ground elevations above the sea water level (SWL) for the considered cross-shore profile near Bremerhaven, Germany. The colours indicate different values for micro-topographical elevations represented by Manning's coefficient.

All values of aquifer parameter are listed in Table 1, where a homogeneous saturated hydraulic conductivity value Ks = 5×10^{-3} m/s (43 m/day) is considered as representative for the gravel/sand aquifer of the entire domain. In addition, uniform value for the longitudinal dispersivity D_L, the lateral dispersivity D_T and the molecular diffusion coefficient D are considered by 100 m, 10 m, and 10^{-9} m^2/s, respectively. Salt concentration in the sea is 25,000 mg/L, which is less than the average seawater concentration of 35,000 mg/L in the North Sea because of water dilution by the river Weser. Therefore, seawater density of 1,018.3 kg/m^3 is considered representative to the salt concentration of 25,000 mg/L, while freshwater (C = 0) density is 1,000 kg/m^3. Viscosity is assumed to be independent from salt concentration, and hence has a constant value of 1.124×10^{-3} kg/m.s. The aquifer storage parameters are 0.005 m^{-1}, 0.18 [-] and 0.2 [-], respectively, for the specific storage, specific yield and the effective porosity n.

The impact of a single storm surge event on coastal flow dynamics and on the investigated coastal aquifers is considered. The storm surge results in overtopping flow over the dyke crest. Subsequently, sea water inundates the hinterland behind the dyke, where the sea water infiltrates into the soil and percolates through the unsaturated (vadose) zone towards the GWT. Therefore, the storm surge event includes the processes of (i) sea level rise (SLR), (ii) overtopping/overflow and ponding, (iii) sea level dropping and pond reduction, and (iv) recovery of aquifer salinity to the initial state (remediation). The considered storm surge (Fig. 4) induces a maximum SLR up to 8.5

Dieses Werk ist copyrightgeschützt und darf in keiner Form vervielfältigt werden noch an Dritte weitergegeben werden.
Es gilt nur für den persönlichen Gebrauch.

m.a.s.l., which is about 1.1 m higher than the dyke crest without consideration of the effects induced by short-waves (e.g. wave runup). Thus, this storm surge event results in hinterland inundation and subsequent vertical SWI behind the dyke.

Table 1: Parameters of the coastal aquifer near Bremerhaven, northern Germany [1,4]

Parameter	Value	Unit
Hydraulic conductivity (*Ks*)	5×10^{-3}	m/s
Longitudinal dispersivity (D_L)	100	m
Transverse dispersivity (D_T)	10	m
Molecular diffusion (*D*)	1×10^{-9}	m^2/s
Seawater concentration	25000	mg/l
Saltwater density (ρ_s)	1018.3	kg/m^3
Freshwater concentration	0	mg/l
Freshwater density (ρ)	1000	kg/m^3
Reference fluid viscosity	1.124×10^{-3}	kg/m.s
Specific storage	0.005	m^{-1}
Specific Yield	0.18	-
Effective porosity (*n*)	0.2	-

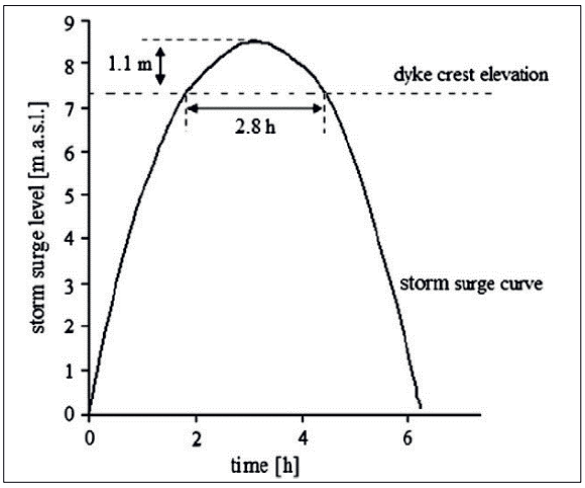

Figure 4: Applied time history of sea level during a storm surge event for the study site near Bremerhaven: the dashed line represents the elevation of the dyke crest [4]

Dieses Werk ist copyrightgeschützt und darf in keiner Form vervielfältigt werden noch an Dritte weitergegeben werden.
Es gilt nur für den persönlichen Gebrauch.

3 State-of-the-art in modelling storm-driven saltwater intrusion at the case study near Bremerhaven

With the global awareness of climate change and expected SLR according to [8, 9], attention is directed towards the scenario of coastal barrier overtopping/breaching, which might induce catastrophic floods and storm-driven saltwater intrusion (SDSWI) accordingly. Using the data provided in Section 2 for the case study of near Bremerhaven, and by utilising the surface-subsurface model HydroGeoSphere (HGS) of [19], Yang et al. [4] studied the effect of storm surge-induced wave overtopping over the dyke in Fig. 3 on aquifer salinity. Using HGS, Yang et al. [4] estimated that a total of 1,045 m^3 of seawater might flow across the dyke during 2.8 h of overtopping. Therefore, a total of 26 tons of salt is delivered onto the hinterland. Seawater flows as far as 3 km inland on the land surface. Simultaneously, the surface water infiltrates into the aquifer, which is considered homogenous with $Ks = 5 \times 10^{-3}\, m/s$, through the unsaturated soil zone (1 m thickness). As a result, salt plumes develop and move vertically downwards within the unsaturated and saturated zones (Fig. 5). However, both the considered precipitation (300 mm/yr) and the seaward flow as shown in Fig. 1 continuously dilute the infiltrated seawater and transport it back into the sea.

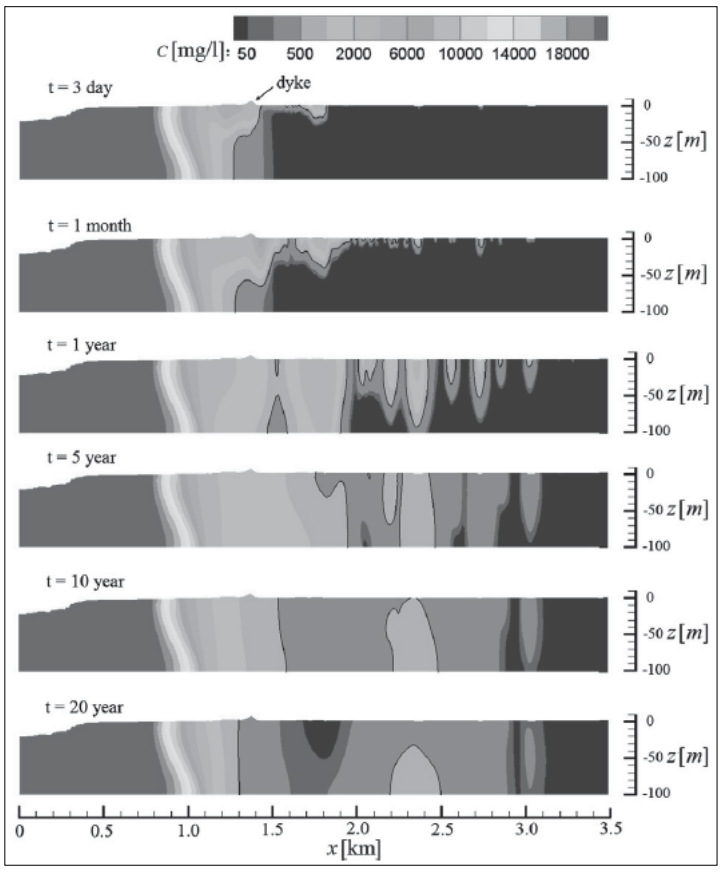

Figure 5: Distribution of salt concentration in the coastal aquifer at different times after the storm surge; Black lines are the iso-concentration lines of 500 mg/L [4]

Dieses Werk ist copyrightgeschützt und darf in keiner Form vervielfältigt werden noch an Dritte weitergegeben werden.
Es gilt nur für den persönlichen Gebrauch.

Fig. 5 presents the distribution of the salt concentration at different times after the onset of the storm surge. After 3 days of the inundation behind the dyke, seawater reached the aquifer behind the dyke, where the maximum salt concentration for human drinking water of 500 mg/L according the specifications of the World Health Organization [20] can be found at 16 m depth. After one month, numerous plume fingers developed in the aquifer up to 1,700 m behind the dyke, and the upper 35 m of the aquifer water is contaminated with a salt concentration of > 500 mg/L. After one year, the salt concentration of 500 mg/L has reached the bottom of the aquifer, such that groundwater of the entire aquifer within the distance of 1,700 m from the dyke has become unfit for drinking. After 5 years, the horizontal extent of the contaminated aquifer has reduced to 1,000 m behind the dyke due to the seaward flow of fresh groundwater. After 10 years, concentrations in most parts of the aquifer have dropped below 500 mg/L, such that groundwater has recovered to be suitable for drinking. However, natural remediation by the seaward flow of fresh groundwater is relatively slow. Even after 20 years, concentrations greater than 500 mg/L can still be found close to the aquifer bottom.

In order to study the effect of aquifer heterogeneity on the migration of salt plumes, Yang et al. [5] run again the surface-subsurface model of [4] for near Bremerhaven by considering aquifer heterogeneity as described in Fig 6a. With a scenario of total dyke failure (an assumed failure mechanism) during a storm surge event, a total of 2,272 m^3 (per meter dyke length) of seawater flowed to the inland. Therefore, a total of 57 tons (per meter dyke length) of salt is delivered onto the hinterland. Seawater flows as far as 7 km horizontally to inland on the land surface. As a result, the salinized area of the aquifer is expanded up to 2,050 m landward because of the expansion of inundation extent. The study of Yang et al. [5] has also shown that the nature of aquifers heterogeneity has a significant effect on the fate of the salt plumes, which is in line with the laboratory experiments of [21]. Moreover, the study showed that the natural remediation process takes more than 20 years as shown in Fig 6b.

In a 3D modelling study by [6] for the same study area near Bremerhaven, a breach of the dyke is assumed with fixed dimensions (fixed width of 100 m). As a result, the inland discharge estimated based on this scenario fed the hinterland to calculate the inland flood extent, water depths and the subsequent SWI. This study also reported that the NRP takes more than 20 years. The open channels in the study area are also simulated and showed an important effect on the increase of the contamination extent because they act as preferential pathways for landwards movement of salt water. However, the surface extent of the seawater, and the SWI extent accordingly, may be retreated by the land topography, as proved by [22].

Dieses Werk ist copyrightgeschützt und darf in keiner Form vervielfältigt werden noch an Dritte weitergegeben werden.
Es gilt nur für den persönlichen Gebrauch.

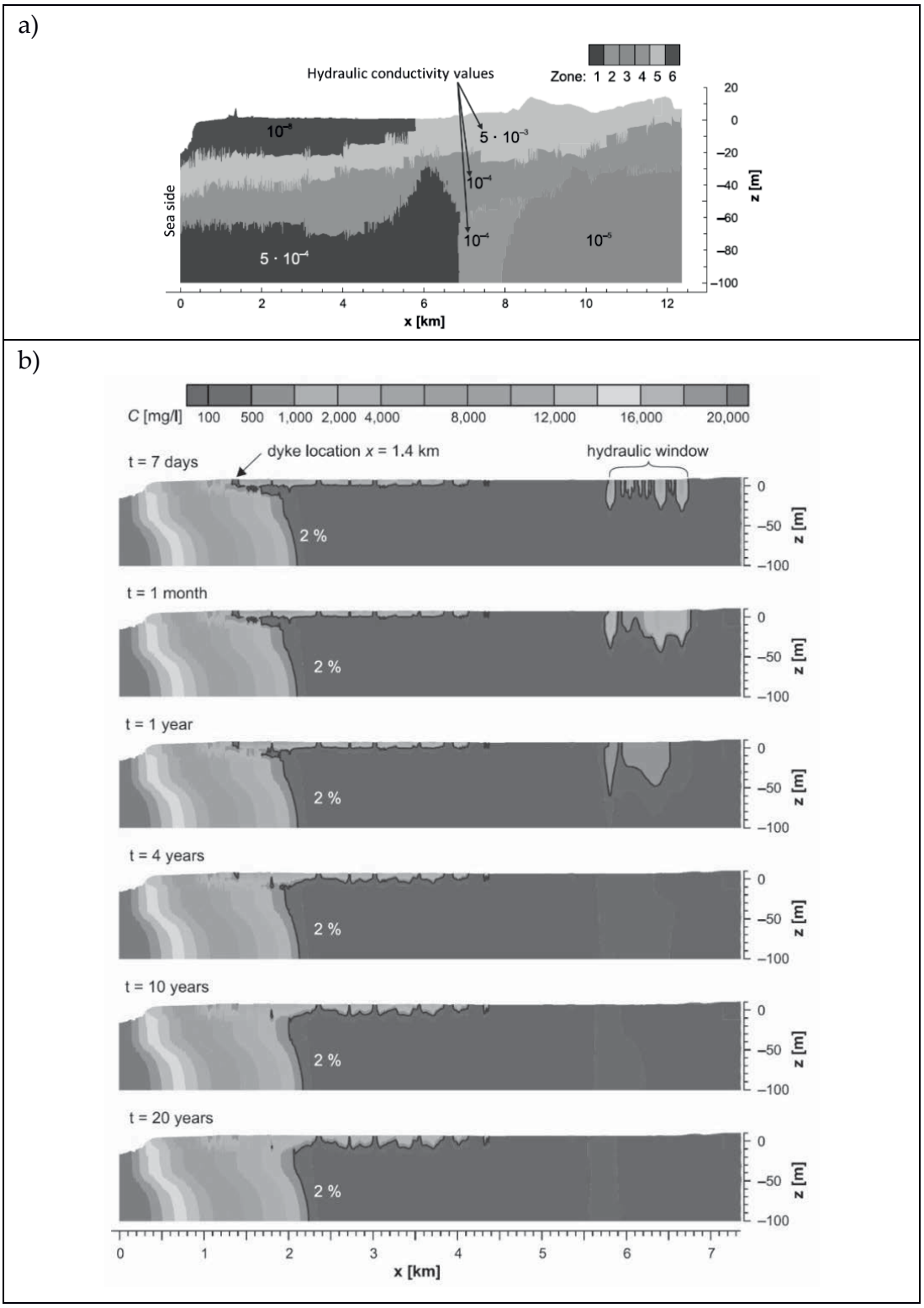

Figure 6: Effect of aquifer heterogeneity on SWI near Bremerhaven: (a) Six different zones of hydraulic conductivity to incorporate geological heterogeneity; Numbers are the hydraulic conductivities [m/s] for each zone and (b) Distribution of salt concentration in the coastal aquifer of soil heterogeneity described in (a) at different times after the storm surge. Black lines are the 2% salt concentration (500 mg/L) of that in seawater (25,000 mg//L) [5]

Dieses Werk ist copyrightgeschützt und darf in keiner Form vervielfältigt werden noch an Dritte weitergegeben werden.
Es gilt nur für den persönlichen Gebrauch.

The most recent studies of [1, 16] for the same study area near Bremerhaven have critically discussed the modelling methodology presented in the studies of [4-6] that is utilising the HGS model. It was shown that the use of a diffusive wave approximation of the nonlinear shallow water equations (e.g., [23]) to predict surface flow in HGS might result in an underestimation of the inland discharge over/through the overtopped/breached coastal barrier, which might accordingly lead to inaccurate prediction of the flood extent, the subsequent contamination extent, and remediation. As a result, these more recent studies proposed a new modelling methodology, utilizing the hydro-geo-morphodynamic open source model XBeach of [24] in order to simulate in combination the breaching/overtopping of coastal barriers and induced inundation of the hinterland as proposed by [25], whilst SWI is modelled separately by the SEAWAT code, which is built in the Visual Modflow graphical interface, so that the outcomes of XBeach are "manually" transferred as input data to SEAWAT. By applying this modelling methodology to the case study of near Bremerhaven with and without allowing the morphological evolution (*Morpho on* and *Morpho off*, respectively), Elsayed [1] predicted that an inland water volume of 2,196 m^3 propagates and extends for 5 km behind the dyke in the hinterland due to the water overflow event, as shown in Fig. 7. Thus, 54.9 tons of salt are supplied to the hinterland. These results were identical for both cases with and without allowing the morphological evolution because of the high Manning coefficient over the dyke crest, which does not permit high flow velocities over the dyke, and thus the dyke remains uneroded as the flow velocity remains always under the threshold effective velocity for sediment stirring according to Shields criterion [26]. The latter volumes for the inland discharge and salt mass are more than twice the values estimated by [4] using the surface module of HGS. Such significant differences arose from the fact that inland discharges calculated using HGS are based on a diffusive wave approximation of the NLSWEs, which ignores the inertial terms in the two momentum equations of the NLSWEs. For the very high overflow velocities over coastal barriers during overtopping and overflow conditions, neglecting the inertial terms (local and convective accelerations) might reduce inland discharges, as the high flow velocities over the barrier are not considered in the calculation because of the diffusive wave approximation. XBeach, however, uses all terms of the NLSWEs, including the inertial terms, and hence accounts for the flow velocities over the dyke, thus calculating more inland discharges. Bearing on a diffusive wave approximation in the surface calculations of HGS represents indeed one of the weaknesses in Yang's studies. In fact, such incorrect estimation of the inland flow rates in Yang's study results in an incorrect simulation of the flood propagation, induced water depths and flood extent, as proved by [25]. Thus, incorrect estimation of flood extent and water depths might also affect the results of the subsurface flow and the contaminant transport.

Dieses Werk ist copyrightgeschützt und darf in keiner Form vervielfältigt werden noch an Dritte weitergegeben werden.
Es gilt nur für den persönlichen Gebrauch.

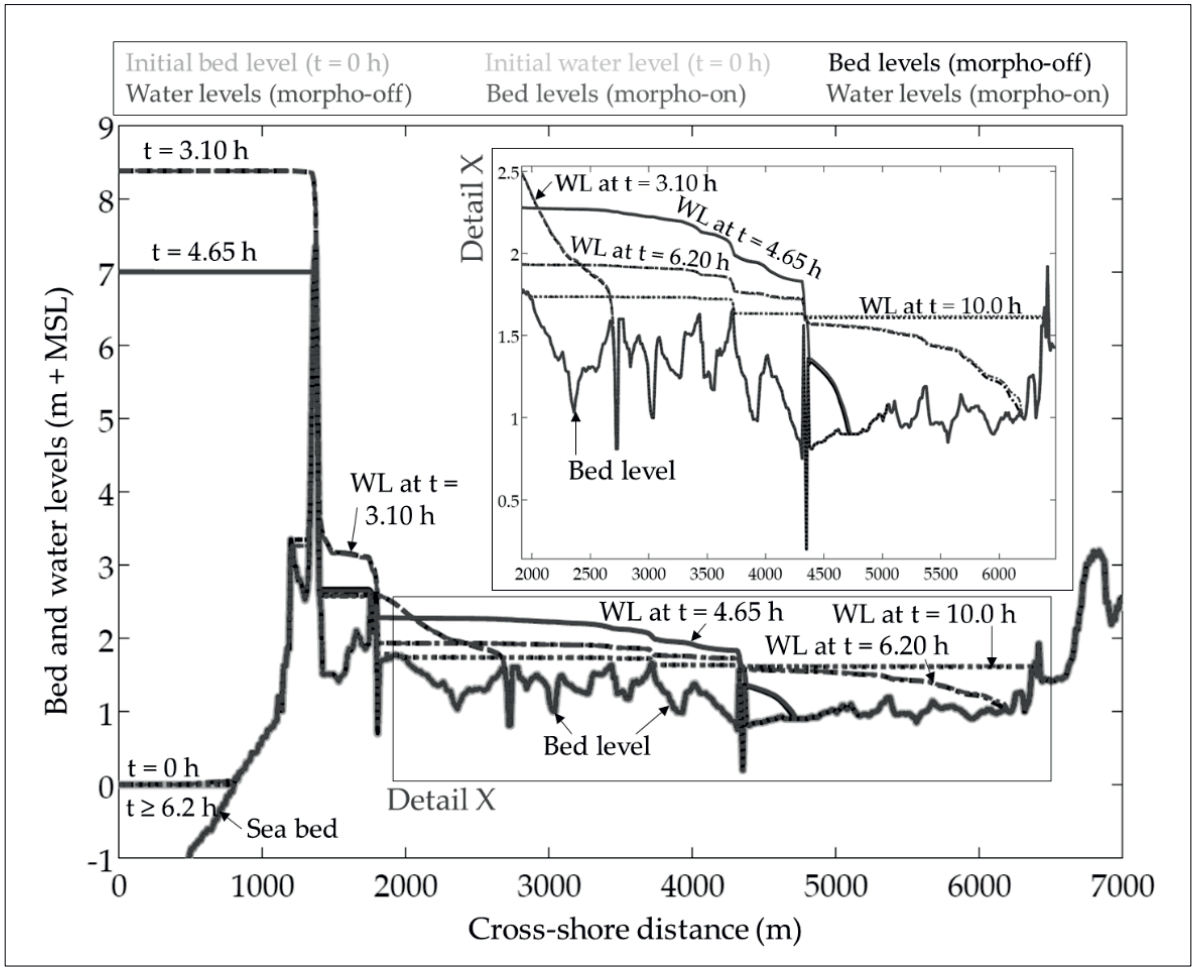

Figure 7: Evolution of the bed level (BL) and water levels (WL) for the cross-shore profile in Fig. 3 under the effect of the storm surge event in Fig. 4 with and without considering the morphological evolution

Using the XBeach-SEAWAT modelling approach, Elsayed [1] reported that the overtopped seawater takes 4 days to infiltrate behind the dyke to the aquifer and to induce a disorder of the salt mass budget of the Bremerhaven aquifer due to this coastal flood. Moreover, he explained such defection using the three curves in Fig. 8, namely: the accumulative (total) source in mass curve, the accumulative (total) sink out mass curve, and the curve of total mass remaining in the aquifer. The latter curve represents indeed the mismatch between the two former curves, and, therefore, its values can be read separately from the vertical axis on the right.

The increase of the source in mass during the percolation interval of 4 days (starting from t=1,825 at the end of the warming up time of the model to t=1,829) is totally stored in the aquifer, as represented by the curve of total mass remaining in the aquifer. This stored mass sinks out the aquifer gradually until the aquifer is totally remediated after 44.3 years. The latter means that freshwater zones in the aquifer, which are affected by the vertical leakage of salt water, will return to its initial state (0 mg/L of salt concentration) after this very long time. This recovery is due to the natural remediation of the aquifer owing to the seaward directed flow in addition to the recharged

Dieses Werk ist copyrightgeschützt und darf in keiner Form vervielfältigt werden noch an Dritte weitergegeben werden.
Es gilt nur für den persönlichen Gebrauch.

part of rain precipitation on the ground surface. In fact, seaward directed freshwater flow dilutes the infiltrating salt water and moves it seaward gradually until the aquifer is totally remediated. Indeed, latter processes are extremely slow, and hence very long intervals are needed for total aquifers recovery.

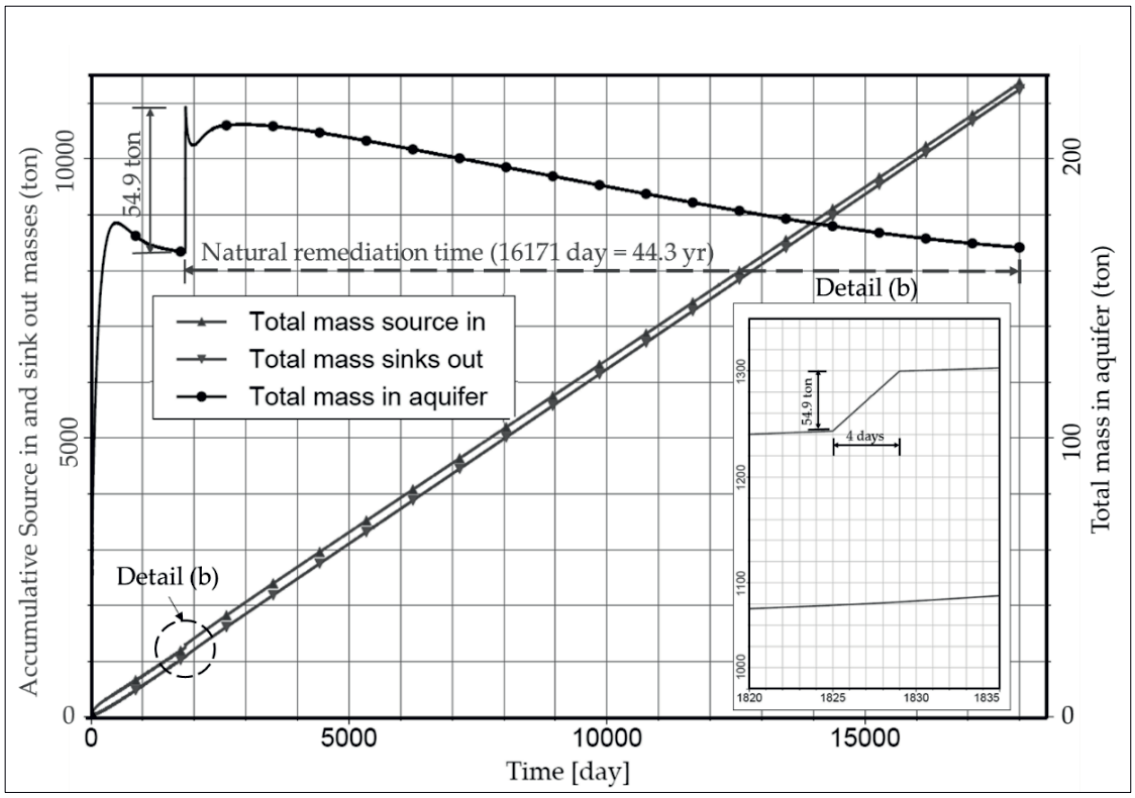

Figure 8: Accumulative salt masses along the fifty years of simulation: Accumulative salt entering the aquifer as a source in, accumulative salt leaving the aquifer as sink out and accumulative salt mass remaining in the aquifer. Detail (b) shows the increase of the source in starting from t = 1,825 days (5 years of warming up) to t = 1,829 days (5 years + 4 days) because of the vertical SWI, which results in an increase of the total mass in the aquifer by 54.9 tons during the inundation interval (4 days). The aquifer is remediated naturally after 44.3 years

4 Management of flood-induced saltwater intrusion into freshwater aquifer near Bremerhaven

Most studies associated with SDSWI are limited to the determination of the time interval for the natural remediation process after such events; no suitable structural mitigation measures are proposed to control this type of SWI and to shorten long remediation intervals. In fact, besides being a major limitation for the usability of contaminated groundwater for drinking and other subsistence purposes, crops in hinterlands may suffer stress, thereby not grow properly, or may die due to salt intolerance [27, 28], thus leading to a decrease in the agricultural yield [29, 30]. Given their vulnerability, sustainable management of coastal fresh groundwater reserves is of paramount importance.

Dieses Werk ist copyrightgeschützt und darf in keiner Form vervielfältigt werden noch an Dritte weitergegeben werden.
Es gilt nur für den persönlichen Gebrauch.

Management of coastal aquifers involves decisions regarding the amount of water to be extracted and/or injected into the aquifer [31], taking into account the interplay between the conditions of the aquifer and economic, social factors and, in some cases, environmental impacts [16]. For instance, some studies (e.g., [32, 33]) have listed many strategies/approaches for controlling lateral SWI into coastal aquifer systems, which is either in the form of upconing induced by excessive pumping and/or in the form of landward shifting of the salt-freshwater interface because of a long-term SLR or a long-term decrease of the groundwater table. These strategies are listed in Fig. 9.

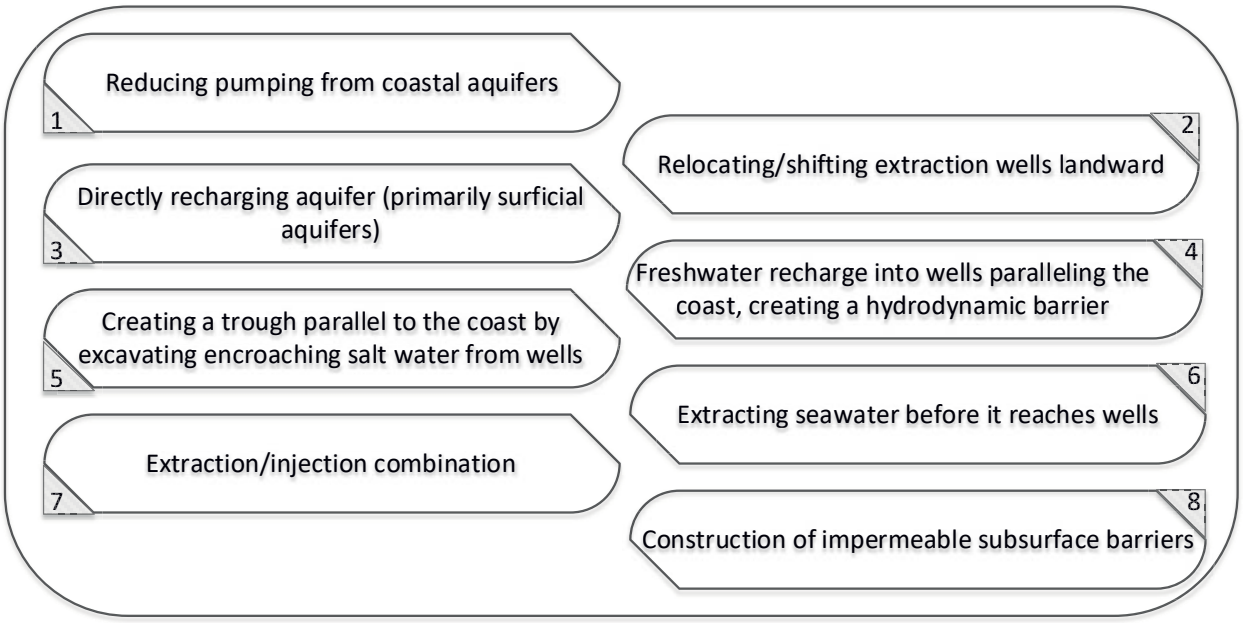

Figure 9: Common strategies to manage saltwater intrusion into coastal aquifers

Each of these methods can be applied to certain situations, and the method used depends on the specific problem to be solved. Moreover, simulation tools are often used to evaluate the effectiveness of possible decisions. Nevertheless, none of the previous traditional techniques for managing lateral SWI is suitable for managing vertical SWI induced by coastal inundation. For instance, Illangasekare et al. [34] attempted to overcome SWI induced by the 2004 tsunami in Sri Lanka using widespread pumping of wells to remove seawater. The latter approach was effective in some areas, but over-pumping has led to upconing of the saltwater interface and rising salinity rather than its removal from the upper part of the saturated zone. In addition, the purged well water was often discharged on the land surface close to the wells, allowing the contaminated water to re-enter the aquifer and the wells after vadose zone infiltration. For that reason, Elsayed and Oumeraci [14] suggested using subsurface drainage system (Fig. 10), especially in flood-prone agriculture areas.

Dieses Werk ist copyrightgeschützt und darf in keiner Form vervielfältigt werden noch an Dritte weitergegeben werden.
Es gilt nur für den persönlichen Gebrauch.

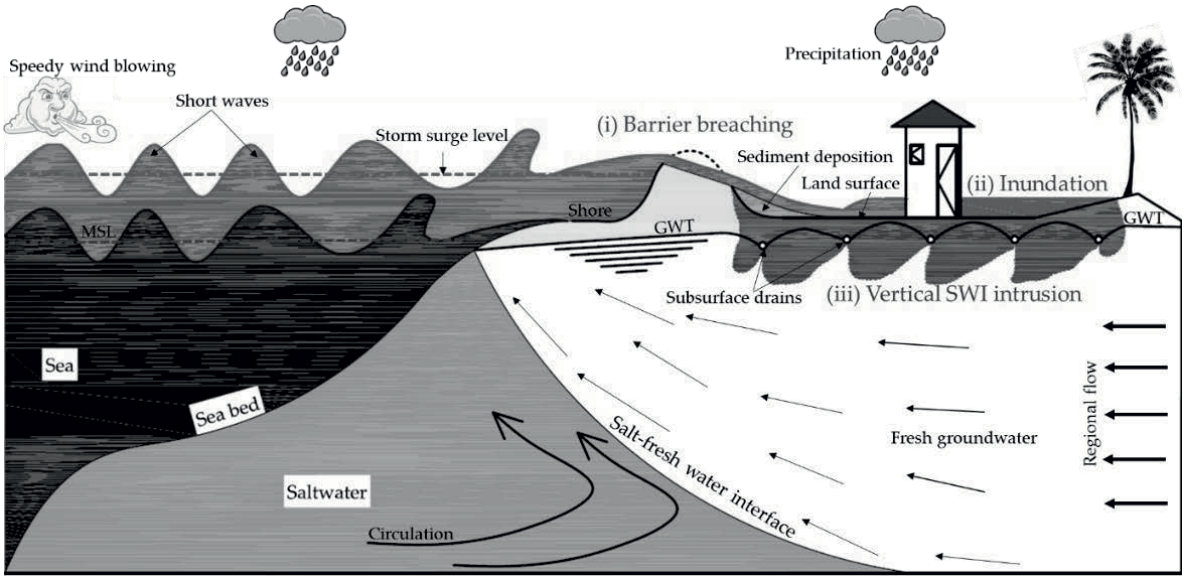

Figure 10: Schematic illustration of the flow of salt water through soil with respect to salt leaching and subsurface drainage during and after a storm-induced coastal flood [35]

The drainage, in general, would absorb the contaminated water before reaching the fresh groundwater. However, surface drainage is repulsive, since it could enlarge the contamination extent because surface drains would act as preferential pathways for landwards movement of salt water, as shown by Yang et al. [6]. For that reason, Elsayed [1] and Elsayed and Oumeraci [14] suggested and numerically tested the feasibility of using subsurface drainage system as shown in Fig. 10. The simulated subsurface drainage system collected part of the infiltrating salt water, especially during intervals of higher drain conductance, which are often taking place during higher infiltration rates from the land surface. Nevertheless, the rest is escaping downward among the drains, as shown in Fig. 10. By comparing both panels of Fig. 11 for saltwater distribution in the aquifer near Bremerhaven for both undrained and drained situations at the same time (t = 1 year after the flood event), one may notice that drainage has proved its efficiency in confining the high salt concentration near to the ground surface. In fact, drainage was capable of controlling the unwanted deeper infiltration of the high salt concentrations in the aquifer. Thus, Elsayed [1] reported that highly concentrated salt water is collected from the shallow zones within the three years after flooding. Moreover, he reported that shorter remediation intervals (< 3 years) might be achieved in case of using closer drains, as the wider drains spacing allows more escaping of the saltwater to the deeper freshwater in the aquifer. However, the efficient role of the drainage in shortening the remediation time of the vertical intrusion is often at the expense of more lateral intrusion (as shown in Fig. 11 by comparing the 50% iso-concentration contour in panel (a) for undrained and in panel (b) for drained conditions) because of the drainage-induced lowering of the GWT during intervals of higher drains conductance.

Dieses Werk ist copyrightgeschützt und darf in keiner Form vervielfältigt werden noch an Dritte weitergegeben werden.
Es gilt nur für den persönlichen Gebrauch.

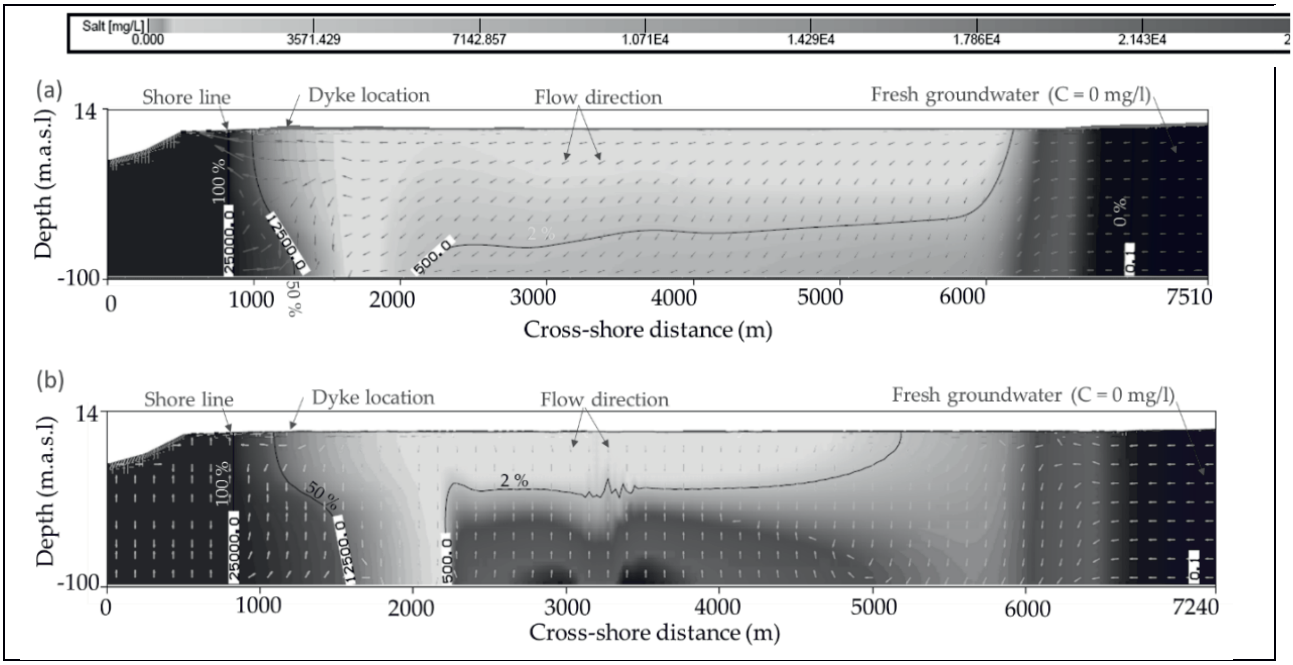

Figure 11: Salt distribution in the aquifer near Bremerhaven after one year of the flood event (a) with no drainage applied and (b) with subsurface drains. Salt-freshwater interface, represented by the 50% iso-concentration contour, and the iso-concentration contour of 500 mg/L (2%) are shown on each panel. The interface shifts landward in panel (b) due to the drainage induced lowering of the groundwater table

The effect of the drainage on the lateral saltwater intrusion might be explained using Fig. 12, which compares the mass of the salt remaining in Bremerhaven aquifer under both drained and undrained conditions. The mass remaining in the aquifer during the three (out of five) years of the warming up phase (the first 3 years eliminate the effect of the assumed initial conditions) is the same with and without drainage because the drains conductance is set at zero. During the following two years, which are also before applying the flood effect, the salt mass remaining in the aquifer increases with the drainage than without it. The latter is because the drainage reduces the GWT, leading to a lateral shift in the salt-freshwater interface landward, as shown in Fig. 11 by comparing panels a and b. During and after the flood by one year, the conductance value is the highest (= 2 m^3/d*m, as shown in Fig. 12), but the mass of salt in the aquifer is increasing dramatically than without drainage. This increase extends to the second year of flooding until it reaches its peak with the reduction of the conductance value from 1 to 0.06 m^3/d*m. With the latter reduction, the mass in the aquifer decreases gradually. Nevertheless, the remaining salt mass in the aquifer in the case of using subsurface drainage keep on higher than without drainage even after the 45 years after the flood event.

Dieses Werk ist copyrightgeschützt und darf in keiner Form vervielfältigt werden noch an Dritte weitergegeben werden.
Es gilt nur für den persönlichen Gebrauch.

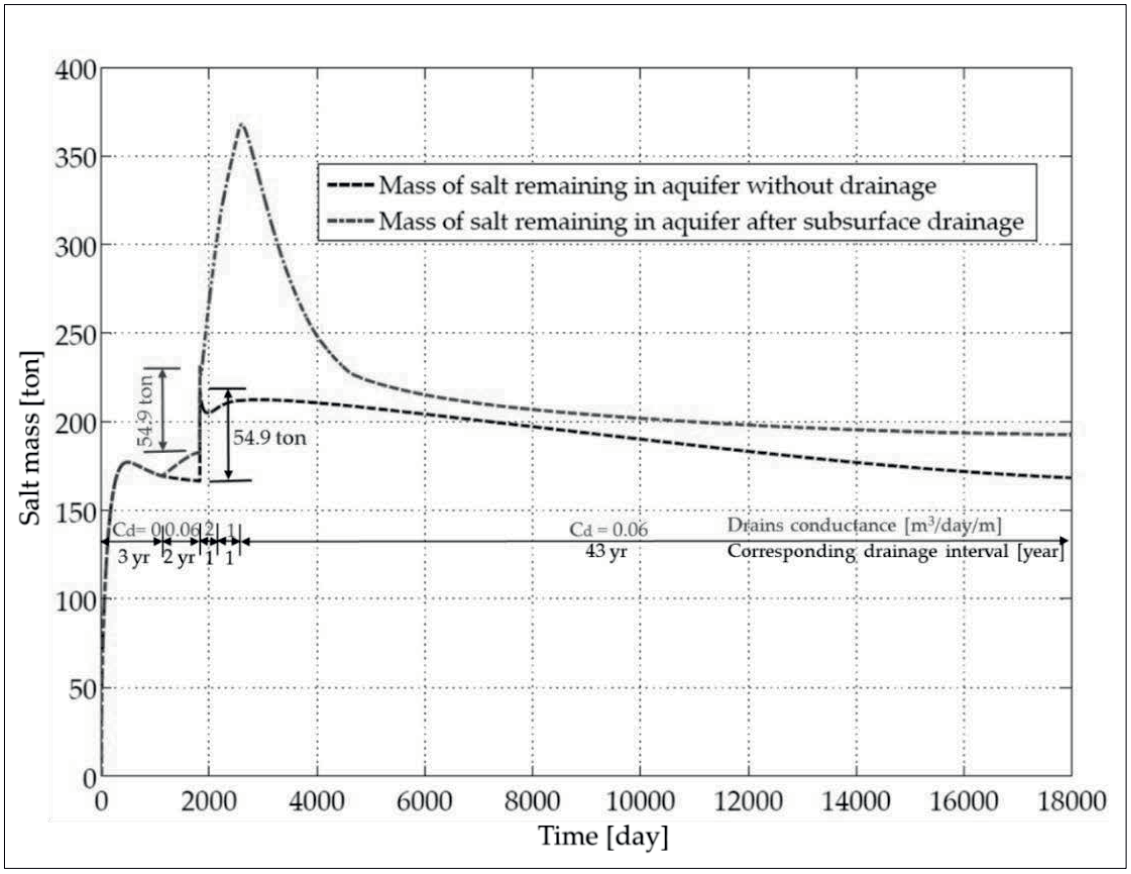

Figure 12: Comparison between salt masses remaining in the aquifer after and before the inundation with and without subsurface drains. In the case of drainage, more salt intrudes laterally to the aquifer, especially during higher conductance intervals

5 Summary and Conclusions

In this study, the implications of storm surge-induced barrier overtopping/breaching for coastal aquifer contamination are explored through a case study near Bremerhaven, Germany. Vertical saltwater intrusion induced by coastal inundation may increase the salinity of the originally fresh groundwater. The latter may significantly reduce the water quality and the environmental values of groundwater, thus possibly hindering any possible sustainable development in coastal zones. In fact, storm-driven saltwater intrusion can result in widespread aquifer contamination that could last for several years until it gets remediated naturally. Storm-surge driven saltwater intrusion (SDWI) often starts with a coastal barrier breaching or even overtopping, inducing inland inundation and subsequent vertical intrusion of seawater in coastal aquifers. An overflow event for 2.8 h near Bremerhaven may contaminate the freshwater aquifers for four decades until they are remediated naturally under the effect of precipitation and subsequent seaward directed flow. The extent of the subsurface contamination is a function of the flood extent.

Common management strategies to shorten long remediation intervals after a storm-driven saltwater intrusion event are found inappropriate for SDSWI mitigation. Therefore, Elsayed [1] proposed and numerically tested a subsurface drainage system. The model results showed that

Dieses Werk ist copyrightgeschützt und darf in keiner Form vervielfältigt werden noch an Dritte weitergegeben werden.
Es gilt nur für den persönlichen Gebrauch.

vertically intruding salt water is efficiently absorbed before contaminating the deeper aquifers. This counter-measure did not only reduce the vertical extent of the contamination, but also allowed to shorten significantly the natural remediation interval. Moreover, by lowering the groundwater table, the subsurface drainage system might improve the agricultural yield and also reduce the area of impact of salt water on possible organisms. On the other hand, the achieved lower groundwater table and shorter remediation interval are often accompanied by an increased lateral intrusion due to the defection in the hydrostatic equilibrium between the mean sea level and the groundwater table. The importance and implications of this effect, which are generally less significant as those of the two aforementioned mitigated effects, need however to be considered for the specific case under study.

6 Acknowledgements

This research is a part of the PhD study of the first author, which is supported by the DAAD in the frame of the Exceed-Swindon Project at Technische Universität Braunschweig. This support is gratefully acknowledged. The data for the case study of near Bremerhaven is gratefully provided by Prof. Dr. Thomas Graf and Dr. Jie Yang. The support of the Exceed-Swindon Project for the first author to attend the INECEP summer school in Mexico is also so much appreciated. The authors would like also to acknowledge the revision of this paper by Prof. Dr. Müfit Bahadir.

7 References

1. Elsayed, S.M.: Breaching of Coastal Barriers under Extreme Storm Surges and Implications for Groundwater Contamination. Leichtweiß-Institute for Hydraulic Engineering and Water Resources, vol. Ph.D. Technische Universität Braunschweig, Braunschweig (2017). Freely avaiable at: https://dx.doi.org/10.24355/dbbs.084-201710161043
2. Giambastiani, B.M.S., Colombani, N., Greggio, N., Antonellini, M., Mastrocicco, M.: Coastal aquifer response to extreme storm events in Emilia-Romagna, Italy. Hydrological Processes 31, 1613-1621 (2017)
3. Ranasinghe, R.: Assessing climate change impacts on open sandy coasts: A review. Earth-Science Reviews 160, 320-332 (2016)
4. Yang, J., Graf, T., Herold, M., Ptak, T.: Modelling the effects of tides and storm surges on coastal aquifers using a coupled surface–subsurface approach. Journal of Contaminant Hydrology 149, 61-75 (2013)
5. Yang, J., Graf, T., Ptak, T.: Sea level rise and storm surge effects in a coastal heterogeneous aquifer: a 2D modelling study in northern Germany. Grundwasser 20, 39-51 (2015)
6. Yang, J., Graf, T., Ptak, T.: Impact of climate change on freshwater resources in a heterogeneous coastal aquifer of Bremerhaven, Germany: A three-dimensional modeling study. Journal of Contaminant Hydrology 177, 107-121 (2015)

Dieses Werk ist copyrightgeschützt und darf in keiner Form vervielfältigt werden noch an Dritte weitergegeben werden.
Es gilt nur für den persönlichen Gebrauch.

7. de Winter, R.C., Ruessink, B.G.: Sensitivity analysis of climate change impacts on dune erosion: case study for the Dutch Holland coast. Climatic Change 141, 685-701 (2017)

8. Parry, M., Canziani, O., Palutikof, J., van der Linden, P.J., Hanson, C.E.: Climate change 2007: impacts, adaptation and vulnerability. Cambridge University Press Cambridge (2007)

9. Stocker, T.: Climate change 2013: the physical science basis: Working Group I contribution to the Fifth assessment report of the Intergovernmental Panel on Climate Change. Cambridge University Press (2014)

10. Vousdoukas, M.I., Mentaschi, L., Voukouvalas, E., Verlaan, M., Feyen, L.: Extreme sea levels on the rise along Europe's coasts. Earth's Future 5, 304-323 (2017)

11. Izaguirre, C., Losada, I.J., Espejo, A., Diez-Sierra, J., Díaz-Simal, P.: Coastal flooding risk associated to tropical cyclones in a changing climate. Application to Port of Spain (Trinidad and Tobago). Natural Hazards and Earth System Sciences Discussions. 2017, 1-24 (2017)

12. Oumeraci, H., Kortenhaus, A., Burzel, A., Naulin, M., Dassanayake, D., Jensen, J., Wahl, T., Mudersbach, C., Gönnert, G., Gerkensmeier, B.: XtremRisK—Integrated flood risk analysis for extreme storm surges at open coasts and in estuaries: Methodology, key results and lessons learned. Coastal Engineering Journal Vol. 57, No. 1 (2015) 1540001 (23 pp)

13. Ujeyl, G., Rose, J.: Estimating Direct and Indirect Damages from Storm Surges: The Case of Hamburg–Wilhelmsburg. Coastal Engineering Journal Vol. 57, No. 6 (2015) 1540006 [26 pp]

14. Elsayed, S.M., Oumeraci, H.: Modelling and Mitigation of Storm-Induced Saltwater Intrusion: Improvement of the Resilience of Coastal Aquifers Against Marine Floods by Subsurface Drainage. Submitt. to J. Environ. Model. Softw. (2017)

15. Violette, S., Boulicot, G., Gorelick, S.M.: Tsunami-induced groundwater salinization in southeastern India. Comptes Rendus Geoscience 341, 339-346 (2009)

16. Werner, A.D., Bakker, M., Post, V.E.A., Vandenbohede, A., Lu, C., Ataie-Ashtiani, B., Simmons, C.T., Barry, D.A.: Seawater intrusion processes, investigation and management: Recent advances and future challenges. Advances in Water Resources 51, 3-26 (2013)

17. Holding, S., Allen, D.M.: Wave overwash impact on small islands: Generalised observations of freshwater lens response and recovery for multiple hydrogeological settings. Journal of Hydrology 529, 1324-1335 (2015)

18. Wilson, A.M., Moore, W.S., Joye, S.B., Anderson, J.L., Schutte, C.A.: Storm-driven groundwater flow in a salt marsh. Water Resources Research 47, n/a-n/a (2011)

19. Therrien, R., McLaren, R., Sudicky, E., Panday, S.: HydroGeoSphere: a three-dimensional numerical model describing fully-integrated subsurface and surface flow and solute transport. Groundwater Simulations Group, University of Waterloo, Waterloo, ON (2010)

20. World Health Organization: Guidelines for drinking-water quality. World Health Organization (2004)

Dieses Werk ist copyrightgeschützt und darf in keiner Form vervielfältigt werden noch an Dritte weitergegeben werden.
Es gilt nur für den persönlichen Gebrauch.

21. Vithanage, M., Engesgaard, P., Jensen, K.H., Illangasekare, T.H., Obeysekera, J.: Laboratory investigations of the effects of geologic heterogeneity on groundwater salinization and flush-out times from a tsunami-like event. Journal of Contaminant Hydrology 136, 10-24 (2012)

22. Yu, X., Yang, J., Graf, T., Koneshloo, M., O'Neal, M.A., Michael, H.A.: Impact of topography on groundwater salinization due to ocean surge inundation. Water Resources Research 52, 5794-5812 (2016)

23. Collier, N., Radwan, H., Dalcin, L., Calo, V.M.: Diffusive Wave Approximation to the Shallow Water Equations: Computational Approach. Procedia Computer Science 4, 1828-1833 (2011)

24. Roelvink, D., Reniers, A., van Dongeren, A., van Thiel de Vries, J., McCall, R., Lescinski, J.: Modelling storm impacts on beaches, dunes and barrier islands. Coastal Engineering 56, 1133-1152 (2009)

25. Elsayed, S.M., Oumeraci, H.: Combined Modelling of Coastal Barrier Breaching and Induced Flood Propagation Using XBeach. Hydrology 3, 32 (2016). Freely available at: http://www.mdpi.com/2306-5338/3/4/32

26. Shields, A.: Anwendung der Aehnlichkeitsmechanik und der Turbulenzforschung auf die Geschiebebewegung (Application of similarity principles and turbulence research to bed-load movement). PhD Thesis Technical University Berlin (1936)

27. Faneca Sànchez, M., Bashar, K., Janssen, G., Vogels, M., Snel, J., Zhou, Y., Stuurman, R.J., Oude Essink, G.: SWIBANGLA: Managing salt water intrusion impacts in coastal groundwater systems of Bangladesh. Deltares (2015)

28. Felisa, G., Ciriello, V., Di Federico, V.: Saltwater Intrusion in Coastal Aquifers: A Primary Case Study along the Adriatic Coast Investigated within a Probabilistic Framework. Water 5, 1830-1847 (2013). Freely available at: http://www.mdpi.com/2073-4441/5/4/1830

29. Fakhruddin, S.H.M.: Flood impact on agriculture risk management. vol. Ph.D. Politecnico di Milano, Milan, Italy (2016). Freely available at: http://hdl.handle.net/10589/122609

30. Williams, V.J.: Identifying the economic effects of salt water intrusion after Hurricane Katrina. Journal of Sustainable Development 3, 29 (2010)

31. Kourakos, G., Mantoglou, A.: An efficient simulation-optimization coupling for management of coastal aquifers. Hydrogeology Journal 23, 1167-1179 (2015)

32. Gaaloul, N., Pliakas, F., Kallioras, A., Schuth, C., Marinos, P.: Simulation of seawater intrusion in coastal aquifers: Forty five-years exploitation in an eastern coast aquifer in NE Tunisia. The Open Hydrology Journal 6, 31-44 (2012)

33. Kumar, C.: Sea water intrusion in coastal aquifers. EPRA International Journal of Research and Development. SSN: 2455-7838, Vol 1, 27-31 (2016)

Dieses Werk ist copyrightgeschützt und darf in keiner Form vervielfältigt werden noch an Dritte weitergegeben werden.
Es gilt nur für den persönlichen Gebrauch.

34. Illangasekare, T., Tyler, S.W., Clement, T.P., Villholth, K.G., Perera, A., Obeysekera, J., Gunatilaka, A., Panabokke, C., Hyndman, D.W., Cunningham, K.J.: Impacts of the 2004 tsunami on groundwater resources in Sri Lanka. Water Resources Research 42, (2006)

35. Elsayed, S.M., Oumeraci, H.: Effect of beach slope and grain-stabilization on coastal sediment transport: An attempt to overcome the erosion overestimation by XBeach. Coastal Engineering 121, 179-196 (2017)

Dieses Werk ist copyrightgeschützt und darf in keiner Form vervielfältigt werden noch an Dritte weitergegeben werden.
Es gilt nur für den persönlichen Gebrauch.

SUBMARINE GROUNDWATER DISCHARGES AND THEIR INFLUENCE ON BENTHIC COVER AND REEF RUGOSITY AT PUERTO MORELOS REEF LAGOON

Arlett Rosado-Torres[1], Ismael Mariño-Tapia[1], César Acevedo-Ramírez[1]

[1]Laboratorio de Procesos Costeros y Oceanografía Física, Centro de Investigación y de Estudios Avanzados del Instituto Politécnico Nacional, Antigua Carretera a Progreso, Km. 6, Col. Cordemex. Mérida, Yucatán, México, C.P. 97310, arlett.rosado@cinvestav.mx

Keywords: Bathymetry, Benthic Cover, Coral, Macroalgae, Rugosity

Abstract

The present study shows evidence of continental inputs of water flowing directly into the reef crest through Submarine Groundwater Discharges (SGD) and its effect on the ecosystem in reef lagoon of Puerto Morelos, Quintana Roo. Using oceanographic instrumentation, high resolution bathymetric profiles were obtained to characterize reef rugosity, videotransects to estimate benthic cover through morpho-functional groups (stony corals, gorgonians, macroalgae, sponges, seagrass, and substrate), and salinity and temperature measurements to determine the influence of SGD. In addition, a CTD Diver was installed fixed on the sea bottom to study the dispersion of SGD on the reef and its lagoon. Measurements show consistent decrements of salinity with one month duration (during October-November 2016) reaching minimum values of 9.4 psu at sites influenced by SGD. These sites show contrasting effects as compared with the reference sites (i.e., Limones), such as a macroalgae-dominated benthic cover and reduced rugosity, especially where the macroalgae is present. Evidence of this is observed in the rugosity index obtained for the reference profiles. The results corroborate the negative influence of SGD on the reef, which could strengthen the demand for better sewage treatment practices in the area.

1 Introduction

In the Caribbean, most reefs have undergone a phase shift [1, 2] that occurs when scleractinial coral cover is reduced in favor of macroalgae dominance [3]. Algae develop in excess as they grow faster than corals, suffocate polyps, and compete with these and other reef habitants for space, light and nutrients [2, 4]. Thus, with increasing algal cover, the available substrate for coral recruitment is significantly reduced [5], and may adversely affect coral survival and distribution [6], and even the structural complexity of the reef system [1]. The change in structural complexity (decrease in bottom rugosity) generates significant losses in reef ecosystem services (i.e., coastal protection and species shelter) [7, 8]. The causes of phase shift are multiple; however, recent studies suggest that continental inputs may be contributing significantly [9].

The reef lagoon of Puerto Morelos is heavily influenced by Submarine Groundwater Discharges (SGD), which have been recognized as a gateway for nutrients, heavy metals, radionuclides and organic compounds [10-14], and depending on the geohydrological conformation, SGD can occur

Dieses Werk ist copyrightgeschützt und darf in keiner Form vervielfältigt werden noch an Dritte weitergegeben werden.
Es gilt nur für den persönlichen Gebrauch.

diffusely through the sea floor, or more punctually in patches or by submarine springs [15, 16]. Nowadays, there is little quantitative information available regarding SGD into the sea because measurements are difficult to perform, given the evident temporal and spatial variability of flows and that discharge sites are not always obvious [10, 16]. As almost all coastal zones are subject to flow of groundwater either as submarine springs or disseminated seepage, coastal areas are likely to experience environmental degradation [10]. SGD is potentially important to this areas because of the likely high concentrations of nutrients in groundwater compared to seawater [16], and even a small flow of groundwater can thus raise coastal concentrations [10, 16-18]. Transport of nutrients to coastal waters may trigger algae blooms, including harmful algae blooms, having negative impacts on the economy of coastal zones [18].

Therefore, the aim of this work is to present the influence of SGD on reefs using hydrodynamic, water quality, and rugosity parameters determined from transects perpendicular to the reef and from data obtained from oceanographic instruments anchored for at least 5 months.

2 Materials and Methods

Study Site

The coastal zone of the Yucatan Peninsula is characterized by a scarce and absent surface relief due to its geology, consisting of highly porous limestone (secondary porosity). This generates an underground hydrographic regime on the coast translates into multiple SGD that flow into wetlands, coastal lagoons and directly into the coastal sea, and has a significant impact on the composition, abundance and structure of marine biological communities due to the contributions of brackish water, nutrients, and contaminants [14]. The Puerto Morelos reef lagoon is located on the north-eastern coast of the Yucatan Peninsula, ~25 km south of Cancun (Fig. 1a), and is considered a protected marine area (Fig. 1b). The coast off Puerto Morelos is fringed by a reef that stretches about 4 km in length alongshore, creating a reef lagoon, whose width varies between 550 and 1,500 m [19].

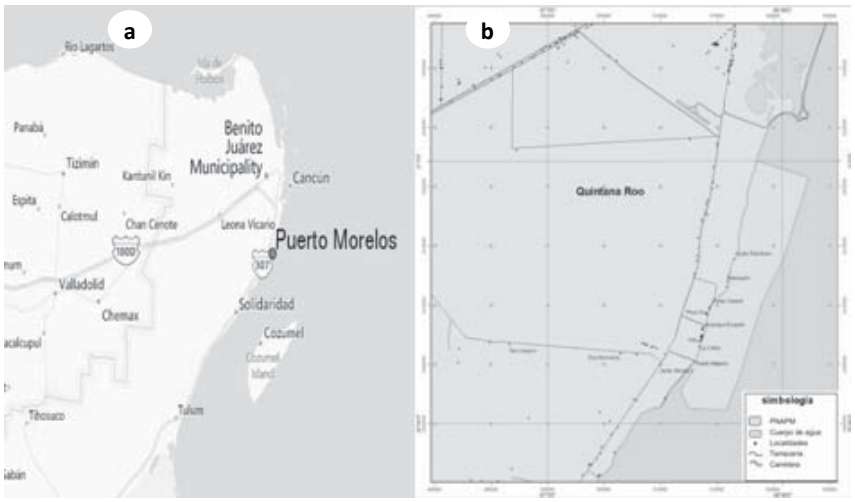

Figure 1: (a) Location of Puerto Morelos, Q. Roo, México; (b) Coastal Protected Park of Puerto Morelos

Dieses Werk ist copyrightgeschützt und darf in keiner Form vervielfältigt werden noch an Dritte weitergegeben werden.
Es gilt nur für den persönlichen Gebrauch.

Brief State-of-the-Art Review

Previous studies found high nitrate levels in the lagoon, which evidences the inadequate sewage disposal practices realized on Puerto Morelos, and the highly dynamic connection of the aquifer with coastal systems [11]. These authors proposed that this interaction occurs as shown in Fig. 2, where SGD plays an important role. In the same sense, Rosado-Torres [12] evaluated the effect of groundwater discharges on benthic communities, suggesting that there is a distribution gradient of benthic communities as a function of distance to SGD due to fluctuations of different environmental factors such as substrate characteristics, solar exposure, nutrient concentration, waves, and currents, among others [20]. In addition, other studies [21] compared the transformation of waves through sites of different rugosity, finding a slightly higher percentage of wave height reduction in the site with greater rugosity, demonstrating its importance as a form of natural protection of the coast.

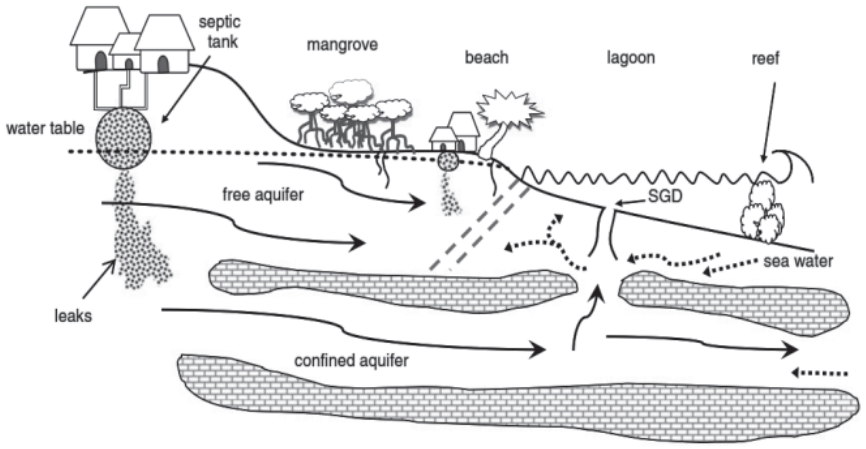

Figure 2: Aquifer interactions between inland human activities and coastal ecosystems in the region [11]

Methodology

Cross-reef profiles of high resolution bathymetry, salinity, temperature, nitrates, benthic coverage (through videotransects), and currents were obtained, which allowed the identification of nutrient inputs by continental and submarine discharges, characterization of the seafloor, and structural complexity of the reef (Fig. 3a). The measuring system incorporates a differential GPS (dGPS), a CTD, an Acoustic Doppler Current Profiler (M9), and a submersible camera (GoPro Hero) (Fig. 3b). These profiles were made by swimming on the reef crest and with the help of boats inside the lagoon.

Dieses Werk ist copyrightgeschützt und darf in keiner Form vervielfältigt werden noch an Dritte weitergegeben werden.
Es gilt nur für den persönlichen Gebrauch.

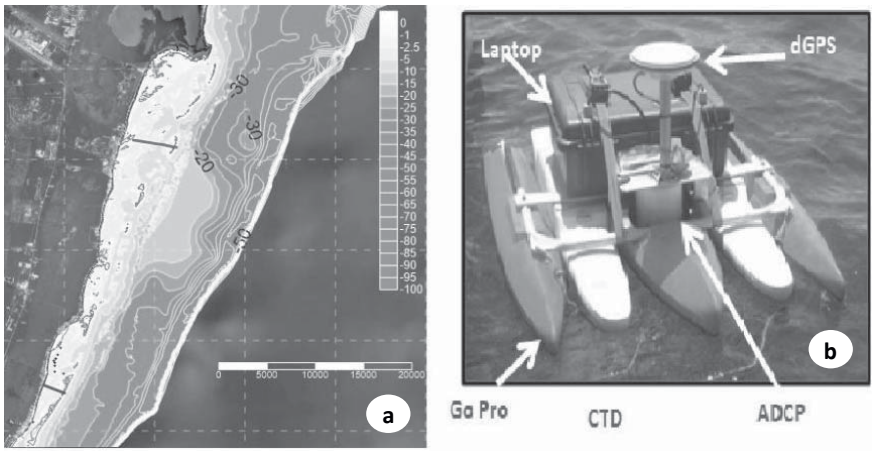

Figure 3: (a) Two of the perpendicular transects along the lagoon; (b) Measuring system with the instruments

Since it is common to find a time lag in the ADCP and dGPS registers, the first step is the synchronization and debugging of both registers. Once the data match, the time series of the GPSd (surface movement of the water by wave) is subtracted from the vertical beam of the ADCP in order to obtain the bottom relief. Rugosity estimates were made using high resolution bathymetry and dGPS. The measured bathymetric path was divided into small-scale (less than 30 m) and large-scale (greater than 30 m) vertical variations using a smooth filter with a 30 m cut-off point. Applying the low-pass filter, that is small-scale variations, will find shapes and objects such as individual coral colonies, sets of colonies, coral debris, algae patches, etc., while at large scales intrinsic form of the reef and the shape of the lagoon are found. To obtain the rugosity, the signal of small scale variations was used, since the interest is focused on the rugosity of the surface of the reef, and it is not considered to study the intrinsic form of the coral reef. Lowe *et al.* [22] proposed the rugosity index as 4 times the standard deviation of the small scale profile in 5 m windows with a flow filter. To link the information provided by the ADCP, this is the shape of the profile with the benthic cover, and complements what is obtained with videotransects that are taken with the GoPro camera. Videotransects were evaluated through the CPCe software (Coral Point Count with Excel Extensions). Characterization of the substrate and taxa present in the sampling points was done by grouping them into six morpho-functional groups (MFG): stony corals, gorgonians, macroalgae, sponges, seagrasses and substrate [23]. Also, samples of water were taken to analyse nitrates, nitrites, ammonium, phosphates, sulphates, and chlorides to quantify the nutrients and to calibrate the SUNA.

Five ADCPs were installed in a cross-reef profile from the fore reef to the beach in order to identify the possible pathways of SGD dispersion and persistent nutrient influence that might favour macroalgae populations and affect the structural complexity of the reef. Only the data obtained from a CTD Diver installed in the fore reef of the profile called "UNAM", located in front of the Instituto de Ciencias del Mar y Limnología of the Universidad Nacional Autónoma de México in Puerto Morelos, are presented in this paper.

Dieses Werk ist copyrightgeschützt und darf in keiner Form vervielfältigt werden noch an Dritte weitergegeben werden.
Es gilt nur für den persönlichen Gebrauch.

3 Results and Discussion

Calculating the rugosity index in two contrasting profiles of the Puerto Morelos lagoon, Figure 4 shows a higher value for the profile called "Limones" compared to "UNAM", being that in the latter the SGD is located.

The top image ("Depth"), it has the shape of the sea floor, while in the second ("Rugosity index"), the rugosity index associated with the profile is observed. As the result of the benthic cover for the entire profile will not be presented, both IR and benthic cover will have the same length from open sea to lagoon, because the analysis focused on the first zone, corresponding to the fore reef, crest reef, back reef and only part of the lagoon. The percentages of benthic coverage obtained by analyzing the videotransects taken with the GoPro camera are also presented in order to link them with both the bathymetric signal and the IR. The profile of the 14.6 km north of the UNAM station of Puerto Morelos is located in an area known as "Limones", which is designated as the best preserved site in the region. It presents the highest value of IR (1.62 m) due to stony corals, which is observed in the figure of benthic coverings, where the darkest colors in the first 500 m indicate a greater coverage of these. Also, there is not much coverage of macroalgae, as indicated by the lighter colors for this MFG. This privileged condition for Limones could be occurring because it is in an area where there are two mouths (or discontinuities of the barrier reef), and, therefore, a constant water change occurs. Also, there is no evidence yet that in this part of the lagoon there is any SGD from the aquifer.

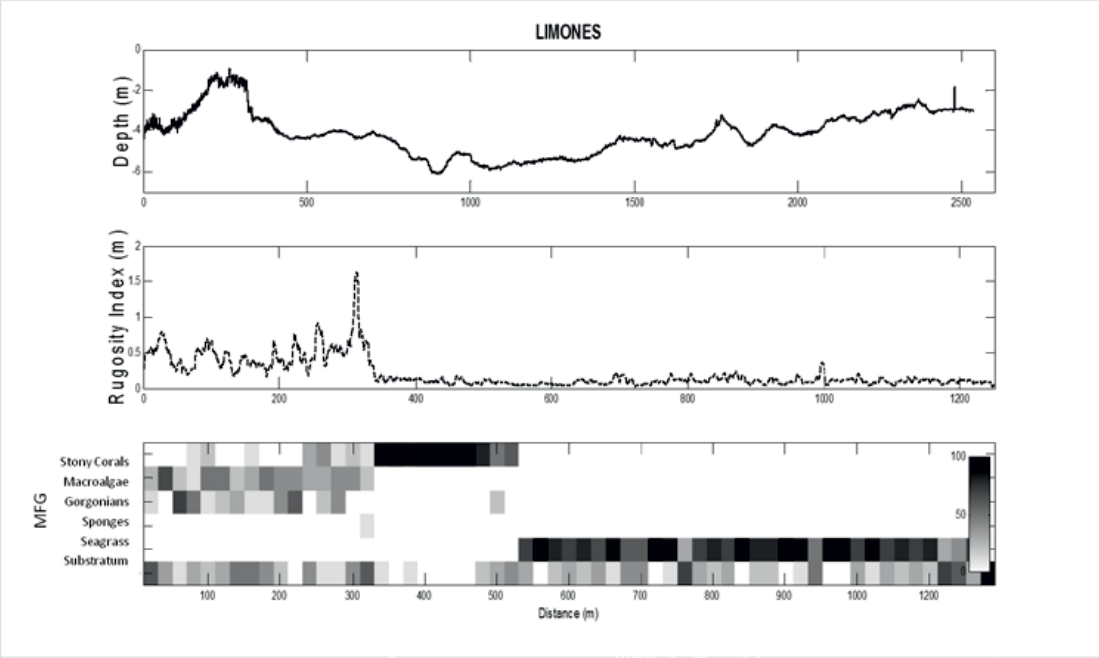

Figure 4a: Bathymetry, rugosity index and benthic covering from "Limones" profile

Dieses Werk ist copyrightgeschützt und darf in keiner Form vervielfältigt werden noch an Dritte weitergegeben werden.
Es gilt nur für den persönlichen Gebrauch.

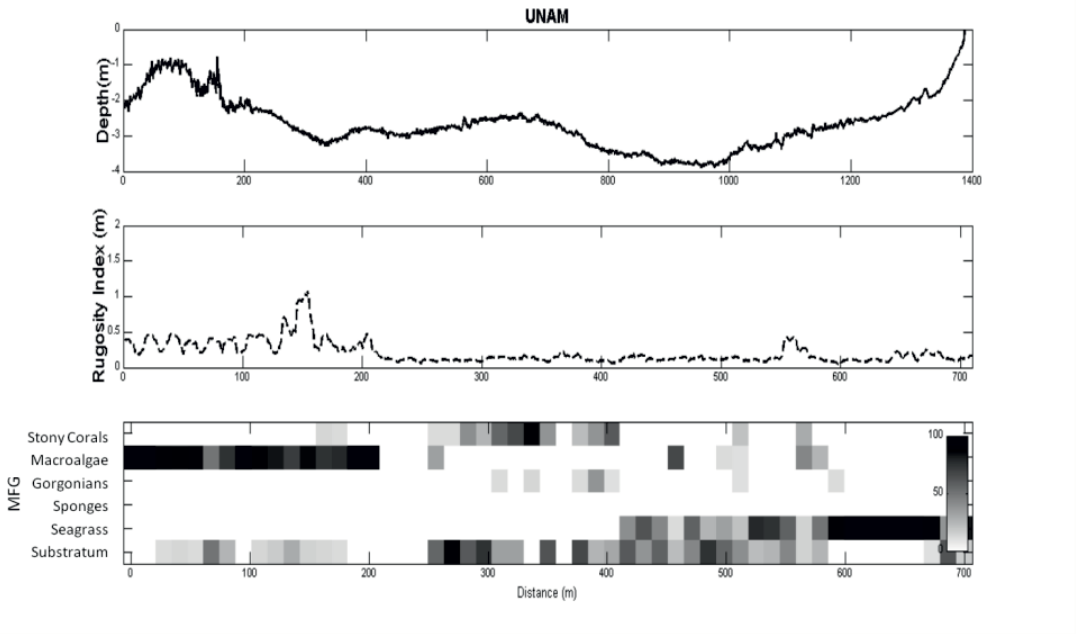

Figure 4b: Bathymetry, rugosity index and benthic covering from "UNAM" profile

On the other hand, it is the UNAM profile that has the lowest IR (1.08 m), which is mainly caused by macroalgae, as seen in the figure of benthic coverings, where the darkest colors are indicated in the MFG macroalgae in the first 400 m of the profile, and lighter colors are observed for the stony corals in this same section of the profile. It is important to note that the width of the lagoon in this part is smaller than that of Limones, being this one of 1400 m of fore reef to beach, whereas Limones has a length of 2500 m. For the above, it is suggested that in this profile there is a greater influence of the human settlements present on the coast. Also, unlike the previous profile, at least one SGD is in this zone, which is confirmed by the results obtained from the anchoring of the CTD Diver in the fore reef.

Regarding the water samples, the results show that, for the UNAM profile, the surface concentrations reached 7.45 ± 0.004 mg/L of N-NO_3, being the highest value of nitrates for all profiles analyzed. The concentrations were in the range of 0.01 to 5.01 mg/L in May and August, 2016. These results coincide with those found by other authors [11], according to which SGD are an important nutrient entry pathway into the system.

Through a simple linear regression (Figure 5) it was observed that the coral cover is inversely proportional to the macroalgal cover. This is due to the fact that the more presence of macroalgae, the coral reef will be reduced. To perform this regression, the rugosity values of three profiles were taken into account in addition to the UNAM and the Limones.

Dieses Werk ist copyrightgeschützt und darf in keiner Form vervielfältigt werden noch an Dritte weitergegeben werden.
Es gilt nur für den persönlichen Gebrauch.

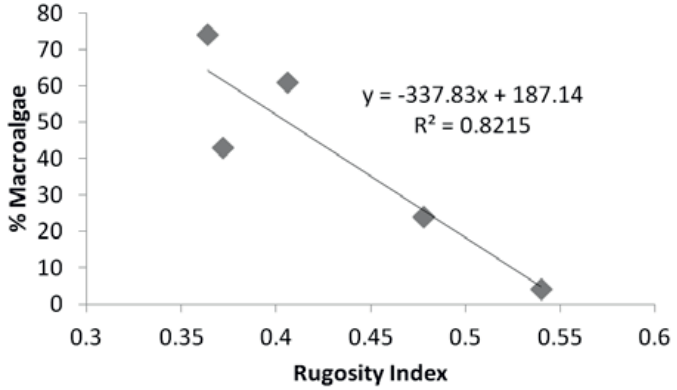

Figure 5: Simple Linear Regression between macroalgae cover and rugosity index from UNAM, Limones and other three profiles

Groundwater flow occurs mainly through coastal springs [24], who seem to be responsible for a greater macroalgal coverage and a marked decrease in salinity in the site of study. In the year 2013, the first suspicion of the presence of a SGD in the UNAM profile had been in the fore reef. With a CTD moored during 13 days, salinities of 21 to 24 ups were observed (Mariño-Tapia, personal communication, January 2016), when the average value of salinity for Puerto Morelos was 36 ups. Thus, from October 2016 to January 2017, a CTD Diver was placed at this same point in order to verify the existence of the SGD. The salinity results indicate, firstly, that there is a SGD in this area, and it was active most of the month October, and then late November and early December (Figure 6).

The nitrate results for the water sample of the UNAM profile, its high macroalgae cover, low coral rugosity, and the low salinity values found, are indicative for the presence of a SGD at this site. However, further water samples from other field work have yet to be analyzed and more comprehensive analyses of benthic cover in other profiles in the reef lagoon of Puerto Morelos to be considered.

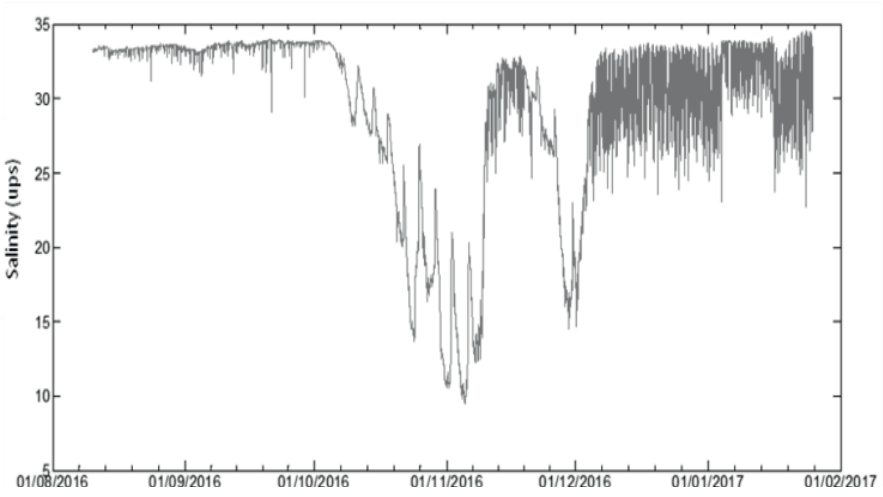

Figure 6: Salinity values in a SGD located in the fore reef from Puerto Morelos

Dieses Werk ist copyrightgeschützt und darf in keiner Form vervielfältigt werden noch an Dritte weitergegeben werden.
Es gilt nur für den persönlichen Gebrauch.

4 Conclusions

An intense Submarine Groundwater Discharge located in the fore reef from UNAM profile was active from October 2016 to January 2017, reaching salinity values as low as 9.4 ups. The largest macroalgae cover is linked to this intense SGD. There is an inverse relationship between macroalgae cover and rugosity index. In this sense, Limones, considered the best conserved reef in the Mesoamerican Barrier Reef, has low macroalgae cover, and large rugosity. Profiles influenced by continental water have the lowest values of rugosity and higher macroalgae cover, linking them to the loss of the coastal protection service of the reef.

5 References

1. Alvarez-Filip, L., Dulvy, N.K., Gill, J.A., Côté, I.M., Watkinson, A.R.: Flattening of Caribbean coral reefs: region-wide declines in architectural complexity. Proceedings of the Royal Society B: Biological Sciences 276, 3019 (2009)
2. Gardner, T.A., Cote, I.M., Gill, J.A., Grant, A., Watkinson, A.R.: Long-term region-wide declines in Caribbean corals. Science 301, 958+ (2003)
3. Hughes, T.P.: Catastrophes, phase shifts, and large-scale degradation of a Caribbean coral reef. Science 265, 1547+ (1994)
4. Garza-Pérez, J.R., Mata-Lara, M., García-Guzmán, S., Schirp-García, E.A.: Reporte de caracterización y evaluación de estado de condición arrecifal, Akumal, Quintana Roo. Programa de Investigación Espacial en Ambientes Costeros y Marinos. UMDI-Sisal, Facultad de Ciencias, Universidad Autónoma de México (2010)
5. García-Salgado, M., Camarena, T.L., Gold, B.G., Vásquez, M., Galland, G., Nava, G., Alarcón, D.G., Ceja, M.V.: Proyecto para la conservación y uso sostenible del Sistema Arrecifal Mesoamericano (SAM). Belice-Guatemala-Honduras-México. En: Línea Base del Estado del Sistema Arrecifal Mesoamericano. Documento Técnico del SAM 18: 1-200, (2006)
6. Tanner, J.E.: Competition between scleractinian corals and macroalgae: An experimental investigation of coral growth, survival and reproduction. Journal of Experimental Marine Biology and Ecology 190, 151-168 (1995)
7. Hernández-Landa, R.C., Acosta-González, G., Núñez-Lara, E., Arias-González, J.E.: Spatial distribution of surgeonfish and parrotfish in the north sector of the Mesoamerican Barrier Reef System. Marine Ecology 36, 432-446 (2015)
8. Marino-Tapia, I., Silva, R., Enriquez, C., Mendoza-Baldwin, E., Escalante-Mancera, E., Ruiz-Rentería, F.: Wave transformation and wave-driven circulation on natural reefs under extreme hurricane conditions. Coastal Engineering Proceedings 1, 28 (2011)
9. Suchley, A., McField, M.D., Alvarez-Filip, L.: Rapidly increasing macroalgal cover not related to herbivorous fishes on Mesoamerican reefs. PeerJ 4, e2084 (2016)

Dieses Werk ist copyrightgeschützt und darf in keiner Form vervielfältigt werden noch an Dritte weitergegeben werden.
Es gilt nur für den persönlichen Gebrauch.

10. Burnett, W.C., Aggarwal, P.K., Aureli, A., Bokuniewicz, H., Cable, J.E., Charette, M.A., Kontar, E., Krupa, S., Kulkarni, K.M., Loveless, A., Moore, W.S., Oberdorfer, J.A., Oliveira, J., Ozyurt, N., Povinec, P., Privitera, A.M.G., Rajar, R., Ramessur, R.T., Scholten, J., Stieglitz, T., Taniguchi, M., Turner, J.V.: Quantifying submarine groundwater discharge in the coastal zone via multiple methods. Science of the Total Environment 367, 498-543 (2006)

11. Hernández-Terrones, L., Rebolledo-Vieyra, M., Merino-Ibarra, M., Soto, M., Le-Cossec, A., Monroy-Ríos, E.: Groundwater Pollution in a Karstic Region (NE Yucatan): Baseline Nutrient Content and Flux to Coastal Ecosystems. Water, Air, & Soil Pollution 218, 517-528 (2011)

12. Rosado-Torres, A.A.: Efecto de las descargas de agua subterránea en la laguna arrecifal de Puerto Morelos, Quintana Roo. vol. M.Sc., pp. 96. Facultad de Ingeniería-Universidad Autónoma de Yucatán (2013)

13. Santos, I.R.S., Burnett, W.C., Chanton, J., Mwashote, B., Suryaputra, I.G., Dittmar, T.: Nutrient biogeochemistry in a Gulf of Mexico subterranean estuary and groundwater‐derived fluxes to the coastal ocean. Limnology and Oceanography 53, 705-718 (2008)

14. Troccoli, G.L.E.: Cambios estructurales del fitoplancton costero tropical en una zona cárstica: perspectivas en escala espacial. Instituto de Ciencias del Mar y Limnología. Unidad Académica Mazatlán, vol. Ph.D. UNAM (2001)

15. Graniel, E., Irany, V.M., González-Hita, L.: Dinámica de la interfase salina y calidad del agua en la costa nororiental de Yucatán. Ingeniería 8, 15-25 (2004)

16. Stieglitz, T.: Submarine groundwater discharge into the near-shore zone of the Great Barrier Reef, Australia. Marine Pollution Bulletin 51, 51-59 (2005)

17. Johannes, R.E.: The ecological significance of the submarine discharge of groundwater. Marine Ecology Progress Series 365-373 (1980)

18. Laroche, J., Nuzzi, R., Waters, R., Wyman, K., Falkowski, P., Wallace, D.: Brown Tide blooms in Long Island's coastal waters linked to interannual variability in groundwater flow. Global Change Biology 3, 397-410 (1997)

19. Coronado, C., Candela, J., Iglesias-Prieto, R., Sheinbaum, J., López, M., Ocampo-Torres, F.J.: On the circulation in the Puerto Morelos fringing reef lagoon. Coral Reefs 26, 149-163 (2007)

20. Pech, D., Ardisson, P.-L., Hernández-Guevara, N.A.: Benthic community response to habitat variation: A case of study from a natural protected area, the Celestun coastal lagoon. Continental Shelf Research 27, 2523-2533 (2007)

21. Franklin, G.L.: Effects of rugosity on wave-dominated coral reef environments. vol. Ph.D., pp. 167. Centro de Investigación y de Estudios Avanzados del Instituto Politécnico Nacional. Unidad Mérida (2015)

Dieses Werk ist copyrightgeschützt und darf in keiner Form vervielfältigt werden noch an Dritte weitergegeben werden.
Es gilt nur für den persönlichen Gebrauch.

22. Lowe, R.J., Falter, J.L., Bandet, M.D., Pawlak, G., Atkinson, M.J., Monismith, S.G., Koseff, J.R.: Spectral wave dissipation over a barrier reef. Journal of Geophysical Research: Oceans 110, (2005)

23. Aronson, R.B., Swanson, D.W.: Video surveys of coral reefs: uni and multivariate applications. Proceedings of the 8th International Coral Reef Symposium 2, 1441-1446 (1997)

24. Beddows, P.A., Smart, P.L., Whitaker, F.F., Smith, S.L.: Beddows, P.A., P.L. Smart, F.F. Whitaker, S.L. Smith: Density stratified groundwater circulation on the Caribbean coast of the Yucatan Peninsula, Mexico. Karst Waters Institute Special Publication 7: 129-134, (2002). vol. 7. Karst Waters Institute Special Publication (2002)

Dieses Werk ist copyrightgeschützt und darf in keiner Form vervielfältigt werden noch an Dritte weitergegeben werden.
Es gilt nur für den persönlichen Gebrauch.

GROUNDWATER ECOSYSTEMS SERVICES FOR INDUSTRIAL USE IN COASTAL AQUIFER

Jéssica Formentini[1], Malva Andrea Mancuso[2]

[1]Postgraduate Program in Environmental Engineering (PPGEAMB), *Universidade Federal de Santa Maria* – (UFSM) (Federal University of Santa Maria), Number 1000, Roraima Avenue, University City, Camobi district, postcode: 97105-900, Santa Maria City, RS, Brazil, jeformentini@yahoo.com.br

[2]Federal University of Santa Maria, Frederico Westphalen campus (UFSM – FW)

Keywords: Aquifer Barrier Marine, Groundwater, Hydrodynamics, Industrial exploitation, Wetlands.

Abstract

Protection of groundwater resources involves the conservation of water quality and quantity in order to save it for the future generations, based on the incorporation of management and planning measures aiming at the conservation of systems and the appropriate use of lands. Thus, it is ensured that potentially impacting activities should not be installed in places that present higher hydrogeological risk. The beverage industry demands large volumes of water in the production process. When groundwater is used to supply the industry, a productive aquifer with good physical-chemical and bacteriological water quality can minimize the production costs. This study aims to develop a conceptual hydrodynamic model for Coxilha das Lombas Aquifer and to estimate the area needed to supply groundwater to the brewing company. The hydrodynamic study indicated the presence of an unconfined and a semi-confined aquifers. Regional groundwater flows from NW to SE. Groundwater withdrawal by the industry is 3.2 times greater than the natural recharge that infiltrate into the aquifer in the company's property. There is risk of reduction on groundwater discharge to the adjacent and non-adjacent wetlands ecosystems,

1 Introduction

The economic development of the beverage industry is directly related to the quality of the raw material used: water. In its production process, this industrial sector requires a large amount of good quality water, which can lead to the extraction of high groundwater volumes to cover the demand.

Overexploitation of an aquifer can cause negative effects related to the deactivation and loss of wells as well as the increase of production costs of water linked to the decrease of the production capacity of abstraction, besides changes on physical and chemical water quality and the risks of land subsidence. In addition, overexploitation can lead to reduce the water discharge in adjacent wetlands [1-5].

Dieses Werk ist copyrightgeschützt und darf in keiner Form vervielfältigt werden noch an Dritte weitergegeben werden.
Es gilt nur für den persönlichen Gebrauch.

Wetlands are ecosystems of extreme ecological importance because of their diversity of environmental goods and services. In the Coastal Plain Geomorphologic Province of Rio Grande do Sul State (PCRS), South of Brazil, there are wetland ecosystems in areas with dunes and coastal lagoons deposits [6]. To preserve and to protect the quality of the environment in these water dependent ecosystems, the Decree nº 38,917/98 created the Environmentally Protected Area (APA) Banhado Grande - Chico Lomã, Banhado dos Pachecos and Banhado Grande [7], and the Decree nº 41,559/2002 created the Unit of Conservation Refúgio de Vida Silvestre Banhado dos Pachecos [8].

Most of the studies carried out in these areas are related to conservation and protection of these ecosystems, without considering the connection between surface water and groundwater [9-13].

The relationship between wetlands ecosystems with the underlying aquifers can assume a relationship of dependence, mainly during drought periods, when the surface water levels of humid areas rely on groundwater discharge from the underlying aquifers [14].

One of the problems observed in the area concerns the urban and economic development that increased after 1998, when 1,800 families settled in the base of Refúgio de Vida Silvestre Banhado dos Pachecos and on surrounding areas. Also, it was authorised the placement of two important industrial units, the brewing industry and the manufacturing industry of packaging, both with high water demands [15].

The industrial activities in that region are dependent on the groundwater extraction from the Coxilha das Lombas aquifer, which constitutes the main source of water for local suppliers. This aquifer is also an important source of freshwater for overlying ecosystems, as is the case with the Refúgio de Vida Silvestre Banhado dos Pachecos [16]. Therefore, this study aims to develop a conceptual hydrodynamic model for Coxilha das Lombas Aquifer and to estimate the area needed to supply groundwater to the brewing company.

2 Materials and Methods

2.1 Study area

The study area is located between the coordinates 50° 53'0'' west and 30°9'30' south, in the eastern region of Rio Grande do Sul state (Brazil), in Águas Claras county, Viamão city (Figure 1).

To the north, the watershed has Gravataí River as an important surface water body that regionally flows from east to west, discharging the waters into the Jacuí Delta towards Guaíba Lake. The Gravataí River and its tributaries supply surface water for Banhado Grande wetland [17].

To the south, there is the Middle Coastal Basin watershed, belonging to the Coastal Hydrographic Region with a large number of lagoons, many of them interconnected. Due to the influence of the sea water, which reach the lagoons through the Pato's Lagoon, the fresh water ecosystem presents high fragility [18].

Dieses Werk ist copyrightgeschützt und darf in keiner Form vervielfältigt werden noch an Dritte weitergegeben werden.
Es gilt nur für den persönlichen Gebrauch.

The region is heavily drained by surface waters. Viamão County is surrounded by the Pato's Lagoon to the south and the Gravataí River to the north. It stands out springs, wetlands and water bodies, such as Alexandria, Estância, Dorneles, Feijó, Fiúza, Itapuã, Gravatá, Taquara, Varejão and São Gravatá streams [19].

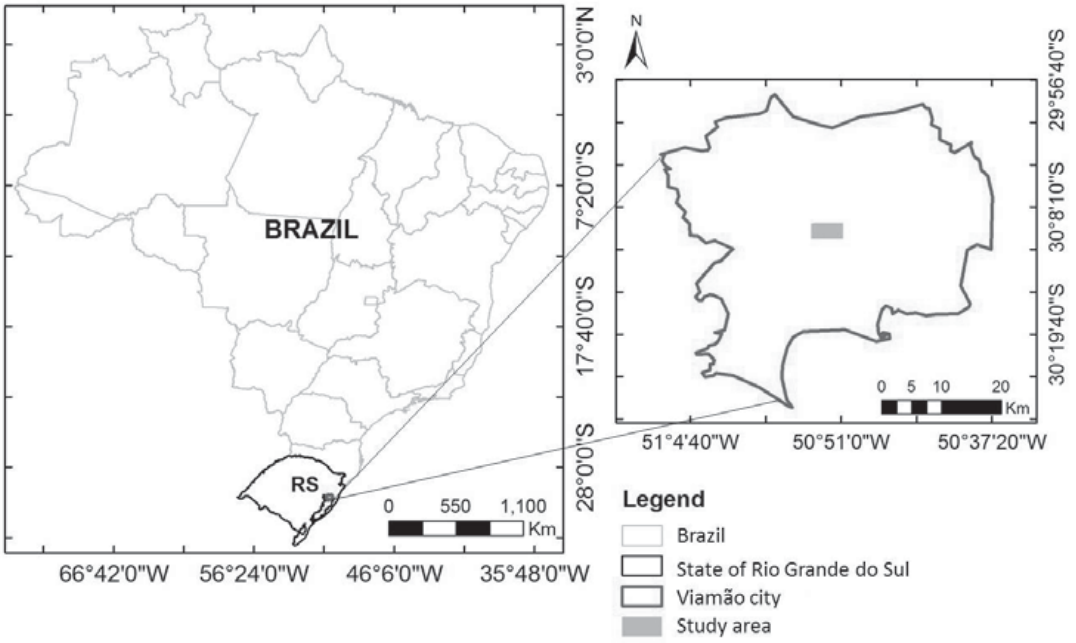

Figure 1: Location of the studied area in Viamão city (RS, Brazil)

Water for agricultural use withdraws big volumes of surface water in the Middle Coastal Basin. In 2007, the extraction for rice irrigation reached 1,202 hm^3/yr, which is approximately 99.3% of the water demand in the watershed of 1,211 hm^3/yr. Concerning the use of groundwater, 75% of the total demand, or 2.93 hm^3/yr is intended to fresh water supply, and 25% or 0.98 hm^3/yr is intended for industrial use [20].

The Coastal Plain Geomorphologic Province of Rio Grande do Sul (PCRS) has its genesis related to the sea levels fluctuations of the Atlantic Ocean, mainly from the Quaternary. The sediments were accumulated in the flood plain, creating two different depositional systems: the alluvial deposits and the transgressive-regressive system "lagoon-barrier". These are the Pleistocene systems "lagoon-barrier" I, II and III, and the "lagoon-barrier" IV, from Holocene [21, 22].

The area of interest in this study is the Quaternary Aquifer Marine Barrier, known as Coxilha das Lombas Aquifer. This area belongs to the "lagoon-barrier" Pleistocene I system, which recorded the first transgressive-regressive Pleistocene event. It is located on the northwest of the coastal plain (NE- SW), and it has 150 km length and 5 km to 10 km width, approximately [21].

The Barrier System I is composed mainly of wind sedimentary deposits. The Lagoon System I surrounds the Barrier and has lagoons on pluvial and fluvial sedimentary deposits from different geological ages [21]. The underlying aquifer of unconsolidated sands has fine to medium

Dieses Werk ist copyrightgeschützt und darf in keiner Form vervielfältigt werden noch an Dritte weitergegeben werden.
Es gilt nur für den persönlichen Gebrauch.

granulometry with little clay matrix. The aquifer has high productivity, with specific capacity above 4 $m^3/h*m$ [23].

The hydrogeological studies of the aquifer indicate flow directions from the Barrier System to the Lagoon System I and Lagoon System II, classified as natural discharge zones for the Gravataí River (located in lagoons terraces) and the Banhado Grande wetland (located above a confined clayey layers) [17]. In addition to this contribution, the discharge of Coxilha das Lombas Aquifer supplies adjacent aquifers (confined and unconfined) in the east and west direction; however, during periods of drought, the aquifer receives contributions from surface systems showing reversed flow [16].

Regionally, Coxilha das Lombas is an unconfined aquifer with unconsolidated sediments and good permeability. However, it has clayey lenses, which can generate hydraulic confinement. Groundwater levels indicate confinement conditions [24]. In 2008, Georepp and Uniper companies [25] identified an aquitard in the study area with silty clays and sandy clays layers, and a large volume of water storage with slow movement.

As for the hydrodynamic characteristics, the Coxilha das Lombas Aquifer presents variable values for the transmissivity coefficient. This parameter was estimated as 96.0 m^2/d [26], 96.0 m^2/d [24], 2,505 m^2/d, and 992 m^2/d [25], based on several pump tests. For this study, a mean transmissivity of 1,200 m^2/d was adopted for Coxilha das Lombas Aquifer. The hydraulic conductivity was estimated in 12 m/d, considering 100 m as the average thickness of the saturated zone [25]. In relation to the aquifer porosity, an average value of 30% was estimated due to the high permeability of the geological formation of the aquifer [24].

The recharge of Coxilha das Lombas Aquifer was estimated by means of the Chloride Method (balance of chlorine) in approximately 200 mm/year, considering an average annual rainfall of 1,330 mm/yr and an estimated evapotranspiration of 1,100 mm/yr. It should be emphasized that the method was applied to one well only, but the authors point out that this value can be extrapolated to the whole aquifer because of its textural and granulometric homogeneity [16].

In 2006, the recharge to Coxilha das Lombas Aquifer was estimated as 163 mm/yr, considering the contribution area of 417 km^2, 1,368 mm/yr of precipitation, and an average evapotranspiration of 1,141 mm/yr [27]. In 2012, the meteorologic recharge was estimated through water balance in 131.4 mm/yr, considering the annual rainfall of 1,375 mm, runoff of 260.4 mm/yr, and the evaporation of 983 mm/yr [17].

The permanent reserve of Coxilha das Lombas Aquifer was estimated in 9.0x106 m^3/km^2, for an area of 152 km^2 and a saturated zone with mean thickness of 60 m and 15% of effective porosity [17].

Dieses Werk ist copyrightgeschützt und darf in keiner Form vervielfältigt werden noch an Dritte weitergegeben werden.
Es gilt nur für den persönlichen Gebrauch.

2.2 Databases used

In order to elaborate the conceptual hydrogeological and hydrodynamic model of Coxilha das Lombas Aquifer on the central zone of Viamão, the following databases were used:

a) *Cartography*: Geological Map of Rio Grande do Sul State, Scale 1:770.000 [23]; Hydrogeological Map of Rio Grande do Sul State, Scale 1:750.000 [28]; Continuous vector cartographic basis of Rio Grande do Sul State, scale 1:50.000 [29];

b) *Underground hydrodynamics*: Executive project of the pump system to the exploitation of underground spring. Águas Claras do Sul Brewery, Viamão – RS [26]; Complementary documentation referring to the Decree nº. 645/2007. Poço 08's Report [30]; Semestral Report – Groundwater collection system [31] and registered wells on the Groundwater Information System – SIAGAS, from CPRM [32].

Hydrogeological data for the conceptual model were obtained from drilling reports, pumping tests, and geophysical tests. Based on existing data, the hydrostratigraphic units, the water budget, the potentiometric map, and the groundwater flow direction were defined [26, 30-32].

The potentiometric map and the groundwater flow direction on the industrial zone were defined from the hydraulic head registered on the drilling report of the pumping wells [26, 30, 32]. Also, groundwater levels and the aquifer layered were estimated based on the resistivity data from the geophysical survey (SEVs) [33].

The integration of the basis and the data analysis was performed by using both the software ArcGIS 10.2.1 [34] and the software Groundwater Modeling System – GMS 9.1 [35].

3 Results and Discussion

The industrial zone of beverage production is located in Viamão county and has 9 wells drilled to supply water for the needs of beer production (VIM01 the VIM09). Today, two wells are inactive and 7 others alternate pumping for groundwater extraction.

Adjacent to the industry, there are 7 wells for multiple uses of groundwater (VIM10 the VIM16) (Figure 2). The wells have depths between 84 m and 140 m, with a mean of 113 m, and a hydraulic head between 23.9 m and 114 m, with a mean hydraulic head of 40.4 m.

The geology of the aquifer indicates sandstones formation with intercalated local layers of clayed sandstones, silts and clays. From the geological description and the geophysical studies of the boreholes, it is possible to define Coxilha das Lombas as an unconfined aquifer locally, but as a semi-confined aquifer regionally. Through the interpretation of pumping tests from the wells drilled in the industrial zone [26, 30], it was noticed that the aquifer behave as an unconfined aquifer in some wells and as a semi-confined aquifer in others.

Dieses Werk ist copyrightgeschützt und darf in keiner Form vervielfältigt werden noch an Dritte weitergegeben werden.
Es gilt nur für den persönlichen Gebrauch.

In the studied area, the potentiometric map of Coxilha do Lombas Aquifer indicates hydraulic head between 30 and 45 m and groundwater flow from NW to SE. Locally, groundwater contributes to the discharge of rivers, draining towards Lagoa dos Patos.

The operation regime of the system depends on the demand of water. In winter months, a reduction of groundwater consumption used by the industry in relation to summer months occurs. For example in 2010, an average of 6,016 m^3/d was exported during the period from May to August and 7,706 m^3/d during the period from September to April [25].

In 2005, counting with five operating wells, industrial production of beer extracted from the aquifer 168,309 m^3/month of water (5,533 m^3/d, approximately), which results in 2,019,708 m^3/yr, approximately. Despite the elevated extracted volumes, authors highlight that the static level of Coxilha das Lombas Aquifer has kept itself relatively stable, presenting downgrade of 2 m at most during the pumping [27].

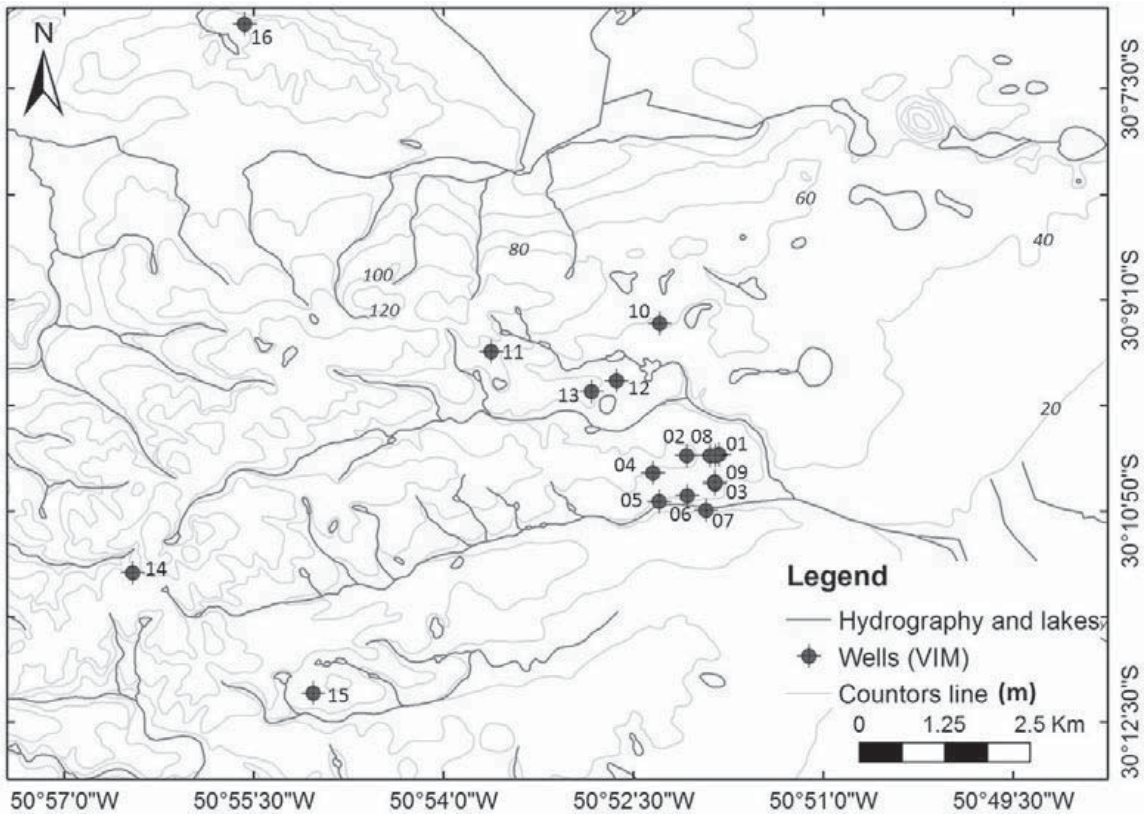

Figure 2: Pumping wells locations in the industrial area (VIM01 to VIM09) and adjacent (VIM10 to VIM16)

In 2009, the annual groundwater consumption was approximately 2,216,687 m^3, and in 2010, around 2,606,749 m^3. The lowest extraction was in June 2009 with 4,243 m^3/d, and the highest extraction was in December 2010 with 9,012 m^3/d [25].

Dieses Werk ist copyrightgeschützt und darf in keiner Form vervielfältigt werden noch an Dritte weitergegeben werden.
Es gilt nur für den persönlichen Gebrauch.

On the first half of 2016, the industry withdraw 120,871 m³/month of groundwater through the operation of 6 wells, pumping 1.2 to 10.7 h/d each, with an extraction of 109 to 262 m³/h*well. Groundwater static levels (N.E) and dynamic levels (N.D) data, did not show regional downgrade near by the brewing company [31].

It's estimated in $1.3x10^5$ m³ /yr per km² the regulatory reserve of Coxilha das Lombas Aquifer, based on the recharge rate of 131.6 mm/year, or around 9.6% from the precipitation (1,375 mm/yr) [17]. Considering 3.49 km² the area of the company, the recharge into that area would be $4.6x10^5$ m³/yr.

However, with an annual consumption of $1.45x10^6$ m³, the area that is necessary for supplying the annual demand of the brewing industry is around 3.2 times the size of the company's property.

4 Conclusions

From the conceptual hydrogeological model, it was possible to identify two aquifer systems in the studied area, an unconfined aquifer underlined by a semi-confined aquifer with interlayers of fine materials such as silt and clay. The groundwater has hydraulic heads between 30 and 45 m, and the groundwater regionally flows from NW to SE.

Regarding to the influence into the aquifer by the brewing industry, the hydraulic balance indicates that it is necessary to use the regulatory reserve of a recharge area 3.2 times greater than the actual property of the industry in order to maintain the beer production process. The consequences for the aquifer exploitation might lead to the reduction of the reserves in adjacent zones as well as to the reduction of the discharge to the surface dependent ecosystems.

Based on the location of the pumping wells and in the hydrodynamics of the aquifer, there is a risk of reduction on groundwater discharge to the adjacent and non-adjacent wetlands ecosystems, since the wells are pumping water from the lower semi confined aquifer, which has regional groundwater flow.

5 Acknowledgement

The authors would like to thank DAAD and Exceed Swindon for financial support for the participation at this Summer School 2017; to the Institute of Technological Research - IPT (New Talents Program - 02/2015), financially supported by the Foundation of the Technological Research Institute; to the AMBEV industry; and to the Water Resources Laboratory of Federal University of Santa Maria - UFSM.

Dieses Werk ist copyrightgeschützt und darf in keiner Form vervielfältigt werden noch an Dritte weitergegeben werden.
Es gilt nur für den persönlichen Gebrauch.

6 References

1. Esteller, M.V., Diaz-Delgado, C.: Environmental effects of aquifer overexploitation: A case study in the highlands of Mexico. Environmental Management 29, 266-278 (2002)
2. Hani, A.: Impact of aquifer intensive use on groundwater quality and on wetlands on coastal aquifer. 777-784 (2003)
3. Pedrera, A., Martos-Rosillo, S., Galindo-Zaldívar, J., Rodríguez-Rodríguez, M., Benavente, J., Martín-Rodríguez, J.F., Zúñiga-López, M.I.: Unravelling aquifer-wetland interaction using CSAMT and gravity methods: The Mollina-Camorra aquifer and the Fuente de Piedra playa-lake, southern Spain. Journal of Applied Geophysics 129, 17-27 (2016)
4. Sahuquillo, A.: La explotación intensa de los acuíferos en la cuenca baja del Segura y en la cuenca del Vinalopó. Ingeniería del agua 20, 13-13 (2016)
5. Simonato, M.: Água subterrânea em áreas urbanas: potencialidade, problemas e desafios. 27, 133-134 (2008)
6. Zank, C.: Diagnóstico De Fauna Do Litoral Médio Do Rio Grande Do Sul E Zoneamento Temático Do Meio Biótico. (2013)
7. Departamento De Meio Ambiente: APA do Banhado Grande. http://meioambiente.pmsap.com.br/unidade/12.
8. Instituto Chico Mendes de Conservação da Biodiversidade: Decreto nº 41559, de 24 de abril de 2002. Cria o Refúgio de Vida Silvestre Banhado dos Pachecos e dá outras providências. http://www.icmbio.gov.br.
9. Aydos, B.B.: Produção rural em unidades de conservação: a situação da área de proteção ambiental do Banhado Grande, RS. pp. 1-60 (2015)
10. Brack, P.: Vegetação e Paisagem do Litoral Norte do Rio Grande do Sul: patrimônio desconhecido e ameaçado, Porto Alegre (2006)
11. Burger, M.I.: Situação e ações prioritárias para a conservação de Banhados e áreas úmidas da zona costeira. (2010)
12. Carvalho, A.B.P., Ozorio, C.P.: Avaliação sobre os banhados do Rio Grande do Sul, Brasil. Revista de Ciências Ambientais 1, 83-95 (2007)
13. Etchelar, C.B.: Análise do processo erosivo no Banhado Grande, Município de Glorinha -RS. pp. 72-72 (2014)
14. Rubbo, M.: Análise do potencial hidrogeológico do aquífero cenozóico da bacia hidrográfica do Rio Gravataí - RS. pp. 1-116 (2004)
15. Martins, S.: Espaço periurbano fragmentado: dinâmica e desenvolvimento socioespacial em Águas Claras, Viamão/RS. pp. 214-214 (2014)

Dieses Werk ist copyrightgeschützt und darf in keiner Form vervielfältigt werden noch an Dritte weitergegeben werden.
Es gilt nur für den persönlichen Gebrauch.

16. Herlinger Jr, R., Viero, A.P.: Estimativa da recarga do aqüífero coxilha das lombas através do método balanço de cloretos. pp. 1-11. (Year)

17. Bourscheid.: Plano de Recursos Hídricos da Bacia Hidrográfica do Rio Gravataí. Relatório Final - RS. BOURSCHEID Engenharia e Meio Ambiente S. A., Porto Alegre. (2012)

18. Secretária Do Ambiente E Desenvolvimento Sustentáve: Unidades de Conservação Estaduais. Área de Proteção Ambiental do Banhado Grande. 2010. http://www.sema.rs.gov.br/conteudo.asp?cod_menu=174.

19. Viamão: Câmara Municipal de Viamão. História de Viamão. http://camaraviamao.rs.gov.br/site/historia_viamao.html.,

20. Ecoplan: Relatório Síntese da Fase A. Diagnóstico e Prognóstico Hídrico das Bacias Hidrográficas do Rio Grande do Sul. Plano Estadual de Recursos Hídricos do Rio Grande do Sul (PERH/RS). DRH/SEMA. (2007)

21. Tomazelli, L.J., Villwock, J.A.: Mapeamento Geológico de Planícies Costeiras: o Exemplo da Costa do Rio Grande do Sul. Gravel 3, 109-115 (2005)

22. Villwock, J.A., Tomazelli, L.J., Loss, E.L., Dehnhardt, E.A., Horn F, N.O., Bachi, F.A., Dehnhardt, B.A.: Geology of the Rio Grande do Sul coastal province. International symposium on sea-level changes and quaternary shorelines 79-97

23. Serviço Geológico Do Brasil: Mapa Hidrogeológico do Rio Grande do Sul. SOPS-SEMA-DRH/RS-CPRM. CPRM. Diretoria de Hidrologia e Gestão Territorial. Escala 1:750.000. Porto Alegre. (2005)

24. Freitas, M.A.d., Costa, C.T., Tedesco, M.A.C.M.A.H.d.: Estudo do comportamento e potencialidade do aqüífero relacionado à barreira marinha em Viamão-RS utilizando modelagem computacional. pp. 17-17. (Year)

25. Itaquy, B.D.M.: Utilização de técnicas de otimização para a gestão do uso da água subterrânea – aplicação na fábrica de águas claras do sul da ambev. pp. 62-62 (2013)

26. Água E Solo: Projeto executivo do sistema de bombeamento para exploração do manancial subterrâneo. Cervejaria Águas Claras do Sul, Viamão – RS. (1998)

27. Collischonn, B., Kirchheim, R.: Quantificação Da Recarga E Das Reservas Do Aqüífero Coxilha Das Lombas (Rs) Através De Balanço Hídrico. pp. 1-18. (Year)

28. Serviço Geológico Do Brasil: Mapa Geológico do Estado do Rio Grande Do Sul. Escala 1:750.000. Porto Alegre. (2006)

29. Hasenack, H., Weber, E.o.: Base cartográfica vetorial contínua do Rio Grande do Sul - escala 1:50.000. Porto Alegre: UFRGS Centro de Ecologia. 1 DVD-ROM. (2010)

30. Georepp – Hidrogeologia Ambiental: Documentação complementar referente Portaria nº: 645/2007. Poço 08. (2007)

Dieses Werk ist copyrightgeschützt und darf in keiner Form vervielfältigt werden noch an Dritte weitergegeben werden.
Es gilt nur für den persönlichen Gebrauch.

31. Ambev: Relatório Semestral – Sistema de captação de água subterrânea. Viamão. (2016)
32. Cprm – Serviço Geológico Do Brasil: Sistema de Informações de Águas Subterrâneas. Banco de dados. (2017)
33. Oliveira, A.B.B.M.d.: Definição de topo e base da região central do aquífero Coxilha Das Lombas (Município de Viamão/RS) através da integração de dados geofísicos e geológicos. Porto Alegre. pp. 78-78 (2016)
34. ESRI: ESRI.: ArcGIS for Server, v.10.2.1. (2013)
35. AQUAVEO: Groundwater Modeling System (GMS), v. 9.1. (2014)

Dieses Werk ist copyrightgeschützt und darf in keiner Form vervielfältigt werden noch an Dritte weitergegeben werden.
Es gilt nur für den persönlichen Gebrauch.

GROUNDWATER FLUCTUATIONS AND THEIR INTERACTIONS WITH RIVERS AND WETLANDS IN COASTAL ZONES

Iris Neri-Flores[1], Patricia Moreno-Casasola[2], Luis Alberto Peralta[3], Oscar A. Escolero[4], Roberto Monroy[2]

[1] Universidad Veracruzana/INECOL. Calz. A. Ruíz Cortines. #455. Boca del Río, Veracruz. México, irisneri@gmail.com

[2] INECOL, Xalapa, Veracruz, México

[3] Instituto Tecnológico de Veracruz, Veracruz, México

[4] Instituto de Geología, UNAM, Ciudad de México

Keywords: Flooding, Groundwater-surface water interaction, Wetlands

Abstract

Groundwater and surface interactions affect recharge and discharge processes, and are of great ecological importance and affect humans. This study was carried out on the coastal plain of the state of Veracruz, Mexico in order to understand seasonal variation in groundwater, its interaction with surface water and with the vegetation of flooded areas. Piezometer data were used with historical data from hydrometric stations and land use data from remote image analysis. Five ways that groundwater, surface water and vegetation interact are: (1) groundwater reflects the river's behaviour and the presence of riparian vegetation, (2) the area with river discharge, influence from the sea and groundwater has mangroves, (3) where the contribution of the river is superficial, but the contribution of groundwater flow is in the opposite direction, a discharge zone is formed, (4) the watershed discharging into the sea and groundwater flowing in the opposite direction indicates that the dune lakes are fed by groundwater, and (5) the aquifer rises where soil is mainly sandy (urban coastal zone). The region's management plan should take into account that flooding in the area results from groundwater and surface water, so solutions should include implementing both engineering and environmental solutions together.

1 Introduction

Groundwater and surface water are complex and must be understood as an integral part of the hydrological cycle. The mechanisms of interactions between groundwater and surface water affect recharge-discharge processes; they are of great ecological significance and have important human impacts [1]. The vegetation cover of a given location may be directly or indirectly affected, and in certain cases, controlled by groundwater flow owing to the effects of the latter on soil moisture and salinity in the area [2]. It is also known that the groundwater flow is the principal component in many coastal wetlands and lagoons [3, 4]. In the Veracruz coastal zone, groundwater levels depend on local flows, which respond quickly to precipitation and increase river flow as evidenced

Dieses Werk ist copyrightgeschützt und darf in keiner Form vervielfältigt werden noch an Dritte weitergegeben werden.
Es gilt nur für den persönlichen Gebrauch.

by groundwater flooding [5]. In Moreno-Casasola [6], one can find the background for the environmental setting for the study area, with descriptions of coastal freshwater wetlands and mangroves in the coastal zone of Veracruz and their relationship to the main functions of these ecosystems such as productivity, hydrological services, carbon sequestration, and connectivity.

Wetlands play an important role in the hydrological cycle, influencing groundwater recharge, low flows, evaporation, and floods. Worldwide, this has led to formulating and implementing policies to conserve and to manage the wetlands that deliver these key environmental services, especially with the aim of reducing flood risk. Wetland type, landscape location and configuration, soil characteristics, topography, soil moisture status, and management all influence whether these wetlands provide flood reduction services or not [3].

The main objective of this study was to understand the seasonal variation in groundwater fluctuation, its interactions with surface water, and its relationship to the vegetation of flooded areas through conceptual hydrogeological modelling. Groundwater and surface water are not isolated components of the hydrologic system, but rather interact in a variety of physiographic landscapes and climates. It is essential to understand and to model these interactions not only for the conservation and restoration of tropical wetlands, but also to understand the dynamics of flooding in coastal regions.

The Gulf of Mexico is very vulnerable to extreme weather because of its lowlands, which are covered by extensive mangroves, marshes, and swamps, as well as beaches and dunes. The region is impacted by hurricanes every year [6, 7]. The littoral zone of the state of Veracruz covers approximately 720 km, and is the second longest in the Gulf of Mexico and the Caribbean. It has several coastal cities, among them the Port of Veracruz (96º20'W – 95º 55'W, 19º15'N – 18º 55'N), which is the most important commercial port in the region. It is surrounded by the cities of Veracruz and Boca del Río, which have a combined population of 690,214 inhabitants (data from 2010 [8]). The cities have spread over dunes and wetlands [9], even though the area has recurrent flooding that has taken lives and affected properties. For example, in 1999 and in 2005, there were floods in October, when the rainy season had already ended, and the soil became saturated to capacity and was not able to absorb any more water, and this increased the extent of flooding [9]. In September 2010, flooding produced by a local river occurred one day after Hurricane Karl made landfall, and it is still remembered as "a dry flood" because it occurred on a sunny day [10]. The rains had fallen on mountains further inland.

The coastal plain of Veracruz has extensive wetlands. There are mangroves, salt marshes, freshwater forested wetlands, broadleaf marshes, cattail marshes, and flooded pastures in areas that used to have freshwater wetlands and even mangroves. Within these types of wetlands floristic composition, soil type, the degree of water fluctuation, salinity, etc. cover a wide range of variation [6, 11-15]. Wetlands provide important goods and environmental services to society, including carbon sequestration, water depuration, and flood peak reduction; they act as nurseries for important fisheries and offer sources of drinking water, among others [3, 6, 16-19].

Dieses Werk ist copyrightgeschützt und darf in keiner Form vervielfältigt werden noch an Dritte weitergegeben werden.
Es gilt nur für den persönlichen Gebrauch.

The study site is located in the coastal zone of Veracruz-Boca del Río (Figure 1). This site is experiencing accelerated population growth because of port dynamics and the tourism activity, and is in constant need of new construction and infrastructure. This has led to the disappearance and degradation of dunes and wetlands, where the terrain has been levelled and the wetlands drained and filled with rocks and earth to create sites for urban development.

The importance of wetlands for flood mitigation has recently begun to be locally appreciated. Several protected sites have been designated in recognition of the ecological importance of the coastal zone in the area. The first site to be designated as a protected area was a large reef, known as the *Parque Nacional Sistema Arrecifal Veracruzano* Biosphere Reserve (the Veracruz National Park Reef System Biosphere Reserve), and this was followed by a mangrove site called *Arroyo Moreno* (Moreno Stream). More recently, a freshwater marsh called *Tembladeras* was designated as a state protected area and the newest one, is called *Corredor Biológico Multifuncional Archipiélago de Lagunas Interdunarias de la zona conurbada de los municipios Veracruz y La Antigua, Veracruz* (the Multifunctional Biological Corridor Archipelago of Interdune Lagoons in the surroundings of the municipalities of Veracruz and La Antigua, Veracruz), formed by dune lakes. The first and last are also Ramsar sites**.** The growth of the city is a constant threat to these and other wetland ecosystems.

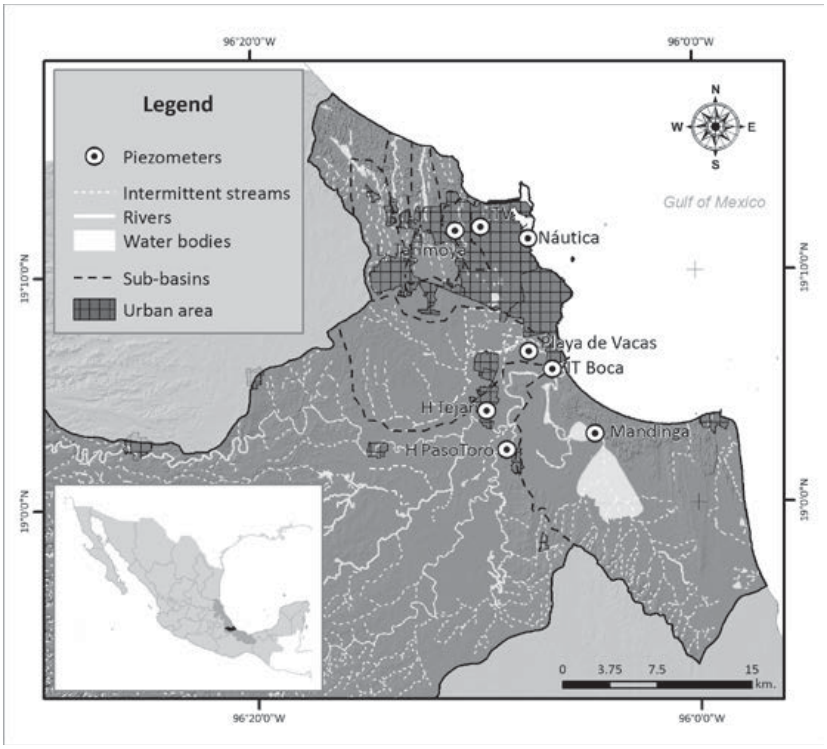

Figure 1: Location of the Veracruz-Boca del Río coastal zone (inset). The Jamapa (H. Tejar) and Cotaxtla (H. Paso del Toro) rivers, and piezometer locations. The piezometer in HTejar was located closest to the river; three more were installed in ItBoca located 25 m away from and perpendicular to the river channel, ItBocam is 115 m away and ItBocae 245 m away

Dieses Werk ist copyrightgeschützt und darf in keiner Form vervielfältigt werden noch an Dritte weitergegeben werden.
Es gilt nur für den persönlichen Gebrauch.

2 Materials and Methods

The methodology involved the hydrological analysis of the data from the hydrometric stations of the Jamapa River (28040) and the Cotaxtla River (28039) shown in Table 1. These data were obtained from BANDAS (*Banco Nacional de Datos de Aguas Superficiales* curated by CONAGUA).

Table 1: Hydrometric stations.

Station	River	UTMx	UTMy	Data period	Number of years with complete records	Critical scale (m)
28039	Cotaxtla	800621	2107599	1952-2006	45	6.15
28040	Jamapa	799082	2110754	1952-2006	54	6.7

The sub-basins were delimited using a Mexican digital elevation model and the hydrography (scale 1:5000) provided by INEGI (2008).

Groundwater fluctuations were analysed by monitoring measurements taken by 10 piezometers we installed for this purpose. Groundwater level was measured every two weeks and the data taken for this paper were for the period from March (dry season) to July 2017 (wet season). The piezometers were located in each sub-basin that would help us further our understanding of groundwater flux (Figure 1).

To identify the groundwater elevation seven piezometers were selected. A two-band GPS, linked to the RGNA (Geodesic Active National Net) was used to obtain elevation. Table 2 shows the data for each piezometer. Depth varied from 1.03 m to 7.10 m. PVC height refers to the PVC tube that protrudes above soil level, the height of which was taken into account to obtain the depth of the water table. ND means No Data. The data are in meters.

Table 2: Piezometer characteristics.

Number	Name	UTMx	UTMy	Depth (m)	PVC height (m)	PVC height (m a.s.l.)
P1	ITV	798528.5	2125328.1	4.60	1.10	ND
P3	Playa de Vacas	802376.1	2115457.6	4.35	0.18	3.4
P4	Mandinga	807618.6	2108955.2	1.94	1.14	4.9
P5a	Itboca e	804256.7	2113928.3	2.86	0.69	4.3
P5b	Itboca m	804238.7	2114062.0	1.58	1.25	ND
P5c	Itboca b	804215.4	2114145.8	1.03	0.97	3.4
P6	H Tejar	799021.7	2110755.9	7.10	1.02	9.9
P7	H PasoToro	800602.5	2107655.6	6.51	1.13	9.4
P8	Náutica	802310.0	2124425.4	2.08	0.61	3.8
P10	L. Tarimoya	796490.6	2125028.8	1.20	1.17	11.2

Dieses Werk ist copyrightgeschützt und darf in keiner Form vervielfältigt werden noch an Dritte weitergegeben werden.
Es gilt nur für den persönlichen Gebrauch.

For the spatial classification of the vegetation we used Rapid Eye perception remote images with a spatial resolution of 5 m for the year 2014. A supervised classification was run to identify the following classes in vector format: cloud forest, pine forest, pine-oak forest, pastures in high mountains, secondary forest, coffee grown under tree shade, pasture, tropical dry forest, tropical rainforest of medium height, riparian vegetation, forest plantations, sugar cane, other crops, wetlands, dune vegetation, bare soil, water bodies, and urban zones.

3 Results

3.1 Hydrological functioning

The Jamapa and Cotaxtla rivers belong to the Jamapa and Cotaxtla river basins, respectively. The latter joins the Jamapa River and discharges into the Mandinga Lagoon and the sea. This lagoon also receives contributions from the rainwater that the dune systems to the south receive. The sub-basin of Arroyo Moreno discharges into the Jamapa River. In the area of the North sub-basins, runoff flows from south to north and discharges into the sea. The zone with dune lakes and the urban zone belong to the aquifer system of alluvial and sand sediments. Figure 2 shows the hydrological functioning in the study area.

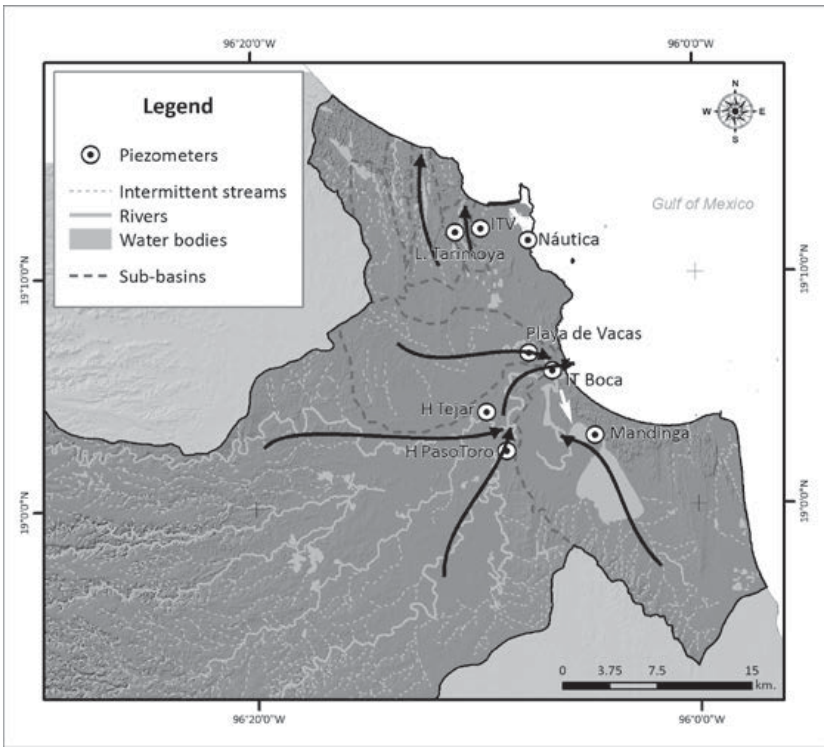

Figure 2: Hydrological functioning, showing directions of water flow in the study area on the Gulf coast of Veracruz, Mexico.

3.2 Hydrometric stations

These stations recorded data from 1951 to 2006, for both the Jamapa and Cotaxtla rivers (hydrometric stations 28040 and 28039, respectively). The monthly flow rate was calculated taking into account the dry season from November to May, the rainy season from June to September,

Dieses Werk ist copyrightgeschützt und darf in keiner Form vervielfältigt werden noch an Dritte weitergegeben werden.
Es gilt nur für den persönlichen Gebrauch.

and a flow decrease in August due to a short but very dry period, locally known as the *canícula.* The hydrological parameters indicate a yearly flow rate of 42.1 m^3/s for the Cotaxtla River and 17.9 m^3/s for the Jamapa River, as shown in Figure 3.

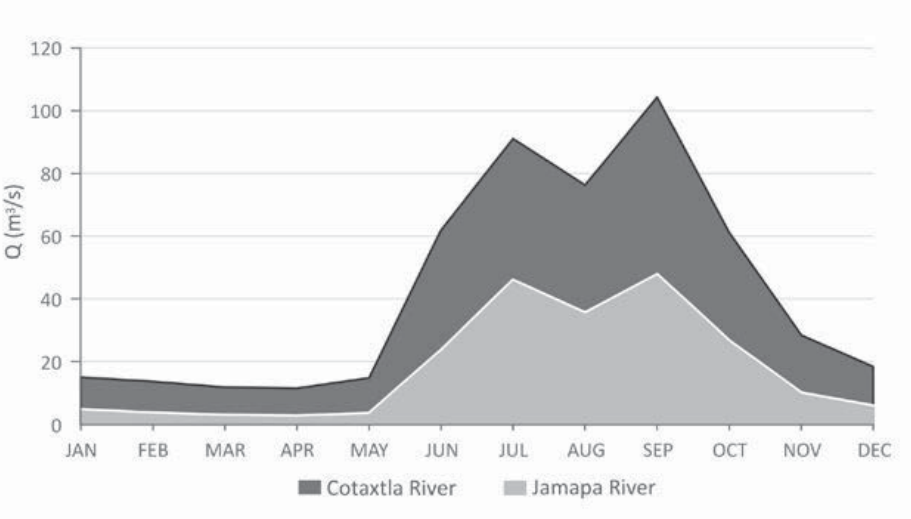

Figure 3: Hydrographs for the Jamapa River (station 28040) and the Cotaxtla River (station 28039), showing the monthly flow rate in m^3/s.

The sub-basins in the study area are:

- *Jamapa and Cotaxtla*: These two sub-basins are characterized by diverse wetland vegetation (freshwater marshes, flooded pastures established in former wetlands, and riparian vegetation) and agricultural zones;
- *Mandinga* is characterized by diverse wetland vegetation (mangroves, freshwater marshes, riverine wetlands, and flooded pastures established on former wetlands), grasslands on dunes, and agricultural zones;
- The *Arroyo Moreno* is characterized by wetlands (mangroves, salt marshes, and pastures established on former wetlands), agricultural areas, and pastures;
- The *North Sub-basins* are characterized by wetlands (freshwater marshes, flooded freshwater forests, and flooded pastures established on former wetlands) and pastures; and
- *Urban coastal zone*: This area is where the majority of the population is located and most of the economic activities occur.

Dieses Werk ist copyrightgeschützt und darf in keiner Form vervielfältigt werden noch an Dritte weitergegeben werden.
Es gilt nur für den persönlichen Gebrauch.

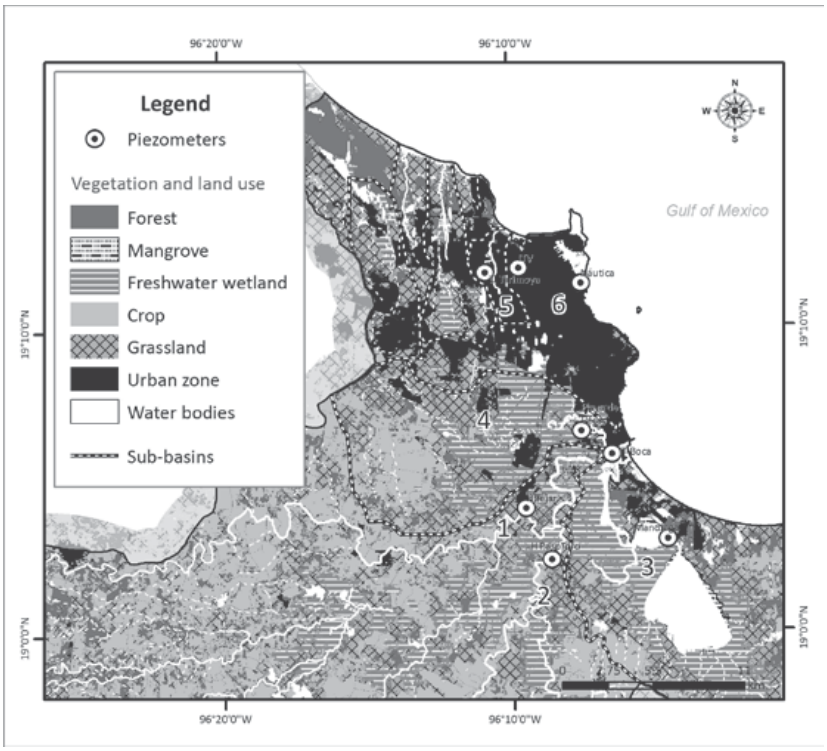

Figure 4: Vegetation and land use in each sub-basin. Each sub-basin is marked with a dashed line and numbered: 1. Jamapa, 2. Cotaxtla, 3. Mandinga, 4. Arroyo Moreno, 5. North Sub-basins, and 6. Urban coastal areas. Vegetation types are indicated (see legend). Grasslands represent the flooded pastures resulting from cattle ranching in wetlands.

3.3 Groundwater fluctuations

To identify the relationship between groundwater and surface water, piezometer data were analysed for the sub-basins: Jamapa (piezometers Tejar and IT Boca, with three piezometers at the latter site), Cotaxtla (piezometer Paso del Toro), A. Moreno (piezometer Playa de Vacas), Mandinga (piezometer Mandinga), and North Sub-basins (piezometer Laguna Tarimoya). In the coastal zone, there was also a piezometer close to the coastline (Nautica).

3.3.1 Jamapa River Sub-basin

Groundwater fluctuations indicate that there is a correlation between the levels in El Tejar and those in ITBoca, which are separated by approximately 12 km. This means groundwater level is related to variations in river discharge. Figure 5 shows that the lowest groundwater levels occurred in May and increased in June (rainy season). The piezometer in HTejar was located closest to the river; three more were installed in ItBoca in order to identify the local influence of groundwater. ItBocab is located 25 m away from and perpendicular to the river channel, ItBocam is 115 m away and ItBocae 245 m away.

Dieses Werk ist copyrightgeschützt und darf in keiner Form vervielfältigt werden noch an Dritte weitergegeben werden.
Es gilt nur für den persönlichen Gebrauch.

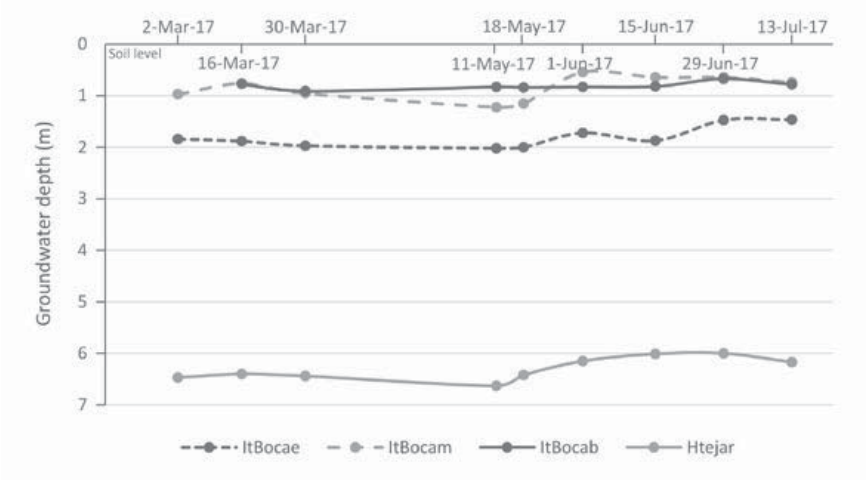

Figure 5: Groundwater fluctuation in the Jamapa River Sub-basin.

3.3.2 Cotaxtla River Sub-basin

Groundwater variation for the Cotaxtla River as recorded by the piezometer had a similar pattern and level to that of the Jamapa River. Figure 6 shows that the minimum level occurred in May with a groundwater depth of 7.01 m and in June of 4.5 m, indicating the groundwater level rose by 2.51 m. In July there was a drop in groundwater level, even though it was still the rainy season.

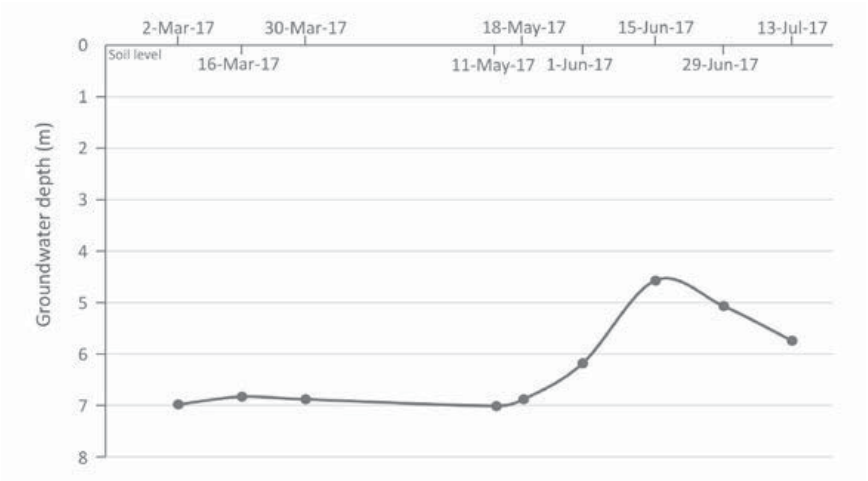

Figure 6: Groundwater fluctuation in the Cotaxtla River Sub-basin.

3.3.3 Arroyo Moreno Sub-basin

The Natural Protected Area of Arroyo Moreno is located in this sub-basin. Figure 7 shows the data from the piezometer located next to the mangrove reserve. The minimum groundwater depth was recorded in May (2.31 m) and it rose in July, reaching 0.82 m. There was water fluctuation and an increase in groundwater level of 1.49 m.

Dieses Werk ist copyrightgeschützt und darf in keiner Form vervielfältigt werden noch an Dritte weitergegeben werden.
Es gilt nur für den persönlichen Gebrauch.

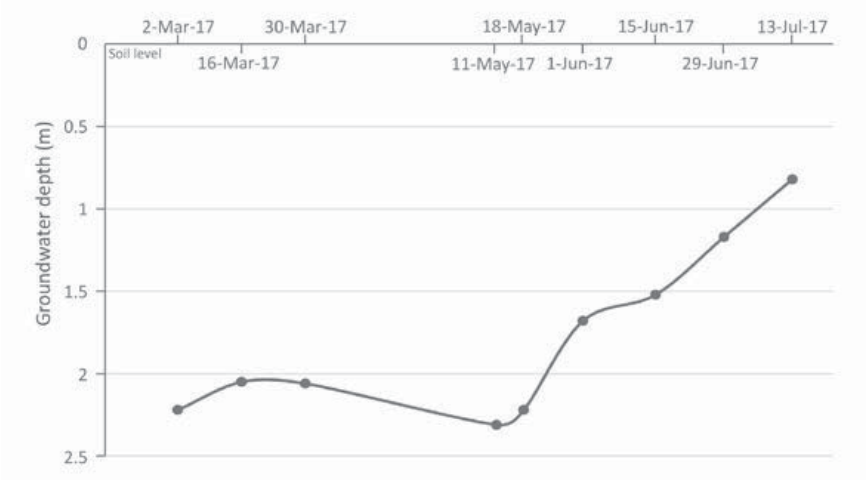

Figure 7: Groundwater fluctuation in the Arroyo Moreno Sub-basin.

3.3.4 Mandinga Sub-basin

This sub-basin has contributions from the Jamapa River, from the sea, and also recharges from water percolating through the dune systems. The piezometer shows the minimum groundwater levels occurred in May (1.57 m depth) and continuously increased until July (0.82 m depth), as shown in Figure 8.

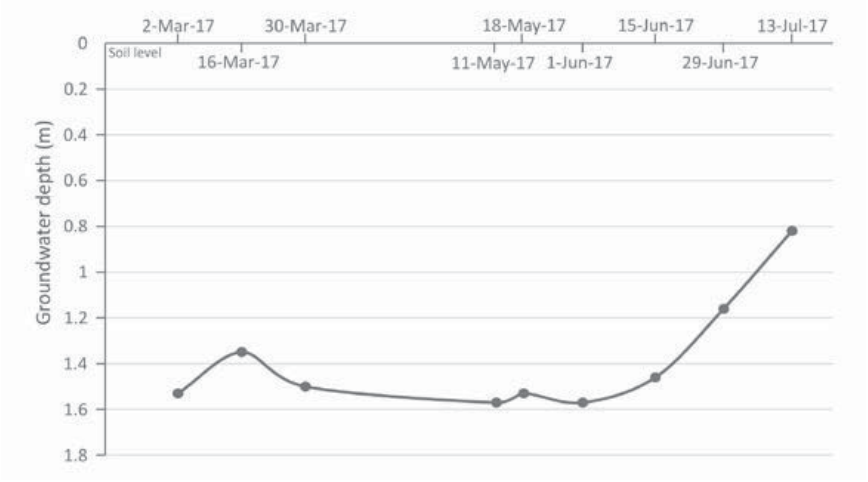

Figure 8**:** Groundwater fluctuation in the Mandinga Sub-basin.

3.3.5 North Sub-basins

These sub-basins include part of the dune lakes that lie within the natural protected area. The piezometer for the North Sub-basins revealed a similar pattern to those of Mandinga and Arroyo Moreno, with the lowest groundwater levels occurring in May after which they increase continuously until June-July. The Tarimoya piezometer shows flooding caused by the rise in groundwater (Figure 9).

Dieses Werk ist copyrightgeschützt und darf in keiner Form vervielfältigt werden noch an Dritte weitergegeben werden.
Es gilt nur für den persönlichen Gebrauch.

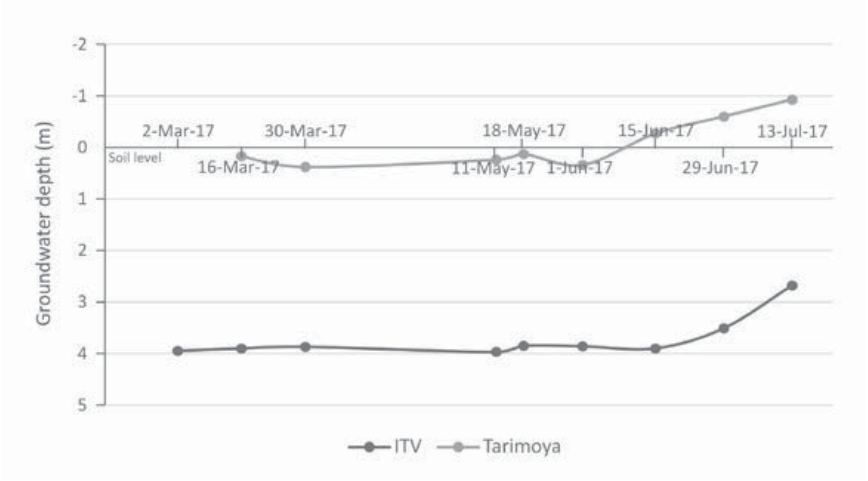

Figure 9: Groundwater fluctuation in the North Sub-basins.

3.3.6 Urban coastal zone

This sub-basin includes the rest of the dune lakes that lie within the natural protected area. The Tembladeras site is located in this zone, and belongs to the protected area.

The piezometer in the urban zone is located just 150 m from the coast. The groundwater level was low, at 1.2 m, from March to mid-May and then started to rise. In July, the groundwater got closer to the surface (Figure 10).

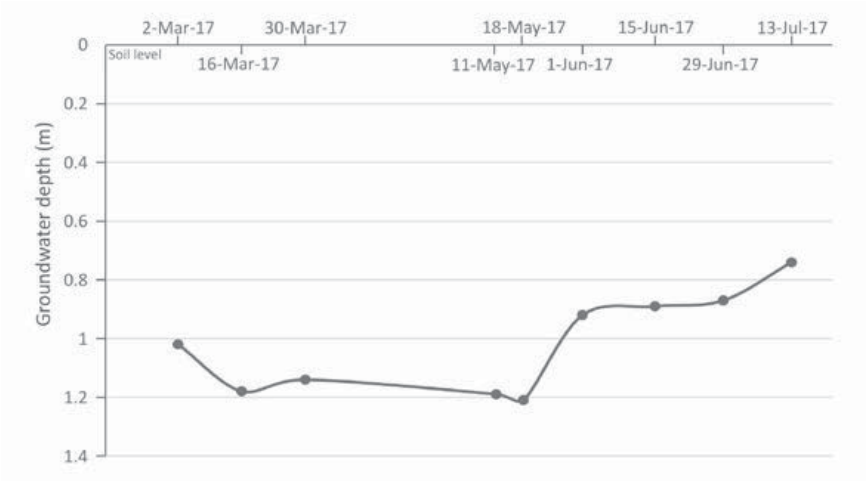

Figure 10: Groundwater fluctuation in the urban coastal zone.

3.4 Net groundwater flow

The analysis of groundwater flow indicates that there is a flow from Mandinga to the mouth of the Jamapa River. There is also a flow from Mandinga to the zone of Paso del Toro (in the confluence zone of the Jamapa and Cotaxtla rivers). The zone of Arroyo Moreno (Playa de Vacas) has contributions from the north, from the east, from the Jamapa River and from Boca del Río, which means that this is a zone of groundwater flow discharge. In the area of the North Sub-basins, there

Dieses Werk ist copyrightgeschützt und darf in keiner Form vervielfältigt werden noch an Dritte weitergegeben werden.
Es gilt nur für den persönlichen Gebrauch.

is a flow from the north to the lagoons, indicating that dune lakes in the urban zone are fed by groundwater. There is also groundwater discharge to the sea.

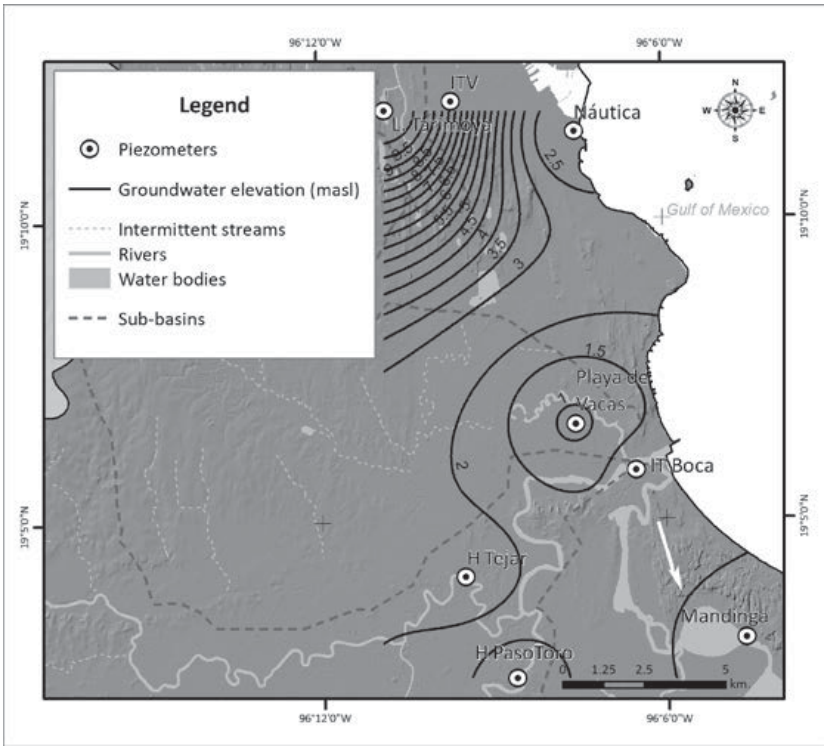

Figure 11: This map shows the water flow according to the piezometer data for the dry season. Numbers indicate groundwater elevation (m a.s.l.). See text for explanation.

4 Discussion

The results reveal five different cases or set of conditions that help to understand the relationship between the surface water, groundwater and vegetation.

4.1 The confluence of the Jamapa and Cotaxtla rivers

There is a river-aquifer relationship: when river flow increases, groundwater level also increases. [20, 21] identified zones with high infiltration that create connections between the river and the aquifer, thus contributing to the base flow of the river. Therefore, the piezometers located close to the river can be utilized as a river monitoring site that can provide early flood warnings to the local inhabitants. The advantages of this monitoring methodology are its low cost and easy installation, which can also be replicated at different places along the river. Neri [21] found that the river-aquifer influence takes place over one kilometer of transverse distance from the river. This means that modifying the riverbank will affect the aquifer. At this confluence, net groundwater indicates a discharge between the confluence of the Jamapa and Cotaxtla rivers with the presence of wetland vegetation. Riparian vegetation used to dominate the area, but has been felled to increase the area for cattle pastures. There probably used to be a freshwater forested wetland like the one found in the Apompal Lagoon in the county of Jamapa [11] that borders the study area, but it was also cut down and only isolated trees remain. The amount of water flow does not allow

Dieses Werk ist copyrightgeschützt und darf in keiner Form vervielfältigt werden noch an Dritte weitergegeben werden.
Es gilt nur für den persönlichen Gebrauch.

the growth of in-channel vegetation that might offer greater resistance and help to attenuate the movement of flood waters. Freshwater marshes are the dominant wetlands along the floodplain, and are characterized mainly by *Typha domingensis*, *Pontederia sagittata,* and *Thalia geniculata*, as well as flooded pastures. Mouw [22] found that discharge zones are the most productive sites with a greater variety of a vegetation types.

4.2 Mandinga

This site has contributions from the superficial water of the Jamapa River and the sea. A contribution of surface water from north to south was detected, but there is also a groundwater contribution from south to north. This produces an ideal area for wetland establishment with the presence of mangroves [12] and salt marshes, but also freshwater wetlands, when there is less salinity from the groundwater. Figure 12 shows the mangroves.

Figure 12: Mangroves in the Mandinga Lagoon

4.3 Arroyo Moreno

The superficial hydrology of this sub-basin has a contribution from west to east; however, the groundwater flow shows a discharge zone. This functioning has to be taken into account because during the rainy season or when the river floods, the groundwater will flow in the direction of the flooding. So, this site could function as an attenuation zone during extreme events. The vegetation in this site is mainly mangroves and flooded pastures with a continuous increase in groundwater level during the rainy season. Unfortunately, urbanization has been encroaching upon this wetland (i.e., advancing gradually beyond usual or acceptable limits) and reducing the environmental services that this wetland can provide. Figure 13 shows an image of the current situation of the mangroves.

Dieses Werk ist copyrightgeschützt und darf in keiner Form vervielfältigt werden noch an Dritte weitergegeben werden.
Es gilt nur für den persönlichen Gebrauch.

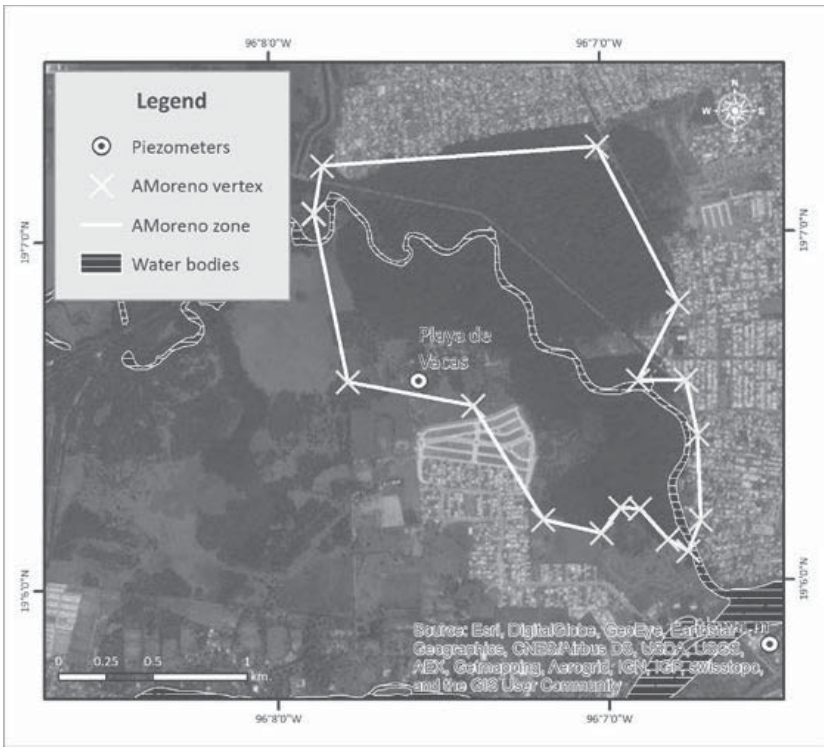

Figure 13: This Google image shows the current situation of the mangroves, which are being encroached upon by urban development from the city of Boca del Río. The Jamapa River is shown in the southern part of the image.

4.4 North Sub-basins

The watershed of the North Sub-basins receives runoff from south to north, but the groundwater flows are in the opposite direction. This is an important piece of information that should be taken into account for groundwater management. In this sub-basin, there is no connection between the surface water and the groundwater. However, the dune lakes are fed by groundwater. The Tarimoya dune lake (Figure 14) had groundwater flooding during the rainy season. These lagoons are considered discharge zones, and they all have wetlands, mainly freshwater marshes and floating vegetation.

Figure 14: Freshwater marshes and flooded pastures bordering the Tarimoya dune lake.

Dieses Werk ist copyrightgeschützt und darf in keiner Form vervielfältigt werden noch an Dritte weitergegeben werden.
Es gilt nur für den persönlichen Gebrauch.

The dune lake in La Mancha (in the municipality of Actopan) is located 60 km north of the city of Veracruz, and for this dune lake Peralta and Yetter [4, 14, 15] showed that groundwater was present throughout the year and was the main source of water feeding the wetlands, dune lakes, and even the mangroves. Yetter [4] found that groundwater originated from distant (the Manuel Díaz mountain range) and nearby source (local sand dune systems).

4.4 Urban coastal zone

The piezometer in the coastal zone showed an increase of groundwater with higher levels during the rainy season. This indicates a saturation of soil pores, which prevents further water infiltration, except for water that replaces the water that is slowly flowing out. On the coast, there is a discharge of groundwater to the sea. This contribution prevents sea water intrusion, which is another very important wetland ecosystem service, especially considering climate change scenarios.

4.5 Flooding in the urban area

The cities of Veracruz and Boca del Río have been constructed over dunes and wetlands (Figure 13), and have high densities of urbanization. These wetlands are fed by groundwater as the research results show, but also by rainwater and superficial water, storm water flow in the streets, and overflow from the Jamapa River are important inputs. Although urbanization has spread over the wetlands, water from these sources continues to flow every year, and floods homes where the wetlands were transformed into residential areas.

To deal with flooding, the government has mainly built infrastructure to drain the water through channels and pumps. Their policies are based on the idea that river overflow is the main problem in Veracruz and Boca del Río. The data indicate that there are strong surface-groundwater interactions and these are responsible for floods. The results obtained in our study indicate that wetland restoration should also be part of flood mitigation policies, along with a commitment to protecting the remaining wetlands and even the flooded pastures. Campos [23, 24] showed that wetland soils, especially freshwater wetlands, store seven to eight times their weight in water. Forested freshwater swamps store between 557 and 889 L/m^3, which means that huge volumes of water are stored in a single cubic meter of soil. Broadleaf freshwater marshes store between 708 and 862 L/m^3, cattail marshes 535-698 L/m^3, flooded pastures 590-679 L/m^3, and mangroves 512-656 L/m^3. These data indicate the importance of wetlands, for storing water and reducing inundations peaks, in floodplain wetlands [23, 25].

Figure 4 shows the extensive distribution of wetlands around the cities, many of which have been transformed into flooded pastures for cattle ranching [26]. They form a belt, which stores water in the soil and releases it slowly into deeper aquifers and into the sea. These wetlands help to mitigate flood peaks. Acreman [3] indicated that floodplain wetlands slow down flood wave speed and store large quantities of water, primarily on the surface, that later flow back into the river, evaporate, or recharge the water table.

Dieses Werk ist copyrightgeschützt und darf in keiner Form vervielfältigt werden noch an Dritte weitergegeben werden.
Es gilt nur für den persönlichen Gebrauch.

The Tembladeras protected natural area is a freshwater marsh designated to help regulate floods. It is a first attempt in this region to use wetlands in conjunction with hydraulic infrastructure to reduce the risks to local inhabitants. Fifty years ago, the US Corps of Engineers [27] showed that the flood reduction function of 3,800 hectares of floodplain storage on the Charles River, in the state of Massachusetts, saved US$ 17 million worth of downstream flood damage each year. Dune lakes, despite their small size, can also help, especially if serious measures are taken to halt city encroachment. As they are surrounded by urbanization and are widely distributed in the city of Veracruz, dune lakes can also function as early warning systems when groundwater levels increase.

Aquifers are the primary source of drinking water. Groundwater extraction has significantly facilitated social development and economic growth, enhanced food security, and alleviated drought in many farming regions. But it has also depressed water tables, degraded ecosystems, and led to a deterioration in groundwater quality [17], including salinization. Thus, the water stored in the soil is also important for preventing salt water intrusion.

Flood control in the Veracruz-Boca del Río area implies continuing the research on different types of wetlands and the role they play in flood peak mitigation. It also implies developing a management plan for using built infrastructure along with natural and constructed wetlands to improve living conditions for inhabitants. The judicious management of floodplain storage enhances flood reduction. This type of management includes planting of shrubs and trees to increase roughness, and building structures that allow water onto the floodplain, but slow its flow back to the river [3]. The management plan should include several types of actions, such as the detailed mapping of all of the sub-basins, wetland types, and low-lying areas. These maps will help to define areas where urbanization can take place with no concern of flooding, and areas where it should be forbidden. Wetland types that help reduce flood peaks should be restored and conservation strategies developed. The management plan should include different participants, such as local NGOs, environmental and local authorities, and people with technical expertise, among others. Ample participation is needed to ensure a management plan that works and can be legally enforced. Policies for flood risk reduction should reflect a holistic view in which engineering and environmental solutions work hand-in-hand.

5 Conclusions

Several conclusions can be drawn from the present study. There are important interactions between surface water, groundwater, and vegetation. During the rainy season, the groundwater rises and interacts with the surface water from the two rivers in the study area. This interaction can be utilized as a monitoring system because an increase in groundwater level can indicate flooding. Water from several sub-basins flows into the urban area, and there is evidence that dune lakes are large capacity groundwater discharge zones.

This study identifies five ways that groundwater, surface water and vegetation interact: (1) the groundwater reflects the river's behavior and the presence of riparian vegetation (i.e. the

Dieses Werk ist copyrightgeschützt und darf in keiner Form vervielfältigt werden noch an Dritte weitergegeben werden.
Es gilt nur für den persönlichen Gebrauch.

confluence of the Jamapa and Cotaxtla rivers), (2) areas with river discharge, sea water intrusion and groundwater have mangroves (Mandinga), (3) where the contribution of the river is superficial but groundwater flow is in the opposite direction, there is a discharge zone. In extreme events this site could function as an attenuation zone (Arroyo Moreno), (4) when watershed discharges to the sea and groundwater flows in the opposite direction, this indicates that the dune lakes are fed by groundwater (North Sub-basins), (5) an aquifer where the soil is mainly sand (urban coastal zone). There are four natural protected areas in this region: Arroyo Moreno, Tembladeras, the dune lakes and the reef zone. Groundwater discharge to the sea modifies the salinity in certain areas of the littoral zone, prevents sea water intrusion, and contributes to the conditions that have allowed reefs to develop and spread in the area.

Dune systems are important areas for rain water infiltration. Parts of them should be conserved as such, and not urbanized. Large areas of the cities are exposed to flooding from both groundwater and surface water. A variety of wetland types are abundant in the sub-basins and store water in the soil, but during the rains they become saturated, so wetland restoration should form part of flooding mitigation policies.

Flood control implies developing a management plan with a comprehensive framework and ample participation by the different stakeholders, using both built infrastructure and wetlands, and emphasizing research on wetland flood mitigation, restoring wetland vegetation to increase roughness, and defining areas for urban growth. The management plan should take into account that flooding in the area results from the interaction of groundwater and surface water, and affects a large urban area. This region offers an opportunity for engineering and environmental approaches to join forces to reduce the risks people are exposed to, while maintaining the environmental services provided by wetlands.

6 Acknowledgements

This study is part of the project: “Evaluación *integral de la vulnerabilidad al cambio climático de la Cuenca del río Jamapa, Veracruz y sus repercusiones en el sistema cafetalero, en poblaciones de la Cuenca baja vulnerables a inundaciones*” funded by SEMARNAT-CONACYT (249270). The authors thank Jaime Omar Sánchez Zaletas, Alejandro García Suárez (Tecnológico de Veracruz) and Gabriela Maldonado Enríquez (Universidad Veracruzana) for technical support, and are grateful to the “Excellence Center for Development Cooperation-Sustainable Water Management”, the TU Braunschweig, the German Academic Exchange Service (DAAD) and the German Federal Ministry for Economic Cooperation and Development (BMZ) for funding and also for technical support provided by the Project “Higher Education Excellence in Development Cooperation-EXCEED,” and for the opportunity to participate in the EXCEED-SWINDOW Summer School “Integrating Ecosystems in Coastal Engineering Practice (INECEP)”.

Dieses Werk ist copyrightgeschützt und darf in keiner Form vervielfältigt werden noch an Dritte weitergegeben werden.
Es gilt nur für den persönlichen Gebrauch.

7 References

1. Marios, S.: Interactions between groundwater and surface water: the state of the science. Hydrogeology Journal 10, 52-67 (2002)
2. Tóth, J.: Groundwater as a geologic agent: an overview of the causes, processes, and manifestations. Hydrogeology journal 7, 1-14 (1999)
3. Acreman, M., Holden, J.: How Wetlands Affect Floods. Wetlands 33, 773-786 (2013)
4. Yetter, J.C.: Hydrology and geochemistry of freshwater wetlands on the Gulf Coast of Veracruz, México. MSc. Thesis. pp. 174. University of Waterloo, Ontario, Canada (2004)
5. Neri, F.I.: Inundaciones por agua subterránea en zonas costeras. Caso de estudio: acuífero de Veracruz. Boletín de la Sociedad Geológica Mexicana 66, 247-261 (2014)
6. Moreno-Casasola, P.: Servicios ecosistémicos de las selvas y bosques costeros de Veracruz: México. Instituto de Ecología A.C.-OIMT-CONAFOR. Xalapa (2016)
7. Ortiz Pérez, M.A., Méndez Linares, A.P.: Escenarios de vulnerabilidad por ascenso del nivel del mar en la costa mexicana del Golfo de México y el Mar Caribe. Investigaciones geográficas 39, 68-81 (1999)
8. INEGI: Censo general de población y vivienda 2010. In (Vol. 2015). Ciudad de México, D.F.: INEGI (Instituto Nacional de Estadística, Geografía) (2010)
9. Tejeda, M.A.: Panorámica de las inundaciones en el Estado de Veracruz durante 2005. In: Inundaciones 2005 en el estado de Veracruz. pp. 9-20. INECC-Universidad Veracruzana. Xalapa (2007)
10. Tejeda, M.A., Betancourt, T.L.: Inundaciones 2010 en el estado de Veracruz:México pp. 578. Consejo Veracruzano de Investigación Científica y Desarrollo Tecnológico. Xalapa (2012)
11. Infante Mata, D., Moreno-Casasola, P., Madero-Vega, C., Castillo-Campos, G., Warner, B.G.: Floristic composition and soil characteristics of tropical freshwater forested wetlands of Veracruz on the coastal plain of the Gulf of Mexico. Forest Ecology and Management 262, 1514-1531 (2011)
12. López-Portillo, J.: Atlas de las costas de Veracruz: manglares y dunas [costeras]. Gobierno del Estado de Veracruz, Secretaría de Educación (2011)
13. Moreno-Casasola, P., Cejudo-Espinosa, E., Capistrán-Barradas, A., Infante-Mata, D., López-Rosas, H., Castillo-Campos, G., Pale-Pale, J., Campos-Cascaredo, A.: Composición florística, diversidad y ecología de humedales herbáceos emergentes en la planicie costera central de Veracruz, México. Boletín de la sociedad botánica de México 29-50 (2010)
14. Peralta Pelaez, L.A., Moreno-Casasola, P., López Rosas, H.: Hydrophyte composition of dune lakes and its relationship to land-use and water physicochemistry in Veracruz, Mexico. Marine and Freshwater Research 65, 312-326 (2014)

Dieses Werk ist copyrightgeschützt und darf in keiner Form vervielfältigt werden noch an Dritte weitergegeben werden.
Es gilt nur für den persönlichen Gebrauch.

15. Peralta-Peláez, L.A., Moreno-Casasola, P.: Floristic composition and diversity of wetland vegetation in dune lakes in Veracruz. Boletín de la sociedad botánica de México 85, 89-101 (2009)

16. Bullock, A., Acreman, M.: The role of wetlands in the hydrological cycle. Hydrology and Earth System Sciences 7, 358-389 (2003)

17. Gleeson, T., VanderSteen, J., Sophocleous, M.A., Taniguchi, M., Alley, W.M., Allen, D.M., Zhou, Y.: Groundwater sustainability strategies. Nature Geoscience 3, 378-379 (2010)

18. Herrera Silveira, J.A., Camacho Rico, A., Pech, E., Pech, M., Ramírez Ramírez, J., Teutli Hernández, C.: Dinámica del carbono (almacenes y flujos) en manglares de México. Terra Latinoamericana 34, 61-72 (2016)

19. Moreno-Casasola, P.: Servicios ecosistémicos de las selvas y bosques costeros de Veracruz: México. Instituto de Ecología A.C-OIMT-CONAFOR. Xalapa (2016)

20. Fleckenstein, J.H., Niswonger, R.G., Fogg, G.E.: River-Aquifer Interactions, Geologic Heterogeneity, and Low-Flow Management. Ground Water 44, 837-852 (2006)

21. Neri, F.I.: Dinámica del agua subterránea-agua superficial y su relación con las inundaciones en zonas costeras. PhD thesis. Ciencias de la Tierra, Instituto de Geología. UNAM, pp. 183 (2017)

22. Mouw, J.E.B., Stanford, J.A., Alaback, P.B.: Influences of flooding and hyporheic exchange on floodplain plant richness and productivity. River Research and Applications 25, 929-945 (2009)

23. Campos C, A., Hernández, M.E., Moreno-Casasola, P., Cejudo Espinosa, E., Robledo R, A., Infante Mata, D.: Soil water retention and carbon pools in tropical forested wetlands and marshes of the Gulf of Mexico. Hydrological Sciences Journal 56, 1388-1406 (2011)

24. Campos, C.A., Pale Pale, J., Juárez Eusebio, A.: Servicios hidrológicos de los suelos de humedal: la capacidad de almacenamiento de agua. In: Moreno-Casasola, P. ed. Servicios ecosistémicos de las selvas y bosques Costeros de Veracruz: México. Instituto de Ecología A.C-OIMT-CONAFOR. Xalapa. 130-142 (2016)

25. Bullock, A., Acreman, M.: The role of wetlands in the hydrological cycle. Hydrology and Earth System Sciences 7, 358-389 (2003)

26. Moreno-Casasola, P., Rosas, H.L., Rodríguez-Medina, K.: From tropical wetlands to pastures on the coast of the Gulf of Mexico. Pastos 42, 185-217 (2014)

27. US Corps of Engineers. An overview of major wetland functions and values. US Fish and Wildlife Service, FWS/OBS-84/18 (1972)

Dieses Werk ist copyrightgeschützt und darf in keiner Form vervielfältigt werden noch an Dritte weitergegeben werden.
Es gilt nur für den persönlichen Gebrauch.

THE MULTI-CHANNEL ESTUARINE SYSTEM OF THE AMAZON AND PARÁ RIVERS

Laíssa R. S. Baltazar[1], Marcos N. Gallo[1], Susana B. Vinzón[1]

[1]Laboratory of Cohesive Sediments Dynamic – LDSC, Postgraduate Program of Naval and Oceanic Engineering– PENO/COPPE, Federal University of Rio de Janeiro, Brazil, baltazar.ocean@gmail.com

Keywords: Amazon River; Multi-channel estuaries; Numerical modelling; Straits of Breves; Tide

Abstract

Tides play an essential role in estuarine hydrodynamics, being important for navigation, water management and the sustainable use of natural resources. This study aims to analyze the behavior of the tidal propagation along the main two channels and the inner straits of the Amazon estuary in terms of water levels and flow velocities. The Amazon River with an average discharge of $1.7x10^5$ m³/s flows through two main branches, North and South, towards the ocean. The Tocantins River, of which the average discharge is $1.3x10^4$ m³/s, flows to the Para River. Around Marajo Island, the Amazon South channel meets the Para River at the mouth and they are also connected through a set of channels, the Straits of Breves. Tidal propagation along this multi-channel system is modulated by the incident tidal amplitude and phase, and the amplitude and phase of the rivers' discharges. However, the tidal response could be more complex due to the exchange between the two hydrographically distinct estuaries, which are connected by tidal channels. A numerical model (Delft3D) and available data from several tidal gauges are used to investigate the tidal propagation. The results show: (a) the formation of a tide convergence zone, and (b) a greater influence of the Amazon River in flow velocity directions than that of the Para River. An analysis of the levels and currents (H-v diagrams) of tides at the convergence zone is also presented to understand the wave tide behavior.

1 Introduction

Water circulation in the estuary is an important factor for diverse studies of practical interest, such as sediment transport, pollutant dispersion and determination of levels and currents for safety navigation. Tidal information is thus important, as it plays an essential role in estuarine hydrodynamics. However, estuarial and coastal settings often have complex geometric patterns of channels subject to tidal forcing from both ends [1]. Few studies have focused on the exchange between two hydrographically distinct estuaries connected by tidal channels [1].

The circulation patterns of water through these systems are controlled by the magnitude and phasing of tidal forcing [1], while the connected channels enable the change of water, sediments, and nutrients between them. When tidal channels join, the tidal waves that propagate landward in the net channels affect each other. The velocity amplitudes and phases of the flow in the tidal channels are not necessarily the same, and even for equivalent tidal forcing in the multi-channel system, residual fluxes may be the result of differences in depth, length, convergence width, or

Dieses Werk ist copyrightgeschützt und darf in keiner Form vervielfältigt werden noch an Dritte weitergegeben werden.
Es gilt nur für den persönlichen Gebrauch.

bottom roughness of the connected channels [2]. The estuary morphology and the pressure gradient influences the tidal meeting point in the channels, which may be a barotropic convergence zone, favorable for sediment and nutrient accumulation [1, 3-6]. Another main feature of tidal propagation in estuaries is the amplification and dampening of the tidal range with distance along the channel. In addition, as tidal waves propagate in a convergent channel, the single incident tidal wave may turn a standing wave with a phase lead close to 90° between the horizontal and vertical tides [7].

1.1 Study area

The study area is depicted in Figure 1 and includes the two estuaries of the Amazon and Tocantins Rivers. The Tocantins River flows to the ocean in a complex system called the Pará River. The average discharge of the Amazon, measured at the last riverine station (Óbidos city), is $1.7x10^5$ m^3/s, with maximum and minimum about $2.7x10^5$ m^3/s and $6x10^4$ m^3/s, respectively. 76% and 73% of the Amazon River flows through the South Channel during maximum and minimum discharge periods, respectively [8].The Tocantins River has an average discharge of $1.3x10^4$ m^3/s, with maximum and minimum of $5x10^4$ m^3/s and $1.5x10^3$ m^3/s, respectively [8-10]. The maximum discharge of the Tocantins River anticipates the Amazon River in about 3 months. The tidal propagation along the Amazon River reaches up to 800 km. Tocantins Rivers is dammed for electricity generation 400 km from the ocean, where the tidal wave stops. These two basins are connected by a net of channels, called the Straits of Breves, with the two main channels called the Breves (East) and the Tajapuru (West).

Water from the Amazon River flows toward Pará River via the Straits of Breves, contributing to the dynamics of the salt intrusion, particularly in the dry season of Tocantins [10, 11]. [10, 12] also found a residual flow from the Amazon to the Pará River in the rainy (June) and dry (November) season.

The tide in the study area is classified as macro-tidal, with a range between 4 and 6 m at the mouth of the Amazon and over than 4 m at the Para River mouth, and is semi-diurnal, with a wave relationship (the quotient of the diurnals to semi-diurnals harmonics) of 0.1 [8, 13].

This estuarine system has great social and economic importance for the region, for example, fishing and navigation, since the mouths of the Amazon and Para Rivers are the entrance to several ports and other waterways. Therefore, it is necessary to investigate the tidal propagation at the Straits of Breves more comprehensively, as this is fundamental for the understanding of sediment transport and currents. The lack of data for inside the multi-channel of the Straits of Breves makes the study of the tides in this region complex.

Previous research addressing convergent tides in a channel and discharge patterns of multi-channel estuaries has provided some knowledge [1, 2, 4, 5, 14-16], although no one study area of these works is on the same spatial scale of the Amazon-Para estuary system. Moreover, most of the studies at the Amazon or Pará estuaries are focused on a specific area or on each system

Dieses Werk ist copyrightgeschützt und darf in keiner Form vervielfältigt werden noch an Dritte weitergegeben werden.
Es gilt nur für den persönlichen Gebrauch.

separately [12, 17-20]. Even with the inclusion of the net connection importance, the collected data were limited to points at the beginning or the end of the Straits of Breves.

There are still gaps in the knowledge concerning tidal behavior inside these multi-channels, where the tidal convergence zone is located and how this is influenced by the discharge of the system, the influence of the spring/neap tide and the dry/flood rivers discharge over the tide amplitudes and velocities. The objectives of the present study are to clarify these processes.

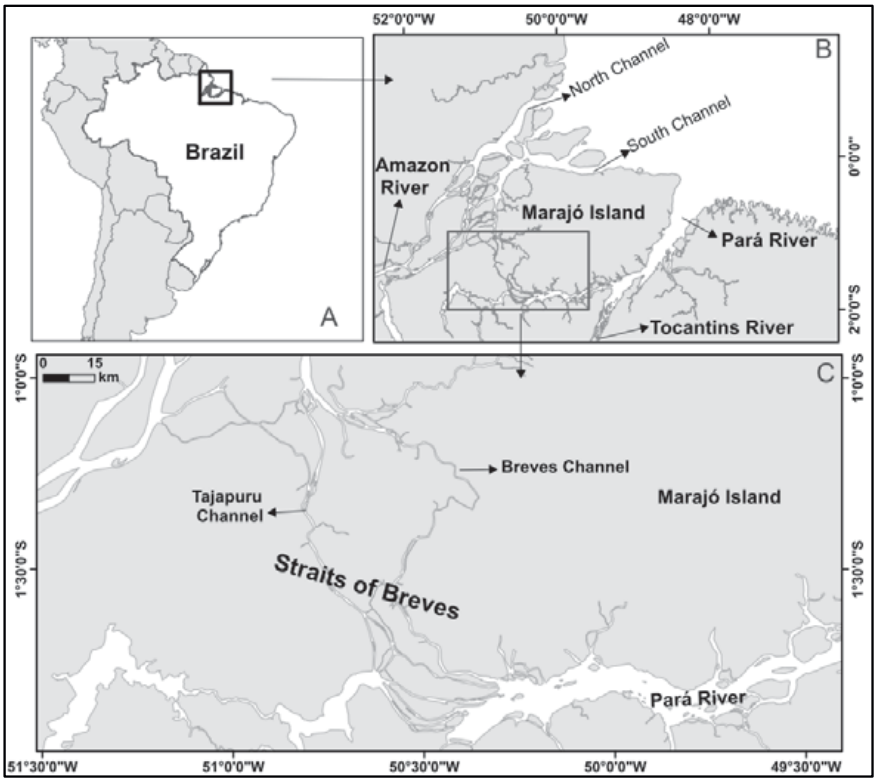

Figure 1: (A) location of the study area (B) South Amazon channel and Pará River connected through Straits of Breves, rounding Marajó Island. (C) Detail of the Straits of Breves, with two main channels, Tajapuru and Breves.

2 Methodology

A numerical model was developed covering the whole system, from the ocean boundary to the last riverine stations (Figure 2), an area of 920 by 1000 km. Delft3D numerical code was used in its vertical averaged mode (2DH module).

A database was built, containing water levels, cross section discharges during a tidal cycle within the estuary, river discharges, tidal constituents along the sea boundary, bathymetry and bottom roughness. Water level information for 16 gauge stations was provided by the Directory of Hydrography and Navigation (DHN- Brazilian Navy), Hydrology and Geochemistry at Amazon Basin Project (HiBAm) and Scientific and Technological Research Institute of Amapá State (IEPA). The model river discharge inputs included the major tributaries: Amazon, Xingu, Tocantins, Jari,

Dieses Werk ist copyrightgeschützt und darf in keiner Form vervielfältigt werden noch an Dritte weitergegeben werden.
Es gilt nur für den persönlichen Gebrauch.

Araguari, Anapu, Acará and Guamá Rivers, considering monthly climatology, based on the National Water Agency (ANA) database [21]. Tidal constituents provided by global model FES2014, which uses satellite data assimilation [22], were used for the sea boundary conditions. The series of amplitudes and phases of the eight main constituents (M2, S2, N2, O1, K1, M4, P1, and K2) were calculated at 29 boundary points, and then interpolated for each cell along the boundary (Figure 2). The bathymetry data base was built from Nautical Charts provided by the Brazilian Navy and bathymetric surveys conducted by the Laboratory of Cohesive Sediment Dynamics, of the Federal University of Rio de Janeiro (LDSC) [23]. The digitalized nautical charts were referred to Mean Sea Level (MSL). The bottom roughness distribution was based on sediment characteristics obtained in the literature [8, 21].

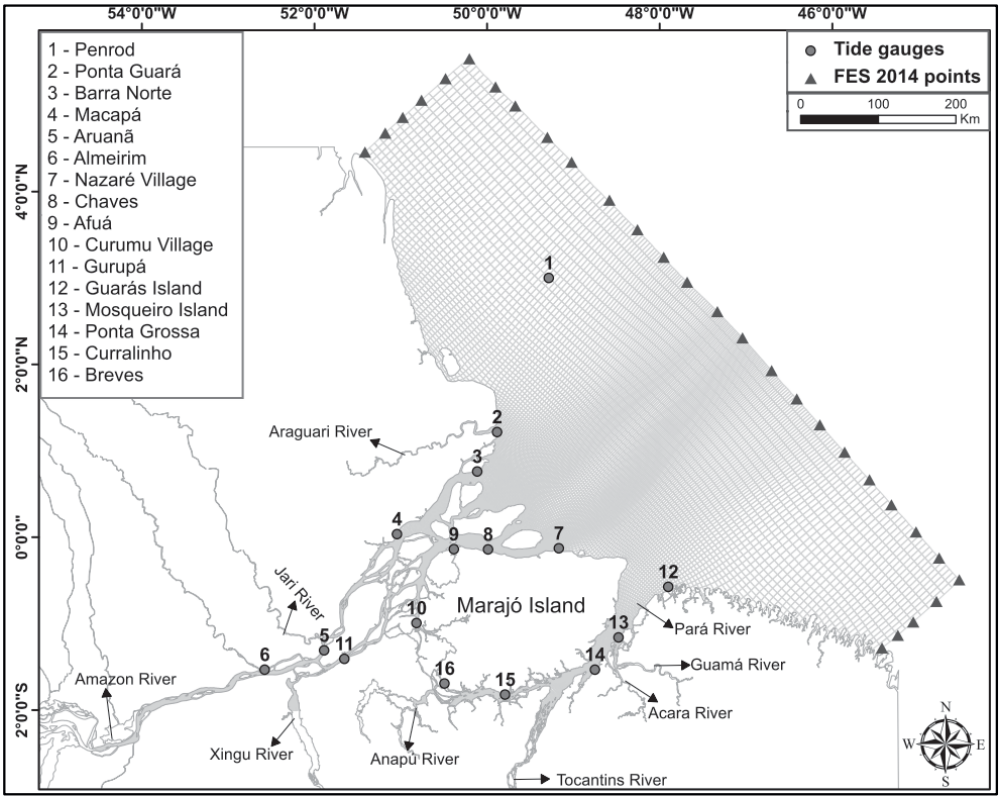

Figure 2: Grid of the numerical model. Triangles indicate the location where tidal constituents were obtained from FES2014; circles indicate the location of tidal gauges; and arrows indicate the location of discharge measurements.

During the process of calibration, amplitude/phase constituents at the boundary were adjusted in order to match the observed data at the Penrod Station (#1). Roughness was also locally modified in the inner estuary, to adjust the model to the observed tidal measurements. Since the tidal data were not simultaneous, obtained during different river discharges, the calibration considered the results obtained in a simulation of a whole year. Modeled tidal series correspond to 2016, while the river discharge corresponds to a typical year (monthly climatology). The comparison between data and model results was then made based on the river discharge at the time of the tidal measurements. The calibration was based on the Pearson correlation and mean square error

Dieses Werk ist copyrightgeschützt und darf in keiner Form vervielfältigt werden noch an Dritte weitergegeben werden.
Es gilt nur für den persönlichen Gebrauch.

(MSE) between the two time series: the model simulation results for 2016 and the tidal series calculated from the data harmonic analysis for the same year. The tool for the harmonic analysis/predict was t_tide / t_predict functions of MatLab® [24].

The time series resulting from the numerical model were compared with data time series, predicted for the simulation year (2016). Data sets were separated according to the river discharge. Thus, stations with long time series were sectioned in maximum, mean or minimum river discharges. Table 1 shows a summary of those comparisons, in terms of the Pearson correlation (%) and mean square error (MSE). 7 stations showed correlations of over 95%, and 13 stations showed correlation over 90%. The lowest correlation was obtained at Curumu Village, where large phase differences were observed. The time series are shown in Figure 3.

Table 1: Pearson correlation (%) and MSE (m) between simulation results and data time series, predicted for the simulation year (2016). Qmax = maximum river discharge; Qave = mean river discharge; Qmin = minimum river discharge.

Tide Gauge	**Correlation (%)**	**MSE (m)**	**Correl_mean (%)**	**MSE_mean (m)**
Penrod (Qave)	97.4	0.031		
Ponta Guara (Qave)	95.9	0.125		
Barra Norte (Qmax)	96.9	0.131	94.2	0.184
Barra Norte (Qave)	93.3	0.177		
Barra Norte (Qmin)	92.4	0.243		
Macapa (Qmax)	95.9	0.056		
Aruana (Qave)	88.3	0.033		
Almeirim (Qave)	79.4	0.007		
Nazare Village (Qmax)	93.8	0.217	95.6	0.145
Nazare Village (Qave)	97.3	0.072		
Chaves (Qave)	96.2	0.094		
Curumu Village (Qave)	69.7	0.248		
Gurupa (Qmax)	92.5	0.023	91.9	0.040
Gurupa (Qave)	91.4	0.058		
Guaras Island (Qave)	94.0	0.223		
Mosqueiro Island (Qave)	96.5	0.060		
Ponta Grossa (Qave)	93.4	0.105		
Curralinho(Qave)	94.9	0.048		
Breves (Qmax)	91.6	0.030	90.8	0.030
Breves (Qave)	87.7	0.033		
Breves (Qmin)	93.2	0.027		

Dieses Werk ist copyrightgeschützt und darf in keiner Form vervielfältigt werden noch an Dritte weitergegeben werden.
Es gilt nur für den persönlichen Gebrauch.

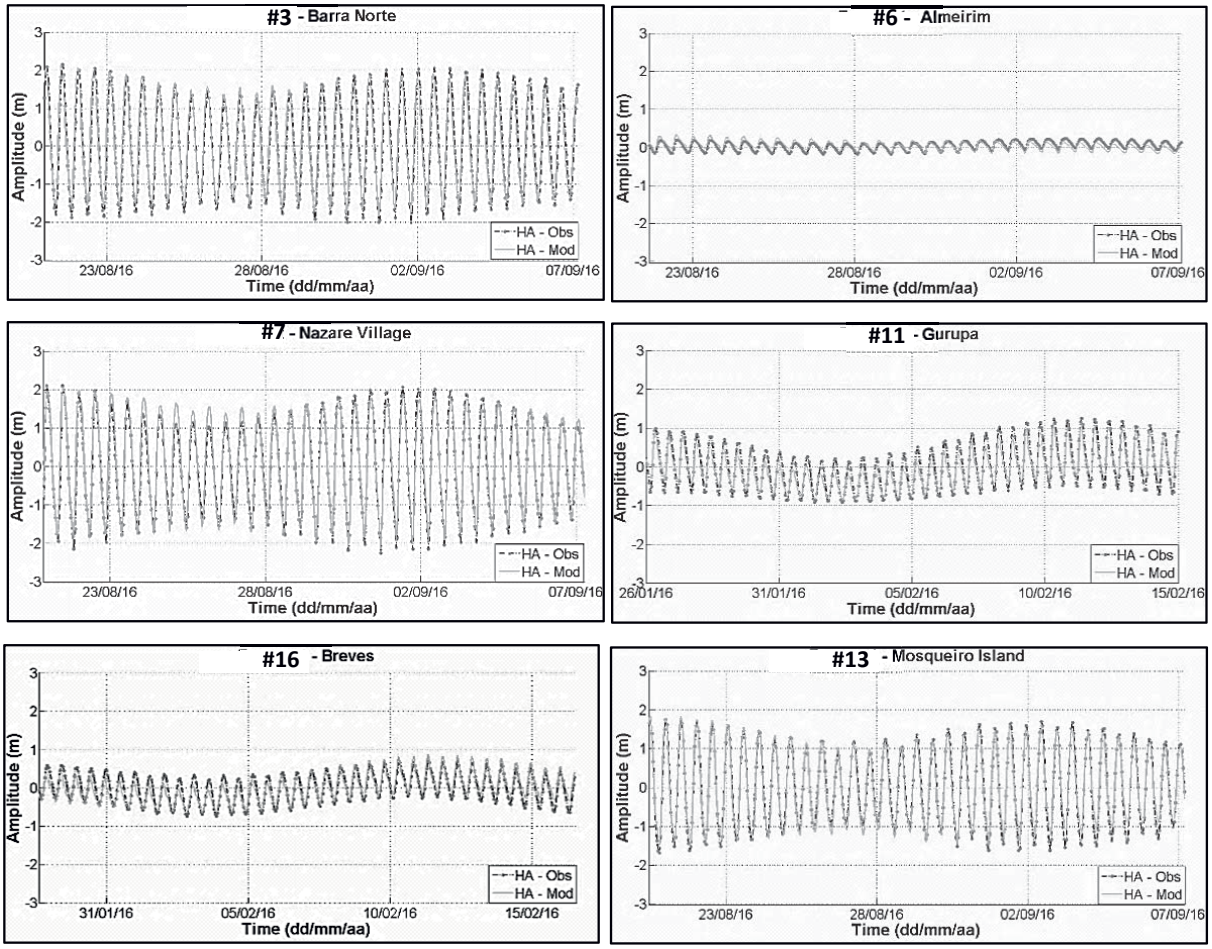

Figure 3: Comparison of simulation results (solid line) and data time series (dots), predicted for the simulation year (2016). The locations of the stations can be seen in Figure 2.

3 Results and Discussion

Figure 4 shows the stations where the tidal propagation was analyzed. The stations are numbered anticlockwise, from gauge station #7 (Nazare Village) to #13 (Mosqueiro Island). Velocities are considered in positive direction following this orientation (anticlockwise is positive and clockwise is negative).

Dieses Werk ist copyrightgeschützt und darf in keiner Form vervielfältigt werden noch an Dritte weitergegeben werden.
Es gilt nur für den persönlichen Gebrauch.

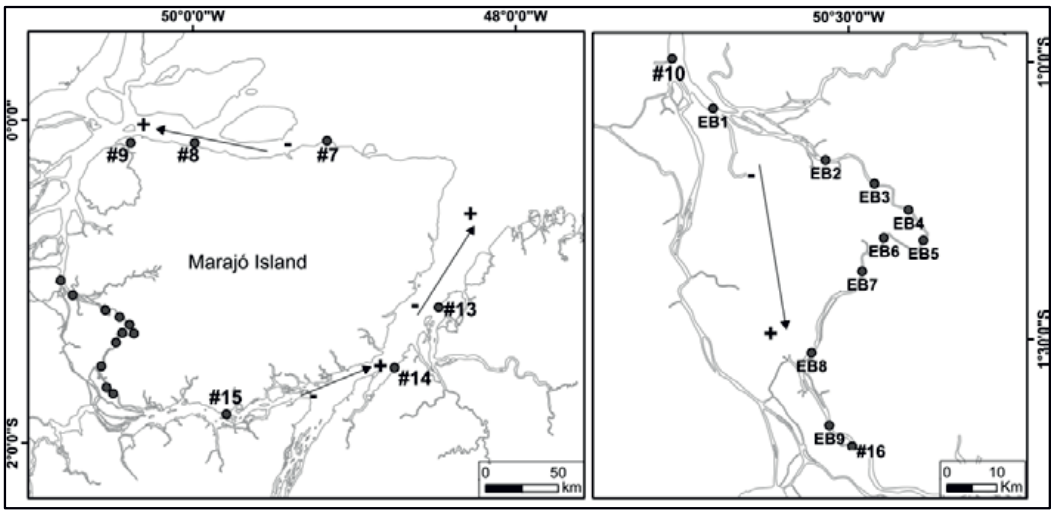

Figure 4: Left: Stations where tidal propagation was analyzed. The arrows show the direction for the mean resulting flow, starting at #7 (Nazare Village) to #13 (Mosqueiro Island). Velocities are positive when oriented anticlockwise. Right: Breves channel, detail of stations between #10 (Curumu Village) and #16 (Breves) where tides propagating along the South Channel and the Para River meet.

3.1 Phase behavior

The increase of the main tidal constituent, M_2 phase, was considered to observe the place where tides meet and propagation along the two channels. Figure 5 shows the phase behavior along the Breves channel. The harmonic analysis of model results is presented for the Amazon River discharge for high water stage (245,414 m^3/s, averaged for June), mean stage (172,383 m^3/s averaged for September), and low water stage (125,141 m^3/s averaged for November).

The two stations at the entrance to Breves channel, #10 Curumu Village and #16 Breves, are almost in phase, when the observed data and simulations results are compared. For the stations in the inner part of the channel (EB1 to EB9), the variation of the M_2 phase was ≈30°, disregarding the river discharge. The station where the phase reaches its maximum value, which corresponds to the tidal meeting location, was station EB7. This station is ≈ 72.5 km and 70.5 km away from the entrance of the South Channel and Pará River, respectively. The results also showed that the difference of the phase, considering the increasing in the Amazon River discharge, was 2.21° at Station #9 Afua and 1.52° inside the Straits of Breves, both between maximum and mean discharge (Figure 5).

Dieses Werk ist copyrightgeschützt und darf in keiner Form vervielfältigt werden noch an Dritte weitergegeben werden.
Es gilt nur für den persönlichen Gebrauch.

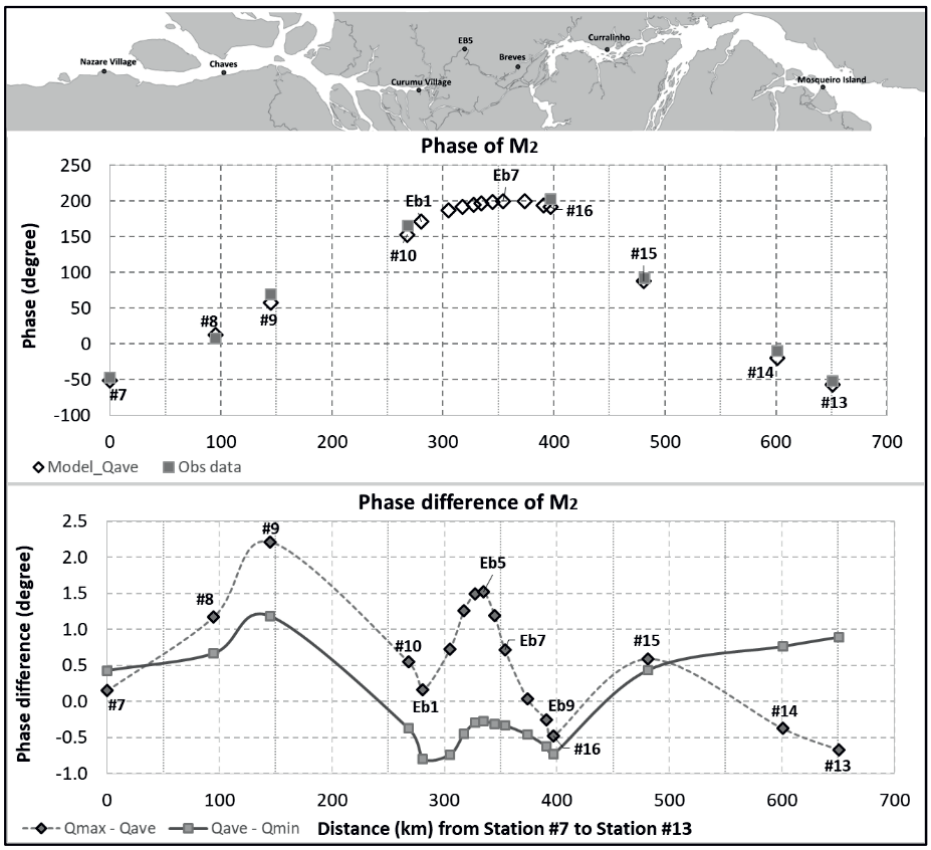

Figure 5: Phase of M_2 component. The upper graph shows the phase of observed data (square) and simulation results with mean discharge (black diamond). The bottom graph shows the difference of M_2 phase considering the Amazon River discharges: maximum – mean (Qmax-Qave) (diamond) and mean – minimum (Qave-Qmin) (square).

3.2 Amplitude behavior

The analysis of amplitudes allowed to identify the features of the wave elevation through the channels toward tide convergence zone. The tidal amplitude falls from the South Channel and Para River to the entrance of the Breves Channel, since the bottom roughness and river flow damped it. Inside the Breves Channel, however, there is an inversion in this behavior, with an increase in the amplitudes. Figure 6 shows this amplitude behavior for a 3.5-day period, where the tide amplitude from the #7 (Nazare Village) and #13 (Mosqueiro Island) stations decreases to upward and turning to increase up to a maximum of around 300 km. Spring tides amplify this feature.

Dieses Werk ist copyrightgeschützt und darf in keiner Form vervielfältigt werden noch an Dritte weitergegeben werden.
Es gilt nur für den persönlichen Gebrauch.

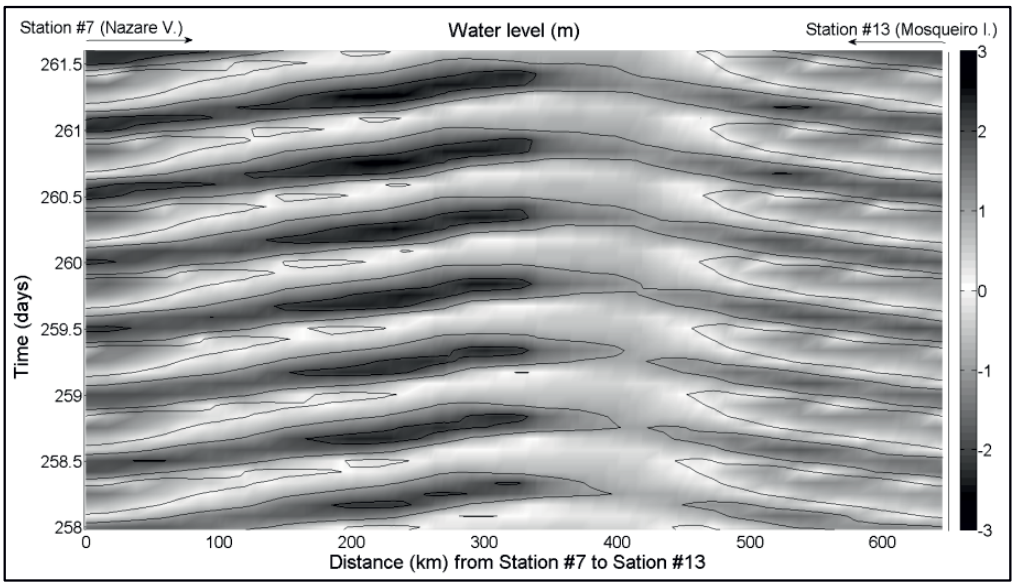

Figure 6: Hovmöller diagram of the water level (m) throughout the channels (#7 to #13), passing from neap tide to spring tide. The black arrow indicates the direction of the tidal wave propagation.

Considering the M_2 harmonic amplitude (Figure 7), it is possible to observe that the site with larger amplitudes in the Breves Channel is around the points EB2-EB3 (≈300-320 km). Moreover, the difference in M_2 amplitude, considering the increase of Amazon River discharge, was 0.04 m (maximum – mean – minimum) at Station #8.

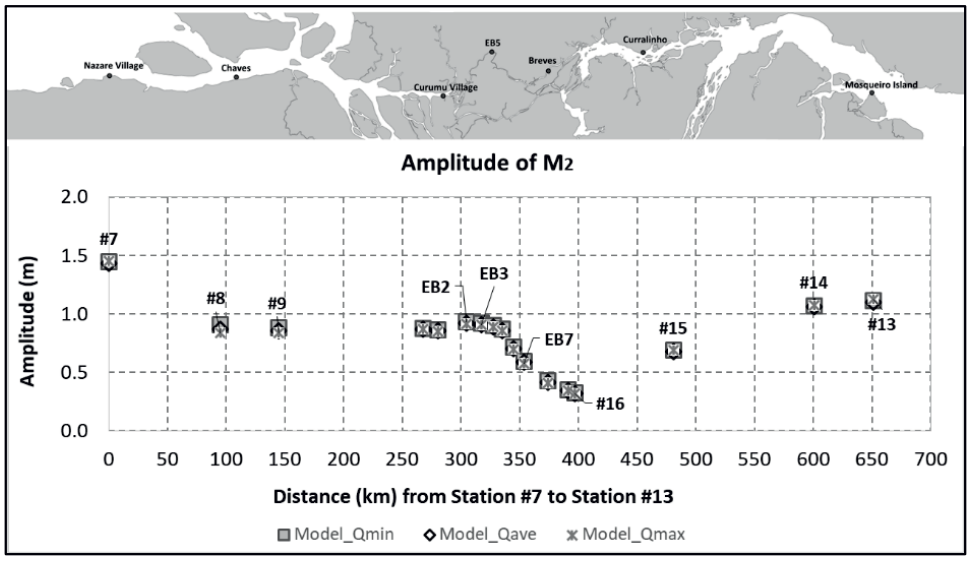

Figure 7: Amplitude of M2 component from Nazaré Village (#7) to Mosqueiro Island (#13), with the black arrow indicating the direction of the tidal wave propagation. The harmonic analysis of the model results are shown for minimum (Model_Qmin), mean (Model_Qave) and maximum (Model_Qmax) discharges.

Dieses Werk ist copyrightgeschützt und darf in keiner Form vervielfältigt werden noch an Dritte weitergegeben werden.
Es gilt nur für den persönlichen Gebrauch.

3.3 Height and velocity analysis (H-v diagrams)

The tide wave amplitude tends to increase up-estuary, but, at the same time, an effective decrease as result of energy dissipation due roughness may occur. Then, the tide wave inside most of the estuaries is a complex composition of progressive and standing waves [25]. The following analysis enables the understanding of the wave tide behavior as it propagates inside the Breves connection channel. At most of stations along the Amazon and Para channels, the tide has a typical progressive wave shape, at which the maximum velocities (positives or negatives) occur during extreme water levels (high or/low water, respectively). At the stations at the entrance to the Breves channel (#10, EB1, EB9 and #16), the tide has maximum velocities close to ebb/flood mid-tide. Since the maximum levels do not coincide with zero velocities, that could be mixed progressive-standing wave behavior (Figure 8).

Considering the seasonality of the rivers, the variation is more noticeable when the Amazon River discharge increases in high water season. Generally, the elevation of the mean level and a small reduction of tidal range occur. However, comparing the results of the first stations in the South Channel (Station #8) and Para River (Station #13), the greater influence on tide propagation of the Amazon River than the Para River is clear. It is more evident when the directions of the velocities are considered in the maximum discharge season, where the velocities at Station #13-EB8 show positive and negative directions with tidal ebbing and flooding, respectively. On other hand, the velocities at stations EB3-EB6 are only positive, with a magnitude reduction during tidal ebbing. Station EB5 has different patterns of H-v relation when compared with the other stations, with magnitude velocity very similar during ebb and flood tides. This is probably associated with the channel morphology at this station.

Dieses Werk ist copyrightgeschützt und darf in keiner Form vervielfältigt werden noch an Dritte weitergegeben werden.
Es gilt nur für den persönlichen Gebrauch.

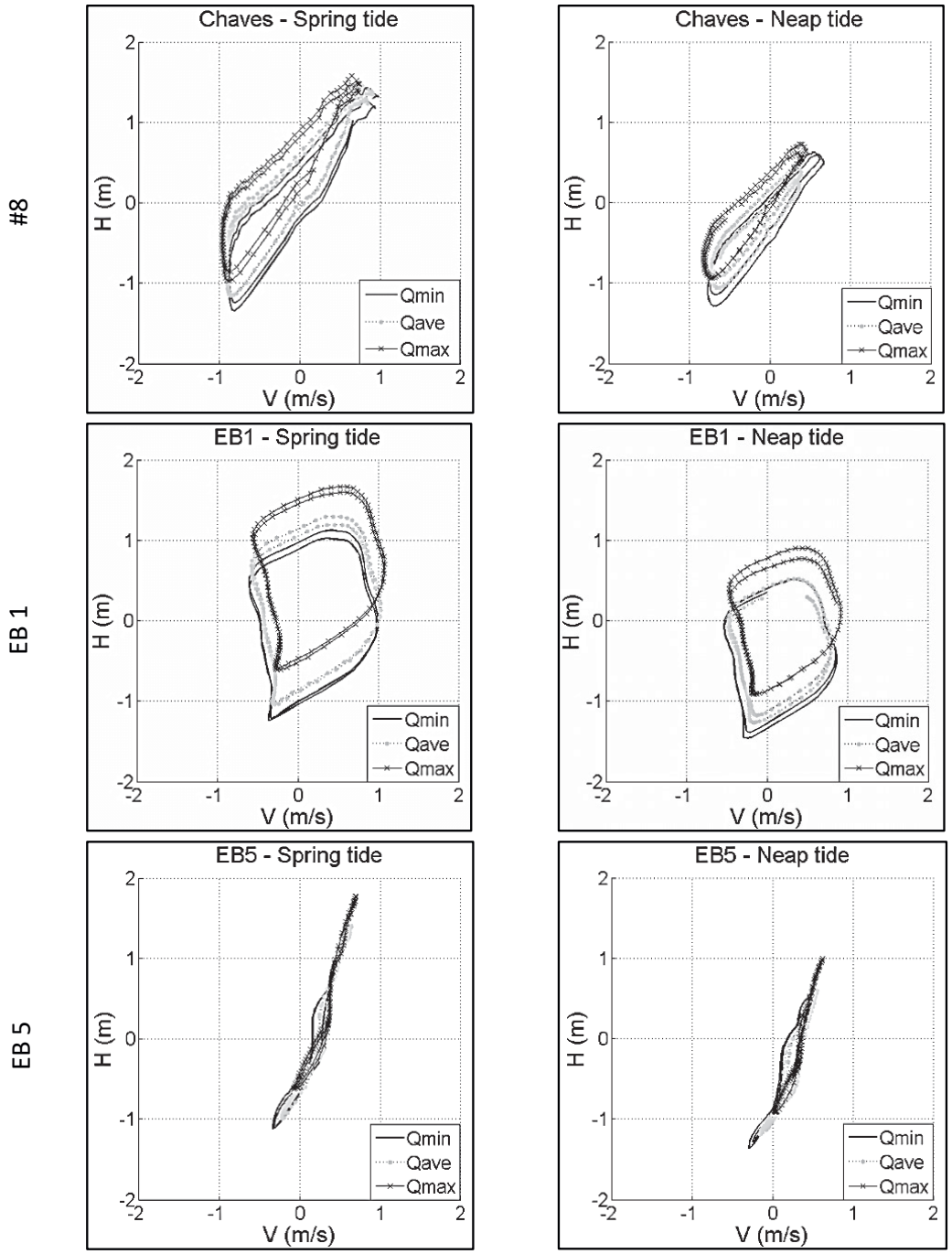

Figure 8: H-v diagrams of model results at #8, EB1 and EB5 stations, for spring tide (left) and neap tide (right). The different lines represent different Amazon River discharges, minimum (Qmin), mean (Qave) and maximum (Qmax). The locations of the stations can be seen in Figure 4.

Dieses Werk ist copyrightgeschützt und darf in keiner Form vervielfältigt werden noch an Dritte weitergegeben werden.
Es gilt nur für den persönlichen Gebrauch.

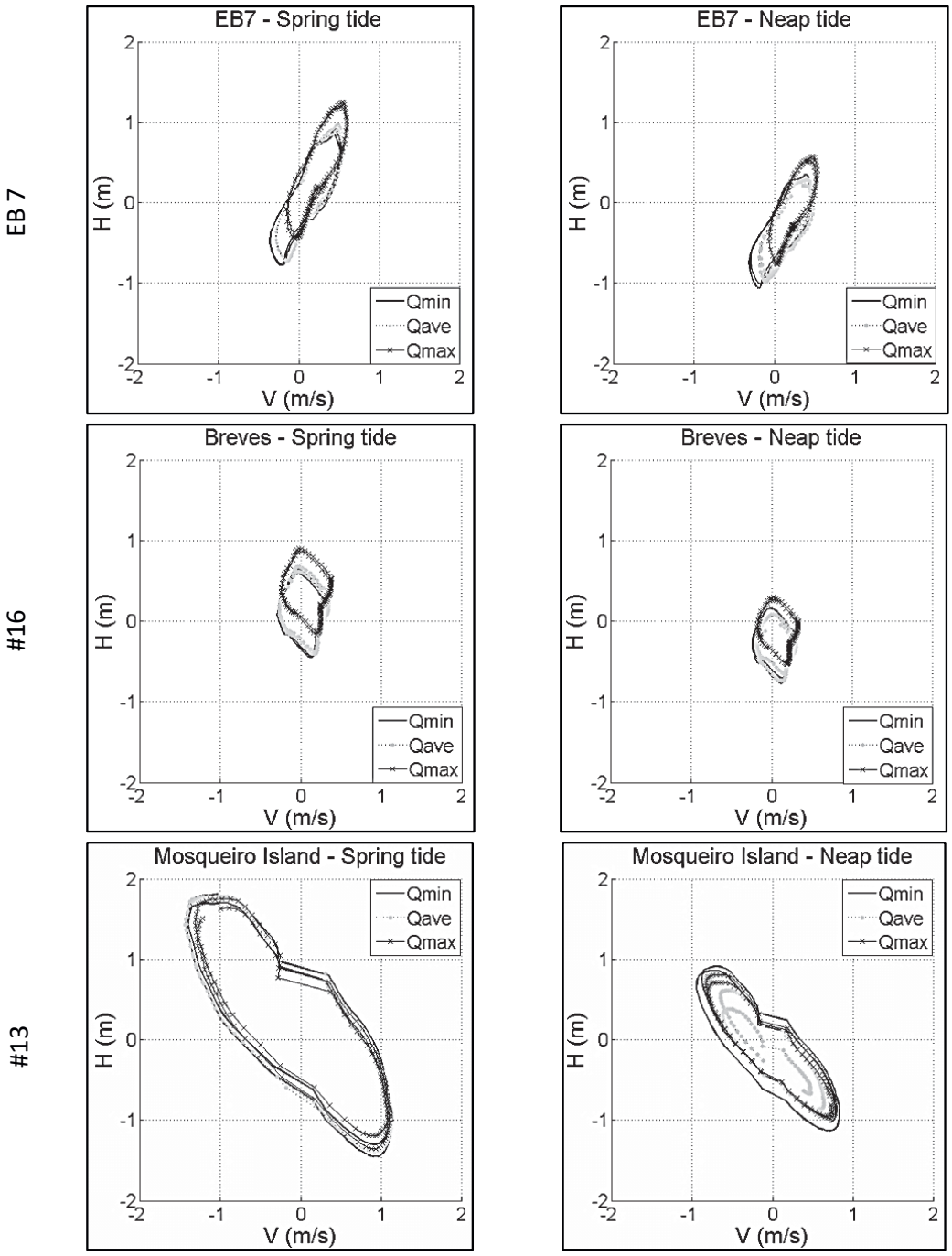

Figure 8: (Continued) H-v diagrams of model results at EB7, #16 and #13 stations, for spring tide (left) and neap tide (right). The different lines represent different Amazon River discharges, minimum (Qmin), mean (Qave) and maximum (Qmax). The locations of the stations can be seen in Figure 4.

Dieses Werk ist copyrightgeschützt und darf in keiner Form vervielfältigt werden noch an Dritte weitergegeben werden.
Es gilt nur für den persönlichen Gebrauch.

4 Conclusions

This research contributes to improving knowledge about multi-channels which are influenced by rivers and tides, as well as to understanding these parameters for the Strait of Breves, which may help decision making for environmental management and navigation. The results show the location of the convergence zone (station EB7) and the influence of the Amazon River on the Straits of Breves region, affecting the tide levels and currents. The tide evaluation, from progressive to mixed progressive-stationary behavior as it propagates into the Straits of Breves, may indicate the influence of one tidal wave over that of the other, in an opposite direction. The stations with low velocities, in the middle of the Straits of Breves, may indicate the places where the accumulation of sediments and nutrients is most likely, as pointed out by [6]. Finally, the influence of discharge on tide is seen clearly at all stations, generally reducing the velocities and amplitudes of the tides and increasing the residual flow from the Amazon to the Para River.

5 Acknowledgements

Thanks to all colleagues from the Lab (LDSC/UFRJ). The authors also thank the DAAD and Exceed Swindon that made participation at the Summer School INECEP event possible. The CNPq are also acknowledged for their support during the research.

6 References

1. Warner, J.C., Schoellhamer, D., Schladow, G.: Tidal truncation and barotropic convergence in a channel network tidally driven from opposing entrances. Estuarine, Coastal and Shelf Science 56, 629-639 (2003)
2. Buschman, F.A., Hoitink, A.J.F., van der Vegt, M., Hoekstra, P.: Subtidal water level variation controlled by river flow and tides. Water Resources Research 46, 1-12 (2009)
3. Maciel, M.A.: Modelagem do padrao de escoamento no canal da passagem - Vitoria_ES. MSc. Thesis. Universidade Federal do Espírito Santo, Vitória (2004)
4. Nascimento, T.F., Chacaltana, J.T.A., Piccoli, F.P.: Análise da Influência do Alargamento de um Estreitamento na Hidrodinâmica do Canal da Passagem, Vitória-ES, Através de Modelagem Numérica. Brazilian Journal of Water Resources 18, 31-39 (2013)
5. Rigo, D.: Análise do escoamento em regiões estuarinas com manguezais – medições e modelagem na baía de Vitória, ES. PhD Thesis. Universidade Federal do Rio de Janeiro, Rio de Janeiro (2004)
6. Traynum, S., Styles, R.: Exchange Flow between Two Estuaries Connected by a Shallow Tidal Channel. Journal of Coastal Research 24, 1260-1268 (2008)
7. Lu, S., Tong, C., Lee, D.-Y., Zheng, J., Shen, J., Zhang, W., Yan, Y.: Propagation of tidal waves up in Yangtze Estuary during the dry season. Journal of Geophysical Research: Oceans 120, 6445-6473 (2015)

Dieses Werk ist copyrightgeschützt und darf in keiner Form vervielfältigt werden noch an Dritte weitergegeben werden.
Es gilt nur für den persönlichen Gebrauch.

8. Gallo, M.N.: A influência da vazão fluvial sobre a propagação da maré no estuário do rio Amazonas. MSc. Thesis. Universidade Federal do Rio de Janeiro, Rio de janeiro (2004)

9. Agência Nacional de Águas: Atlas Geográfico Digital de Recursos Hídricos. Sistema Nacional de Informações sobre Recursos Hídricos. http://www.snirh.gov.br/atlasrh2013livro/ (2013)

10. Costa, M.S.: Aporte hídrico e do material particulado em suspensão para a Baía do marajó: influência dos rios Amazonas e Tocantins. Msc. Thesis. Universidade Federal do Pará, Belém (2013)

11. Barthem, R.B., Schwassmann, H.O.: Amazon River Influence on the Seasonal Displacement of the Salt Wedge in the Tocantins River Estuary, Brazil, 1983 - 1985. Boletim Museu Paraense Emílio Goeldi I, (1994)

12. Silva, I.O.: Disribuição da Vazão Fluvial no Estuário do Rio Amazonas. MSc. Thesis. Universidade Federal do Rio de Janeiro, Rio de Janeiro (2009)

13. Rollnic, M., Rosário, R.P.: Tide propagation in tidal courses of the Pará river estuary, Amazon Coast, Brazil. Journal of Coastal Research 65, 1581-1586 (2013)

14. Buschman, F.A., Hoitink, A.J.F., van der Vegt, M., Hoekstra, P.: Subtidal flow division at a shallow tidal junction. Water Resources Research 46, 1-12 (2010)

15. Nguyen, A.D.: Salt Intrusion, Tides and Mixing in Multi-channel Estuaries. PhD. Thesis. Taylor & Francis/Balkema Netherlands (2008)

16. Sassi, M.G., Hoitink, A.J.F., de Brye, B., Vermeulen, B., Deleersnijder, E.: Tidal impact on the division of river discharge over distributary channels in the Mahakam Delta. Ocean Dynamics 61, 2211-2228 (2011)

17. Baltazar, L.R.S., Menezes, O.B., Rollnic, M.: Contributions to the Understanding of Physical Oceanographic Processes of the Marajó Bay - PA, North Brazil. Journal of Coastal Research 64, 1443-1447 (2011)

18. Borba, T.A.C., Rollnic, M.: Runoff quantification on Amazonian Estuary based on hydrodynamic model. Journal of Coastal Research 75, 43-47 (2016)

19. Gallo, M.N., Vinzon, S.B.: Generation of overtides and compound tides in Amazon estuary. Ocean Dynamics 55, 441-448 (2005)

20. Prestes, Y.O., Rollnic, M., Souza, M., Rosario, R.P.: Volume transport in the tidal limit of the Pará River, Brazil. 17th Physics of Estuaries and Coastal Seas, Porto de galinhas (2014)

21. Molinas, E.: Dinâmica da frente salina e residuais de velocidade na plataforma continental interna amazônica. MSc. Thesis. Universidade Federal do Rio de Janeiro, Rio de Janeiro (2014)

22. ANVISO with CNES supports: FES2014. https://www.aviso.altimetry.fr/en/data/products/auxiliary-products/global-tide-fes.html (2014)

Dieses Werk ist copyrightgeschützt und darf in keiner Form vervielfältigt werden noch an Dritte weitergegeben werden.
Es gilt nur für den persönlichen Gebrauch.

23. PIATAM-OCEANO: Oceanografia Geológica. In: Coleção Síntese do Conhecimento Sobre a Margem Equatorial Amazônica, v. 4. Projeto Piatam Oceano, Federal Fluminense University (UFF), Niterói, Brazil. (2008)

24. Pawlowicz, R., Beardsley, B., Lentz, S.: Classical tidal harmonic analysis including error estimates in MATLAB using T_TIDE. Computers & Geosciences 28, 929-937 (2002)

25. Miranda, L.B., Castro, B.M., Kjerfve, B.: Princípios de Oceanografia Física de Estuários. Editora da Universidade de São Paulo, São Paulo (2002)

Dieses Werk ist copyrightgeschützt und darf in keiner Form vervielfältigt werden noch an Dritte weitergegeben werden.
Es gilt nur für den persönlichen Gebrauch.

EROSION OF PUERTO COLOMBIA COAST BY MARITIME ACTIVITIES

Marianella Bolívar[1], Germán Rivillas-Ospina[2], Carlos Pinilla[3], Gabriel Ruiz[4], Juan Pablo Rodríguez[5], Rodolfo Silva[6], Yeison Berrío[1], Oriana Daza[1], Juan Martín[7]

[1]Universidad Del Norte, Civil and Environmental Engineering Department, Sustainable Development Institute, Km 5 Puerto Colombia, Barranquilla, Atlántico, Colombia, bmarianella@uninorte.edu.co

[2]Universidad Del Norte, Civil and Environmental Engineering Department – PIANC COLOMBIA, Sustainable Development Institute, Km 5 Puerto Colombia, Barranquilla, Atlántico, Colombia.

[3]Universidad Del Norte, Physics Department, Km 5 Puerto Colombia, Barranquilla, Atlántico, Colombia.

[4]Departamento de Recursos del Mar, Centro de Investigación y Estudios Avanzados – Politécnico Nacional, Carretera Puerto Progreso Km, Mérida, Yucatán, México.

[5]Universidad Antonio Nariño, Civil Department, Calle 58A bis # 37 - 94 Bogotá, Colombia

[6]Instituto de Ingeniería, Universidad Nacional Autónoma de México, 04510, Ciudad de México, México

[7]Universidad Del Norte, History and Social Studies Department, Km 5 Puerto Colombia, Barranquilla, Atlántico, Colombia

Keywords: coastal processes, hard structures, Puerto Colombia coast, ecosystems, wave climate

Abstract

In this article, coastal processes are analysed using Landsat Satellite images to assess conditions caused by the construction of coastal works. The littoral cells were implemented according to geomorphological and hydrological factors and the use of regressive models such as the Digital Shoreline Analysis System (DSAS), an extension of ArcGIS 10.3, in order to estimate the changes in the coastline such as erosion and sedimentation rates. The results of this study show that the equilibrium of the system was lost given that the natural conditions allow the natural generation of soft sandy beaches has been irreversibly altered by human activities.

1 Introduction

The beaches of Puerto Colombia municipality show serious erosive and sedimentary processes that affect tourist activities and the marine ecosystem. In the area around Bocas de Ceniza and Puerto Caiman, in the municipality of Puerto Colombia, in Northern Colombia [1] developed a methodology of coastal analysis based on elements of cartography, geology, geomorphology, and

Dieses Werk ist copyrightgeschützt und darf in keiner Form vervielfältigt werden noch an Dritte weitergegeben werden.
Es gilt nur für den persönlichen Gebrauch.

the multi–temporal interpretation of the shoreline and the sand bars. Images from 1935 to 2009 were used to classify the coastal dynamics, sedimentation, and erosion processes. This technique was based on the use of remote sensors, Geographic Information System (SIG), and field work. Three morphodynamic cells were defined along the shoreline with steep slopes and coastal erosion processes, excessive constructions, and intense processes of sedimentation with the formation of extensive sand bars. The results suggested a migration of the sand bars and the beach from northeast to southeast, with the disappearance of the Puerto Colombia beaches being highly likely.

The coastal wetlands of Turkey were studied using multi-temporal Landsat Satellite images, analysing quantitatively the evolution of the shoreline with a ArcGIS 10.2.2 extension and Digital Shoreline Analysis System (DSAS) [2]. It is important to highlight that in the years 1989, 1999 and 2009 important changes in the littorals bars occurred going from sedimentation and erosion processes, identified with maximum values 20.68 m/yr in the Yumurtalik wetland to the disappearance of the Gediz delta in 1975 by sedimentation process.

Sheik and Chandrasekar [3] studied the changes along the coast between Kanyakumari and Tuticorin in the south of India and related them to the hydrodynamic and morphology processes caused by the Tsunami of 2004. They used satellite images from 1999, 2001, 2003, 2005, 2007 and 2009, and the tools of ERDAS IMAGINE 9.1 in order to correct the deviations that emerge from the image analysis, such as radiometric and geometric distortions, presence of noise, and sensor velocity. For the reconstruction of the shoreline, Digital Shoreline Analysis System (DSAS) was used, calculating erosion rates with the analysis of the parameters End Point Rate (EPR), Linear Regression Rate (LRR), and Least Median of Squares (LMS). The results showed that the natural and anthropogenic processes on the coast modified the original configuration and the dynamics of the profile variation through erosion and sedimentation.

In a study along the Buenos Aires coast, Bunicontro et al. [4] noted the absence of studies focusing on environmental criteria when considering the effects of human activities that disturb the hydrodynamic conditions of the area, producing a regression of the cliffs and other coastal erosion processes. In this research, the installation of hard structures from 1980 was noticed, regression of the shoreline causing other changes to the natural dynamics of local and regional hydrodynamic process, the morphology of the beach, and increasing environmental pressures on the coast related to human activities and ecology. This study also analysed the evolution of coastal systems, their functions and consequences, comparing the area with other areas, which had not been altered. This study was undertaken between 1975 and 1985 using aerial photographs from the Geodesic Department of Buenos Aires and satellite images of Google Earth from 2003, 2009 and 2011.

[5] described and assessed the functionality of coastal protection strategies implemented on the Caribbean Colombian coast, particularly coastal management. The authors presented scenarios of present and future conditions, emphasizing the major trends (sediment imbalance, sand mining,

Dieses Werk ist copyrightgeschützt und darf in keiner Form vervielfältigt werden noch an Dritte weitergegeben werden.
Es gilt nur für den persönlichen Gebrauch.

ecosystem destruction, and coastal constructions) for users, property owners, and coastal managers. They concluded that erosion problems here are related to sedimentary imbalances, extreme waves, ecosystem destruction, and rising sea level. Overall, the authors stated that the strategies implemented to combat erosion are generally hard structures, especially in major concentration in tourist populated cities. Nearly 90% of these structures were not successful and caused disruption to natural conditions, producing impacts such as a reduction in sediment supply, an increase in erosion, damage to natural landforms, and new points of erosion [5].

The objective of this work is to study the anthropogenic impacts of maritime activities on the beaches in the vicinity of Puerto Colombia. In order to propose solutions to restore the ecosystem in integrated manner it will discuss the concept of green infrastructure to the extent, permitted by current regulations, encouraging the re-establishment of sediment transport, dune vegetation and evolution of the coast. Finally, restoration measures are proposed based on the diagnostics of the system.

2 Materials and Methods

The municipality of Puerto Colombia is located in the Atlantic Department in the Northeast of the metropolitan area of Barranquilla District. It has an urban area of 22 km^2 and a rural area of 50 km^2. The area has warm, dry and semi-dry weather, with aridity trend due to low precipitation. The coastal zone of this department is devoid of vegetation, and is in part covered by small dunes (Figure 1), *INVEMAR & CRA* [6].

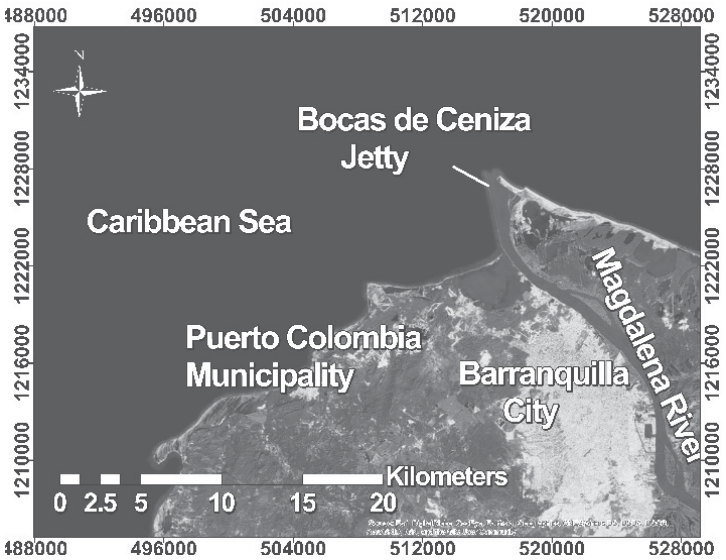

Figure 1: Location of Puerto Colombia

An effective way to analyse the morphological changes on beaches in the long term is to define the littoral cells and to describe the main characteristics that govern the physical dynamics of the system such as hydrology, river inputs, sediment properties, submarine canyons, spits, cliffs, and tidal channels.

Dieses Werk ist copyrightgeschützt und darf in keiner Form vervielfältigt werden noch an Dritte weitergegeben werden.
Es gilt nur für den persönlichen Gebrauch.

Plan view analysis of the littoral zone close to Puerto Colombia was performed by dividing the coastal bar into spatial cells in order to find the cause of the present sediment imbalance. The main feature regulating shoreline processes is wind generated waves, although tides, currents, and the beach configuration also play an important role in the coastal environment.

In this study, the human interventions on the coast have been taken into account, characterizing the coastal infrastructure (harbours, groins, etc.), navigation channels, and their impacts on coastal process. This research seeks to analyse the basic concepts and to define the study zone through sub-cells in order to understand how the sediment is transported along the coast of Puerto Colombia. The sub-cells are described as follows:

2.1 Punta Roca - Country Beach

This cell is located between Punta Roca cliff (11 ° 2 ' 54.99 ' N and 74 ° 55 ' 17.05 ' W) and the first groin of the “Playa del Country” beach at 11 ° 2 ' 19.10 ' N and 74 ° 55 ' 23.47 ' W. It is limited to the east by the Mallorquín coastal wetland cell (Figure 2A). Its length is 973 m, and it is 1 m above sea level (a.m.s.w.l).

According to [7], this zone is formed by silt and sand of medium grain size, sometimes including fragments of shells and molluscs, and does not exceed the thickness of 5 m. The sediment is composed of quartz, plagioclases, muscovite, and some lithic fragments and ferromagnesian minerals (amphiboles and pyroxenes).

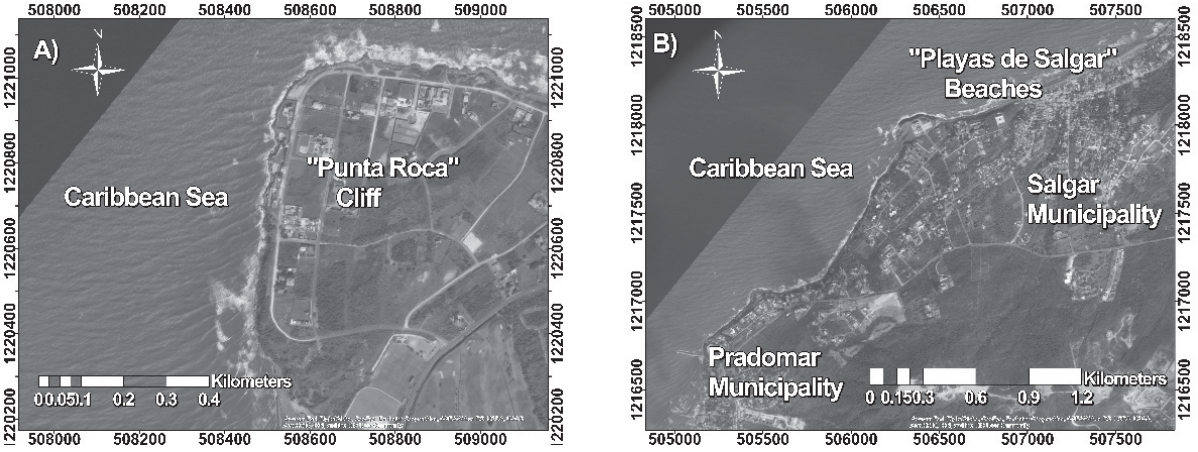

Figure 2: (A) Sub-cell of the sector Punta Roca cliff to breakwater located on the Country Beach, (B) Sub-cell of Salgar beach – Pradomar beach.

The area is a coastal bar, 57 m long and 100 m wide. The beach profile has slopes of 0.3% on average. The beach was formed from sediment transported from the Magdalena river [8]. At the eastern end of this coastal cell, the beach presents a battery of 12 groins that disrupt the sediment transport to the next sub-cell.

Dieses Werk ist copyrightgeschützt und darf in keiner Form vervielfältigt werden noch an Dritte weitergegeben werden.
Es gilt nur für den persönlichen Gebrauch.

2.2 Salgar beach –Pradomar beach

This urbanised coastal cell stretches from Salgar beach (11 ° 1 ' 10.23 ' N and 74 ° 56 ' 13.85 ' W) to the groin located at (11° 0' 23.08' N and 74° 57' 10.21' W) on Pradomar beach (Figure 2B). Its length is 2.58 km and its altitude 2 m a.m.s.w.l. The marine deposits here constitute one of the most important marine geomorphological forms of the area, showing a great sand mobility over the last 40 years with crests of beaches that are old coastlines.

The beach is formed by medium or fine-grained sands, light to dark grey, the darker due to the greater concentration of heavy metals [1]**.** It also has a cliff of soft rock, 2,207 m [8], and there is a low threat of flooding. The aquifers belong to two Caribbean basins (part of the Balboa wetland – Grande stream, and the Mallorquín wetland) with water regulation rates of 0.14 and 0.11 m/s, respectively. Its relative hydraulic vulnerability is moderate [9]. Again, at the end of this coastal cell, a battery of 7 groins was placed on the beach, modifying the coastal processes and altering the sediment sources.

2.3 Puerto Colombia Harbour – "Arroyo Caña" rivermouth

This cell is located from the port of Puerto Colombia (10°59'19.94"N and 74°57'37.53"W) to the mouth of the "Arroyo Caña" river (10°58'53.06"N and 74°58'39.93"W). Its extension is 2.12 km and its altitude 1 m a.m.s.w.l (Figure 3C). The area contains the river mouths of "Arroyo Grande" and "Arroyo Caña", which come from upstream of the basin and feed to the Balboa wetland. This littoral cell is located at west of Puerto Colombia, near to the urban area, which generates high anthropogenic pressure on the water body. The urban area is 160 ha [7] and has a perimeter of 25,782 m. Morphological changes in the coastline are the result of the construction of breakwater of Bocas de Ceniza. This coastal zone is composed of marshes, wetlands, swamps, and mangrove forests associated with dunes formed by ancient coastal bars. The cell has a Hidrobia biomass in the swamp, and Pendozonobioma on the beaches and dunes. The morphodynamic behaviour is responsible for the geomorphology evolution of the zone, which varies between dry seasons with high energy large swells, and wet seasons with low energy waves [6]**.**

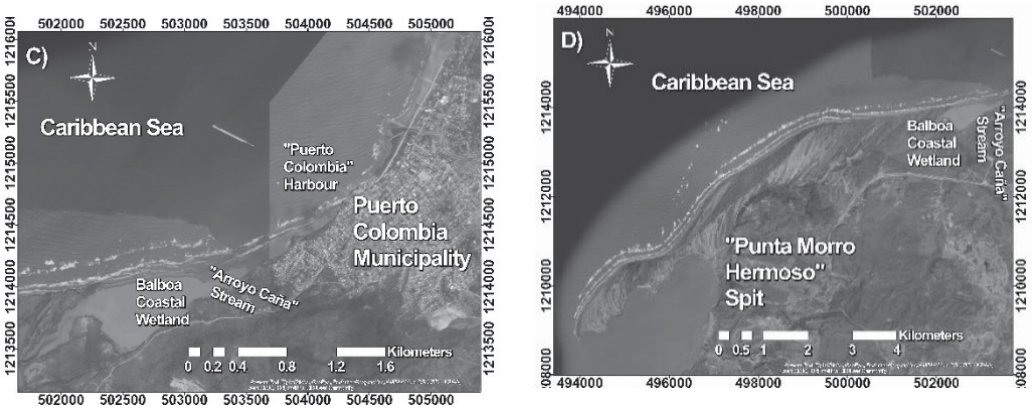

Figure 3: (C) Sub-cell of Puerto Colombia Pier- Mouth of Arroyo Caña, (D) Sub-cell of Arroyo Caña river mouth – Punta Morro Hermoso.

Dieses Werk ist copyrightgeschützt und darf in keiner Form vervielfältigt werden noch an Dritte weitergegeben werden.
Es gilt nur für den persönlichen Gebrauch.

2.4 Arroyo Caña rivermouth– Punta Morro Hermoso Spit

The fourth cell runs from the mouth of the "Arroyo Caña" river (10°58'53.06"N and 74°58'39.93"W) to "Punta Morro Hermoso" spit (10°56'14.78"N and 75° 3'12.26"W). This cell has an extension of 10.9 km and a height of 1 m a.m.s.w.l (Figure 3D). There is a small community called "El Morro" that is part of a beach complex. There are also coastal marshes (Type M, Unit Geomorphological) associated with ancient deltaic deposits of the Magdalena River. The cell also contains the "Ostión" and "Cucumbito" streams, whose aquifers are close to the beaches. Water bodies, an intertidal zone, cliffs, swamps, and coral reefs are important geomorphological features [8]**.** Threats of landslides, storms, erosion, deposition, flood risk, and meteorological events are all present here.

The methodology of this study is based on erosion processes analysis, using the software ArcGIS® tools from historical shoreline positions, created through digitalization of Landsat images from 1984, 1988, 1989, 1990, 2008, and 2016 for the coastal cells in Puerto Colombia. Erosion and sedimentation rates are evaluated with the Digital Shoreline Analysis System (DSAS), a powerful tool that calculates the change rates using statistical methods. In order to estimate the potential erosion, a baseline was defined and orthogonal transects along the coastal cell were built in the domain. Finally, the erosion rates were estimated with the Endpoint Rate (EPR) interpolation method.

3 Results and Discussions

3.1 Morphological Response of the Coastal Cells

The most important morphological features in the zone are sandy beaches, coastal spits, coastal wetlands, cliffs, rivers, and coastal dunes. The main sediment source is from rivers, and the main affectations are due to human interventions; the battery of groins and ports. Field data found that wind action generates sandy dunes, and currents activate the transport of cohesive material (silts and clays) along the coastal zone. In the Colombian Caribbean storm surges associated with hurricanes produce high waves that also erode the coastline.

The natural equilibrium of the system, which allows it to adjust to new physical conditions, has been altered mainly by coastal infrastructure that affects sediment sources and causes erosion. The non-equilibrium of the beach does not allow the retrieval of sediments due to the absence of a sand contribution from the river or the transversal currents originated from gravitational waves.

The study area has changed importantly along the coastline. Due to the installation of remedial measures, related to short term politician decisions, sedimentation takes place caused by littoral drift at the right side of the hard structures. This intensive erosion increased over time (Figure 4).

Dieses Werk ist copyrightgeschützt und darf in keiner Form vervielfältigt werden noch an Dritte weitergegeben werden.
Es gilt nur für den persönlichen Gebrauch.

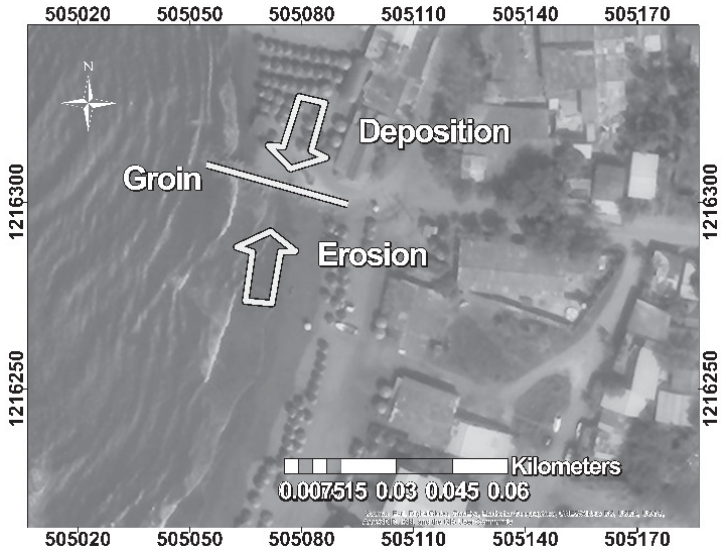

Figure 4: Erosion/sedimentation processes caused by coastal structures.

In 1926, modifications to the system were induced by the building of protective structures close to Barranquilla port, in the Magdalena river mouth (Bocas de Ceniza). The coastal structures induced relevant changes to the sediment sources in the region. Consequently, anthropogenic factors affected the zone and contributed to the modification and destruction of habitats, pollution and the overexploitation of the natural resources, and led to the human interventions undertaken in the municipality of Puerto Colombia.

The extraction of materials from the beaches and rivers for use in buildings, such as sands and gravel (1) creates a loss of the sediments necessary to supply sand to the beaches, and (2) leads to coastal erosion. Moreover, recent modifications in the mangrove ecosystem was found to be caused by indiscriminate felling of the trees. This reduces the natural protection the mangroves provide against erosion and alters the nesting places and the biologic exchanges of species. The effects of waves and currents on the low terraces or swamps are also increased, as is the case at the Country beach.

The urban infrastructure in the intertidal zone, such as houses, restaurants, roads, ports, and protective structures promote disturbances on the coast, represented by loss of sediment that generate coastal erosion processes on the beach (Figure 5 and Figure 6).

Dieses Werk ist copyrightgeschützt und darf in keiner Form vervielfältigt werden noch an Dritte weitergegeben werden.
Es gilt nur für den persönlichen Gebrauch.

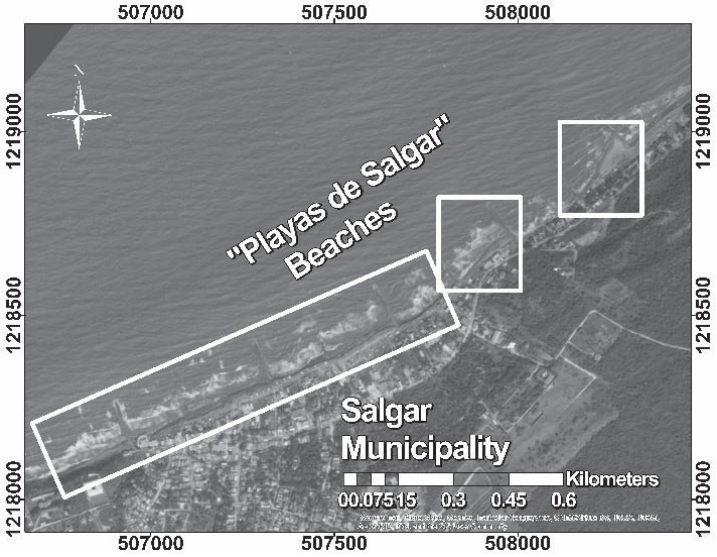

Figure 5: Salgar Beach – Pradomar beach sector

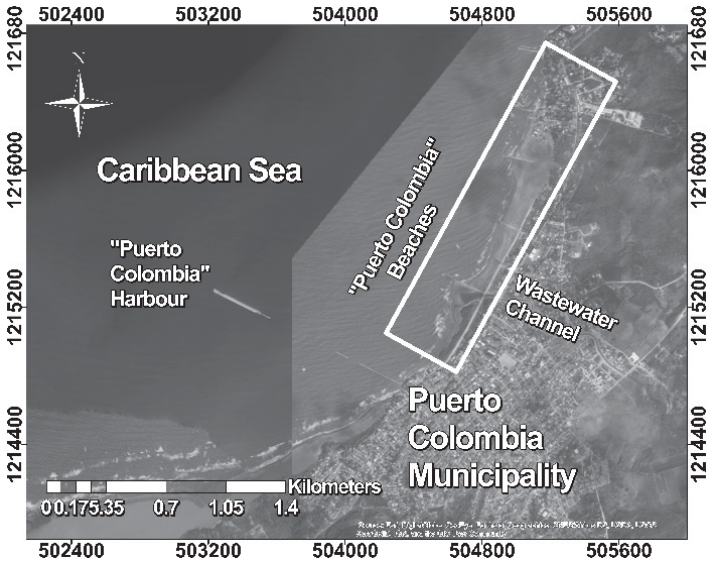

Figure 6: Puerto Colombia Harbour - Arroyo Caña Rivermouth Sector

Despite the erosion problems, the material removed from the coastal sub-cells is transported to the west of the littoral cell, as seen in the sedimentation processes found close to “Punta Morro Hermoso”. The formation of the Isla Verde spit, as was known in 1935, is an example of accretion process.

The increase in the number of coastal protection structures (groins and breakwaters) generated unwanted environmental and social effects on the landscape, shoreline, subaquatic vegetation, and economic activities of the population in the coastal zone. However, there was no mitigation of the negative erosional impacts. Figure 7 shows the locations of the coastal structures.

Dieses Werk ist copyrightgeschützt und darf in keiner Form vervielfältigt werden noch an Dritte weitergegeben werden.
Es gilt nur für den persönlichen Gebrauch.

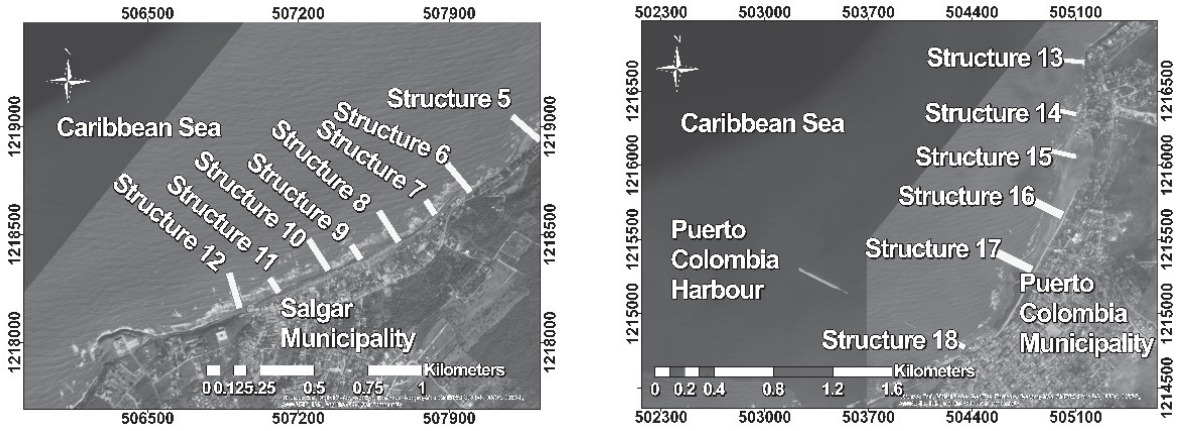

Figure 7: Groins locations at the Puerto Colombia coast

3.2 Shoreline change analysis

The evolution of the coastline was carried out using the Digital Shoreline Analysis System (DSAS) tool from 1984 to 2016 (Figure 8), which uses base layers of polylines in order to represent the shoreline at a particular point in time. The model generates a series of measures of statistical adjustment based on the comparison of the shoreline positions, known as Net Shoreline Movements (NSM), Shoreline Change Envelopes (SCE), End Point Rate (EPR), Linear Regression Rate (LRR), and Weighted Linear Regression Rate (WLR). Temitope (2014) [11] found that although none of these tools determine the morphodynamic forcings, they have proven to be effective means to facilitate an in-depth analysis of the temporary movement and historical positions of the coastline and its geomorphology.

In Figure 8, it can be noted that the first cell shows a significant recession of the coastline from 1989 to 2008. In the cell 2, the coastline from the beaches of Salgar to the beaches of Pradomar, the shoreline regression is less than in sub-cell 1, producing negative changes only in the northwest. Cell 3 shows a uniform regression from 1989 until 2016 on average, but it is higher than the erosion presented in the coastline of cell 1. Finally, in cell 4, there is deposition from 1996 to now, forming a new “Isla Verde” spit between the municipalities of Puerto Colombia and Tubará.

3.3 Analysis of the erosion/accretion potential

In the middle and late nineteenth century, the city of Puerto Colombia had a sea port, built at Sabanilla in 1820. However, due to the existence of the coastal bar that sheltered it (“Ancient Isla Verde”, Figure 9) and the sedimentation produced by the Magdalena River, it was relocated at Puerto Belillo in 1882 and finally to Puerto Colombia in 1893. In order to make maritime navigation possible on the Magdalena River, a jetty was built later at the river mouth between 1922 and 1936, locating the port 20 km upstream. However, new coastal protection structures were built in the last 14 km on the banks of the river in order to stabilize and to deepen the navigation inland waterway (Figure 10).

Dieses Werk ist copyrightgeschützt und darf in keiner Form vervielfältigt werden noch an Dritte weitergegeben werden.
Es gilt nur für den persönlichen Gebrauch.

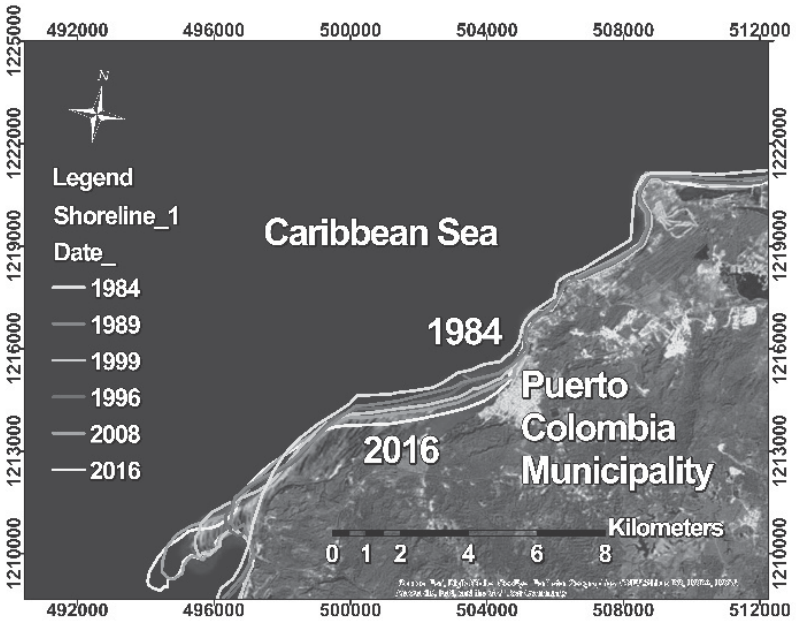

Figure 8: Shoreline Analysis

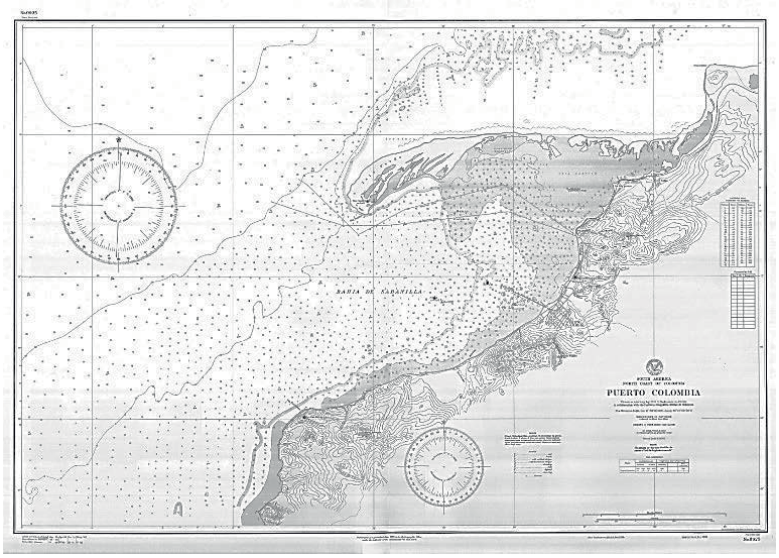

Figure 9: Cartography of the Municipality of Puerto Colombia in 1820 (Source: [12])

The new river mouth is located in front of a submarine canyon, and the design of the jetties did not consider this. Therefore, a large percentage of the sediment that the river transports is leading to the canyon. There is thus a sediment deficit at the site, where the sediments are very relevant for the natural maintenance of the beaches of the Atlantic. These engineering works led to the disappearance of the old “Isla Verde”.

Dieses Werk ist copyrightgeschützt und darf in keiner Form vervielfältigt werden noch an Dritte weitergegeben werden.
Es gilt nur für den persönlichen Gebrauch.

Figure 10: Western Tajamar of Bocas de Ceniza. (Source [10])

On the other hand, as shown in Figure 11A and 11B for the years 1973 and 1989, a process of sediment accumulation on the beaches of Puerto Colombia is shown. In 1989, a progressive accumulation of sediment formed the littoral spit seen in Figure 11B. All the material eroded from the old “Isla Verde” was deposited in a new location close to “Punta Morro Hermoso”, in sub-cell 4.

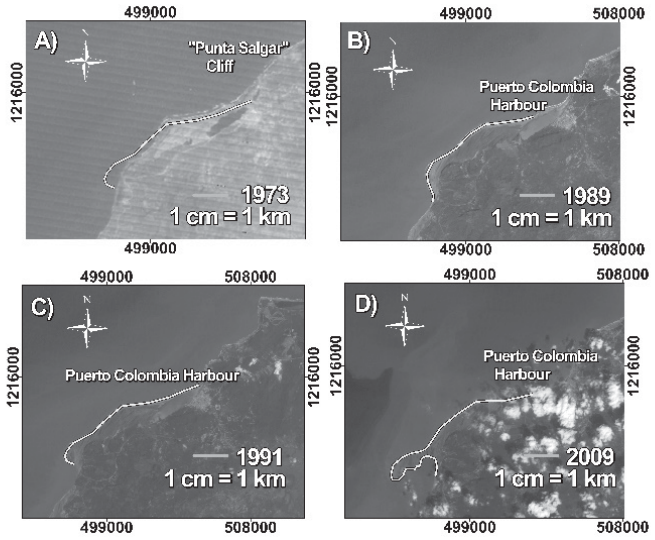

Figure 11: Coastal arrow analysis in the years (A) 1973, (B) 1989, (C) 1991, (D) 2009

As seen in Figure 11C for 1991, the new “Isla Verde” spit is more pronounced in front of the municipalities of Juan de Acosta and Tubará. In this sense, the longshore sediment transport builds the Galerazamba spit. Meanwhile, as seen in Figure 11D for 2009, the coastal spit has evolved, with a sedimentation rate of 0.01 m/yr, and with erosion in the north-western part, where it is very narrow.

Dieses Werk ist copyrightgeschützt und darf in keiner Form vervielfältigt werden noch an Dritte weitergegeben werden.
Es gilt nur für den persönlichen Gebrauch.

In the first coastal cell (Figure 12), which starts at Punta Roca and runs to the first groin on the Country beaches, there are rates of 0.01 m/yr accretion and, on the west side, erosion of 0.30 m/yr. The Pradomar beach cell has an erosion rate of between 0.30 and 0.55 m/yr and small sedimentation rates of between 0.01 and 0.13 m/yr.

However, the littoral cell that includes the harbor of Puerto Colombia to the “Arroyo Caña” river mouth has the highest erosion rates (0.83–0.98 m/yr.). Finally in contrast, the littoral cell from “Arroyo Caña” river to “Punta Morro Hermoso” has sedimentation rates of between 0.01 and 0.30 m/yr, and some points have an erosion between 0.55 and 0.83 m/yr, forming the coastal spit by the sediment transport that comes from the Magdalena River.

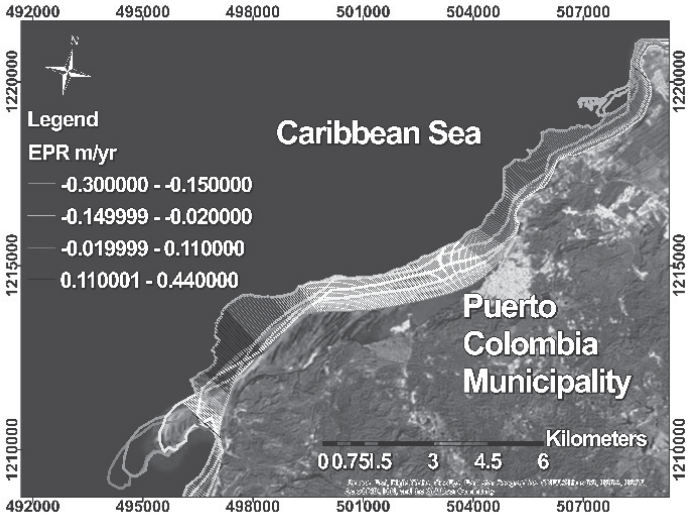

Figure 12: Erosion/sedimentation process in Puerto Colombia coasts

The results of the implementation of the theoretical model show that the equilibrium of the system was lost. The natural conditions that allow the generation of soft sandy beaches in harmony with the marine climate has been altered by human activities.

4 Conclusions

Initiatives to prevent or to mitigate environmental and physical impacts on the coastal zones are recommended. The lack of knowledge about the morphodynamic and ecological interplay has brought about many environmental problems. Plans for people in areas of risk, regulations to restrict new building developments in the area, and the removal of the groins that do not serve their purpose are needed. Hydro-morphodynamic numerical simulations can be used in order to understand the coastal processes, and eco-friendly solutions must be proposed to restore the shoreline as erosive processes, which can generate significant damage and loss of the territory, and affect coastal infrastructure, human live and ecosystem equilibrium.

Dieses Werk ist copyrightgeschützt und darf in keiner Form vervielfältigt werden noch an Dritte weitergegeben werden.
Es gilt nur für den persönlichen Gebrauch.

5 Acknowledgements

This work was carried out by the Institute for Sustainable Development (IDS) and the Coast and Ports Group of Universidad Del Norte - Barranquilla, Colombia. Carlos Pinilla thanks COLCIENCIAS for funding (Proy. Code XML ID 121571051568). The authors are also grateful to the Federal Ministry for Economic Cooperation and Development, Germany (BMZ), German Academic Exchange Service (DAAD), Excellence Center for Development Cooperation, Sustainable Water Management (EXCEED/ SWINDON), and Technical University of Braunschweig (TUBS) for their financial and technical support,which enabled participation at the Summer School INECEP, September 2017 in Puerto Morelos, Mexico.

6 References

1. Vargas Cuervo, G.: Procesos de erosión y sedimentación costera entre Bocas de Ceniza y Puerto Colombia, Colombia. XX Seminario Nacional de Hidráulica e Hidrología, pp. 1-12, Barranquilla, Colombia (2012)
2. Kuleli, T., Guneroglu, A., Karsli, F., Dihkan, M.: Automatic detection of shoreline change on coastal Ramsar wetlands of Turkey. Ocean Engineering 38, 1141-1149 (2011)
3. Sheik, M.: A shoreline change analysis along the coast between Kanyakumari and Tuticorin, India, using digital shoreline analysis system. Geo-spatial Information Science 14, 282-293 (2011)
4. Bunicontro, M.P., Marcomini, S.C., López, R.A.: The effect of coastal defense structures (mounds) on southeast coast of Buenos Aires province, Argentine. Ocean & Coastal Management 116, 404-413 (2015)
5. Rangel-Buitrago, N., Williams, A., Anfuso, G.: Hard protection structures as a principal coastal erosion management strategy along the Caribbean coast of Colombia. A chronicle of pitfalls. Ocean & Coastal Management 1-18 (2017) (In press)
6. Posada Posada, B.O.: Diagnóstico de la erosión en la zona costera del Caribe colombiano. INVEMAR, Santa Marta, Colombia (2008)
7. Escolar Vega, A.: Ecosistemas Acuaticos del Departamento Del Atlantico http://cinto.invemar.org.co/alfresco/d/d/workspace/SpacesStore/10217db5-a414-4b60-aee3-c47dd8d3c614/Ecosistemas%20acu%C3%A1ticos%20del%20departamento%20del%20Atl%C3%A1ntico?ticket=TICKET_d597a06ee2deab7b64127ba0607323496929fc49. (2007) (Accessed on 30-Oct-2017)
8. Rangel-Buitrago, N.G., Posada-Posada, B.O.: Geomorfología y procesos erosivos en la costa norte del departamento de Córdoba, Caribe colombiano (Sector Paso Nuevo-Cristo Rey). Boletín de Investigaciones Marinas y Costeras-INVEMAR 34, 101-119 (2005)
9. INVEMAR - Oficina de Planeación: PLAN DE ACCIÓN INVEMAR. Santa Marta (Magdalena), Colombia, pp. 1-96. (2016),

Dieses Werk ist copyrightgeschützt und darf in keiner Form vervielfältigt werden noch an Dritte weitergegeben werden.
Es gilt nur für den persönlichen Gebrauch.

http://www.invemar.org.co/documents/10182/43106/PLAN+DE+ACCI%C3%93N+INVEMAR+2016.pdf/a8ae035c-2e67-4d75-aa5b-3c66953ea796. (Accessed on 30-Oct-2017),

10. Google: Google Earth. www.google.com/earth/download/ge/. (Accessed on 30-Oct-2017)
11. Oyedotun, T.: Shoreline geometry: DSAS as a tool for historical trend analysis. In: Geomorphology, B.S.f. (ed.) Geomorphological Techniques, pp. 2047-0371 (2014)
12. Alvarado Ortega, M.: Barranquilla, ciudad con río y mar. Barranquilla Cómo vamos, pp. 22. (2009), www.barranquillacomovamos.co/copy/images/stories/pdf/ciudad/Barranquilla.pdf. (Accessed on 30-Oct-2017)

Dieses Werk ist copyrightgeschützt und darf in keiner Form vervielfältigt werden noch an Dritte weitergegeben werden.
Es gilt nur für den persönlichen Gebrauch.

METHODOLOGY FOR THE DETERMINATION OF EROSION AND DECREASE OF COASTAL VULNERABILITY

Román Alejandro Canul Turriza[1], Edgar Mendoza[1]

[1]Engineering Institute, National Autonomous University of Mexico UNAM, Circuito Escolar s/n, Edif. 5. Ciudad Universitaria, 04510, Coyoacán, México, DF, RCanulT@iingen.unam.mx

Keywords: beach, Campeche, coast, erosion, vulnerability

Abstract

For more than three decades, the tourism development at the coast of Campeche has lacked a management plan that considers its conservation and sustainability. As a result, several areas feature tourist and urban infrastructure that is severely pressing the coastal system. Specifically Chenkan, which is a RAMSAR site dedicated to the conservation of the sea turtle, is suffering chronic erosion problems and increased vulnerability due to anthropogenic interventions in the coast. The present study analyzes data from a survey of 10 beach profiles with an average spacing of 300 m in longitudinal direction and 60 m in transversal direction for the calculation of erosion/deposition volumes and the grain size distribution, and statistical values of 330 sediment samples. In addition, Quickbird images from 2009 to 2013 were used in order to evaluate the coastline evolution. The results obtained so far show the seasonal variability of the coastline and of the sediment grain size.

1 Introduction

Erosion is one of the many impacts caused by humans in coastal systems. This alteration is relevant because it diminishes the resistance and resilience of these ecosystems [1]. Chronic erosion is identified by the retreat of the coastline and the permanent loss of sediment volume in the beach profile. This phenomenon is the main cause of the destruction of beaches, which results in severe alteration of ecosystems and loss of environmental services.

A beach in chronic erosion process is also characterized by changes in its width and slope. In these beaches, cantilevers and vertical terraces are commonly seen [2]. In addition, other features can be found such as scarps, concave areas, and tidal ridges [3]. The coastline of the state of Campeche, which is 523 km long, presents areas with chronic erosion rates. The worst of them are reported to be up to 7 m/yr [4].

Within the coast of Campeche, one of the most affected areas by erosion is Chenkan, where 5.3 m per year of beach were lost during the period of 1970 to 2005 [5]. This erosive process has been exacerbated by the increase in the frequency and intensity of hydrometeorological phenomena (north and hurricanes), among other factors [5, 6].

Dieses Werk ist copyrightgeschützt und darf in keiner Form vervielfältigt werden noch an Dritte weitergegeben werden.
Es gilt nur für den persönlichen Gebrauch.

In spite of the erosive process, the coast of Campeche has a high tourist potential given its natural resources and beauty [7]. Anthropogenic activities, morphological changes, and beach erosion have affected the complex and delicate coastal ecosystems of Chenkan [6], increasing the vulnerability of coastal populations. This work aims to diagnose the present erosion process in Chenkan.

2 Materials and Methods

2.1 Study area

Chenkán is a RAMSAR site located on the Sabancuy - Champotón stretch of Federal Highway 180, and adjacent to Terminos Lagoon Flora and Fauna Protection Area (APFFLT) (Figure 1). In its area, three climatic periods are found: February to May dry season, June to September rainy season, and October to January the "Nortes" season [8]. A Center for the Conservation of Sea Turtles (CPCTM Spanish name) is also located in Chenkan. The beach of Chenkan is highly dynamic, always showing small width, but in the last 30 years, the coastline has shown a dominant process of erosion.

In recent years, the geomorphology of Chenkan has been modified by anthropogenic intervention mainly by changes of land use and construction of coastal protection infrastructure. The impact of these modifications coupled with the previous erosion is high as the beach width continues to reduce causing habitat loss of the different species that are located on the coast.

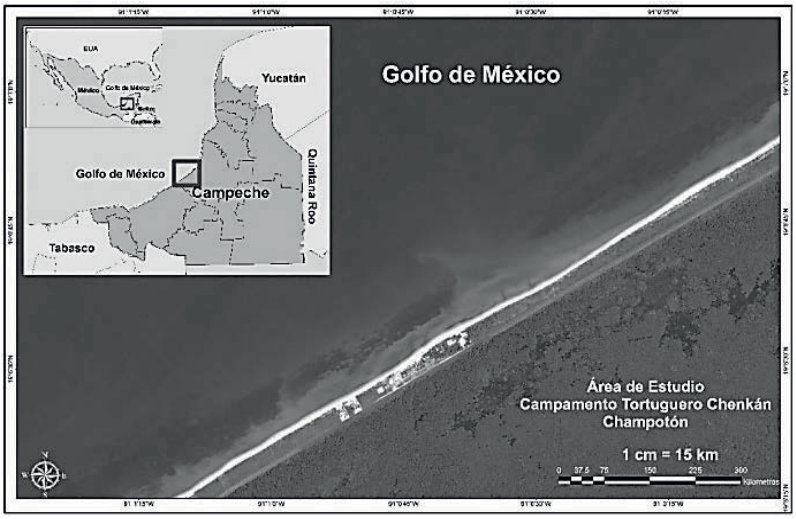

Figure 1: Location of the study area

In order to diagnose the erosion, a simple methodology was followed: (1) analysis of satellite images to evaluate the coastline evolution, (2) analysis of sediment samples in each climatic period (dry, rainy and "Nortes") from 2013 to 2015, and (3) performing topographic surveys of the beach from 2013 to 2015 [9].

Dieses Werk ist copyrightgeschützt und darf in keiner Form vervielfältigt werden noch an Dritte weitergegeben werden.
Es gilt nur für den persönlichen Gebrauch.

2.2 Coastline evolution

9 Quickbird images were analyzed (the only available without clouds), which cover the period from March 2009 to October 2013. These images were processed in order to identify natural or artificial obstacles that would alter the littoral sediment transport. Other elements were also identified such as bars, dunes, and aspects the dry beach width.

From the images, the coastline was digitized (using ArcGis sofware) in order to estimate its spatial and temporal changes and to obtain the areas of accretion and erosion, following Torres et al., 2010 procedure [10]. The analysis was focused on two areas: close to the Turtle Camp area and another place nearby, where coastal protection infrastructure has been built (Figures 2 and 3).

Figure 2: Approach to the area of Turtle Camp

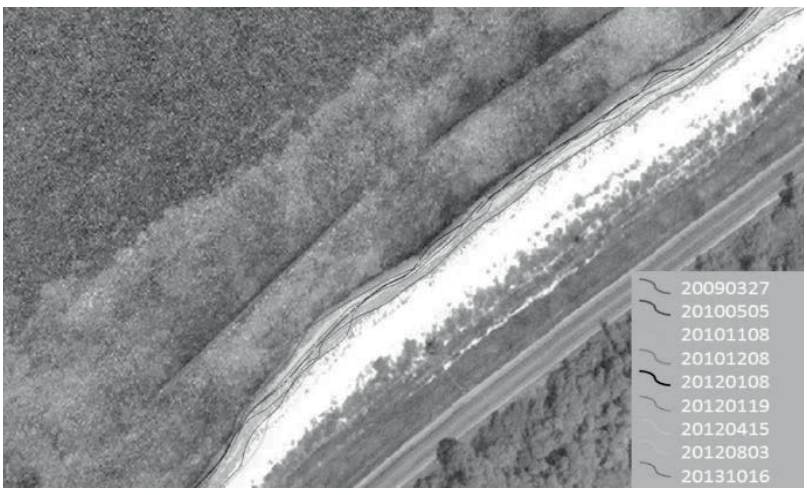

Figure 3: Approach to the coastal protection zone

The base (T0) polygon was that for the year 2009, and the areas of accretion and erosion were calculated per year, followed by a summation of the areas by year and period (Table 2).

Dieses Werk ist copyrightgeschützt und darf in keiner Form vervielfältigt werden noch an Dritte weitergegeben werden.
Es gilt nur für den persönlichen Gebrauch.

2.3 Characterization of beach profiles

For recording the beach profiles, a differential GPS was used. Nine surveys were carried out, as given in Table 1.

Table 1: Fieldworks

Fieldworks	Date
1	2013 / 06 / 27
2	2013 / 08 / 23
3	2013 / 11 /07
4	2013 /12 / 12
5	2014 / 02 / 20
6	2014 / 06 / 05
7	2014 / 07 / 30
8	2014 / 10 / 24
9	2015 / 03 / 21

Fieldworks 1 and 2 are representative for the rainy season 2013, 3 and 4 for the "Nortes" season 2013, 5 for the dry season 2014, the 6 and 7 for the rainy season 2014, 8 is "Nortes" season of 2014, and 9 dry season of 2015. After the post-processing, x, y, and z coordinates of each measured point were obtained. Ten profiles with an average spacing of 300 m in the longitudinal direction and an average length of 60 m in the cross-shore direction, covering a length of 3 km, corresponding to the area with the highest sea turtle nesting were measured (Figure 4).

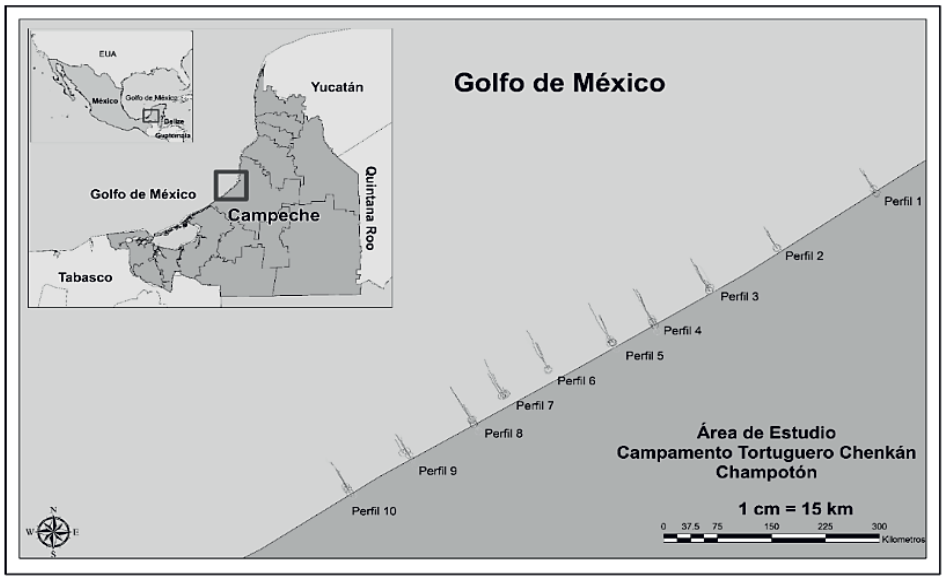

Figure 4: Measured profile location

Cluster analysis [11] was used to group the profiles based on the width of the dry beach measured between fieldworks. In addition, the areas above mean sea level, and erosion or deposit volumes

Dieses Werk ist copyrightgeschützt und darf in keiner Form vervielfältigt werden noch an Dritte weitergegeben werden.
Es gilt nur für den persönlichen Gebrauch.

were calculated for a unit beach width associated with a profile, following the procedure proposed by Ramírez, 2007 [12].

2.4 Characterization of sediment

Four zones of the beach profile were sampled: dune, swash zone and submerged bar (two samples located at 1.0 m and 1.5 m depth, respectively). The breaking zone was not sampled because the study area is characterized by a low energy wave. The sediment characterization was done in phases: (1) material collection, (2) mechanical granulometric analysis by sieving [13], (3) Statistical analysis, and (4) ANOVA. For this, 330 samples distributed along the profiles were processed (Figure 5).

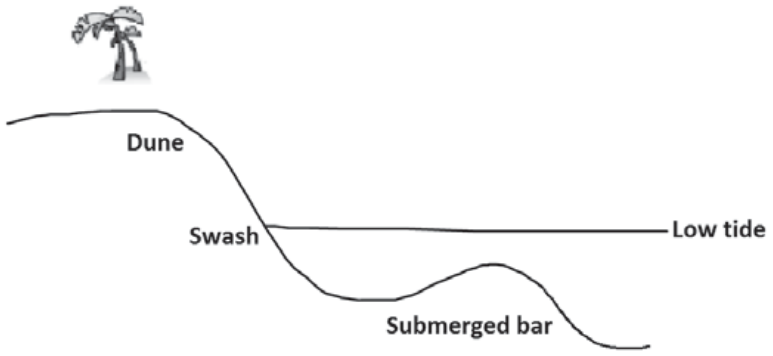

Figure 5: Profile sampling zones

The descriptive statistical analysis of the sediments was performed by the arithmetic moments method to obtain the values of the median, geometric mean, variance, standard deviation, coefficient of variation, bias, and kurtosis using the Sandy tool [14]. The arithmetic mean by zone and climatic season was analyzed for the years 2013 and 2014; subsequently, a classification was made based on the Udden - Wentworth classification [15].

An ANOVA analysis was also carried out to establish if there are significant differences between the size of the D_{50} and climatic times and profiles.

2.5 Integration of measured parameters

The determination of the geomorphological aspects of the coastline enables to identify the evolution of the coastline as well as elements that influence the feedback mechanisms of the system. The evaluation of the sediment properties and zoning of them allow to identify the areas with erosion and deposition as well as to elucidate the possible displacement of the sediment in the beach. The determination of the volumes of erosion or deposition and the displacement of the coastline allow determining the dominant process (erosion or deposit) and the influence of anthropogenic and natural elements in the study area.

Dieses Werk ist copyrightgeschützt und darf in keiner Form vervielfältigt werden noch an Dritte weitergegeben werden.
Es gilt nur für den persönlichen Gebrauch.

3 Results

3.1 Coastline evolution

Regarding the characterization of Chenkan beach (2009), it was found that the construction of marine structures is closely related to the interruption of the existing cross-shore sediment transport, which led to a change in the coastline. For example, in the characterization of the coastline of the year 2010, it is observed that the beach had an average accretion of 10 m. In addition, a wavy coastline was developed in front of the structures, and protrusions and lows were formed. This shows that these structures govern the behavior of the coastline in the studied area (Figure 6).

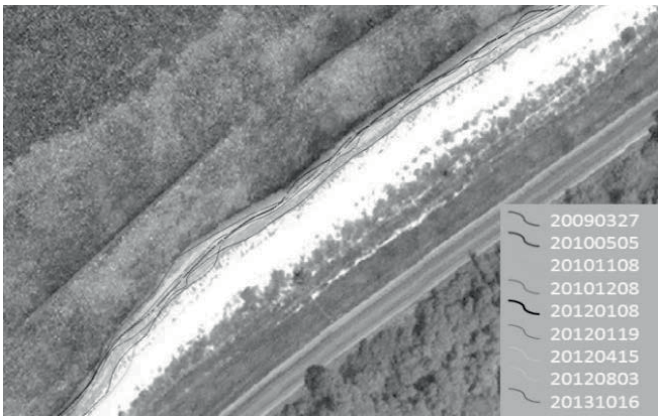

Figure 6: Changes in the coastline for the zone of structures

The conditions mentioned above are maintained for the year 2011. However, in 2012 it is observed that the coastline presents undulation and recoil in front of the structures; in addition, a reduction of the seagrass area was observed. Finally, in the characterization of the year 2013, there is a greater reduction of dry beach width and the placement of coastal structures.

In contrast to areas with coastal structures, the presence of seagrass was associated with areas of less erosion or that could maintain the sedimentary balance (Figure 7).

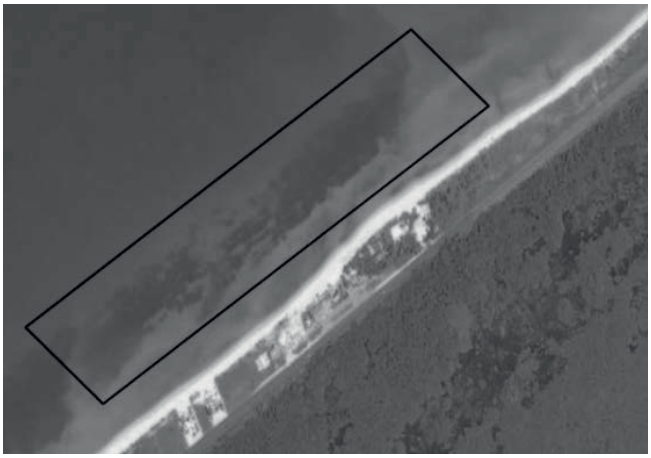

Figure 7: Image of the year 2011. In the box: area of seagrass

Dieses Werk ist copyrightgeschützt und darf in keiner Form vervielfältigt werden noch an Dritte weitergegeben werden.
Es gilt nur für den persönlichen Gebrauch.

Table 2 presents the calculated areas for each of the drawn polygons. The total column represents a summation of the accretion and erosion areas per year. It is observed that, for the period analyzed, the eroded area is greater than the accretion one. Comparing the dry seasons of 2010 and 2012, an accretion of 692 m^2 was obtained, while from the comparison of the period of north 2010 and 2011 a decline of 5,586 m^2, and from 2011 to 2013 a decline of 15,816 m^2 were identified.

Table 2: Balance of back and accretion areas obtained with the digitalization of satellite images

Image	Retreat (m^2)	Accretion (m^2)	Total (m^2)
20100505	-2,655	1,312	-1,343
20101208	-63	11,511	11,448
20120108	-6,173	586	-5,587
20120415	-8,647	82	-8,565
20120803	-4,936	425	-4,511
20131016	-3,867	715	-3,152
TOTAL (m^2)	-26,341	1,4631	-11,710

3.2 Characterization of beach profiles

Figure 8 show that, in general, the profiles have a gentle slope (0.2%). However, during the "Nortes" season, the width of the dry beach is reduced and steps of up to 2 m are formed in some profiles, while others have a beach increment (Figure 9).

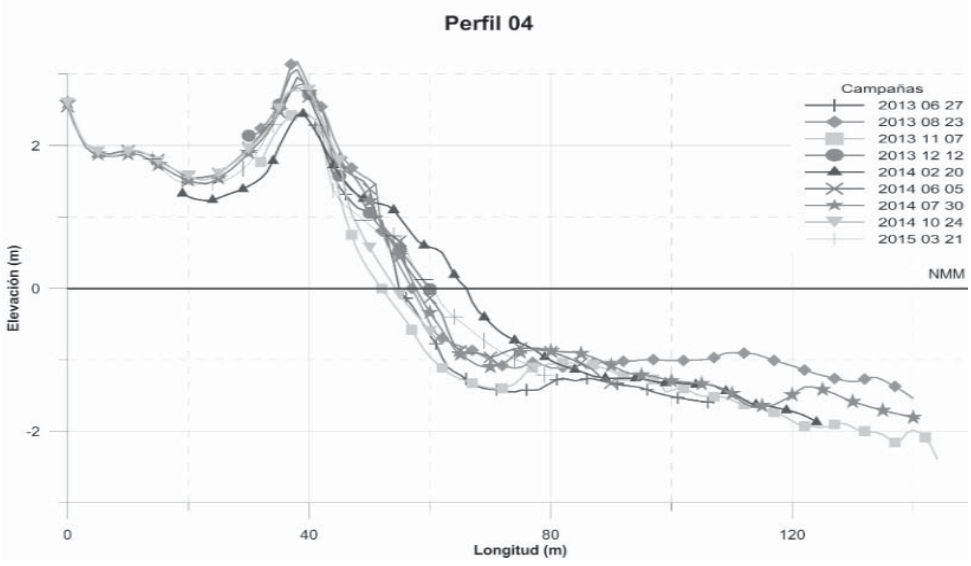

Figure 8: Profile variation

In Chenkan, two kinds of profiles can be clearly identified: the storm profile and the accretion profile. The first one originates during the rainy and "Nortes" seasons, while the second one occurs in the dry season.

Dieses Werk ist copyrightgeschützt und darf in keiner Form vervielfältigt werden noch an Dritte weitergegeben werden.
Es gilt nur für den persönlichen Gebrauch.

Figure 9: Beach scarp measured during the campaign of June 5, 2014. Average height 2 m.

The dry (average) beach width measured for each season is presented in Table 3, calculated from the point of intersection between the profile and the mean sea level.

Table 3: Average dry beach width measured

Dry beach width (m)	Survey
44.9	2013/06/27
56.5	2013/08/23
53.2	2013/11/07
55.7	2013/12/12
53.8	2014/02/20
54.4	2014/06/05
53.8	2014/07/30
52.9	2014/10/24
53.9	2015/03/21

Some profiles show a retreat of up to 11.5 m. For each profile, the area above sea level was calculated in order to quantify, how much material has been lost or gained between surveys. Table 4 shows the values corresponding to profile 04.

Dieses Werk ist copyrightgeschützt und darf in keiner Form vervielfältigt werden noch an Dritte weitergegeben werden.
Es gilt nur für den persönlichen Gebrauch.

Table 4: Area above mean sea level for profile 04

Area (m^2)	Survey
16.8	2013/06/27
22.2	2013/08/23
11.4	2013/11/07
20.6	2013/12/12
25.7	2014/02/20
21.7	2014/06/05
21.0	2014/07/30
15.0	2014/10/24
18.0	2015/03/21

While the volumes for a calculated unit beach width are presented in Table 5, a volume equivalent to -40.77 m^3 was obtained during the 2 years of measurement. Comparing the rainy season and the "Nortes" for the years 2013 and 2014, a volume loss of 20.10 m^3 was obtained for rainfall and -7,363 m^3 for the "Nortes".

Table 5: Volume of erosion or deposit for unitary beach width

Volume (m^3)	Campaign
----------	2013/06/27
44.0	2013/08/23
-92.0	2013/11/07
73.2	2013/12/12
-77.8	2014/02/20
26.8	2014/06/05
-2.9	2014/07/30
-2.3	2014/10/24
-9.8	2015/03/21
$\sum = \mathbf{-40.8}$	

From the Cluster analysis, the zoning of the profiles was obtained based on the measured dry beach length, using the Pearson correlation coefficient and the unweighted average agglomeration method (Figure 10).

Dieses Werk ist copyrightgeschützt und darf in keiner Form vervielfältigt werden noch an Dritte weitergegeben werden.
Es gilt nur für den persönlichen Gebrauch.

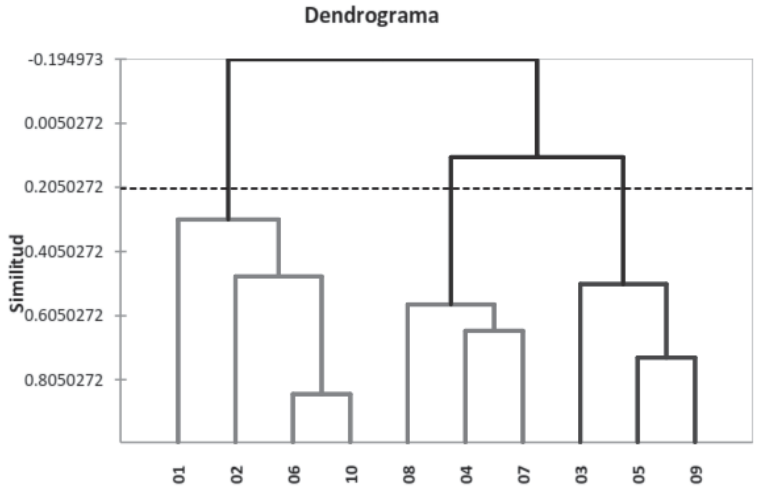

Figure 10: Profile zoning dendrogram

Figure 10 shows that the profiles are separated into three groups: the first group (profiles 01, 02, 06 and 10) is characterized by profiles in retreat; the second group (profiles 04, 07 and 08) is characterized by profiles in accretion and; the third group (profiles 03, 05 and 09) is characterized by profiles that present negligible variation.

3.3 Sediment characterization

From the grain size distribution and considering the D50 of the sediments, common processes were found. These include fine grain accumulation (0.25 to 0.125 mm) in the submerged zone after the bar, the presence of medium size sand (0.5 to 0.25 mm) in the dune, the transition from medium sand to coarse sand in the wash zone (1 to 0.5 mm), and a mixture in the submerged zone before the bar.

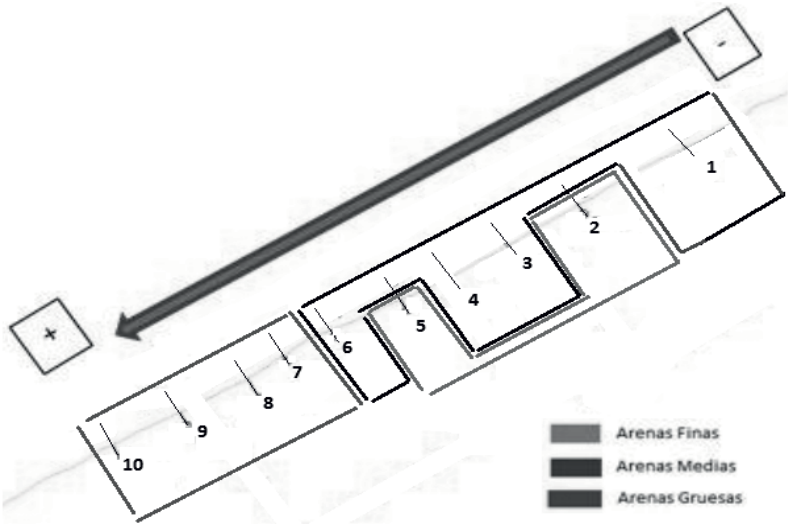

Figure 11: Percentile 50 (mm) for the submerged zone before the bar (North 2013). The arrow and the signs indicate the direction of the gradient of sediment grain size.

Dieses Werk ist copyrightgeschützt und darf in keiner Form vervielfältigt werden noch an Dritte weitergegeben werden.
Es gilt nur für den persönlichen Gebrauch.

Figure 11 shows the zoning of the nominal diameter values D50 for the area submerged before the bar by profile in the north season. In this figure, three zones are identified: fine sands (profiles 02 and 05), medium sands (profiles 01, 03, 04 and 06), and coarse sand (profiles 07 to 10).

The size of the sediment in the dune zone, in the washing area and in the bar decreases from dry season (from 0.353 to 0.312 mm, from 0.644 to 0.427 mm, from 0.776 to 0.615 mm, respectively). In contrast, in the submerged area after the bar, the sediment is preserved as fine.

To identify if changes in sediment size are significant, a temporal and spatial analysis was performed for the different zones. From the ANOVA for the temporal analysis of the zones it was obtained that there is no significant difference between climatic seasons except for the submerged zone before the bar, where there is a difference between the norths and rainy seasons. In general, the tendency of the D50 is to decrease from the rainy season to the dry season.

From the ANOVA for spatial analysis it is observed that there is no significant difference of the D50 between profiles, however, the tendency for the dune and wash zones is to decrease from profile 01 to 10 while in submerged areas the tendency is inversely. D50 diameter increases from profile 1 to 10.

3.4 Integration of measured parameters

In Chenkan, the beach presents an erosive behavior that has worsened with the presence of structures poorly planned, which is reflected in the regression of the coastline result of the measurements of profiles. This process is causing increasing the vulnerability of turtle nesting in the area by reducing the dry beach width as well as the vulnerability of existing tourist and urban infrastructure.

4 Discussion

The changes in the profiles are due to their natural evolution; however, the presence of anthropogenic elements has modified the action of currents and waves affecting transverse transport of sediments. During the dry season, the width of dry beach is reduced and the profiles come to present steps of up to 2 m of unevenness, which leads to a change in the slope of the dry beach. This variation in the slope of the profile in the “Nortes” season coincides with that described by Crevenna Recánces in 2006 [6], which found a profile of beach with steep slope, small width and scarps of up to 1 m height.

The change in slope and dry beach width is due to energy dissipation under storm conditions, where sea level rise displaces the zone of dissipation from the break zone to the dune zone. There is a transfer of fine sand from the dry beach to the submerged beach, forming the sand bar. The finest sediments are placed after the bar, where there is no influence of the waves. During the dry season, the material of the bar is transported to the dry beach causing a partial recovery of it.

Dieses Werk ist copyrightgeschützt und darf in keiner Form vervielfältigt werden noch an Dritte weitergegeben werden.
Es gilt nur für den persönlichen Gebrauch.

The analysis of satellite images for the period 2009-2013 of the coastline allowed finding a regression of the line especially in the northern part of the study area, originated by the increase of structures that allow the sediment to exit the system, but not his return. This change can be established as erosive.

Chenkan presents a natural evolution that can be analyzed through the climatic seasons that occur in the area. However, if it is analyzed over a longer period, it is possible to identify shifting in the coastline. Because the nesting densities of turtle species are high in Chenkan beach, changes in slope and sediment size affect nesting success. The presence of coastal structures reduces the number of nesting, and the reduction of dry beach width forces the species to lay their eggs in areas affected by the tide and the waves.

5 Conclusions

The profiles 4 and 5 that are protected by natural elements present less variation between climatic times. During the dry and rainy season, the dry beach presents a setback due to the effects of storm surge and waves. However, in the dry season, a recovery is observed.

In the rainy season, D50 diameter presents a slight increase from profile 1 to 10, while during the dry season the behavior is the reverse, so that the longitudinal transport occurs from northeast to southwest for the “Nortes” season. In general, the change in the coastline has an erosion behavior.

6 Acknowledgement

This publication is one of the results of the Regional Network Latin America of the global collaborative Project “EXCEED – Excellence Center for Development Cooperation – Sustainable Water Management in Developing Countries”. The authors would like to acknowledge the support of German Academic Exchange Service, DAAD and the Instituto de Ingeniería of the Universidad Nacional Autónoma de México for their participation in this EXCEED project.

7 References

1. Charlier, R.H., De Meyer, C.P.: Coastal erosion: response and management. vol. 70, pp. 6-18. Springer Science & Business Media (1998)
2. Márquez, R.: Las tortugas marinas y nuestro tiempo. La ciencia para todos. México, DF: Fondo de Cultura Económica. Los Cabos: Prospective for a Natural and Tourism Paradise (2002)
3. Salazar-Vallejo, S.: Calentamiento global y efectos costeros. Ava. Cient 25, 10-20 (1998)
4. Ortíz Pérez, M.A.: Retroceso reciente de la línea de costa del frente deltaico del río San Pedro, Campeche-Tabasco. Investigaciones geográficas 25, 7-23 (1992)
5. Márquez -García, A.: Variación de la línea de costa en la región de Isla Aguada - Chenkán, México. En V. Guzmán, F. Cuevas, F. Abreu - G., B. González - G., A. García, & R. Huerta,

Dieses Werk ist copyrightgeschützt und darf in keiner Form vervielfältigt werden noch an Dritte weitergegeben werden.
Es gilt nur für den persönlichen Gebrauch.

Resultados de la reunión del grupo de trabajo de la tortuga de carey en el Atlántico mexicano. Memorias. CONANP/EPC/APFFLT/PNCTM, pp. 224, Veracruz (2008)

6. Bolongaro, A., Márquez, A., Torres, V., García, A.: Vulnerabilidad de sitios de anidación de tortugas marinas por efectos de erosión costera en el estado de Campeche. Vulnerabilidad de las zonas costeras mexicanas ante el cambio climático. Semarnat-INE, UNAM-ICMyL 514 (2010)
7. Alpuche Gual, L.: Clasificación de playas campechanas para su manejo integral y desarrollo sostenible. Universidad Autónoma de Campeche (2014)
8. Yanez-Arancibia, A., Day Jr, J.: Ecology of coastal ecosystems in the southern Gulf of Mexico: The Terminos Lagoon Region. Inst Cienc Del Mar y Limnol UNAM, COSAT Ecol Inst LSU. Editorial Universitaria, Mexico DF (1988)
9. Woolf, P.: Topografía. alfaomega (1997)
10. Torres-Rodríguez, V., Márquez-García, A., Bolongaro-Crevenna, A., Chavarría-Hernández, J., Exposito-Díaz, G., Márquez-García, E.: Tasa de erosión y vulnerabilidad costera en el estado de Campeche debido a efectos del cambio climático. Vulnerabilidad de las Zonas Costeras Mexicanas ante el Cambio Climático (segunda edición): Universidad Autónoma Metropolitana-Iztapalapa, UNAM-ICMyL, Universidad Autónoma de Campeche 413-432 (2011)
11. Legendre, P., Rogers, D.J.: Characters and Clustering in Taxonomy: A Synthesis of Two Taximetric Procedures. Taxon 21, 567-606 (1972)
12. Ramírez González, E.A.: Evolución Morfodinámica de la Playa Comprendida Entre Punta Cancún y Punta Nizuc en el Estado de Quintana Roo, México. Facultad de Ingeniería, vol. M.Sc. Thesis. UNAM, Mexico (2007)
13. Juárez Badillo, E., Rico Rodríguez, A.: Mecánica de Suelos Tomo I. Fundamentos de la Mecánica de Suelos. 3a edición, Editorial Limusa (1976)
14. Ruiz-Martínez, G., Rivillas-Ospina, G.D., Mariño-Tapia, I., Posada-Vanegas, G.: SANDY: A Matlab tool to estimate the sediment size distribution from a sieve analysis. Computers & Geosciences 92, 104-116 (2016)
15. Wentworth, C.K.: A Scale of Grade and Class Terms for Clastic Sediments. The Journal of Geology 30, 377-392 (1922)

Dieses Werk ist copyrightgeschützt und darf in keiner Form vervielfältigt werden noch an Dritte weitergegeben werden.
Es gilt nur für den persönlichen Gebrauch.

COASTAL EROSION CONTROL IN FRINGE MANGROVES AFFECTED BY LOGGING IN THE COLOMBIAN CARIBBEAN

David Alejandro Sánchez-Núñez[1], José Ernesto Mancera Pineda[2], Gladys Bernal[3]

[1]Universidad Nacional de Colombia sede Caribe, Calle 25 # 2-55, Playa Salguero, Santa Marta, dasanchezn@bt.unal.edu.co

[2]Universidad Nacional de Colombia, sede Bogotá, Cr 45 # 26-85

[3]Universidad Nacional de Colombia, sede Medellín, Cr 80 # 65-233-Campus Robledo, Medellín

Keywords: Caribbean, Disturbance, Ecosystem services, Erosion rates, Fringe mangroves

Abstract

Fringe mangroves are able to reduce erosion by wave dissipation, sediment retention and soil development. Indicators of mangrove ecosystem integrity and reported erosion/accretion rates were analyzed to identify the relation between potential erosive predictors and reported erosion rates. Two of the three sites studied had mangrove tree mortality levels (23% and 30%) above the expected threshold (13% and 14%, respectively) due to natural mortality and logging; a result that indicate a suboptimum condition of ecosystem integrity. Relatively high erosion rates of -9 m/yr are found in a highly exposed location with suboptimum ecosystem integrity. Accretion rates of +0.2 m/yr are found in a protected location with an acceptable condition of ecosystem integrity. In Punta Las Playitas, a location with relatively low exposition to waves, high exposed setting and suboptimum ecosystem integrity, erosion rates are between -0.2 and -1.5 m/yr. It is concluded that Interaction between ecosystem integrity, wave energetic conditions and sediment delivery may define sediment balance in mangrove vegetated shores. it is necessary to identify acceptable thresholds of logging intensity and river sediment delivery to improve coastal adaptation, mangrove persistence and to establish soft engineering solutions to erosion using mangroves.

1 Introduction

Mangroves are plants adapted to live in the transition zone between terrestrial and marine domains and, therefore, to thrive in brackish, anoxic and unconsolidated soils along coastlines [1]. In such transition zones, mangroves can occupy different geomorphological settings such as estuaries, lagoons, deltas, and low carbonate islands [2]. Further, mangroves within each geomorphological province are also distributed between physiographic settings according to their position, and in turn, to the degree of influence by tides and waves [3]. Fringe mangroves are located along the coastline facing daily tides, basin mangroves are located inland and are influenced by spring tides and used to have higher salinities, while riverine mangroves have more fresh water influence and are located along tidal rivers. Fringe mangroves, in continuous contact with wind-waves, are the most important physiographic types for coastal erosion control [4]. Basin

Dieses Werk ist copyrightgeschützt und darf in keiner Form vervielfältigt werden noch an Dritte weitergegeben werden.
Es gilt nur für den persönlichen Gebrauch.

mangroves also protect the coast and control erosion but in less frequent and more extreme conditions, when swell waves or storm surges are present and the area of waves influence go further inland.

Sedimentation in mangroves occurs in the space available for potential sediment accumulation or accommodation space [2]. This area comprises the intertidal zone and can be modified by mangroves. Sedimentation accretion within the mangrove progressively diminishes the accommodation space if there is a positive soil elevation change. In fringe mangroves, close to the seaward, the accommodation space is higher, while in basin mangroves, close to the landward, the accommodation space is smaller [2]. However, basin mangroves are usually located in depressions. Under such topographic conditions, the accommodation space for sediments to deposit may be considerable.

Mangrove structures affect the horizontal and vertical hydrodynamics due to the projected area of obstacles, pneumatophores, trunks and prop roots, that oppose to water flow [5]. Structures such as prop roots and pneumatophores generate a complex hydrology with jets, eddies and stagnation zones that favor sedimentation of particles [6]. The current speed is lower within mangrove root zones. Models have shown that resident time of water particles in mangrove roots compared to areas lacking vegetation is higher, the higher the flow velocity [6, 7].

In neotropical mangroves, *Rhizophora mangle* predominate in fringe mangroves as this species tolerate higher inundation regimes [8], loose soils, where the prop roots are designed to anchor the trees, and lower salinities up to 60 g/L. *Avicennia germinans* and *Laguncularia racemosa* that tolerate lower inundation regimens [8] and higher salinities up to 80 g/L and 90 g/L, respectively, are predominant in basin mangroves. Therefore, in fringe mangroves, prop roots are the predominant structures that oppose to water flow, while in basin mangroves, pneumatophores are the predominant structures that modify the hydrodynamics. Prop roots promote higher sediment deposition rates than pneumatophores, but mangrove soils, where pneumatophores predominate, experience higher soil elevation, possibly due to a better sediment-binding capacity of fine roots associated with pneumatophores [9].

Sedimentation rates of fine particles in mangroves are found also to be directly related to the turbidity level and the mean sea level as both are associated with sediment availability [10]. Mangroves promote sedimentation of clay flocs by the induced friction of vegetation and, therefore, are expected to diminish the turbidity of coastal waters [6]. However, from vertical accretion observations at different mangroves densities, it is expected than there is a threshold in mangrove density that favor erosion instead of deposition at high flow rates [11].

In general, fringe mangrove structures enhance processes such as wave energy dissipation and sediment deposition [12]. Wave height diminishes between 1.4 and 11% in the first 10 m of mangroves depending on the degree of projected area of vegetal structures [13]. On the other hand, sediment deposition rates have shown to be between 1.3 and 20.8 mm/yr, and vertical

Dieses Werk ist copyrightgeschützt und darf in keiner Form vervielfältigt werden noch an Dritte weitergegeben werden.
Es gilt nur für den persönlichen Gebrauch.

accretion rates (soil superficial changes) from +1.6 to +8.6 mm/yr that counterbalance soil shallow subsidence and erosive dynamics generating net soil level changes between -1.3 and 5.9 mm/yr [12, 14].

Wave water flow and sediment interactions have been studied in fringe mangroves very scarcely, where horizontal erosion or accretion occurs, despite it has been found that mangroves reduce erosion rates of around 33% along Thailand coasts (from 3 m/yr to 2 m/yr) [15]. Wave height dissipation within mangroves depends on the degree of projected area of vegetation and on the incident wave velocity [16, 17]. However, it is still unknown, to which degree fringe mangroves favor sediment deposition, sediment retention and modify sediment dynamics as result of wave dissipation and interaction with longshore currents.

The aim of this paper is to review the relationship between ecological-management conditions of fringe mangroves and coastal erosion, and to understand the impact of logging on ecosystem integrity and on coastal erosion control mechanisms

2 Materials and Methods

2.1 Study area

The Sinu River delta is located at the southwest of the Morrosquillo Gulf, Department of Cordoba, at the Colombian Caribbean coast. The deltaic system was declared a special management district (a special Colombian protection category) in order to protect their biodiversity and to foster sustainable use of ecosystems [18]. Currently, there live around 650 fishermen and 70 mangrove loggers along with their families depending partially or completely on coastal ecosystems [19].

The integral management district has 8,6 ha of mangroves from a total extension of 27,2 ha and is considered to be the better preserved and second largest mangrove cover in the Colombian Caribbean [20]. Four mangrove species are present in the system, *Rhizophora mangle*, *Avicennia germinans*, *Laguncularia racemosa* and *Pellicera rhizophorae*. *Conocarpus erecta*, a species considered associated to mangroves, is also present [18].

The Sinu River has an average water flow of 402 m^3/s and delivers in average 3 kt/d of total suspended sediments since 2000. A gradual and progressive reduction of the sediment yield delivered by the Sinu River since 1984 was found, when this variable started to be recorded (Fig. 1). Although the URRA dam began operating in 2000 and fragmented the river flow in 1999, the reduction in the suspended sediment yield of the river was attributed to regional causes as other rivers in the Colombian Caribbean coast without dams experiencing the same pattern at the same time [21]. The authors also stated a sediment deliver decline from 1984 to 2000 and an increase from 2000 to 2015, suggesting that the dam did not affect the total suspended sediment yield. Despite there are no noticeable changes in the sediment yield due to URRA dam operation, water flow extremes were softening (Fig. 2), a pattern that supports previous suggestions of water flow regulation by the URRA dam [22].

Dieses Werk ist copyrightgeschützt und darf in keiner Form vervielfältigt werden noch an Dritte weitergegeben werden.
Es gilt nur für den persönlichen Gebrauch.

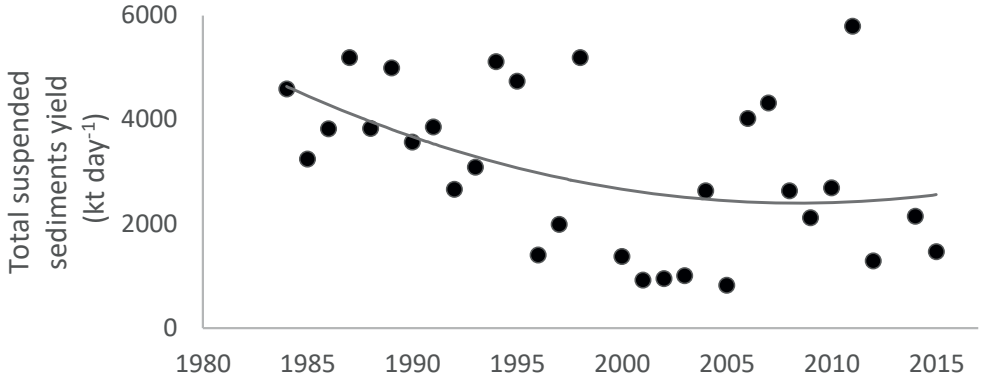

Figure 1: Total suspended sediment yield of the Sinu River between 1984 and 2015. Data from IDEAM, the Colombian hydrology and meteorology research Institution.

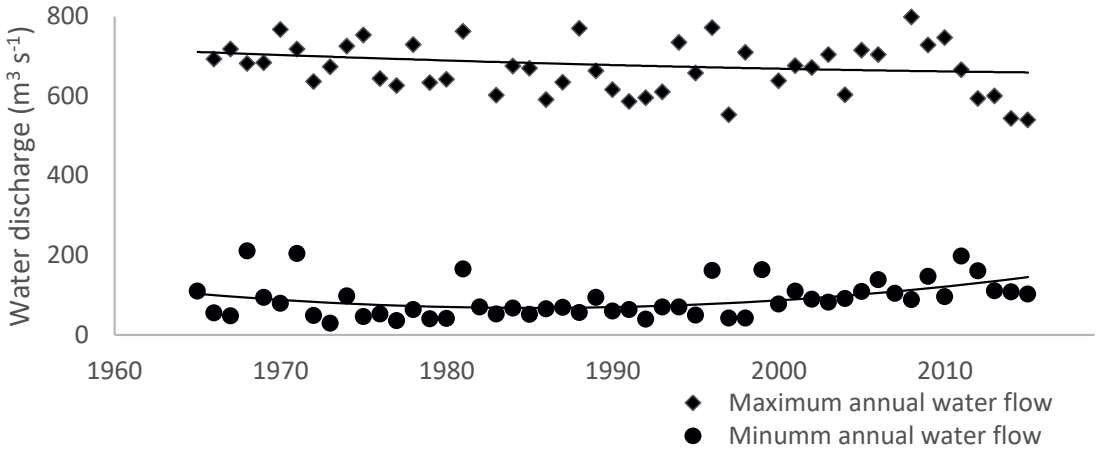

Figure 2: Minimum and maximum annual water discharge of the Sinu River between 1965 and 2015. Data from IDEAM, the Colombian hydrology and meteorology research Institution

On an annual basis, water flow is lower between January and April, when the average monthly water flow lies between 150 m/s and 200 m/s. In contrast, during July and October, the maximum peaks of monthly average water flow are about 550 - 580 m/s [23]. When the trade winds and the Caribbean current are active, turbidity flume extends to the southeast of the delta, while during the months of higher river water flow and in the absence of the trade winds, turbidity flume extends towards the east of the delta [23].

The river delta has changed its position six times in the last 2,350 years. The last change occurred in 1938, when the river mouth moved towards the east to its current location at Tinajones [24]. Such movement generated strong changes in plant coverage. The Cispata Bay lost fresh water influence while experiencing marine water intrusion, soil salinization and increase in mangrove extension [25].

The climate in the Sinu River delta is semiarid according to Thornthwaite classification, with a water deficit of 519 mm during the dry season between December and February, when the

Dieses Werk ist copyrightgeschützt und darf in keiner Form vervielfältigt werden noch an Dritte weitergegeben werden.
Es gilt nur für den persönlichen Gebrauch.

evapotranspiration exceeds the precipitation rates [26]. Average annual precipitation is about 1,267 mm with peaks in May during the minor wet season, and in September during the major wet season (160 mm and 180 mm, respectively) and, therefore, corresponds to a bimodal pattern [23]. The average temperature is around 27.1 ^{o}C [27].

Wind speed is higher during the major dry season between December and March compared with the rest of the year due to the influence of the trade winds and records a maximum peak in March (7.5 m/s), a second peak in July (4.5 m/s), and a minimum in September (4.1 m/s). During the dry season, predominant wind directions are north-northeast, north, and north-northwest with a predominance of 41.7%, 35.8%, and 17.7%, respectively, while during the rest of the year, main wind directions are north-northeast, north-northwest, south-southeast, and north with a predominance of 20.1%, 17.4%, 11.0%, and 6.6%, respectively [23].

In the Morrosquillo Gulf, 62% of 70 km of the shore experience erosion [28]. During the dry season, wind waves driven by the trade winds and swell waves are considered to be important erosive agents [29]. Elevated seas, known locally as “mar de leva” are generated by cold fronts, low pressures, and the passage of hurricanes at a distance from the coast [30]. There are up to four swell wave events between January and February [29].

The most frequent sea states go from northeast toward south-west and from north towards south. During a neutral ENSO condition year, significant wave heights range between 0.8 and 1.6 m with peaks in February and March (1.6 m) and July (1.2 m) [31]. The predominant ocean current, which is in the southeast direction, change to the northeast during the wet season influenced by the Panama countercurrent [29]. In the southwest of the Morrosquillo Gulf, where the Sinu River delta is located, a longshore current from west toward east predominates, especially during the dry season [32]. Tide is semidiurnal with an amplitude lower than 40 cm [29].

Continental shelf is broad and reach about 50 km up to the external border located between 100 m and 200 m of depth [33]. On the other hand, the shallow platform in the area is of about 1 km and of low slope (<1^{o}) [34].

2.2 Fringe mangrove settings selection

Fringe mangroves in the Sinu River delta are located in Punta Mestizos, Punta Las Playitas, and the internal lagoons of Cispata Bay that also include Cienaga Nisperal and Cienaga La Flotante. They cover 3.9 km, 2.9 km, and 62.3 km, respectively, along the coast (Fig. 3). The extension of fringe mangroves along the margins of internal lagoons can be easily recognized by the presence of oysters that are associated with salinities between 25 g/L and 35 g/L [35], and are attached to mangrove roots up to 55 m from the lagoon borders. Logging is frequent, selective and of small scale in fringe mangroves. Fisherman cut *Rhizophora mangle* trees for stakes and poles to be used in fishing arts and construction. Average diameter of trees logged is about 8.1 cm.

Dieses Werk ist copyrightgeschützt und darf in keiner Form vervielfältigt werden noch an Dritte weitergegeben werden.
Es gilt nur für den persönlichen Gebrauch.

Fringe mangroves in Punta Mestizos are a highly exposed to waves, while they are protected in the internal lagoons of Cispata Bay by coastal morphology. Punta las Playitas has an intermediate wave exposition condition compared with the other locations, and mangroves are located in the swash zone. Punta Mestizos and the internal lagoons of the Cispata Bay receive sediment supplies from the Sinu River and from caño Grande, respectively. Punta las Playitas has lower sediment supplies than the other locations.

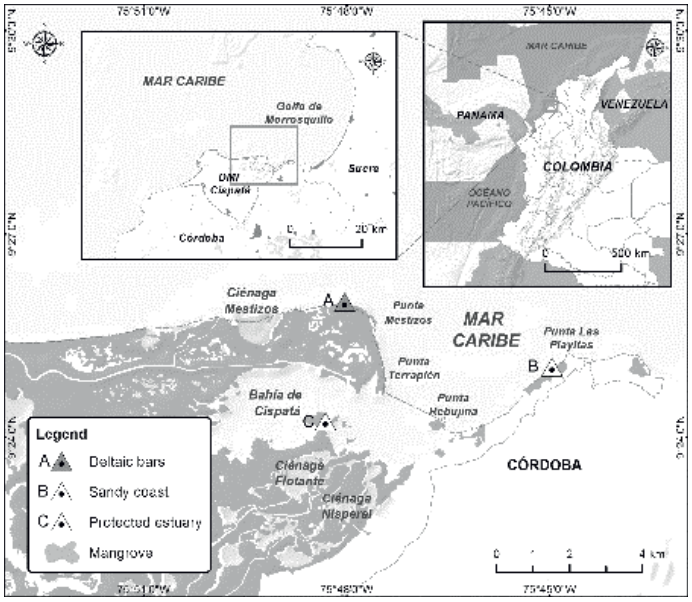

Figure 3: Study area and location of fringe mangrove settings within the delta of the Sinu River

2.3 Mangrove integrity and erosion rates

Mangrove height, diameter at breast height, was assessed in 10 plots of 49 m^2 according to standard procedures and considering alive, logged, and dead trees [36]. Four plots were located in Punta Mestizos, four in Punta las Playitas, and two in la Bahia de Cispata in the mangrove structure survey. Mortality rate found, including logging and natural causes, was compared with the expected mortality according to the development of the forest at each location [37]. It is considered that a higher basal area of forest implies higher development. Long trend erosion rates at each location were assessed from studies that measure erosion rates based on remote sensor images and differential GPS.

3 Results and Discussion

Fringe mangroves protect from coastal erosion through wave dissipation, sediment retention and soil development [12, 13]. However, responses of this ecosystem to erosion agents such as wind waves and swell waves must be complex, since there are several distinguishable environmental-management conditions that affect fringe mangroves along the Caribbean coast. Therefore, there is a high degree of uncertainty about the response of mangroves to erosion agents and sea level rise, and to the adoption of soft engineering solutions to erosion using mangroves.

Dieses Werk ist copyrightgeschützt und darf in keiner Form vervielfältigt werden noch an Dritte weitergegeben werden.
Es gilt nur für den persönlichen Gebrauch.

Colombia fringe mangroves in the Caribbean coast are distributed at least in three environmental and management gradients: (i) sediment supply, (ii) degree of exposition of the coast, and (iii) ecosystem integrity or health. Sediment supply depends on the closeness to river mouths or channels, directions of longshore currents, surface currents, and presence of dams along rivers and levees in river mouths that enhance navigability but limit sediment transport.

The degree of exposition depends on the position of fringe mangroves to the breaking wave zone. Mangroves of archipelagos, such as those in San Andres Island or Islas del Rosario, which are protected from sea wave by coral reefs barriers, do not face the full energy of wind waves, but a wave energy dissipated by coral reefs and seagrasses. Fringe mangroves in internal lagoons or bays such as Cienaga Grande de Santa Marta or Cispata Bay are also protected from direct impact of waves by coastal morphology (Fig. 3).

In contrast, there are mangroves fully exposed to waves as those in Punta Mestizos in the Sinu River complex (Fig. 4). Mangrove seedlings cannot establish in highly energetic coasts, as they need favorable hydrodynamic conditions. Establishment of mangrove in these locations occurred under previous favorable hydrodynamic and/or sedimentary conditions. Punta Mestizos received a high sediment load, when the Delta was located in the Cispata Bay just 4 km far between 1849 and 1938, and when the river delivered a high amount of sediments before 2000 (Fig. 1, Fig. 2). In fact, fishermen state that there was a sand barrier in Punta Mestizos of about 5 m around 1996 that does not exist currently. Similarly, fringe mangroves of Isla de Salamanca are sediment starving because a high proportion of the Magdalena River sediment flume was interrupted and re-diverted towards the sea by a directional levee.

Figure 4: Mangroves in the highly exposed coast of Punta Mestizos in the Sinu River delta complex, 2016

On the other hand, mangroves integrity is affected by natural and anthropogenic disturbances, among which selective logging may be the most important in the tropics due to its widespread geographical presence and difficulty to manage, as this is usually a subsistence activity and population dedicated to this activity is highly vulnerable given their high levels of illiteracy [38, 39]. Logging may cause changes in forest structure, composition, function, succession, and in turn,

Dieses Werk ist copyrightgeschützt und darf in keiner Form vervielfältigt werden noch an Dritte weitergegeben werden.
Es gilt nur für den persönlichen Gebrauch.

ecosystem integrity [40-42]. While widespread tree logging may generate peat collapse or vertical erosion in mangroves [43], the effect of selective logging, which is the typical logging management carried out by coastal communities, is unknown.

Through its development, mangrove forest experiences a process known as self-thinning, in which some trees die naturally by competition. In a younger mangrove forest, tree density and competition is higher, while in a mature state few individuals remain and tree density is lower [44]. Based on that, it may be expected that low logging intensities may have no effects on the ecosystem integrity, and in turn, on mechanisms of coastal erosion control. Even positive effects on soil development can be expected, when competition is reduced. However, above a threshold, selective logging may generate peat collapse and a mid-term to long-term decrease in vegetation projected area. In consequence, selective logging may affect sediment deposition and wave dissipation as prop roots facilitate such mechanisms [8, 16].

Furthermore, in the presence of other disturbances, even low intensity logging may affect ecosystem integrity and the mechanisms of coastal erosion control. In the Sinu River complex, fringe mangroves locations experience different rates of selective logging (Fig. 5). In Punta Mestizos and Punta las Playitas, logging disturbance in combination with other natural disturbances such as wave impact and arboreal termites generate a level of mortality higher than expected for the development state of those mangroves (Table 1). In such locations, logging exacerbates natural disturbance and impact mangrove integrity up to a level beyond a threshold for a normal condition mangrove.

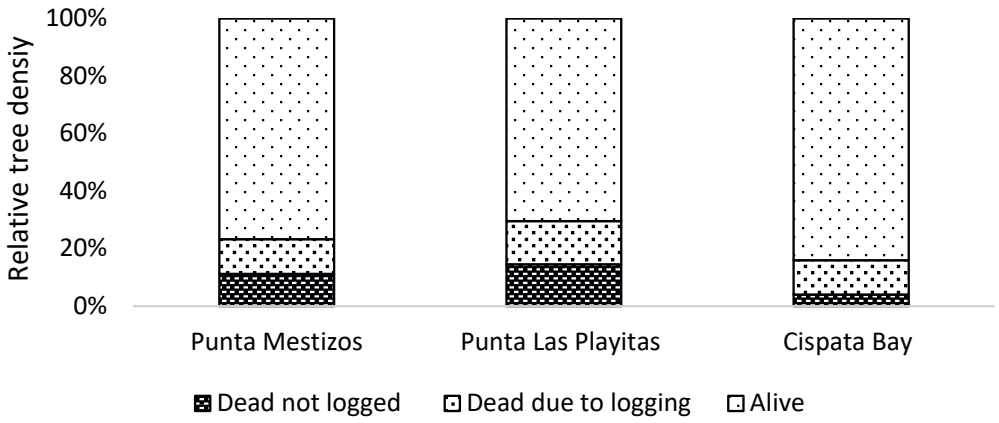

Figure 5: Relative density of alive and dead trees in fringe mangroves in the Sinu River mangrove complex

In the Sinu River mangrove delta complex, fishermen mainly cut trunks of *R. mangle* in a position above the higher prop roots along fringe mangroves. After logged, dead trunks and prop roots can remain standing for several years despite *R. mangle* does not re-sprout. However, in fringe mangroves, the continual impact by waves accelerates the decaying process, and in a mid-term, the projected area responsible of wave dissipation is reduced. Depending on the hydrodynamic

Dieses Werk ist copyrightgeschützt und darf in keiner Form vervielfältigt werden noch an Dritte weitergegeben werden.
Es gilt nur für den persönlichen Gebrauch.

conditions, mangroves will recover after a disturbance or even not. It may be expected that mangrove regeneration could be hampered in highly energetic settings and favored in protected conditions.

Table 1: Ecological integrity in fringe mangroves of the Sinu River mangrove delta complex estimated from the difference between expected mortality and found mortality rates. DBH: Diameter at breast height

Locality	Forest development, (average DBH in cm)	Expected mortality in relation to forest development (in %) according to [37]	Found mortality (in %)	Mangrove integrity
Cispata Bay	5.1	> 25	16.0	Good
Punta Las Playitas	10.6	13 – 14	29.6	Regular
Punta Mestizos	9.5	14 – 15	23.3	Regular

Mangroves are considered ecosystem engineers that responded to past coastal dynamics showing mechanisms that counterbalanced up to certain point past sea level rates and, therefore, generate habitat stability [45]. In Belice, mangroves protected by a coral reef barrier, developed soil vertically at a rate that followed sea level rise during Holocene and were able to persist [46]. In fact, some authors found mangrove peat up to 10 m depth and up to 8000 years old in Twin Cays, Belice, that correspond to past continual development of peat by mangrove root growth. Such pattern occurred in a low carbonate setting with just autochthonous sediments supplies.

Fringe mangroves have variable vertical accretion rates from 1.6 to 8.6 mm/yr, which are related to sediment deposition of autochthonous and allochthonous sediments [12]. Furthermore, these authors also report variable rates of subsurface change (belowground changes) from -9.7 to 2.4 mm/yr, related to root growth [12]. Here, it is hypothesized that such variance in fringe mangroves is related to complex dynamics between sediment supply, exposition of the coast, and mangrove integrity.

Woodroffe *et al*. [2] pointed out that mangroves, from a macroscale perspective, are located in estuaries, lagoons, deltas, and low carbonate islands along open coast locations with moderate wave processes, and along sheltered locations. These authors also indicated that mangrove classification after Lugo and Snedaker [3] as basin, fringe, riverine, dwarf, and overwashed is appropriate from a mesoscale perspective. Such macroscale and mesoscale classification is inappropriate to predict responses to erosive agents and to sea elevation change, and sedimentary, energetic hydrodynamic exposition, and integrity conditions of mangroves should be better predictors.

Positive rates of soil elevation change and horizontal accretion should occur in protected fringe mangroves and/or in systems with high sediment supply and ecosystem integrity. On the other

Dieses Werk ist copyrightgeschützt und darf in keiner Form vervielfältigt werden noch an Dritte weitergegeben werden.
Es gilt nur für den persönlichen Gebrauch.

hand, high rates of vertical erosion, also known as peat collapse and horizontal erosion should be present in localities highly exposed to erosive agents, and/or with sediment starvation and poor ecosystem integrity. Such predictive pattern can be appreciated in the Sinu delta system regarding horizontal erosion, as higher erosion rates of 9 m/yr occur in fringe mangroves of Punta Mestizos [23], a highly exposed location with an ecosystem integrity below an acceptable threshold. Sediment delivery to this location has decreased, as described before, and surely the hydrodynamic conditions do not allow enough sediment deposition to counterbalance wind wave energy. In contrast, accretion rates of 0.2 m/yr are found in the internal estuary of Cispata Bay [47], a protected location with an acceptable condition of ecosystem integrity. Here, conditions of integrity and hydrodynamics would favor sediment deposition.

On the other hand, Punta Las Playitas, a location with lower exposition to waves than Punta Mestizos, ecosystem integrity below an acceptable threshold occurs due to logging as described before. Here, erosion rates are between -0.2 and -1.5 m/yr [45], and mangroves interact only with the wave swash zone. However, such interaction seems to favor sediment retention and to keep low erosion rates.

4 Conclusions

From the perspective of management and decision-making, there is a need to identify thresholds in mangrove logging intensity and sediment supply that ensure minimum or tolerable impacts on ecosystem integrity and provision of ecosystem services [48, 49]. In addition, such thresholds should consider exacerbated erosive dynamics expected from sea level rise and extreme weather events in order to model and to manage locally and regionally mechanisms of coastal erosion control by mangroves, and to improve coastal adaptation and mangrove persistence. Furthermore, it is necessary to better understand sediment dynamics within mangroves, considering particular mangrove species, and environmental and management gradients that affect fringe mangroves and microtidal conditions of the Caribbean in order to establish soft engineering solutions to erosion using mangroves.

5 Acknowledgements

Authors thank DAAD and Exceed Swindon organizing the summer school “Integrating ecosystems in coastal engineering practice - INECEP” and for the financial support to participate. The Instituto de Investigaciones Marinas y Costeras-INVEMAR funded field work during 2015 and COLCIENCIAS (Contract FP44842-141-2016) provide financial support. This research was performed at the Caribbean headquarters of the Universidad Nacional de Colombia.

6 References

1. Tomlinson, P.B.: The botany of mangroves. Cambridge University Press (2016)
2. Woodroffe, C.D., Rogers, K., McKee, K.L., Lovelock, C.E., Mendelssohn, I., Saintilan, N.: Mangrove sedimentation and response to relative sea-level rise. Annual Review of Marine Science 8, 243-266 (2016)

Dieses Werk ist copyrightgeschützt und darf in keiner Form vervielfältigt werden noch an Dritte weitergegeben werden.
Es gilt nur für den persönlichen Gebrauch.

3. Lugo, A.E., Snedaker, S.C.: The ecology of mangroves. Annual Review of Ecology and Systematics 5, 39–64 (1974)

4. Everard, M., Jha, R.R., Russell, S.: The benefits of fringing mangrove systems to Mumbai. Aquatic Conservation Marine and Freshwater Ecosystems 24, 256-274 (2014)

5. Mazda, Y., Wolanski, E.: Hydrodynamics and modeling of water flow in mangrove areas. . Coastal Wetlands: an integrated ecosystem approach, pp. 231-262. Elsevier, Amsterdam (2009)

6. Furukawa, K., Wolanski, E., Mueller, H.: Currents and sediment transport in mangrove forests. Estuarine Coastal Shelf Science 44, 301–310 (1977)

7. Kathiresan, K.: How do mangrove forests induce sedimentation ? Revista de Biología Tropical 51, 355-360 (2003)

8. Krauss, K.W., Lovelock, C.E., McKee, K.L., Lo, L., Ewe, S.M.L., Sousa, W.P.: Environmental drivers in mangrove establishment and early development : A review. Aquatic Botany 89, 105-127 (2008)

9. Krauss, K.W., Allen, J.A., Cahoon, D.R.: Differential rates of vertical accretion and elevation change among aerial root types in Micronesian mangrove forests. Estuarine, Coastal and Shelf Science 56, 251-259 (2003)

10. Willemsen, P.W.J.M., Horstman, E.M., Borsje, B.W., Friess, D.A., Dohmen-janssen, C.M.: Geomorphology Sensitivity of the sediment trapping capacity of an estuarine mangrove forest. Geomorphology 273, 189-201 (2016)

11. Spenceley, A.P.: The role of pneumatophores in sedimentary processes. Marine Geology 24, M31-M37 (1977)

12. Krauss, K.W., McKee, K.L., Lovelock, C.E., Cahoon, D.R., Saintilan, N., Reef, R., Chen, L.: Tansley review How mangrove forests adjust to rising sea level. New Phytologist 202, 19-34 (2014)

13. McIvor, A., Möller, I., Spencer, T., Spalding, M.: Reduction of wind and swell waves by mangroves. Natural Coastal Protection Series: Report 1. Cambridge Coastal Research Unit Working Paper 40, 2050-7941. (2012)

14. Adame, M.F., Neil, D., Wright, S.F., Lovelock, C.E.: Sedimentation within and among mangrove forests along a gradient of geomorphological settings. Estuarine, Coastal and Shelf Science 86, 21-30 (2010)

15. Thampanya, U., Vermaat, J., Sinsakul, S., Panapitukkul, N.: Coastal erosion and mangrove progradation of Southern Thailand. Estuarine, coastal and shelf science 68, 75-85 (2006)

16. Horstman, E., Dohmen-Janssen, M., Narra, P., van den Berg, N.-J., Siemerink, M., Balke, T., Bouma, T., Hulscher, S.: Wave attenuation in mangrove forests; field data obtained in Trang, Thailand. Coastal Engineering Proceedings 1, 40 (2012)

Dieses Werk ist copyrightgeschützt und darf in keiner Form vervielfältigt werden noch an Dritte weitergegeben werden.
Es gilt nur für den persönlichen Gebrauch.

17. Mazda, Y., Wolanski, E., King, B., Sase, A., Ohtsuka, D., Magi, M.: Drag force due to vegetation in mangrove swamps. Mangroves Salt Marshes 1, 193-199 (1997)

18. Corporación Autónoma Regional de Los Valles del Sinú y del San Jorge – CVS e Instituto de Investigaciones Marinas y Costeras - INVEMAR: Plan integral de manejo del Distrito de Manejo Integrado (DMI) bahía de Cispatá - La Balsa- Tinajones y sectores aledaños del delta estuarino del río Sinú, departamento de Córdoba. Editores: Rojas, G. X y P. Sierra-Correa. Serie de Publicaciones Especiales No. 18 de INVEMAR, Santa Marta. (2010)

19. Guillen, K., Sánchez-Núñez, D., Olivero, W., Contreras, A.: Valoración integral delservicio de control de la erosión que presta el manglar en el DMI de Cispata. Línea de Valoración Económica-VAE. Instituto de Investigaciones Marinas y Costeras "José Benito Vives de Andreis" –INVEMAR, Santa Marta. (2015)

20. Sánchez-Páez, H., Ulloa-Delgado, G., Tavera-Escobar, H., Gil-Torres, W.: Plan de manejo integral de los manglares de la zona de uso sostenible sector estuarino de la bahía de Cispatá departamento de Córdoba. OIMT. CVS. CONIF. Ministerio de Ambiente, Vivienda y Desarrollo Territorial, Bogotá. (2005)

21. Restrepo-López, J.C., Ortiz-Royero, J.C., Otero-Díaz, L., Ospino-Ortiz, S.R.: Transporte de sedimentos en suspensión en los principales ríos del Caribe colombiano: magnitud , tendencias y variabilidad. Revista de la Academia Colombiana de Ciencias Exactas, Físicas y Naturales 39, 527-546 (2015)

22. Ruiz-Ochoa, M., Bernal, G., Polanía, J.: Influencia del Río Sinú y el Mar Caribe en el sistema lagunar de Cispatá. Boletín de Investigaciones Marinas y Costeras-INVEMAR 37, 29–49 (2008)

23. INVEMAR-GEO: Aportes sedimentarios del río Sinú y su relación con los procesos costeros del Departamento de Córdoba. Santa Marta. (2015)

24. Robertson, K., Chaparro, J.: Evolución histórica del río Sinú. Cuadernos de Geografía, vol. 7, pp. 70–87 (1998)

25. Castaño, A., Urrego, L., Bernal, G.: Dinámica del manglar en el complejo lagunar de Cispatá (Caribe colombiano) en los últimos 900 años. Revista de Biología Tropical 58, 1347-1366 (2010)

26. Rangel-Ch, O.: Colombia diversidad biótica IX Ciénagas de Córdoba: biodiversidad, ecología y manejo ambiental. Bogotá: Instituto de Ciencias Naturales (2010)

27. Ramírez, J.A., Molina, E., M., B.: Anillos anuales y clima en Rhizophora mangle L. de la Bahía de Cispatá, Colombia. Revista Facultad Nacional de Agronomía 63, 5639-5650 (2010)

28. Rangel, N., Galeano, E., Coca, O.: Estudios para la prevención y mitigación de la erosión costera. Convenio MADS-INVEMAR. Informe Técnico Final para Ministerio de Ambiente y Desarrollo Sostenible, Santa Marta, DTC. (2012)

Dieses Werk ist copyrightgeschützt und darf in keiner Form vervielfältigt werden noch an Dritte weitergegeben werden.
Es gilt nur für den persönlichen Gebrauch.

29. INVEMAR, CVS, CARSUCRE: Formulación del Plan de Manejo Integrado de la Unidad Ambiental Costera Estuarina del Río Sinú y Golfo de Morrosquillo, Caribe Colombiano. Informe Técnico. Fase I – Caracterización y Diagnóstico. Santa Marta. (2001)

30. Bernal, G., Osorio, A., Urrego, L., Peláez, D., Molina, E., Zea, S., Montoya, R., Villegas, N.: Occurrence of energetic extreme oceanic events in the Colombian Caribbean coasts and some approaches to assess their impact on ecosystems. Journal of Marine Systems 164, 85-100 (2016)

31. Osorio, A.F., Montoya, R.D., Ortiz, J.C., Peláez, D.: Construction of synthetic ocean wave series along the Colombian Caribbean Coast: A wave climate analysis. Applied Ocean Research 56, 119-131 (2016)

32. CIOH: Estudio geológico y sedimentológico del Golfo de Morrosquillo. Informe Final. Centro de Investigaciones Oceánicas e Hidrográficas, Cartagena de Indias (1993)

33. INVEMAR-CARSUCRE: Diagnóstico de la Erosión Costera en el Departamento de Sucre, Caribe Colombiano. Informe Final Fase I, Informe Final Fase II. Convenio de Cooperación No. 022, Santa Marta. (2009)

34. Correa, D., Acosta, S., Bedoya, G.: Análisis de las causas y monitoreo de la erosión litoral en el Departamento de Córdoba, Corporación autónoma de los valles de Sinú y San Jorge-CVS. Universidad EDAFIT, Medellín (2007)

35. Gómez, H., Arias, L., Pérez, C., Dueñas, P., Frías, J., Silva, L., Perea, L., Vallejo, A., Daza, P., Torres, M.: Fundamentos de Acuicultura Marina. Santafé de Bogotá: INPA, 1995. (1995)

36. CARICOMP: Manual of methods for mapping and monitoring of physical and biological parameters in the coastal zone of the Caribbean. CARICOMP Data Management Center, University of West Indies, Kingston, Jamaica. (2001)

37. Jimenez, J.A., Lugo, A.E., Cintron, G.: Tree mortality in mangrove forests. Biotropica 17, 177-185 (1985)

38. De la Rosa, I.: Sostenibilidad integral del manglar con comunidades locales en un área protegida (DMI Bahía Cispatá). Pre memorias simposio 5. Visiones institucionales y comunitarias frente al uso y ocupación de las áreas protegidas. II Congreso Colombiano de Áreas Protegidas. Parques Nacionales Naturales de Colombia, Bogotá. (2014)

39. Nguyen, T.P., Luom, T.T., Parnell, K.E.: Mangrove allocation for coastal protection and livelihood improvement in Kien Giang province, Vietnam: Constraints and recommendations. Land Use Policy 63, 401-407 (2017)

40. Blanco, J.F., Estrada, E., Ortiz, L.F., Urrego, L.E.: Ecosystem-wide impacts of deforestation in mangroves: The Urabá Gulf (Colombian Caribbean) case study. International Scholarly Research Network Ecology 255, 1359-1366 (2012)

Dieses Werk ist copyrightgeschützt und darf in keiner Form vervielfältigt werden noch an Dritte weitergegeben werden.
Es gilt nur für den persönlichen Gebrauch.

41. Ferwerda, J., Ketner, P., McGuinness, K.: Differences in regeneration between hurricane damaged and clear-cut mangrove stands 25 years after clearing. Hydrobiologia 591, 35-45 (2007)

42. Hauff, R.D., Ewel, K.C., Jack, J.: Tracking human disturbance in mangroves: estimating harvest rates on a Micronesian Island. Wetlands Ecology and Management 14, 95-105 (2006)

43. Lang'at, J.K.S., Kairo, J.G., Mencuccini, M., Bouillon, S., Skov, M.W., Waldron, S., Huxham, M.: Rapid losses of surface elevation following tree girdling and cutting in tropical mangroves. PLoS One 9, e107868 (2014)

44. Tang, S., Meng, C.H., Meng, F.-R., Wang, Y.H.: A growth and self-thinning model for pure even-age stands: theory and applications. Forest Ecology and Management 70, 67-73 (1994)

45. McKee, K.L., Cahoon, D.R., Feller, I.C.: Caribbean mangroves adjust to rising sea level through biotic controls on change in soil elevation. Global Ecology and Biogeography 16, 545-556 (2007)

46. Feller, I.C., Lovelock, C., Berger, U., McKee, K., Joye, S., Ball, M.: Biocomplexity in mangrove ecosystems. Annual Review of Marine Science 2, 395-417 (2010)

47. Rangel-buitrago, N.G., Anfuso, G., Thomas, A.: Ocean & Coastal Management Coastal erosion along the Caribbean coast of Colombia : Magnitudes , causes and management. Ocean and Coastal Management 114, 129-144 (2015)

48. Lee, S.Y., Primavera, J.H., Dahdouh‐Guebas, F., McKee, K., Bosire, J.O., Cannicci, S., Diele, K., Fromard, F., Koedam, N., Marchand, C.: Ecological role and services of tropical mangrove ecosystems: a reassessment. Global Ecology and Biogeography 23, 726-743 (2014)

49. Lovelock, C.E., Fernanda, M., Bennion, V., Hayes, M., Reef, R., Santini, N., Cahoon, D.R.: Estuarine , Coastal and Shelf Science Sea level and turbidity controls on mangrove soil surface elevation change. Estuarine, Coastal and Shelf Science 153, 1-9 (2015)

Dieses Werk ist copyrightgeschützt und darf in keiner Form vervielfältigt werden noch an Dritte weitergegeben werden.
Es gilt nur für den persönlichen Gebrauch.

DESIGN OF STRATEGIES FOR THE CONTROL OF BEACH EROSION WITH AN ECOSYSTEM-BASED MANAGEMENT APPROACH

Angel Gabriel Kuc Castilla[1], Edgar Mendoza[1], Debora Lithgow[1], Rodolfo Silva[1]

[1]Engineering Institute, National Autonomous University of Mexico, Circuito Escolar s/n, Ciudad Universitaria, Coyoacan, Mexico D.F., C.P. 04510, AKucC@iingen.unam.mx

Keywords: coastal erosion, anthropization

Abstract

Coastline evolution was studied in Sabancuy beach through the use of satellite images, from which the areas of beach erosion and accretion were determined in a period of 10 years (2004 - 2014). The beach at the east side of the access channel was found to have a growth area of 129,109 m^2, while the beach in the west side of the channel shows an area loss of -23,790 m^2.The degree of anthropization of the study area was determined to evaluate the effect of the transformation by human action on the different biological systems. It was found that 50% of the study area is covered with natural vegetation, 36% is occupied by agricultural areas, 8% corresponds to secondary vegetation, and lastly, 6% corresponds to urban settlements. Based on this information, a first proposal of possible strategies for beach erosion control is presented.

1 Introduction

Sabancuy is a beach of fine sand with shallow and transparent waters, calm waves, and soft bottom slope that has developed inside the estuary of the same name. In the Sabancuy estuary, an artificial channel was built with breakwaters on both sides in order to serve the communication with the sea (Sabancuy inlet). The channel was expected to improve the ecological interactions of this habitat, and also to maintain and to increase the efficiency of the existing fishing operation.

The phenomenon seen after the construction of these structures is that longitudinal sediment transport (east-west directed) was interrupted for the construction of the breakwaters, causing a process of sedimentation on the beach east and an erosive process on the west beach. This also caused the saturation in the retention capacity of the east breakwater, causing the entrance of parts of the sediment into the communication channel, while the other part continues its way westwards. These coastal dynamics led to the construction of protection barriers on the west beach of the access channel with the objective of reducing erosion [1].

The objective of this work is to propose strategies for coastal erosion control, considering the interconnections between the physical environment and the coastal ecosystems in order to maximize the protection service provided by both the engineering (rigid and flexible) and the coastal ecosystems, for which the evolution of the coastline and the degree of modification of the ecosystem by anthropogenic effects were analyzed.

Dieses Werk ist copyrightgeschützt und darf in keiner Form vervielfältigt werden noch an Dritte weitergegeben werden.
Es gilt nur für den persönlichen Gebrauch.

2 Materials and methods

2.1 Study area

Sabancuy estuary is located in the eastern region of Terminos Lagoon [2] and consists of five areas: El Pujo, San Nicolás, Ensenada Polcai, Santa Rosalía, and the populated area of Sabancuy. It has two inlets of communication, the first one with Terminos Lagoon in El Pujo, where there are marshes with extensive floodplains, and the second one located towards Polcai cove, and is an artificial channel that flows into the adjacent coast area [3] (Figure 1).

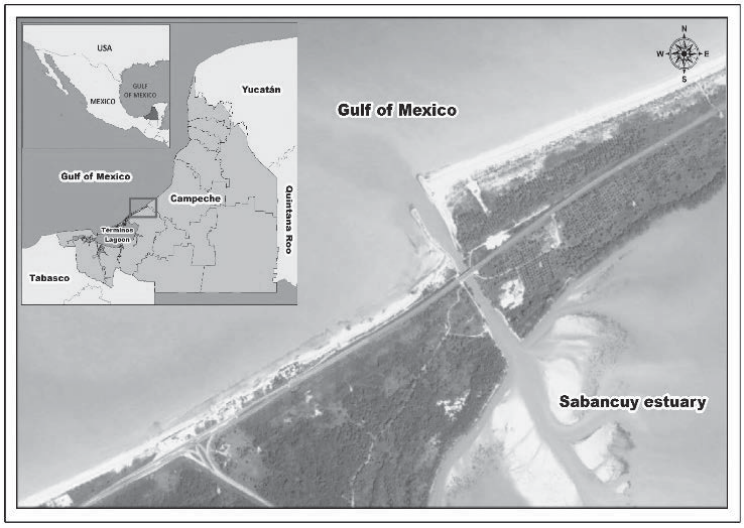

Figure 1: Location of Sabancuy in the State of Campeche

According to INEGI, 2010 [4], the population of Sabancuy consists of 7,286 inhabitants, 3,705 men and 3,581 women, Sabancuy presents two main routes of communication: the federal road 180 (78 km) and the local highway, which communicates the town with other communities to the interior and connects with federal highway 186 in the section Villahermosa - Escárcega.

The climate of the region is warm-humid with three climatic seasons defined as dry season from February to April, rainy season from May to October, and "Nortes" or winter storms season from November to January [5]. Thus, during the dry season, the beaches are generally stable, and the erosion process restarts during the rainy and "Nortes" season. The most severe erosion episodes occur in the period of "Nortes" [6].

Sabancuy is an erosive beach, where a breakwater that prevents the free transit of coastal sediments to the west was constructed [7]. Sabancuy sands present abundant fragments of carbonate shells of different sizes and a high content of clear lithic fragments with little abundance of quartz and feldspar. These types of minerals are deposited by the runoff of the different rivers bordering the area. They are classified as medium sand to fine gravel with grain sizes ranging from 0.05 to 5.0 mm [8]. In Sabancuy, a regression of -211.2 m (1974-2005) has been found with an erosion rate of 6.8 m/yr [6] (Figures 2 and 3). In the Sabancuy estuary, the maximum velocity of the currents is between 0.080 - 0.087 m/s [9].

Dieses Werk ist copyrightgeschützt und darf in keiner Form vervielfältigt werden noch an Dritte weitergegeben werden.
Es gilt nur für den persönlichen Gebrauch.

Figure 2: Sabancuy beach, 2015

Figure 3: Sabancuy beach, 2016

Due to the fact that the access channel to the Sabancuy estuary was blocked by sediments provided by the tides and waves, dredging works of 324,685 m^3 and 88,666 m^3 of sediment were performed in 2007 and 2008, respectively.

2.2 Coastline evolution

Changes in the coastline are due to multiple factors that may have different origin (natural or anthropogenic), spatio-temporal scale, and permanence. That is, such changes can be temporary or permanent, can occur suddenly or for decades, and be local or regional.

For the analysis of the variation of the coastline, satellite images were used, which were obtained from the Google Earth database for the years 2004 and 2014.

Dieses Werk ist copyrightgeschützt und darf in keiner Form vervielfältigt werden noch an Dritte weitergegeben werden.
Es gilt nur für den persönlichen Gebrauch.

ArcGIS software was used to geo-reference the satellite images from control points and subsequently converted to the Universal Transverse Mercator (UTM) projection for zone 15 north on a spheroid defined by WGS84 (World Geodetic System 84). From the georeferenced images, the coastline was manually digitized, considering the intertidal zone interpreted from each of the satellite images, later the digitized lines were exported to AutoCAD program for processing and analysis.

In order to determine the areas of erosion/accretion between two images of different dates, the method of reference areas was used. This method consists of drawing a polygon that serves as baseline data. The vertices, where this polygon starts and ends are taken as reference in each image. Then, the continental area (m^2) of each polygon, produced by the intersection of the coastlines, is obtained.

The quantification of erosion/accretion processes was done by calculating the difference of continental areas between two images. In this case, a negative sign indicates erosion and a positive sign denotes accretion [6] (Figure 4).

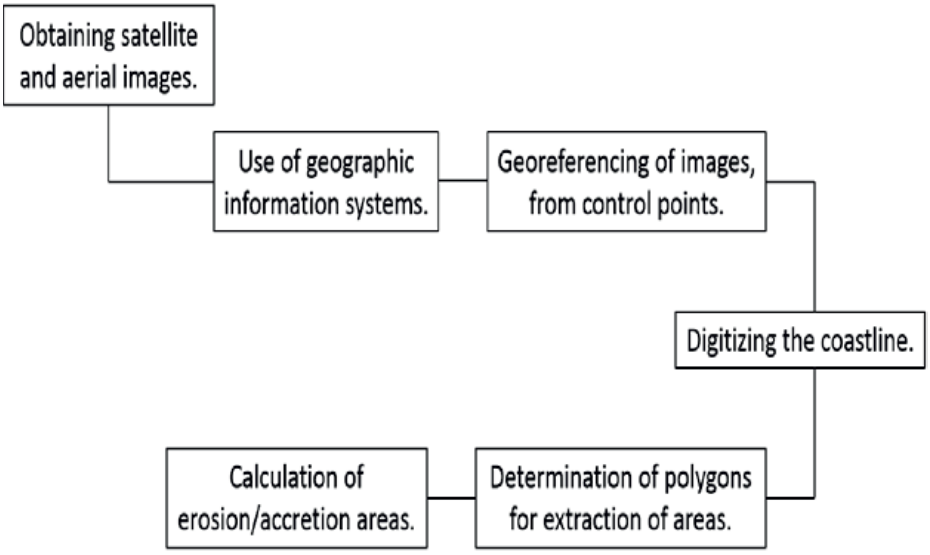

Figure 4: Diagram for the analysis of satellite images

2.3 Determination of the Relative Integrated Anthropization Index (INRA)

The concept of anthropization is understood as the degree of modification of an original ecosystem by anthropogenic effects, added to the difficulty that this modification represents for the ecosystem to regenerate, and the amount of anthropogenic elements it contains. In order to estimate the relative degree of anthropization, the method proposed by [9] was applied to the vegetation cover of the study area. For this, maps of land use and vegetation should be available in the study area.

First, the units of analysis (UA) were defined, that is the area, to which an anthropization value has to be assigned. In this study, the size of each UA is 1 km^2. Once the area to be analyzed was

Dieses Werk ist copyrightgeschützt und darf in keiner Form vervielfältigt werden noch an Dritte weitergegeben werden.
Es gilt nur für den persönlichen Gebrauch.

located and its respective UA defined, it was proceeded to divide each into a hundred equal parts, which are called subunits of analysis (SUA). The next step was to identify all interventions that generate a decrease or alteration in the ecosystem within each SUA, for which the INEGI land usage map was used. Once the coverages or land uses were defined over the study area, they were grouped into categories and assigned a value between 0 (without anthropogenic modification) and 1 (fully intervened) (Table 1).

Table 1: Partial anthropization values and corresponding coverages

Category	Anthropized value	Type of coverage identified
A	0.00	Natural vegetation
B	0.25	Disturbed vegetation
C	0.50	Agricultural area
D	0.75	Scattered urban settlements (rural areas)
E	1.00	Urban zone

Modified from Martínez-Dueñas, 2010 [9].

Once the anthropization values for each subunit of analysis (SUA) were identified, the relative degree of anthropization per unit of analysis (UA) was estimated, based on the following expression:

$$\mathrm{INRA} = \left(\frac{\Sigma \mathrm{SUA}'}{\mathrm{n}}\right).100$$

Where are

$\Sigma \mathrm{SUA}' =$ Sum of the value of partial anthropization of all SUA, and n = Total number of SUA.

The final value of the anthropization index (INRA) varies from 0 – 100, where 0 equals units with null anthropization and 100 to a high degree of anthropization (Table 2). The units defined within the study area were classified in agreement with the proposed ones by [10], as shown in Table 2.

Table 2: Anthropization degree intervals

INRA	Degree of anthropization	Landscape Features
100	Transformed	Landscape with urban matrix
75	Heavily altered.	Landscape with semi-artificial urban matrix with low density and patches of secondary vegetation
50	Altered	Landscape with semi-transformed matrix with patches of secondary vegetation
25	Semi-Transformed	Landscape with natural matrix with scarce patches of alteration
0	Natural	Landscape with matrix without obvious alteration

Source: Mateo Rodríguez y Ortiz Pérez, 2001 [10].

Dieses Werk ist copyrightgeschützt und darf in keiner Form vervielfältigt werden noch an Dritte weitergegeben werden.
Es gilt nur für den persönlichen Gebrauch.

In order to facilitate the interpretation of large extensions, a method based on the concept of pictorial unit (pixel) was used, where the analyzed subunits and analyzed units take the characteristics of pixels (texture, color, etc.) equivalent to the value or category of anthropization within them.

3 Results and Discussion

3.1 Coastline evolution

The images used for the analysis of the changes in the coastline are from 2/28/2004 and 12/9/2014, which correspond to rainy and "Nortes" season, respectively. As a result of the satellite images analyses, the areas of accretion and erosion are shown in Table 3, obtained for a period of 10 years (2004 - 2014) as well as the balance of sediments between zones.

Table 3: Balance of areas of accretion and erosion obtained with digitalized satellite images

Period	Zone	Accretion (m^2)	Erosion (m^2)	Sediment balance (m^2)
2004-2014	East beach	129,109	0	129,109
	West beach	778	24,568	-23,790

The results show that the beach at the east side is in accretion, having gained 129,109 m^2 of dry beach (Figure 5), and in the opposite case, the beach of the west zone is in constant retreat, having lost -23,790 m^2 of dry beach (Figure 6). This corresponds to the expected response of the coast to structures such as that are placed in Sabancuy.

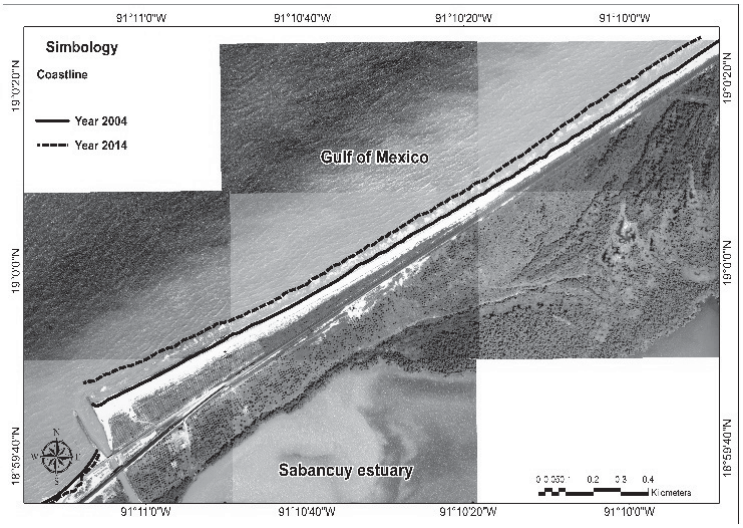

Figure 5: Beach east side

Dieses Werk ist copyrightgeschützt und darf in keiner Form vervielfältigt werden noch an Dritte weitergegeben werden.
Es gilt nur für den persönlichen Gebrauch.

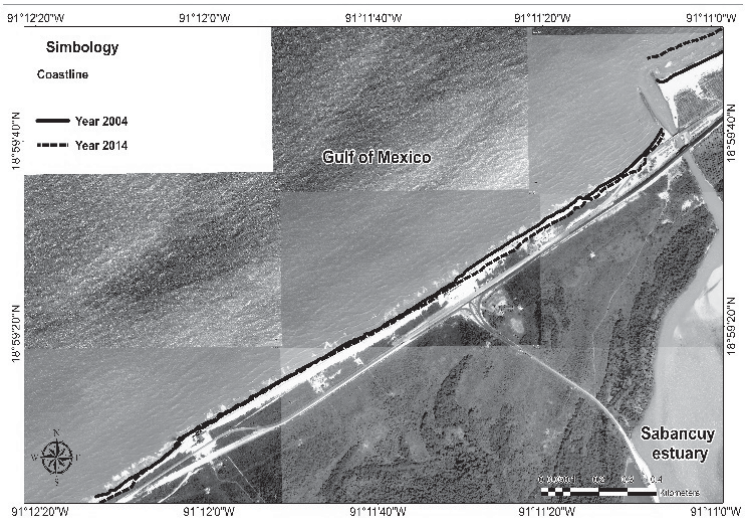

Figure 6: Beach west side

3.2 Relative Integrated Anthropization Index (INRA)

From the land use map of the INEGI scale 1: 250, 000, series V, it was possible to differentiate 6 types of coverage in the study area.

- Mangrove
- Body of wáter
- Secondary vegetation
- Cultivated grassland
- Human settlements
- Urban zone

The study area was divided into 30 units of analysis (UA) of 1 km^2 each and these in turn were divided into 100 subunits of analysis (SUA).

The results show that the most frequent category was A (0.00), corresponding to the zones of natural vegetation, occupying 50% of the total area of study (Table 4). The next most extensive coverage was C (0.50), corresponding to the agricultural area, which occupies 36% of the total area of study. Secondary vegetation B (0.25) covers 8 % of the study area. Finally, the category of urban zone E (1.00) corresponds to the population of Sabancuy, covering 6% of the area of study.

The information for each cell of 0.01 km^2 (SUA) is presented cartographically in Figure 7, where a specific color has been assigned for each category of anthropization.

Dieses Werk ist copyrightgeschützt und darf in keiner Form vervielfältigt werden noch an Dritte weitergegeben werden.
Es gilt nur für den persönlichen Gebrauch.

Table 4: Number of cells (SUA) occupied by each category of anthropization, with which the INRA of the units of analysis (UA) was calculated.

UA	A (0.00)	B (0.25)	C (0.50)	D (0.75)	E (1.00)	INRA
1	40	60	0	0	0	15
2	35	65	0	0	0	16.25
3	62	38	0	0	0	9.5
4	67	33	0	0	0	8.25
5	63	37	0	0	0	9.25
6	99	1	0	0	0	0.25
7	100	0	0	0	0	0
8	100	0	0	0	0	0
9	100	0	0	0	0	0
10	100	0	0	0	0	0
11	100	0	0	0	0	0
12	100	0	0	0	0	0
13	30	0	61	0	9	39.5
14	30	0	0	0	70	70
15	30	0	7	0	63	66.5
16	31	0	69	0	0	34.5
17	55	0	45	0	0	22.5
18	60	0	40	0	0	20
19	6	0	92	0	2	48
20	0	0	78	0	22	61
21	23	0	67	0	10	43.5
22	68	0	32	0	0	16
23	100	0	0	0	0	0
24	49	0	51	0	0	25.5
25	0	0	100	0	0	50
26	0	0	100	0	0	50
27	0	0	100	0	0	50
28	17	0	83	0	0	41.5
29	43	0	57	0	0	28.5
30	8	0	92	0	0	46
Total	1516	234	1074	0	176	
%	50	8	36	0	6	

Dieses Werk ist copyrightgeschützt und darf in keiner Form vervielfältigt werden noch an Dritte weitergegeben werden.
Es gilt nur für den persönlichen Gebrauch.

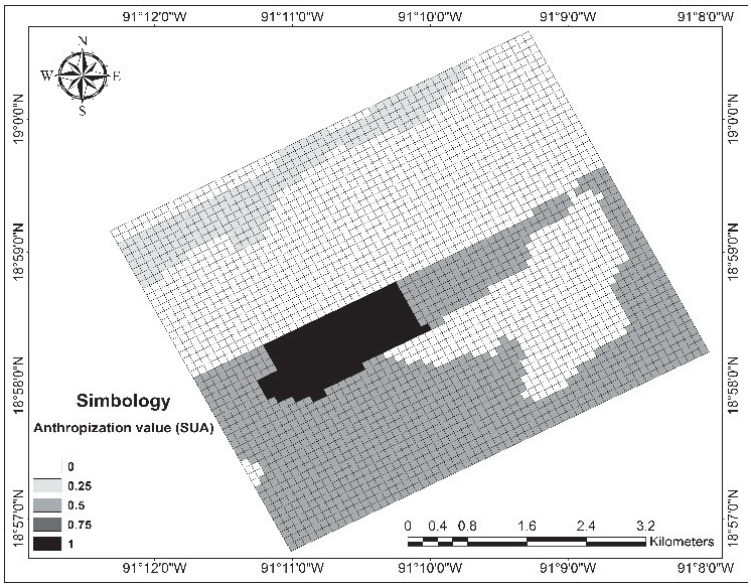

Figure 7: Partial anthropization degree (subunits of analysis SUA)

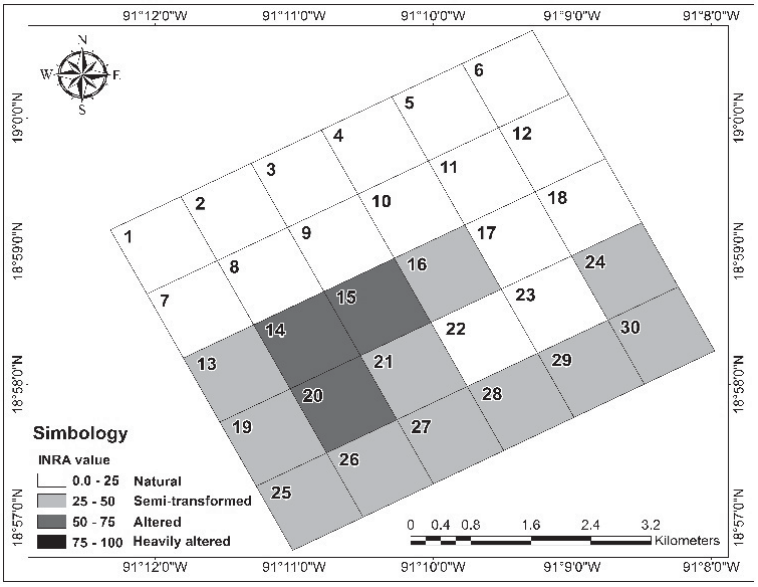

Figure 8: Degree of anthropization for each of the units of analysis (UA)

The highest values of anthropization are found in UAs 14 (70%), 15 (66.5%), and 20 (61%). The lowest values of anthropization are found in UAs 7 to 12 and 23 (0%), where they are mangrove forest and the water body of the estuary (Figure 8). In summary, it can be said that there is an anthropization gradient, which is greater inland and decreases as one moves towards the coast.

3.3 Proposed of strategies for the control of erosion

The results show that the beach located on the west side of the access channel to the Sabancuy estuary had a significant retreat in the coastline in a period of 10 years (2004-2014), which indicates that it is the area, where it is necessary to implement measures to control the erosion process.

Dieses Werk ist copyrightgeschützt und darf in keiner Form vervielfältigt werden noch an Dritte weitergegeben werden.
Es gilt nur für den persönlichen Gebrauch.

An alternative proposed herein is to make an artificial nourishment of the beach creating an area that allows the establishment of mangroves. The material is expected to be borrowed from dredging areas in the interior of the Sabancuy estuary. In the same way, it is proposed to place structures in order to stimulate the sedimentation and to protect from the energy of the waves to the reforested zone.

As a second alternative, the creation of a system of dunes covered with native vegetation was analyzed that help in the retention of the sediment placed. As in the first proposal, the material to perform the filling can be obtained from dredging work inside the estuary.

3.4 Discussion

From the analysis of the satellite images in the period 2004 - 2014, it was observed that there is a retreat of the coastline in the western sector of the access channel to the estuary. The retreat of the coastline is the result of the breakwater built in the channel that communicates the estuary with the sea, retaining the transport of sediments, generating an accretion zone on the east side, and causing an erosive process on the west side.

A number of studies have shown that mangroves and coastal dunes help with sediment retention, reduce stream velocity and wave energy, and dampen flooding [11-14]. For this reason, mangrove planting is proposed as a strategy for erosion control in the Sabancuy beach, for filling and mangrove reforestation as well as for creation of dunes.

Although the present study gives an overview of the situation, in which the study area is located, where the area to be intervened was detected, a more detailed analysis is necessary to determine if the proposals for erosion control will be feasible or not.

The analysis of the degree of anthropization of the study area allows knowing if the ecosystem that is intended to place once existed in the site or if they still exist but is degraded or fragmented.

However, it is necessary to evaluate if the conditions of the site are necessary for the placement of proposed alternatives, such as to determine the period of flood or hydroperiod (frequency and duration of flooding of a certain area), the microtopography, the interstitial salinity and of water, the sediment characteristics, the wave pattern and intensity, among others. So, it is necessary to work with an interdisciplinary group in order to obtain the best possible solution.

4 Conclusions

It was found that the east beach had a growth of 129,109 m^2, while the west beach had a retreat of -23,790 m^2. It was also determined that 50% of the study area is in the natural state, 36% occupied by agricultural areas, 8% by secondary vegetation, and only 6% by urban settlements.

Given that the beach is far from being stable, the proposed solution is to use the material that is dredged from the access channel to nourish the beach. This solution can be combined with the

Dieses Werk ist copyrightgeschützt und darf in keiner Form vervielfältigt werden noch an Dritte weitergegeben werden.
Es gilt nur für den persönlichen Gebrauch.

construction of a vegetated dune in order to re-establish the ecosystem connectivity and, with a submerged small structure, to generate a perched beach profile. This combination of interventions would fall into a soft engineered solution and will, in the mid-term, generate a window of opportunity for the placing of another ecosystem based alternative.

5 Acknowledgements

This work was done in the Institute of Engineering in the National University of Mexico. Authors are thankful to German Academic Exchange Service (DAAD), Excellence Center for Development Cooperation, Sustainable Water Management (EXCEED/ SWINDON), and National University of Mexico (UNAM) for their financial and technical supports, enabling to participate at the Summer School on Integrating Ecosystems in Coastal Engineering Practice (INECEP).

6 References

1. Gobierno del Estado de Campeche: Manifestación de impacto ambiental modalidad particular para la rehabilitación de las escolleras y obras de dragado de mantenimiento en Sabancuy, municipio de Carmen, Campeche. (2008)
2. Carranza-Edwards, A., Gutiérrez-Estrada, M., Rodríguez-Torres, R.: Unidades morfotectónicas continentales de las costas mexicanas. Anales del Instituto de Ciencias del Mar y Limnología, Universidad. Nacional Autónoma de México, vol. 2, pp. 81-88 (1975)
3. Villalobos-Zapata, G.J., Mendoza Vega, J.: La Biodiversidad en Campeche: Estudio de Estado. Comisión Nacional para el Conocimiento y Uso de la Biodiversidad (CONABIO), Gobierno del Estado de Campeche, Universidad Autónoma de Campeche, El Colegio de la Frontera Sur. México (2010)
4. INEGI: Censo de Población y Vivienda 2000. http://www.beta.inegi.org.mx/proyectos/ccpv/2010/ (2010)
5. Agraz Hernández, C.M., Chan Keb, C.A., Iriarte-Vivar, S., Posada Venegas, G., Vega Serratos, B., Osti Sáenz, J.: Phenological variation of Rhizophora mangle and ground water chemistry associated to changes of the precipitation. Hidrobiológica 25, 49-61 (2015)
6. Torres-Rodríguez, V., Márquez-García, A., Bolongaro-Crevenna, A., Chavarría-Hernández, J., Exposito-Díaz, G., Márquez-García, E.: Tasa de erosión y vulnerabilidad costera en el estado de Campeche debido a efectos del cambio climático. Vulnerabilidad de las Zonas Costeras Mexicanas ante el Cambio Climático (segunda edición): Universidad Autónoma Metropolitana-Iztapalapa, UNAM-ICMyL, Universidad Autónoma de Campeche 413-432 (2011)
7. Carranza-Edwards, A., Márquez-García, A.Z., Tapia-Gonzalez, C.I., Rosales-Hoz, L., Alatorre-Mendieta, M.Á.: Cambios morfológicos y sedimentológicos en playas del sur del Golfo de México y del Caribe noroeste. Boletín de la Sociedad Geológica Mexicana 67, 21-43 (2015)

Dieses Werk ist copyrightgeschützt und darf in keiner Form vervielfältigt werden noch an Dritte weitergegeben werden.
Es gilt nur für den persönlichen Gebrauch.

8. Martínez, M.L., Moreno-Casasola, P., Espejel, I., Jiménez-Orocio, O., Infante-Mata, D., Rodríguez-Revelo, N.: Diagnóstico de las dunas costeras de México. pp. 45-54. Comisión Nacional Forestal, Mexico (2014)

9. Martínez-Dueñas, W.A.: INRA-Índice integrado relativo de Antropización: Propuesta técnica-conceptual y aplicación. Intropica 5, 37-46 (2010)

10. Mateo Rodríguez, J.M., Ortiz Pérez, M.A.: La degradación de los paisajes como concepción teórico-metodolgica. Instituto de Geografía, UNAM (2001)

11. Barbier, B.E.: Valuing Ecosystem Services for Coastal Wetland Protection and Restoration: Progress and Challenges. Resources 2, 213-230 (2013)

12. Gedan, K.B., Kirwan, M.L., Wolanski, E., Barbier, E.B., Silliman, B.R.: The present and future role of coastal wetland vegetation in protecting shorelines: answering recent challenges to the paradigm. Climatic Change 106, 7-29 (2011)

13. Koch, E.W., Barbier, E.B., Silliman, B.R., Reed, D.J., Perillo, G.M.E., Hacker, S.D., Granek, E.F., Primavera, J.H., Muthiga, N., Polasky, S., Halpern, B.S., Kennedy, C.J., Kappel, C.V., Wolanski, E.: Non-linearity in ecosystem services: temporal and spatial variability in coastal protection. Frontiers in Ecology and the Environment 7, 29-37 (2009)

14. Shepard, C.C., Crain, C.M., Beck, M.W.: The Protective Role of Coastal Marshes: A Systematic Review and Meta-analysis. PLOS ONE 6, e27374 (2011)

Dieses Werk ist copyrightgeschützt und darf in keiner Form vervielfältigt werden noch an Dritte weitergegeben werden.
Es gilt nur für den persönlichen Gebrauch.

IDENTIFYING MULTIFUNCTIONAL RESTORATION AREAS FOR COASTAL LANDSCAPE CONSERVATION IN MEXICO

Debora Lithgow[1,3], M. Luisa Martínez[2], Rodolfo Silva[3], Juan B. Gallego-Fernández[1]

[1]Departamento de Biología Vegetal y Ecología, Universidad de Sevilla, 41080, Sevilla, España

[2]Instituto de Ecología, INECOL, Xalapa, Veracruz, México, marisa.martinez@inecol.edu.mx

[3]Instituto de Ingeniería, Universidad Nacional Autónoma de México, CU, 04510 CDMX, México

Keywords: sandy beaches, coastal dunes, biosphere reserve, Marismas Nacionales, perturbation, restoration

Abstract

Overpopulation and inadequate management of the world's coastlines have seriously degraded numerous sandy beaches that provide valuable ecosystem services to society. The recovery of coastal ecosystem services is one potential adaptation strategy to address both current threats and future threats from climate change. However, the implementation of restoration projects is a complex process that involves multiple variables (i.e., ecological, geomorphological, and socio-economic variables) that vary widely per site. In the present study, the ReDune index was applied in Marismas Nacionales, a UNESCO-designated Biosphere Reserve located on the Mexican Pacific Coast, in order to identify sandy beaches that require restoration and can be feasibly restored. The results highlight the flexibility and versatility of the ReDune index, which can be applied in sites with differing sedimentary, ecological, and human pressures and characteristics. Also, the index clearly distinguished between locations, where restoration is urgent, and those, where it is not. Further research is required to choose the appropriate strategies for restoring the indicated sites. Ultimately, the considered restoration alternatives should be flexible and enhance the resilience of the complex beach systems of Marismas Nacionales.

1 Introduction

Latin American coastal areas are prime targets for the development of commerce, industry, housing and tourism. However, these activities trigger rapid population growth and unplanned development, which may conflict with the aims of coastal conservation or threaten the capacity of coastal ecosystems to provide a range of ecosystem services [1]. This conservation of coastal areas is especially relevant in Latin America, as this region includes six of the ten most biodiverse countries in the world: Brazil, Colombia, Peru, Mexico, Ecuador and Venezuela (1st, 2nd, 4th, 5th, 6th and 9th place, respectively). Although the region's biodiversity is not evenly distributed, the overall richness and economic importance of the region's ecosystems and natural capital are undeniable [2].

Dieses Werk ist copyrightgeschützt und darf in keiner Form vervielfältigt werden noch an Dritte weitergegeben werden.
Es gilt nur für den persönlichen Gebrauch.

The conservation of ecosystems including beaches and dunes has been increasingly recognized to play a significant role in reducing socioeconomic vulnerability and increasing the capacity of regions to adapt to extreme natural events and climate change [3]. In Mexico, the loss of ecosystem protection services is a critical issue, as the socioeconomic losses derived from storms and hurricanes have increased over time [4].

Despite socioeconomic vulnerability to natural hazards, natural resources management in Mexico has failed to sustainably use coastal resources or to effectively manage associated ecosystems. For example, the second most intense hurricane recorded worldwide (hurricane Patricia, category 5) made landfall on the Mexican Pacific Coast in 2015 and destroyed thousands of hectares of crops and houses. However, unplanned coastal development has since continued in the area, indicating a lack of recognition of the ecosystem services provided by coastal systems and of the dependence of economic activities on ecosystem services. Consequently, coastal dunes are not considered to be priority areas for conservation or restoration, and are frequently excluded from Natural Protected Areas [5].

During recent decades, some approaches such as ecosystem-based management (EBM) and green infrastructure (GI) have been promoted to address both conservation and development goals. In this respect, EBM and GI can provide solutions to coastal problems such as flooding and erosion, while avoiding the negative effects of "hard" engineering projects [1]. A green infrastructure project is any construction (natural, semi-natural or artificial) that contributes to the conservation or restoration of biological diversity or enhances the provision of ecosystem services [1, 6]. In comparison to traditional solutions, solutions based on GI are more flexible and resilient under changing conditions, ensure ecosystem functioning and better respond to social demands [7, 8]. Furthermore, preserving the multifunctionality of ecosystems enables numerous benefits to be obtained from the same area [9]. In this context, restoration actions using GI that are based on an EBM approach are one strategy for ensuring ecosystem health, resilience and sustainability, while simultaneously meeting economic, social and developmental demands [10].

EBM is based on several common principles that have three general aims [11]: (1) sustainability, (2) ecological health, and (3) inclusion of humans in ecosystems. Therefore, EBM projects are based upon diverse ecological, human and management perspectives. In particular, 15 common principles that characterize EMB were identified in a literature review [12]. In descending order of frequency of mentioning in the literature, EBM should seek to (1) consider ecosystem connections, (2) use appropriate spatial and temporal scales, (3) implement adaptive management techniques, (4) rely on scientific knowledge, (5) implement integrated management techniques, (6) involve stakeholders, (7) consider the dynamic nature of ecosystems, (8) preserve ecological integrity and biodiversity, (9) foster sustainability, (10) recognize the coupling of social and ecological systems, (11) ensure that decisions reflect societal choice, (12) consider distinct boundaries, (13) be interdisciplinary, 14) (implement appropriate monitoring strategies, and (15) acknowledge uncertainty [12].

Dieses Werk ist copyrightgeschützt und darf in keiner Form vervielfältigt werden noch an Dritte weitergegeben werden.
Es gilt nur für den persönlichen Gebrauch.

The ambitious goals and heterogeneous principles of EBM may complicate its execution. Several challenges may be related to the shift from unilateral targets to multilateral ones (i.e., a shift from the conservation of biodiversity to the conservation and maintenance of ecosystem services), the establishment of restoration objectives, the coordination of multi-jurisdictional projects, wherein stakeholders may have varying objectives or, finally, transdisciplinary collaborations across sectors that have not traditionally worked with one another [13].

The implementation of an EBM approach in restoration projects requires the consideration of factors such as cost, time and required human resources. This process also requires the identification of priority restoration sites, which is a challenging task that requires the integral evaluation of complex data. Also, ideally, the decision to restore a site must be accepted and easily understood by experts from different disciplines and by decision makers. To this end, several indices have been created to allow non-specialists to use and to integrate multidisciplinary approaches [14-16]. Different studies of beaches and coastal dunes have relied on multidisciplinary indices to assess the complexity and vulnerability of coastal systems [16-20] or the impact of tourism [21-23]. For example, the ReDune index [24] was designed to account for the numerous variables that should be considered during coastal dune restoration efforts. This index can also be applied to decide between three management interventions: restoration, rehabilitation, or conservation. Finally, in cases, where more than one coastal dune system is being evaluated, this index can determine the site(s) with the greatest need for restoration.

The goal of the present study was to evaluate the degree of perturbation and the need for restoration of a 90 km beach along the coast of the Marismas Nacionales Biosphere Reserve in Nayarit. The conservation and restoration of coastal ecosystems are particularly important at this site, as Marismas Nacionales is the largest wetland area along the Mexican Pacific Coast and contains several endangered species that are dependent on the connection of wetlands, beaches and dunes. In addition, many local livelihoods depend on the ecosystem services provided by this marine system, which offers flood protection and enables the operation of fisheries, for example.

2 Methods

2.1 Study area

Marismas Nacionales (MaNas) is a large estuarine complex (220,000 ha) located on the northwestern Mexican Pacific Coast in the alluvial plain of Nayarit and southern Sinaloa (22°15’04’’, 22°17’07’’ N and 105°11’05’’, 105°13’36’’ W). The climate is subtropical warm sub-humid, or type Aw under the Köopen classification, with an average annual rainfall above 1,550 mm and an average annual temperature of 26–28 °C. MaNas was identified as one of the areas with the highest geomorphological and biological diversity in Mexico [25]. The area has a complex topography and encompasses multiple natural systems such as beaches, coastal dunes, dune-slacks, lagoons, herbaceous wetlands and mangroves, which have been threatened by agriculture, cattle ranching, aquaculture and touristic development (Figure 1).

Dieses Werk ist copyrightgeschützt und darf in keiner Form vervielfältigt werden noch an Dritte weitergegeben werden.
Es gilt nur für den persönlichen Gebrauch.

Figure 1: Complex landscapes in Marismas Nacionales: (a) connected dunes and wetlands, (b) mangrove forest and beach, (c) dry forest along the San Pedro River, and (d) aquaculture ponds built over herbaceous wetlands and dunes

The MaNas Biosphere Reserve (MaNas-BR) was accepted as part of UNESCO's Man and Biosphere Program in 2010 and has a total area of 133,000 ha, including a core zone of 208.79 ha (Figure 2). The MaNas-BR is currently inhabited by 2,219 people in four localities [25]. In total, 321 localities (233,825 inhabitants) are located throughout the coastal plain.

Uncoordinated governmental efforts to increase productivity and to alleviate poverty in the region have inadequately assessed environmental and economic trade-offs and largely promoted economic activities such as agriculture and shrimp farming, resulting in the modification of the hydrosedimentary flux of the region.

2.2 Assessing restoration needs with the Restoration of Coastal Dunes Index

The Restoration of Coastal Dunes Index (ReDune) was applied in 90 sites along the coast of Marismas Nacionales. The ReDune index is a weighted checklist that was developed with the help of a multidisciplinary expert panel that included geomorphologists, ecologists and anthropologists. The index is integrated by 36 hierarchically-organized indicators that are grouped into two general categories: elements with a positive influence on foredunes and those with a negative influence (Figure 3). The elements with a positive influence facilitate ecosystem recovery, e.g., societal interest in conservation actions may encourage the implementation of restoration projects. Meanwhile, the elements with a negative influence have a detrimental impact on foredunes, e.g., the presence of high degree of perturbation or other factors that cause stress to a system.

Dieses Werk ist copyrightgeschützt und darf in keiner Form vervielfältigt werden noch an Dritte weitergegeben werden.
Es gilt nur für den persönlichen Gebrauch.

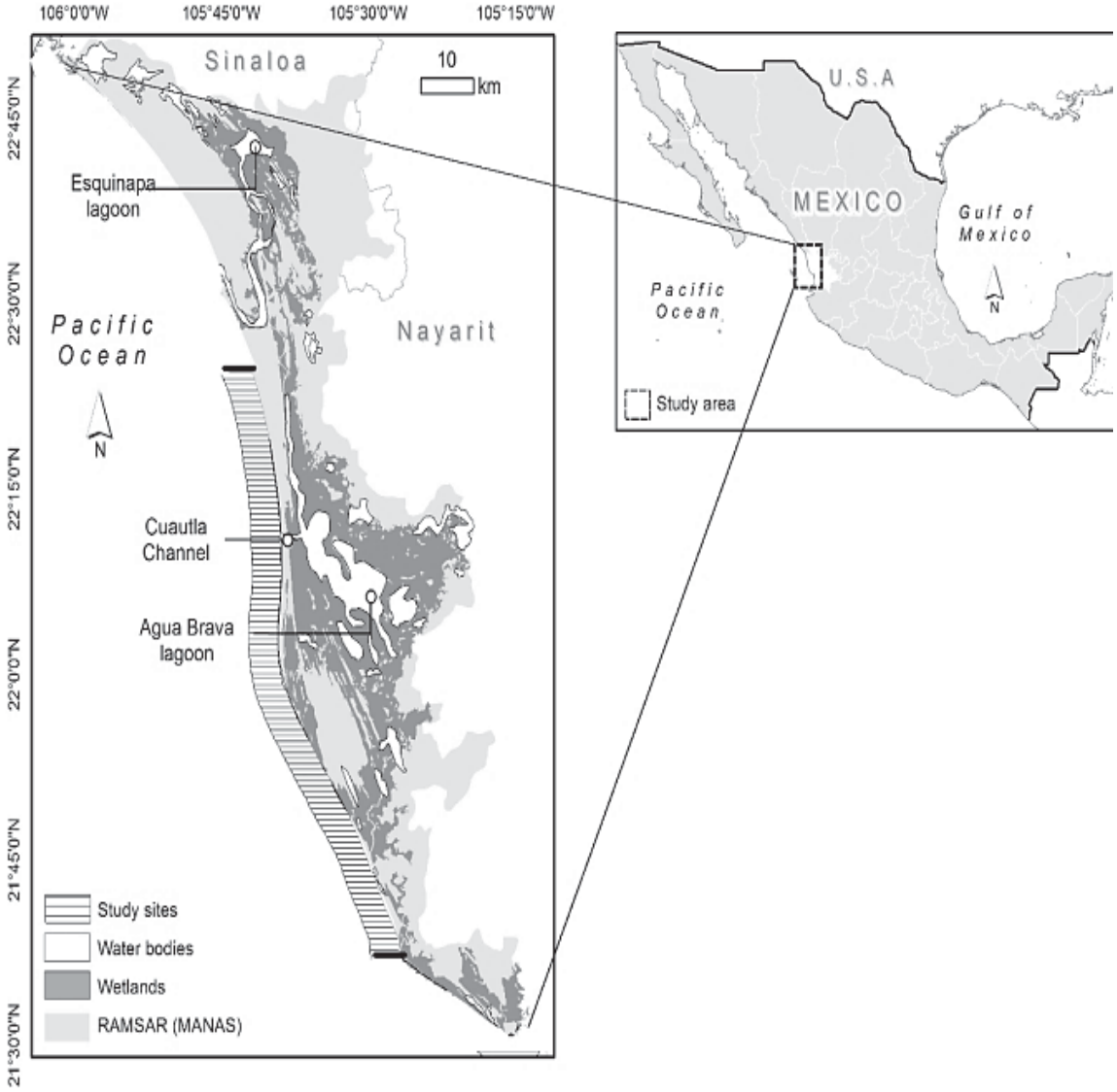

Figure 2: Location of the study area: Marismas Nacionales, Nayarit, and distribution of water bodies, wetlands and RAMSAR site.

At each site, the beach and foredune were inspected and a 200 m long segment was selected based on two factors: the environmental conditions (physical and ecological) of the fragment including the degree of human pressure had to be homogeneous, and the site had to be representative of the area in general. Then, at each site, a checklist was followed in order to obtain all variables required for calculating the indicators of the ReDune index.

3 Results and Discussion

3.1 Main findings

Of the 90 study sites, 30 were in a good state of conservation, while 54 presented signs of degradation but also qualified as potential restoration sites. The remaining 6 sites were seriously degraded, and their biotic and/or abiotic conditions negated the possibility of affordable or

Dieses Werk ist copyrightgeschützt und darf in keiner Form vervielfältigt werden noch an Dritte weitergegeben werden.
Es gilt nur für den persönlichen Gebrauch.

successful restoration efforts within the short to medium term. However, these latter sites could be candidates for rehabilitation or the introduction of green infrastructure (Figure 4).

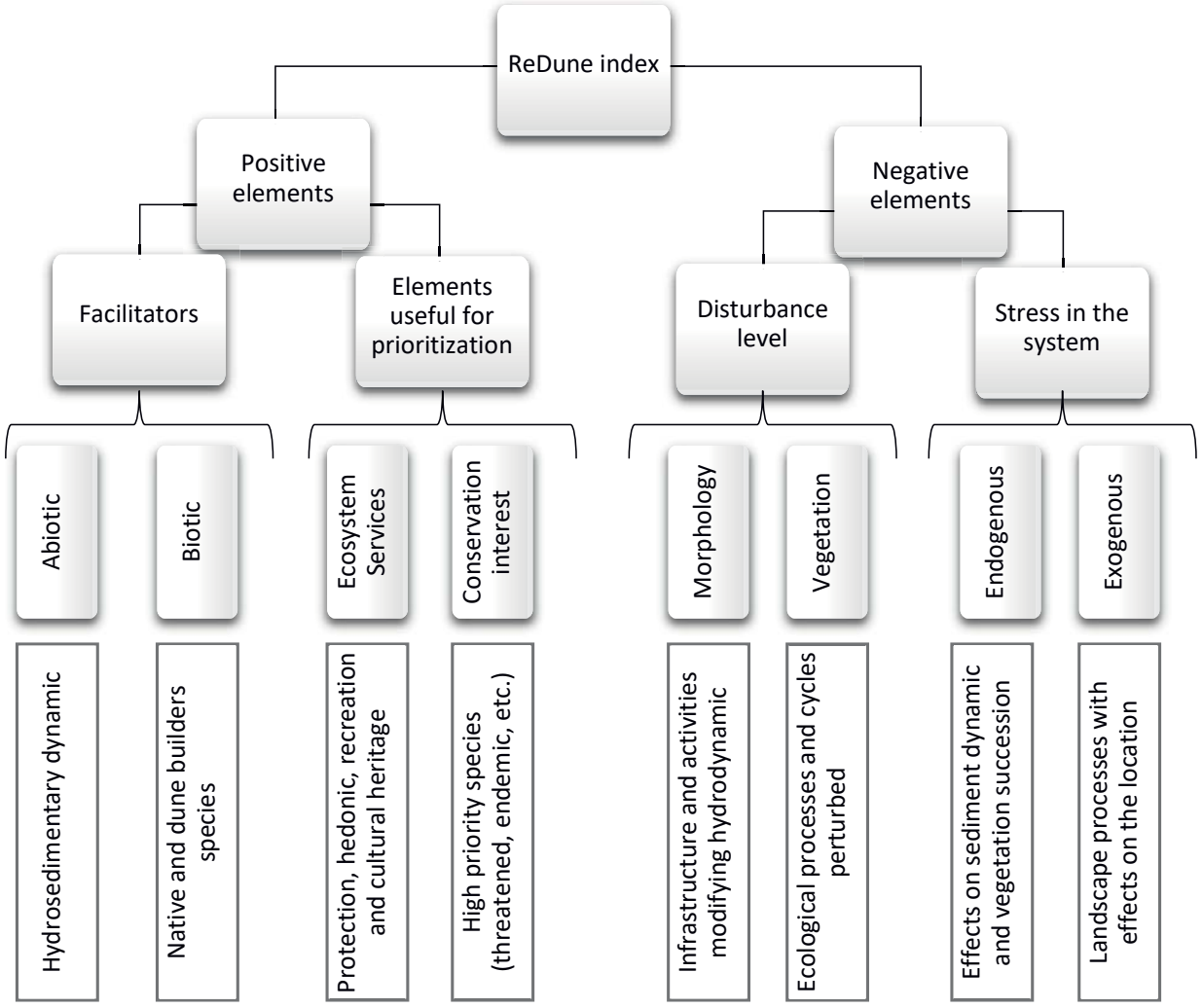

Figure 3: Elements considered in the ReDune index.

3.2. Sites in a good state of conservation

One-third of the sites did not have notable signs of perturbation. These sites had wide, dry beaches with a high rate of sediment transport to the foredune in addition to an extensive vegetation cover of native and dune-builder species. Also, these sites were inaccessible to tourists.

3.3. Sites in need of restoration

More than half of the sites were in need of restoration and also deemed suitable for restoration efforts. The majority of these sites had a low degree of urbanization in addition to artificial channels that had been dredged to facilitate navigation between the sea and nearby water bodies, resulting in modifications to the dune slacks. Such channels affect the complex hydrosedimentary dynamics of coastal systems and cause erosion.

Dieses Werk ist copyrightgeschützt und darf in keiner Form vervielfältigt werden noch an Dritte weitergegeben werden.
Es gilt nur für den persönlichen Gebrauch.

Also, human pressures were evident at some sites, including cattle tramping, the presence of temporary structures (stilt houses) on foredunes, and coconut plantations (Figure 5). However, the stress factors in these cases can be controlled, and existing perturbations may be reversible. Likewise, at these sites, propagules of dune plants were present in nearby dune systems, which can potentially facilitate restoration. Finally, the existence of human interests that are at risk was another factor used to prioritize restoration interventions at these sites.

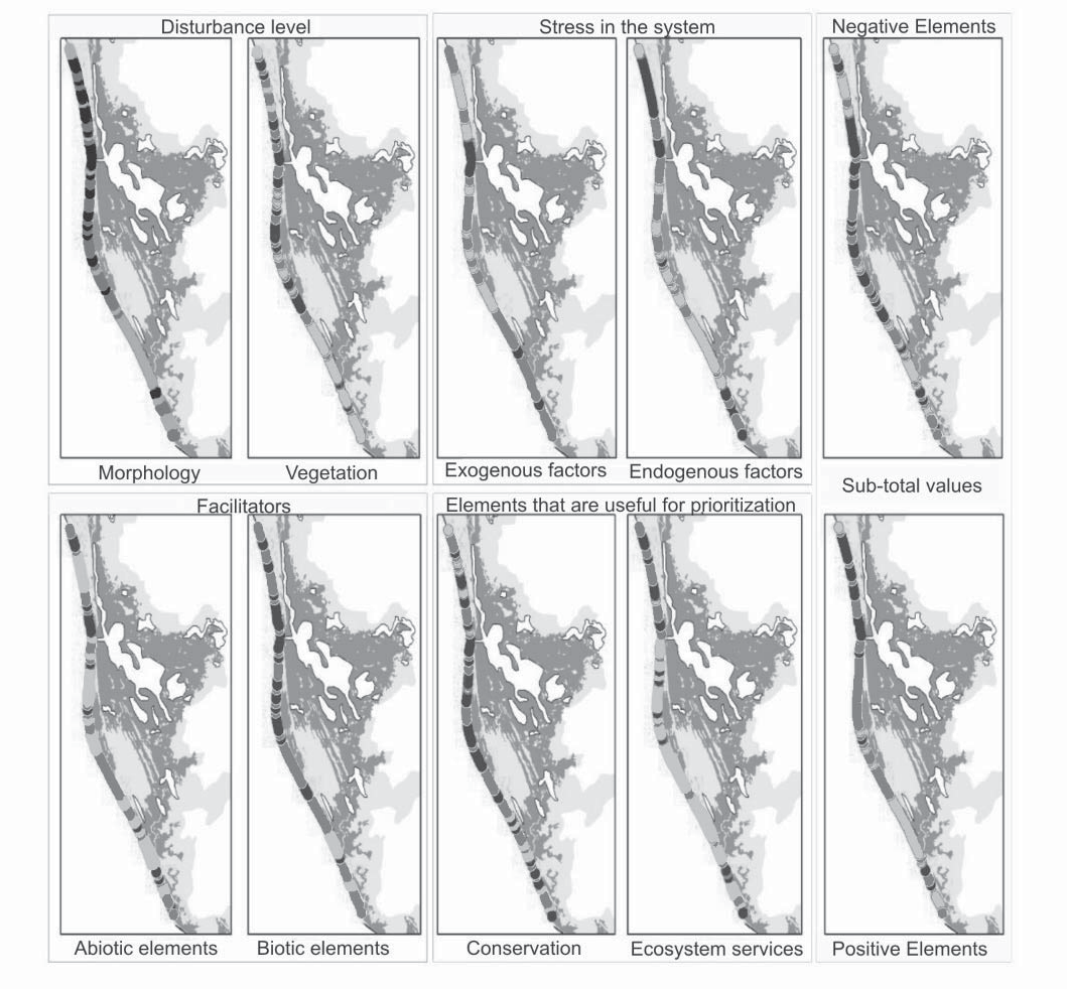

Figure 4: Redune index variables evaluated at 90 study sites. The darker dots indicate higher values in each variable.

3.4. Sites with a need for rehabilitation with green infrastructure

Less than 10% of evaluated sites did not have restoration potential. This was mainly due to high levels of stress at these sites (e.g., the presence of urban areas) or the presence of poorly planned coastal infrastructure that had interrupted sedimentary dynamics. The most infamous project in the area is the Cuautla Channel. This originally small breaching channel was constructed to connect the sea with the Agua Brava Lagoon in 1970. The channel has continuously grown and is currently almost 600 m wide and 15 m deep [26], causing extreme erosion and property loss (Figure 5). More recently, the construction of breakwaters and small dredging channels has significantly

Dieses Werk ist copyrightgeschützt und darf in keiner Form vervielfältigt werden noch an Dritte weitergegeben werden.
Es gilt nur für den persönlichen Gebrauch.

modified the sediment dynamics of some beaches. Most sites in this latter category do not have the necessary elements for restoration since their hydrosedimentary dynamics have been modified or interrupted. However, because of the risk to human infrastructure, rehabilitation actions, including the implementation of green infrastructure projects, are strongly recommended.

Figure 5: (a) Coconut plantation and cattle ranching over dunes, (b) loss of foredune, (c) erosion caused by the Cuautla Channel, and (d) infrastructure built behind dunes without erosion problems

4 Conclusions

The ReDune index was applied to 90 sites along the coast of the Marismas Nacionales Biosphere Reserve. The index distinguished sites in a good state of conservation (30 sites), degraded sites that are candidates for restoration (54 sites), and highly degraded sites, where rehabilitation is the only viable option (6 sites). Accordingly, this index facilitates the prioritization of restoration or rehabilitation actions upon considering various elements at coastal sites with different levels of degradation.

After selecting the priority restoration sites, the strategies for implementing restoration efforts should be based on an ecosystem-based approach. The implementation of green infrastructure represents one good strategy to restore or to rehabilitate sites. Projects developed according to the principles of ecosystem-based management or green infrastructures follow the same rationale: Functional ecosystems (healthy, resilient, etc.) must be preserved or recovered, when needed, in order to ensure the provision of multiple ecosystem services. From this perspective, the restoration of multiple ecosystem services is a desirable outcome of ecological restoration efforts. Also, the restoration or preservation of the multifunctionality of coastal ecosystems enables several benefits to be obtained from the same spatial area. Therefore, under this mode of restoration, multiple objectives can be met: the protection/recovery of landscape

Dieses Werk ist copyrightgeschützt und darf in keiner Form vervielfältigt werden noch an Dritte weitergegeben werden.
Es gilt nur für den persönlichen Gebrauch.

interconnectivity, the maintenance of ecosystem integrity, the conservation of biodiversity, and the provision of socio-economic benefits including jobs for local inhabitants.

5 Acknowledgments

This research was supported by the Mexican National Council of Science and Technology (CONACYT) through the postdoctoral fellowship (CONACYT-224619) awarded to DL. Also, the authors thank the EXCEED-SWINDON project, DAAD and their respective institutions for the support provided. This publication is one of the results of the Summer School on "Integrating Ecosystems in Coastal Engineering Practice-INECEP-2017," funded by the Federal Ministry for Economic Cooperation and Development, Germany, the EXCEED-SWINDON project, and DAAD.

6 References

1. Everard, M., Jones, L., Watts, B.: Have we neglected the societal importance of sand dunes? An ecosystem services perspective. Aquatic Conservation: Marine and Freshwater Ecosystems 20, 476-487 (2010)
2. Silva, R., Lithgow, D., Esteves, L.S., Martínez, M.L., Moreno-Casasola, P., Martell, R., Pereira, P., Mendoza, E., Campos-Cascaredo, A., Winckler Grez, P.: Coastal risk mitigation by green infrastructure in Latin America. Proceedings of the Institution of Civil Engineers-Maritime Engineering 1-16 (2017)
3. Nordstrom, K.F., Jackson, N.L.: Foredune Restoration in Urban Settings. In: Martínez, M.L., Gallego-Fernández, J.B., Hesp, P.A. (eds.) Restoration of Coastal Dunes, pp. 17-31. Springer Berlin Heidelberg, Berlin, Heidelberg (2013)
4. Lithgow, D., Martínez, M.L., Silva, R., Geneletti, D., Gallego-Fernández, J.B., Cerdán, C.R., Mendoza, E., Jermain, A.: Ecosystem Services to Enhance Coastal Resilience in Mexico: The Gap between the Perceptions of Decision-Makers and Academics. Journal of Coastal Research SI 77, 116-126 (2017)
5. Lithgow, D., de la Lanza, G., Silva, R.: Ecosystem-Based Management strategies to improve aquaculture in developing countries: Case study of Marismas Nacionales. Ecological Engineering (2017), in press, https://doi.org/10.1016/j.ecoleng.2017.1006.1039
6. Wickham, J.D., Riitters, K.H., Wade, T.G., Vogt, P.: A national assessment of green infrastructure and change for the conterminous United States using morphological image processing. Landscape and Urban Planning, 94, 186-195 (2010)
7. Andersson, E., Barthel, S., Borgström, S., Colding, J., Elmqvist, T., Folke, C., Gren, Å.: Reconnecting Cities to the Biosphere: Stewardship of Green Infrastructure and Urban Ecosystem Services. AMBIO 43, 445-453 (2014)
8. Snäll, T., Lehtomäki, J., Arponen, A., Elith, J., Moilanen, A.: Green Infrastructure Design Based on Spatial Conservation Prioritization and Modeling of Biodiversity Features and Ecosystem Services. Environmental Management 57, 251-256 (2016)

Dieses Werk ist copyrightgeschützt und darf in keiner Form vervielfältigt werden noch an Dritte weitergegeben werden.
Es gilt nur für den persönlichen Gebrauch.

9. Pakzad, P., Osmond, P.: Developing a Sustainability Indicator Set for Measuring Green Infrastructure Performance. Procedia - Social and Behavioral Sciences 216, 68-79 (2016)

10. Curtin, R., Prellezo, R.: Understanding marine ecosystem based management: A literature review. Marine Policy 34, 821-830 (2010)

11. Arkema, K.K., Abramson, S.C., Dewsbury, B.M.: Marine ecosystem-based management: from characterization to implementation. Frontiers in Ecology and the Environment 4, 525-532 (2006)

12. Long, R.D., Charles, A., Stephenson, R.L.: Key principles of marine ecosystem-based management. Marine Policy 57, 53-60 (2015)

13. Wasson, K., Suarez, B., Akhavan, A., McCarthy, E., Kildow, J., Johnson, K.S., Fountain, M.C., Woolfolk, A., Silberstein, M., Pendleton, L., Feliz, D.: Lessons learned from an ecosystem-based management approach to restoration of a California estuary. Marine Policy 58, 60-70 (2015)

14. Barbosa de Araújo, M.C., da Costa, M.F.: Environmental Quality Indicators for Recreational Beaches Classification. Journal of Coastal Research 24, 1439-1449 (2008)

15. Botero, C., Pereira, C., Tosic, M., Manjarrez, G.: Design of an index for monitoring the environmental quality of tourist beaches from a holistic approach. Ocean & Coastal Management 108, 65-73 (2015)

16. McLachlan, A., Defeo, O., Jaramillo, E., Short, A.D.: Sandy beach conservation and recreation: Guidelines for optimising management strategies for multi-purpose use. Ocean & Coastal Management 71, 256-268 (2013)

17. García-Mora, M., Gallego-Fernández, J., Williams, A., Garcia-Novo, F.: A coastal dune vulnerability classification. A case study of the SW Iberian Peninsula. Journal of coastal research 17, 802-811 (2001)

18. Martínez, M.L., Gallego-Fernández, J.B., García-Franco, J.G., Moctezuma, C., Jiménez, C.D.: Assessment of coastal dune vulnerability to natural and anthropogenic disturbances along the Gulf of Mexico. Environmental Conservation 33, 109-117 (2006)

19. Muñoz-Vallés, S., Gallego-Fernández, J.B., Dellafiore, C.M.: Dune Vulnerability in Relation to Tourism Pressure in Central Gulf of Cádiz (SW Spain), a Case study. Journal of Coastal Research 27, 243-251 (2011)

20. Williams, A.T., Alveirinho-Dias, J., Garcia Novo, F., García-Mora, M.R., Curr, R., Pereira, A.: Integrated coastal dune management: checklists. Continental Shelf Research 21, 1937-1960 (2001)

21. Leatherman, S.P.: Beach Rating: A Methodological Approach. Journal of Coastal Research 13, 253-258 (1997)

Dieses Werk ist copyrightgeschützt und darf in keiner Form vervielfältigt werden noch an Dritte weitergegeben werden.
Es gilt nur für den persönlichen Gebrauch.

22. Micallef, A., Williams, A.T., Gallego-Fernandez, J.B.: Bathing Area Quality and Landscape Evaluation on the Mediterranean Coast of Andalucia, Spain. Journal of Coastal Research SI 61, 87-95 (2011)

23. Phillips, M.R., House, C.: An evaluation of priorities for beach tourism: Case studies from South Wales, UK. Tourism Management 30, 176-183 (2009)

24. Lithgow, D., Martínez, M.L., Gallego-Fernández, J.B.: The "ReDune" index (Restoration of coastal Dunes Index) to assess the need and viability of coastal dune restoration. Ecological Indicators 49, 178-187 (2015)

25. Comisión Nacional de Áreas Naturales Protegidas (CONANP): Programa De Manejo Reserva De La Biosfera Marismas Nacionales Nayarit. CONANP, Mexico City, Mexico, 199p: http://www.conanp.gob.mx/datos_abiertos/DGCD/118.pdf (2013)

26. Ochoa, C.F., Baldwin, E.M., Casarín, R.S., Martínez, G.R.: Hydro-morphologic Revision of the Cuautla Channel at Nayarit, Mexico. CLEAN – Soil, Air, Water 40, 920-925 (2012)

Dieses Werk ist copyrightgeschützt und darf in keiner Form vervielfältigt werden noch an Dritte weitergegeben werden.
Es gilt nur für den persönlichen Gebrauch.

ELEMENTS INDUCING COASTAL SQUEEZE ON THE COAST OF SABANCUY, CAMPECHE, MEXICO

Debora L. Ramírez-Vargas[1], Edgar Mendoza[1], Debora Lithgow[1,2], Rodolfo Silva[1]

[1]Instituto de Ingeniería, Universidad Nacional Autónoma de México, CU, 04510 CDMX, México. DRamirezV@iingen.unam.mx

[2]Departamento de Biología Vegetal y Ecología, Universidad de Sevilla, 41080, Sevilla España

Keywords: coastal squeeze, coastal ecosystems, hard structures, land use change, sea level rise

Abstract

The term coastal squeeze describes the process, in which rising sea levels and other factors, such as increased storminess and coastal subsidence, push coastal habitats landward. Also, the presence of hard structures along coastlines can create static, artificial margins between the land and the sea, restricting coastal habitats to a narrowed zone. Rising ground levels with respect to the coastal plain, which may be caused by impeded hydrosedimentary flow, can also form additional natural barriers. In particular, the coast of Mexico is vulnerable to increasing sea levels, yet other more rapidly occurring processes could be inducing coastal squeeze to a greater extent, such as coastal subsidence, extreme hydro-meteorological phenomena, land use changes and erosion stemming from the retention of sediments in upper coastal basins. The objective of this study was to analyze coastal squeeze along the coast of Sabancuy in the state of Campeche, Mexico, through identifying the variables for the first time that are determinative of coastal squeeze in this area. The processes examined land use changes, storm incidence and the presence of hard structures, among other factors, which have rapidly increased in the study area in recent years and have caused the loss of coastal ecosystems. Ultimately, one of the goals is to create a methodology that can quantitatively measure the effects of coastal squeeze in different coastal zones. This study presents the first steps: the identification of variables that influence coastal squeeze and an assessment of their importance. The resulting methodology would serve as a tool for decision makers and for the sustainable management of coasts.

1 Introduction

Coastal squeeze is the process, in which the functioning of the intertidal zone of a coastline is reduced or completely lost. This process can be caused by natural and anthropogenic factors, whether marine or terrestrial [1-3]. Natural processes that impact coastal squeeze are related to the sea, to the tide, to storms and rising sea levels (*e.g.*, the increased eustatic rise of sea levels as a result of coastal subsidence). The main anthropogenic factor that causes coastal squeeze is the increasing development of urban, commercial and tourist infrastructure in the coastal zone. Coastal infrastructure is a static barrier that prevents the inland migration of coastal systems

Dieses Werk ist copyrightgeschützt und darf in keiner Form vervielfältigt werden noch an Dritte weitergegeben werden.
Es gilt nur für den persönlichen Gebrauch.

(Figure 1), thereby reducing resilience to extreme events (*e.g.*, hurricanes) and lowering the capacity of coastal systems to adapt to natural phenomena (*e.g.*, subsidence). Natural static barriers such as cliffs also prevent the inland migration of coastal ecosystems.

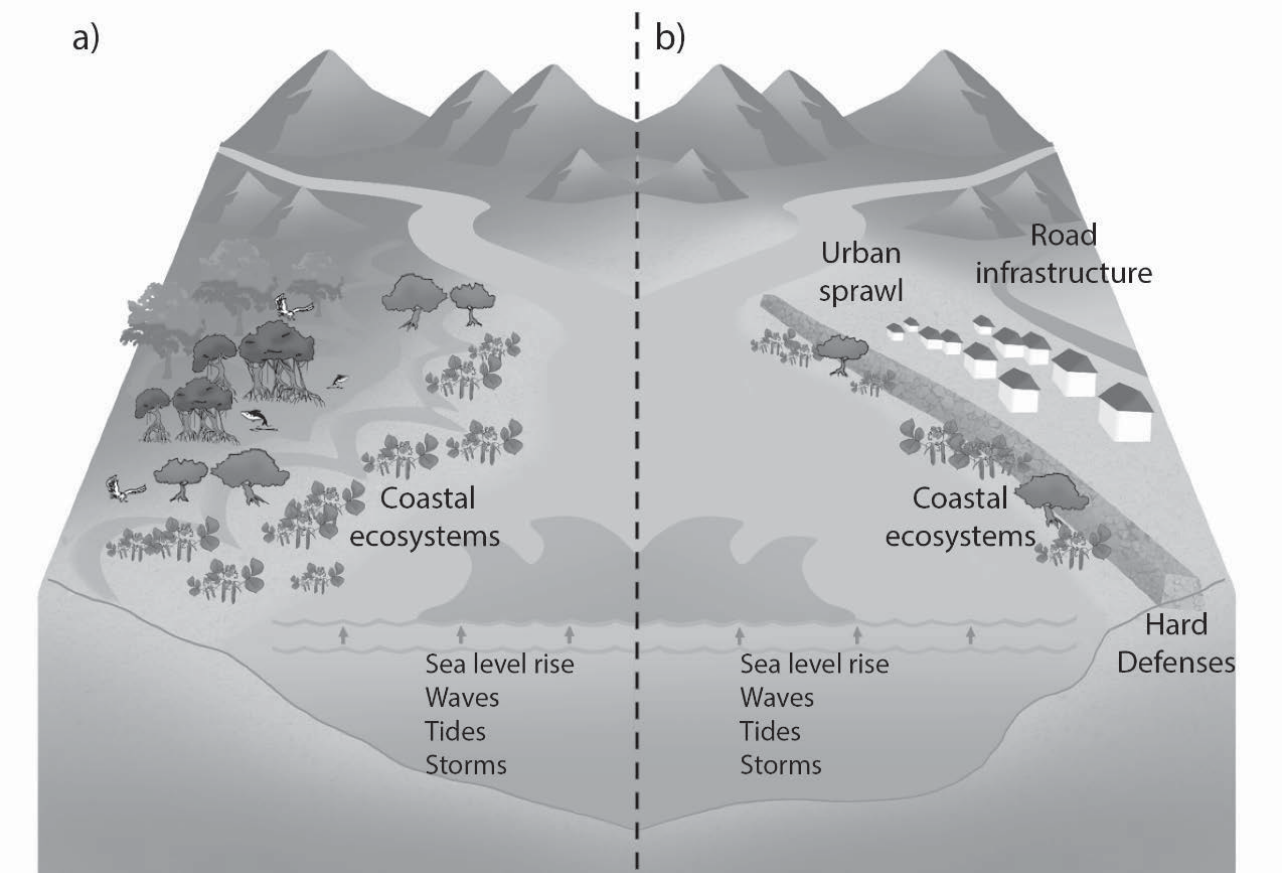

Figure 1: Illustration of coastal squeeze. (a) Healthy coastal ecosystems can adapt to new conditions (*e.g.*, rising sea level) by migrating landward. (b) The presence of artificial static barriers (*e.g.*, infrastructure) can squeeze coastal ecosystems within a narrowed area and prevent the landward migration of these ecosystems. (Source: [4], modified)

In addition, coastal squeeze creates competition between the ecosystems located in the intertidal zone, endangering their health, integrity and resilience. Wetlands, beaches and dunes are among the ecosystems most threatened by coastal squeeze despite the recognized value of these ecosystems. The loss of these ecosystems is a pressing concern, as they provide a wide array of ecosystem goods and services, including carbon sequestration, water purification, coastal protection, flood regulation and biodiversity support. In recent years, several studies have demonstrated that coastal dunes contribute to the delivery of ecosystem services such as protection against floods, recreation, salinization prevention and drinking water protection. In addition, existing ecosystems can be used in nature-based solutions to address numerous environmental, social and economic challenges [5-7].

Dieses Werk ist copyrightgeschützt und darf in keiner Form vervielfältigt werden noch an Dritte weitergegeben werden.
Es gilt nur für den persönlichen Gebrauch.

At one point, coastal squeeze was considered to be solely caused by climate change and rising sea levels [2]. However, at the end of the 1980s, the construction of coastal protection works was observed to contribute to erosion [2]. Anthropogenic modifications were then increasingly recognized to produce a narrowing of the intertidal zone. Subsequently, other elements that generate coastal squeeze are identified, such as changes in land use or in the duration and intensity of storms [3, 8] The origin and consequences of coastal squeeze are examined from numerous perspectives. The present study aims to explore coastal squeeze from biological, ecological, socioeconomic, ecosystem management and climate change perspectives, which are the most addressed ones in the academic literature.

While the effects of climate change on sea levels and on coastal ecosystems are globally recognized and extensively covered in the literature [9], such studies are mostly performed in northern European countries, where higher impacts are expected from rising sea levels. Undoubtedly, the coasts of Mexico and, especially, the Gulf of Mexico are vulnerable to climate change and associated rises in sea levels. Nevertheless, coastal squeeze in this region may be even more influenced by processes occurring at a faster rate, e.g., disordered urban growth, erosion resulting from the retention of sediments in upper coastal basins or extreme hydrometeorological phenomena. Therefore, the objective of the present study was to identify the factors that induce coastal squeeze along the coast of Sabancuy, Campeche, Mexico, and to suggest a method for their quantification.

2 Materials and Methods

2.1 Study area

Campeche has 523 km of coastline, a continental shelf of 51,100 km^2 (second largest nationally) and 2,200 km^2 of coastal lagoons. The main economic activities of the state are fishing, beekeeping, agriculture and livestock ranching [10]. Campeche is a highly biodiverse state [11] that has experienced increasing environmental deterioration in recent years as a result of human activities, including the establishment of recreational sites and tourist infrastructure on the coast. The Términos Lagoon is located at 91°00' and 92°22' W and 18°25' and 19°00' N. This lagoon forms part of the Grijalva-Usumacinta hydrological region and has an average annual precipitation of 1,426.8 mm and an average annual temperature of 26.9 °C [12]. The lagoon has an area of 1,971 km^2, a length of 70 km, a width of 26 km and an average depth of 3.5 m [13]. Two mouths, one to the west of Del Carmen (4 km long) and one to the east of Puerto Real (3.3 km long), connect the lagoon to the sea.

The Sabancuy Estuary (18°59'10" N and 90°10'31" W) is located in the eastern portion of Términos Lagoon. The estuary has an extension of 470 km^2 (Figure 2) and two mouths: The first mouth connects to the extensive floodplains of the Términos Lagoon, and the second one connects to an artificial channel that flows toward an adjacent coastal area [14].

The surface hydrology is characterized by waterlogged conditions and low water flow including sinking ground levels, high salt content and the presence of small permanent lagoons. The area

Dieses Werk ist copyrightgeschützt und darf in keiner Form vervielfältigt werden noch an Dritte weitergegeben werden.
Es gilt nur für den persönlichen Gebrauch.

contains several landforms of less than 10 m in height that slightly incline toward the coast, creating extensive plains and small undulations called “cuyos,” which are small mounds with distinct soil conditions [15].

The localities of Isla Aguada and Sabancuy are located in the Sabancuy Estuary and have a population of 6,204 and 7,286 inhabitants, respectively. The main economic activity in these localities is fishing, although some agricultural activities are also present [16].

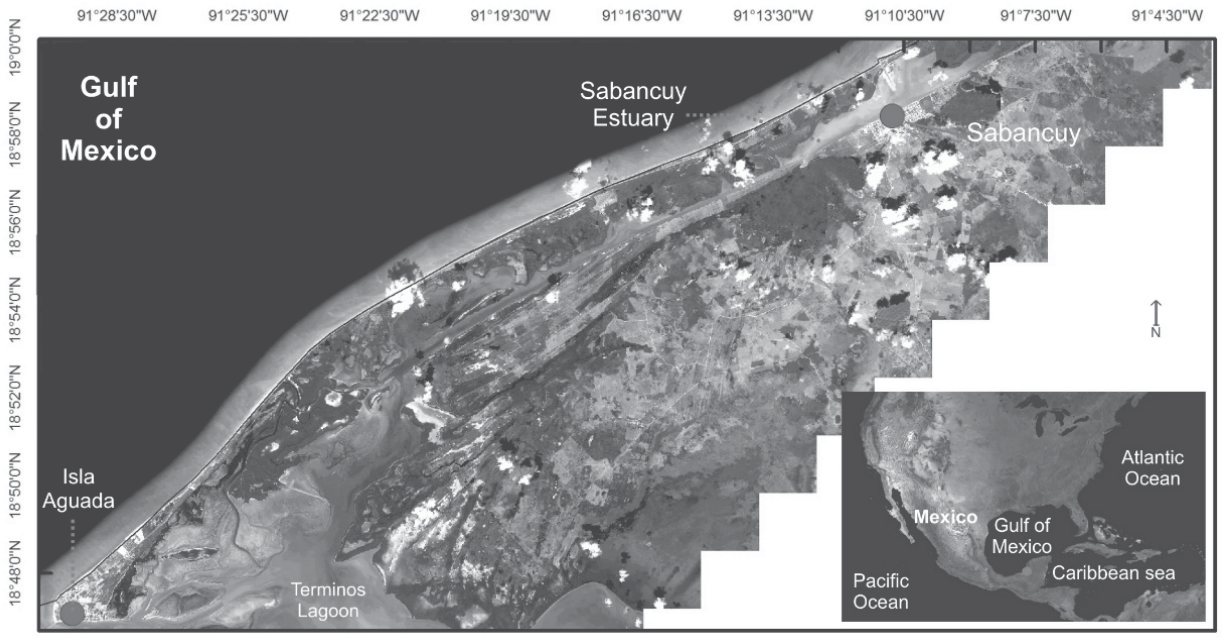

Figure 2: Location of the Sabancuy Estuary in the Gulf of Mexico. The remaining natural vegetation (seagrasses and mangrove forests) and the presence of hard structures that have caused erosion at the public beach are shown.

The transport of sediments is from east to west, corresponding with the division of the Sabancuy coastline into two parts. The eastern portion is composed of private properties and has a beach wider than 40 meters that is protected by a seawall along a channel used by fishermen. The western portion serves as a pubic beach, which is less than 20 meters in width, and is protected by two hard structures. This latter side of the beach experiences erosion stemming from the placement of seawalls that prevent the transport of sediment to this area.

2.2 Identification of variables inducing coastal squeeze

The variables that induce coastal squeeze were identified, based on the definition of coastal squeeze and scientific articles that have evaluated coastal squeeze in the study area. The factors causing coastal squeeze were confirmed in satellite images of Google Earth. First, all factors were divided into natural or anthropogenic, and then the factors were further divided into those related to land or to water. According to the literature, the most important natural variables affecting coastal squeeze are raising sea level, waves, tides, storms and erosion. The most important

Dieses Werk ist copyrightgeschützt und darf in keiner Form vervielfältigt werden noch an Dritte weitergegeben werden.
Es gilt nur für den persönlichen Gebrauch.

anthropogenic variables are land use changes, population density, infrastructure development and fishing. Table 1 details the variables that are the key determinants of coastal squeeze in the study area. The methodology for evaluating these variables in the study area is described in greater detail at following.

Table 1: Variables for quantifying coastal squeeze

Natural variable		Anthropogenic variable	
Variable	Unit	Variable	Unit
Sea level rise	Meters (m)	Land use changes	Square meters (m^2)
Wave height	Meters (m)	Population density	Habitant/square meters (m^2)
Frequency and intensity of storms	Years	Infrastructure development (roads and bridges, houses, hotels, beaches and recreation areas)	Square meters (m^2)
Erosion	Meters (m)	Coastal protection works	Square meters (m^2)
Accretion	Meters (m)	Fishing	National currency ($)

A database of the variables identified as determinants of coastal squeeze was created. The next task was to determine the relative importance of each variable that can be based on the degree, to which the identified variables impact coastal squeeze in the study area. The method for quantifying coastal squeeze should reflect the degree of the resulting ecological and socio-economic effects in the study area.

The variables of storms and coastal subsidence were deemed as the main variables that induced coastal squeeze in the study area. Climate change and the associated rise in sea levels are other important factors that affect coastlines around the world. Nevertheless, in the study zone, the factors that most impacted ecosystem loss appeared to be operating in the shorter term such as storms and the development of infrastructure along the coast.

According to the identified variables and their impacts on the study area, the ways were highlighted, in which these different variables could be used to quantify coastal squeeze as part of the first steps in formulating a quantitative methodology.

Dieses Werk ist copyrightgeschützt und darf in keiner Form vervielfältigt werden noch an Dritte weitergegeben werden.
Es gilt nur für den persönlichen Gebrauch.

3 Results and Discussion

The variables identified in the satellite images [16] included natural processes such as sediment transport and the direction of sediment transport as well as the distribution of local vegetation. However, the anthropogenic variables were most represented in the images including the development of new localities, roads and infrastructure (Figure 3).

In Figure 4, several additional variables inducing coastal squeeze in the study area are evident (e.g., land use changes and hard structures). These variables are described, based on data obtained from government institutions and their corresponding databases. Other variables were based on studies previously performed in the study area and the documented effects of different processes such as erosion.

In the following paragraphs, the variables determined to influence coastal squeeze in the study area are described. The identification of these variables is perhaps the one of the most important steps in this process, as all coastal zones are unique in their hydrosedimentary dynamics and physical processes.

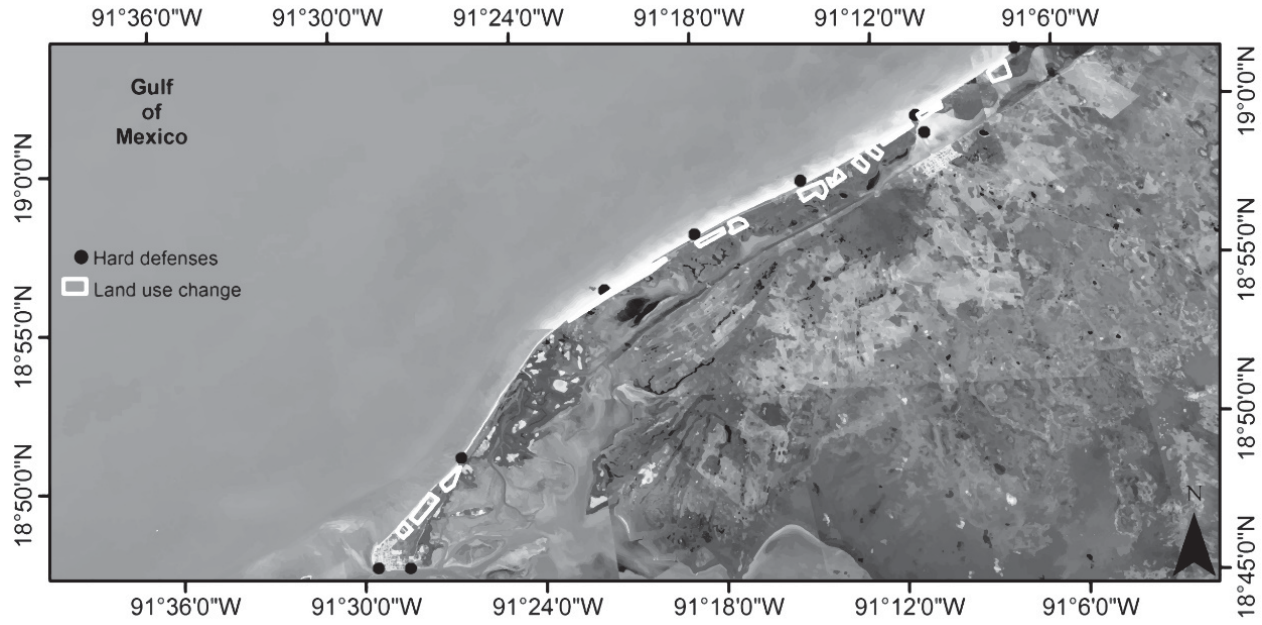

Figure 3: Land use changes and the location of hard defences for storm protection (breakwaters, harbour works, *etc.*) in Sabancuy, Campeche

The results indicated that the frequency and intensity of storms, which is a natural factor, is the variable with the greatest influence on coastal squeeze. Meanwhile, land use change is the most impactful anthropogenic variables. At the following, the identified variables and the data to be included in the quantitative model are listed.

Dieses Werk ist copyrightgeschützt und darf in keiner Form vervielfältigt werden noch an Dritte weitergegeben werden.
Es gilt nur für den persönlichen Gebrauch.

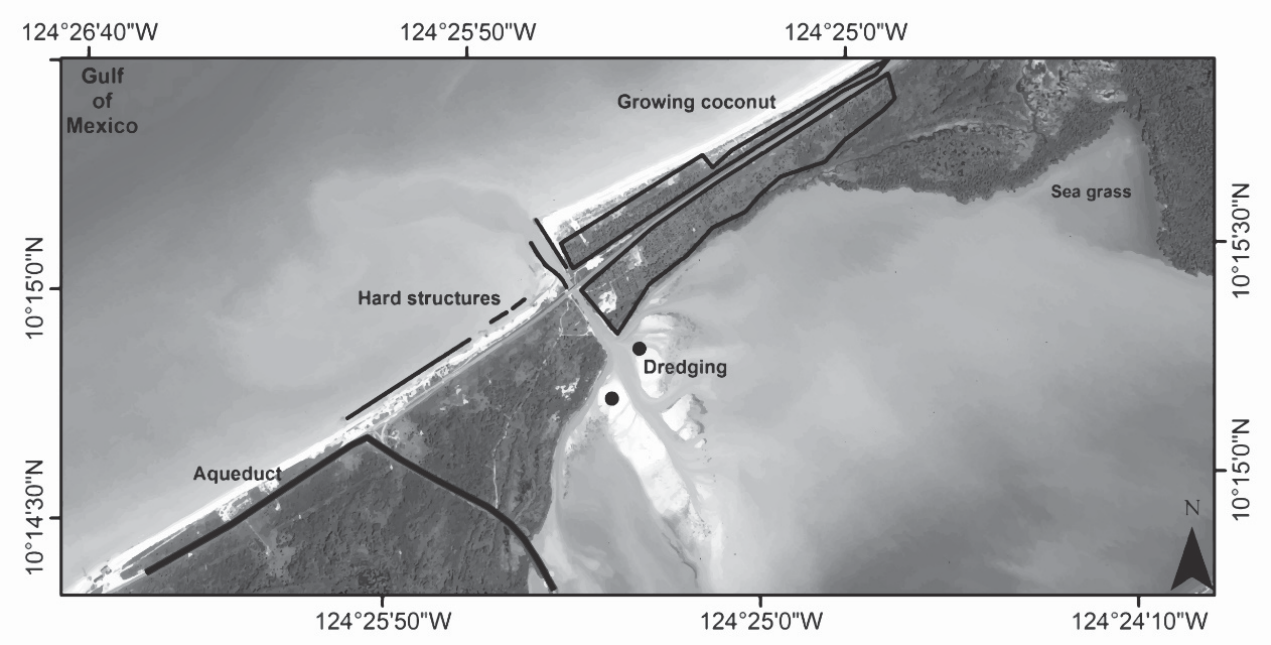

Figure 4: Variables inducing coastal squeeze in the study area

The *natural variables* that are most determinative of coastal squeeze are as follows:

- *Sea level rise*: Several scenarios for sea level increase are considered (8 cm by 2030, 13.5 cm by 2050, and 33 cm by 2100) [17, 18].
- *Waves*: The normal conditions of waves versus those of storm surges are considered in order to determine their relationship with other variables. The data obtained from one study [19] indicated that waves have a height of 65 to 100 cm and approach the coastline every 7 to 10 seconds.
- *Frequency and intensity of storms*: A bibliographic search identified all extreme events recorded in the area and their associated socioeconomic effects. Since 1961, an extraordinary storm occurred in the area every 7 years. However, since the passage of Hurricane Isidore in 2002, no additional storms have affected the zone. This may be due to the El Niño and La Niña phenomena [17].
- *Erosion and accretion*: Digital images of different years (2004, 2005, 2014, and 2016) were considered [20]. From satellite images, erosion can be observed at the western portion of the study area, while accretion can be observed at the eastern portion, which is likely caused by the two breakwaters located at the mouth of the Sabancuy Estuary. The erosion to the west is greater than 10 m and, therefore, coincides with the accretion phenomenon to the east [21].

The resulting *anthropogenic variables* that are determinative of coastal squeeze are as follows:

- *Land use changes*: Digital images of different years (2004, 2005, 2014 and 2016) were considered [21]. Changes to land once occupied by vegetation were observed, including the replacement of vegetation with localities or agriculture activity. However, in future work, it is aimed to delimit and to classify land uses and vegetation in order to generate descriptive

Dieses Werk ist copyrightgeschützt und darf in keiner Form vervielfältigt werden noch an Dritte weitergegeben werden.
Es gilt nur für den persönlichen Gebrauch.

maps of land use changes that would enable such changes to be observed and to be quantified in m^2 [22].

- *Population density*: The population density for the state of Campeche is 16 inhabitants/km^2 [23]. In the following step, it is aimed to quantify the rate of population growth in the coastal region.
- *Infrastructure development and coastal protection works*: Environmental Impact Manifestations (MIAs) detailing the works to be carried out in the Federal Terrestrial Maritime Zone were analyzed [24]. After identifying the works, a database was compiled in order to identify the potential impacts, as listed in the MIAs, in addition to modifications of coastal sites, required investment and the objectives of the works. Nine structures were identified impacting the environment, although six will likely have a high impact and induce coastal squeeze, including roads, an aqueduct, a dredged channel and breakwaters (Figure 4).
- *Fishing*: Fishing activity contributes 10% of the Mexico's gross domestic product [23]. It is aimed to obtain data from the government agency of CONAPESCA [25], which records fishery production at local and national levels.

The greatest threat facing coastal areas is coastal squeeze [9, 26]. Beaches are caught between rising sea levels, erosion and increasing coastal developments. The resulting narrowing of beaches prevents the migration of coastal ecosystems inland [27, 28], leading to the degradation of coastal ecosystems and to the declining provision of ecosystem services such as protection from storms. Infrastructure is another threat in coastal areas. Based on initial results of the study, it is suggested to use fuzzy logic methods. Such a methodology can be used in order to determine whether or not coastal squeeze exists in a given area and to propose different solutions that would preserve both coastal ecosystems and key economic activities. The concrete benefits of this tool rest on its ability to be applied in numerous coastal areas and its use of a mathematical model, which will enable greater precision.

If sea levels increase in the absence of coastal structures, the intertidal zone can move inland without loss or reduction of the habitats in this zone. However, when coastal defense works are present, the landward movement of ecosystems is limited. Therefore, in combination with increasing sea level, coastal habitats are squeezed. An ongoing process of coastal squeeze could potentially lead to the disappearance of coastal ecosystems [1].

Studies around the world modelled and predicted changes in the flooding or erosion of coasts with increasing escarpment or inclination as well as changes at beaches that reduced the areas following increasing sea level [1, 3, 8, 9]. Other studies also noted the effects of the construction of artificial structures or the increasing duration and intensity of storms [29, 30]. Interestingly, rocky coasts or cliffs, where the shore is completely steep, constitute about 80% of the world's oceanic coasts, yet these coasts have not been studied [9, 30]. In these cases, a static natural barrier is also present, and rising sea level could similarly generate coastal squeeze [31].

Dieses Werk ist copyrightgeschützt und darf in keiner Form vervielfältigt werden noch an Dritte weitergegeben werden.
Es gilt nur für den persönlichen Gebrauch.

The major ecosystems threatened by coastal squeeze are dunes and wetlands. The disappearance of these ecosystems is worrying because they provide a wide variety of ecosystem goods and services such as hurricane protection. In addition to coastal squeeze, coastal ecosystems are degraded by numerous natural and anthropogenic causes. For example, erosion, salinization, drought, groundwater extraction, pollution from agricultural and urban runoff, and construction of borders and dams, among others [30].

Beaches and coastal dunes are dynamic ecosystems capable of responding to different factors, wherein natural perturbations form part of the dynamics of these ecosystems [5, 32]. The capacity of coastal ecosystems to resist external agents of perturbation without losing their current or potential functions (resistance) will depend on numerous morphological, ecological and socioeconomic factors [33]. However, the presence of infrastructure on the coast, for example, modifies coastal morphology and functioning, and thereby limits the capacity of associated ecosystems to respond to perturbations [3, 29].

The coast of Sabancuy is endangered by the development of infrastructure, land use changes and the construction of protection structures, which cause erosion and changes in the dynamics of sediment transport. Subsequent actions in the study area will determine whether local ecosystems are lost or conserved. A methodology for quantifying coastal squeeze would represent a useful tool for decision makers and serve to identify the main variables that influence coastal squeeze at a particular site. The first steps toward forming a quantitative methodology are highlighted in the present study.

4 Conclusions

The present study identified the natural and anthropogenic elements that induce coastal squeeze along the coast of Sabancuy. The identification of the influencing variables is an important part of determining the best model for quantifying the effects of these variables on coastal squeeze. Such a methodology would enable decision makers and planners to identify priority areas for conservation, given limited funding, and also to determine the most impactful variables that should be addressed in order to reduce coastal squeeze at a particular site.

The variables analyzed in this study suggest that the coast of Sabancuy is undergoing a process of coastal squeeze that could eliminate or degrade the associated coastal ecosystems and species, and also endanger infrastructure and human lives because of the growing risk of erosion and flooding events.

5 Acknowledgments

DRV sincerely thanks DAAD and Exceed Swindon for the opportunity and financial support to participate at the INECEP 2017 summer school program to acquire the knowledge shared by its participants. Also, DRV wishes to thank CONACyT for her fellowship [CVU546729]. All authors are thankful for the support received from their respective institutions.

Dieses Werk ist copyrightgeschützt und darf in keiner Form vervielfältigt werden noch an Dritte weitergegeben werden.
Es gilt nur für den persönlichen Gebrauch.

6 References

1. Black, Veatch: Coastal squeeze study. Report produced for the Environment Agency (2006)
2. Doody, J.P.: 'Coastal Squeeze': An Historical Perspective. Journal of Coastal Conservation 10, 129-138 (2004)
3. Pontee, N.: Defining coastal squeeze: A discussion. Ocean & Coastal Management 84, 204-207 (2013)
4. Alexandra Fries: Integration and Application Network, University of Maryland Center for Environmental Science (ian.umces.edu/imagelibrary/).
5. Lithgow, D., Martínez, M.L., Gallego-Fernández, J.B., Hesp, P.A., Flores, P., Gachuz, S., Rodríguez-Revelo, N., Jiménez-Orocio, O., Mendoza-González, G., Álvarez-Molina, L.L.: Linking restoration ecology with coastal dune restoration. Geomorphology 199, 214-224 (2013)
6. Thorslund, J., Jarsjö, J., Jaramillo, F., Jawitz, J.W., Manzoni, S., Basu, N.B., Chalov, S.R., Cohen, M.J., Creed, I.F., Goldenberg, R., Hylin, A., Kalantari, Z., Koussis, A.D., Lyon, S.W., Mazi, K., Mård, J., Persson, K., Pietroń, J., Prieto, C., Quin, A., Van Meter, K., Destouni, G.: Wetlands as large-scale nature-based solutions: Status and challenges for research, engineering and management. Ecological Engineering 108, 489-497 (2017)
7. Van der Biest, K., De Nocker, L., Provoost, S., Boerema, A., Staes, J., Meire, P.: Dune dynamics safeguard ecosystem services. Ocean & Coastal Management 149, 148-158 (2017)
8. Doody, J.P.: Coastal squeeze and managed realignment in southeast England, does it tell us anything about the future? Ocean & Coastal Management 79, 34-41 (2013)
9. Schleupner, C.: Evaluation of coastal squeeze and its consequences for the Caribbean island Martinique. Ocean & Coastal Management 51, 383-390 (2008)
10. PED-Campeche: Plan Estatal de Desarrollo de Campeche. pp. 136. Gobierno del estado de Campeche. Comité de Planeación para el Desarrollo del Estado (COPLADE). Edición: Secretaría de Planeación (www.campeche.gob.mx), Mexico (2015)
11. Villalobos-Zapata, G.J., Mendoza Vega, J.: La Biodiversidad en Campeche: Estudio de Estado. Comisión Nacional para el Conocimiento y Uso de la Biodiversidad (CONABIO), Gobierno del Estado de Campeche, Universidad Autónoma de Campeche, El Colegio de la Frontera Sur. México (2010)
12. Garcia, E.: Clasificación climática de Köppen, UNAM. Instituto de Geografía. UNAM (1973)
13. Yanez-Arancibia, A., Day Jr, J.: Ecology of coastal ecosystems in the southern Gulf of Mexico: The Terminos Lagoon Region. Inst Cienc Del Mar y Limnol UNAM, COSAT Ecol Inst LSU. Editorial Universitaria, Mexico DF (1988)
14. Posada-Vanegas, G., Vega-Serratos, E., Silva-Casarín, R.: Peligros naturales en el estado de Campechecuantificación y protección civil. CENAPRED (2013)

Dieses Werk ist copyrightgeschützt und darf in keiner Form vervielfältigt werden noch an Dritte weitergegeben werden.
Es gilt nur für den persönlichen Gebrauch.

15. González Solis, A., Torruco Gómez, D.: La fauna béntica del Estero de Sabancuy, Campeche, México. Revista de Biología Tropical 49, 31-45 (2001)

16. INEGI: Censo de Población y Vivienda. INEGI (2010)

17. IPCC: Climate change 2007. The physical science basis: Contribution of Working Group I to the Fourth Assessment Report of the IPCC. pp. 333. Cambridge University Press: Cambridge, UK (https://www.ipcc.ch/publications_and_data/publications_ipcc_fourth_assessment_report_wg1_report_the_physical_science_basis.htm) (2007)

18. Vázquez-Botello, A., Gutiérrez, S., Galaviz, J.R., Luis, J., Botello, A.V., Villanueva-Fragoso, S., Gutiérrez, J., Galaviz, J.L.R.: Vulnerabilidad de las zonas costeras mexicanas ante el cambio climático (2010)

19. Ruiz, G., Mendoza, E., Silva, R.: Caracterización del régimen del oleaje y viento de 1948-2007 en el litoral mexicano. Ingeniería del agua Vol. 16, Núm. 1 (2009), (2009)

20. Google Earth. Image©: DigitalGlobe. Image ©2017. TerraMetrics. Data 510, NOAA, U.S. Navy, NGA, GEBCO., (2017)

21. Torres, V., Márquez García, A., Bolongaro Crevenna Recaséns, A., Chavarria Hernández, J., Márquez García, E., Expósito Díaz, G.: Tasa de erosión y vulnerabilidad costera en el estado de Campeche debidos a efectos del cambio climático (2010)

22. CONABIO: Portal de Geoinformación, Sistema Nacional de Información Sobre Biodiversidad. http://www.conabio.gob.mx/informacion/gis/ (2017)

23. INEGI: Información por entidad. http://cuentame.inegi.org.mx/monografias/informacion/camp/poblacion/densidad.aspx?tema=me&e=04 (2017)

24. Secretaría de Medio Ambiente y Recursos Naturales: Gaceta Ecológica (Listado de proyectos que ingresan a evaluación de Impacto Ambiental). http://sinat.semarnat.gob.mx/Gaceta/aniosgaceta (2017)

25. CONAPESCA: Sistema de Información de Pesca y Acuacultura (SIPESCA). https://www.gob.mx/ conapesca/acciones-y-programas/sistema-de-informacion-de-pesca-y-acuacultura-sipesca (2017)

26. Defeo, O., McLachlan, A., Schoeman, D.S., Schlacher, T.A., Dugan, J., Jones, A., Lastra, M., Scapini, F.: Threats to sandy beach ecosystems: A review. Estuarine, Coastal and Shelf Science 81, 1-12 (2009)

27. Dugan, J.E., Defeo, O., Jaramillo, E., Jones, A.R., Lastra, M., Nel, R., Peterson, C.H., Scapini, F., Schlacher, T., Schoeman, D.S.: Give Beach Ecosystems Their Day in the Sun. Science 329, 1146 (2010)

28. Galbraith, H., Jones, R., Park, R., Clough, J., Herrod-Julius, S., Harrington, B., Page, G.: Global Climate Change and Sea Level Rise: Potential Losses of Intertidal Habitat for Shorebirds. Waterbirds: The International Journal of Waterbird Biology 25, 173-183 (2002)

Dieses Werk ist copyrightgeschützt und darf in keiner Form vervielfältigt werden noch an Dritte weitergegeben werden.
Es gilt nur für den persönlichen Gebrauch.

29. Martínez-Vázquez, L.M., Mendoza-González, G., Silva-Casarín, R., Mendoza-Baldwin, E.: Land use changes and sea level rise may induce a “coastal squeeze” on the coasts of Veracruz, Mexico. Global Environmental Change 29, 180-188 (2014)

30. Torio, D.D., Chmura, G.L.: Assessing Coastal Squeeze of Tidal Wetlands. Journal of Coastal Research 29, 1049-1061 (2013)

31. Jackson, A.C., McIlvenny, J.: Coastal squeeze on rocky shores in northern Scotland and some possible ecological impacts. Journal of Experimental Marine Biology and Ecology 400, 314-321 (2011)

32. Bimal, P., Harun, R.: Climatic Hazards in Coastal Bangladesh: Non-Structural and Structural Solutions. pp. 342. Butterworth-Heinemann (2016)

33. Reggiani, A., Nijkamp, P., Lanzi, D.: Transport resilience and vulnerability: The role of connectivity. Transportation Research Part A: Policy and Practice 81, 4-15 (2015)

Dieses Werk ist copyrightgeschützt und darf in keiner Form vervielfältigt werden noch an Dritte weitergegeben werden.
Es gilt nur für den persönlichen Gebrauch.

CHALLENGES AND STRATEGIES TO MODEL MARINE LITTER IN THE GUANABARA BAY

Gabriela V. Buraschi[1], Marcos N. Gallo[1]

[1]Cohesive Sediments Dynamics Laboratory (LDSC), Coastal and Oceanographic Engineering Area (PEnO/COPPE), Federal Univ. of Rio de Janeiro CT 203, P.O. Box 68508, Rio de Janeiro, Brazil, gvburaschi@oceanica.ufrj.br

Keywords: analytical-numerical 3D model, floating macro marine litter, Guanabara Bay, modeling marine litter, particle tracking model

Abstract

The problem of floating macro marine litter (FMML) in Guanabara Bay was globally evidenced when the 2016 Olympic Games were held in the city of Rio de Janeiro. This problem also occurs on the beaches of *Ilha do Fundão*, where the campus of the Federal University of Rio de Janeiro is located, which is part of the bay. When it is required to evaluate the dynamics, transport and spatial distribution of the FMML in this particular sector, and in the bay in general, certain challenges present themselves. That is, the modeling of flows between the coasts and the interface with the ocean, the monitoring, distribution and quantification of floating litter on the beaches, and when they are in the marine environment, the scale problems of the processes, which the numerical models cannot represent, as well as the validation of the results with limited data from surveys, among others. This work discusses the challenges for FMML modeling in coastal areas and, likewise, evaluates possible strategies for solving them. For that, some strategies for modeling were proposed, such as the use of a 3D analytical-numerical hydrodynamic model, coupled to a Lagrangian particle tracking model, combined with observed experimental data.

1 Introduction

1.1 Marine litter pollution

Pollution with marine litter is a complex worldwide concern, causing environmental, economic, health, social and aesthetic impacts [1, 2]. According to the UN Environment Program [1], marine litter consists of items that are persistent, manufactured or processed solid materials discarded into the sea or rivers, or on beaches. Especially, the plastic marine debris is widely documented. Recently, it was estimated that ~8 million metric tons of mismanaged plastic waste have entering the ocean each year [3]. Studies estimated ~5 trillion particles to be present in the ocean [4]. The tendencies and presence of marine debris in oceanic and coastal regions are increasing, and the problem will require a number of local and regional solutions [5].

Modeling the dynamics of marine debris on local, regional and global scales is an extremely difficult task and, in order to improve the models, many processes must be studied and considered [6]. The classical techniques of modeling the transport of floating debris combine numerical

Dieses Werk ist copyrightgeschützt und darf in keiner Form vervielfältigt werden noch an Dritte weitergegeben werden.
Es gilt nur für den persönlichen Gebrauch.

models that describe the ocean circulation and hydrodynamics models in order to simulate the water movement in more detail. For describing the interaction between the marine litter and the water, the models combine the hydrodynamic and advection-diffusion components. The first component uses tides and winds forcing and calculates the currents, sea-levels and tidal ranges for each element for a certain time step. The wind is an important forcing for litter material with higher buoyancy [7, 8]. Sea and river currents influence the routes and velocities of the marine litter [9, 10]. On the other hand, storms and tides play significant roles on debris transportation and deposition on the beaches and coastlines [11]. The second component makes use of a Lagrangian scheme for tracking the particles, which are transported by the predicted currents in each time step, and spread them laterally based on a calculated value of the horizontal diffusion coefficient. The size and shape, hence the volume, of a litter item together with its density determine the buoyancy, which is a deciding factor [12].

At present, the modeling of transport of floating debris have reasonable results only because of many assumptions or numbers of unknowns, as for example, the variability of the oceanic forcing and of the wind, the values of the wind drift coefficient and the resuspension of some floating debris by waves [13]. Moreover, the use of simplistic initial conditions based on bulk average inputs, and poorly known contribution of floating debris from urban rivers, and commercial and recreating shipping are other assumptions [13-16]. This means that in most cases simple or more complex statistical strategies are used to suppose the input of marine litter into the system.

Critchell and Lambrechts [17] found that the physical characteristics of the source location is the most important effect on the destination of the plastic debris. Also, they determined that the rate of degradation of macroplastics into microplastics have a considerable influence on the result, as well as the diffusivity, used to parameterize the sub-grid scale movements, and the relationship between debris resuspension/re-floating from beaches and the wind shadow created by high islands. Settling and wind drift velocity are less relevant processes in order to determine the fate of debris. Another factor that affects the accumulation rate of debris is the orientation of beaches to the prevailing wind direction [13].

Hardesty et al. [5] documented some of the available ocean circulation models and oceanographic datasets used for marine debris modeling/tracking, and many simulation studies are made about this issue. Most of them focus on the spatial location, consistency of distributions of marine litter, and on drift simulations across the oceans [10, 18-21]. However, the management of marine debris occurs over the smaller spatial scales of government jurisdictions. Models of marine debris must match the scale, of which management can be applied or policy implemented, especially along the coast [22]. In the literature, quite some studies developed forecasting models in order to predict the accumulation at coastlines, and only a few propagation studies have been found [13, 17, 23]. Advanced research can figure out new engineering solutions to efficiently capture debris near shore [11].

Dieses Werk ist copyrightgeschützt und darf in keiner Form vervielfältigt werden noch an Dritte weitergegeben werden.
Es gilt nur für den persönlichen Gebrauch.

The present case study aims to discuss the problems faced to model the floating marine macro litter (FMML) in the Guanabara Bay as well as to evaluate different strategies for solving them. Furthermore, with particular interest in the *Ilha do Fundão* area, it is proposed to combined use of different modeling approaches: observed data and a hydrodynamic model (SisBaHiA®), configured for the estuarine system, coupled to a Lagrangian particle-tracking model to simulate the transport of marine litter and its distribution along the coastline.

1.2 Study area and diagnostic

The Guanabara Bay is a tropical estuarine system, located on the south eastern coast of Brazil, in the state of Rio de Janeiro. The bay has a semi-circular format and covers an area of approximately 380 km^2. The bay has a narrow entrance and extends longitudinally 30 km to the north, with a maximum transverse extension in the E-W direction of 28 km. The deepest sites are along the main navigation channel, the bottom can reach more than 40 m, but around 84% of the bay's water is shallower than 10 m [24]. The bottom sediments of the Guanabara Bay are composed of sand, muddy sand, sand mud and mud [25, 26], distributed in response to bottom topography, shoreline configuration, tidal currents and sediment sources [27].

The mean freshwater discharge is 350 m^3/s [25, 28]. That discharge presents a variation with minimum values during the winter and maximum in summer [25]. The renewal time of 50% of the bay water volume is 11.4 days, although in the inner part of the bay, this time could be much longer, mainly in neap tides and dry periods. It can be classified as a tidal dominated estuary, subject to a mixed tidal regime with semidiurnal predominance. The mean tidal range is 0.7 m and extreme high water spring goes up to 1.3 m with no significant spatial variability. Regarding mixing processes, the bay presents a salt wedge in some inner regions, while in other regions, characterized by the absence of a well-defined salt gradient, it presents partially mixed waters [29]. Although dominated by tides, winds also play an important role on water circulation, modifying the surface currents in the shallower regions of the bay.

The estuarine system still maintains 40% of the original mangrove area, half of which is relatively well preserved in the Guapimirim Environmental Protection Area, on the northeastern shore of Guanabara Bay (Figure 1). Most part of the mangroves is degraded by urbanization and irregular occupation of the shorelines. One of the most drastic impacts on the environment is the pollution caused by the lack of sewage treatment in the metropolitan area of Rio de Janeiro. The amount of raw sewage discharged in the bay exceeds 20 m^3/s [30]. The floating debris, which accumulates on the shorelines and mangroves within the bay, is another noticeable impact. Particularly, the island *Ilha do Fundão* and surrounding areas are potential sources of marine litter, as they are close to a biggest slums complex, where solid urban waste collection is not efficient. This is an artificial island, where the University City of the Federal University of Rio de Janeiro is located. The island is situated within the municipality of the City of Rio de Janeiro, but it is a federal area, therefore, the local government has no jurisdiction. Consequently, the university must hire a cleaning service for the University City.

Dieses Werk ist copyrightgeschützt und darf in keiner Form vervielfältigt werden noch an Dritte weitergegeben werden.
Es gilt nur für den persönlichen Gebrauch.

The ecological consequences related to the pollution of Guanabara Bay remain unknown, partly because of the poor representation of the water circulation within the bay, especially in the inside of their channels, streams and drainage channels. Many studies report the contamination of its waters, sediments and biota by heavy metals and organic compounds [31-33]. However, there is poor knowledge regarding the floating debris distribution, classification and density. Some authors reported the microplastic pollution problem on their beaches [34, 35]. Besides, few investigations quantified, identified and analyzed the marine debris in certain places in the bay [36-38].

Several actions were implemented by the State Government of Rio de Janeiro in order to mitigate the floating debris problem. As of 2007 and in the context of the reception of the Pan American Games in 2007, the State Government created the "*Ecobarreira*" Project, placing floating barriers at strategic points at the mouths of some rivers to collect floating debris that has been discarded. Nonetheless, the technological level adopted in the *eco-barriers* is quite simple, of questionable efficiency and seems to be little resistant to deal with the great accumulation of debris [36]. At the present time, there are 17 *eco-barriers* installed around the bay, but in fact, 3 are working [39]. Several are already broken. As a consequence, these measures that were taken by the policymakers were insufficient, probably due to the lack of studies on floating debris impacts and the influence of hydrodynamics in spreading them.

1.3 Background modeling for macro marine litter in the Guanabara Bay

In the context of the competitions for the 2016 Olympics, held in the City of Rio de Janeiro, a modeling for the distribution of floating litter particles was made upon request of city's State Secretariat of Environment [39]. This performance assisted in the management of the monitoring service of the "*ecoboats*", collectors of the floating debris in the bay. A 3D hydrodynamic model was used, coupled to a Lagrangian particle-tracking model in order to simulate the transport of floating litter particles from source regions under the effect of winds and currents at 30 cm depth. The probabilistic strategy was that the source contributed uniformly and continuously [39]. Another approach to monitoring of floating litter and forecasting system for the Guanabara Bay is available in the internet (http://guanabaralimpa.deltares.nl/). It is about *Guanabara Limpa* Project created by the Government of Rio de Janeiro and Deltares (Center for Coastal Research) as well as other local research institutions and government agencies. It was created to monitor and to forecast the system Guanabara Bay, in addition to support the *ecoboats* that removed floating litter in the bay in preparation of the Olympics of the 2016. Despite being available on the web, this project was interrupted due to lack of resources. The system provides a four-day forecast of surface currents, wind and sea-levels for the bay, but the forecast of the concentration of floating debris is not available. Furthermore, the model has not good resolution in certain places of the bay, for example, around the *Ilha do Fundão* and *Canal do Fundão*, which are potential sources of marine litter. The models use different strategies to simulate the trajectory of marine litter, but both use hypothetical amounts of litter as input of the simulation.

Dieses Werk ist copyrightgeschützt und darf in keiner Form vervielfältigt werden noch an Dritte weitergegeben werden.
Es gilt nur für den persönlichen Gebrauch.

2 Available background information & data

Regarding the data acquisition for the hydrodynamic characterization, short-time ADCP and bathymetric surveys have been conducted inside the bay since 2015, especially surrounding *Ilha do Fundão* area. Other available data include a tide station located in the south of the *Ilha do Fundão*. This station register levels every 5 minutes since October 2016, and the data are used for the correction of local bathymetry and the determination of level of residence on the beaches in the island; 2 month of ADCP data were acquired outside the Guanabara Bay during the summer and winter of 2012–2013; wind data of Galeão Airport (2016-2017); mean discharges of the main rivers.

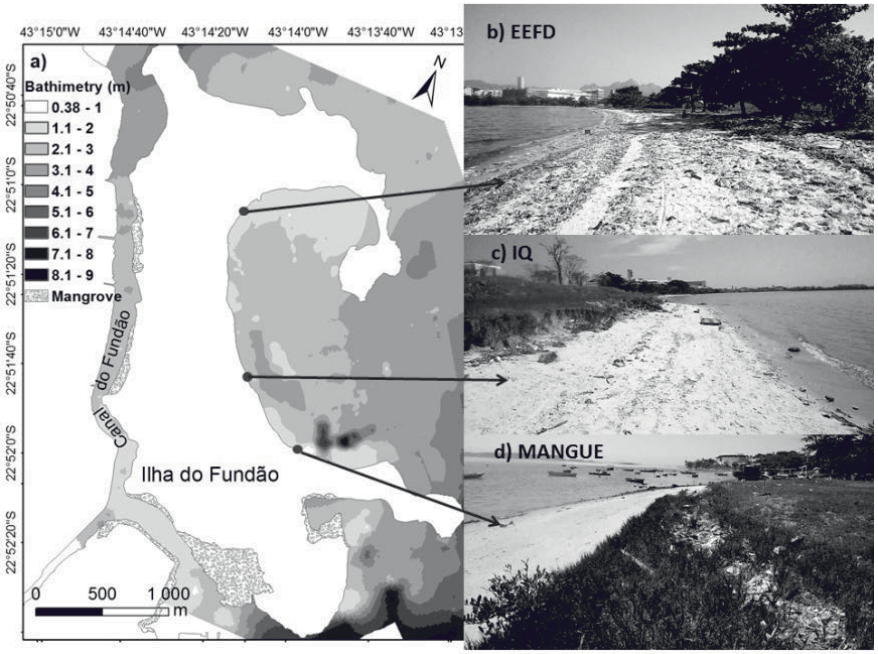

Figure 1: (a) Bathymetry detail in the *Ilha do Fundão*; (b) Beach of the Faculty of Physical Education of UFRJ (EEFD); (c) Beach of the Institute of Chemistry of UFRJ (IQ); (d) Mangue beach

In order to monitoring, classifying and quantifying the FMML, direct and indirect methodologies were used. Direct methods consisted of the direct sampling of material on the beaches at the University City. At the same time, a GoPro Hero 3 camera was used to indirectly quantify and to observe the FMML distribution in the area. This was carried out in three different places of the *Ilha do Fundão* (Figure 1 b-d) in different periods of tide (ebb, flood, spring and neap tides). Moreover, the sources were evaluated and the frequencies that the marine litter arrive on the beaches were determined.

Until now, 11 collection fields were sampled approximately every 15 days between the months of March and July. This was made at different distances of tide in order to assess the variability and influence on the transportation and deposition of litter item on beaches and along coastline. Table 1 shows some characteristics of the beaches sampled and the average amount of litter found per

Dieses Werk ist copyrightgeschützt und darf in keiner Form vervielfältigt werden noch an Dritte weitergegeben werden.
Es gilt nur für den persönlichen Gebrauch.

square meter in *Ilha do Fundão*. It should be noted that approximately 90% of the litter found on beaches is plastic. Others data coming from previous studies are also used [36, 37].

Table 1: Characteristics and estimated quantities of the garbage collection sectors in *Ilha do Fundão*

Sector	Length (m)	Area (m²)	Litter Average (kg/m²)	TOTAL (Tn)
EEFD	406	6,980	2.0	14.2
IQ	1520	13,950	0.3	3.7
MANGUE	520	2,243	1.9	4.3

3 Discussion

According to Hardesty et al. [5], one of the challenges to model coastal environment is the fluxes between the coasts and ocean interface, and the challenges of monitoring the distribution and quantification of floating debris both before it arrives and once it is already in the marine environment. Another issue is that global data on wind, tides, waves, pressure, and other processes currently exist that are identified as critically important. The challenge is how to bring these typically coarse data sets down to the coastal or finer scales. Additionally, one large uncertainty is in the rate of suspension/resuspension off/on shore of particles of litter as well as data on coastal dynamic and morphodynamic occur on scales that model cannot reproduce due to the resolution. In the same way, there is usually a conflict between spatial scale of the transport of marine litter and the discretization scales used in the hydrodynamic model.

Another issue to be solved is the strategy to be used in order to represent the process when the marine litter arrives on the coastline (beaching), and then it is recaptured by the action of tides or and waves; these processes occur on an even smaller scale. One more important issue in the FMML simulation is its heterogeneity in terms of size, type, density, and how to model it. The most critical point of the marine litter modeling studies is the validation of the results with data from field surveys [40]. This is the model accuracy. Data on the distribution of floating litter are limited and sparse in the Guanabara Bay in order to validate the simulations, and it is a problem that the modeling is facing. Even, it is not certain that all the garbage found on the beaches comes from the bay. Combining empirical data and modeling approaches can be useful to help predicting or forecasting their behavior and fate. This is one of the strategies proposed to the model FMML in Guanabara Bay.

3.1 Strategies to model FMML in the Guanabara Bay

In this work, the SisBaHiA® model is proposed for the hydrodynamics (*Sistema Base de Hidrodinâmica Ambiental*) (www.sisbahia.coppe.ufrj.br). This is a system of computational models registered by the Coppetec Foundation, which manages agreements and research contracts for the coordination of Graduate Programs and Engineering Research (COPPE) of the Federal University of Rio de Janeiro (UFRJ). The SisBaHiA has a hydrodynamic model of lineage FIST (*Filtered in Space*

Dieses Werk ist copyrightgeschützt und darf in keiner Form vervielfältigt werden noch an Dritte weitergegeben werden.
Es gilt nur für den persönlichen Gebrauch.

and Time). The spatial discretization can be accomplished by means of quadratic finite elements, quadratic triangular, or the combination of both, which allows optimized spatial discretization and an excellent representation of complex bathymetry and contours. The model consists of two modules: one 2DH and the other 3D. It solves the complete Navier-Stokes equations with shallow water approximation, considering the hydrostatic pressure approach. The 2DH calculates vertically averaged currents and the free surface elevation and, for reasons of numerical efficiency, FIST3D always includes this module. The 3D calculates the three-dimensional velocity field with two methodology options. One of them is the complete 3D model, totally numeric and salinity and temperature data are required. The other option is an analytical-numerical 3D model, which is an approach that uses the 2DH and calculates logarithmic profile in each point of the grid. This option is more computationally efficient, but only includes the advective acceleration of the 2DH module. The velocity profiles are computed through a solution that is a function of the vertical 2DH velocities, free surface elevation, equivalent roughness bottom of the 2DH module, and the wind velocity acting on the free surface of the water. The last option is the most appropriate and is chosen for FMML modeling in the Guanabara Bay.

In Lagrangian model of SisBaHiA, the particles are represented by a cloud with numerous particles, and the main problem is to compute the position in the continuous space of each particle. Since the position space of the particles is continuous, the scales conflict disappears because the discretization of the hydrodynamic model is only used for interpolations of the velocity field. SisBaHiA have two modules to Lagrangian transport. One of them is deterministic, it is a general-purpose model for simulating advective-diffusive transport with kinetic reactions (MTLADR module) for selected layers of 3D or 2DH flows. It is ideal for simulating the transport of scalar that may be floating, mixed or occupying only one layer in the water column. This model is especially suitable for simulations of transport and for determination of drift tendencies of floating debris, determination of the mass and height of deposited material. The transport may be conditioned by minimum velocity values, or bottom shear stress exerted only by currents, or bottom shear stress exerted simultaneously by waves and currents. The model admits the use of any kind of kinetic decay reaction, or simulates processes of loss of material by bioaccumulation in biota, for example; but these mechanisms still need to be better studied for debris in marine waters. However, it would allow adding other terms of marine litter losses mechanisms in the environment, such as loss of material by UV radiation and subsequent fragmentation and/or consumption by biota. The second Lagrangian transport model in SisBaHiA is probabilistic. It is coupled to the previous model and enables obtain probabilistic results computed from *N* events, or results over a period of time *T*. This module provides areas most likely to accumulate FMML.

Finally, in addition to the traditional methods of FMML data collection (monitoring and quantifying with direct method), this work makes use of other technologies, such as camera and drones, not only to quantify, moreover, to observe the spatial and temporal distribution.

Dieses Werk ist copyrightgeschützt und darf in keiner Form vervielfältigt werden noch an Dritte weitergegeben werden.
Es gilt nur für den persönlichen Gebrauch.

4 Conclusions

The use of an analytical-numerical 3D model can efficiently resolve FMML modeling in the Guanabara Bay, and simplify the problem, since salinity and temperature data are not required. The combined use of techniques, for instance, numerical models and observed data, can significantly improve the uncertainties involved in the modeling of the hydrodynamic and dynamics, transport, and spatial and temporal distribution of FMML. The application of traditional methodologies in addition to new technologies, such as cameras and drones can provide a better view of the sources of discharge of marine litter. It can also lead to a better understanding, where efforts should be focused in order to prevent litter from entering coastal environments.

Other data coming from experimental work can improve the understanding of FMML movement, for instance, small scale experiments in the laboratory in order to simulate the action of waves over macro marine litter, the influence of the wind on objects that float on the surface and others, those travel in the next layers, the observation of the movement of objects with different densities, among other research.

5 Acknowledgements

This work was done thank the financial support provided by the Rectory of UFRJ and CAPES through the aid of Ciências do Mar II 1977/2014 for the accomplishment of field work, and the support of the LDSC group.

Authors are also thankful to Federal Ministry for Economic Cooperation and Development, Germany (BMZ), German Academic Exchange Service (DAAD), Exceed SWINDON and Technical University of Braunschweig (TUBS) for their financial and technical supports, enabling to participate at the Summer School on Integrating Ecosystem in Coastal Engineering Practice (INECEP) held in September 18-29, 2017, in Puerto Morelos, México.

6 References

1. Cheshire, A., Adler, E., Barbière, J., Cohen, Y., Evans, S., Jarayabhand, S., Jeftic, L., Jung, R., Kinsey, S., Kusui, E.: UNEP/IOC Guidelines on Survey and Monitoring of Marine Litter. UNEP Regional Seas Reports and Studies, no. 186; IOC Technical Series no. 83: XII+ 120 pp. (2009)
2. European Commission: Overview of EU Policies, Legislation and Initiatives Related to Marine Litter. SWD 365. Brussels, 31.10.2012. Commission Staff Working Document (2012)
3. Jambeck, J.R., Geyer, R., Wilcox, C., Siegler, T.R., Perryman, M., Andrady, A., Narayan, R., Law, K.L.: Plastic waste inputs from land into the ocean. Science 347, 768 (2015)
4. Eriksen, M., Lebreton, L.C.M., Carson, H.S., Thiel, M., Moore, C.J., Borerro, J.C., Galgani, F., Ryan, P.G., Reisser, J.: Plastic Pollution in the World's Oceans: More than 5 Trillion Plastic Pieces Weighing over 250,000 Tons Afloat at Sea. PLOS ONE 9, e111913 (2014)

Dieses Werk ist copyrightgeschützt und darf in keiner Form vervielfältigt werden noch an Dritte weitergegeben werden.
Es gilt nur für den persönlichen Gebrauch.

5. Hardesty, B.D., Harari, J., Isobe, A., Lebreton, L., Maximenko, N., Potemra, J., van Sebille, E., Vethaak, A.D., Wilcox, C.: Using Numerical Model Simulations to Improve the Understanding of Micro-plastic Distribution and Pathways in the Marine Environment. Frontiers in Marine Science 4, 30 (2017)

6. Turra, Maximenko, Potemra: Modeling marine debris movement and transport. Technical Proceedings of Fifth International Marine, Honolulu, Hawaii, USA. https://marinedebris.noaa.gov/sites/default/files/5imdc_proceedings_final.pdf (2011)

7. Astudillo, J.C., Bravo, M., Dumont, C.P., Thiel, M.: Detached aquaculture buoys in the SE Pacific: potential dispersal vehicles for associated organisms. Aquatic Biology 5, 219-231 (2009)

8. Hinojosa, I.A., Rivadeneira, M.M., Thiel, M.: Temporal and spatial distribution of floating objects in coastal waters of central–southern Chile and Patagonian fjords. Continental Shelf Research 31, 172-186 (2011)

9. Galgani, F., Leaute, J.P., Moguedet, P., Souplet, A., Verin, Y., Carpentier, A., Goraguer, H., Latrouite, D., Andral, B., Cadiou, Y., Mahe, J.C., Poulard, J.C., Nerisson, P.: Litter on the Sea Floor Along European Coasts. Marine Pollution Bulletin 40, 516-527 (2000)

10. Martinez, E., Maamaatuaiahutapu, K., Taillandier, V.: Floating marine debris surface drift: Convergence and accumulation toward the South Pacific subtropical gyre. Marine Pollution Bulletin 58, 1347-1355 (2009)

11. Pallister, Gaudet: Storm influenced marine debris movement into Prince William Sound, Alaska. Technical Proceedings of Fifth International Marine, Honolulu, Hawaii, USA. https://marinedebris.noaa.gov/sites/default/files/5imdc_proceedings_final.pdf (2011)

12. Browne, M.A., Galloway, T.S., Thompson, R.C.: Spatial Patterns of Plastic Debris along Estuarine Shorelines. Environmental Science & Technology 44, 3404-3409 (2010)

13. Critchell, K., Grech, A., Schlaefer, J., Andutta, F., Lambrechts, J., Wolanski, E., Hamann, M.: Modelling the fate of marine debris along a complex shoreline: Lessons from the Great Barrier Reef. Estuarine, Coastal and Shelf Science 167, 414-426 (2015)

14. Carlson, D.F., Suaria, G., Aliani, S., Fredj, E., Fortibuoni, T., Griffa, A., Russo, A., Melli, V.: Combining Litter Observations with a Regional Ocean Model to Identify Sources and Sinks of Floating Debris in a Semi-enclosed Basin: The Adriatic Sea. Frontiers in Marine Science 4, 78 (2017)

15. Rech, S., Macaya-Caquilpán, V., Pantoja, J.F., Rivadeneira, M.M., Jofre Madariaga, D., Thiel, M.: Rivers as a source of marine litter – A study from the SE Pacific. Marine Pollution Bulletin 82, 66-75 (2014)

16. Woodring, Enache, Pick-Aluas: Global Ocean Alert System: focusing on the world's river mouth outflows as a source of marine debris. Technical Proceedings of Fifth International

Dieses Werk ist copyrightgeschützt und darf in keiner Form vervielfältigt werden noch an Dritte weitergegeben werden.
Es gilt nur für den persönlichen Gebrauch.

Marine, Honolulu, Hawaii, USA. https://marinedebris.noaa.gov/sites/default/files/5imdc_proceedings_final.pdf (2011)

17. Critchell, K., Lambrechts, J.: Modelling accumulation of marine plastics in the coastal zone; what are the dominant physical processes? Estuarine, Coastal and Shelf Science 171, 111-122 (2016)
18. Lebreton, L.C.M., Borrero, J.C.: Modeling the transport and accumulation floating debris generated by the 11 March 2011 Tohoku tsunami. Marine pollution bulletin 66, 53-58 (2013)
19. Lebreton, L.C.M., Greer, S.D., Borrero, J.C.: Numerical modelling of floating debris in the world's oceans. Marine Pollution Bulletin 64, 653-661 (2012)
20. Neumann, D., Callies, U., Matthies, M.: Marine litter ensemble transport simulations in the southern North Sea. Marine Pollution Bulletin 86, 219-228 (2014)
21. Potemra, J.T.: Numerical modeling with application to tracking marine debris. Marine Pollution Bulletin 65, 42-50 (2012)
22. Vegter, A.C., Barletta, M., Beck, C., Borrero, J., Burton, H., Campbell, M.L., Costa, M.F., Eriksen, M., Eriksson, C., Estrades, A.: Global research priorities to mitigate plastic pollution impacts on marine wildlife. Endangered Species Research 25, 225-247 (2014)
23. Yoon, J.-H., Kawano, S., Igawa, S.: Modeling of marine litter drift and beaching in the Japan Sea. Marine pollution bulletin 60, 448-463 (2010)
24. Figueiredo Jr, A., de Toledo, M., Cordeiro, R., Godoy, J., T. da Silva, F., C. Vasconcelos, S., A. dos Santos, R.: Linked variations in sediment accumulation rates and sea-level in Guanabara Bay, Brazil, over the last 6000 years. Palaeogeography, Palaeoclimatology, Palaeoecology 415, 83-90 (2014)
25. Amador, E.: Baía de Guanabara e ecossistemas periféricos: homem e natureza. Reproarte Gráfica e Editora, Rio de Janeiro. (1997)
26. Quaresma, V., Dias, G., Baptista Neto, J.: Caracterização da ocorrência de padrões de sonar de varredura lateral e sísmica de alta freqüência (3, 5 e 7, 0 kHz) na porção sul da Baía de Guanabara. Brazilian Journal of Geophysics 18, 201-213 (2000)
27. Soares-Gomes, A., Da Gama, B., Neto, J., G Freire, D., Cordeiro, R., Machado, W., Bernardes, M., Coutinho, R., Thompson, F., Pereira, R.: An environmental overview of Guanabara Bay, Rio de Janeiro. Regional Studies in Marine Science (2016)
28. Kjerfve, B., De Lacerda, L.D., Dias, G.: Baía de Guanabara, Rio de Janeiro, Brazil. Coastal marine ecosystems of Latin America 107-117 (2001)
29. Kjerfve, B., Ribeiro, C.H., Dias, G.T., Filippo, A.M., Quaresma, V.D.S.: Oceanographic characteristics of an impacted coastal bay: Baía de Guanabara, Rio de Janeiro, Brazil. Continental Shelf Research 17, 1609-1643 (1997)

Dieses Werk ist copyrightgeschützt und darf in keiner Form vervielfältigt werden noch an Dritte weitergegeben werden.
Es gilt nur für den persönlichen Gebrauch.

30. Júnior, J.T.A., de Campos, T.M.P., Pires, P.J.M.: Sediment Characteristics of an Impacted Coastal Bay: Baía de Guanabara, Rio de Janeiro, Brazil. Journal of Coastal Research Special Issue 71, 41-47 (2014)

31. Christensen, J., Tomasi, G., Scofield, A., de Fatima Guadalupe Meniconi, M.: A novel approach for characterization of polycyclic aromatic hydrocarbon (PAH) pollution patterns in sediments from Guanabara Bay, Rio de Janeiro, Brazil. Environmental Pollution 158, 3290-3297 (2010)

32. Covelli, S., Protopsalti, I., Acquavita, A., Sperle, M., Bonardi, M., Emili, A.: Spatial variation, speciation and sedimentary records of mercury in the Guanabara Bay (Rio de Janeiro, Brazil). Continental Shelf Research 35, 29-42 (2012)

33. Neto, J., Xaver Gingele, F., Leipe, T., Brehme, I.: Spatial distribution of heavy metals in surficial sediments from Guanabara Bay: Rio de Janeiro, Brazil. Environmental Geology 49, 1051-1063 (2006)

34. Castro, R.O., Silva, M.L., Marques, M.R.C., de Araújo, F.V.: Evaluation of microplastics in Jurujuba Cove, Niterói, RJ, Brazil, an area of mussels farming. Marine Pollution Bulletin 110, 555-558 (2016)

35. Gomes de Carvalho, D., Neto, J.: Microplastic pollution of the beaches of Guanabara Bay, Southeast Brazil. Ocean & Coastal Management 128, 10-17 (2016)

36. Bernardino, D., Franz, B.: Lixo flutuante na Baía de Guanabara: passado, presente e perspectivas para o futuro. Desenvolvimento e Meio Ambiente 38, (2016) http://revistas.ufpr.br/made/article/view/47024

37. Ferreira, J., Silva, C., Resende, A.: Clean bay project: monitoring of marine environments degraded by solid waste in Guanabara Bay, Rio de Janeiro, Brazil. Journal of Integrated Coastal Management 11, 103-113 (2011)

38. da Silva, M.L., Sales, A.S., Martins, S., de Oliveira Castro, R., de Araújo, F.V.: The influence of the intensity of use, rainfall and location in the amount of marine debris in four beaches in Niteroi, Brazil: Sossego, Camboinhas, Charitas and Flechas. Marine Pollution Bulletin 113, 36-39 (2016)

39. PROOCEANO: Plano de Gestão do serviço de supervisão dos Ecobarcos. Technical report. Rio de Janeiro. June 19. (2016)

40. Politikos, D.V., Ioakeimidis, C., Papatheodorou, G., Tsiaras, K.: Modeling the Fate and Distribution of Floating Litter Particles in the Aegean Sea (E. Mediterranean). Frontiers in Marine Science 4, 191 (2017)

Dieses Werk ist copyrightgeschützt und darf in keiner Form vervielfältigt werden noch an Dritte weitergegeben werden.
Es gilt nur für den persönlichen Gebrauch.

DESALINATION PLANTS – THE ENVIRONMENTAL IMPACT ON CORAL REEFS IN THE NORTHERN RED SEA

Manuela König[1]

[1]Leichtweiß-Institute for Hydraulic Engineering and Water Resources, Technische Universität Braunschweig, Beethovenstraße 51a, 38106 Braunschweig, Germany, ma.kg.in.hg@t-online.de

Keywords: Coral Reefs, Desalination, Numerical Modeling, SWRO

Abstract

Desalination techniques could be a solution to face the problems of water scarcity. In 2015, 300 million people could be supplied with freshwater by desalinated water as well as a huge capacity of industry waters. Nevertheless, the technique comes with a variety of disadvantages. This paper examines the emissions of desalination plants and their environmental impacts on the marine organisms of corals. Basis of this paper is a case study of Höpner & Lattermann (2003) [1] about chemical loads of desalination plants in the northern Red Sea. It was found that the brine that is lead into the ocean can heavily influence the marine ecosystem. In this paper, the idea of an assessment tool is extended. The paper is structured as a literature research and combines the existing issues with the idea of a numerical tool as guidance within the planning of new plants. The objective of this guide should be to optimize the system in order to decrease environmental impacts. Central of the discussion is that for each plant a holistic and individual solution has to be found. Combining all aspects in one assessment approach is complex, but this challenge should be seen as a chance to preserve nature.

1 Introduction

Nowadays, society is faced with many environmental challenges. The decline of freshwater resources is one of the most dominant issues. Various changes in the ecosystem concerning extreme weather conditions and the concern to cover the economies' and societies' demands for water put a lot of pressure on humanity. Combined with developments such as the increasing world population, sustainable innovations are needed. Moreover, an increasing need of food raises water demand from industries and agriculture.

The water resources of the earth are distributed unequally, not only geographically but also divided into a mere 2 % of fresh water and 98 % salt water [2]. Considering this, desalination plants seem as a choice to cover water demands in the future, especially in arid and semi-arid areas. The huge potential of the technique can be seen by reviewing the worldwide capacity of desalination plants. The capacity increased from 44.1 Mm^3/d in 2007 [3] up to 86.5 Mm^3/d in 2015 [4]. Already in 2015, 300 million people were dependent on desalination technique for their water supply [4].

Dieses Werk ist copyrightgeschützt und darf in keiner Form vervielfältigt werden noch an Dritte weitergegeben werden.
Es gilt nur für den persönlichen Gebrauch.

Therefore, desalination techniques are an innovative solution to supply humanity with freshwater using global saltwater resources. With a capacity of 21 Mm³/d, representing 48% of the worldwide capacity, desalination plants are quite common in the Gulf region. The Red Sea holds 13% of the worldwide desalination capacity and will be the region focused on in this paper [3].

The aim of this case study [1] was to collect data and to estimate the impact of the detected plants on the marine environment. The results were used for an impact assessment. This paper is based on data from Lattemann and Höpner [3, 5, 6] as well as on further ideas on numerical investigations from [7, 8]. On the basis of this information the aim of this paper is to extend the idea of an assessment tool [3] as guidance within the planning process of new desalination plants. A holistic discussion concerning the important issues as well as advantages and disadvantages is held.

2 Materials and Methods

The data used in the case study [1] was collected from 21 desalination plants that were chosen from the International Desalination Association (IDA) in its "Worldwide Desalting Plants Inventory Report" from 2000. The World Conservation Monitoring Center provided appropriate GIS maps with the location of the plants as well as the coral reefs distribution [1].

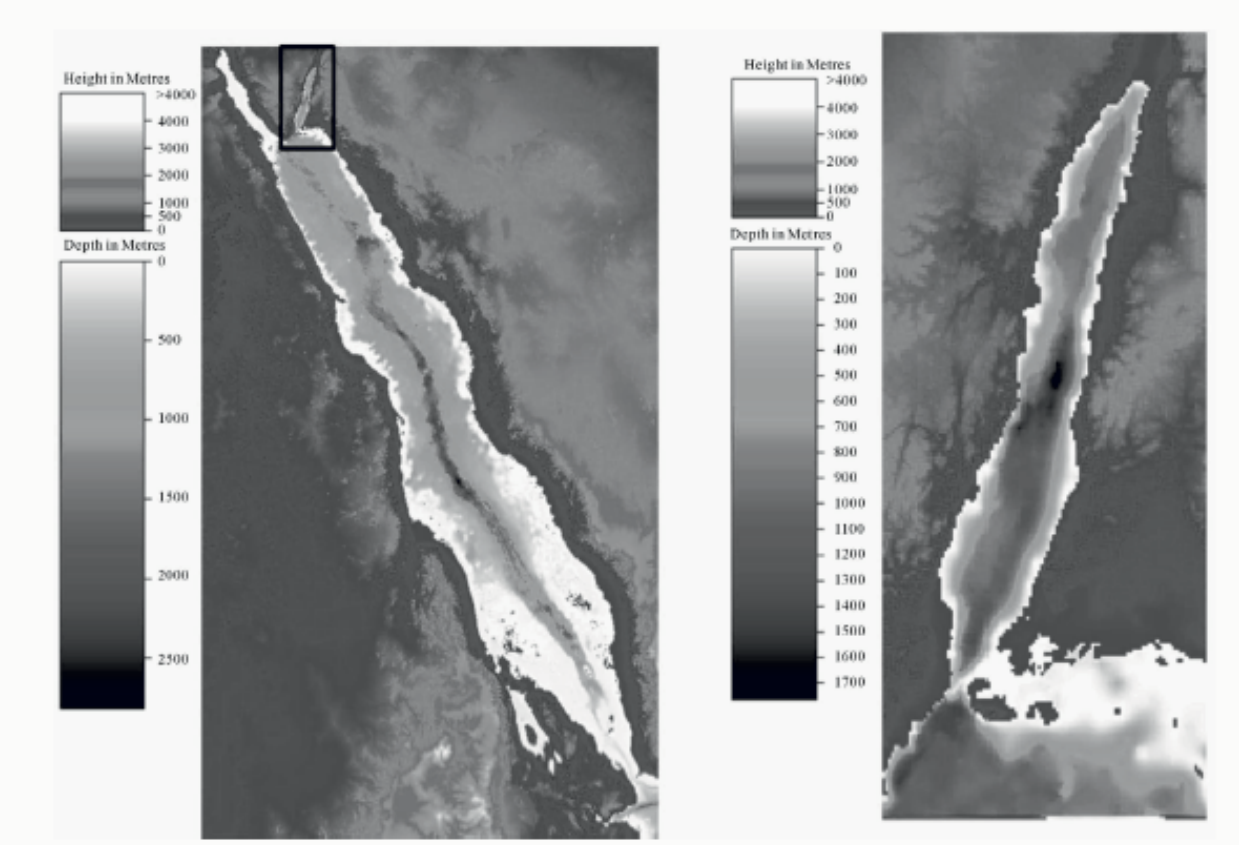

Figure 1: Map with bathimetry of the Red Sea (left panel) and the Gulf of Aqaba (right panel) [9]

Dieses Werk ist copyrightgeschützt und darf in keiner Form vervielfältigt werden noch an Dritte weitergegeben werden.
Es gilt nur für den persönlichen Gebrauch.

2.1 Study area

The Red Sea located in the Middle East is connected to the Mediterranean Sea via the Suez Channel in the north and to the Indian Ocean via the Gulf of Aden. The Gulf of Aqaba is located in the north-eastern part of the Red Sea. Due to little flow exchange with other seas, water contents in the northern Red Sea and the Gulf of Aqaba are concentrated [1].

The Red Sea is known for its coral reefs as a unique ecosystem. As a favoured holiday destination for snorkelling, tourism is an important source of income for the surrounding countries [10]. The coral reefs in this region are considered some of the most diverse coral reefs worldwide [11], and therefore, should be protected. The biggest part of the coral reefs belong to the Kingdom of Saudi Arabia [11], and with 92% most desalination plants of the Red Sea region are located there [3].

2.2 Overview of desalination plants

Desalination methods can be divided into three basic categories: Chemical, distillation and membrane processes [12]. There are more detailed methods and variations of each, but there it is referred to [3, 6, 12]. For the decision, which method is most appropriate for each individual setting, different aspects of hydrodynamic, morphology, meteorology and ecology have to be thoroughly analyzed in order to get a holistic overview. The design of each desalination plant with its single modules is variable and unique. For each plant, an individual concept is used taking into account the existing circumstances.

2.2.1 Chemical Process

The ion exchange method is a chemical process used to desalinate water. A solid and a liquid phase lead to the exchange of the contained ions. The feedwater with Na^+ and Cl^- ions constitutes the liquid phase. To remove Na^+ and Cl^- from the sea water, a solid ion exchanger phase is used, exchanging Na^+ versus H^+ and Cl^- versus OH^-, both together forming non-ionized water H_2O. In terms of worldwide capacity, the distribution of desalination plants using chemical processes is minor [3, 13].

2.2.2. Distillation Process

The distillation process is a thermal technology relying on the usage of evaporation and condensation. The Multi-Stage-Flash (MSF) method is one of the most commonly used. 14 Mm^3/d are produced daily, which amounts to 32% of the capacity worldwide [3].

The intake water passes through several flashing stages. At first, the saltwater is heated up to 120 °C. It then flows into a “brine pool”, where the water evaporates [12]. On its way to condensate, the produced vapour is used to heat up cold saltwater. In the next stage, the resulting brine is treated again in the same way. With every stage the feedwater’s salt concentration grows. The Multiple-Effect-Distillation (MED) is a forerunner of the MSF method. 8% of the worldwide capacity in desalination uses this technique. The thermal plants are always coupled with a power plant using the waste heat. For the production of 1 m^3 desalted water approximately 47 kWh thermal energy is needed [12].

Dieses Werk ist copyrightgeschützt und darf in keiner Form vervielfältigt werden noch an Dritte weitergegeben werden.
Es gilt nur für den persönlichen Gebrauch.

2.2.3 Membrane Process

The membrane desalination processes can be divided into pressure and electrical driven ones. Their common feature is that all of them work with a semi-permeable membrane that holds back specific contents like salt, minerals, metals and bacteria. The membrane consists of porous materials such as ceramics, metals or synthetics [13].

The desalination method used the most worldwide (51% of the global capacity) is the seawater reverse osmosis (SWRO). The SWRO uses the different osmotic pressures of fresh and salt water to its advantage. A semi permeable membrane separates the salty feedwater and the produced fresh water. Wherefore a huge pressure of 80 to 100 bar is applied on the salt [5]. Typically, seawater has a salinity concentration in between 30,000 and 40,000 ppm [3].

To protect the sensitive membrane, a pre-treatment of the feedwater is needed. The pre-treatment consists of multi-media filtration removing large particles, organic matter, bacteria and oil. The problems of precipitation and scaling are faced by adding chemicals. Also oxidants need to be removed [6, 14].

In comparison to the distillation processes, the membrane techniques are less energy consuming. The energy needed for SWRO is approximately 3-4 kWh/m³ [14]. Also, this process runs with electrical energy and is not necessarily dependent on a coupled power plant. But the technique is more chemical and material intensive [14].

2.3 State-of-the-art

The IDA, the European Desalination Society (EDA) as well as other regional and local associations are collecting and providing information concerning desalination. Regular knowledge exchanges, seminars and courses are organized. Their continuous work on a transfer of experience and information is indispensable.

Facing the problem of high salinity in the outfall areas, the design of outfall structures has to be taken into account. By optimizing the structure, the brine could be diluted while releasing back into the ocean. Floating rates that are adapted to the seasonal conditions of the environment or pipes with several holes are an option. For the variability of in- and outfall structures, the book “Intakes and Outfalls for Seawater Reverse-Osmosis, Desalination Facilities, Innovations and Environmental Impacts” [14] is a collection of different articles. The focus is also given on “assessment and reduction of environmental impacts” [14].

One of the articles deals with a stepwise approach of numerical modeling for desalination effluent discharges [7]. [7] is using the software Delft3D Flexible Mesh developed by Deltares for numerical investigations. In general, Delft3D is a tool that is used among others for “Recirculation of cooling water from power and desalination plants including the release of bio-fouling chemicals such as chlorine” [15]. The water quality can be simulated and may help to evaluate the impact of desalination plants on the environment and to give recommendations on planning options.

Dieses Werk ist copyrightgeschützt und darf in keiner Form vervielfältigt werden noch an Dritte weitergegeben werden.
Es gilt nur für den persönlichen Gebrauch.

3 Results and discussion

3.1 Problems

The negative impacts of desalination plants can be roughly divided into the impact resulting from the structure itself, the desalination process and the therefore occurring stress on the surrounding ecosystem.

The plant construction itself affects the soil and underground of the marine environment. The intake and outfall structures are an intrusion into the marine ecosystem. Through impingement and entrainment, marine organisms are endangered [3]. Furthermore, desalination is an energy intensive process. If energy is provided using non-renewable processes, for example through coal combustion, the well-known negative impacts are resulting.

Another factor that puts the marine environment at risk is the discharge of the brine [5]. The brine is produced during the process of the desalination and released back into the ocean. It contains the used chemicals – being partly toxic – and their by-products, which leads to a decrease in diversity of the ecosystem in long term time scale [6].

The measured parameters like the salinity depend on the type of desalination plant and the hydrodynamic water conditions. The values are influenced by the capacities of the plant, the hydrodynamic and bathymetry, water composition and diffuser design. For example, shallow waters as the Mediterranean Sea have lower water exchange compared with deep water regions. Therefore, the dilution of the critical compounds is less and the impact on the marine environment higher.

The considered case study focuses on the brine components of chlorine, copper and antiscalants that are used for disinfection purposes or for avoiding corrosion. The data of the 21 analysed plants (MSF and SWRO) summarized total amounts of 2.7 kg/d chlorine, 36 kg/d cupper and 9.48 kg/d antiscalants for the total area in the Northern Red Sea [1]. Metals accumulate in the surrounding sediment [1]. Depending on the recovery rate of a SWRO desalination plant, the salinity of the brine can be twice as high as of the feedwater. In other studies, a raised salinity was detected up to some kilometres from the desalination plant [16]. It shows that the negative impact of releasing brine into the ocean is spreading quite far.

Another problem arising in desalination plants is biofouling. In order to prevent biofouling chemicals, most commonly elemental chlorine is added after the intake. But as oxidants like chlorine damage the membrane, the water needs to be de-chlorinated with sodium bisulfate before it enters the proper membrane process. The US Environmental Protection Agency recommends a chlorine content of 7.5 µg/L in seawater as a long term threshold criterion. Measurements detected concentrations between 200 and 500 µg/L around SWRO plants. Chlorine or formaldehyde are also added to disinfect the produced freshwater [6].

Dieses Werk ist copyrightgeschützt und darf in keiner Form vervielfältigt werden noch an Dritte weitergegeben werden.
Es gilt nur für den persönlichen Gebrauch.

As cleaning chemicals, either alkaline or acidic substances *"such as detergents (e.g., dodecylsulfate, dodecylbenzene sulfonate) or oxidants (e.g., sodium perborate, sodium hypochlorite)"* [6] can be applied. In order to prevent scale formation, antiscalants of different chemical composition are used. They may not have a toxic influence on the marine environment, but raise the concentration of nutrients in the brine. This can result in eutrophication. To remove suspended material and to protect the membrane during the filtration, coagulants like $FeCl_3$ help to accumulate the substances.

Thermal desalination processes such as MSF do not use as many chemicals but heated brine also needs to be treated. The temperature of brine was measured with up to 10 to 15°C higher than the water body into the brine was released in [6, 16]. This has a negative impact on the aquatic life around the plant.

It is controversial that the water quality is negatively influenced by the brine that is released back into the ocean, although desalination plants take the feedwater from the same area. For the listed reasons, adaptive solutions to ensure the intactness of the surrounding environment are urgently needed. The negative impact on the ecosystem is most evidently reflected in the change of salinity and temperature, which further affect the function of the ecosystem itself.

Due to the released brine, the marine environment is heavily influenced and losses in biodiversity are detected. Even small changes in the long-term habitat conditions result in high stress levels for the organisms. Studies show that in the outfall areas the *posidonia oceanic* had problems with leaf necrosis, and a *"decreased carbohydrate storage in leaf tissues"* [6] was detected. A decreased density of organisms like seagrass, phytoplankton and corals is an immense problem, too. Moreover, the accumulation of metals in mussels due to corrosion in the plants is a serious issue.

3.2 Solution

A sustainable and holistic optimization of the technology is urgently needed in order to reduce the negative impact of deslination plants on the environment and marine ecosystem. In Missimer et al., (2015) [14] it is highlighted, that the greening of the desalination process should be an important objective for the coming years. But reaching this aim is also a challenge.

One method to improve the technique is the positioning and the design of the outfall construction. There is a variation of design of intake and outfall structures, varying from onshore and offshore, subsurface and deep constructions [14]. Moreover, the subsurface construction can be built as a single pipe or a multiport diffuser. These multiport diffusers are becoming standard today and are used more and more [14].

The reduction of the brine toxicity itself should also be a priority. It is important to find alternative options for the used chemicals and - if possible – to substitute those through eco-friendly alternatives.

Dieses Werk ist copyrightgeschützt und darf in keiner Form vervielfältigt werden noch an Dritte weitergegeben werden.
Es gilt nur für den persönlichen Gebrauch.

Apart from detailed module improvements, a holistic supporting system should become a standard within the planning of desalination plants. As an existing tool, Lattemann (2010) developed in her PhD Thesis a *"decision support system for seawater desalination plants"* [3]. It is a tool with the aim to reduce the environmental impact. An extension to this existing tool could be a numerical model. The simulation of different scenarios is an option to identify the desalination plant with the least impact on the environment. The tool meant to be a rough recipe, guidance or instruction with an approach to classify different situations.

Two projects are described in [7, 8]. [7] uses a tiered approach that is becoming more detailed and complex with each step. Another option may be a coupling of different models. [8] uses a combination of a near field mixing model (CORMIX) and a transport process in the far field model (DELFT3D). It is highly recommended to use a coupled approach. Using two systems in combination can help compensating the disadvantages of each model.

A three-dimensional model is mandatorily needed, because the gradient of the horizontal and vertical circumstances are high [9]. Especially in the surface area, vertical gradients of water temperature and salinity are high.

During the preparation, a detailed step-by-step time schedule for the whole project should be defined. An open but critical communication is irreplaceable for the planning process. Although time and money consuming, data collection through field studies, measurements and monitoring programs should not be neglected. A meticulous and detailed measurement work is needed for the resulting data. It is important for the reliability and credibility of the results to get as much data about the different aspects as possible [7, 17]. Important aspects that need to be considered are:

- *Hydrodynamics* (Tide, water levels, current flow velocities and directions, discharges from rivers),
- *Water quality* (Temperature, salinity, pH-level, concentration of substances and nutrients, chlorine, dissolved oxygen, ammonia),
- *Habitat* (Specie samples, thresholds to chemicals),
- *Meteorology* (Wind velocities and directions, air temperature, precipitation and evaporation rates).

3.3 Discussion

The idea to use a numerical tool to mitigate the environmental impacts of desalination plants is a first step towards an aware planning process. Especially the integration of the ecosystem into the planning of desalination plants seems difficult. Also, social aspects like conflicts about water supply within regions of water scarcity make that even more complex. When drinking water is urgently needed, environmental impacts are often neglected. Today, the pressure on the desalination industry is very high and is thought to increase in the future [9]. The awareness for sustainable and integrated solutions needs to be communicated through associations such as the IDA.

Dieses Werk ist copyrightgeschützt und darf in keiner Form vervielfältigt werden noch an Dritte weitergegeben werden.
Es gilt nur für den persönlichen Gebrauch.

In order to break down the complexity of modeling a desalination plant and simulating the impacts on the marine environment, the system can be divided. By separating single specialized modules of the desalination plant the model can be built up more easily. Results then are only combined in the evaluation. An official guideline developed by experts could help in the practical implementation. The tool can be used to help find the optimal location for building a new desalination plant with the minimum environmental impacts.

To avoid exceptions, it has to be clearly defined when a system will be improved and the aim of less environmental impact is reached. The results from a numerical investigation should be arranged in a matrix for good visualization and comparison issues.

Moreover, there are some uncertainties within numerical modeling that need to be considered. A model can only represent reality to a certain extend. A lot of assumptions need to be taken, depending on adjustments of the used software and database. It is important to keep up transparency and to describe all uncertainties and problems while modeling. Therefore, numerical investigations are still not state-of-the-art, but only used for scientific purposes. Nevertheless, numerical results may be helpful for first estimations in planning processes.

4 Conclusions

The desalination technique is essential for a secure water supply in Arabic countries [17]. Desalination plants provide water in arid areas and thus enable life there. Nevertheless, the processes come with a range of disadvantages.

The environmental impacts mostly through the salty or heated brine, which is released into the ocean, are immense. The protection of the coral reefs in the Red Sea or a sensitive ecosystem in general, should be focused on. Climate change and rising sea temperature already threaten coral reefs. Releasing toxic or heated brine poses an even greater threat. Therefore, a holistic, sustainable and integrated solution is needed.

In order to find this solution, a numerical tool including a guideline with model set-up recommendations could support the planning process of desalination plants. Nevertheless, the development and implementation of such a tool is a complex task. But it can be seen as a chance to reduce the environmental impacts of the desalination technique and to protect marine life.

Prospectively, a detailed development plan should be framed. It is preferable if the development could be a working closely together with governmental and justice instances. A combined system including regular controls and monitoring systems lead to a growing focus on protecting the environment. The overall objective is that the innovative technology of desalination can be used in more areas of the world, where people have crucial problems with freshwater scarcity.

5 Acknowledgement

I wish to thank Exceed Swindon and DAAD for the financial support, giving me the opportunity to attend to the INECEP Summer School in Puerto Morelos.

Dieses Werk ist copyrightgeschützt und darf in keiner Form vervielfältigt werden noch an Dritte weitergegeben werden.
Es gilt nur für den persönlichen Gebrauch.

6 References

1. Hoepner, T., Lattemann, S.: Chemical impacts from seawater desalination plants—a case study of the northern Red Sea. Desalination 152, 133-140 (2003)
2. Gleick, P.H.: Water resources. Encyclopedia of climate and weather 2, 817-823 (1996)
3. Latteman, S.: Development of an environmental impact assessment and decision support system for seawater desalination plants. CRC press (2010)
4. IDA: International Desalination Association, (2016). http://idadesal.org/desalination-101/desalination -by-the-numbers/, (access on 07/03/2016)
5. Höpner, T., Lattemann, S.: Desalination of seawater, Global change: Enough water for all? Wissenschaftliche Auswertungen Hamburg 384, 277-280 (2007)
6. Lattemann, S., Höpner, T.: Environmental impact and impact assessment of seawater desalination. Desalination 220, 1-15 (2008)
7. Bleninger, T., Morelissen, R.: Tiered Modeling Approach for Desalination Effluent Discharges. Intakes and Outfalls for Seawater Reverse-Osmosis Desalination Facilities, pp. 397-449. Springer (2015)
8. Niepelt, A., Bleninger, T., Jirka, G.: Desalination brine discharge modeling-Coupling of hydrodynamic models for brine discharge analysis. 5th International Conference on Marine Waste Water Discharges and Coastal Environment, Croatia, (2008)
9. Ahmed, A.S.M., Abou-Elhaggag, M.E., El-Badry, H.: Hydrodynamic modeling of the Gulf of Aqaba. Journal of Environmental Protection 3, 922 (2012)
10. Sawall, Y., Al-Sofyani, A.: Biology of Red Sea corals: metabolism, reproduction, acclimatization, and adaptation. The Red Sea, pp. 487-509. Springer (2015)
11. Spalding, M.D., Ravilious, C., Green, E.P.: World atlas of coral reefs University of California Press. Berkeley Los Angeles (2000)
12. DME: Deutsche Meereswasserentsalzung e.V. (2015), http://www.dme-ev.de/onlineseminar-englisch/, (access on 31/05/2017)
13. Younos, T., Tulou, K.E.: Overview of desalination techniques. Journal of Contemporary Water Research & Education 132, 3-10 (2005)
14. Missimer, T.M., Jones, B., Maliva, R.G.: Intakes and Outfalls for Seawater Reverse-Osmosis Desalination Facilities: Innovations and Environmental Impacts. Springer (2015)
15. Deltares, (2017) https://www.deltares.nl/academy/delft3d-block-2a/ (access on 02/07/2017)
16. Roberts, D.A., Johnston, E.L., Knott, N.A.: Impacts of desalination plant discharges on the marine environment: A critical review of published studies. Water Research 44, 5117-5128 (2010)
17. Mohamed, K.A.: Environmental impact of desalination plants on the environment. In: 13th International Water Technology Conference, IWTC, 13, 951-964 (2009)

Dieses Werk ist copyrightgeschützt und darf in keiner Form vervielfältigt werden noch an Dritte weitergegeben werden.
Es gilt nur für den persönlichen Gebrauch.

ECONOMIC VALUATION OF MANGROVE AREAS A STUDY CASE IN NORTHEAST OF BRAZIL

Nadia Selene Zamboni[1,2], Adriana Rosa Carvalho[1,2]

[1]Department of Ecology, Federal University of Rio Grande do Norte– UFRN, nselenezamboni@gmail.com

[2]Fishing Ecology, Management and Economics, http://feme-group.blogspot.com.br

Keywords: ecosystem services, mangroves, opportunity cost, replacement cost, valuation

Abstract

Brazil has the second largest mangrove area on earth with high socioeconomic and ecological importance. However, these forests are suffering a decline due to sea level rise, human occupation and lack of preservation policies, putting at risk the quality of several ecosystem goods and services that they provide, such as carbon storage service that contribute to the climate change mitigation. A way to avoid more degradation and to promote the preservation of mangroves is doing an economic valuation of their ecosystem services. Through this study case, performed in the Ponta do Tubarão Sustainable Development Reserve - RDSPT (Rio Grande do Norte), it was aimed to estimate the opportunity and replacement costs associated with the carbon storageservice, and the dynamics of loss and gain of mangrove areas as a consequence of the coastline progression and human perturbation over 30 years. It was found that an increase of mangrove areas from 1984 to 2014 occured, leading to a higher carbon storagecapacity. Carbon storageservice of the RDSPT mangroves also affords 75% more profit than the wind energy sector. It was found that the restoration of the lost areas would cost approximately € 377 millon by reforesting the core areas and patches near the beach strip.

1 Introduction

Growing in the intertidal zone and occupying coastal and estuarine areas in many tropical places, mangroves are one of the most productive, diverse and biologically complex ecosystems on the planet [1, 2]. Besides, they afford many benefits to people, supplying a variety of ecosystem goods and services that include provisioning (e.g., food, raw materials, pharmaceutical resources), regulating (e.g., flood, storm and erosion control, coastal protection and shoreline stabilization, water purification and waste treatment), supporting (e.g., habitat, biodiversity, nursery, nutrient cycling), and cultural services (e.g., recreation and tourism, aesthetic and spiritual values, education and research) [3-5]. Furthermore, mangroves provide ecosystem services that contribute to climate change mitigation, being an efficient source and sink for carbon dioxide [4, 6]. This contributes significantly to the global carbon budget [7, 8]. The total economic value of all the ecosystem services provided by mangroves is estimated in approximately US$ 186 million each year [9].

Dieses Werk ist copyrightgeschützt und darf in keiner Form vervielfältigt werden noch an Dritte weitergegeben werden.
Es gilt nur für den persönlichen Gebrauch.

Despite the socioeconomic and ecological importance of mangroves, the range and quality of these ecosystems is declining worldwide [10]. A similar scenario is observed in Brazil, which despite having the second largest mangrove area in the world [11-14], about 25% of his total mangrove forests have already been destroyed [15]. One of the most affected areas is the northeast coast [16, 17].

The creation of shrimp and fish farms, the overharvesting of wood for charcoal and fuel, the industrial and tourism development, among others anthropogenic activities resulted in significant changes in the coastline. Moreover, the erosion of seaward mangrove fringes, increasing saline intrusion and increasing wind driven sand transport resulted in significant changes in mangrove cover along that part of the Brazilian coast [18, 19].This current scenario of mangroves degradation and loss caused by coastal use and occupation, coupled with the effects of rise in sea level, leads to a decline in their potential to sequester and to store carbon, resulting in economic damage [20].

Even though there has been an improvement in the knowledge about the regulating service of carbon sequestration worldwide in the last years [21, 22], there is a scarcity of economic assessments of a potential carbon-credit system [23]. This is even more incipient in Brazil, since there is a political inaction related to the protection of carbon storage ecosystems and the ecosystem services that they provide.

This absence of information in the existing market prices leads to an undervaluation of mangrove ecosystems both in private and public decision-making, reinforcing the relevance of developing valuation studies of the carbon storage ecosystem service by employing these values appropriately in coastal management, conservation and restoration [4]. But, there are intentions from the Reducing Emissions from Deforestation and Forest Degradation (REDD) to financially reward developing countries for keeping carbon stored in their natural forests [24], making essential the inclusion of mangrove protection measures in Brazilian policies.

Cost-benefit analyzes of different mangrove uses allow avoiding the destruction of these ecosystems by making stakeholders aware of the ecological and economic value of them [25]. In this context, economic valuation of mangrove ecosystem can be useful for indicating the ‘opportunity cost’ of other land-use practices [26] and the ‘replacement cost’ as a benefit of restoring the lost mangroves areas. Both ways estimate the cost-benefit of conservation and help in land-use decision making.

The Ponta do Tubarão Sustainable Development Reserve (RDSPT) was selected as a case study because it is located in the northern littoral of Rio Grande do Norte state in northeastern Brazil, a region known for suffering intense erosive processes and anthropogenic actions [27, 28] that affect adversely the action of natural processes on the ecosystems associated with the geo-environmental units present in the region [28].

Dieses Werk ist copyrightgeschützt und darf in keiner Form vervielfältigt werden noch an Dritte weitergegeben werden.
Es gilt nur für den persönlichen Gebrauch.

These processes of erosion and degradation of the coastline threaten reducing and even making the mangroves disappear [27]. Moreover, the integrity of the RDSPT has been compromised by the construction of wind farms and oil extraction. Both activities have increased dramatically in the long term (20 to 100 years) and have been widespread [29], jeopardizing the maintenance of the region's ecological balance and compromising the sources of income of the local communities [30].

Considering the scarce of economic assessments of mangroves within the RDSPT, strategies of management of these areas were planned. The present work aims to estimate the opportunity and the replacement costs, associated with the dynamics of loss and gain of mangrove areas along the coastline of the RDSPT as a consequence of the coastline progression and resource exploration over 30 years. The economic values were correlated to the monetary worth of the carbon sequestered by the mangrove forests. This valuation study intends to promote the conservation and management of mangrove ecosystems, while allowing the maintenance of the carbon storage service benefits and other ecosystem services provided by mangroves such as coastal protection, therefore, reducing the costs of erosion containment.

2 Materials and Methods

2.1 Study Area

The Ponta do Tubarão Sustainable Development Reserve (RDSPT) is a protected area located on the northern coast of the state of Rio Grande do Norte, between the cities of Macau and Guamaré (Fig. 1). Delimited by the UTM coordinates Zone 24 South (5° 6' 54" S, 36° 38' 2" W and 5° 5' 42" S, 36° 19' 30" W), it has a total area of 12,940 ha [31].

This region has an intense sedimentary dynamics and is formed by oceanic and sheltered sandy beaches, barrier islands and sandy spurs, tidal channels, mobile and vegetated dune fields, mangroves and estuarine areas. Meteooceanographic forcings model the landscape in short and long terms periods, subjected to the trade winds, semidiurnal mesomaric regime and action of coastal drift currents [32]. It is a sector with a delicate geoenvironmental equilibrium, in which changes in landscapes conformation can result from factors such as the generation and/or disappearance of coastal areas due to erosive trends, displacement of barrier islands and sandy spurs, moving of dune fields and opening and closing of tidal channels in estuarine areas [33].

The mangrove forests are found in the coastal stretches and sheltered areas linked indirectly by the sea, as well as in the interior of lagoons and/or along canals. Some of the species present are the red mangrove (*Rhizhophora mangle* L.), white mangrove (*Laguncularia racemosa* (L.) C. F. Gaertn.), and black mangrove (*Avicennia schaueriana* Stapf & Leech.).Mangroves are usually located at the points of the coast, where the tidal waters arrive with less energy, depositing the fine particulate that they bring into suspension, and forming the substrate necessary for their development [34].

Dieses Werk ist copyrightgeschützt und darf in keiner Form vervielfältigt werden noch an Dritte weitergegeben werden.
Es gilt nur für den persönlichen Gebrauch.

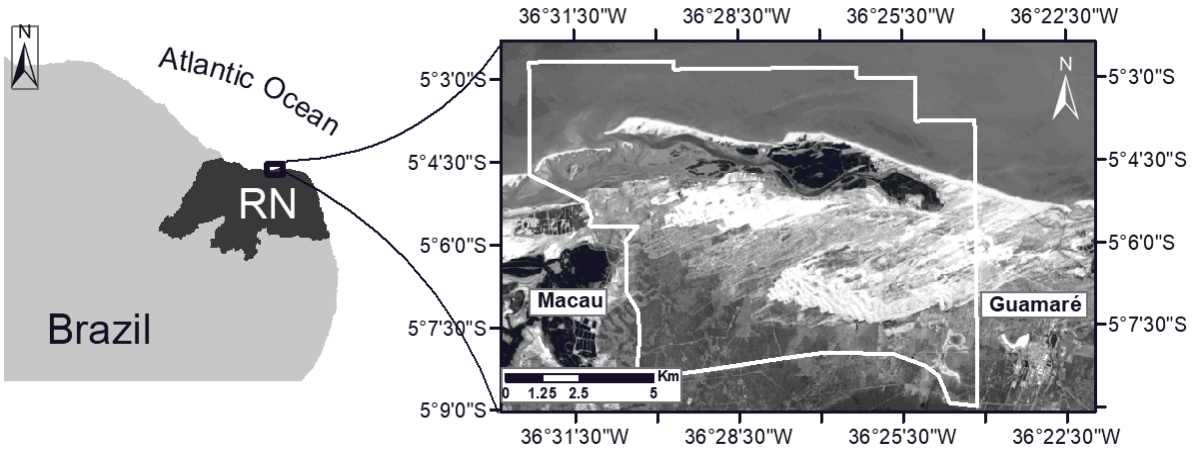

Figure 1:Location of the RDSPT between the cities of Macau and Guamaré, in the state of Rio Grande do Norte, in northeastern Brazil

2.2 Spatial Analysis

The multispectral optical images Landsat 5-TM of day 08/17/1984 and Landsat 8-OLI of day 10/10/2014, both with path/row 214/64 and resolution of 30 m, were provided by Geoprocessing (GEOPRO) Lab of the Geology Department of Federal University of Rio Grande do Norte. The images were treated with DIP (Digital Image Processing) techniques using the software ER-Mapper 7.1®, allowing to characterize the geoenvironmental units of the study area, highlighting the mangrove areas and differentiating them from dunes and other coverages. The application of the colored compositions of the multispectral bands in the color systems Red-Green-Blue (RGB) also permitted to distinguish the urban areas. The images were then interpretated using the software ArcGis 10.2®.

Through a supervised classification,it was possible to delimit and to quantify the mangrove areas. Prior information about the different classes and their locations was get from GEOPRO Lab´s works, which provided field data and land cover types information.For the multitemporal analysis of the evolution of the coastline morphodynamics and the trends of expansion/contraction of the mangroves, a vectorization and quantification of the features was performed, revealing the changes that occurred in 30 years. Thus, it was possible to observe those areas that suffered erosion, accretion and those that remained stable.

2.3 Valuation Analysis

For the economic valuation of the CO_2storage service of the RDSPT mangroves, first the values of CO_2 stored (in tonnes) by three species compositions were determined, previously registered by [35], who also quantified the percentages of coverage and averages of carbon storageper hectare of each species. In turn, the estimates made by the author were based on the works of [24, 36, 37].

Dieses Werk ist copyrightgeschützt und darf in keiner Form vervielfältigt werden noch an Dritte weitergegeben werden.
Es gilt nur für den persönlichen Gebrauch.

Then, the economic values of the quantities of carbon sequestered by each specie in the years 1984 and 2014 were estimated, applying the average value of carbon credit quoted in Brazil in 2014.

After these estimations, the methods of 'opportunity cost' and 'replacement cost' were applied. On the one hand, the opportunity cost method defines the value of an alternative use of the resources, considering the consumption of goods and services that were abdicated. For this, a comparison between the economic values of carbon sequestered by the current mangrove forest and the economic benefits that the wind industry provides to the local population of the RDSPT, translated in jobs generation, were performed. This last aspect was determined following as reference what was calculated by [38], in relation to the indirect jobs of operation and maintenance generated by the wind energy in Brazil, and considering the current minimum wage in Brazil.

It is important to emphasize that the wind industry in the RDSPT is represented by four wind farms (Alegria I, Alegria II, Miassaba II and Miassaba III) distributed within the reserve. Alegria I is the oldest one, operating since 2010, followed by Alegria II and Miassaba III in 2012, and Miassaba II in 2014.

A comparison between the quantity of carbon stored (in tons) per hectare of mangrove and the total amount of CO_2 emissions avoided (in tons) by the wind farms per hectare was also made. Thus, it was evaluated what could be gained with the preservation or conservation of the mangroves instead of a possible expansion of the wind industry.

In order to calculate the amount of CO_2 emissions avoided by the wind farms of the RDSPT, first the amount of energy generated by the wind farms was estimated, following the formula: *[(Power x Time) x Capacity factor = Energy (electricity) generated]*. Subsequently, the average annual CO_2 emission factor of the Brazilian interconnected system was applied, in order to finally obtain the CO_2 emissions reductions.

The other method applied was the replacement cost method, which means the expenditure of replacing or restoring a damaged environment to its original state (useful as a measure of the benefit of restoration). Hence, the cost of restoring those mangrove areas lost in 30 years was estimated, based on the cost values obtained by [39].

3 Results

The resulting images from the PDI treatments with compositions Landsat 5-TM R(6/2) G(5/3) B(4/2) of the year 1984 and Landsat 8-OLI R(7/5) G(6/4) B(5/3) of the year 2014, revealed the existance of different geoenvironmental units such as mobile dunes, beach strip, flood areas with muddy substrate, hyperoxerophilous caatinga vegetation, villages with urban settlement, and mangroves.

Dieses Werk ist copyrightgeschützt und darf in keiner Form vervielfältigt werden noch an Dritte weitergegeben werden.
Es gilt nur für den persönlichen Gebrauch.

The mangrove area of the RDSPT in the year of 1984 was around 503 ha, and this area increased in 2014 by only 3,46%, reaching 521 ha. Although there was forest loss in some parts and gain in others, the final balance shows a slight increase of 18.1 ha (Fig. 2).

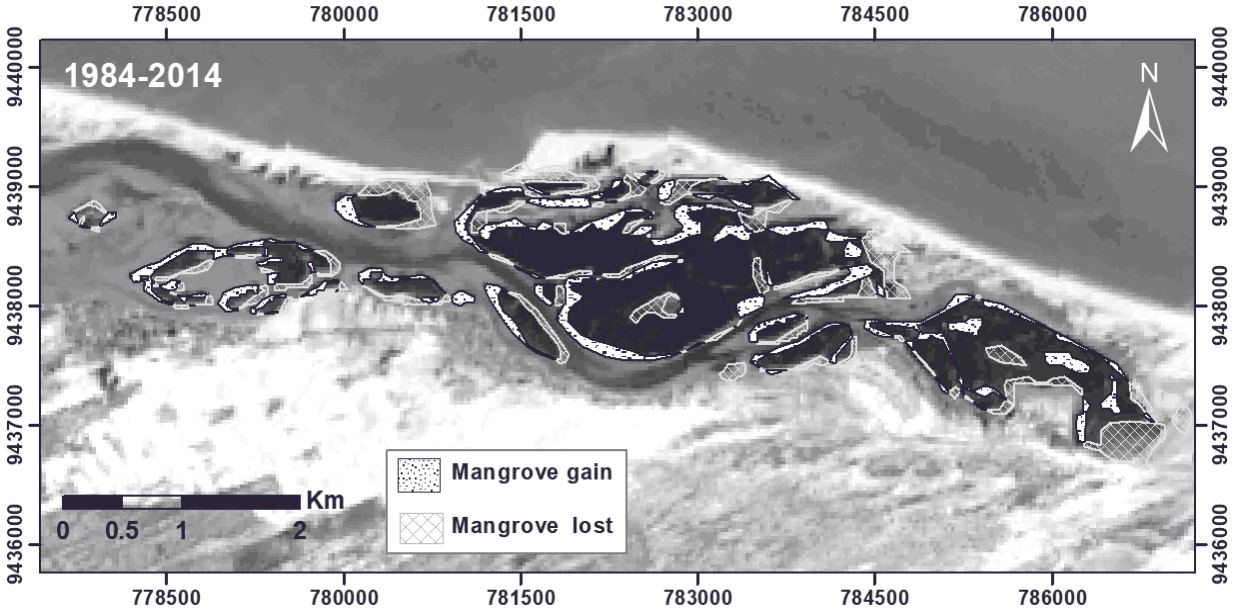

Figure 2: Areas of loss and gain of mangroves in the RDSPT over 30 years

According to [35], the vegetation of the total mangrove area of the RDSPT is constituted by 63% of *Rhizophora mangle*, 25% of *Avicennia shaueriana,* and 12% of mixed species. The author also found that the averages carbon stored per hectare per species are 39,93 t/ha by *R. mangle*, 28.47 t/ha by *A. shaueriana,* and 34.20 t/ha by a mixed forest.

Extrapolating these results to the present research, and following the assumption that the current structure and distribution of species represents the historical pattern for 1984, it could be deduced that the area occupied and the amount of CO_2 stored by the three species in both years are those that are given in Table 1.

Table 1: Amountsof CO_2 stored by the three species distributed in the total mangrove area of the RDSPT in the years 1984 and 2014

	1984		2014		1984-2014
	Area (ha)	CO_2 seq. (t)	Area (ha)	CO_2 seq. (t)	Diff. CO_2 seq. (t)
R.mangle	317	12,657	328	13,111	455
A. shaueriana	126	3,581	130	3,710	129
Mixed florest	60.4	2,065	62.5	2,139	74.2
Total	503	18,302	521	18,960	658

Dieses Werk ist copyrightgeschützt und darf in keiner Form vervielfältigt werden noch an Dritte weitergegeben werden.
Es gilt nur für den persönlichen Gebrauch.

According to historical data provided by the market for carbon credits trading [40], the average value of carbon credit quoted in Brazil in 2014 was of 6.3 €/t CO_2. Thus, when applying this price in the study area, based on the average amount of carbon stored in 1 hectare of mangrove of each specie as previously mentioned, and considering the total area occupied by the three species in each year, the following results come out and are shown in Table 2.

Table 2:Economic values of the quantities of carbon stored by the three species distributed in the total mangrove area of the RDSPT in the years 1984 and 2014

		1984	2014	1984-2014
	Value (€/t CO_2/ha)	Value (2014 €/t CO_2)		
R.mangle	252	79,737	82,602	2,865
A. shaueriana	179	22,560	23,371	810.7
Mixed florest	215	13,007	13,475	467.5
Total		115,304	119,447	4,143

3.1 Environmental Costs and Mangrove Benefits

3.1.1 Opportunity Cost Method

The wind energy in Brazil generates direct and indirects jobs, and within the direct jobs there are the operation and maintenance activities, which are permanent jobs, accounted annualy using the direct job index in (jobs/Megawatts-MW). Following the guidelines established by [38], the participation of these kind of activities in relation to the total of jobs in Brazilian wind energy is less than one job per installed MW (about 0.5 jobs). By hypothesizing that in the existing wind farms in the reserve, most of the local employees may work on maintenance and operation tasks, one can deduce that there are approximately 117 employees or less participating in this activity among the four wind farms.

If one considers that each employee receives a salary equivalent to the current minimum wage in Brazil of R$ 937 or € 255.31 (1 €= R$ 3.67), then the economic benefit produced by the wind energy in the RDSPT is about € 29,957 (Table 3).

Table 3: Economic benefit produced by the wind energy in the RDSPT, translated in jobs generation

Wind Farm	Power (MW)	Jobs (0.5/MW)	Income (€ 255.31)
Alegria I	51.15	25.5	6,529
Alegria II	100.6	50.3	12,848
Miassaba II	14.40	7.2	1,838
Miassaba III	68.47	34.2	8,741
Total		117.3	29,956

Dieses Werk ist copyrightgeschützt und darf in keiner Form vervielfältigt werden noch an Dritte weitergegeben werden.
Es gilt nur für den persönlichen Gebrauch.

Comparing these incomes with the economic benefit provided by the mangroves in 2014, previously estimated in € 119,447, it is obvious that the service of carbon storage by the mangroves affords 75% more profit than the wind energy to the communities of the RDSPT.

Moreover, in view of the capacity of wind farms to avoid CO_2 emissions to the atmosphere, it was possible to estimate these values from the corresponding powers, capacity factors and energy of each wind farm (Table 4), annual time (24 hours x 365 days), and the average annual CO_2 emission factor of the Brazilian interconnected system (81.7 g CO_2/kWh).

With these results, a comparison between the total amount of CO_2 emissions avoided by the wind farms per hectare calculated in 35.49 t CO_2/ha (Table 5), and the quantity of carbon stored by the mangroves per hectare, which can range according to species from 28.47– 39.93 t CO_2/ha.

Table 4: Estimation of the amount of CO_2 emissions avoided by the four wind farms operating in the RDSPT

Wind Farm	Power (kW)	Capacity Factor	Energy (kWh)	CO_2 emissions avoided (t CO_2)
Alegria I	51,150	0.32	430,000,000	11,714
Alegria II	100,650	0.31	273,325,140	22,331
Miassaba II	14,400	0.49	61,356,442	5,013
Miassaba III	68,470	0.45	271,108,334	22,149
Total				61,207

Table 5: Estimation of the relation between the total amount of CO_2 emissions avoided by the wind farms and the occupied area

Wind Farm	Área (ha)	CO_2 emissions avoided (t CO_2)	Relation (t CO_2/ha)
Alegria I Alegria II	1,900	34,045	17.91
Miassaba II	Not reported	5,013	-
Miassaba III	1,260	22,149	17.57
Total			35.48

3.1.2 Replacement Cost Method

Based on [39], who estimated the cost of restoration of mangroves in Potengi estuary, also located in Rio Grande do Norte state, the environmental impairment of mangrove deforestation reaches values between US$ 4.2 millon and 4.6 millon per hectare or about € 3.5 millon - 3.9 millon per hectare (1 € = US$ 1.17). Applying the lower value for the total lost mangrove area in the RDSPT in

Dieses Werk ist copyrightgeschützt und darf in keiner Form vervielfältigt werden noch an Dritte weitergegeben werden.
Es gilt nur für den persönlichen Gebrauch.

30 years, sized in 108.35 ha, and corrected with Brazilian inflation rate (CPI) of this year, estimated in 3% [40], it was found that the restoration and reforestation of this area would cost approximately € 377 millon.

This value comes from a series of steps required during the restore process described by [41], including the improvement and preparation of the soil, plant recovery and maintenance of the vegetation. It also comprises the cost of inputs. The potential areas to be reforested are those that have muddy-sand and muddy substrates with ideal physicochemical properties for planting mangrove species [42, 43]. In the case of the RDSPT mangrove forest, these areas are those that have become flood areas as a consequence of the erosive process, located in core areas and patches near the beach strip (Fig. 3).

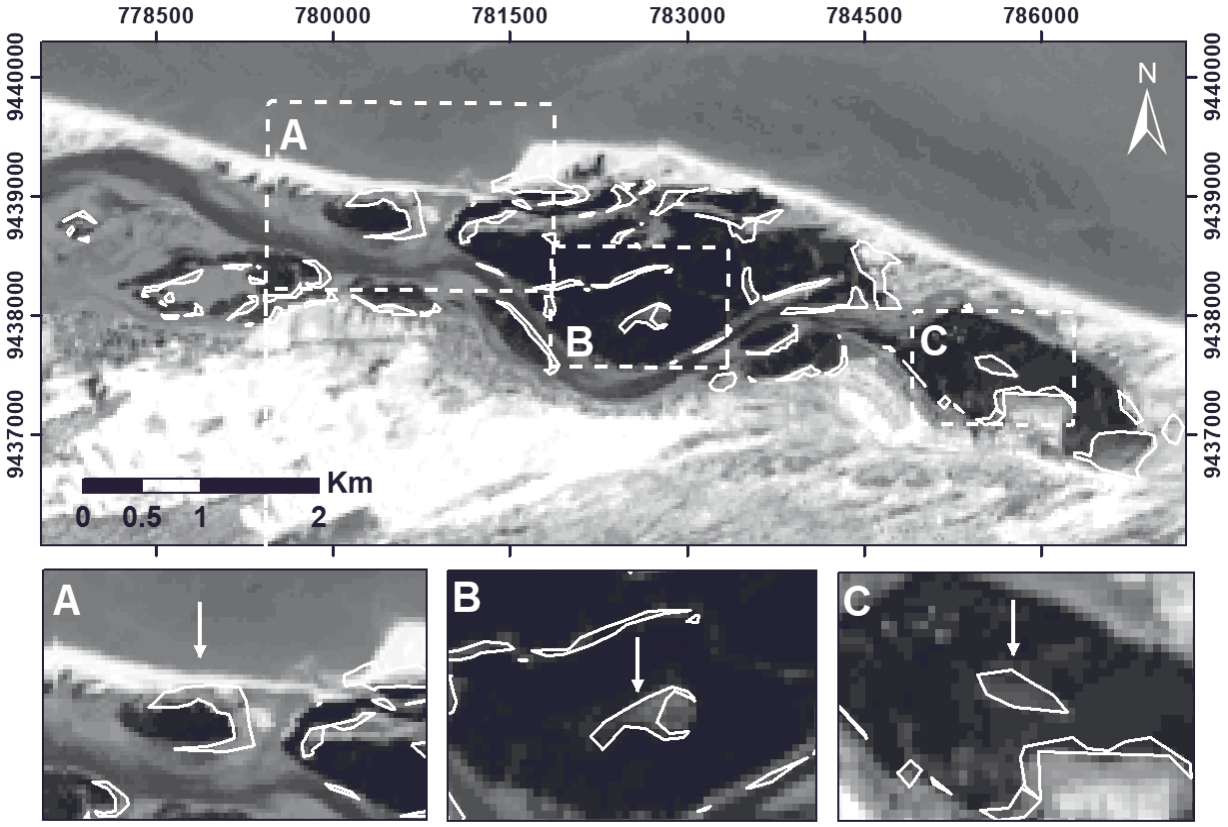

Figure 3: Image Landsat 8-OLI of the year 2014 showing the mangrove areas lost in 30 years. (A) Patches of flood areas near of the beach strip, (B, C) Flooded core areas

4 Discussion

Mapping the spatial distribution of mangroves is always possible, when mangrove areas are accurately identifiable from other geoenvironmental units [44]. It is possible to distinguish mangrove areas from non-mangrove vegetation and other coverages through the application of DIP techniques, which proved to be an efficient tool when it comes to enhancing the target unit. It was possible to highlight and delimit the mangrove areas both in Landsat 5-TM and Landsat 8-OLI, although they presented different colors due to differences in the characteristics of the bands of

Dieses Werk ist copyrightgeschützt und darf in keiner Form vervielfältigt werden noch an Dritte weitergegeben werden.
Es gilt nur für den persönlichen Gebrauch.

each one. The multitemporal analysis performed from a supervised classification and subsequent vectorization revealed changes in the geomorphological features of the study area over time, given by coastal processes.

It is evident that several erosion processes have occurred in the landscape due to sea level rise, mainly in the strip beach, forming barrier islands and river and tidal channels. There is a continuous migration of these barrier islands with preferential alignments and orientations [45]. According to a prognostic study of coastal erosion on the northern coast of Rio Grande do Norte, performed by [46], the erosive process that will occur here in 30 years in the beach strips, with northeast to southwest direction, will lead to a complete disappearance of the islands barriers and sandy bars of the RDSPT. In addition, the authors also affirm that the RDSPT estuary will remain protected for the next 20 years, but due to erosion of barrier islands, local estuarine ecosystems will be compromised. The loss of coastal area and vegetation cover of the estuarine system will cause increasingly sharp instabilities of the coastal zone and loss of marine biodiversity.

The geomorphology changes observed in the study area also brought variations in the mangrove areas. In 30 years, RDSPT´s mangrove areas increased from 503.14 ha to 521.21 ha. This result is similar to those found by [47] at the mouth of the Açu River (near the RDSPT), in which a fluctuation between mangrove loss and gain was observed between 1998 and 2009, but with a final balance of 391.65 ha of increase.The expansion tendency of mangroves that was registered in this research, have been also observed by other researchers in Brazil [48, 49] and worldwide [50, 51, 14]. This may be due to the appearance of new sedimentation areas caused by changes in estuarine dynamics by sea level rise, and changes in sedimentary patterns [18], cited in [39]. Anyway, according to [39], under some circumstances, it is also possible that the new substrate areas do not last long, leading to the loss of mangroves due to erosion process. The increase in extent of some mangroves patches in the RDSPT may be due to the generation of muddy and muddy-sand substrate areas in the tidal and fluvial-estuarine lowlands, with ideal physicochemical properties for the development of mangrove.

With the increase in mangrove areas, an increase in the carbon storage capacity will come . In the RDSPT, the total mangrove area stores almost 19,000 tons of CO_2, contribuiting to the mitigation of gas emissions while providing biodiversity protection, benefits to fisheries, and to coastal protection.

There are programs that reduce emissions from deforestation and degradation, such as REDD programs, being a great opportunity for developing countries like Brazil, to reconsider the potential carbon-credit system that is generated from the carbon sequestration service, encouraging to preserve their forests [52, 23]. In addition, the Kyoto Protocol expects developing countries to commit to reducing emissions through the use of clean energy and acting as CO_2 sequesters through forests. And for this, there is a carbon market known as Clean Development Mechanism, which consists of a carbon credit trading based on sequestration or mitigation projects [47]. Within this framework of the carbon-credit system, it was verified that the RDSPT´s

Dieses Werk ist copyrightgeschützt und darf in keiner Form vervielfältigt werden noch an Dritte weitergegeben werden.
Es gilt nur für den persönlichen Gebrauch.

mangroves provides a CO_2 storage service, of which prices range from € 179,36 to € 251,55 per t $CO_2$and per ha, depending of the species. These prices obtained are within the expected one by [54], who found that the average value for the CO_2 storage service mangroves worldwide, using market prices, is between US$ 100 and US$ 500 per ha and year.

The opportunity and replacement costs estimated in this research, also reinforce the importance of protecting mangroves by maintaining the carbon stores and restoring the degraded areas. Comparing the benefits between mangroves and the wind energy sector in the reserve, it is noticeable, how advantageous is to maintain the intact mangrove areas.

Due to sea level rise and some anthropogenic perturbations, the RDSPT´s mangroves have been oscillating in loss and gain of areas through time, as had been registered by other researchers. At the same time, this study found an increase of some patches and the reduction of others over 30 years, maintaining a good level of CO_2storage. Although the current balance of areas is positive, it is important to apply restoration plans to guarantee and even to improve the continuity of the ecosystem services provided by these forests, that not only include carbon storage, but also coastal protection, among others.

Applying the replacement cost method in the study area, it was found that the costs for restoration and reforestation of the lost mangrove areas would cost about € 377 millon. This amount is much smaller than the costs registered by [39] in Potengi mangrove, estimated in US$ 6.1 billion (€ 5.2billion). Nevertheless, considering that are high values, if there are not enough resources for an active restoration like reforestation, it is possible to resort to a passive recovery, leading to a natural regeneration of the forests. According to [55], this last strategy could be successful at low cost, and at the same time, it would preserve diversity and faunal assemblages.

In order to reach that recovery success it is important to control the conditions of the appropriate humidity and consistency of the substrate [56], and to understand the autecology of the species and the hydrological standards [57]. If it is an assisted recovery, it is also relevant to choose which species and where to reforest, modelling vegetation development and individual interactions [58]. According to [55], restoration using *R. mangle* allows accelerating the recovery of functional groups, ecosystem services and high biomass production, being suitable for sites with high propagule predation. Anyway, it is worth to consider mixed species, and not to restore in a monospecific form [59]. So, it is recommended to use *R. mangle* as a pioneer and to allow the seeds of other species to naturally colonize available soils [45].

The potential areas to be reforested are those that have become flood areas as a consequence of erosion and sea levelrise, located in core areas and patches near the beach strip. The core areas are the main places, where the greatest efforts of restoration should be placed, where conservation of biodiversity, ecological integrity, wilderness and other similar aspects have priority, and it is possible to maintain existing natural qualities or to restore degraded landscapes [60]. Indeed, the core areas function more as indicators of quality than the total area [61]. Other

Dieses Werk ist copyrightgeschützt und darf in keiner Form vervielfältigt werden noch an Dritte weitergegeben werden.
Es gilt nur für den persönlichen Gebrauch.

areas, in which the mangrove recovery could be performed, are the patches near the beach strip, surronding the fragments of small size, increasing the buffer effect of these fragments, which will consequently favor the increase of the core areas.

In the Brazilian northeast, and especially in Rio Grande do Norte, public policies for the recovery and/or preservation of mangroves are still scarce. Therefore, the generation of knowledge is essential for the elaboration of conservation and management plans in order to encourage the government to participate in preservation policies.

5 Conclusions

The expansion tendency observed in the RDSPT´s mangrove areas was registered by many researchers in Brazil. Moreover, the opportunity and replacement costs obtained in this work demonstrate the importance of protecting mangroves by maintaining the carbon stores and restoring the degraded areas. Beyond the high costs for restoration and reforestation of the lost mangrove areas, it is possible to resort to a passive recovery. The potential areas to be reforested are core areas and patches near the beach strip. Further studies are necessary in order to improve the knowledge about the total value of mangroves in the RDSPT, including not only the carbon storage, but also other ecosystem services. It is also necessary to inquire more about the potential locations to restore and to reforest, taking into consideration predictions of coastal erosive process.

6 Acknowledgments

The authors would like to thank to DAAD and Exceed Swindon for making the participation at the INECEP event possible and for the financial support provided. Authors also thank for the contribution given by the Geoprocessing Laboratory (GEOPRO) at the Center of Exact and Earth Sciences at the Federal University of Rio Grande do Norte.

7 References

1. Bann, C.: Economic valuation of tropical forest land use options: a manual for researchers. (1998)
2. Stedman, S.-M., Dahl, T.E.: Status and trends of wetlands in the coastal watersheds of the Eastern United States 1998 to 2004. National Oceanic and Atmospheric Administration, National Marine Fisheries Service (2008)
3. Kumar, P.: The economics of ecosystems and biodiversity: ecological and economic foundations. UNEP/Earthprint (2010)
4. Barbier, E.B., Hacker, S.D., Kennedy, C., Koch, E.W., Stier, A.C., Silliman, B.R.: The value of estuarine and coastal ecosystem services. Ecological Monographs 81, 169-193 (2011)

Dieses Werk ist copyrightgeschützt und darf in keiner Form vervielfältigt werden noch an Dritte weitergegeben werden.
Es gilt nur für den persönlichen Gebrauch.

5. Brander, L.M., Wagtendonk, A.J., Hussain, S.S., McVittie, A., Verburg, P.H., de Groot, R.S., van der Ploeg, S.: Ecosystem service values for mangroves in Southeast Asia: A meta-analysis and value transfer application. Ecosystem Services 1, 62-69 (2012)

6. Alongi, D.M.: Carbon sequestration in mangrove forests. Carbon Management 3, 313-322 (2012)

7. Mcleod, E., Chmura, G.L., Bouillon, S., Salm, R., Björk, M., Duarte, C.M., Lovelock, C.E., Schlesinger, W.H., Silliman, B.R.: A blueprint for blue carbon: toward an improved understanding of the role of vegetated coastal habitats in sequestering CO2. Frontiers in Ecology and the Environment 9, 552-560 (2011)

8. Chung, I.K., Beardall, J., Mehta, S., Sahoo, D., Stojkovic, S.: Using marine macroalgae for carbon sequestration: a critical appraisal. Journal of Applied Phycology 23,877-886 (2011)

9. Rath, A.B.: Mangrove Importance. WWF (2016). Available in: http://wwf.panda.org/about_our_earth/blue_planet/coasts/mangroves/mangrove_importance/

10. Ellison, A.M.: Macroecology of mangroves: large-scale patterns and processes in tropical coastal forests. Trees-Structure and Function 16, 181-194 (2002)

11. Kjerfve, B., Lacerda, L.D.: Mangroves of Brazil. Mangrove ecosystems technical reports ITTO TS-13 2, 245-272 (1993)

12. Kitzmann, D.I.S., Asmus, M.L., Laydner, C.: Gestão Costeira no Brasil. Estado atual e perspectivas. (2004)

13. Magris, R.A., Barreto, R.: Mapping and assessment of protection of mangrove habitats in Brazil. Pan-American Journal of Aquatic Sciences 5, 546-556 (2010)

14. Giri, C., Ochieng, E., Tieszen, L.L., Zhu, Z., Singh, A., Loveland, T., Masek, J., Duke, N.: Status and distribution of mangrove forests of the world using earth observation satellite data. Global Ecology and Biogeography 20, 154-159 (2011)

15. MMA (Ministério de Meio Ambiente): Panorama da conservação dos ecossistemas costeiros e marinhos no Brasil. Brasília: 152 p. Available in: http://www.mma.gov.br/estruturas/205/_publicacao/205_publicacao27072011042233.pdf. Brasília: MMA/SBF/GBA, (2010)

16. Amaro, V.: Diagnóstico e vulnerabilidade ambiental dos estuários do litoral norte e seus entornos. Instituto de Desenvolvimento Econômico e Meio Ambiente-IDEMA. Projeto de Zoneamento Ecológico-Econômico dos estuários do Estado do Rio Grande do Norte e dos seus entornos, SUGERCO/IDEMA, Natal/RN. Amaro, VE (Org.) Relatório Final (2002)

17. Souto, M.V.S., Castro, A., Grigio, A., Amaro, V., Vital, H.: Multitemporal analysis of geoenvironmental elements of the coastal dynamics of the region of the Ponta do Tubarão,

Dieses Werk ist copyrightgeschützt und darf in keiner Form vervielfältigt werden noch an Dritte weitergegeben werden.
Es gilt nur für den persönlichen Gebrauch.

City of Macau/RN, on the basis of remote sensing products and integration in GIS. Journal of Coastal Research 39, 1618-1621 (2006)

18. Lacerda, L., Marins, R.: River damming and changes in mangrove distribution. ISME/Glomis Electronic Journal 2, 1-4 (2002)
19. Maia, L., Lima, J.: Hydrogeochemical Characterisation of Groundwater Saline Intrusion in the Western Shore of Ceará, North-Eastern Brazil. Environmental Geochemistry in Tropical and Subtropical Environments, pp. 277-291. Springer (2004)
20. Beaumont, N., Jones, L., Garbutt, A., Hansom, J., Toberman, M.: The value of carbon sequestration and storage in coastal habitats. Estuarine, Coastal and Shelf Science 137, 32-40 (2014)
21. Spalding, M., Kainuma, M., Collins, L.: World atlas of mangroves. A collaborative project of ITTO, ISME, FAO, UNEP-WCMC.UNESCO-MAB, UNU-INWEH and TNC. Earthscan, London (2010)
22. Murray, B.C., Pendleton, L., Jenkins, W.A., Sifleet, S.: Green payments for blue carbon: Economic incentives for protecting threatened coastal habitats. Nicholas Institute for Environmental Policy Solutions, Report NI 11 (2011)
23. Siikamäki, J., Sanchirico, J.N., Jardine, S.L.: Global economic potential for reducing carbon dioxide emissions from mangrove loss. Proceedings of the National Academy of Sciences 109, 14369-14374 (2012)
24. Estrada, G.C.D., Soares, M.L.G., Santos, D.M.C., Fernandez, V., de Almeida, P.M.M., de Medeiros Estevam, M.R., Machado, M.R.O.: Allometric models for aboveground biomass estimation of the mangrove *Avicennia schaueriana*. Hydrobiologia 734, 171-185 (2014)
25. D'Croz, L., Kwiecinski, B.: Contribución de los manglares a las pesquerías de la Bahía de Panamá. Revista de Biologia Tropical 28, 13-29 (1980)
26. Vo, Q.T., Künzer, C., Vo, Q.M., Moder, F., Oppelt, N.: Review of valuation methods for mangrove ecosystem services. Ecological Indicators 23 ,431-446 (2012)
27. Neves, C.F., Muehe, D.: Vulnerabilidade, impactos e adaptação a mudanças do clima: a zona costeira. Parcerias Estratégicas 13,217-296 (2010)
28. Lima, E.: Vulnerabilidade da zona costeira de Pititinga, Rio do Fogo, Rio Grande do Norte. Universidade Federal do Rio Grande do Norte, M.Sc. Thesis, (2013)
29. Teixeira, M.G., Venticinque, E.M.: Fortalezas e fragilidades do Sistema de Unidades de Conservação Potiguar. Desenvolvimento e Meio Ambiente 29 (2014)
30. Dantas, S.T.P.d.L., Amaro, V.E.: Caracterização físico-química e avaliação das concentrações de elementos maiores e traços em sedimentos areno-lamosos do estuário de Diogo Lopes, litoral setentrional do estado do Rio Grande do Norte, Brasil (2012)

Dieses Werk ist copyrightgeschützt und darf in keiner Form vervielfältigt werden noch an Dritte weitergegeben werden.
Es gilt nur für den persönlichen Gebrauch.

31. IDEMA – Instituto de Desenvolvimento Econômico e Meio Ambiente do Rio Grande do Norte: Mapeamento geoambiental da Reserva de Desenvolvimento Sustentável Ponta do Tubarão. Relatório Técnico, Natal. (2004)

32. Vital, H., dos Santos Neto, F., Saraiva Plácido Junior, J.: Morfodinâmica de um Canal de Maré Tropical: Estudo de Caso na Costa Norte Rio Grandense, Nordeste do Brasil. Revista de Gestão Costeira Integrada-Journal of Integrated Coastal Zone Management 8, 113-126 (2008)

33. Santos, M.S.T., Amaro, V.E.: Dinâmica sazonal de processos costeiros e estuarinos em sistema de praias arenosas e ilhas barreira no Nordeste do Brasil. Revista Brasileira de Geomorfologia 14, 151-162(2014)

34. Macedo, R.K.: Metodologias para a sustentabilidade ambiental. ANÁLISE AMBIENTAL: estratégias e ações (1995)

35. Costa, B.C.P.d.: Sensoriamento remoto em suporte ao mecanismo de desenvolvimento limpo (MDL) em manguezais do litoral setentrional do Rio Grande do Norte, Brasil (2016)

36. Soares, M.L.G., Schaeffer-Novelli, Y.: Above-ground biomass of mangrove species. I. Analysis of models. Estuarine, Coastal and Shelf Science 65, 1-18 (2005)

37. Rodrigues, D.P., Hamacher, C., Estrada, G.C.D., Soares, M.L.G.: Variability of carbon content in mangrove species: Effect of species, compartments and tidal frequency. Aquatic Botany 120, 346-351 (2015)

38. Simas, M., Pacca, S.: Energia eólica, geração de empregos e desenvolvimento sustentável. Estudosavançados 27, 99-116 (2013)

39. Ferreira, A.C., Lacerda, L.D.: Degradation and conservation of Brazilian mangroves, status and perspectives. Ocean & Coastal Management 125, 38-46 (2016)

40. INVESTING.COM: Available in: https://br.investing.com/.

41. Galli, F.: Valoração de Danos Ambientais-Subsídio para Ação Civil. Série Divulgação e Informação 193, 230-244(1996)

42. DANTAS, S.: Caracterização Ambiental de Bancos Areno-Lamosos nos Campos Petrolíferos de Macau e Serra (RN), como Subsídio às Medidas Mitigadoras ao Processo Erosivo. 103 f. Dissertação (Mestrado em Ciência e Engenharia de Petróleo)–Programa de Pós-graduação em Ciência e Engenharia de Petróleo. Universidade Federal do Rio Grande do Norte. Natal-RN (2009)

43. Dantas, S., Amaro, V., Costa, B.: Mangrove reforestation as a mesotidal coastal protection and clean development mechanism on Macau-Serra oil Field, Potiguar Basin, Northeast Brazil. Journal of Coastal Research SI 64, 1268-1271 (2011)

44. Green, E.P., Clark, C.D., Mumby, P.J., Edwards, A.J., Ellis, A.: Remote sensing techniques for mangrove mapping. International Journal of Remote Sensing 19, 935-956 (1998)

Dieses Werk ist copyrightgeschützt und darf in keiner Form vervielfältigt werden noch an Dritte weitergegeben werden.
Es gilt nur für den persönlichen Gebrauch.

45. Nascimento, M.C.d.: A erosão costeira e sua influência sobre a atividade petrolífera: alternativas sustentáveis na mitigação de impactos ambientais. Universidade Federal do Rio Grande do Norte (2009)

46. Franco, C.d.M., Amaro, V., Souto, M.d.S.: Prognóstico da erosão costeira no Litoral Setentrional do Rio Grande do Norte para os anos de 2020, 2030 e 2040. Revista de Geologia 25, 37-54 (2010)

47. Amaro, V.E., Júnior, J.R.: Avaliação ecológico-econômica do manguezal na foz do rio Açu/RN: o sequestro de carbono e a importância da aplicação de práticas preservacionistas. Geologia 25, 71-84(2012)

48. Lacerda, L.D.d., Menezes, M.O.T.d., Molisani, M.M.: Changes in mangrove extension at the Pacoti River estuary, CE, NE Brazil due to regional environmental changes between 1958 and 2004. Biota Neotropica 7, 67-72 (2007)

49. Maia, L., LACERDA, L.d., Monteiro, L., Souza, G.: Atlas dos manguezais do nordeste do Brasil. Fortaleza: SEMACE 1, 125 (2006)

50. Benfield, S.L., Guzman, H.M., Mair, J.M.: Temporal mangrove dynamics in relation to coastal development in Pacific Panama. Journal of Environmental Management 76, 263-276 (2005)

51. Cavanaugh, K.C., Kellner, J.R., Forde, A.J., Gruner, D.S., Parker, J.D., Rodriguez, W., Feller, I.C.: Poleward expansion of mangroves is a threshold response to decreased frequency of extreme cold events. Proceedings of the National Academy of Sciences 111, 723-727 (2014)

52. Donato, D.C., Kauffman, J.B., Murdiyarso, D., Kurnianto, S., Stidham, M., Kanninen, M.: Mangroves among the most carbon-rich forests in the tropics. Nature Geoscience 4, 293-297 (2011)

53. Salem, M.E., Mercer, D.E.: The economic value of mangroves: a meta-analysis. Sustainability 4, 359-383 (2012)

54. Estrada, G.C.D., Soares, M.L.G., Fernadez, V., de Almeida, P.M.M.: The economic evaluation of carbon storage and sequestration as ecosystem services of mangroves: a case study from southeastern Brazil. International Journal of Biodiversity Science, Ecosystem Services & Management 11, 29-35 (2015)

55. Ferreira, A.C., Ganade, G., de Attayde, J.L.: Restoration versus natural regeneration in a neotropical mangrove: effects on plant biomass and crab communities. Ocean & Coastal Management 110, 38-45 (2015)

56. Ferreira, A., Pimenta, H., da Silva, L., de Souza, A.: Gestão ambiental de áreas degradadas: um estudo de caso nas nascentes e manguezais do rio Jaguaribe em Natal-RN. Associaçao Brasileira de Engenharia Sanitária e Ambiental (ABES)(ed), Trabalhos Técnicos do 24to Congresso Brasileiro de Engenharia Sanitária e Ambiental. Belo Horizonte, pp. 1-11 (2007)

Dieses Werk ist copyrightgeschützt und darf in keiner Form vervielfältigt werden noch an Dritte weitergegeben werden.
Es gilt nur für den persönlichen Gebrauch.

57. Lewis, R.R., Streever, B.: Restoration of mangrove habitat. WPR Technical Notes Collection (ERDC.TN-WRP-NV-RS-3.2).U.S. Army Engineer Research and Development Center, Vicksburg, MS., (2002)

58. Berger, U., Piou, C., Schiffers, K., Grimm, V.: Competition among plants: concepts, individual-based modelling approaches, and a proposal for a future research strategy. Perspectives in Plant Ecology, Evolution and Systematics 9, 121-135 (2008)

59. Bosire, J.O., Dahdouh-Guebas, F., Walton, M., Crona, B.I., Lewis, R., Field, C., Kairo, J.G., Koedam, N.: Functionality of restored mangroves: a review. Aquatic Botany 89, 251-259 (2008)

60. Noss, R.F., Dinerstein, E., Gilbert, B., Gilpin, M., Miller, B.J., Terborgh, J., Trombulak, S.: Core areas: where nature reigns. Continental conservation: scientific foundations of regional reserve networks. Island Press, Washington, DC 99-128 (1999)

61. McGarigal, K., Cushman, S.A., Neel, M.C., Ene, E.: FRAGSTATS: spatial pattern analysis program for categorical maps (2002)

Dieses Werk ist copyrightgeschützt und darf in keiner Form vervielfältigt werden noch an Dritte weitergegeben werden.
Es gilt nur für den persönlichen Gebrauch.

Dieses Werk ist copyrightgeschützt und darf in keiner Form vervielfältigt werden noch an Dritte weitergegeben werden.
Es gilt nur für den persönlichen Gebrauch.

Dieses Werk ist copyrightgeschützt und darf in keiner Form vervielfältigt werden noch an Dritte weitergegeben werden.
Es gilt nur für den persönlichen Gebrauch.